PTB bericht
Wissenschaftliche Veröffentlichungen
CP-8
Mai 2013

Volker Ebert, Jens Brunzendorf und Viktor Werwein (Hrsg.)

Spectral reference line data for atmospheric monitoring

Proceedings of the EUMETRISPEC workshop held at Wolfenbüttel castle and PTB Braunschweig, Nov. 15–16, 2012

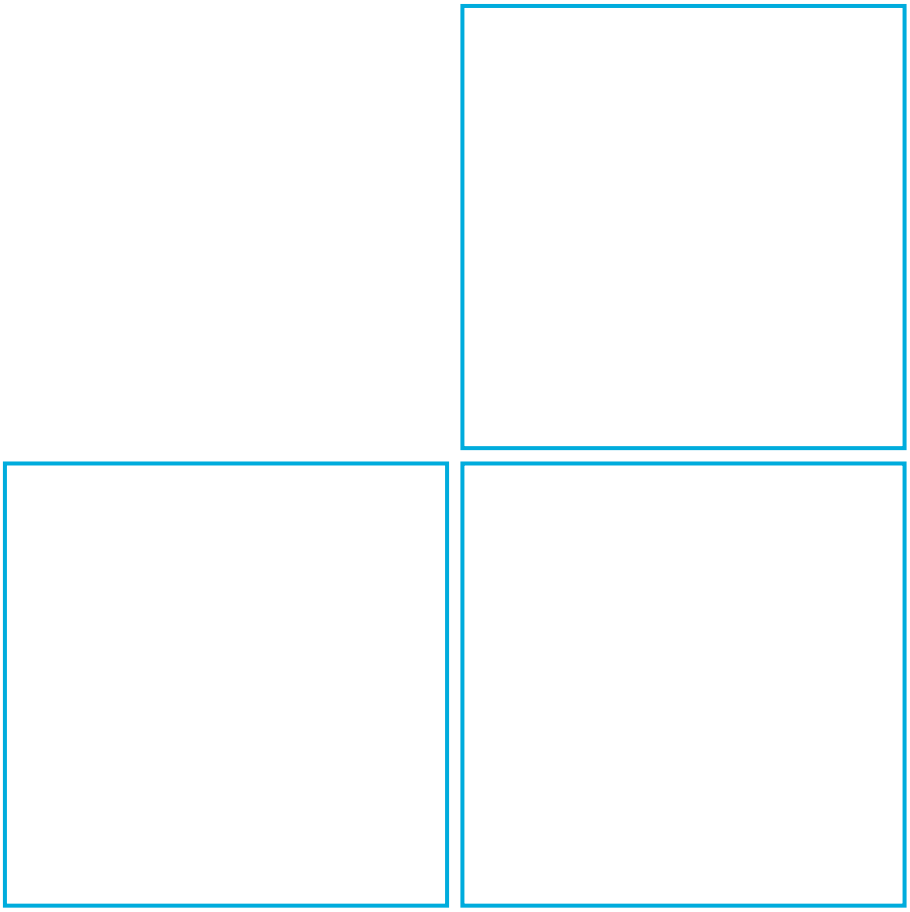

ISSN 1614-953X
ISBN 978-3-95606-034-2

Proceedings

of the EUMETRISPEC workshop held at Wolfenbüttel castle & PTB Braunschweig, November 15th - 16th, 2012

EMRP
European Metrology Research Programme
Programme of EURAMET

The EMRP is jointly funded by the EMRP participating countries within EURAMET and the European Union

EURAMET
European Association of National Metrology Institutes

WORKSHOP PARTICIPANTS

Name	Institution
Alain Barbe, Prof. Dr.	Groupe de Spectrométrie Moléculaire et Atmosphérique, Université de Reims, France
Sigurd Bauerecker, Prof. Dr.	Institut für Physikalische und Theoretische Chemie, Technische Universität Braunschweig, Germany
Manfred Birk, Dr.	Institut für Methodik der Fernerkundung, Deutsches Zentrum für Luft- und Raumfahrt, Germany
Jens Brunzendorf, Dr.	3.22 Metrologische Molekülspektroskopie, Physikalisch-Technische Bundesanstalt, Germany
Bernhard Buchholz	3.22 Metrologische Molekülspektroskopie, Physikalisch-Technische Bundesanstalt, Germany
Alain Campargue, Dr.	Laboratoire Interdisciplinaire de Physique, Université Grenoble, France
Marc Coleman, Dr.	Environmental Measurement, National Physical Laboratory, United Kingdom
Maurizio De Rosa, Dr.	CNR-INO, Istituto Nazionale di Ottica, Italy
Volker Ebert, Prof. Dr.	Head of department 3.2 Gasanalytik und Zustandsverhalten, Physikalisch-Technische Bundesanstalt, Germany
Alexander Fateev, Dr.	Optical Diagnostics Group, DTU Chemical Engineering, Danmarks Tekniske Universitet, Denmark
Edgar Flores, Dr.	Chemistry Department, Bureau International des Poids et Mesures, France
Thomas Forsting	Institut für Physikalische und Theoretische Chemie, Technische Universität Braunschweig, Germany
Karl-Heinz Gericke, Prof. Dr.	Institut für Physikalische und Theoretische Chemie, Technische Universität Braunschweig, Germany
Livio Gianfrani, Prof. Dr.	Dipartimento di Scienze Ambientali, Seconda Università di Napoli, Italy
Iouli E. Gordon, Dr.	Atomic and Molecular Physics Division, Harvard-Smithsonian Center for Astrophysics, USA
Jeremy. J. Harrison, Dr.	Department of Chemistry, University of York, United Kingdom
Axel Keens, Dr.	Bruker Optics, Germany
Maria B. Kiseleva, Dr.	Onderwijsinstituut voor Moleculaire Wetenschappen Radboud Universiteit Nijmegen, Netherlands
Alexander Klein	3.22 Metrologische Molekülspektroskopie, Physikalisch-Technische Bundesanstalt, Germany
Benjamin Kühnreich	Physikalisch-Technische Bundesanstalt and Technische Universität Darmstadt, Germany
Graham Leggett, Dr.	Environmental Division, Tiger Optics LLC, USA
Sven Liebich	3.23 Thermisches Zustandsverhalten und Dichte, Physikalisch-Technische Bundesanstalt, Germany
Daniel Lisak, Prof. Dr.	Instytut Fizyki , Uniwersytet Mikołaja Kopernika, Poland
Christoph Maul, Dr.	Institut für Physikalische und Theoretische Chemie, Technische Universität Braunschweig, Germany
Javis Nwaboh, Dr.	Metrologische Molekülspektroskopie, Physikalisch-Technische Bundesanstalt, Germany

Johannes Ofner, Dr.	Atmosphärische Chemie, Bayreuther Zentrum für Ökologie und Umweltforschung, Germany
Johannes Orphal, Prof. Dr.	Institut für Meteorologie und Klimaforschung, Karlsruher Institut für Technologie, Germany
Stefan Persijn, Dr.	Van Swinden Laboratory (VSL), Netherlands
Jan C. Petersen, Dr.	Dansk Fundamental Metrologi (DFM), Denmark
Andrea Pogany, Dr.	3.22 Metrologische Molekülspektroskopie, Physikalisch-Technische Bundesanstalt, Germany
Anne Rausch, Dr.	3.22 Metrologische Molekülspektroskopie, Physikalisch-Technische Bundesanstalt, Germany
Klaus Schäfer, Dr.	IMK-IFU, Karlsruhe Institute of Technology, Germany
Franz Schreier, Dr.	Institut für Methodik der Fernerkundung, Deutsches Zentrum für Luft- und Raumfahrt, Germany
Anton Serdyukov, Dr.	3.22 Metrologische Molekülspektroskopie, Physikalisch-Technische Bundesanstalt, Germany
Jörn Stenger, Prof. Dr.	Präsidium, Physikalisch-Technische Bundesanstalt, Germany
Geoffrey C. Toon, Dr.	Jet Propulsion Laboratory, California Institute of Technology, USA
Ha Tran, Prof. Dr.	Laboratoire Interuniversitaire des Systèmes Atmosphériques, Université Paris-Est Créteil, France
Markku Vainio, Dr.	Mittatekniikan Keskus (MIKES), Finland
Miroslava Valkova, Dr.	Slovenský Metrologický Ustav (SMU), Slovakia
Ann Carine Vandaele, Dr.	Belgisch Instituut voor Ruimte-Aeronomie, Belgium
Ignacio Vespoli	Institut für Physikalische und Theoretische Chemie, Technische Universität Braunschweig Physikalisch-Technische Bundesanstalt, Germany
Steven Wagner, Dr.	Technische Universität Darmstadt and Physikalisch-Technische Bundesanstalt, Germany
Stefan Welzel, Dr.	Department of Applied Physics, Eindhoven University of Technology, Netherlands
Olav Werhahn, Dr.	3.22 Metrologische Molekülspektroskopie, Physikalisch-Technische Bundesanstalt Physikalisch-Technische Bundesanstalt, Germany
Viktor Werwein	3.22 Metrologische Molekülspektroskopie, Physikalisch-Technische Bundesanstalt Physikalisch-Technische Bundesanstalt, Germany
Oliver Witzel	3.22 Metrologische Molekülspektroskopie, Physikalisch-Technische Bundesanstalt Physikalisch-Technische Bundesanstalt, Germany
Sergei N. Yurchenko, Dr.	Department of Physics and Astronomy, University College London, United Kingdom
Mark A. Zondlo, Prof. Dr.	Department of Civil and Environmental Engineering, Center for Mid-Infrared Technologies for Health and the Environment, Princeton University, USA
Jean-Jacques Zondy, Dr.	Laboratoire national de métrologie et d'essais (LNE), France

INTRODUCTION

This PTB-Report compiles the oral presentations and posters originally performed at the 1st stakeholder workshop organized by the EUMETRISPEC project consortium in Wolfenbüttel & Braunschweig, Germany, 2012 November 15/16.

The EUMETRISPEC project is embedded in the framework of the European Metrology Research Programme (EMRP). It aims to establish a metrology infrastructure for measuring molecular spectral reference line data for atmospheric monitoring. Since the beginning of the EUMETRISPEC project in late 2011, one of the first project goals was to implement and maintain a sustained interrelationship with the atmospheric monitoring, the lab spectroscopy and the spectral data simulation communities as the key stakeholders of the project's aims. Next to the EUMETRISPEC partners' own participations and impacts to scientific conferences, network meetings, or atmospheric bodies, a sequence of stakeholder workshops was intended to serve the EUMETRISPEC consortium's wish of a close collaboration with stakeholders. To streamline the project efforts this first workshop of this sequence was organized already in the initial phase of the project.

The organizing committee intended to attract people from meteorological organizations, from ground- and satellite-based monitoring networks, from field measurement-oriented academia as well as from quantum chemical modeling groups to present their views and needs on spectral reference data for use in atmospheric retrievals or in validation of simulated ab-initio spectral data. The workshop aimed to bring together experience, whishes and needs of environmental monitoring community with metrological points of view and goals of the EMRP project. To date, gathered spectral data, i.e. broad spectra or analyte-specific line-by-line spectral information are very often processed by means of reference data taken from data bases where accuracy and traceability are not in focus or not stated. Consequently, issues based on ill-defined accuracy or lack of traceability can evoke problems for long-term time atmospheric monitoring series or comparability between different remote sensing groups using different sources of line parameters when improving experimental measurement capabilities. Similarly, models that rely on spectral reference data input cannot improve on the reference data's quality. However, due to limitation in funding, lab-based investigations in line parameters are often difficult to realize by atmospheric community groups. So, the European Metrology Research Programme initiated by EURAMET e.V. and funded by the EU identified some possible area herein, where the metrology community could impact to assist the still existing efforts from the other communities.

During the workshop 9 invited 45-min. talks on spectroscopy and metrology key topics were given, accompanied by 6 additional presentations on EUMETRISPEC and the EMRP. Finally, a poster session comprising 21 posters from 91 authors coming from 30 institutions completed the workshop. In total 49 scientists attended the workshop, representing 31 institutions from 12 different nations. The report composed and presented here comprises all talks (part 1 of this report) and all posters (part 2) as they were authorized by the respective authors. We herewith would like to express our gratitude to all contributing speakers ,all poster presenters and all participants for their valuable input and hope that this report will reciprocate some of their efforts and provide a referable source of information for all involved communities. We hope you all come back for the next EUMETRISPEC workshop in 2014.

Braunschweig, February 2013, Olav Werhahn (PTB)

EUMETRISPECs Stakeholder Workshop Agenda

Thursday November 15, 2012 @ Wolfenbüttel Palace

08:30 – 08:40	Welcome
08:40 – 08:55	Jörn Stenger, EMRP Chair, on the "EMRP program"
08:55 – 09:25	Introduction to the EUMETRISPEC project
09:25 – 10:05	Mark Zondlo, Princeton University "*Atmospheric trace gas sensing: Community needs with respect to spectral line data*"
10:05 – 10:35	Coffee break
10:35 – 11:15	Geoffrey Toon, California Institute of Technology "*Ground-based atmospheric monitoring networks using FTIR: Present / future needs of the NDACC and TCCON community with respect to spectral line data*"
11:15 – 11:55	Johannes Orphal, Karlsruhe Institute of Technology "*Satellite-based remote sensing: Community needs with respect to spectral line data*"
11:55 – 13:25	Lunch break
13:25 – 14:05	Iouli Gordon, Harvard-Smithsonian Center for Astrophysics "*Efficient use of laboratory and theoretical spectroscopic data in HITRAN*"
14:05 – 14:30	Johannes Orphal, Karlsruhe Institute of Technology *"The GEISA Spectroscopic Database for Atmospheric Remote Sensing: Content Description and Critical Evaluation"*
14:30 – 15:10	Manfred Birk, German Aerospace Center "*FT-based high resolution lab spectroscopy for atmospheric line data measurements*"
15:10 – 15:40	Coffee break
15:40 – 16:20	Sergei Yurchenko, University College London "*Absorption/emission spectra from first principles: Towards large-scale production of line lists for molecules of atmospheric importance*"
16:20 – 17:00	Ha Tran, Laboratoire Interuniversitaire des Systèmes Atmosphériques "*The role of refined line shape models and line mixing for the extraction of high accuracy spectral line data: Status and need for experimental validation*"
17:00 – 17:20	Stefan Persijn, Van Swinden Laboratory "*Primary Reference Gas Mixtures: Preparation and Analysis*"
17:20 – 17:40	Jean-Jacques Zondy, Laboratoire national de metrologie et d'essais "*EUMETRISPEC work package 1*"
17:40 – 18:00	Jens Brunzendorf, Physikalisch-Technische Bundesanstalt "*EUMETRISPEC work package 2*"
18:00 – 18:20	Jan C. Petersen, Dansk Fundamental Metrologi "*EUMETRISPEC work package 3*"
20:00	Workshop dinner

Friday November 16, 2012 @ PTB Braunschweig

08:15 – 09:00	Bus transfer to PTB
09:00 – 10:45	Poster Session and Coffee
10:45 – 11:30	Daniel Lisak, Nicolaus Copernicus University in Torun "*Cavity ring-down spectroscopy for high-precision molecular line parameters*"
11:30 – 11:45	Conclusion
11:45 – 13:00	PTB laboratory tour

CONTENTS: PART A - TALKS

CONTENTS: PART B - POSTER SESSION

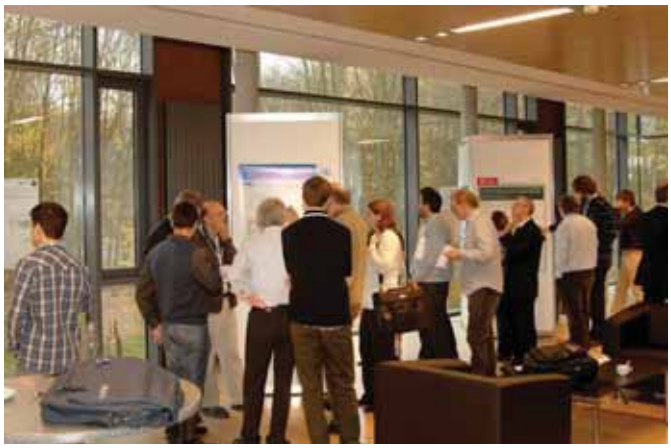

T. Forsting, I. Vespoli, C. Maul ***"Teaching an old dog new tricks: Quantum state selective detection of molecular chlorine by high-resolution cavity ring-down spectroscopy"***	**Poster 10**
J. Hald, L. Nielsen, J. C. Petersen **"*Towards Accurate Determination of Molecular Line Strength - Exemplified by Acetylene*"**	**Poster 11**
G. Leggett, T. Gardiner, R. Robinson **"*The Identification and Quantification of Greenhouse Gas Point Source Emissions Using Cavity Ring-Down Spectroscopy, Complementary to Other Techniques*"**	**Poster 12**
A. Nikitin, L. Brown, K. Sung, M. A Smith, A. Mantz, X. Thomas, L. Regalia, L. Daumont, R. Kochanov, M. Rey, V.G Tyuterev **"*New measurements and analyses of line positions and intensities of CH_3D in the infrared*"**	**Poster 13**
J. Nwaboh, A. Pogány, O. Werhahn, V. Ebert ***"Line strengths and collisional broadening coefficients of CO_2 (@2 µm) and H_2O (@2.7 µm), traceability and uncertainty assessment"***	**Poster 14**
A. Pogany, J. Nwaboh, O. Werhahn, V. Ebert **"*Towards traceability in CO2 line strength measurements at 2.7 µm using tunable diode laser absorption spectroscopy*"**	**Poster 15**
K. Schäfer, R. Harig, T. Blumenstock, N. Höfert, K. Weber **"*Development of a VDI guideline for passive FTIR measurements in the atmosphere*"**	**Poster 16**
E. Starikova, V. Tyuterev , A. Barbe , M.-R. De Backer, X. Thomas, S. A. Taskhun ***"Analysis of the FTS spectrum of $^{16}O_3$ in the range 3300 cm^{-1}: First example of new theoretical modelling for polyad of strongly coupled (220)/(121)/(022) states"***	**Poster 17**
M. Vainio, J. Peltola, M. Merimaa **"*Absolute-frequency measurements of CH_4 and N_2O line centers in the mid-infrared*"**	**Poster 18**
J. Vander Auwera, M. Herman, B. Amyay, K. Didriche, T. Foldes, D. Golebiowski, M. Tudorie, A. Fayt **"*Infrared line parameters for constituents of planetary and stellar atmospheres*"**	**Poster 19**
S. Wagner, P. Ortwein, V. Ebert **"*Spectroscopic Line Data for High Temperature Process Diagnostics in Complex Chemical Matrixes*"**	**Poster 20**
S. Welzel, J. Röpcke, R. Engeln **„ *Mid-IR Chemical Sensing Applied to Reactive Non-Equilibrium Environments*"**	**Poster 21**

PART 1: TALKS

"Introduction to the EUMETRISPEC project on Traceable Reference Spectral Line Data for environmental monitoring"

Volker Ebert

Physikalisch-Technische Bundesanstalt (PTB)

EUMETRISPEC Workshop

on "Traceable spectral reference line data for atmospheric monitoring"

November 15th - 16th, 2012
Wolfenbüttel Castle and PTB

- 1 -

Physikalisch Technische Bundesanstalt

- National Metrology Institute (NMI)
- 2nd largest NMI worldwide
- Federal Ministry of Economics and Technology (BMWi)
- 1900 staff members, 110 PhD students, 600 scientific papers per year, 145 Mio. € budget,
- Locations: **Braunschweig** + Berlin

Metrology:

- Science and application of correct measurement
- Traceability of results to the SI through national standards
- Determination of results with verification of uncertainty

- 2 -

PTB Organisation Chart

PTB

Presidential Board	Presidential Staff	Press and Information Office

Certification centre

QUEST-Institute at PTB

Mechanics and Acoustics	Precision Engineering
Electricity	Ionizing Radiation
Chemical Physics and Explosion Protection	Temperature and Synchrotron Radiation
Optics	Medical Physics and metrological Information Technology
Scientific-technical Cross-sectional Tasks	Administrative Services

- 3 -

Department 3.2

Division 3 „Chemical Physics and explosion protection “ Prof. Dr. K.-D. Sommer

Department 3.2 „ *Analysis and state behaviour of gases* “ Prof. Dr. V. Ebert

WG 3.21 „Humidity“
Dr. N. Böse

Targets :
preparative and analytical humidity research, national humidty standards, Homologation for analytical devices for vehicle exhaust gas analysis for car inspection, Breath alcohol , grain humidty,
soot aerosol diagnostics

WG 3.22 „Metrology of molecular spectroscopy“
Prof. Dr. V. Ebert

Targets :
Molecular, laser and FTIR spectroscopy of gases, laser analytics in industrial as well as environmental applications, e.g. at high pressures and temperatures (gas pipelines , engines ..), field transfer standards, generation of traceable spectral line data

WG 3.23 „Thermal state behaviour and density “
Dr. H. Bettin

WG 3.24 „Avogadro constant “
Dr. H. Bettin

Targets:
Density and volume of solid bodies, gas density, LNG, redefinition of the avogadro and Boltzmann constant

4

Basic capabilities WG 3.22

→ **Laser spectroscopy techniques** and methods

- TDLAS/QCLAS, CEAS/CRDS, develop. fs-comb spectr.
- direct absorption
- cavity enhanced spectroscopy
- direct traceable methods (*TILSAM*)
- TDLAS field instruments (H2O, CH4 , ballon + airplanes)
- line data measurement facility

→ **FTIR-based spectrometry**

- IFS 125HR
- VERTEX 80 FTS

→ **Preparative capabilities**

- two national primary standards for humidity
- national primary standards for alcohol
- dynamic gravimetric preparation of trace mixtures (e.g. SO2..)

5

HAI: Airborne Multi-phase TDL-Hygrometer for HALO

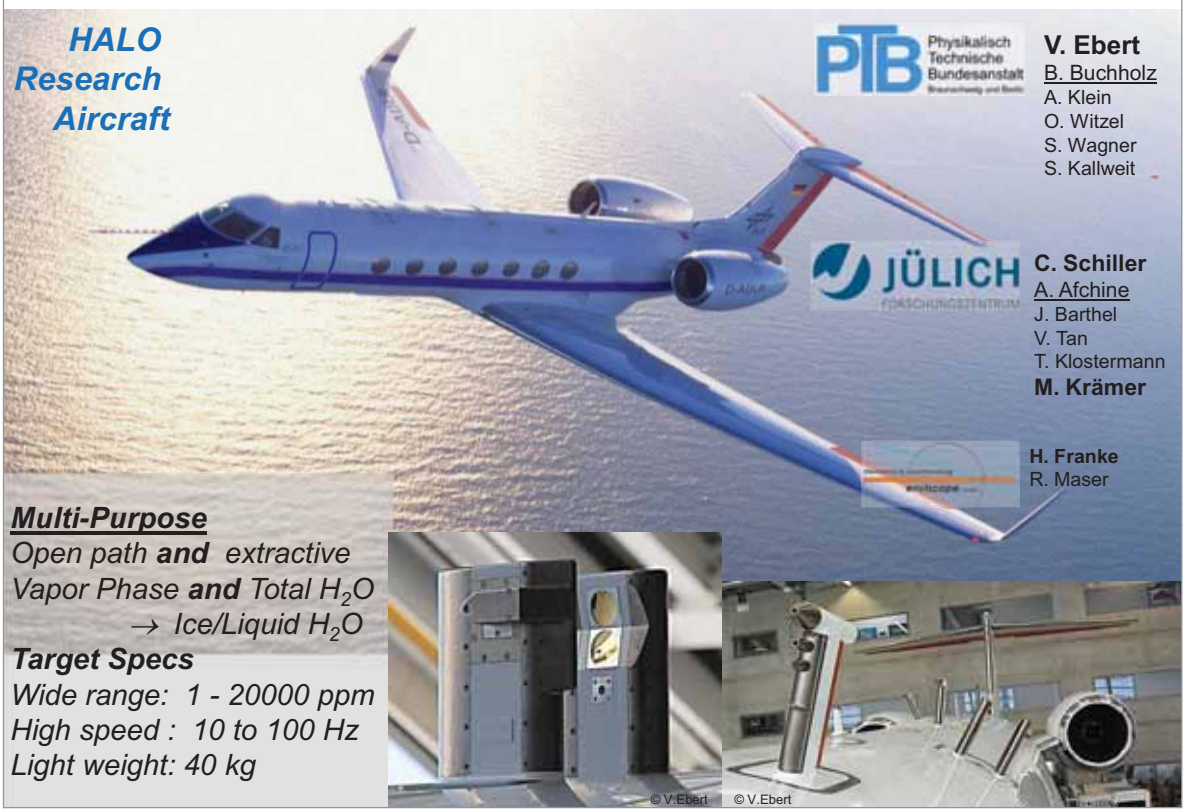

Laser: Spectral Line Data Measurement

H2O 1370nm air broadening: low temperature study

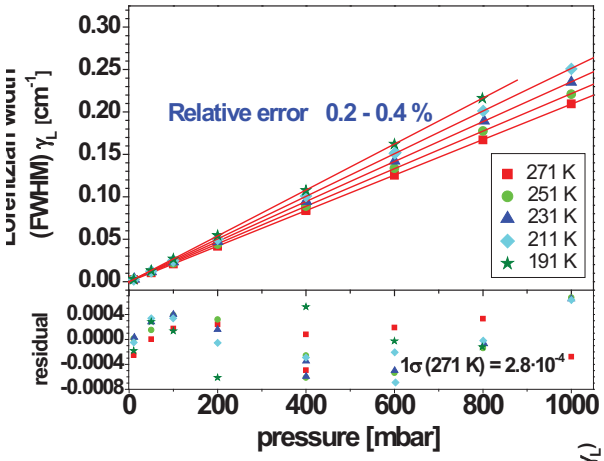

N = 0,732 ± 0,4 %
N = 0,77 ± 10-20 % (HITRAN `04)

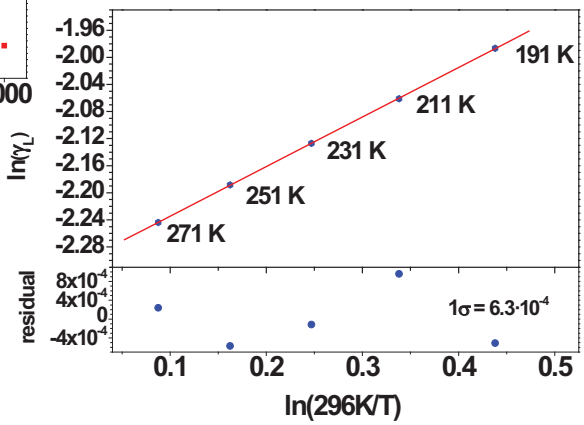

Combustion applications ⇒ In-Spray-Hygrometer

Fire Research

Optimization of
fire suppression systems

Tool:
In-Situ-TDLAS-Diagnostics in
Dense Water Sprays/Fogs

Cooperation:
Naval Research Laboratories, NRL
Washington DC, USA

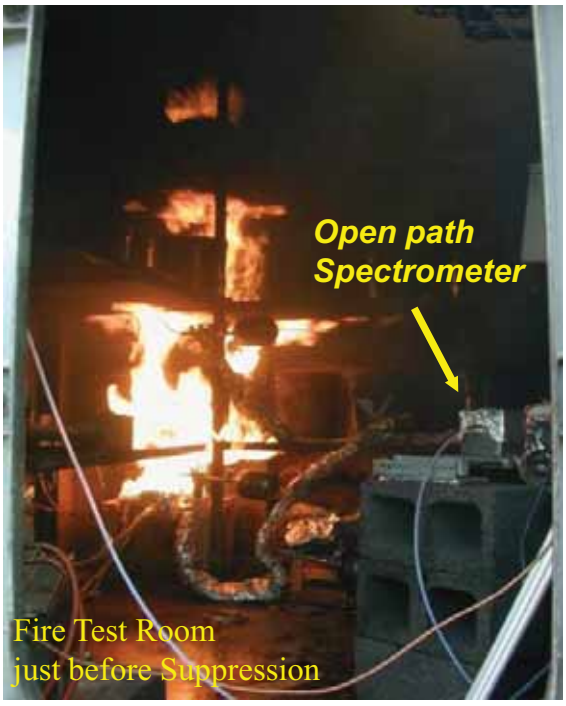

Proc. Comb. Inst. *29, 353-360 (2002)*
31, 799-806 (2006)
Opt. Lett. *31, 900-902 (2006)*

Laser: Line parameter measurement II

Pressure broadening + line strength

HCl-N_2-pressure broadening

γ_{N2}=0.07292(5) cm^{-1}/atm, (1σ= 0,07%)

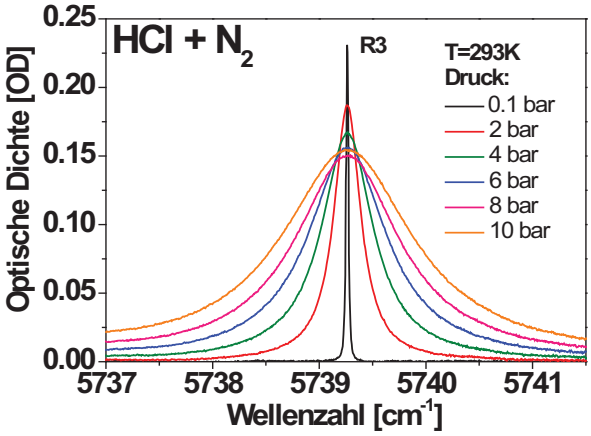

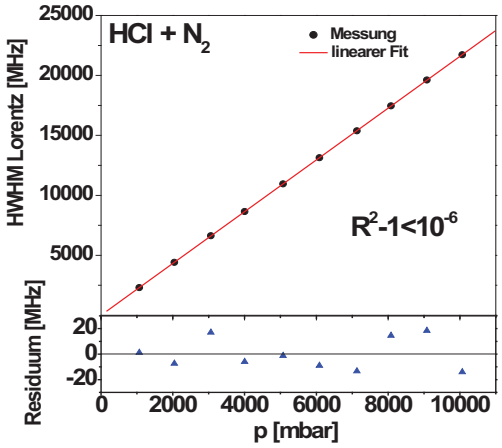

$$\gamma_L = \left(\frac{T_0}{T}\right)^{0.5} \cdot \left(\gamma^0_{HCl} \cdot p_{HCl} + \gamma^0_{fremd} \cdot p_{fremd}\right)$$

γ_{HCl} =0.021787(61) cm^{-1}/atm, HITRAN: +9.6%
γ_{O2} =0.03978(6) cm^{-1}/atm
γ_{He} =0.02113(1) cm-1/atm,
$S(T_0)$ =12.53(11)·10^{-21} cm^{-1}/(molec·cm^{-2}) (1σ= 0,9%)

Ortwein et al. Appl Phys B 2010

FT-IR: Line parameter measurement

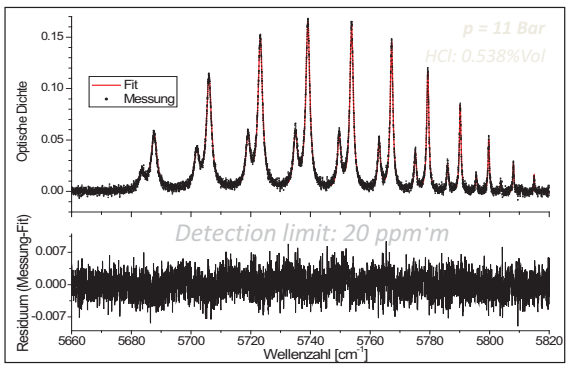

HCl 0-15 bar
(Bruker Vertex 80, own retrieval software)

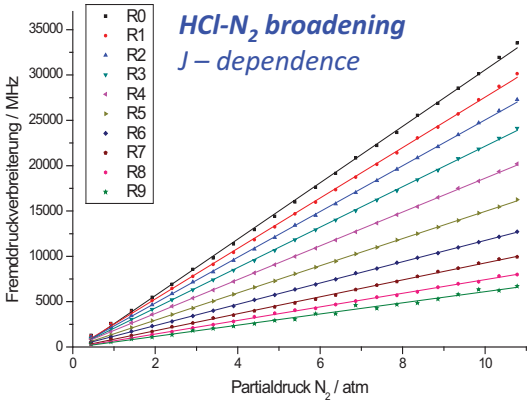

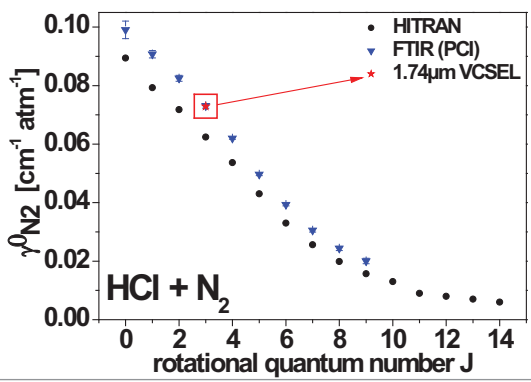

deviation
γ^0_{N2}(VCSEL)/γ^0_{N2}(FTIR): 0.2%

>> Unpublished

WMO

Report on the WMO

Measuremer
for Global Obse
for Climate Cha

Traceability, Stabil

30 March – 1 April 2010
WMO Headquarters
Geneva, Switzerland

Issue 4: Traceable Spectroscopic Data

Current spectroscopic reference standards do not possess the absolute accuracy required to support atmospheric GHG remote sensing with sub-1 % uncertainties.

Consistent and consolidated spectral reference data are not available, e.g. Ozone absorption cross sections for UV (Hartley, Huggins), Visible (Chappuis) and NIR (Wulf band) and IR (10 µm, 5 µm) do not agree within their reported uncertainties.

Recommendations:

- Spectroscopic reference standards should be validated against both laboratory and atmospheric reference spectra.
- Benchmark spectra recorded by different NMIs and laboratories should be made freely available to the research community for testing and verification.
- Spectroscopic reference standards must yield consistent results across all applicable wavelength ranges (UV, Visible, IR).
- Molecular spectroscopic reference standards should use validated, standardized algorithms for line shapes, line mixing, speed dependence, etc.

11

EURAMET

Community connections

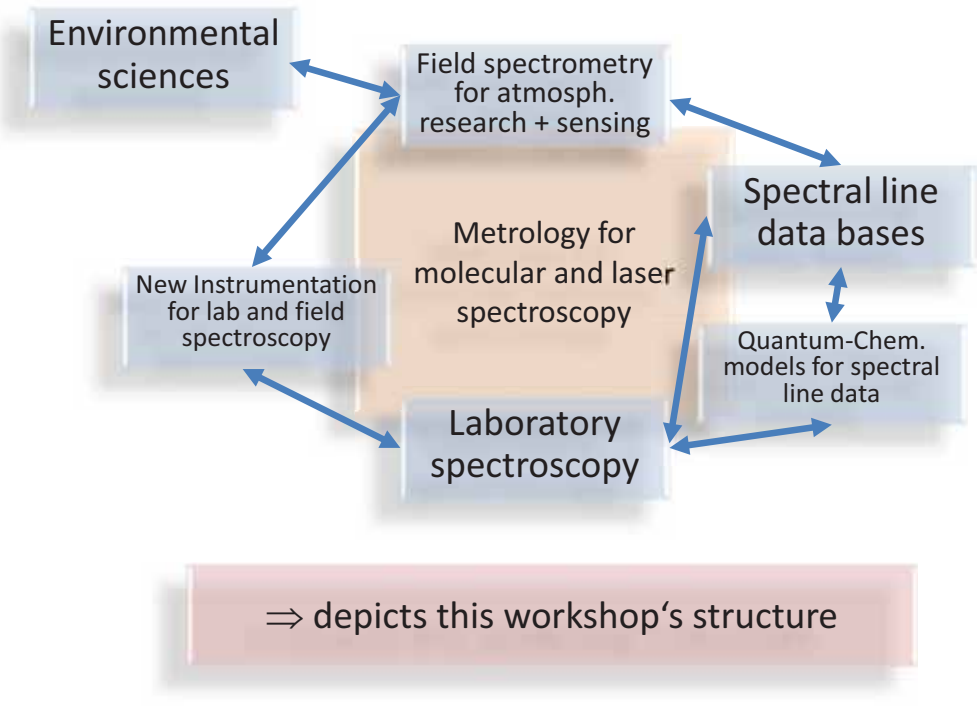

⇒ depicts this workshop‘s structure

12

Workshop Goals

- Foster communication accross community boundaries
- Collect needs of the atmospheric sensing community
- Promote EUMETRISPEC activities as well as lab spectroscopic activities at NMIs + community
- Catalayse cooperation and scientific exchange between spectroscopic and metrology communities

- Have a successfull and fruitfull meeting and a nice time in Wolfenbüttel and Braunschweig

13

Introduction to the EUMETRISPEC project on

Traceable Reference Spectral Line Data for environmental monitoring

V. Ebert, /PTB , Braunschweig, Germany
J Brunzendorf, O Ott, A Rausch, A Serdyukov, V Werwein, O Werhahn /PTB

M. Cadoret /CNAM, J.C. Petersen/DFM, J.J. Zondy/LNE, M. Vainio/MIKES, M. Valkova/SMU, S. Persijn/VSL, *M. Kiseleva /Radboud U.*

1st EUMETRISPEC Stakeholder Workshop
Wolfenbüttel/PTB Nov 14-16 2012

EURAMET

J Brunzendorf, **V. Ebert,** O Ott, A Rausch, A Serdyukov, V Werwein, O Werhahn /PTB
M. Cadoret/CNAM J.C. Petersen/DFM J.J. Zondy/LNE M. Vainio/MIKES
M. Valkova/SMU S. Persijn/VSL *M. Kiseleva - F Harren /Radboud U.*

15

Introduction to the EUMETRISPEC project on

Traceable Reference Spectral Line Data for environmental monitoring

V. Ebert, /PTB , Braunschweig, Germany
J Brunzendorf, O Ott, A Rausch, A Serdyukov, V Werwein, O Werhahn /PTB

M. Cadoret /CNAM, J.C. Petersen/DFM, J.J. Zondy/LNE, M. Vainio/MIKES, M. Valkova/SMU, S. Persijn/VSL, *M. Kiseleva /Radboud U.*

1st EUMETRISPEC Stakeholder Workshop
Wolfenbüttel/PTB Nov 14-16 2012

EMRP
European Metrology Research Programme
Programme of EURAMET
The EMRP is jointly funded by the EMRP participating countries within EURAMET and the European Union

Atmospheric Monitoring

Spectroscopic Instrumentation

Techniques

GLOBAL	LOCAL
FTIR	NDIR
LIDAR	TDLAS
DOAS	QCLAS
Grating	CRDS

Platforms:
satellite, plane, ballon, ship, ground

Monitoring application

Transport processes
Radiation transport
CO2 emission /budget
Atm dynamics , compartment coupling
Climate modell

Spectral reference line data are of highest importance

Atmospheric Monitoring: Instrumentation and Networks

Satellites

- OCO,
- GOSAT,
- Odin/Osiris,
- ACE,
- Aqua/AIRS,
- Aura/TES,
- UVN,
- Envisat/GOMOS
- MERIS
- MIPAS+Sciamachy,
- MERLIN,
- Metop-2/GOME-2,
- HIRS,
- Terra/MOPITT…..

…Some cost up to 3 G€

Ground monitoring networks

- **NDACC : Network for the Detection of Atmospheric Composition Change (NDACC)** ⇒more than 70 high-quality, remote-sensing research stations

- TCCON: Total Carbon Column Observing Network ; > 25 FTIR sites worldwide

- NOVAC
- LIDAR network
- GAW (WMO)

10.01.2013 3

Sources for Spectral Data

- Spectral LBL databases HITRAN/GEISA
  ⇒ *indespensable for env. research*

but

- accuracy of sensors/ atm. data/ climate models
  ⇒ *often limited by spectral data quality*

Causes:

- **data source heterogeneity** in LBL databases like HITRAN

lack of

- **standardisation** of equipment, setups, procedures
- **validated experimental uncertainties**
  (unquoted, incorrect, or unclear)
- **standardized measurement/data retrieval protocols**
- **metrological procedures** in line parameter retrieval

4

HITRAN2008: Statistical error analysis

HITRAN2008 :

- Only coarse "uncertainty" information provided
  - 1% - 5% - 10% - 20% - unreported , undefined , estimated
  - No metrologically based uncertainty figures provided
- Uncertainty Statistics out of 2.7 Mio lines in HIT2008
  - S(T) : U=Better 1%: 0.05% u= 10% and worse: 45%
  - γ_0 : U=Better 1%: 0.02% u= 10% and worse: 68%
- Not traceable

⇒ no traceable line by line data base available

5

Traceable LBL databases ?

NIST + PNNL?

- limited amount of traceable spectral data for gas phase species

But

- do not provide the line-by-line data, but absorption cross sections
- low spectral resolution of only 0,125 cm^{-1} or worse
- cover only single vapour component spectra
- no line identification
- Limited p, T coverage
  - only individual p, T combinations,
  - very limited pressure (around 1000 hPa)
  - very limited temperature range (270 - 350 K),
- No line by line pressure broadening data

⇒ **Cannot fill the gap left by lack of traceability of HITRAN or GEISA**

⇒ **no traceable line by line data base available**

⇒ **EUMETRISPEC initiative**

P.M. Chu, F.R. Guenther, G.C. Rhoderick, W.J. Lafferty, The NIST Quantitative Infrared Database, J. Res. Natl. Inst. Stand. Technol., 104, 59, 1999
S.W. Sharpe et al, Appl. Spectr. 58 1452 2004

6

EMRP ENV06: 2012-2014

Spectral Reference Data for Atmospheric Monitoring

V. Ebert (C.)	**PTB**	**D**
M. Cadoret	**CNAM**	**F**
J.C. Petersen	**DFM**	**DK**
J.J. Zondy	**LNE**	**F**
M. Vainio	**MIKES**	**Fin**
M. Valkova	**SMU**	**SK**
S. Persijn	**VSL**	**NL**
M. Kiseleva	***Radboud U.***	***NL***

„EUMETRISPEC“

⇒ **Eu**ropean **Metr**ology **I**nfrastructure for Traceable **Spec**tral Reference Data in Atmospheric Monitoring

EMRP

The EUMETRISPEC TEAM

J Brunzendorf, **V. Ebert,** O Ott, A Rausch, A Serdyukov, V Werwein, O Werhahn /PTB
M. Cadoret/CNAM J.C. Petersen/DFM J.J. Zondy/LNE M. Vainio/MIKES
M. Valkova/SMU S. Persijn/VSL *M. Kiseleva - F Harren /Radboud U.*

8

Time line

- PRT submitted by NPL and PTB — 28 Mar 2010
- JRP Protocol submitted (7 partners) — 11 Oct 2010
- **Review meeting** / Budapest — 22 Nov 2010
  - Result: *17 PRTs, 9 incl . ENV**06** funded*
- Negotiation meetings started — 16 Jan 2011
- Consortium agreement — Feb 2012
- Contract finalized (Starting date 1.Nov 2011) — Mar 2012
- Kickoff meeting @ PTB — 22. Mar 2012
- 1st Stakeholder Workshop — 14. Nov. 2012

Stakeholder support

EUMETRISPEC: Objectives

- Setup and validate **European spectroscopic infrastructure** for traceable line data measurements
  - –Central high-resolution FT-IR spectrometer facility *(PTB-funds)*
    - •VIS to MIR, 0.002 cm-1 resolution
    - • Special traceable measurements cells and infrastructure *(PTB-funds)*
    - •Setup of reference gas handling facility
    - •Traceability of all measurands including p, T, L, X_i, ($X_{isotopes}$)
  - –Traceable FTIR validation by high-res laser spectroscopy via "satellite" institutes
  - –Facility open to other NMIs and atmospheric community
- Develop **measurement + evaluation protocols** for traceable line data
  - –Metrological code development for full uncertainty evaluations
  - –Dissemination of measurement protocols and uncertainty evaluation
- Provide selected **traceable line data** sets

  Species: CO2, N2O , CH4 ; H20, *HCl, Hbr, HNO3*

  Spectral ranges : FTIR: 0.7 - 12 µm Lasers: 1,25- 2µm, 2.7-4µm , 4.6µm
- Data dissemination to atmosph. monitoring community

EUMETRISPEC: Concept

1st Call ⇒ ***Concentration Phase***

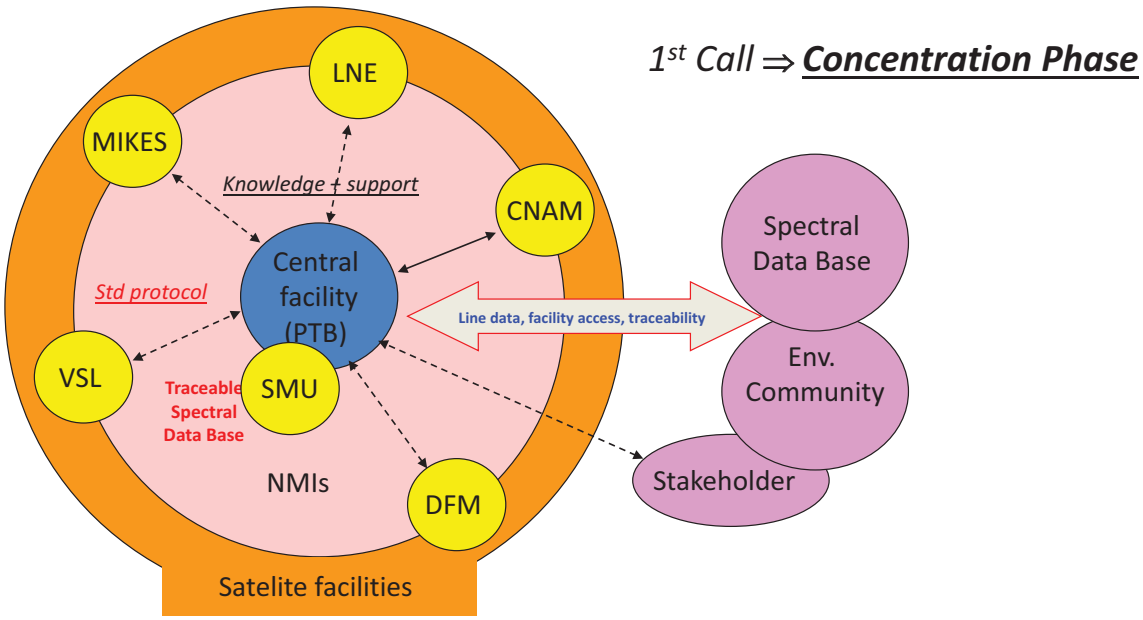

⇒ 4 M€ funding for ⇒280 MM

CF = New Bruker 125 HR at PTB

SF ⇒ WP1 talk

13

Eumetrispec: Parameters to be measured

Species: CO2, N2O , CH4 ; H20, *HCl, Hbr, HNO3*

Spectral ranges :

FTIR: 0.7 - 12 µm **Lasers**: 1,25- 2µm, 2.7-4µm , 4.6µm

Symbol[35]	Spectral parameter	Boundary conditions
S	Absorption line strength	T=296 K,
λ_0	Absolute line centre frequency ≡ Absolute spectral line position	T=296 K; P = 1013 hPa, in air
$d\lambda_0/dp_{air}$	Pressure induced line centre frequency shift ≡ Coefficient of the air-induced pressure shift in line position	T=296 K; in air
γ^0_{air}	Pressure induced line broadening coefficient ≡ collisional line broadening coefficient ≡ Coefficient of air-induced pressure broadening ≡ air broadening coefficient ≡ pressure broadening coefficient	T=296 K; in air
n_{air}	Temperature coefficient of the pressure induced line broadening (γ^0_{air}) ≡ Coefficient of the temperature dependence of the air broadening coefficient	In air

Parameter range : p = 0-1013 hPa T = 300 -220 K

-14- 2012-03-22/23

EMRP European Metrology Research Programme

Work package structure

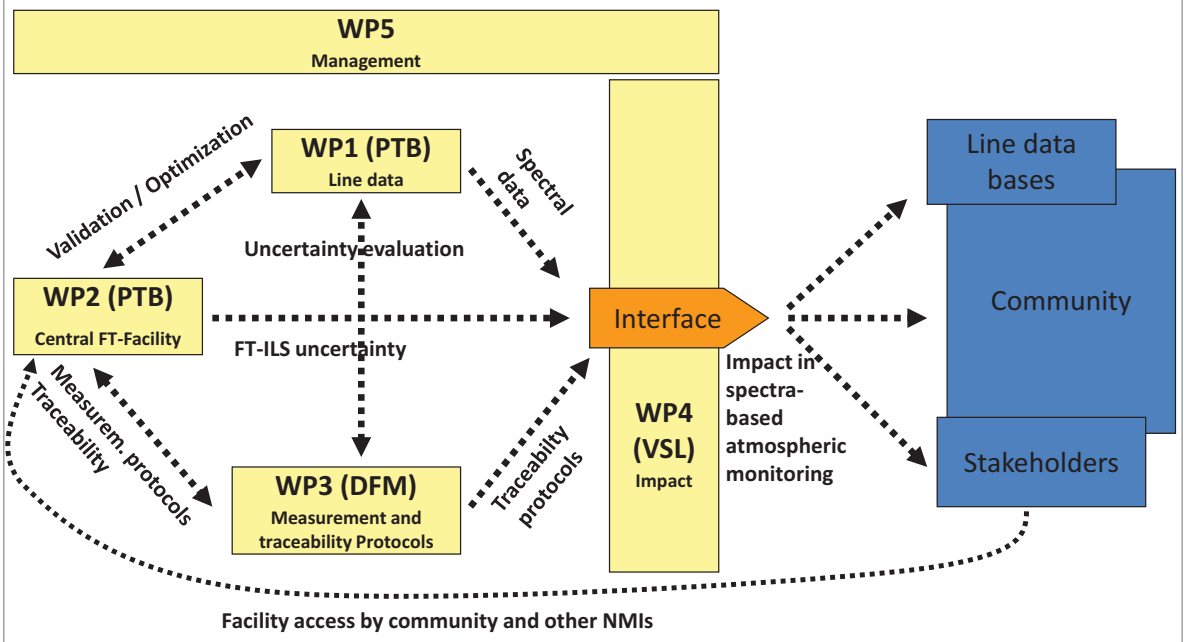

Project implementation/strategy

- **Joint metrology and community effort :**
  - Broad synergies created by sharing knowledge, facilities and tasks
  - Efficient linking of metrological expertise of leading NMIs in spectroscopy
  - Broad experience in FTIR, high res. laser spectroscopy, molecular spectroscopy
  - Full metrology support on all measurands (spectral parameters+ p,T,L,X_i, isotopes)
  - Strong community support:
    22 institutions, 4 community collaborators, open project board
- **Open hardware, software and data infrastructure**
  - Joined central facility setup
  - Inclusion of external expertise by open infrastructure and a JRP management board
  - Facility access open to all interested NMIs / atmospheric monitoring community members (as long as measurement and evaluation protocols are maintained)
- **Long term perspective for European spectroscopy infrastructure**
  - **Stage 1 (EMRP):** Knowledge condensation and validation on one facility, then multiplication
  - **Stage 2 (EMRP):** Facility/capability "multiplication" + capability expansion
    (plus: new Molecules, spectral ranges: UV+THz, dense spectra, cross sections, particles)
  - **Stage 3:** Maintaining of facility network using national funds

Dissemination

- **Kickoff-Meetings, Workshops, project presentations by JRP**
  - Community-open
- Publications in **Journals, community conferences/meetings** (NDACC, TCCON etc)
- **Line data submission to HITRAN/GEISA**
- **Metrological line database**
  - **Web query** on **new spectral data requirements**
  - **Linked to HITRAN / GEISA**
- **Long term community contact** via **collaborations at CF**
- **Standardisation input to**
  - **CIPM**/CCQM**,**
  - **EURAMET**/TCMC,
  - **ISO** (e.g. ISO TC 158)
  - **CEN,**
  - **EU + WMO directives**
  - EMEP Europ. Monitoring and Evaluation program
  - **WMO-GAW** (best practice guides)

Community interaction

- Collect input of atmospheric community needs to ENV06
  - Species, spectral bands/lines, phys-chem conditions you like to be characterized
    - Web interface in preparation
- Share expertise in lab spectroscopy (FTIR , Laser) and metrology
  - community standardization procedures, quality control approaches ..
- Attract and integrate community support in
  - Line assignment, State of the art line shape models / line mixing
  - Further exploitation of traceable spectra / derive other parameters: E“ …
- Announce exp. feedback for spectroscopic models (QC)
- Intercomparison experiments with *community*
  - E.g. via HBr, HCl, N2O reference cells
- Advertise
  - Project web site — www.eumetrispec.org
  - 6 monthly Newsletter .. — sign up on web site
  - stakeholder meetings — 1st: Mid Nov 2012 @ PTB/Braunschweig
  - **PhD/Postdoc positions available** — **see website**
  - Funded collaboration possibilities
    - Next EMRP project call in 2013: ⇒ EUMETRISPEC II ?

18

EUMETRISPEC-Long term?

2nd Call ⇒ ***Multiplication Phase***

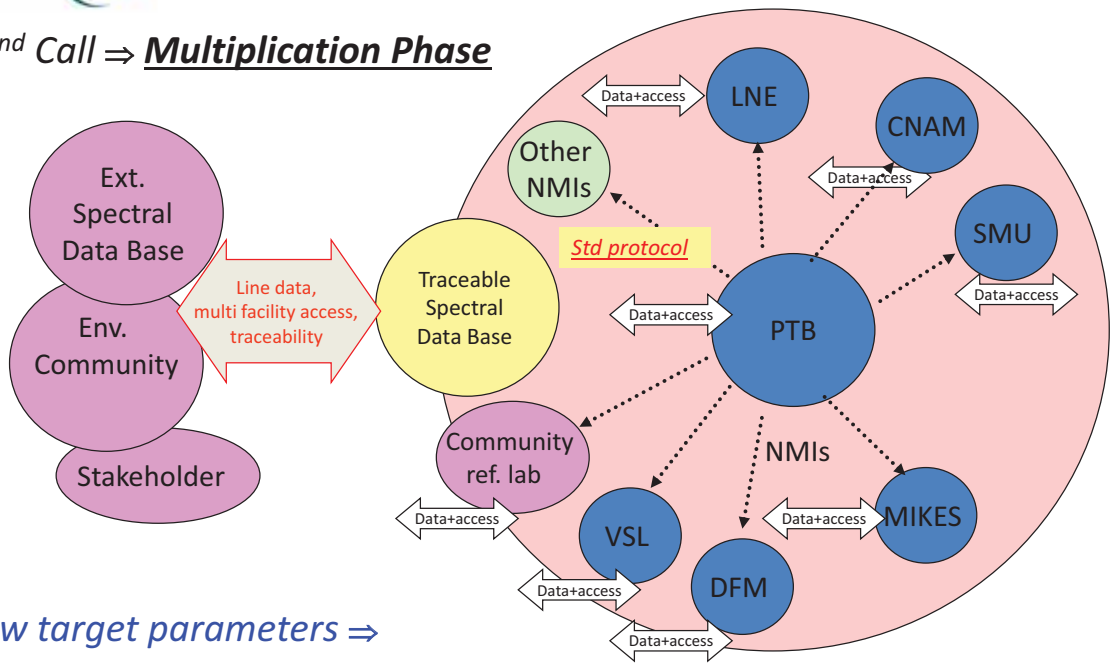

New target parameters ⇒

expand to ⇒ **UV / THz spectral range**

⇒ **heavier molecules ⇒ cross sections**

⇒ ***your proposals ?***

THANK you for your interest

Questions ??

Need further information .. ??

- www.Eumetricspec.org
- Volker.ebert@ptb.de

20

"EMRP and EMPIR: How EUMETRISPEC is embedded in the joint European metrology research"

Jörn Stenger

Physikalisch-Technische Bundesanstalt (PTB)

EMRP and EMPIR

How Eumetrispecs is embedded in the joint European metrology research

Jörn Stenger, EMRP Chair

Motivation for joint research

"Metrology Dilemma"

Growing demand for metrology → NMI DI ← NMI budgets stable or even declining

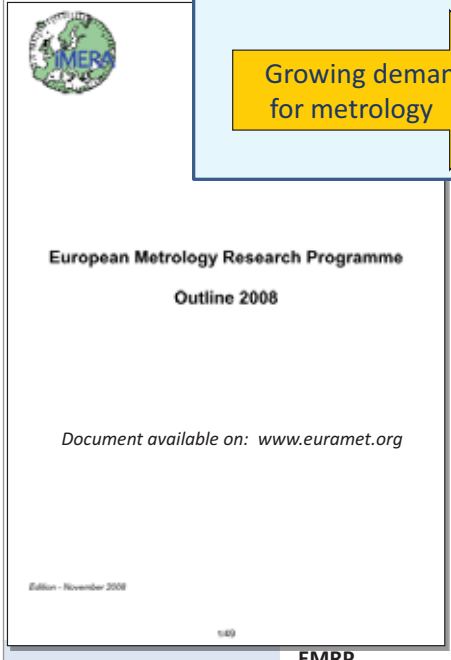

Grand Challenges
- Health
- Energy
- Environment
- New technologies

Fundamental and applied metrology R&D
- Fundamental metrology
- Metrology for industry

Capacity Building and KT

European joint metrology research addresses all fields of application

Secure measurements and reference data

do you get what you pay for?

safely below radiation limits?

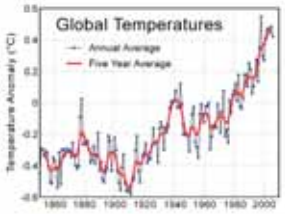

data quality for policy making sufficient?

Do/underpin basic science

do constants of nature drift with time?

Drive innvovation

efficiency? quality control in production?

precise enough to be competitive?

EMRP
Eumetrispecs Stakeholder Workshop, 15 November 2012

3

EURAMET e.V.

European Association of National Metrology Institutes

bilateral cooperations since ≈ 1900
EUROMET since 1990
EURAMET e.V. since 2007

Members:

37 European NMIs

22 of them actively participating in the EMRP

Associates:

- 71 Designated Institutes holding national standards
- JRC

metrologists:
NMIs: ≈5000
DIs: ≈1500

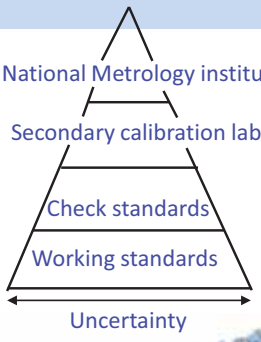

Joint programming of metrology research

- coordination of national metrology research programmes (EMRP with those of 22 member states)
- jointly agreed strategic research agenda
- implemented by EURAMET e.V.
- highly integrated

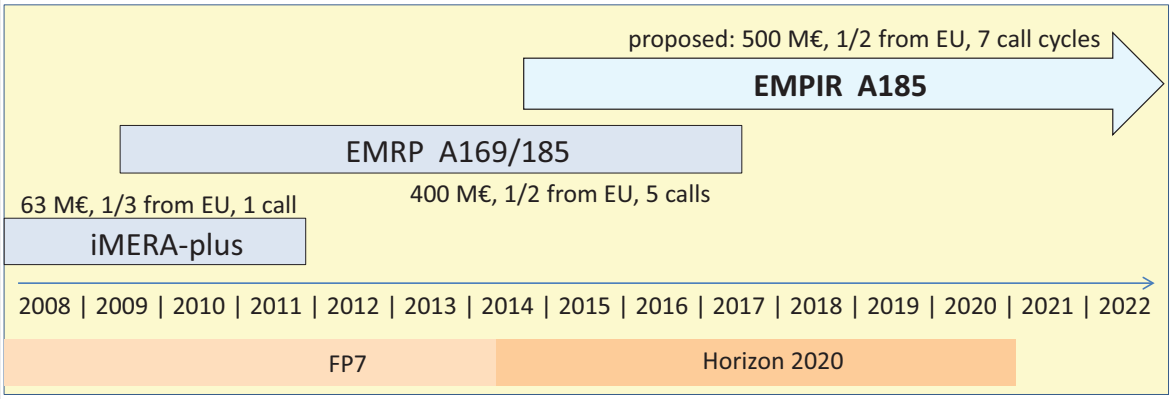

EMRP
Eumetrispecs Stakeholder Workshop, 15 November 2012
5

Funding breakdown of EMRP

DECISION No 912/2009/EC OF THE EUROPEAN PARLIAMENT AND OF THE COUNCIL of 16 September 2009

on the participation by the Community in a European metrology research and development programme undertaken by several Member States

400 M€
200 M€ EU + 200 M€ MS

Researcher Grants
40 M€
36 M€ cash EU +
4 M€ cash MS

Joint Research Projects
344 M€
164 M€ cash EU +
180 M€ in kind MS

Management
16 M€
16 M€ cash MS

EURAMET Secretariat
Braunschweig

EURAMET EMRP-MSU
London

EMRP
Eumetrispecs Stakeholder Workshop, 15 November 2012
6

The science agenda of the EMRP

EMRP ERAnet-plus

Metrology for ...

2007	SI units	21 projects concluded
	Health	
	Length	
	Electromagnetism	

EMRP Article 169/185

Metrology for ...

2009	Energy	9	65 projects running
2010	**Environment**	9	
	Metrology for Industry	17	
2011	Health	11	
	SI broader scope	10	
	New Technologies	9	
2012	Metrology for Industry		review process
	SI broader scope		
	Open excellence call		
2013	Energy		preparation
	Environment		

– typical project size: 3 M€ (full cost)
– about 60 projects more expected in 2012/13 calls

EMRP
Eumetrispecs Stakeholder Workshop, 15 November 2012
7

The Environment call of 2010

MACPoll	Metrology for Chemical Pollutants in Air	Annarita Baldan (VSL)
PartEmission	Emerging requirements for measuring pollutants from automotive exhaust emissions	Dr Martin Thedens (PTB)
solarUV	Traceability for surface spectral solar ultraviolet radiation	Dr Julian Gröbner (SFI DAVOS)
MetEOC	Towards a European Metrology Centre for Earth Observation and Climate	Dr Nigel Fox (NPL)
Ocean	Metrology for ocean salinity and acidity	Petra Spitzer (PTB)
EUMETRISPEC	Spectral Reference Data for Atmospheric Monitoring	Prof Volker Ebert (PTB)
MeteoMet	Metrology for pressure, temperature, humidity and airspeed in the atmosphere	Dr Andrea Merlone (INRIM)
WFDtraceability	Traceable measurements for monitoring critical pollutants under the WFD	Dr Rosemarie Philipp (BAM)
MetroRWM	Metrology for Radioactive Waste Management	Petr Kovar (CMI)

EMRP
Eumetrispecs Stakeholder Workshop, 15 November 2012
8

The Environment call of 2013

Focus on metrological research to improve the quality of data for policy making and regulation, underpin other environmental research initiatives, and stimulate technological innovation. It addresses:

- contamination of water, air and soil
- radiation measurement and protection (including electromagnetic and ionising radiation, and acoustic noise)
- the properties of the atmosphere and oceans, including their constituents, contamination, transport properties and other parameters
- emission control; measurement of gases and particles that have an effect on the climate (CO_2, methane, aerosols...)
- remote sensing for environmental and climate control.

This TP will enable collaborative research for large and transnational monitoring systems. EURAMET wishes to put a focus on climate control and especially welcomes proposals enabling the establishment of a long-term European NMI/DI network coordinating the measurement infrastructure in this area and links to a potential global network.

EMPIR – the successor initiative to EMRP

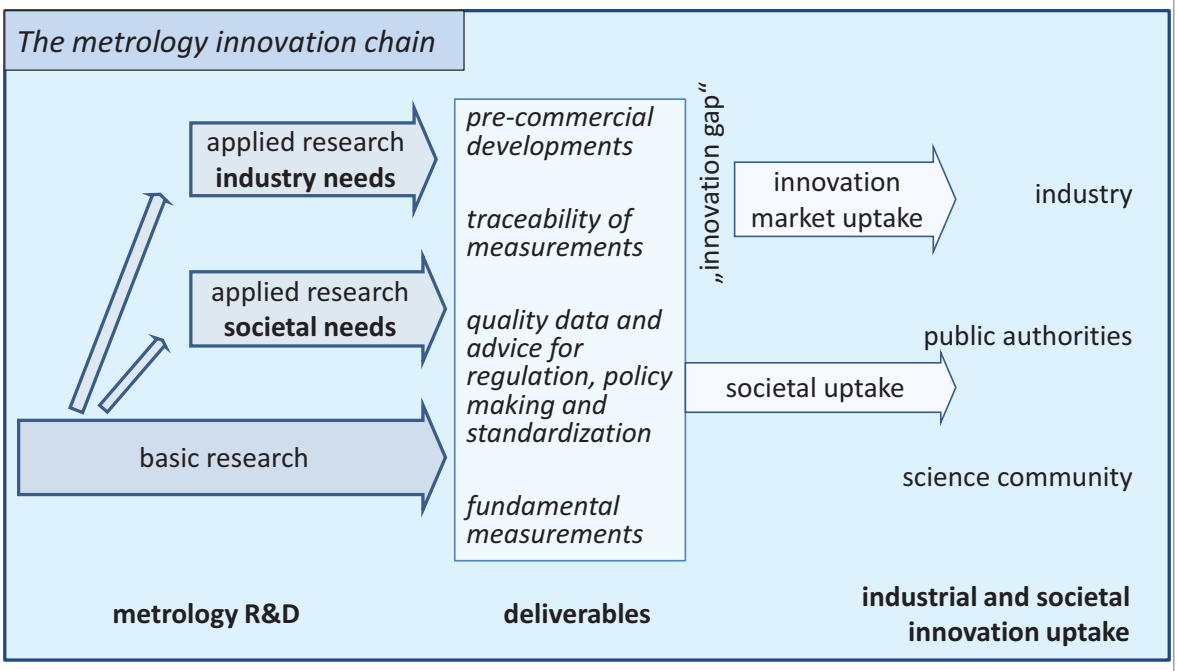

The modules of EMPIR

Module 1: Science	Basic scientific metrology
	Grand challenges Environment, Energy, Health
Module 2: Innovation	Innovation: technology projects
	Innovation: central support for technology and knowledge transfer
Module 3: Pre-normative	R&D focused on metrology needed for European and international documentary standards
Module 4: Capacity building	R&D measurement capabilities
	Non-R&D accompanying measures, mobility

If successful: 7 call cycles starting 2014 or 2015
Envisaged size: 500 M€ (full cost methodology)

EMRP
Eumetrispecs Stakeholder Workshop, 15 November 2012

11

"Atmospheric trace gas sensing: Community needs with respect to spectral line data"

Prof. Dr. Mark A. Zondlo

Princeton University

Prof. Dr. Mark A. Zondlo

Department of Civil and Environmental Engineering, Center for Mid-Infrared Technologies for Health and the Environment, Princeton University
59 Olden Street, 08544 Princeton, NJ, USA
Phone: +1 6092585037
E-mail: mzondlo@princeton.edu

Education and Professional Experience

since 2008	Assistant Professor, Department of Civil and Environmental Engineering, Princeton University, USA; Assoc. Faculty: Department of Atmospheric and Oceanic Sciences, Center for Mid-Infrared Technologies for Health and the Environment, Princeton Institute for the Science and Technology of Materials, Princeton Environmental Institute
2002-2007	Senior Research Scientist, Southwest Sciences, Inc., Santa Fe, New Mexico, USA
1999-2002	Advanced Study Program Postdoctoral Fellow, National Center for Atmospheric Research, Boulder, Colorado, USA
1999-2002	Aerosol and cloud chemistry, National Center for Atmospheric Research, Colorado, USA
1999	Chemistry (physical, atmospheric) Ph.D., University of Colorado, Boulder, Colorado, USA
1994-1999	Graduate Research Assistant, University of Colorado, Boulder, Colorado, USA
1994	Chemistry B.A., Rice University
1992-1993	NSF REU Undergraduate research assistant, University of California, Irvine, USA

Activities, Honors and Awards

- Recent field experiments: NASA SEAC4RS (Thailand), 2012
- PI for VCSEL hygrometer
- Agricultural Nitrous Oxide Flux Study (Michigan), 2012
- PI for QCL N_2O; NSF DC3 (Kansas), 2012
- PI for VCSEL hygrometer; Baltimore Ecosystem Study (Maryland), 2012
- PI for QCL NH_3 and N_2O sensors; NSF TORERO (Chile, Costa Rica), 2012
- PI for VCSEL hygrometer; NSF PREDICT (Saint Croix, Virgin Islands), 2010
- PI for VCSEL hygrometer; NOAA CalNex 2010
- PI for open-path ammonia measurements; NSF HIPPO Global (Arctic-to-Antarctic), 2009-2011
- Reviewer for Journal of Geophysical Research Letters, Journal of Atmospheric and Oceanic Technology, The Journal of Physical Chemistry, Atmospheric Chemistry and Physics, Applied Physics B, NASA, NSF AGS, NOAA AC4, and DOE BER

Atmospheric trace gas sensing: Community needs with respect to spectral line data

Mark A. Zondlo

Department of Civil and Environmental Engineering, Center for Mid-Infrared Technologies for Health and the Environment, Princeton University

Mitigating global climate change and improving air quality require better understanding of the sources, sinks, distribution, and transport of greenhouse gases and air pollutants[1]. Over the past decade, the explosion of laser-based trace gas sensors have provided unique insights into these processes due to their relatively low power consumption, small size, and high-selectivity while maintaining high-precision, high-stability, and well-calibrated measurements. While the successes of commercial and research-grade laser-based sensors are remarkable, there remain significant barriers toward deploying even smaller, lower power, and lightweight sensors. For example, the use of reduced pressure cells to avoid interferences and tightly control the temperature/pressure of the optical cell requires relatively high power pumps and moving parts. Tight thermal control of the other optomechanical and electrical components requires large housings and heating elements.

For both greenhouse gases and aerosol precursors, higher spatial and temporal measurements are needed beyond existing remote sensing data, regional observation networks, and aircraft-based studies[2]. In turn, new sensor technologies require development to fully utilize the capabilities of new observational platforms. For example, local greenhouse gas and air pollutant emissions require dense sensor networks or the agility of platforms such as unmanned aerial vehicles (UAVs) to sample within the atmospheric boundary layer. For carbon cap-and-trade verification, fenceline or perimeter monitoring may be required near and downwind of local sources. The World Meteorological Organization's Global Climate Observation System (GCOS) desires robust, routine chemical measurements on weather balloons. Further in the future, smarphone-sized sensors and applications would revolutionize trace gas monitoring.

Trace gas sensing at ambient pressures and temperatures provides a pathway towards smaller/lighter sensors, but the uncontrolled sampling environments place even more challenging constraints on the spectroscopic measurements themselves. Improved spectroscopic parameters are critical to develop the next generation of atmospheric trace gas optical-based sensors. First, the strongest atmospheric absorption lines of a trace gas – typically the ones with the best characterized spectral parameters – are almost never the most optimal absorption lines under ambient conditions due to other atmospheric absorbers. Second, accurate temperature-dependences of the linestrengths are critical for relevant measurements of greenhouse gases, for which accuracies/precisions/stabilities of one part in one thousand are required. Third, validated spectral data over a wide range of atmospheric temperatures and pressures are needed for aircraft, satellite, and balloon data. Finally, the influence of the broadening of water vapor on spectral lineshapes is necessary for ground-based measurements in the large and rapidly changing absolute humidity of the atmospheric boundary layer.

The influence of spectroscopic data uncertainties on the accuracy of measurements will be demonstrated through case studies of atmospheric measurements of greenhouse gases and air pollutants in the near and mid-infrared. Laser-based sensing applications include an open-path nitrous oxide sensor using a quantum cascade laser at 4.54 μm[3] for understanding agricultural nitrogen emissions, methane emissions from hydraulic gas fracturing and thawing permafrost using quantum cascade and vertical cavity lasers[4], atmospheric ammonia measurements for air quality[5], and water vapor from and upper tropospheric and lower stratospheric water vapor measurements for cirrus cloud formation[6].

[1] IPCC, 2007.
[2] NAS Decadal Survey, 2007.
[3] Tao et al., Opt. Exp., revised, 2012.
[4] A. Khan, D. Schaefer, L. Tao, D. J. Miller, K. Sun, M. A. Zondlo, W. A. Harrison, B. Roscoe, D. J. Lary, Remote Sensing, 4, 2012.
[5] K. Sun, L. Tao, D. J. Miller, M. A. Khan, M. A. Zondlo, Appl. Phys. B, 4, 2012.
[6] S. Tilmes, L. L. Pan, P. Hoor, E. Atlas, M. A. Avery, T. Campos, L. E. Christensen, G. S. Diskin, R.-S. Gao, R. L. Herman, E. J. Hintsa, M. Loewenstein, J. Lopez, M. E. Paige, J. V. Pittman, J. R. Podolske, M. R. Proffitt, G. W. Sachse, C. Schiller, H. Schlager, J. Smith, N. Spelten, C. Webster, A. Weinheimer, M. A. Zondlo, J. Geophys. Res.-Atmos., 115, D14303, 2010.

How are humans changing the Earth's composition and climate?

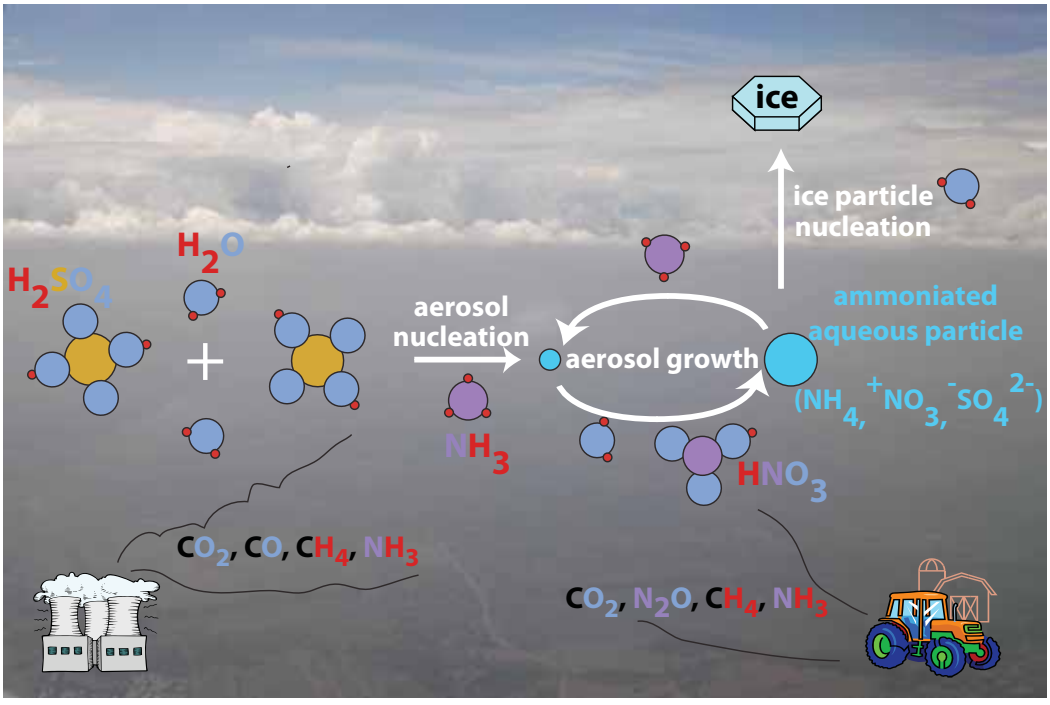

Emissions vary greatly in space and time for greenhouse gases and air pollutants

Motivation

(a) Total budget well constrained but partitioning of sources/sinks are not:

- CO_2
- CH_4
- N_2O

(b) Poorly-constrained:

- H_2O
- SO_4^{2-}, NO_3^- aerosols cloud formation

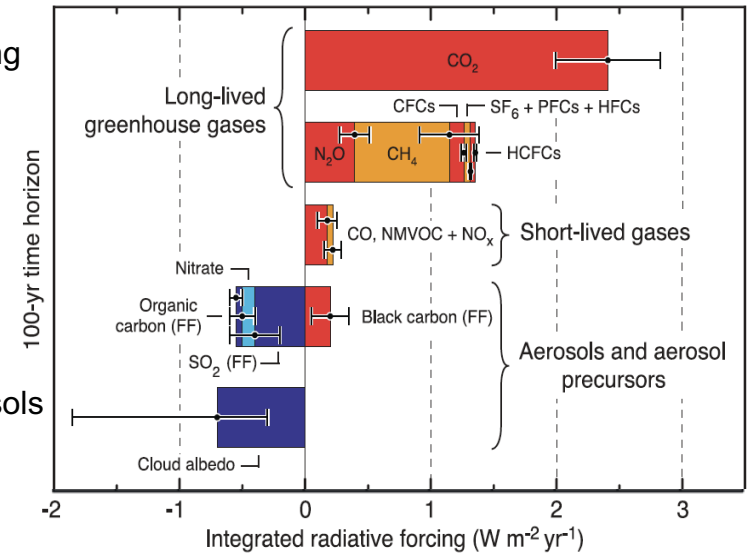

More widespread measurements needed for

(a) most effective mitigation practices (source/sink quantification)

(b) improved understanding of global climate/air quality

New sensor especially needed for atmospheric boundary layer sampling

Atmospheric measurement challenges

Scientific requirements:	H_2O	NH_3	N_2O
accuracy	5%	20%	0.1 ppbv
precision (10 Hz)	< 3%	<3%	0.1%
mixing ratios	1-10^4 ppmv	10^2-10^4 ppt	~325 ppbv
dynamic range	10^6	10^5	100

Engineering requirements

- fast
- selective
- low power
- low volume and mass
- low maintenance
- replicable
- self-calibrating

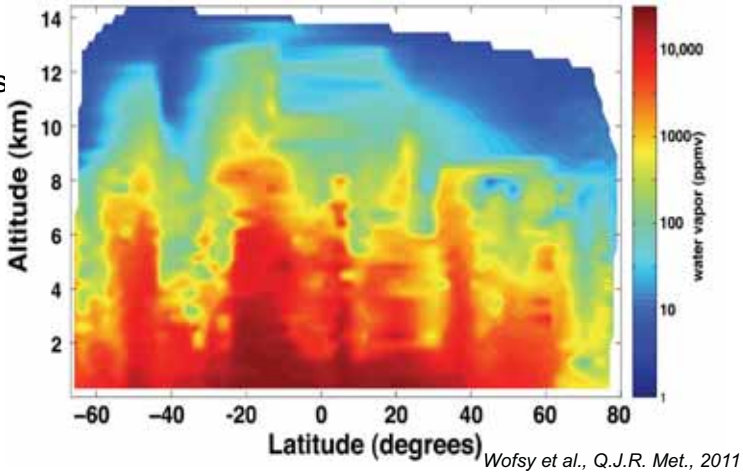

Wofsy et al., Q.J.R. Met., 2011

Laser-based sensors meet these criteria

Beer-Lambert law

$$\frac{I(\lambda)}{I_o(\lambda)} = \exp(-\alpha(\lambda))$$

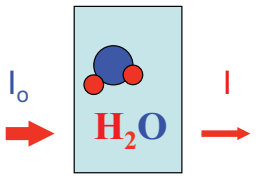

where: $I(\lambda)$ is light intensity after absorption

$I_o(\lambda)$ is incident light intensity

$\alpha(\lambda)$ is absorbance

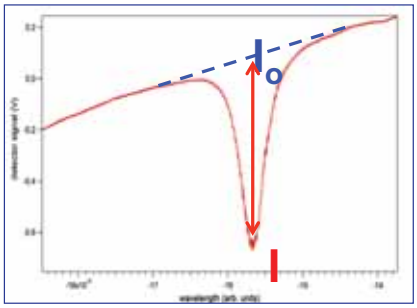

$$\alpha(\lambda) = S(T)\, g(\lambda,T,P)\, N\, \ell$$

where: $S(T)$ is the linestrength σ = cross section

$g(\lambda,T,P)$ is the normalized Voigt lineshape function

N is the absolute concentration

ℓ is the pathlength

Laser-based techniques use direct absorption spectroscopy or derived-forms of it rely upon spectroscopic principles

Laser-based atmospheric trace gas sensors

Successes

- fast response and selective detection
- high-precision and stability (>1:1000)
- far more compact, lower power than GC, MS, etc.
- widespread and successful use

Caveats

- reduced pressure cells with tight thermal/pressure control for narrow absorption lines to achieve high selectivity
- too power hungry, heavy for sensor networks, UAVs, balloons, remote field deployments (100-1000 W, 10s kg)
- inlets/tubing have sampling biases in fast (slow) changing conditions
- require complex calibration methods for routine field use

Next generation TDL-based systems: fast, lightweight, low power, limited field calibration

➔ *consider three examples: H_2O, NH_3, and N_2O*

Open-path detection: advantages and challenges

Open-path detection: gas sampled at ambient conditions, no sample handling

Advantages	Challenges
sampling minimized	spectroscopy over range of temp., pressure
no gas handling	need to know T, P in optical path
no pumps (lower power)	broad lineshapes, interferences from other gases
no inlet delay issues	extreme, changing conditions
fast response	calibration
no phase re-partitioning	mirror/optics need to be relatively clean
	(e.g. sea salt, dew/frost, bugs, mold)

For what applications is this necessary?

1. "Sticky" species (H_2O, NH_3, HNO_3…) where inlet/tubing adsorption is a problem
2. Eddy covariance fluxes (10 Hz) for surface/atmosphere emissions (GHG)
3. Low power, low weight platforms (UAVs, remote field sites) for atmospheric boundary layer sampling (greenhouse gas emissions)

H_2O: most important trace gas species on climate

- stratospheric water vapor trends mask/augment surface temperature trends from anthropogenic greenhouse gases by ~ 30% *(Solomon et al.*, 2010)
- positive feedback on CO_2 doubling (ΔT=+1.5°C → 3.0°C due to H_2O ↑) (*IPCC*, 2007)
- increasing trends in stratosphere, troposphere (100% increase between 2000-2100, Soden *et al.,* 2006, at 200 hPa; 20% at sfc)
- cirrus cloud microphysics not well understood (predicting cirrus cloud formation highly uncertain in cloud and climate models)
- critical roles in chemistry (oxidizing capacity of atmos.)

NSF Gulfstream-V VCSEL hygrometer

Vertical Cavity Surface Emitting Laser, 1854 nm

(Zondlo et al., JGR, 2010)

~ 1000 flight hours, routine on NSF G-V (since 2008)

1854 nm fiberized VCSEL, WMS and direct abs.

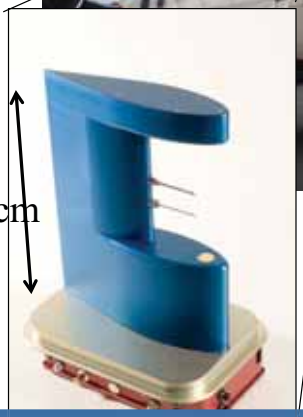

Parameter	Specifications
Dew point range	-110°C to +30°C
Sensitivity (1 Hz)	0.05 ppmv
Frequency	25 Hz
Accuracy	2-10%
Precision	≤ 1%
Power	8 W
Weight	6 kg
Size	25 cm × 16 cm × 5 cm
Operation	unattended
Design	open-path

- optical sensing outside fuselage
- mirrors exposed to environment
- open-path design allows for fine water vapor structure to be observed

Flying laboratory of NSF G-V

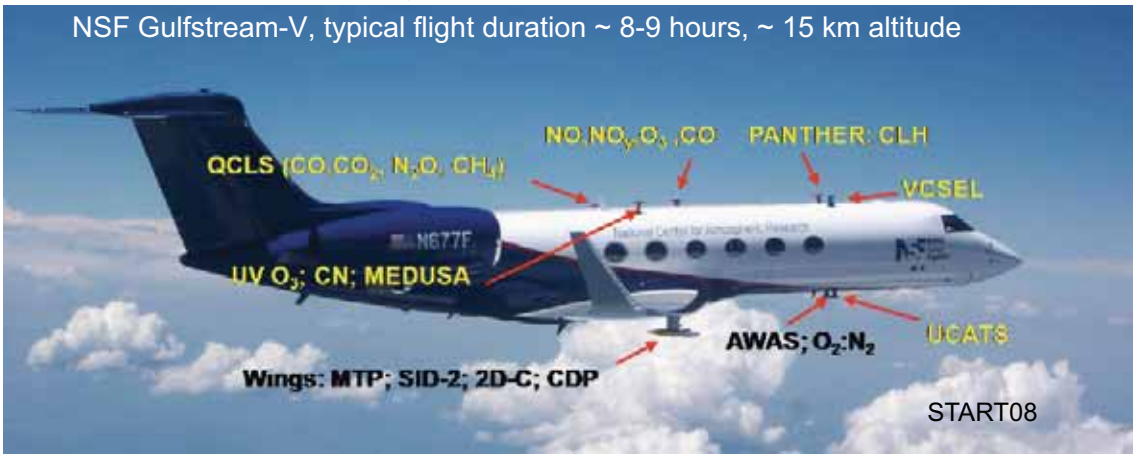

High-altitude, long duration aircraft coupled with open-path, high-sensitivity water vapor measurements provides unique datasets for ice supersaturation:

Field experiment	location	time	focus
NSF START08	N. America	2008	ex-UT/LS
NSF HIPPO	global	2009-2011	pole-to-pole observations
NSF PREDICT	tropical, w. Atlantic	2010	tropical clouds
NSF TORERO	tropical, e. Atlantic	2012	biogenic emissions on UT O_3
NSF DC3	N. America	2012	deep convection
NASA SEAC4RS	SE Asia	2013	deep convection
NSF MPEX	N. America	2013	mid-latitude convection

VCSEL current tuning capabilities

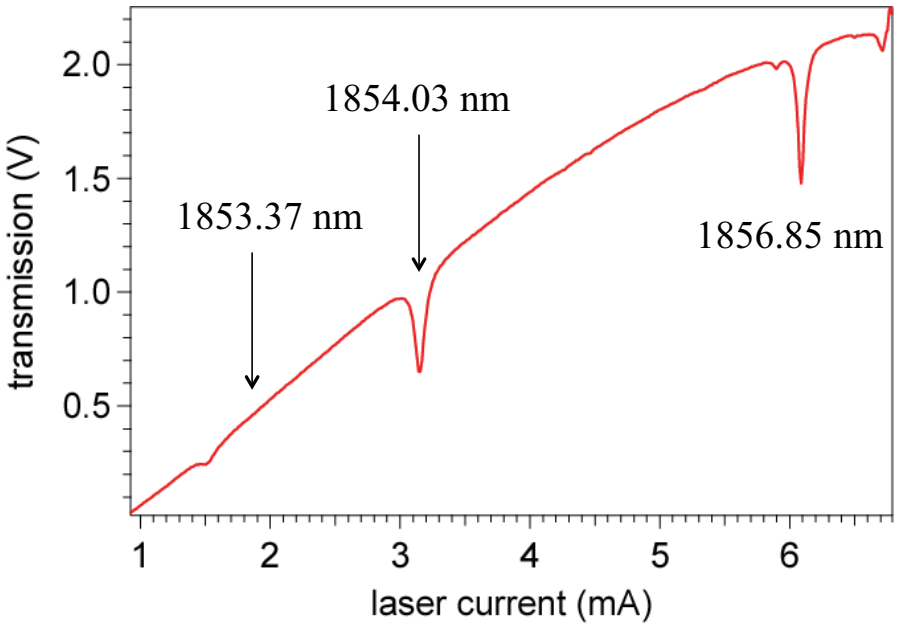

1854.03 nm line (“strong”) for mid-troposphere to lower stratosphere
1853.37 nm compilation (“weak”) of three lines for lower troposphere
Wavelength modulation and direct absorption spectroscopy used

Spectroscopic detection methods

Wavelength modulation spectroscopy (f=250 kHz; 1.5 kHz scan rate)
Modulation depth and scan width change with f(P,T) every second
Normalized peak shape largely invariant
Fit entire trough-to-trough peak shape with stored reference spectrum
Few percent correction to account for differences from reference condition

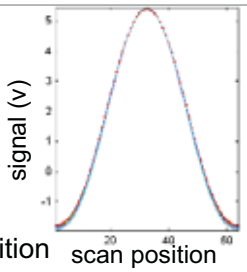

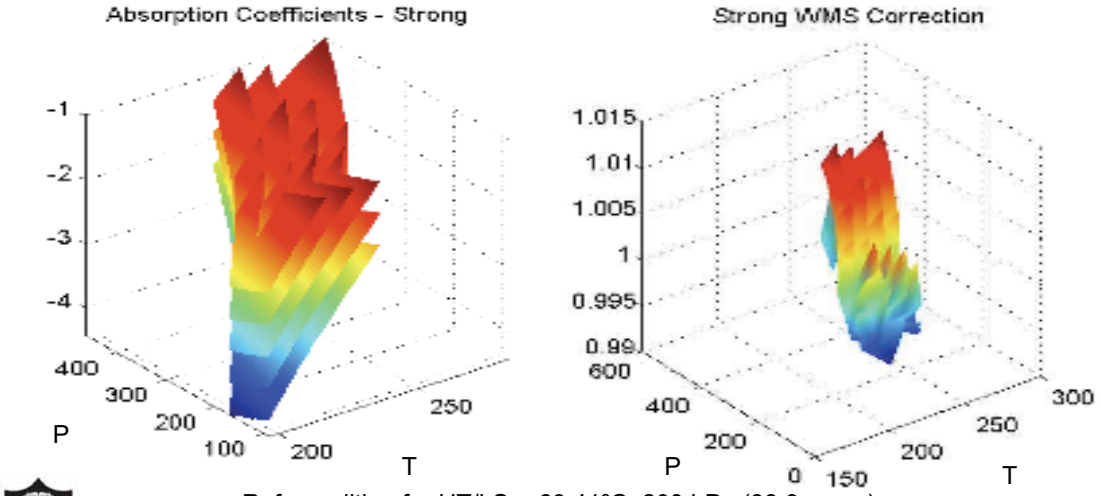

Ref. condition for UT/LS: -63.41ºC, 200 hPa (33.9 ppmv)
Empirical calibrations required

Example: Open vs. close-path sampling

HIPPO-3: 525 hPa, 255 K

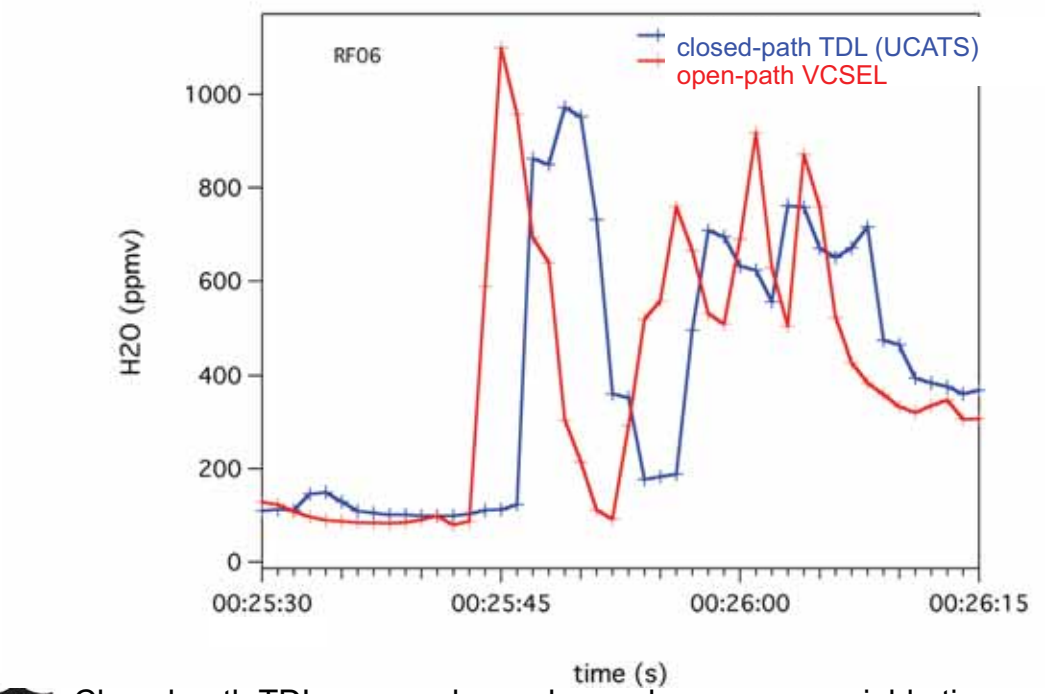

Closed-path TDL sensor shows damped response, variable time lags during HIPPO

How do ice supersaturated regions – the birthplaces of cirrus clouds - form?

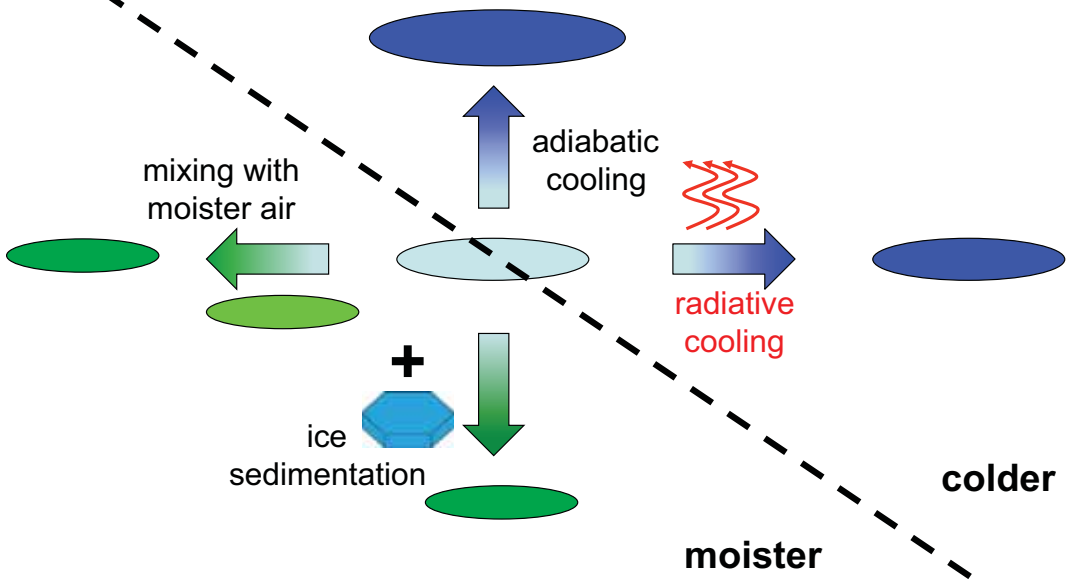

Clouds models initiate ice supersaturation by cooling on a constant water vapor background
(e.g. Jensen *et al.*, 2004; Spichtinger *et al.*, 2009)

Representative ice supersaturated region

Examining only the dRHi into components from temp. and water vapor:

RHi=e/e_s x 100

e is H_2O partial pressure

e_s is saturated ice vapor pressure

$$dRHi = d\frac{e}{e_s} \approx e\,d\frac{1}{e_s} + \frac{1}{e_s}de$$

dRHiT dRHiq

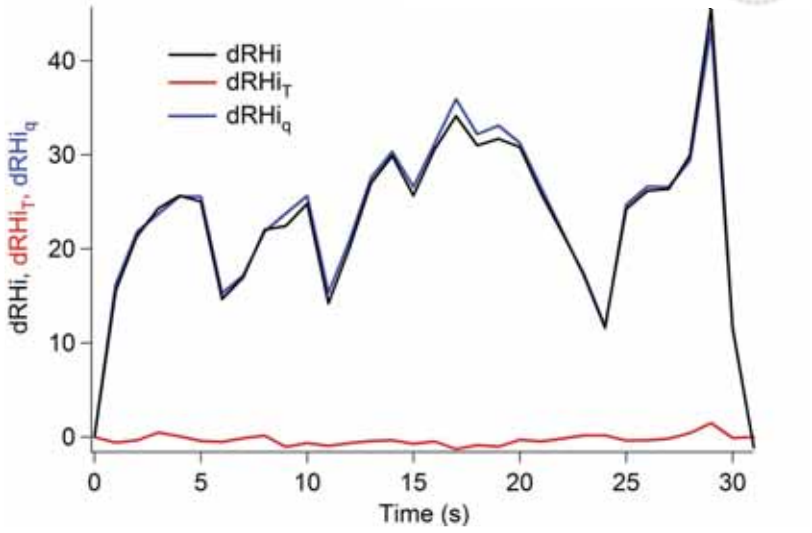

H_2O – not temperature - controls variability in RHi field on scales 0.2-100 km

> 5500 individual ice supersaturated case studies

(Diao et al., *Nature Geo.*, revised, 2012)

Tropospheric Ammonia

- one of the most important species in aerosol chemistry and physics
- ammoniated aerosols important for urban air quality
- largest uncertainties in climate change are impact of aerosols
- severe measurement challenges: parts per *trillion* sensitivies "sticks" to sampling lines/inlets
- rapidly increasing anthropogenic emissions

Requires open-path configuration AND fundamental absorption lines (mid-IR)

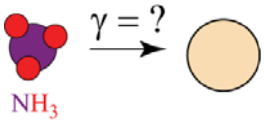

Why open-path for ammonia?

Compare NH_3 vs. a non-"sticky" gas like ethylene

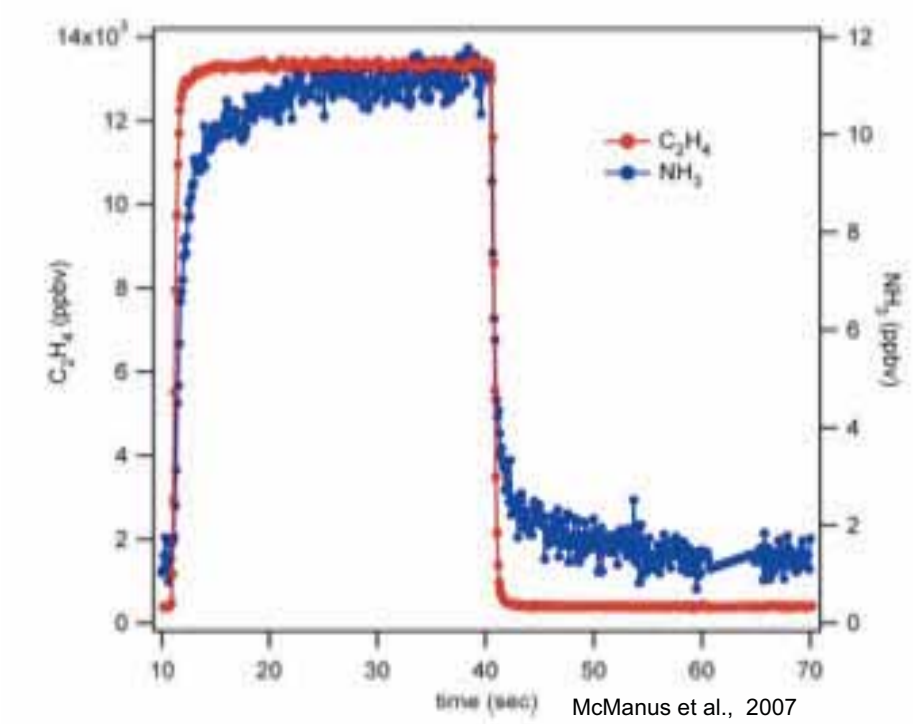

McManus et al., 2007

NH_3 spectroscopy

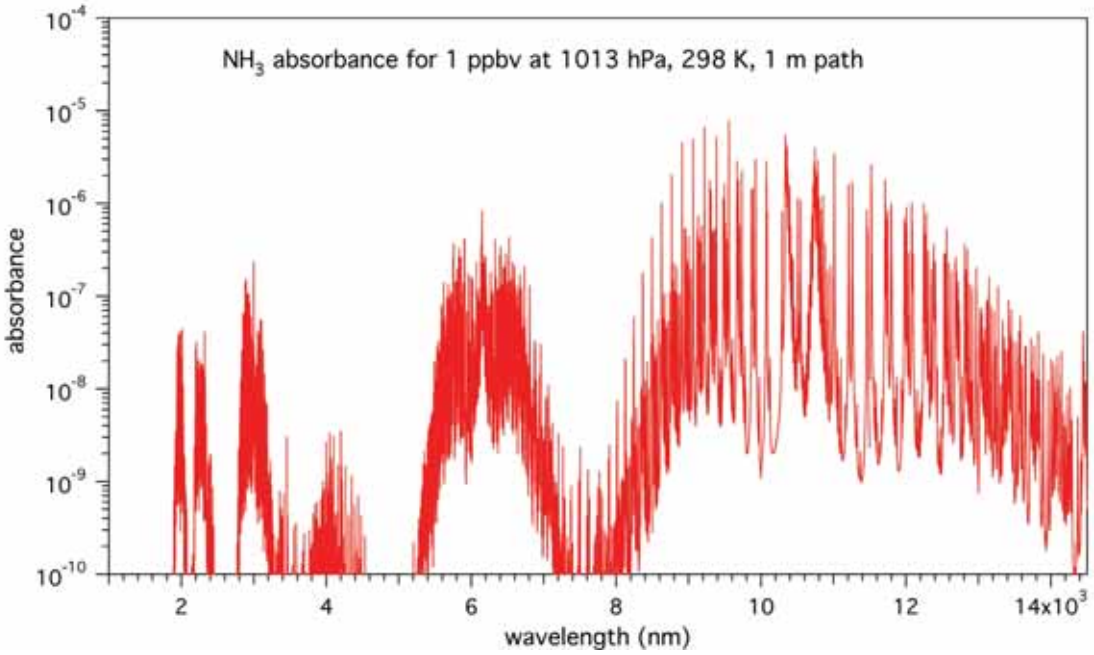

Strongest absorption lines near 10 μm, but are these the best ones?
For ambient detection, need to look at interferences…

Atmospheric spectra at 9.06 μm

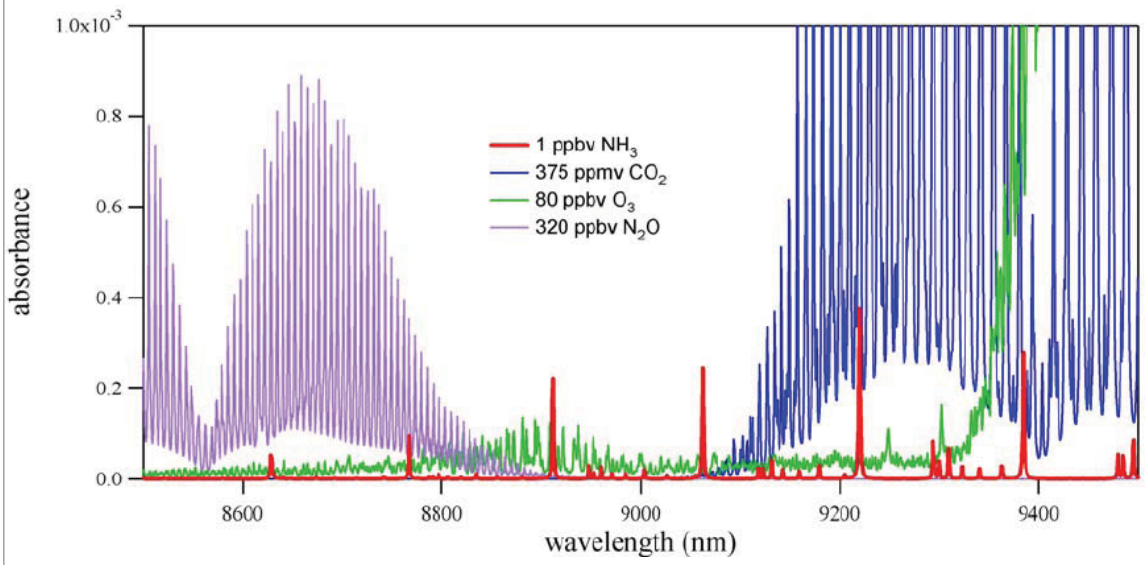

strongest lines have significant interferences at amb. T, P

most optimum line(s) at 9.06 μm

…and water vapor (up to 4%) isn't even included here!!

Optimal NH_3 absorption feature: 9062 nm

Two complications:

a) H_2O sloping background

b) ozone may be interferent at sub ppbv

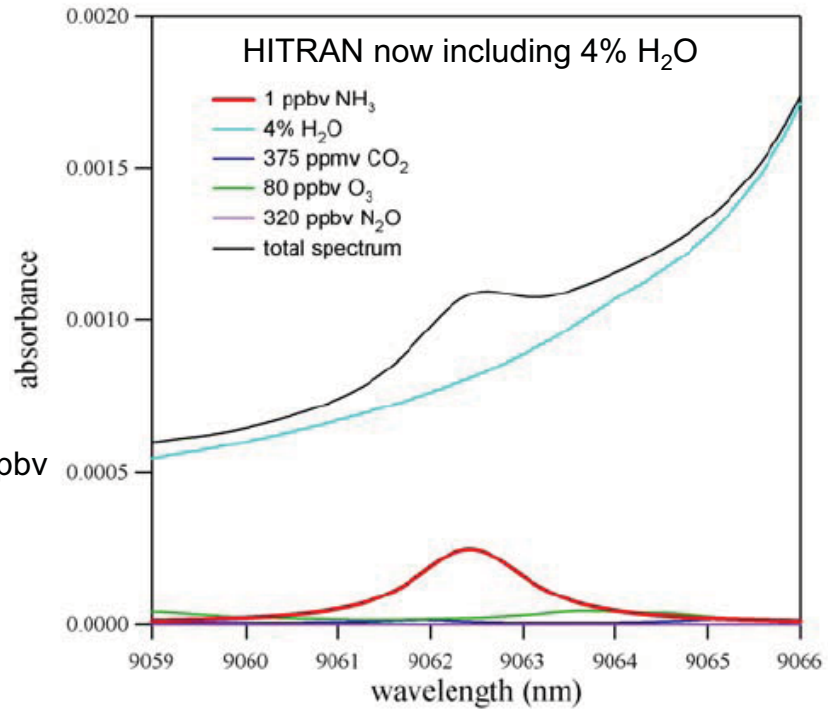

Metric for system drift in open-path configuration: in-line reference cell of a stable gas

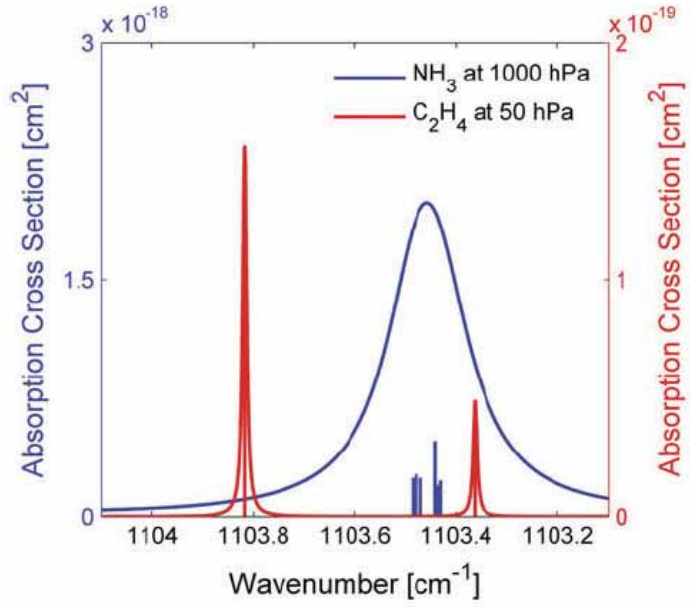

Ethylene (C_2H_4) as a reference absorption signal:

- Stable gas with negligible absorption in atmosphere
- Comparable absorption offset with NH_3 feature
- Little interference w/ NH_3 at reduced pressure
- Need to calibrate line shape parameters

Multiharmonic WMS fitting

$$\nu(t) = i_R \eta_R R(2\pi f_R t) + i_m \eta_m \cos(2\pi f_m t + \phi) + \nu_0$$

η_R is current-to-frequency tuning rate at ramp frequency (f_R)
η_m is current-to-frequency tuning rate at modulation frequency (f_m)
Φ is phase difference between modulation laser frequency and laser intensity
i_R and i_m are amplitude of ramp and modulation of laser current, respectively
R is the sawtooth ramp function
IIR low-pass Butterworth filter to yield nth harmonic signal *(Tao et al., Opt. Letters, 2012a; Sun et al., Appl. Phys. B, 2012)*

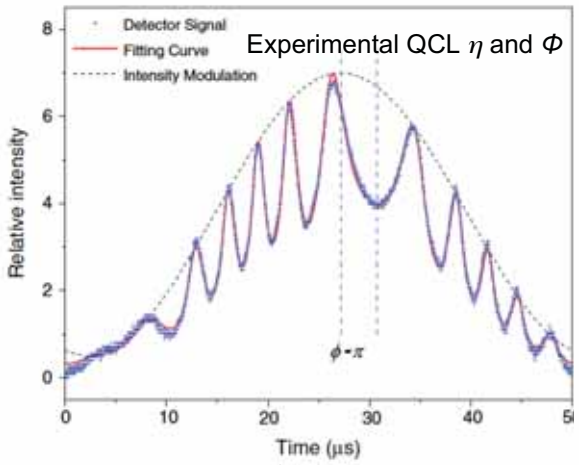

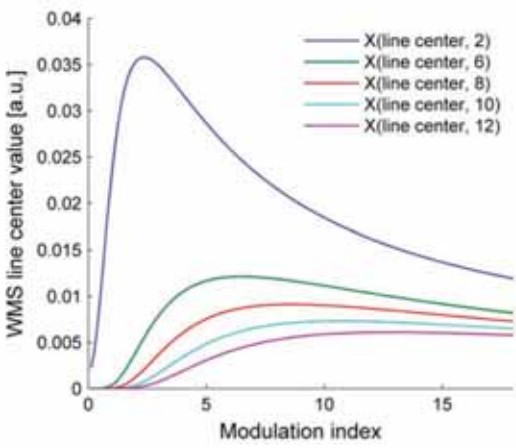

By selecting nth harmonic, can distinguish between broadened ambient NH_3 and reduced-pressure ethylene cell (nth derivative-like of absorption profile)

Spectroscopic Parameters of NH_3 & C_2H_4

Line shape parameters of NH_3 & C_2H_4 are measured experimentally and compared with HITRAN database (Rothman et al. 2009)

HITRAN data generally within 10% of experimental methods except one NH_3 linewidth

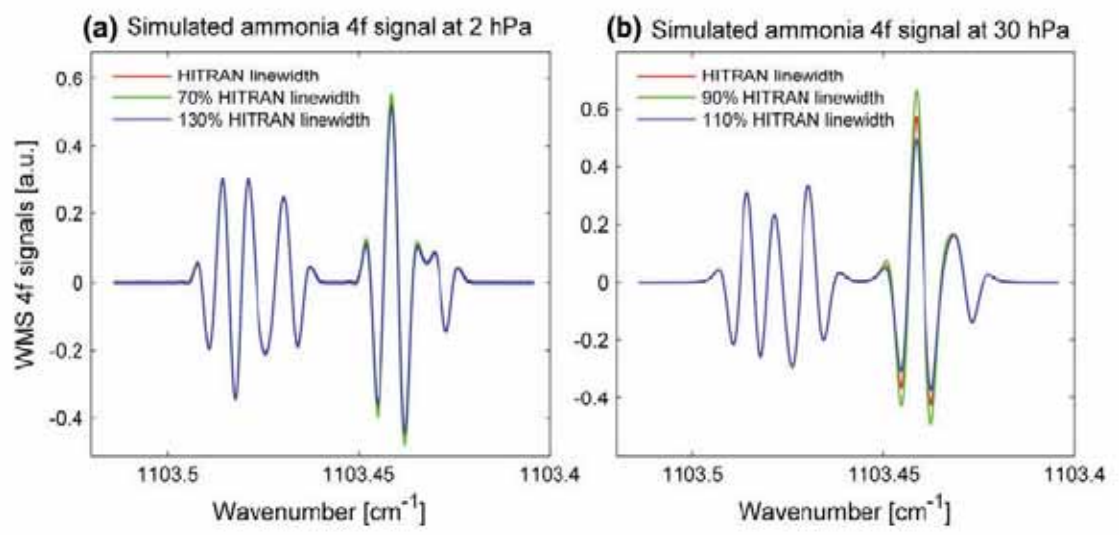

4f signals more sensitive to linewidth at 30 hPa than 2 hPa

Multiharmonic detection for continuous, in-line calibration

2.5 cm, 30 hPa 1% ethylene in N_2 w/ ambient NH_3

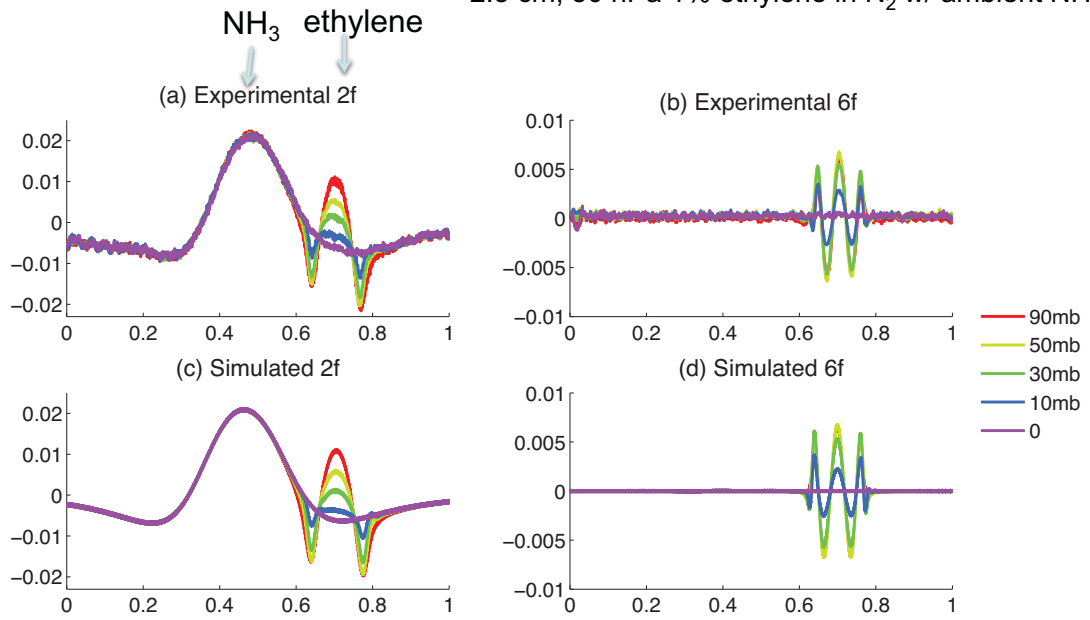

Ethylene 6f in-line reference signal not affected by ambient ammonia

Influence of changes of NH_3 on reference signal

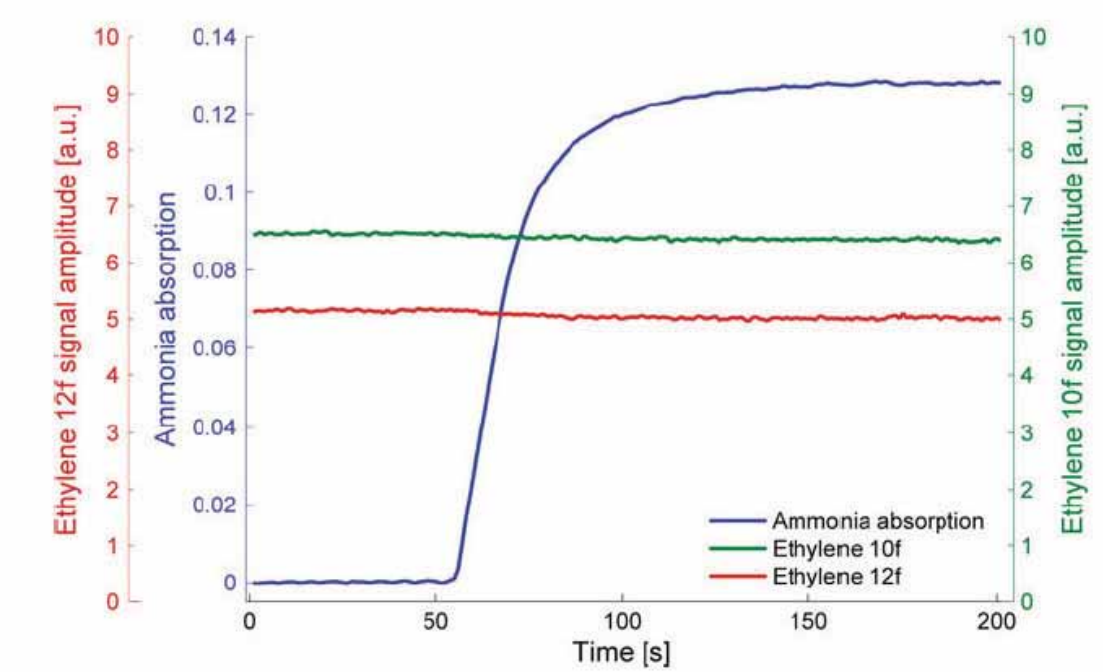

Ammonia absorption changes from 0 to 0.13 with no discernable effect on reference ethylene signals at higher harmonics

9.06 µm QCL open-path ammonia sensor

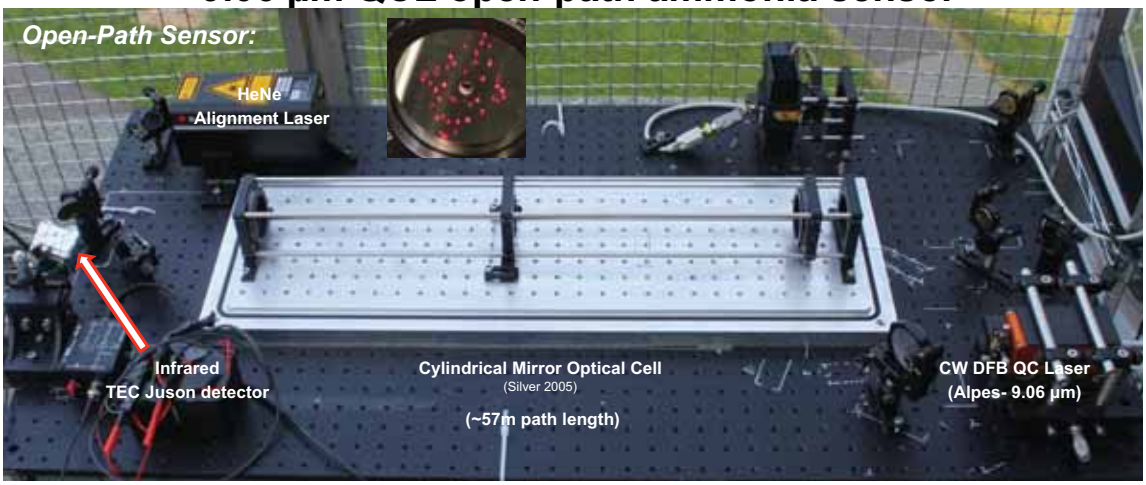

Challenges:

- Interference from other species, i.e. H_2O, CO_2
- Difficult to get the baseline of air-broadened absorption
- No control of T/P
- Calibration: need to enclose the open-path system

Solutions:

- ✓ Detecting ammonia line at 9.06 µm – QC laser (more isolated)
- ✓ Wavelength modulation spectroscopy (WMS)
- ✓ T/P spectroscopic studies
- ✓ In-line ethylene calibration

Ambient NH_3 – Princeton, NJ

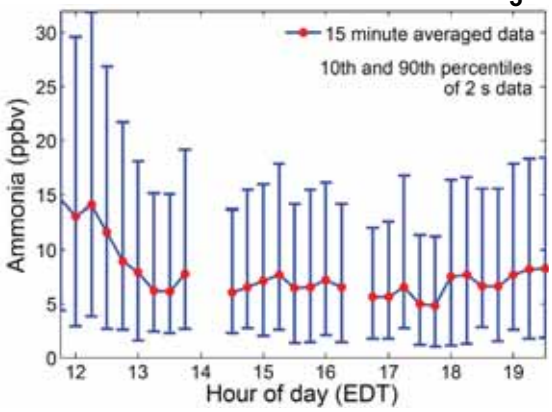

July 22, 2011

Very humid (26ºC dewpoint), hot (41ºC)

Mean: **~ 9 ppbv NH_3**

- Much higher than models, urban emissions are underestimated

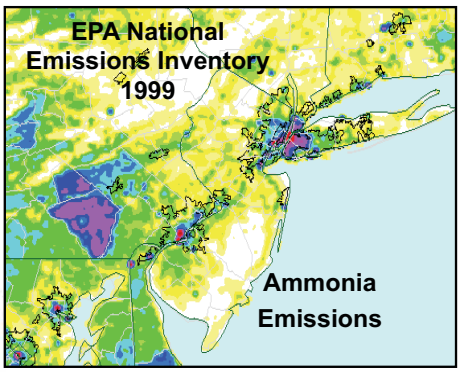

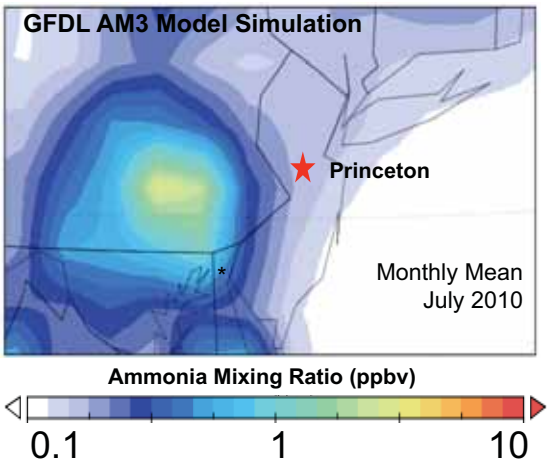

Atmospheric nitrous oxide (N_2O)

- Third most important anthropogenic greenhouse gas
- Emissions have tripled in past 100 years
- Agriculture emissions dominant source but largely unconstrained
- Long atmospheric lifetime of 110 years – long response time
- QC lasers at 4.54 μm can detect N_2O in an open path setup for eddy covariance flux studies

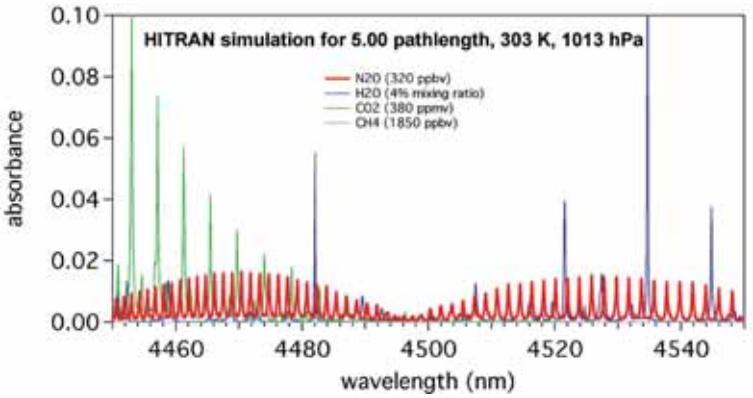

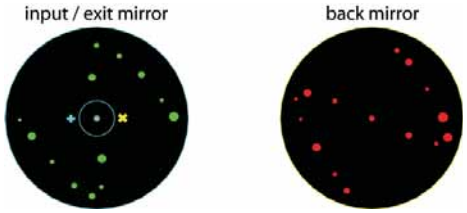

Nitrogen emissions and cycle listed as one of the grand challenges in the 21st century (NAE, 2008)

Global nitrous oxide (HIPPO #1)

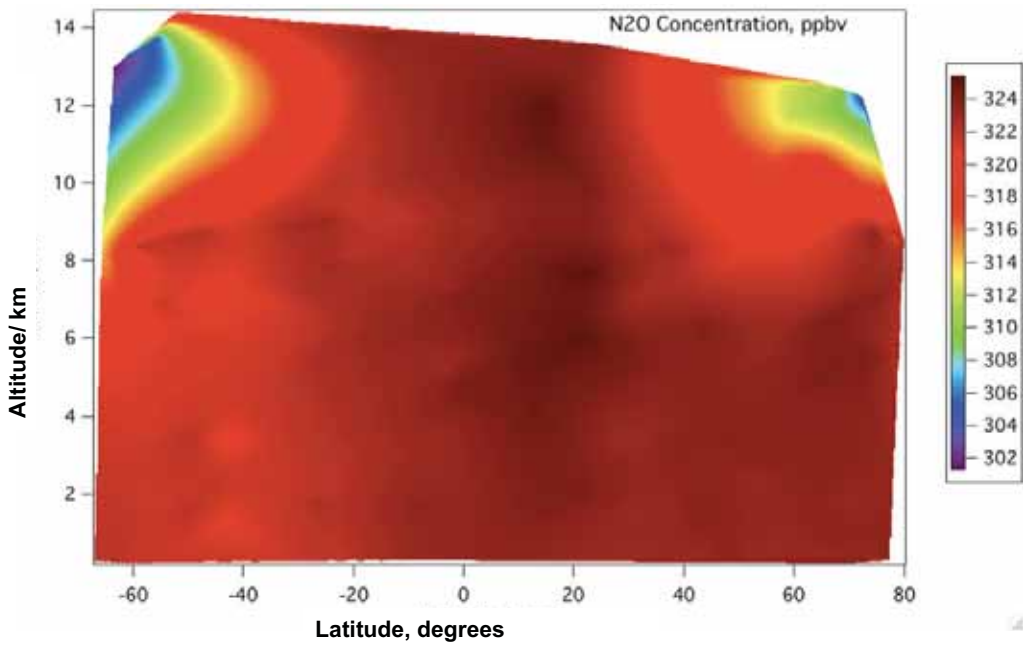

Source: E. Atlas, NSF HIAPER Pole-to-Pole Observations

Nitrous oxide is largely invariant at ~ 325 ppbv in atmosphere

Open-path nitrous oxide

- Room temperature, continuous-wave, single mode QC lasers are great light sources for gas sensing spectroscopic applications.
- 4.5 μm QC laser was selected to detect N_2O at its fundamental vibrational band
- Simultaneous detection of N_2O and CO
  - distinguish between combustion and natural sources of N_2O
- Detection of reference C_2H_2
  - Inline reference signal & calibration

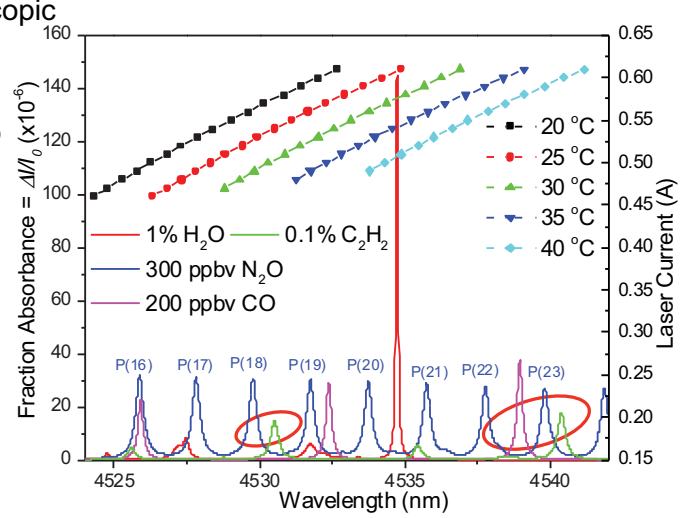

N_2O, CO, and in-line acetylene simultaneous detection

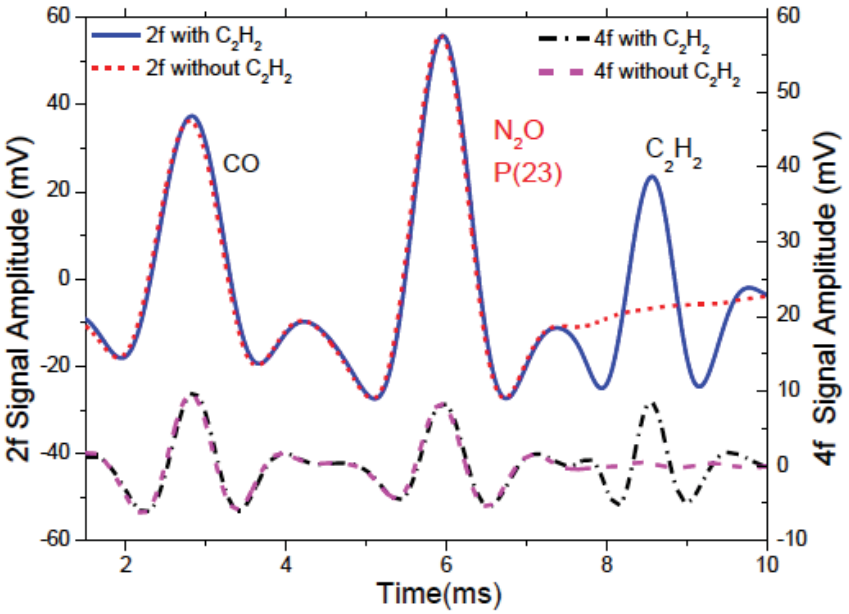

• Simultaneous spectra of three species in one QCL scan range and multiharmonic fits

Laboratory measurements: ambient air

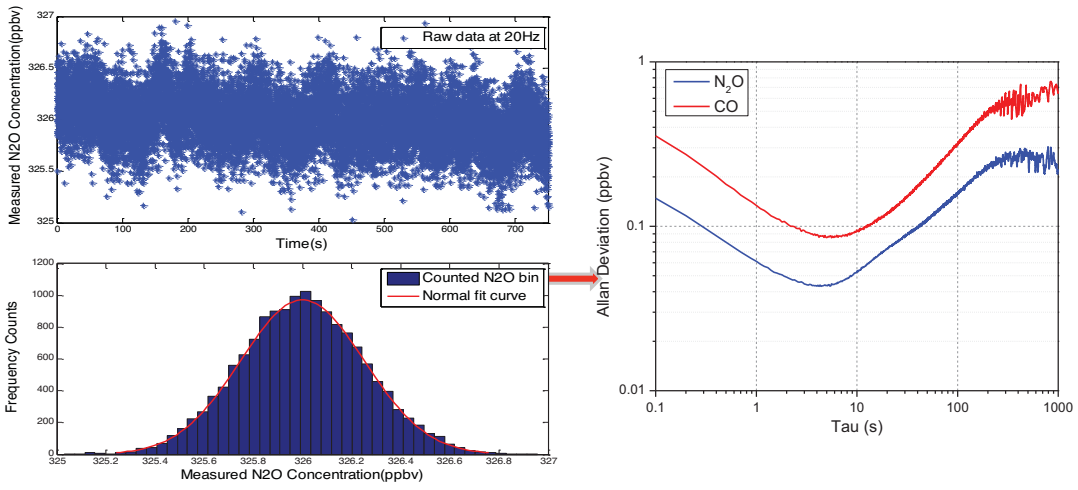

• Data from an overnight test with ambient lab air

• Measured data follows a normal distribution

•Sensitivity of 0.07 ppbv of N_2O and 0.15 ppbv of CO at 1 Hz sample rate

N_2O: Open-path challenges, spectroscopy

• Due to the high-precision/stability needed, even small changes in ambient temperature/pressure influence the measurement

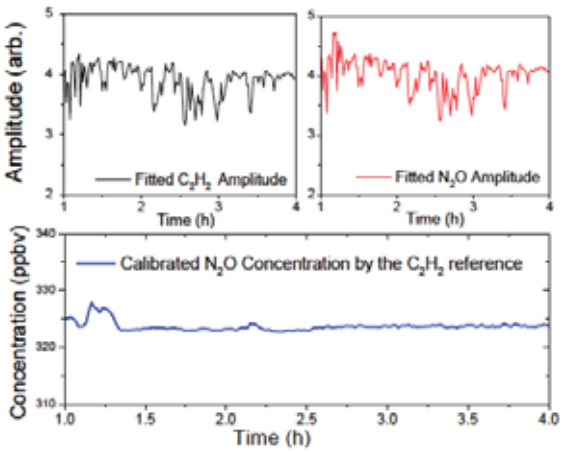

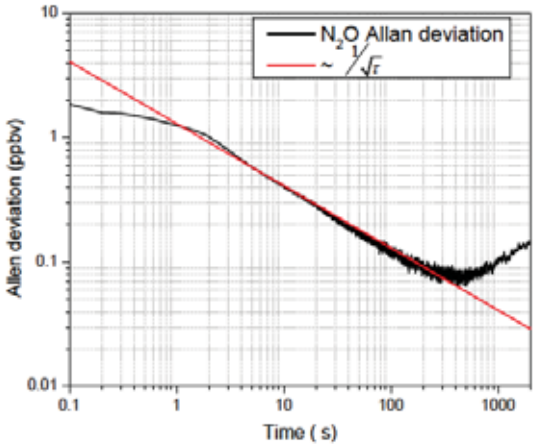

(Tao et al., Opt. Express, revised, 2012b)

• Normalization by in-line acetylene reference signal accounts for field drift of system for long-term stability
• Data also corrected by water vapor broadening
(~ 1% change in signal for 1% change in absolute humidity)

Intercomparison with Los Gatos closed-path sensor

LGR N_2O/CO Sensor

• LGR N_2O/CO sensor is a close-path system based on ICOS with a NIR laser

• gas inlet of LGR sensor was taped close to the sample cell of the WMS sensor

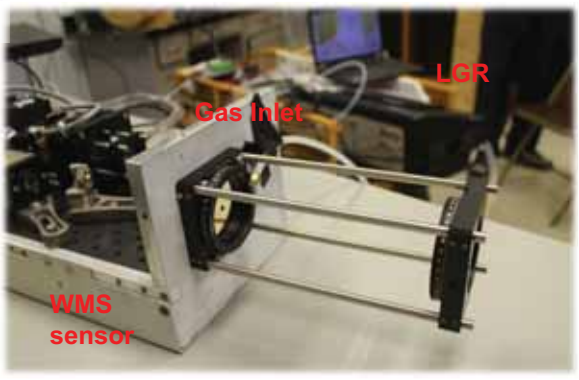

• both sensors measured the N_2O/CO emissions from a nearby car

• LGR sensor: recorded at 2Hz
WMS sensor: recorded at 10Hz

CO and N_2O car exhaust measurements
Open-path challenges II: sampling

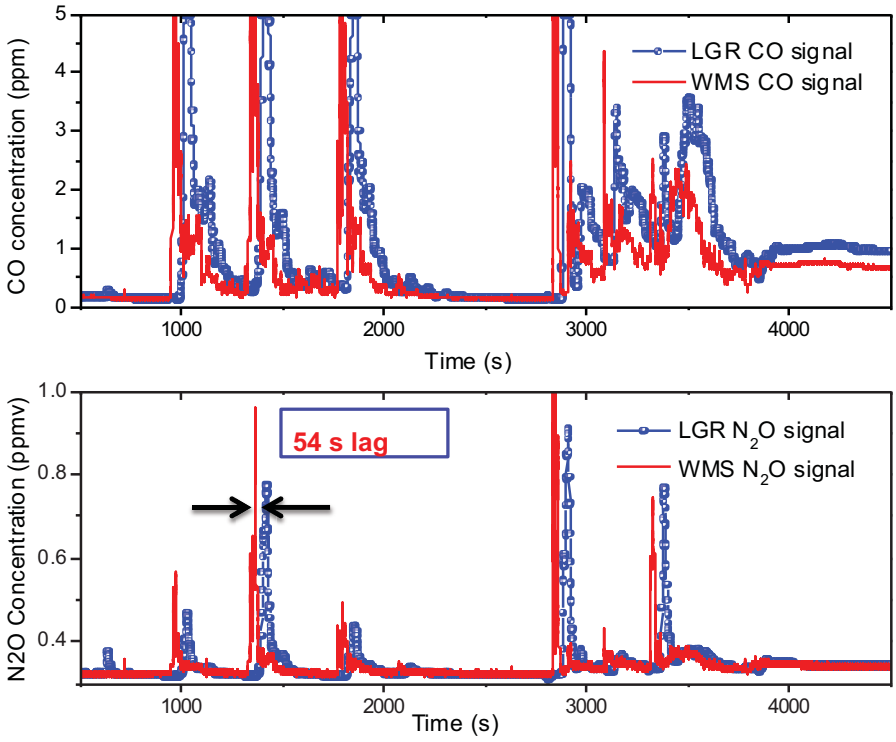

Time-response, sample bias corrected (1 Hz)

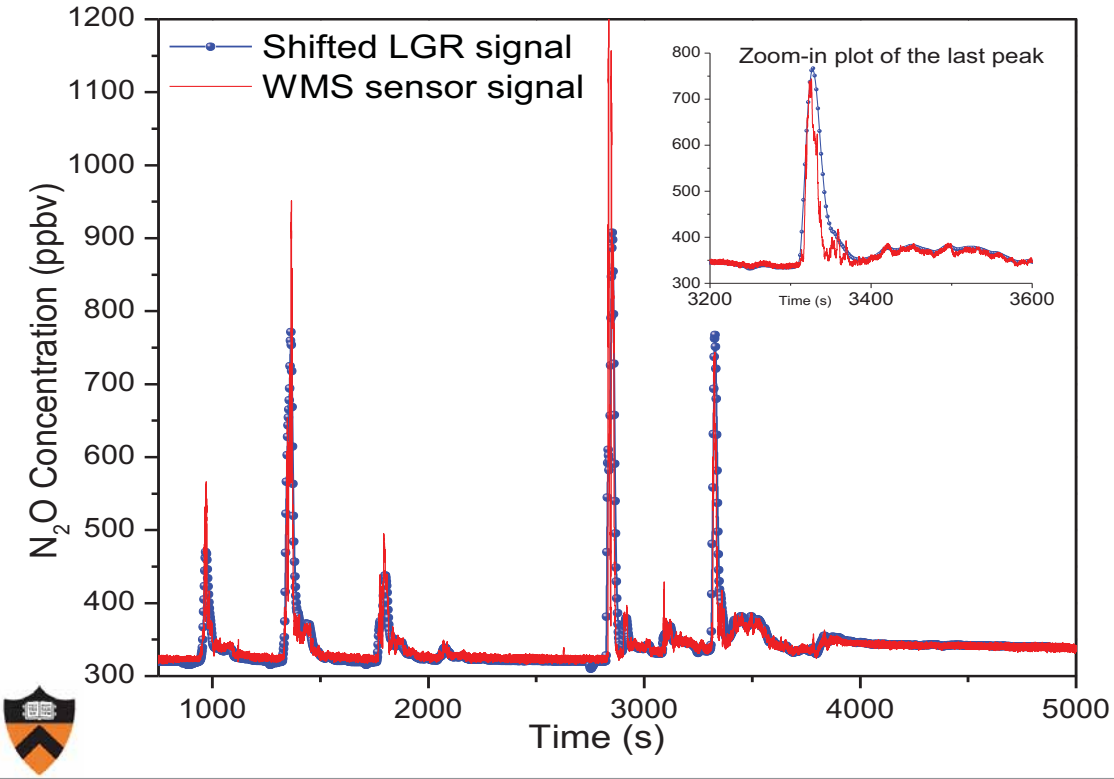

Field tests: flux chamber wetlands and eddy covariance in corn field

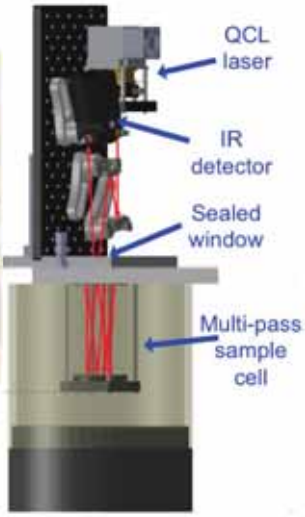

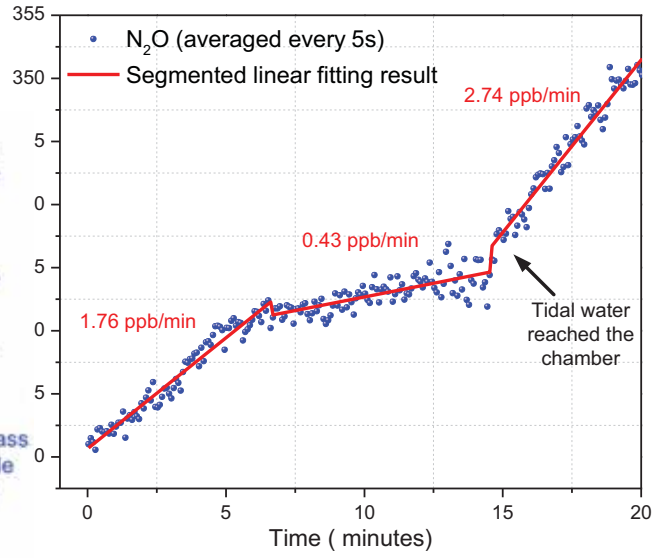

Atmospheric laser-based sensors: spectroscopic needs

All gases:

- more studies of temperature- and pressure-dependence over range of troposphere
- "weak" but isolated lines very important for ambient air detection (most optimum lines most often not the strongest for ambient detection)
- particular attention to "sticky" gases that are challenging to address in laboratory

Greenhouse gases CO_2, CH_4, N_2O (high precision/stability needed):

- water broadening coefficients may significantly bias measurements if incorrect

Atmospheric radicals:

- limited data for species such as NO, NO_2, OH, and HO_2

Ambient pressure detection requires critical attention to spectroscopic parameters for accurate and relevant measurements (pressure-broadened lines, interferences, changing temperature & pressure & humidity)…but it can be done for new sensing platforms and applications

Funding: NSF AGS-1063466; NSF EEC-0540832; NASA NNX09AO51H; USDA 2008-05149

"Ground-based atmospheric monitoring networks using FTIR: Present / future needs of the NDACC and TCCON community with respect to spectral line data"

Dr. Geoffrey C. Toon

Jet Propulsion Laboratory, California Institute of Technology

Dr. Geoffrey C. Toon

Jet Propulsion Laboratory, California Institute of Technology
4800 Oak Grove Drive, 91109 Pasadena, CA, USA
Phone: +1 8183548259
E-mail: geoffrey.c.toon@jpl.nasa.gov

Research

Remote measurements of atmospheric composition: Instrumentation and data analysis

Education and Professional Experience

since 2001	Caltech Faculty: Visiting Associate in Planetary Science, USA	
since 1984	Jet Propulsion Laboratory, USA	
	2008-2012	Group Supervisor, Atmospheric Observations
	since 2006	Senior Research Scientist
	since 1986	Research Scientist, JPL
	1984-1986	NRC Resident Research Associate, JPL
1984	D.Phil. (Atmospheric Physics) University of Oxford, UK	
1978	B.A. Honours (Physics) University of Oxford, UK	

Activities, Honors and Awards

- 8 NASA Achievement Awards

Ground-based atmospheric monitoring networks using FTIR: Present / future needs of the NDACC and TCCON community with respect to spectral line data

Geoffrey C. Toon

Jet Propulsion Laboratory, California Institute of Technology

Improving our understanding of the changing atmosphere requires increasingly accurate measurements of its composition. Two global networks currently make open-path atmospheric composition measurements using the sun as a source. The NDACC-IR network, operational since 1991, measures more than 20 atmospheric trace gases in the mid-IR spectral region (700-4100 cm^{-1}). The TCCON network, operational since 2003, covers the near-IR (4000-8000 cm^{-1}). TCCON measures fewer gases (e.g. CO_2 , CH_4 , CO, N_2O) but strives for higher accuracy and precision (up to 0.2%). Each network uses Fourier Transform spectrometers at more than 20 sites, some of which are common to both networks.

The NDACC-IR and TCCON networks offer an interesting contrast in calibration methodologies. NDACC-IR relies on the spectroscopy for their calibration, such that a 5% error in the line intensities will cause a 5% error in the retrievals. TCCON uses a more complicated calibration procedure that relies on co-located in situ profile measurements and assumptions about diurnal variations to reduce sensitivity to instrumental and spectroscopic errors. This presentation discusses the spectroscopy needs of the TCCON and NDACC-IR networks, and highlights areas in which improvements would be beneficial.

Ground-based atmospheric monitoring networks using FTIR: Spectroscopic needs of the NDACC and TCCON communities

Geoff Toon, Jet Propulsion Laboratory, California Institute of Technology

Will discuss atmospheric remote sensing using direct sunlight with FTIR spectrometers:
NDACC: Network for Detection of Atmospheric Composition Change (1991-present)
TCCON: Total Carbon Column Observing Network (2003-present)

Opinions expressed here are my own and do not necessarily represent the unanimous opinion of the entire NDACC and TCCON communities.

© 2012. All rights reserved

NDACC (formerly NDSC)

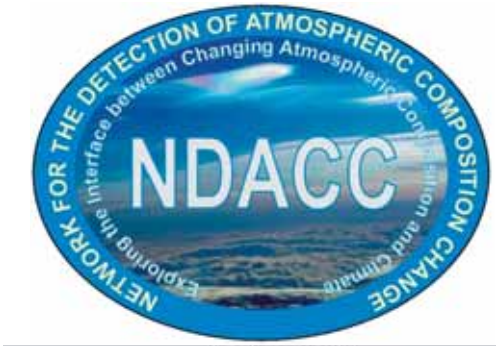

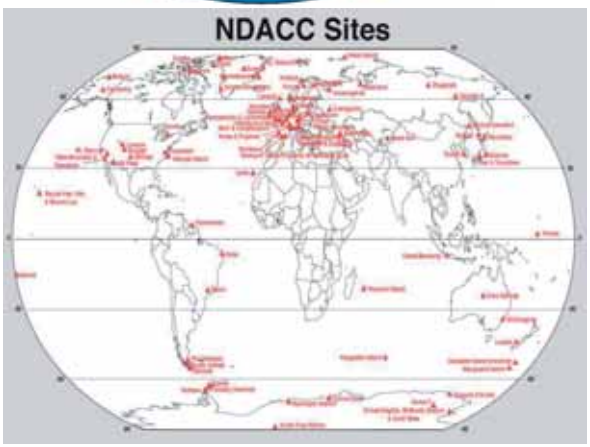

Network for Detection of Atmospheric Composition Change (NDACC) includes:

- O_3 sondes
- UV/Vis spectrometers
- Microwave radiometers
- Lidars
- Dobson-Brewer spectrometers
- Fourier Transform Spectrometers (FTS)

Only FTS will be considered further here

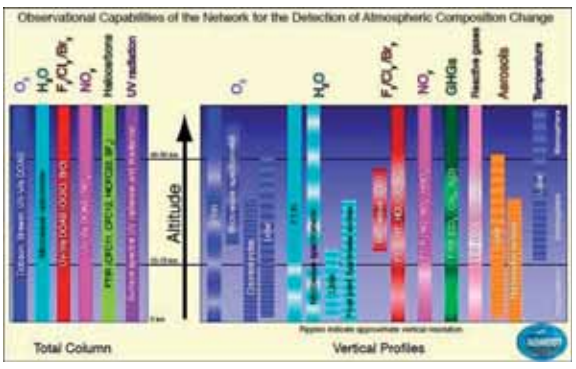

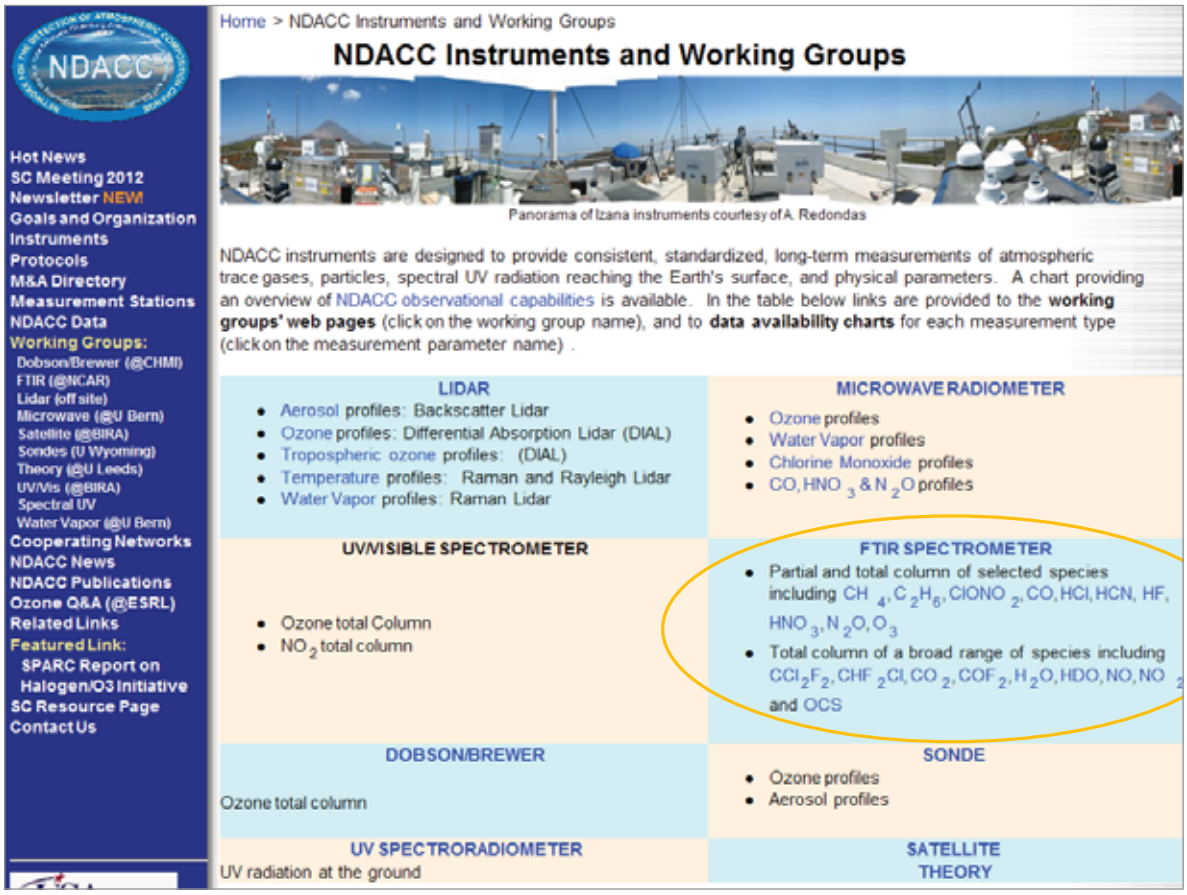

TCCON

Started in 2003 (Park Falls, Wisconsin, USA)

24 sites today (see below)

Main motivation is validation of satellite observations of GHG (OCO, GOSAT)

Uses Bruker IFS125 HR spectrometers

NDACC & TCCON Summary

	NDACC	TCCON
Spectral Coverage	700-4100 cm^{-1}	4000-8000 cm^{-1}
Spectral Resolution	0.003 to 0.009 cm^{-1}	0.02 cm^{-1}
Detectors	HgCdTe & InSb @ 77K	InGaAs @ 300K
Retrieval Method	SFIT2 / PROFITT	GFIT (highly standardized)
Calibration Standard	HITRAN	In Situ profiles
Accuracy Goal	1-10%	0.2-0.5%
Operational	1991-present	2003-present

Main focus of NDACC-FTS is O_3 and weakly absorbing trace gases (e.g. NO, NO_2, HNO_3, $ClNO_3$, HCl, HF, COF_2, OCS, HCN) present at ppb levels. Highest sensitivity is found in 700-4100 cm^{-1} region, where small doppler widths allow profile retrieval. These gases are variable, so moderate accuracy suffices, allowing HITRAN to be primary calibration standard.

TCCON's main focus is CO_2 and CH_4, present at ppm levels. Fundamental bands are saturated, so use overtone/combination bands at higher frequencies. Variations of interest are < 0.2% and so high accuracy is required. HITRAN accuracies are insufficient – a more complex calibration procedure is needed.

Atmospheric Remote Sensing: Accuracy/Precision requirements

For long lived atmospheric gases (e.g. CO_2, N_2O , CH_4) , the variations of interest (e.g., seasonal cycle, inter-hemispheric gradient, sources, sinks) tend to be small in comparison with the accumulated total gas column.

So high fractional accuracy is needed for measurements to be scientifically useful.

For CO_2, column-averaged mole fraction needs to be better than 0.3%
For N_2O, the tropospheric mole fraction needs to be better than 0.2%
For CH_4, the tropospheric mole fraction needs to be better than 0.4%
For shorter-lived gases (e.g. CO) the requirements are less strict (>1%)

The OCO and GOSAT satellite sensors attempt to meet these goals, and ground-based validation networks (e.g. TCCON, NDACC) try to do even better.

Requirements will get stricter in the future as more is learned about these gases.

These goals impose strict requirements on the spectroscopy. Not only for these gases themselves, but also on other interfering absorbers (e.g. H_2O, HNO_3, etc.)

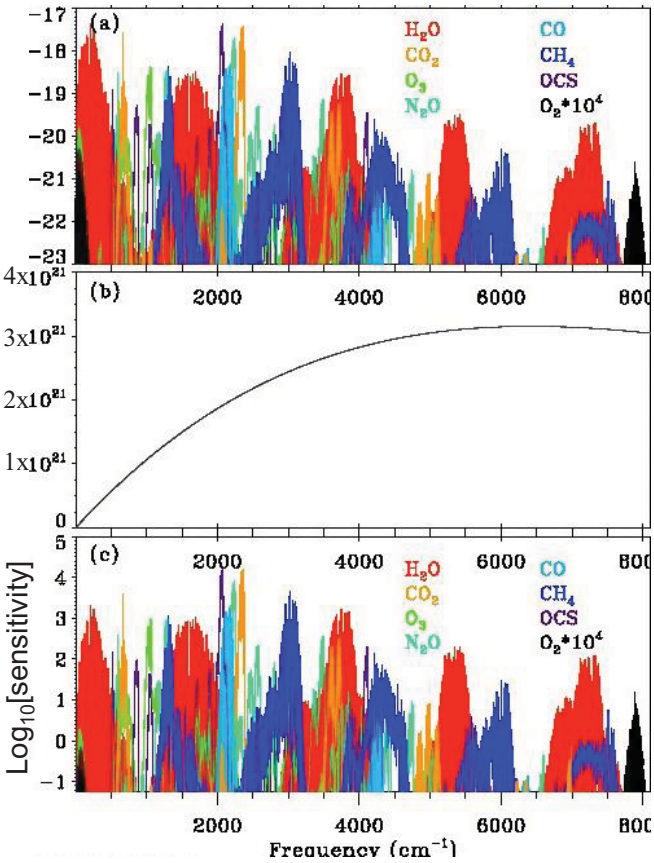

HITRAN Linelist

HITRAN Line Intensities
(integrated in 1 cm^{-1} bins)
Units of $cm^{-1}/(molec/cm^2)$

Solar Planck function
$ph/s/cm^2/sr/cm^{-1}$

Sensitivity:
Absorbed photons per molecule

Spectral Coverage

NDACC covers the 700-4200 cm^{-1} region where the trace molecules of interest have their fundamental absorption bands and hence the highest gas sensitivity.

TCCON covers 4000-8000 cm^{-1} using the weaker overtone and combination bands of CO_2, CH_4, CO, N_2O. This region is also used by OCO and GOSAT.

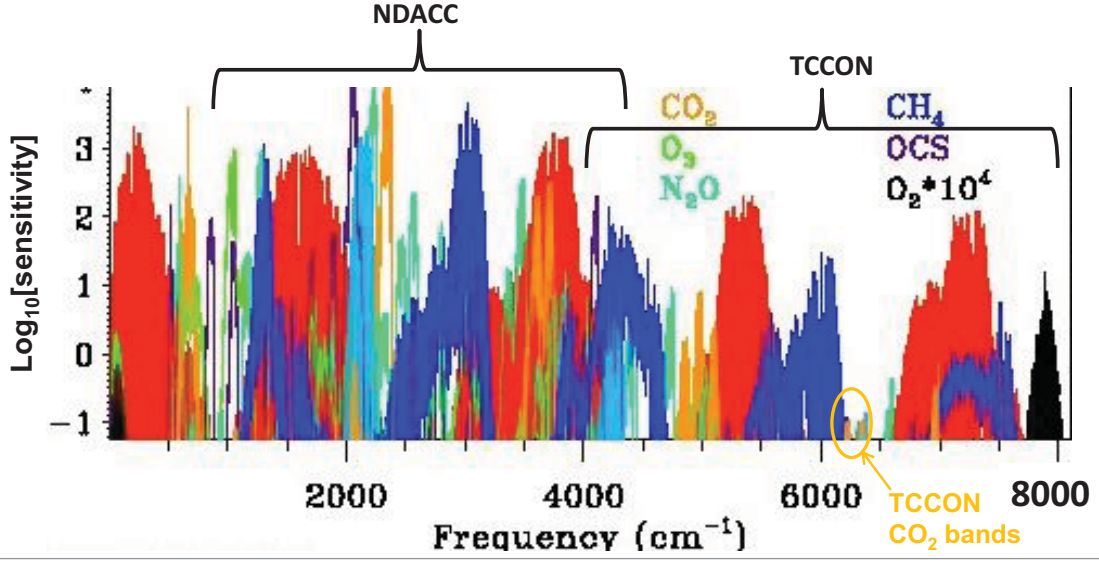

Spectral Fitting Terminology

Both NDACC and TCCON use similar methods to retrieve atmospheric gas amounts

$$\text{Minimize } \chi^2 = \sum_i [y_i - f_i(x)]/\varepsilon_i\}^2 + \sum_k [(x_k - x^a_k)/\varepsilon_k]^2$$

Measured Spectrum — *Calculated Spectrum* — *A Priori constraint*

where *i* is an index over the spectral points, and

$$f_i(x) = \underbrace{\text{Continuum}_i(x_c) \text{ . ILS}}_{\textit{Instrumental}} * \Big(\text{Solar}_i \text{ . } \underbrace{\text{Exp}\{-[\sum_k \sum_l a_{i,k,l}.v^a_{k,l}.g_l \text{ . } p_l \text{ .} x_{k,l}]\}}_{\textit{Atmospheric Transmittance}} \Big)$$

$a_{i,k,l}$ are the absorption coefficients (from HITRAN) for gas *k* and level *l*
$v^a_{k,l}$ are the a priori vmrs, p_l is the atmospheric number density, g_l is the airmass factor

x is the unknown "state vector" containing the unknown atmospheric VMR scale factors ($x_{k,l}$) and the coefficients defining the continuum level (x_c).
If $x_{k,l}$ is assumed to be level-dependent, it is called a "profile retrieval"
If $x_{k,l}$ is assumed independent of level, "profile scaling retrieval"

Spectral Fitting Example

Since the spectra are not radiometrically calibrated, it is necessary to retrieve the instrumental radiometric gain (continuum level), in addition to the atmospheric gases.

The continuum level is represented by a low order polynomial. It represents the responsivity of the instrument and solar planck function as a function of wavenumber.

The solar spectrum is empirically derived from low-airmass solar spectra measured from the ground (Kitt Peak), balloon (MkIV), and Space (ATMOS).

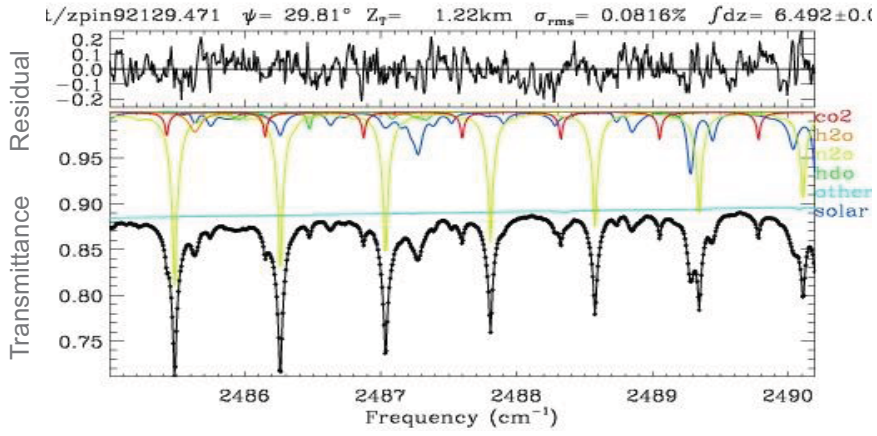

Column Abundances

Having iterated the spectrum fitting to convergence, the vertical column of the gases is computed from

Slant Column of gas k = $\int v^a_{k,l} . g_l \, . \, p_l \, . x_{k.l}$

Vertical Column of gas k = $\int v^a_{k,l} . \, p_l \, . x_{k.l}$

VMR profile of gas k = $v^a_{k,l} \, . x_{k.l}$

For NDACC, these are the reported end products, together with the averaging kernels and a priori vmr profiles.

For TCCON there are additional calibration procedures aimed at reducing the sensitivity of the results to systematic errors, both instrumental and spectroscpic.

TCCON Calibration

TCCON does not rely on the absolute accuracy of the HITRAN spectroscopy.
It uses 4 levels of calibration:

1. Band-to-band biases are quantified and corrected before averaging
2. O_2 column abundances are used to normalize CO_2, CH_4, CO, N_2O columns
3. Empirically remove airmass-dependent biases that are symmetrical about noon
4. Co-located NIST-traceable in situ profiles are used to perform final calibration

Random vs Systematic Errors

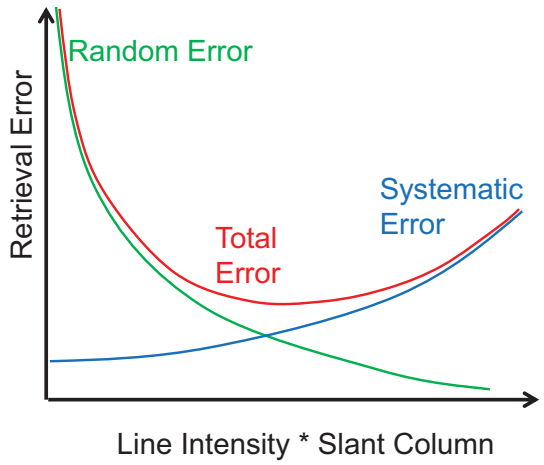

For weak absorptions, random errors dominate. For stronger absorptions (larger intensity or higher airmass) systematic errors dominate. There is an optimum line depth where the retrieval uncertainties are a minimum.

Systematic errors include spectroscopic and instrumental contributions.

1. Correction of line intensity biases

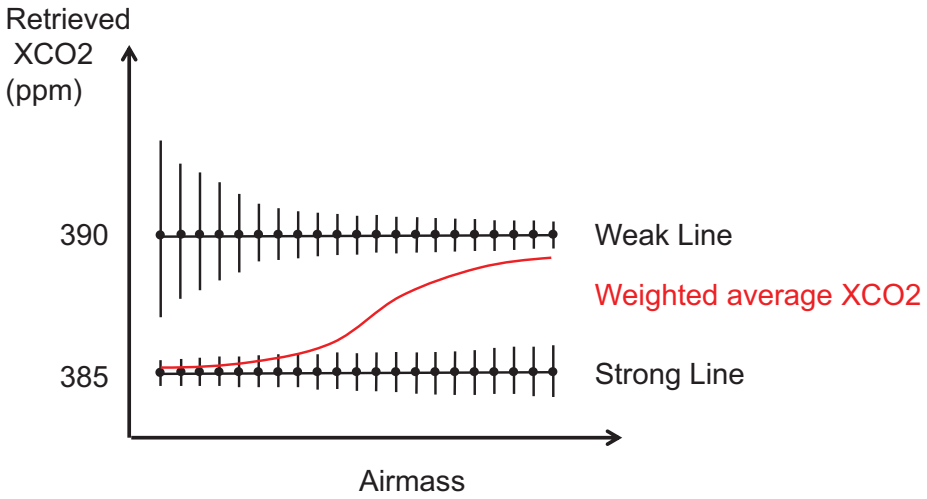

Even though weak and strong lines might each be airmass-independent, their weighted average is not.

Important to correct such biases before weak and strong lines/bands are averaged.

Difficult if weak/strong lines are inter-mingled in same fitting window

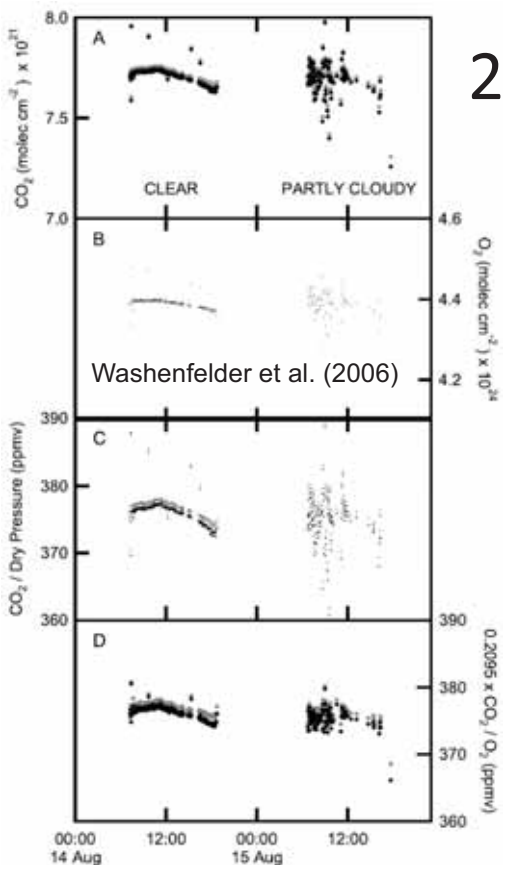

2. Using O_2 as reference

Xgas = gas_column / dry_air_column

Xgas is column-averaged dry air mole fraction is a more useful quantity than the column itself:
- More comparable with in situ measurements
- Less sensitive to surface pressure variations
- Less sensitive to humidity changes

How to compute dry_air_column?
- From surface pressure (P_S/m.g)
- From O_2 column (O2_column/0.2093)

Atmospheric O_2 vmr = 0.2093 globally. The O_2 option gives better results due to cancellation of systematic errors (eg, zero offset, ILS, pointing) common to CO_2 and O_2.

O_2 band at 7900 cm^{-1}. MIR region used by NDACC has no comparable reference gas absorption band (N_2?).

3. Airmass-dependent biases

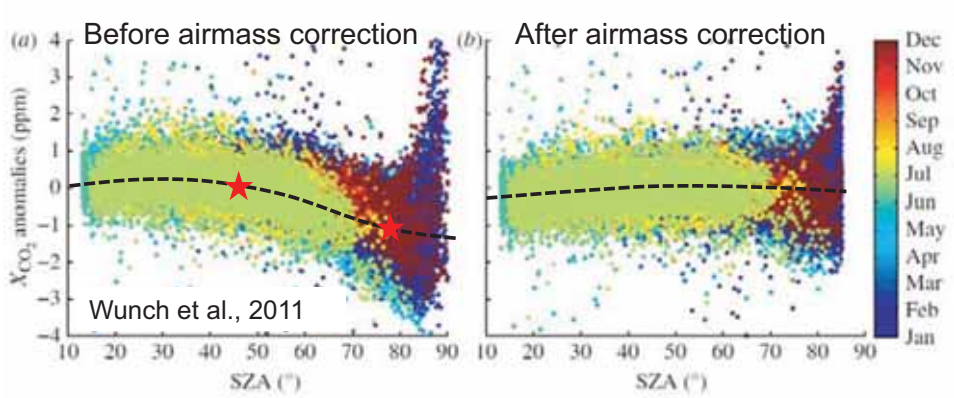

At all TCCON sites, uncalibrated XCO2 is ~1ppm (0.25%) lower at sunrise/set than at noon. Occurs at all times of year, even when exchange of CO_2 with the surface is tiny.

This artifact is highly detrimental to the science by creating false:
- diurnal variations
- seasonal variations at a given site (esp. at higher latitudes)
- latitude variations (between sites)

These artifacts are unacceptable, especially in the SH where the seasonal variations and latitude gradients of interest are < 0.1%. Similar artifacts exist in the raw XCH4.

What causes airmass dependent bias ?

The fact that the airmass-dependent biases are similar at all sites suggest a common cause, unrelated to the site or instrument.

Atmospheric airmass can vary by a factor 35 between noon and sunset/rise (tropics).

Almost all types of spectroscopic errors cause an airmass-dependent component.

Line shape errors (widths, non-voigt, line mixing).

- In saturated lines, the spectral information comes only from the wings (line center is blacked out) and hence the widths are critical
- In weak lines, the information comes from entire line (mainly near line center) hence less sensitive to widths

As already mentioned, any inconsistency between weak and strong lines of the same gas will cause an airmass-dependent artifact:

It is very common for the weak and strong line parameters in the same region to be based on different laboratory spectra. Even in a multi-spectrum fit, the weak lines will be defined primarily by the spectra with large absorber amounts, and vice versa.

In situ profile comparison

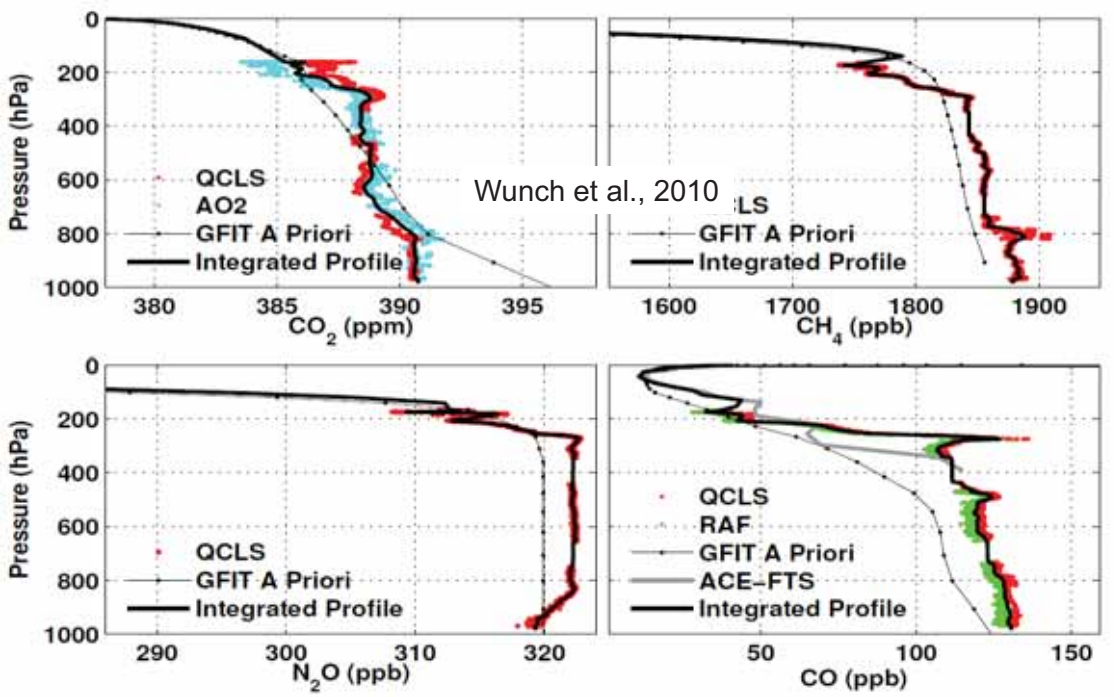

From Wunch et al., 2010

4. In Situ Calibration

CO_2 | CH_4

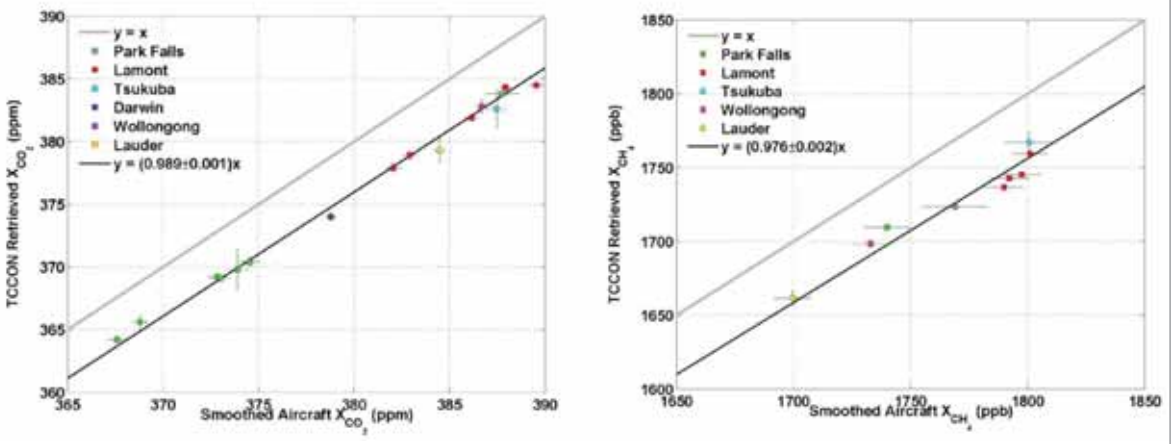

From Wunch et al., 2010

TCCON Calibration Summary

The four calibration techniques explained previously provide the TCCON data a reduced sensitivity to certain types of systematic errors, including spectroscopy.

An error in the mean intensity of the used lines of a given gas has no effect on the final reported TCCON results because of the in situ calibration.

Simple airmass-dependent errors are also removed by the airmass-correction.

Since the low-order spectroscopic errors are calibrated out, what types of remaining spectroscopic errors are TCCON results susceptible to?

Errors and Inconsistencies in the spectroscopy is the main problem.

- Between Weak / Strong line intensities or widths (in same fitted window)
- Missing lines
- Lineshapes (do widths in HITRAN assume Voigt or non-Voigt?)

For the remainder of this presentation we focus on spectroscopic inconsistencies.

Example: Spectroscopic Problem

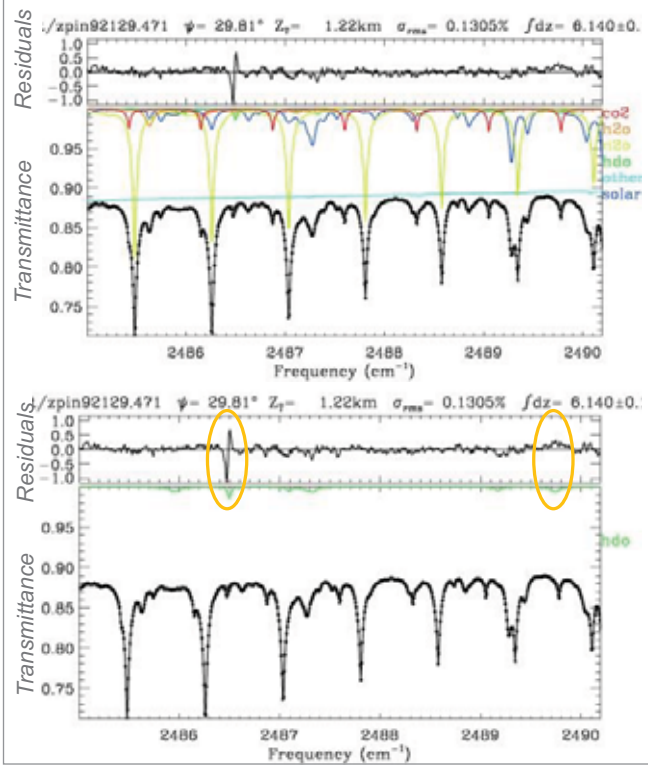

How important are spectroscopic uncertainties in the overall error budget?

Figures left show spectral fits to the 2485-2490 cm^{-1} region used to retrieve CO_2 and N_2O for NDACC. The largest residuals are associated with HDO absorptions.

You might think that, if the offending HDO lines don't directly overlap the N_2O lines (lime green), there would be little effect.

But there is an effect because the HDO-related residuals affect the retrieved continuum, which in turn affects the N_2O.

Fits to Kitt Peak Lab spectra

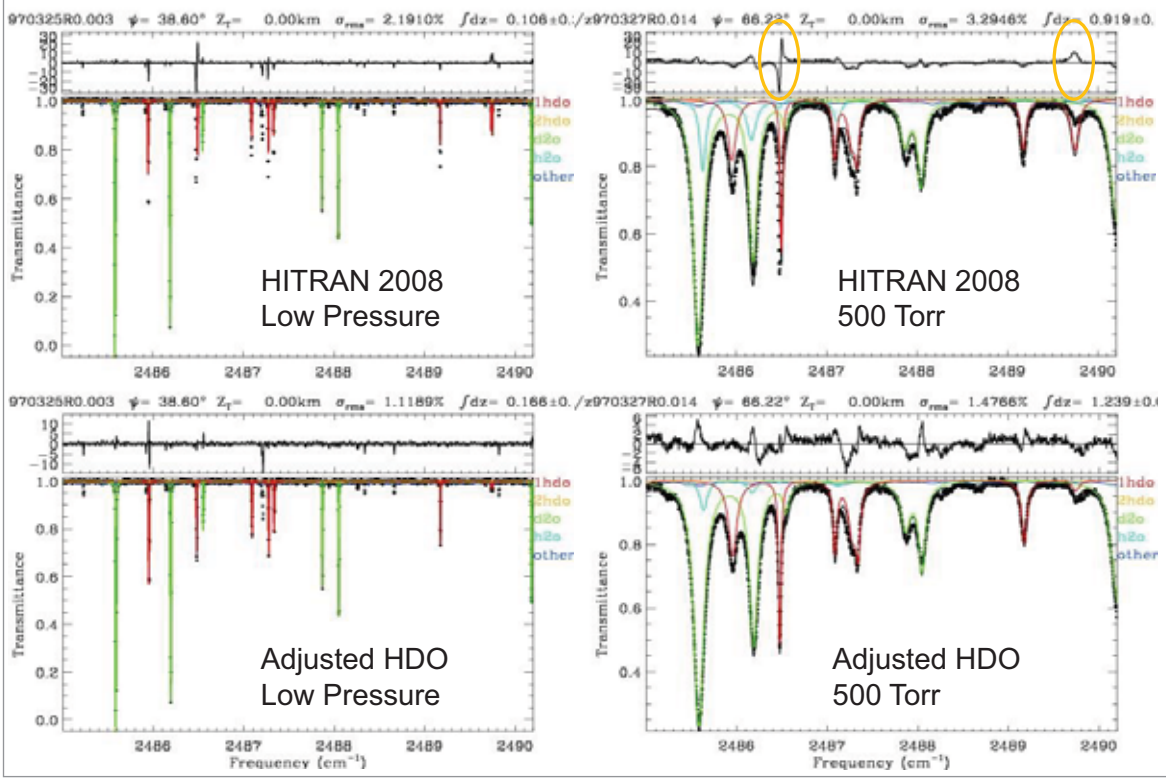

Fits to Kitt Peak Lab Spectra

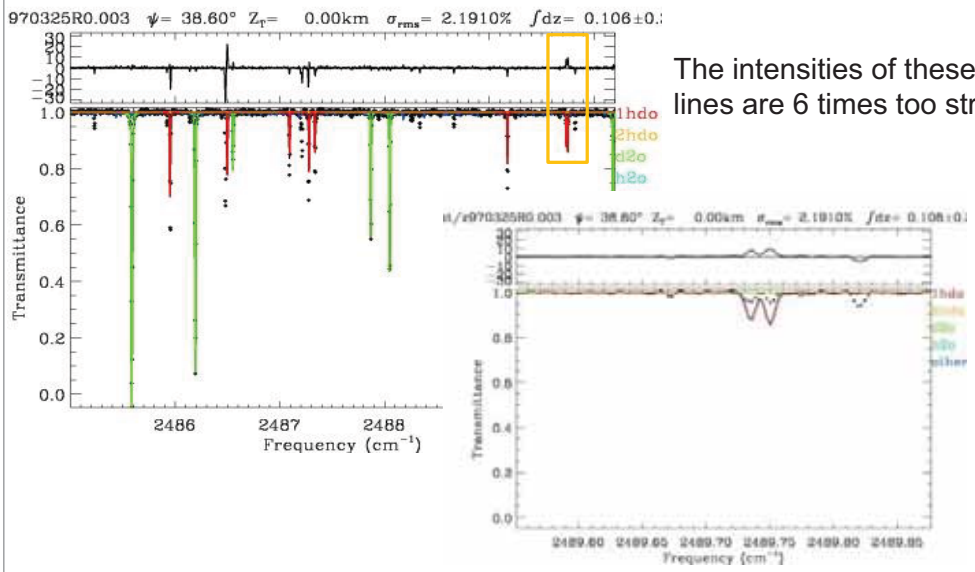

The intensities of these two HDO lines are 6 times too strong.

Why are HDO lines have such large errors when these lab spectra have been available for over 15 years?

This suggests the linelist was never totally checked against lab spectra.

After Fixing HDO lines in this region

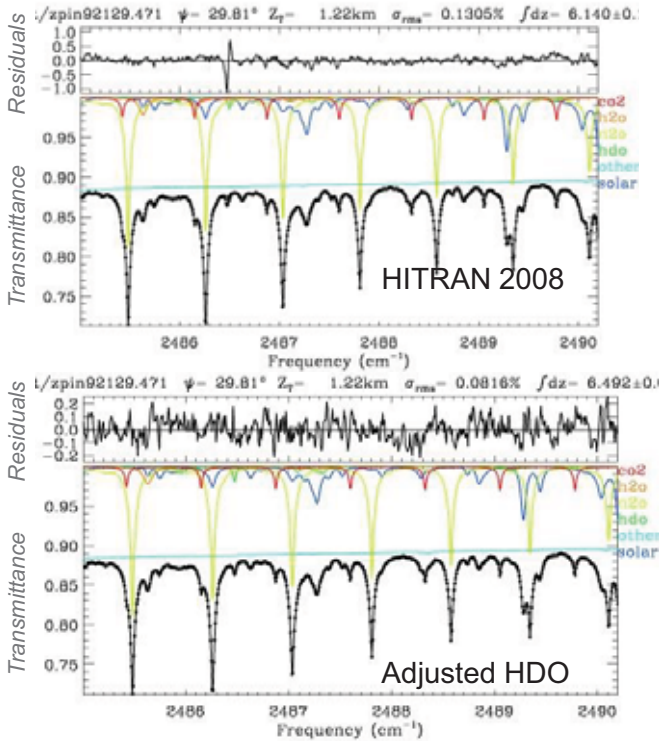

Spectral fit using HITRAN 2008 linelist (shown previously)

After empirically adjusting HDO lines based on fits to Kitt Peak laboratory spectra.

Retrieved CO_2 increases by > 5%
Retrieved N2O changes by > 2%

Use of HITRAN 2008 linelist would cause a large HDO-dependent bias in the retrieved CO_2 and N_2O

Spectrometry versus Spectroscopy

Spectrometry

Spectroscopy **users** (like me) want to achieve good fits to their spectra in order to accurately retrieve the atmospheric composition. I call this **spectrometry.**

I don't care whether this is achieved by empirical cross-section measurements or theoretical linelists, as long as it does a good job.

If I see an obvious, easily-correctable error in the HITRAN linelist, I will try to fix it, recognizing that it is very inefficient to have multiple end-users fix the same problem:

- •Duplication of effort
- •Lack of understanding of methods/assumptions

Far better if the linelist generators (spectroscopists) fixes errors at the beginning.

Spectroscopy

Spectroscopists seem more interested in understanding why the spectrum of a particular gas looks the way it does.

Understanding the fundamental quantum-mechanical basis of molecular spectra is very important, and in the long term will yield better linelists.

Empirical vs Theoretical Approaches

Most spectroscopists seem to favor theoretical approaches to generating linelists

Very few spectroscopists enjoy making high quality (artifact-free) cross-section measurements at dozens of different T/P conditions (very difficult and boring)

Theoretical Approach involves computing the spectroscopic parameters

- • Provides quantum numbers, hence E"
- • Resulting linelist is complete (for the band being analyzed)
- • May be inaccurate for complex molecules

Empirical Approach involves measuring parameters using laboratory spectra has several weaknesses:

- • cannot assign lines, so lab measurement must cover full range of T & P
- • unresolved overlapping lines
- • interfering absorbers, esp H_2O
- • instrumental artifacts (ILS, channel fringes, zero offsets)
- • requires multiple spectra at each P/T to cover large dynamic range

Ideally, a combination of theoretical and empirical methods would be best.

Fit to MkIV Balloon spectrum

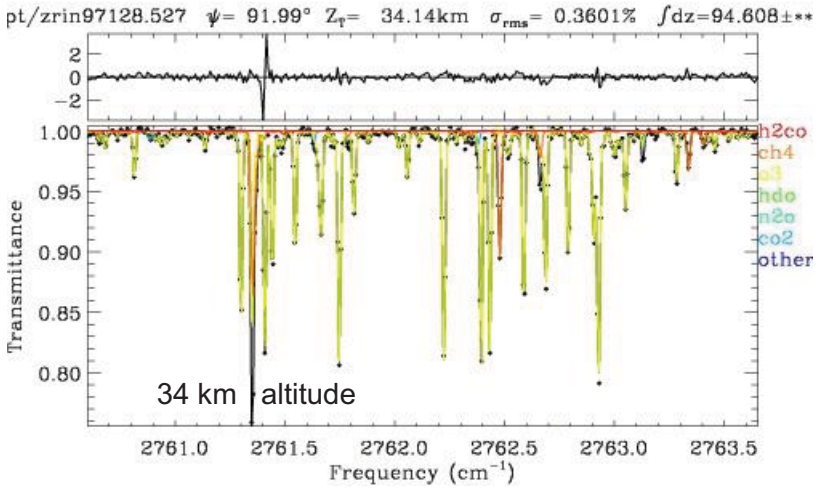

Window used to measure formaldehyde (H_2CO) contains lots of O_3 lines, one of which is in the wrong position, causing large residual.

In least squares fitting, the largest residuals have a disproportionate impact on the retrievals.

Fits to Kitt Peak Lab spectra

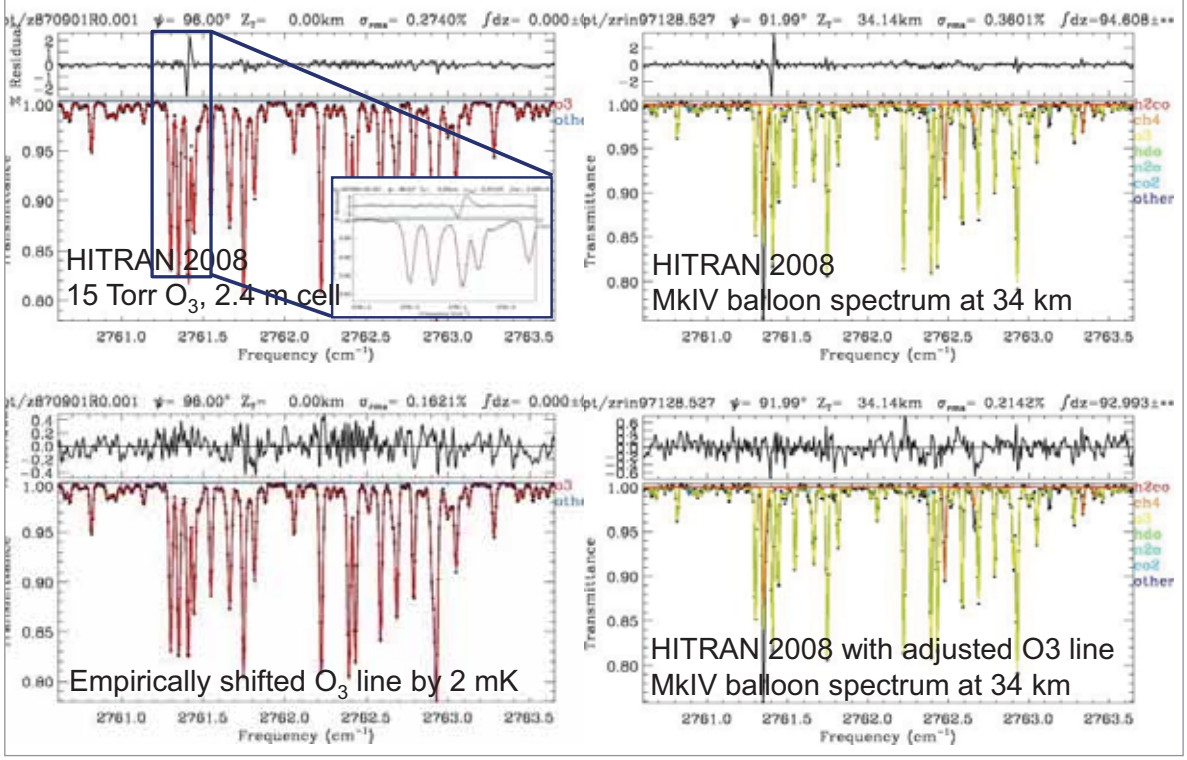

O_3 Laboratory Spectra

The Kitt Peak O_3 spectral fitting residuals are remarkably similar to those in the 34 km MkIV balloon spectrum.

After empirically correcting the position of the wayward O_3 line at 2761.4 cm^{-1}, the Kitt Peak and the MkIV balloon fitting residuals improve by nearly a factor 2.

Although this makes only a 1.5% change to the retrieved H_2CO at 36 km, at lower altitude it is larger (>5%).

The improved fitting residuals reduce the error bars on the retrieved atmospheric profile of H_2CO by nearly a factor 2 at 36 km.

Q: How can one O_3 line position be so poor, when all the others are so good?

A: Resonances have perturbed its energy level

These are dozens of misplaced O_3 lines like this in HITRAN_2008. It is unlikely in the near future, that the theoretical methods used to generate the linelists will be able to capture the resonances.

Therefore empirical corrections will continue to be needed.

Summary (1/2)

To do useful atmospheric science, the measurement accuracy requirements are becoming more stringent. For long-lived atmospheric gases (e.g. CO_2, N_2O, CH_4) the accuracy requirements are now 0.2-0.4%.
But this doesn't mean that all spectroscopic parameters need to be this good.

NDACC bases its calibration directly on the HITRAN spectroscopy.
Width errors are particularly important for profile retrieval.

TCCON attempts to escape some of the spectroscopic limitations by using a complicated calibration methodology:

This allows useful atmospheric measurements to be made with less dependence on the absolute accuracy of the spectroscopy.

But the TCCON calibration process is not "free":

- results become sensitive to O_2 spectroscopic problems
- unable to measure true diurnal variations that are symmetrical about noon
- need co-located in situ profiles measured into stratosphere on sunny days

Summary (2/2)

Good consistency and completeness of the spectroscopy is important, from line to line and from band to band, over a range of airmasses.

Solar occultation measurements (e.g. ACE, MkIV) also require good weak/strong consistency due to the large dynamic range of absorber slant columns.

It is fairly easy to find out where these problems/inconsistencies are by fitting atmospheric solar spectra and laboratory data using the HITRAN linelist.

Problems (residuals) seen in atmospheric solar spectra are also seen in lab spectra.

The problem is how to fix these problems/inconsistencies:
- empirical adjustment (short-term solution)
- request a better theoretical linelist (long-term)

Might have to keep re-doing empirical adjustments every 4 years.

Realistic uncertainties on the theoretical line parameters would facilitate a more automated approach to empirical correction (perturbed lines → large uncertainties)

Need to get linelists validated (and adjustments made) **before** release:
1. Fit existing laboratory spectra
2. Fit atmospheric spectra measured under well-known conditions

Specific Spectroscopy Requests

Parameterizations (pseudo-lines) for gases for which lab data (cross sections) exist, but are too complicated for a theoretical prediction (e.g., C_2H_6, C_3H_8)

More consistent spectroscopy for CH_4, H_2O, HDO over the whole 3 micron region, especially the five windows used by NDACC for CH_4 retrievals.

MW1: 2613.70–2615.40 cm^{-1}
MW2: 2650.60–2651.30 cm^{-1}
MW3: 2835.50–2835.80 cm^{-1}
MW4: 2903.60–2904.03 cm^{-1}
MW5: 2921.00–2921.60 cm^{-1}

Better spectroscopic data for the new HFCs and HCFCs that are used as substitutes for the banned CFCs (Montreal Protocol)

Better line parameters for CF_4 (around 1285 cm^{-1}), and for CCl_4 (790 cm^{-1}).

Consistency between the line parameters in the NIR and the MIR for CO_2, CH_4, CO, N_2O, to make a combined use of NDACC and TCCON data.

Improved consistency between the O_3 line parameters in the 10 um region (NDACC) and in the UV/VIS region (Brewer, DOAS, and many satellite instruments)

HITRAN 2008 contains no $^{13}CH_4$ lines between 3364 and 5898 cm^{-1}

Acknowledgements

NASA Upper Atmosphere Research Program (NDACC, HITRAN)

NASA Carbon Cycle Program (TCCON)

Jim Hannigan, Martine DeMaziere, Ralf Sussmann, Paul Wennberg, Debra Wunch

Spectroscopy community who have contributed to HITRAN

The Importance of Line Shapes

Errors in the line intensities have a very direct and predictable effect on the retrieved column amount (S.X is conserved). Therefore post-analysis corrections are possible. For example, if I'm told that the CO_2 intensities are all to high by 2%, then I can say with certainty that all of my retrieved CO_2 columns are too low by 2%.

Line shape errors (widths, shifts, non-Voigt) are more difficult to deal with.
If I'm told that the widths are all too high by 2%, then the consequences are complex.
•For weakly-absorbing lines, effect on the retrieved columns is probably small (<1%)
•For strongly-absorbing lines the effect will be close to 2%.

The same line may be weak at noon and strong at sunset/rise.

So accurate line shape information is critical, especially for retrievals of tropospheric gases, which have substantial absorber amounts at 1000 mbar.

And since the atmosphere covers 190K to 320K, the temperature-dependence of the line shape is also important.

HCOOH: Ground-based solar spectrum

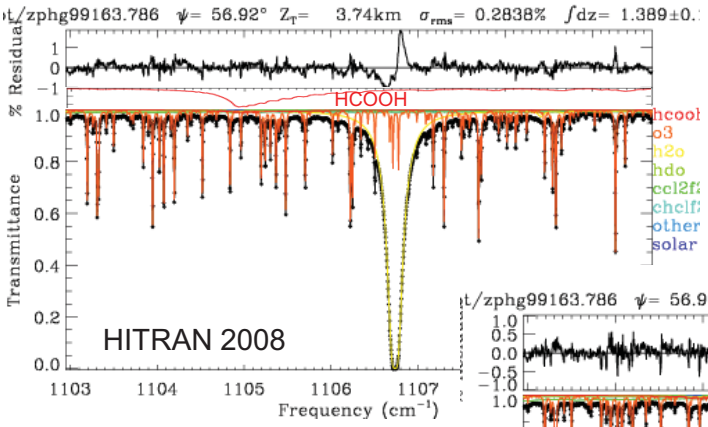

Window used by NDACC for HCOOH retrieval

H_2O line at 1106.7 cm^{-1} produces large residual.

Fixed by changing width and pressure shift

Note Residual scale change

Retrieved HCOOH increases by 40% as a result of H_2O line width shift adjustment

Intensity of H_2O line irrelevant since HCCOH is target gas

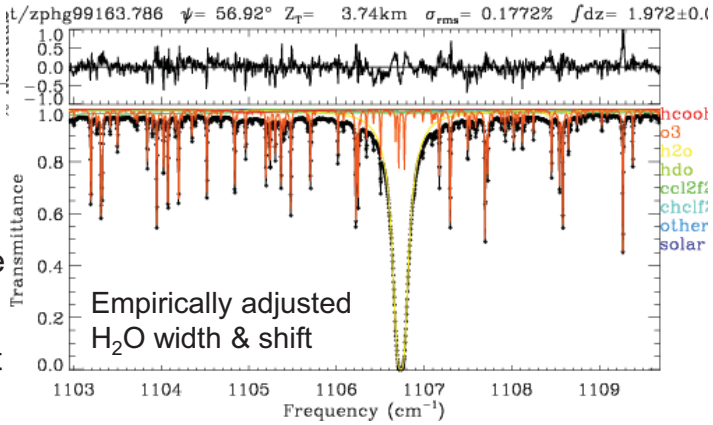

Pseudo-Line-Lists (PLL)

A method of smoothly interpolating/extrapolating in P/T/[illegible] between various laboratory cross-section data. Uses a Voigt lineshape as a basis function.

Useful for molecules for which theoretical calculations are difficult (e.g. C_2H_6, C_3H_8, $ClNO_3$, SF_6, NF_3, N_2O_5, CFCs, HFCs, HCFCs, CH_3COOH).

Contains little spectroscopic insight. Instead is a brute force method (least squares minimization of residuals between lab spectra and simulation)

Interpolates more accurately in P/T than say a polynomial, because it tries to represent the **physics** of partition functions and P-broadening.

So should extrapolate more accurately to conditions outside those encompassed by the original lab data.

Fitting lab spectra during the derivation of the PLL provides opportunity to account for various systematic errors: ILS, contamination, channel fringes, zero-level offsets, etc, and also to identify outlier sspectra and correct /omit them. [An outlier could be caused by an incorrectly tabulated T or P]

Resulting PLL is in HITRAN format – easy to use.

Example: C_2H_6 Pseudo-Line-List

Based on lab cross-section measurements of Harrison and Bernath [2011]

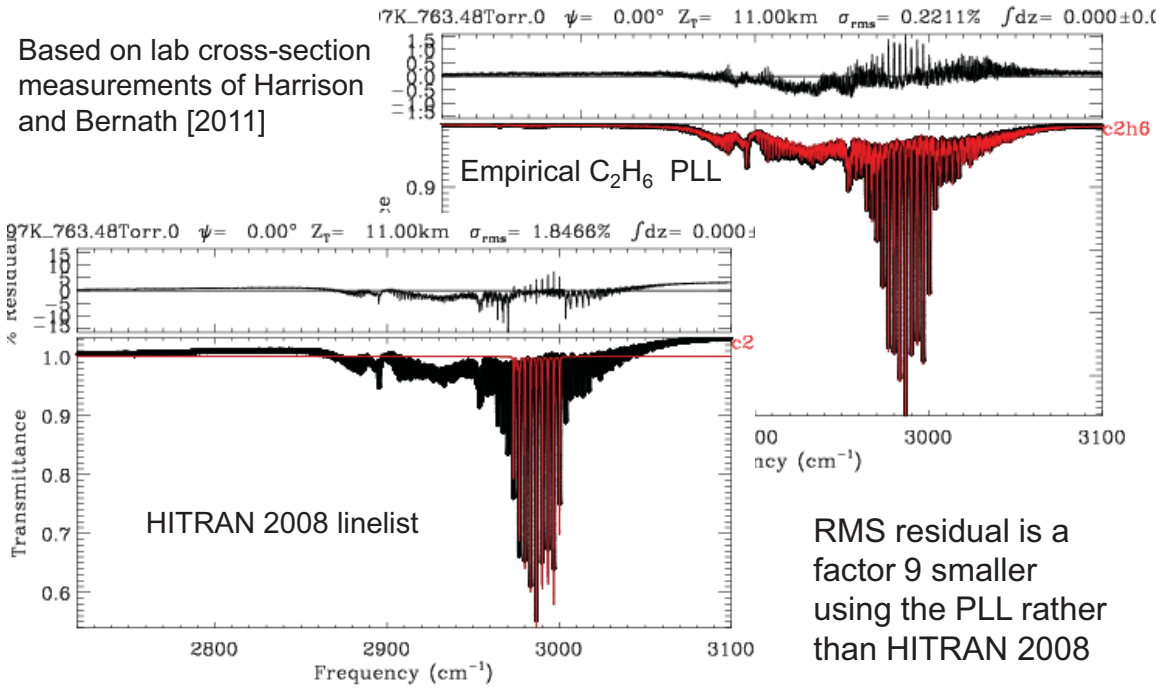

RMS residual is a factor 9 smaller using the PLL rather than HITRAN 2008

"High-resolution remote-sensing of the Earth's atmosphere: Spectroscopic needs and challenges"

Johannes Orphal

Institute for Meteorology and Climate Research,
Karlsruhe Institute of Technology

Prof. Dr. Johannes Orphal

Institut für Meteorologie und Klimaforschung, Karlsruher Institut für Technologie
Hermann-von-Helmholtz-Platz 1, 76344 Eggenstein-Leopoldshafen, Germany
Phone: +49 72160829121
E-mail: orphal@kit.edu

Research

Optical remote-sensing; Atmospheric physics and chemistry; Climate research; High-resolution spectroscopy; Molecular physics; Spectroscopic reference data

Education and Professional Experience

since 2009	Head, Institute for Meteorology and Climate Research (IMK) – Atmospheric Trace Substances and Remote-Sensing (about 75 scientists), KIT, Karlsruhe, Germany
since 2009	Professor of Physics (W3), Karlsruhe Institute of Technology (KIT), Karlsruhe, Germany
2006-2009	Professeur des Universites, Universite Paris-12 (Paris-Est), Creteil, France
2002	Habilitation a Diriger les Recherches, Universite Paris-11 (Paris-Sud), Orsay, France
1999-2005	Charge de Recherche du CNRS, Laboratoire de Photophysique Moleculaire (Orsay), Laboratoire Interuniversitaire des Systemes Atmospheriques, Creteil, France
1995-1999	Research Assistant, Institute of Environmental Physics (IUP) and Institute of Remote-Sensing (IFE), University of Bremen, Germany
1995	Docteur en Sciences (Specialite Lasers et Matieres), avec les felicitations ecrites du jury (president Gerard Megie), Universite Paris-11 (Paris-Sud), Orsay, France
1991-1995	Thesard (PhD student), Laboratoire de Physique Moleculaire et Applications, Universite Paris-11 (Paris-Sud), Orsay, France
1991	Diplom-Physiker (Graduation in Physics), Humboldt-University, Berlin, Germany
1986-1991	Physik-Studium, Humboldt-University, Berlin, Germany
1984-1986	Computer-Operator (with professional certificate), IBM-360 mainframes
1984	Abitur (High School Graduation), Max-Planck-Gymnasium, Berlin, Germany

Activities, Honors and Awards

- Best Experimental Physics Lecture Award, Physics Department, KIT, Karlsruhe, 2012
- Honorary Editor (invited), Science-SoftCon UV/Vis+ Spectra Data Base, 7th edition, Maintal, Germany, 2010
- Invited Senior Fellowship (EU "Transfer of Knowledge" (ToK), University College Cork (UCC), Irland, 2005-2008
- Prix de la Valorisation de la Recherche (Prix du Conseil General de l'Essonne), Universite Paris-11 (Paris-Sud), Orsay, 2004
- The Journal of Molecular Spectroscopy Special Review Lecture, The Ohio State University, Columbus, OH, USA, 2003
- Emmy-Noether Grant of the German Research Foundation (DFG), 1999
- Marie-Curie HCM Fellowship, Commission of the European Community (CEC), 1992-1994
- MICECO (Mission Interministerielle pour la Cooperation en Europe Centrale et Orientale) Grant, awarded by the French Embassy in Berlin, Germany, 1991-1992

High-resolution remote-sensing of the Earth's atmosphere: Spectroscopic needs and challenges

Johannes Orphal

Institute for Meteorology and Climate Research, Karlsruhe Institute of Technology

Remote-sensing of the Earth's atmosphere using spectroscopic techniques provides essential and unique data on variability and trends of important atmospheric constituents related to climate, stratospheric chemistry and tropospheric air pollution, in particular concerning the vertical dimension. In this talk, I will briefly give an overview of existing and future atmospheric sensors and the current needs and challenges for spectroscopy, in particular in the mid- and near-infrared regions.

Karlsruher Institut für Technologie

Spectroscopy needs: atmospheric measurements

Johannes Orphal

INSTITUT FÜR METEOROLOGIE UND KLIMAFORSCHUNG (IMK)
Atmosphärische Spurenstoffe und Fernerkundung (ASF)

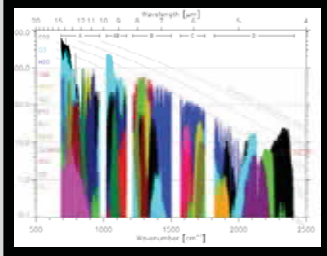

Karlsruher Institut für Technologie

Spectroscopy needs: atmospheric measurements

… with some metaphysical considerations

Johannes Orphal

INSTITUT FÜR METEOROLOGIE UND KLIMAFORSCHUNG (IMK)
Atmosphärische Spurenstoffe und Fernerkundung (ASF)

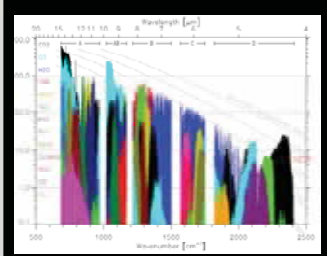

KIT – Universität des Landes Baden-Württemberg und
nationales Forschungszentrum in der Helmholtz-Gemeinschaft

www.kit.edu

High-resolution spectroscopy (Paris-Créteil)

2003 JMS Review Lecture (OSU)

Line positions are measured to 10^{-9} (and better)

Nearly 200 years of technology development:

- the prism spectrometer
- the grating spectrometer (still today)
- interferometers (very high resolution)
- lasers and improvements

2003 JMS Review Lecture (OSU)

Line positions are measured to 10^{-9} (and better)

Nearly 200 years of technology development:

- the prism spectrometer
- the grating spectrometer (still today)
- interferometers (very high resolution)
- lasers and improvements

Line intensities: Count molecules using pressure?

There must be better techniques („oscilloscope“):

- based on the physics (e.g. Rabi oscillations)
- goal: line intensities with <0.01% accuracy
- many new applications will be possible

5 Prof. Dr. Johannes Orphal Institut für Meteorologie und Klimaforschung (IMK)

High-resolution spectroscopy (Paris-Créteil)

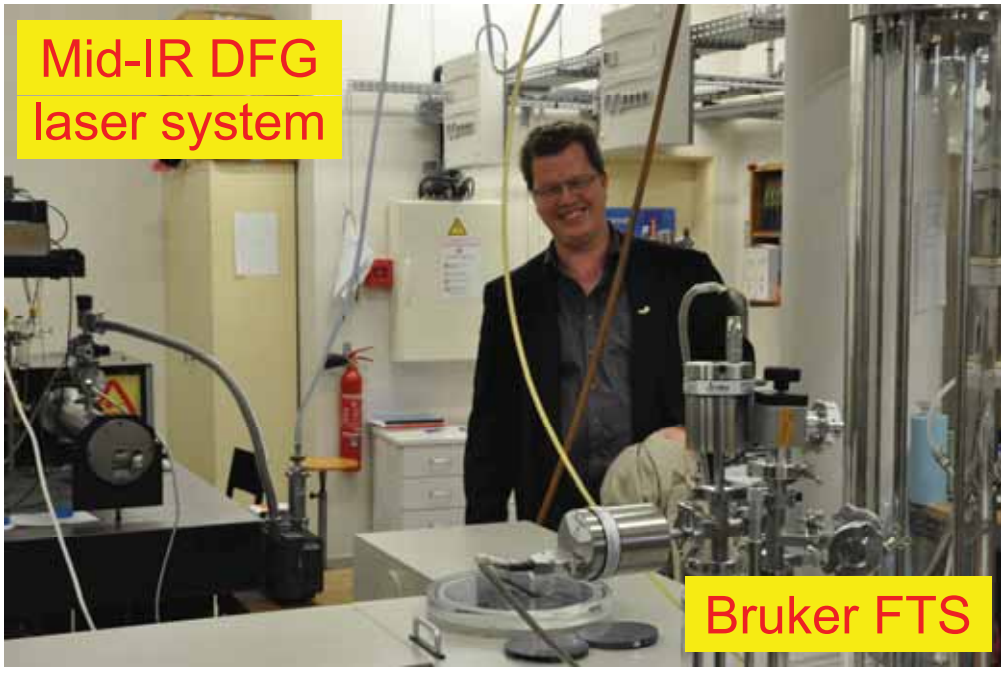

6 09.01.2013 Prof. Dr. Johannes Orphal Institut für Meteorologie und Klimaforschung (IMK)

High-resolution spectroscopy

N_2O, low p, ca. 60 s

obs-clc ×100

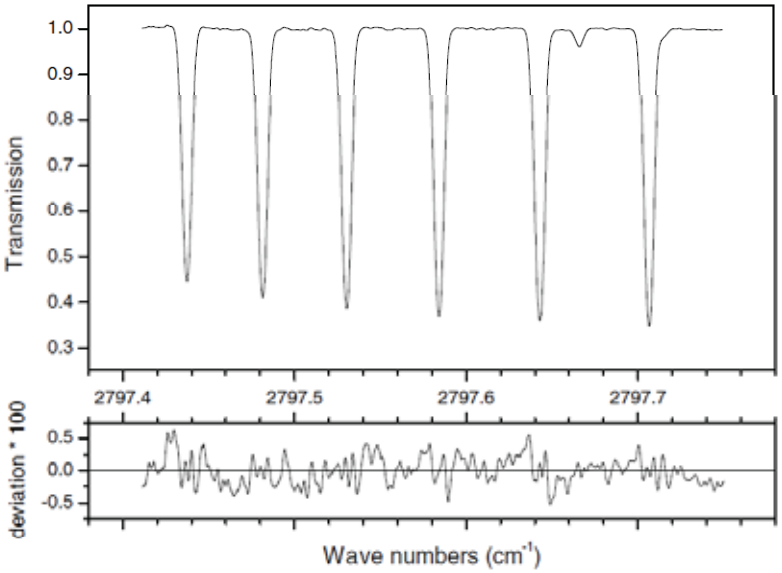

P.-M. Flaud and J. Orphal, „A continuous-wave difference-frequency generation laser operating in the mid-infrared (3-5 microns) region for accurate line intensity measurements", *Infrared Physics & Technology* 51, 322-331, 2008.

HNO_3 laboratory spectroscopy:

A. Perrin, J.-M. Flaud, C. Camy-Peyret, V. Jaouen, R. Farrenq, G. Guelachvili, Q. Kou, F. Le Roy, M. Morillon-Chapey, J. Orphal, M. Badaoui, J.-Y. Mandin, and V. Dana, „Line intensities in the 11 μm and 7.6 μm bands of HNO_3", *Journal of Molecular Spectroscopy* 160, 524-539, 1993.

J.-M. Flaud, A. Perrin, J. Orphal, Q. Kou, P.-M. Flaud, C. Piccolo, and B. Carli, „New analysis of the v_5+v_9-v_9 hot band of HNO_3", *Journal of Quantitative Spectroscopy and Radiative Transfer* 77, 355-364, 2003.

A. Perrin, J. Orphal, J.-M. Flaud, S. Klee, G. Mellau, H. Mäder, D. Walbrodt, and M. Winnewisser, „New analysis of the v_5 and $2v_9$ bands of HNO_3 by infrared and millimetre-wave techniques: line positions and intensities", *Journal of Molecular Spectroscopy* 228, 375-391, 2004.

L. Gomez-Martin, H. Tran, A. Perrin, R. R. Gamache, A. Laraia, J. Orphal, P. Chelin, C. E. Fellows, and J.-M. Hartmann, „Some improvements of the HNO_3 spectroscopic parameters in the spectral region from 600 to 950 cm^{-1}", *Journal of Quantitative Spectroscopy and Radiative Transfer* 110, 675-686, 2009.

HNO_3 laboratory spectroscopy:

A. Perrin, J.-M. Flaud, C. Camy-Peyret, V. Jaouen, R. Farrenq, G. Guelachvili, Q. Kou, F. Le Roy, M. Morillon-Chapey, J. Orphal, M. Badaoui, J.-Y. Mandin, and V. Dana, „Line intensities in the 11 μm and 7.6 μm bands of HNO_3“, *Journal of Molecular Spectroscopy* 160, 524-539, 1993.

J.-M. Flaud, A. Perrin, J. Orphal, Q. Kou, P.-M. Flaud, C. Piccolo, and B. Carli, „**New analysis** of the $v_5+v_9-v_9$ hot band of HNO_3“, *Journal of Quantitative Spectroscopy and Radiative Transfer* 77, 355-364, 2003.

A. Perrin, J. Orphal, J.-M. Flaud, S. Klee, G. Mellau, H. Mäder, D. Walbrodt, and M. Winnewisser, „New analysis of the v_5 and $2v_9$ bands of HNO_3 by infrared and millimetre-wave techniques: line positions and intensities”, *Journal of Molecular Spectroscopy* 228, 375-391, 2004.

L. Gomez-Martin, H. Tran, A. Perrin, R. R. Gamache, A. Laraia, J. Orphal, P. Chelin, C. E. Fellows, and J.-M. Hartmann, „Some improvements of the HNO_3 spectroscopic parameters in the spectral region from 600 to 950 cm^{-1}”, *Journal of Quantitative Spectroscopy and Radiative Transfer* 110, 675-686, 2009.

HNO_3 laboratory spectroscopy:

A. Perrin, J.-M. Flaud, C. Camy-Peyret, V. Jaouen, R. Farrenq, G. Guelachvili, Q. Kou, F. Le Roy, M. Morillon-Chapey, J. Orphal, M. Badaoui, J.-Y. Mandin, and V. Dana, „Line intensities in the 11 μm and 7.6 μm bands of HNO_3“, *Journal of Molecular Spectroscopy* 160, 524-539, 1993.

J.-M. Flaud, A. Perrin, J. Orphal, Q. Kou, P.-M. Flaud, C. Piccolo, and B. Carli, „**New analysis** of the $v_5+v_9-v_9$ hot band of HNO_3“, *Journal of Quantitative Spectroscopy and Radiative Transfer* 77, 355-364, 2003.

A. Perrin, J. Orphal, J.-M. Flaud, S. Klee, G. Mellau, H. Mäder, D. Walbrodt, and M. Winnewisser, „**New analysis** of the v_5 and $2v_9$ bands of HNO_3 by infrared and millimetre-wave techniques: line positions and intensities”, *Journal of Molecular Spectroscopy* 228, 375-391, 2004.

L. Gomez-Martin, H. Tran, A. Perrin, R. R. Gamache, A. Laraia, J. Orphal, P. Chelin, C. E. Fellows, and J.-M. Hartmann, „Some improvements of the HNO_3 spectroscopic parameters in the spectral region from 600 to 950 cm^{-1}”, *Journal of Quantitative Spectroscopy and Radiative Transfer* 110, 675-686, 2009.

HNO_3 laboratory spectroscopy:

A. Perrin, J.-M. Flaud, C. Camy-Peyret, V. Jaouen, R. Farrenq, G. Guelachvili, Q. Kou, F. Le Roy, M. Morillon-Chapey, J. Orphal, M. Badaoui, J.-Y. Mandin, and V. Dana, „Line intensities in the 11 μm and 7.6 μm bands of HNO_3“, *Journal of Molecular Spectroscopy* 160, 524-539, 1993.

J.-M. Flaud, A. Perrin, J. Orphal, Q. Kou, P.-M. Flaud, C. Piccolo, and B. Carli, „**New analysis** of the $v_5+v_9-v_9$ hot band of HNO_3“, *Journal of Quantitative Spectroscopy and Radiative Transfer* 77, 355-364, 2003.

A. Perrin, J. Orphal, J.-M. Flaud, S. Klee, G. Mellau, H. Mäder, D. Walbrodt, and M. Winnewisser, „**New analysis** of the v_5 and $2v_9$ bands of HNO_3 by infrared and millimetre-wave techniques: line positions and intensities”, *Journal of Molecular Spectroscopy* 228, 375-391, 2004.

L. Gomez-Martin, H. Tran, A. Perrin, R. R. Gamache, A. Laraia, J. Orphal, P. Chelin, C. E. Fellows, and J.-M. Hartmann, „**Some improvements** of the HNO_3 spectroscopic parameters in the spectral region from 600 to 950 cm^{-1}”, *Journal of Quantitative Spectroscopy and Radiative Transfer* 110, 675-686, 2009.

11 Prof. Dr. Johannes Orphal Institut für Meteorologie und Klimaforschung (IMK)

HNO_3 laboratory spectroscopy:

A. Perrin, J.-M. Flaud, C. Camy-Peyret, V. Jaouen, R. Farrenq, G. Guelachvili, Q. Kou, F. Le Roy, M. Morillon-Chapey, J. Orphal, M. Badaoui, J.-Y. Mandin, and V. Dana, „Line intensities in the 11 μm and 7.6 μm bands of HNO_3“, *Journal of Molecular Spectroscopy* 160, 524-539, 1993.

J.-M. Flaud, A. Perrin, J. Orphal, Q. Kou, P.-M. Flaud, C. Piccolo, and B. Carli, „**New analysis** of the $v_5+v_9-v_9$ hot band of HNO_3“, *Journal of Quantitative Spectroscopy and Radiative Transfer* 77, 355-364, 2003.

A. Perrin, J. Orphal, J.-M. Flaud, S. Klee, G. Mellau, H. Mäder, D. Walbrodt, and M. Winnewisser, „**New analysis** of the v_5 and $2v_9$ bands of HNO_3 by infrared and millimetre-wave techniques: line positions and intensities”, *Journal of Molecular Spectroscopy* 228, 375-391, 2004.

L. Gomez-Martin, H. Tran, A. Perrin, R. R. Gamache, A. Laraia, J. Orphal, P. Chelin, C. E. Fellows, and J.-M. Hartmann, „**Some improvements** of the HNO_3 spectroscopic parameters in the spectral region from 600 to 950 cm^{-1}”, *Journal of Quantitative Spectroscopy and Radiative Transfer* 110, 675-686, 2009.

Similar efforts for, e.g., HONO, $ClONO_2$, $ClNO_2$, $BrONO_2$, $BrNO_2$, … requirement No. 1 is TIME !

12 Prof. Dr. Johannes Orphal Institut für Meteorologie und Klimaforschung (IMK)

The Earth's atmosphere: not just layers

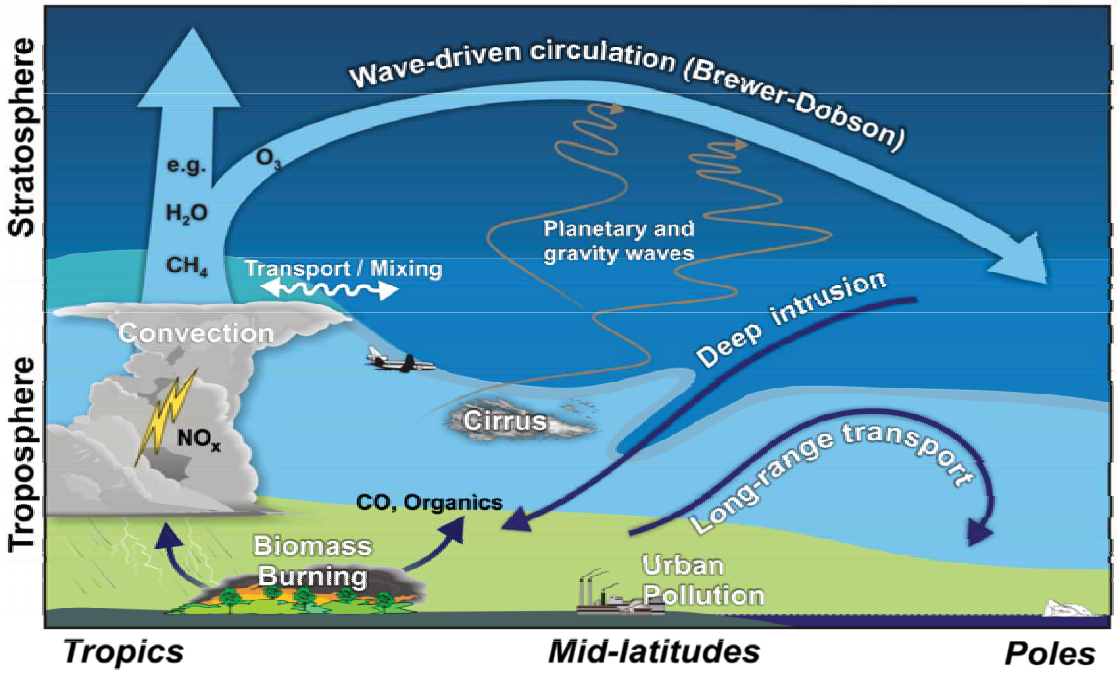

13 09.01.2013 Prof. Dr. Johannes Orphal Institut für Meteorologie und Klimaforschung (IMK)

MIPAS: The Michelson Interferometer for Passive Atmospheric Sounding on Envisat (2002-2012)

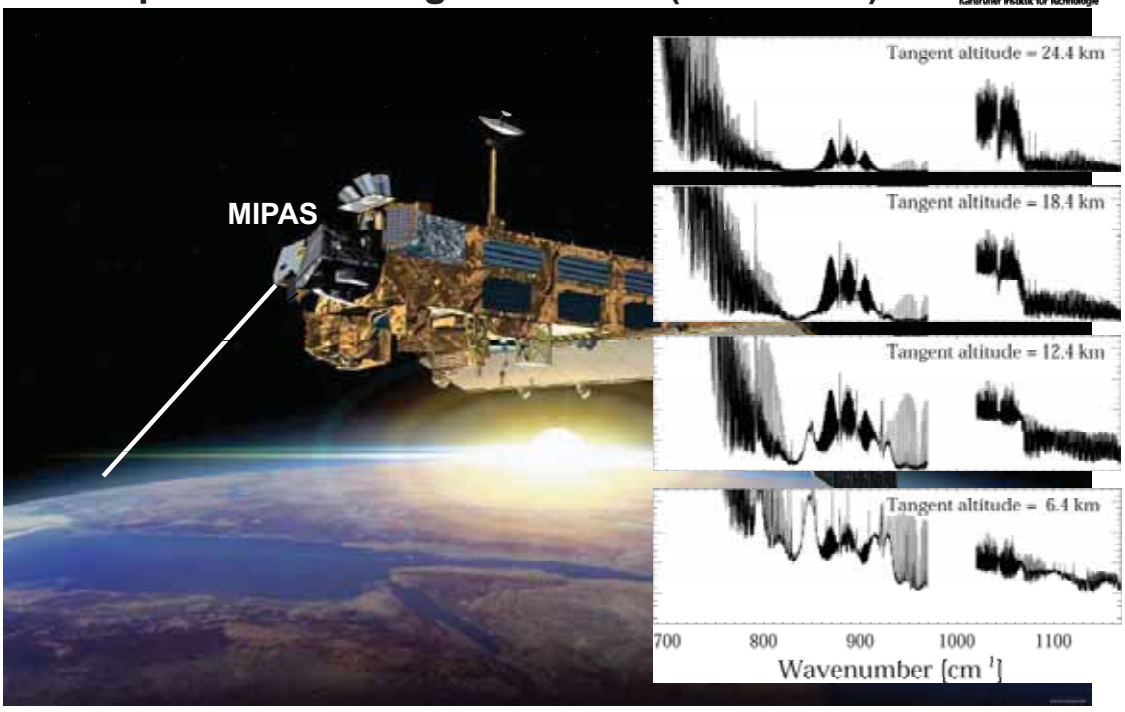

14 09.01.2013 Prof. Dr. Johannes Orphal Institut für Meteorologie und Klimaforschung (IMK)

MIPAS: about 40 atmospheric trace gases

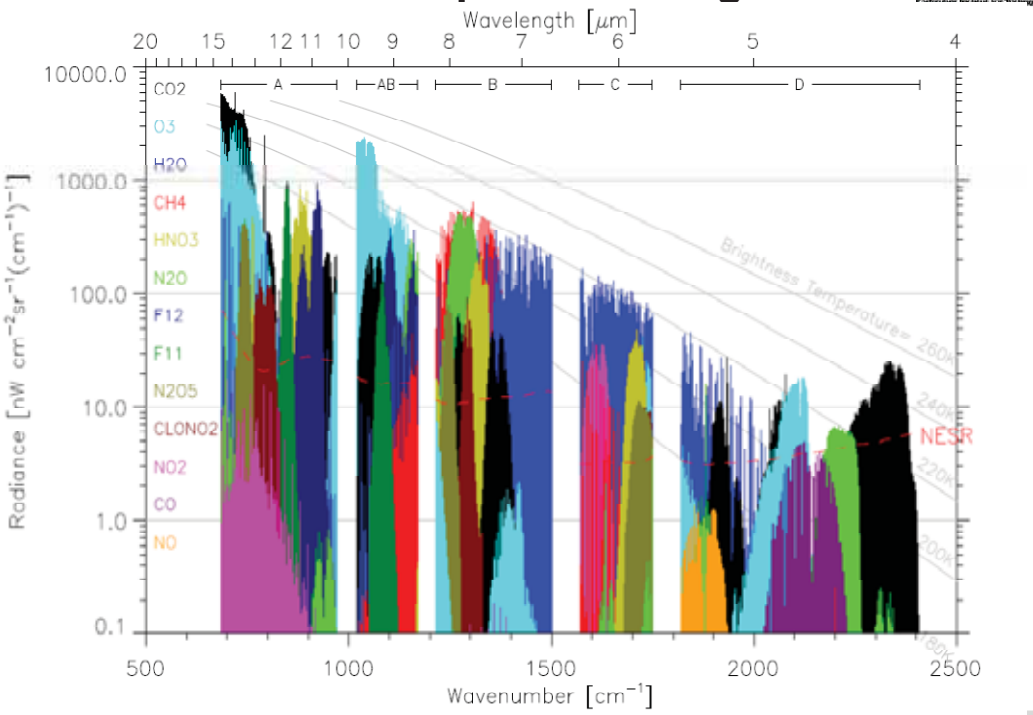

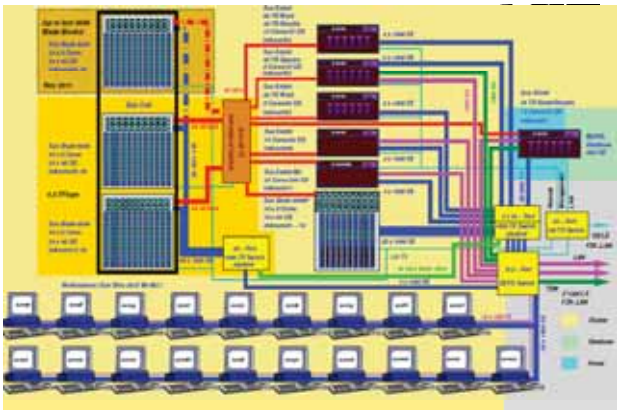

Sun Blade Constellation system

- 384 cores at 2.9 GHz
- 2.3 TB internal memory
- wired over a 72 port 40 Gb/s Infiniband-Switch and 48 1Gb/s Ethernet ports to
- three Sun fileservers (120 TB filespace)

5 Tflops total computing power

Doubled total performance in 2011/2012

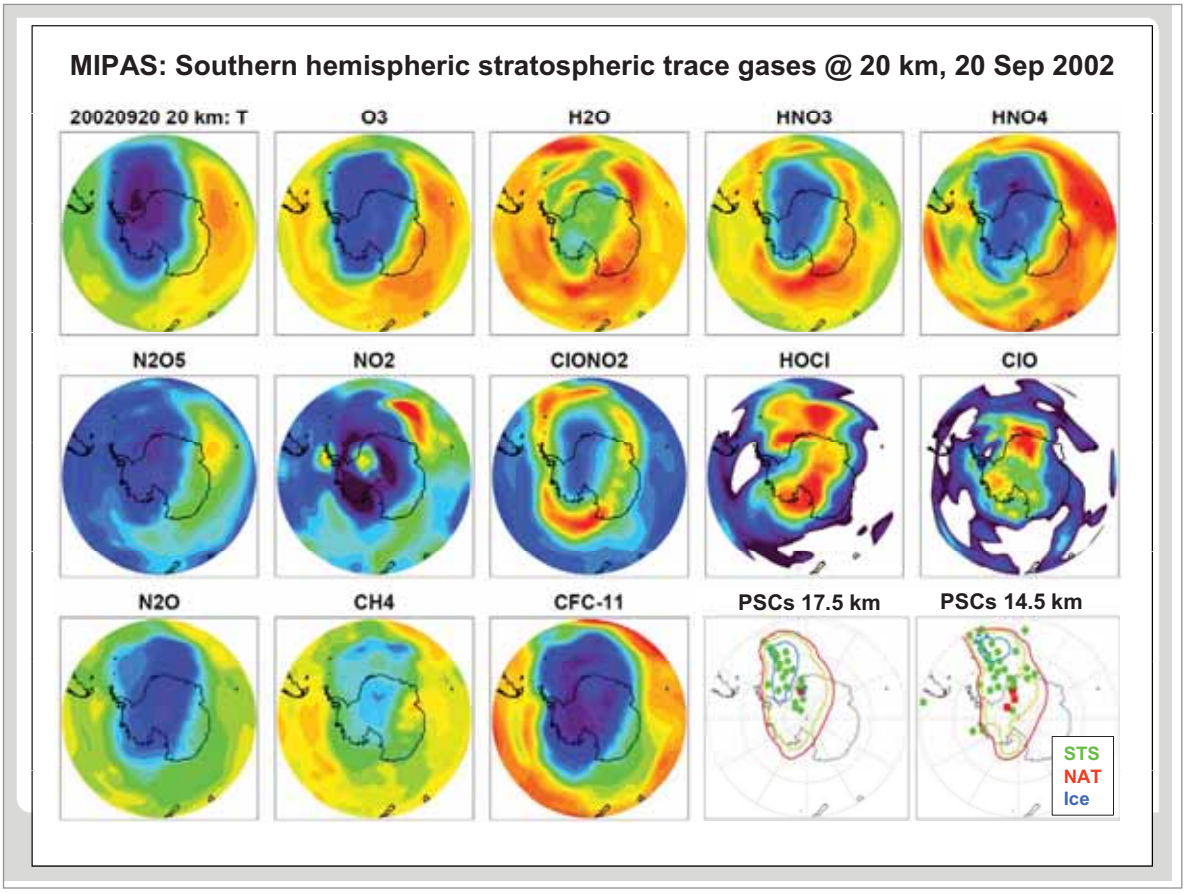
MIPAS: Southern hemispheric stratospheric trace gases @ 20 km, 20 Sep 2002
20020920 20 km: T
O3
H2O
HNO3
HNO4
N2O5
NO2
ClONO2
HOCl
ClO
N2O
CH4
CFC-11
PSCs 17.5 km
PSCs 14.5 km
STS
NAT
Ice

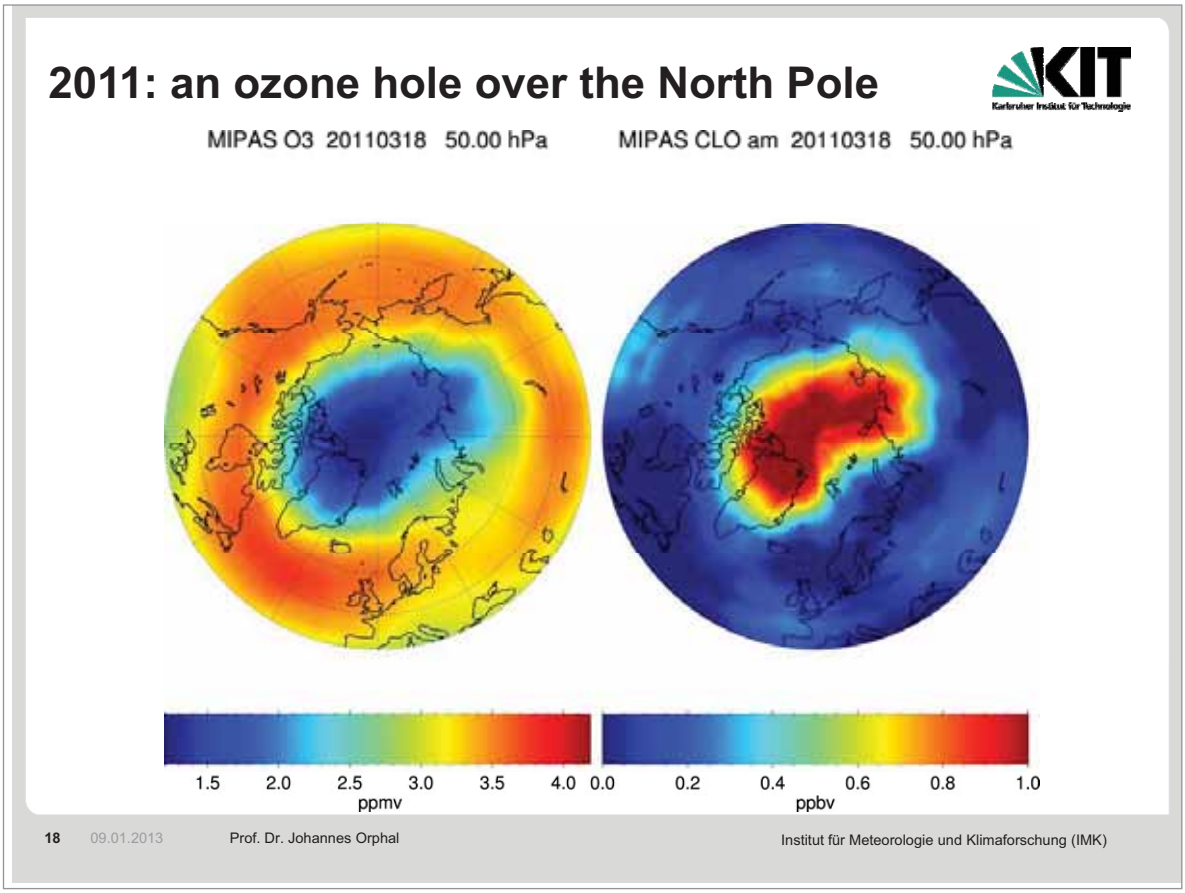
2011: an ozone hole over the North Pole
KIT
Karlsruher Institut für Technologie
MIPAS O3 20110318 50.00 hPa
MIPAS CLO am 20110318 50.00 hPa
1.5 2.0 2.5 3.0 3.5 4.0
ppmv
0.0 0.2 0.4 0.6 0.8 1.0
ppbv
18 09.01.2013 Prof. Dr. Johannes Orphal
Institut für Meteorologie und Klimaforschung (IMK)

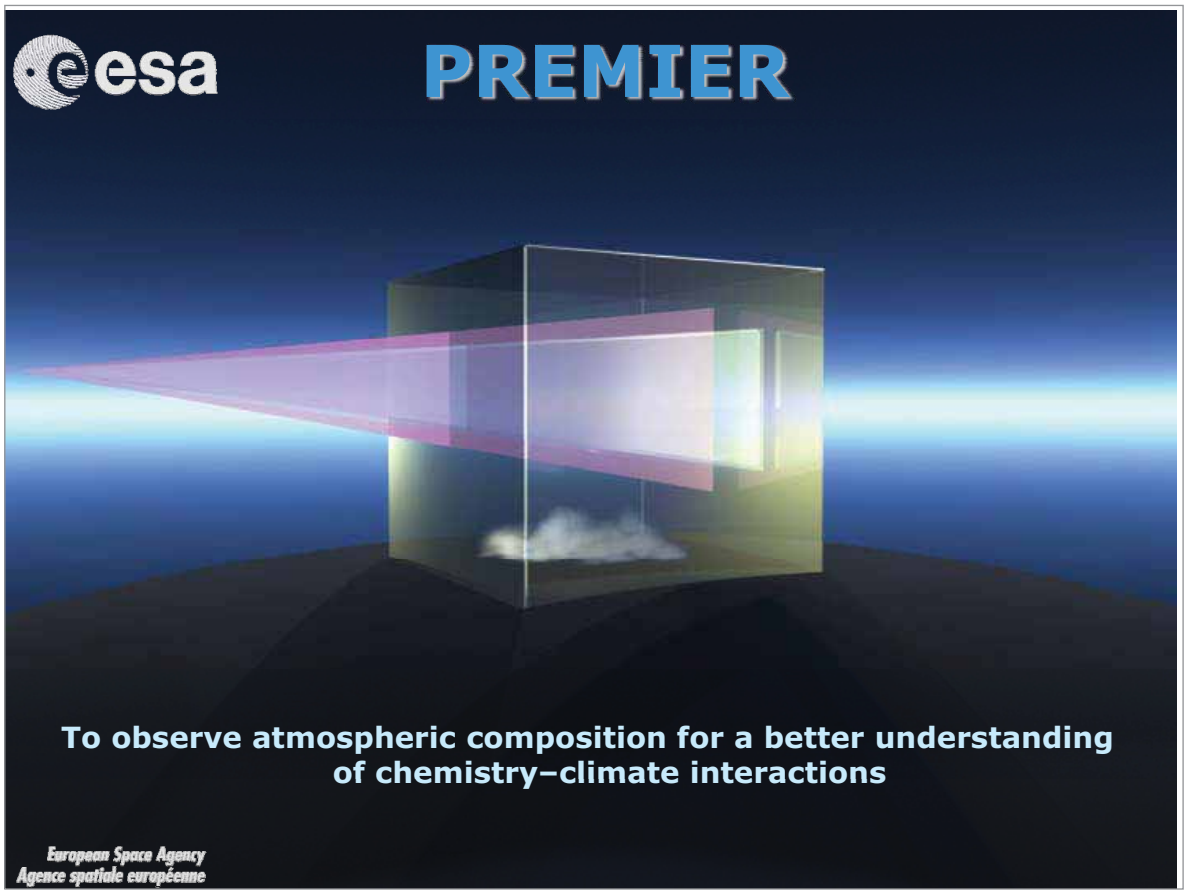
esa
PREMIER
To observe atmospheric composition for a better understanding of chemistry–climate interactions
European Space Agency
Agence spatiale européenne

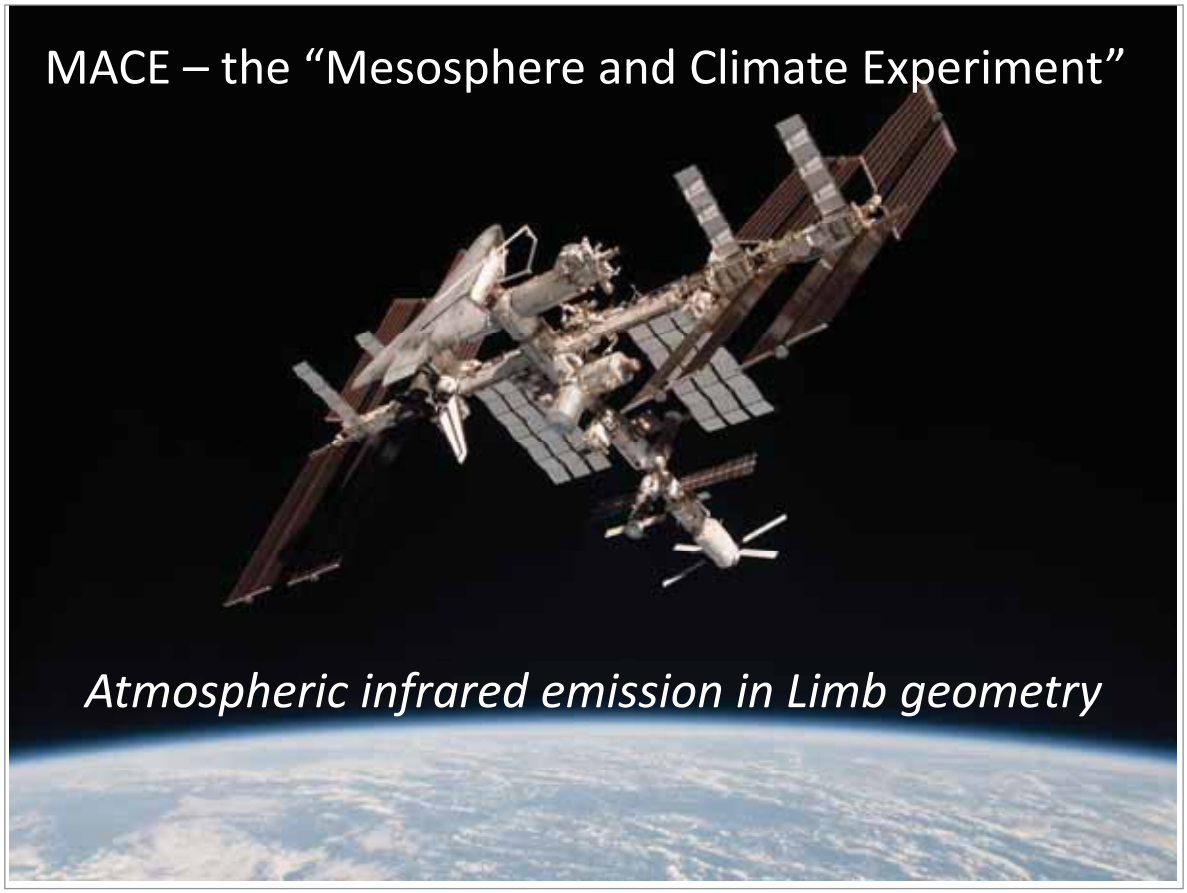
MACE – the “Mesosphere and Climate Experiment”
Atmospheric infrared emission in Limb geometry

Journal of Quantitative Spectroscopy & Radiative Transfer 113 (2012) 1330–1339

Contents lists available at SciVerse ScienceDirect

Journal of Quantitative Spectroscopy & Radiative Transfer

journal homepage: www.elsevier.com/locate/jqsrt

Analysis of averaged broadband residuals between MIPAS-Envisat spectra and line-by-line calculations

J. Plieninger [a,*], T. von Clarmann [a], G.P. Stiller [a], N. Glatthor [a], B. Funke [b], J. Orphal [a]

[a] Institut für Meteorologie und Klimaforschung, Karlsruhe Institute of Technology, Karlsruhe, Germany
[b] Instituto de Astrofísica de Andalucía (CSIC), Gorieta de la Astronomía s/n, 18008 Granada, Spain

ARTICLE INFO

Dedicated to J.-M. Flaud, C. Camy-Peyret and A. Barbe for their contributions to atmospheric spectroscopy and remote sensing
Available online 14 February 2012

Keywords:
Remote sensing
Spectroscopy
MIPAS
Ozone
Nitric acid
Infrared

ABSTRACT

MIPAS-Envisat spectra are compared to broadband spectra calculated with the KOPRA radiative transfer algorithm, using atmospheric temperature and trace gas concentrations which have been derived from small spectral ranges, so called microwindows, of the MIPAS-Envisat spectra. The objective is to detect instrumental problems and inconsistencies in the retrievals as well as in the spectroscopic dataset. The HITRAN 2008 spectroscopic database is used for all calculations. In this paper, we discuss residuals between modelled and measured broadband spectra which are caused by inconsistencies in the HITRAN O_3 and HNO_3 datasets. We conclude that the intensity of the $^{16}O^{16}O^{18}O$ Q-branch around 1090.3 cm^{-1} is too low. HNO_3 spectroscopy has turned out to be largely improved in the HITRAN 2008 version. However, even these spectroscopic data still produce spectral radiances too low at 885.45 and 886.15 cm^{-1}. Generally the calculated spectral radiance in the $\nu_5/2\nu_9$ region is slightly too low.

© 2012 Elsevier Ltd. All rights reserved.

CH_4 lines are visible in averaged residuals

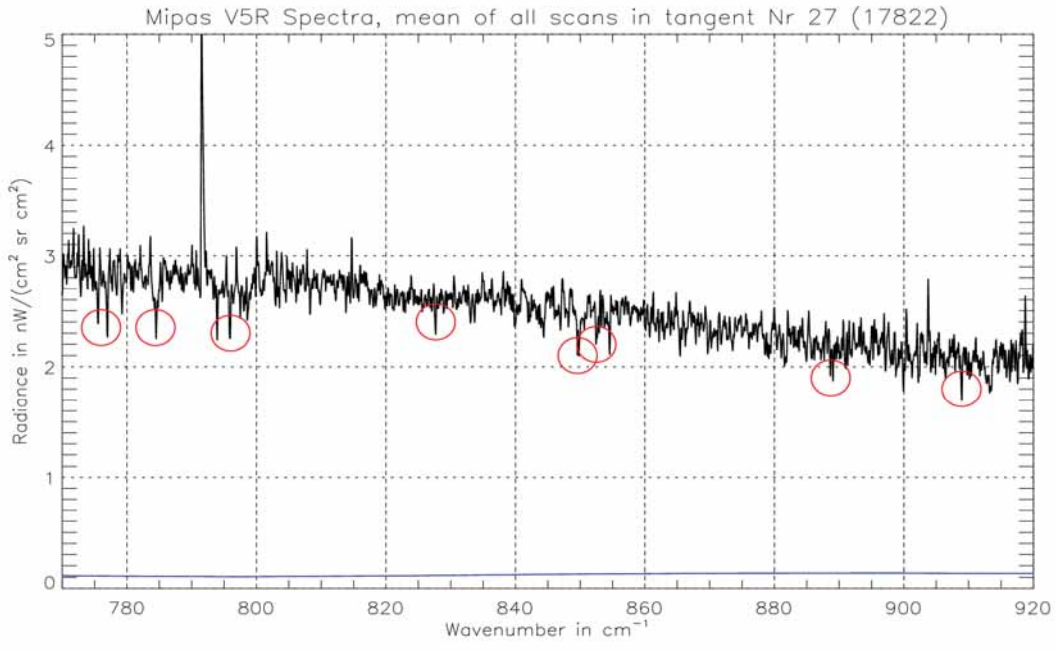

CH_4 lines are visible in averaged residuals

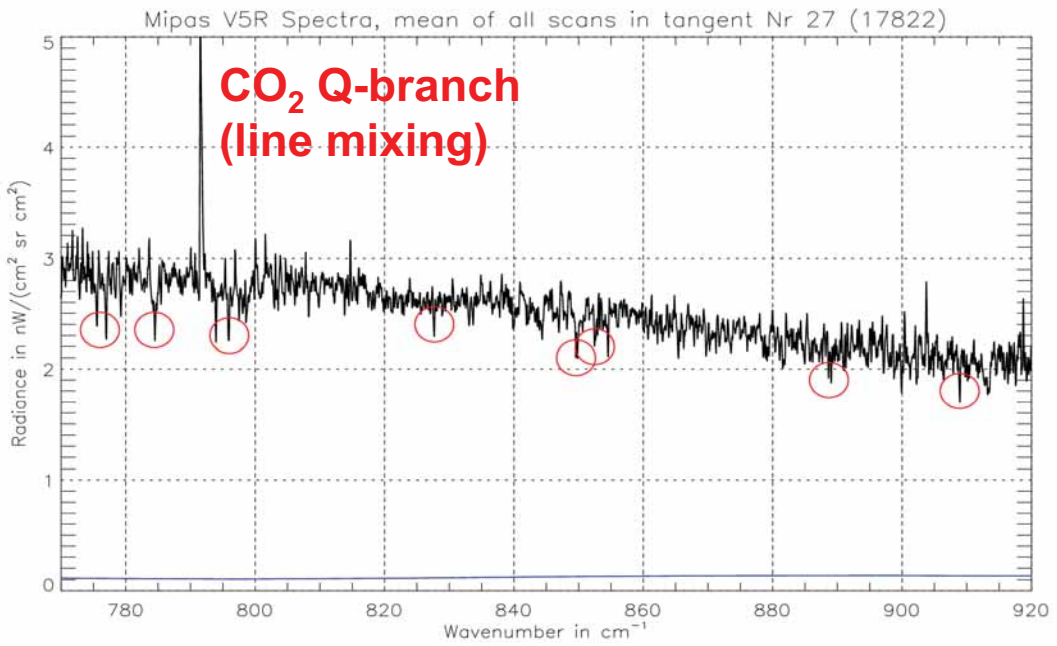

UV-visible absorption cross-sections

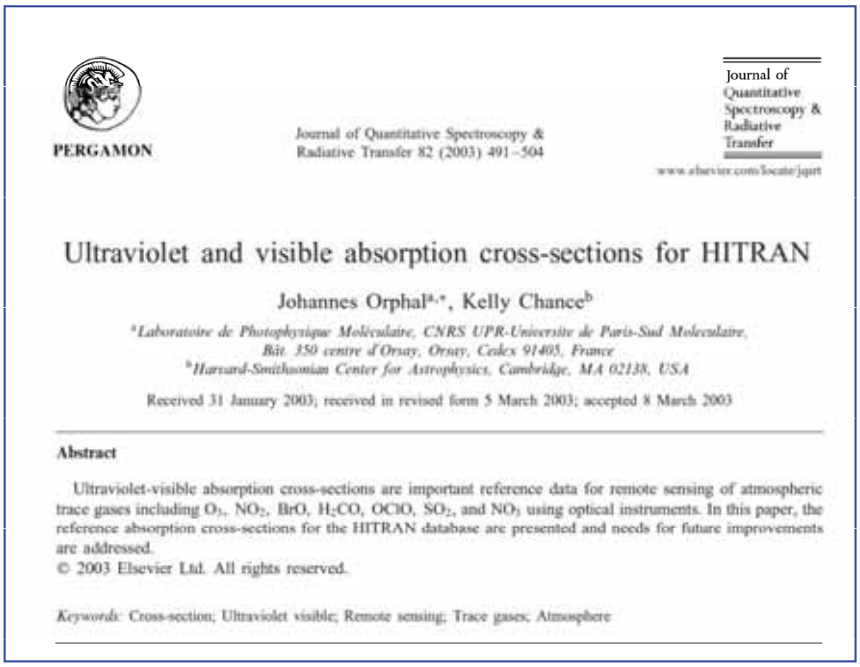

PERGAMON

Journal of Quantitative Spectroscopy & Radiative Transfer 82 (2003) 491–504

Journal of Quantitative Spectroscopy & Radiative Transfer

www.elsevier.com/locate/jqsrt

Ultraviolet and visible absorption cross-sections for HITRAN

Johannes Orphal[a,*], Kelly Chance[b]

[a] *Laboratoire de Photophysique Moléculaire, CNRS UPR-Université de Paris-Sud Moleculaire, Bât. 350 centre d'Orsay, Orsay, Cedex 91405, France*

[b] *Harvard-Smithsonian Center for Astrophysics, Cambridge, MA 02138, USA*

Received 31 January 2003; received in revised form 5 March 2003; accepted 8 March 2003

Abstract

Ultraviolet-visible absorption cross-sections are important reference data for remote sensing of atmospheric trace gases including O_3, NO_2, BrO, H_2CO, OClO, SO_2, and NO_3 using optical instruments. In this paper, the reference absorption cross-sections for the HITRAN database are presented and needs for future improvements are addressed.

© 2003 Elsevier Ltd. All rights reserved.

Keywords: Cross-section; Ultraviolet visible; Remote sensing; Trace gases; Atmosphere

UV-visible absorption cross-sections

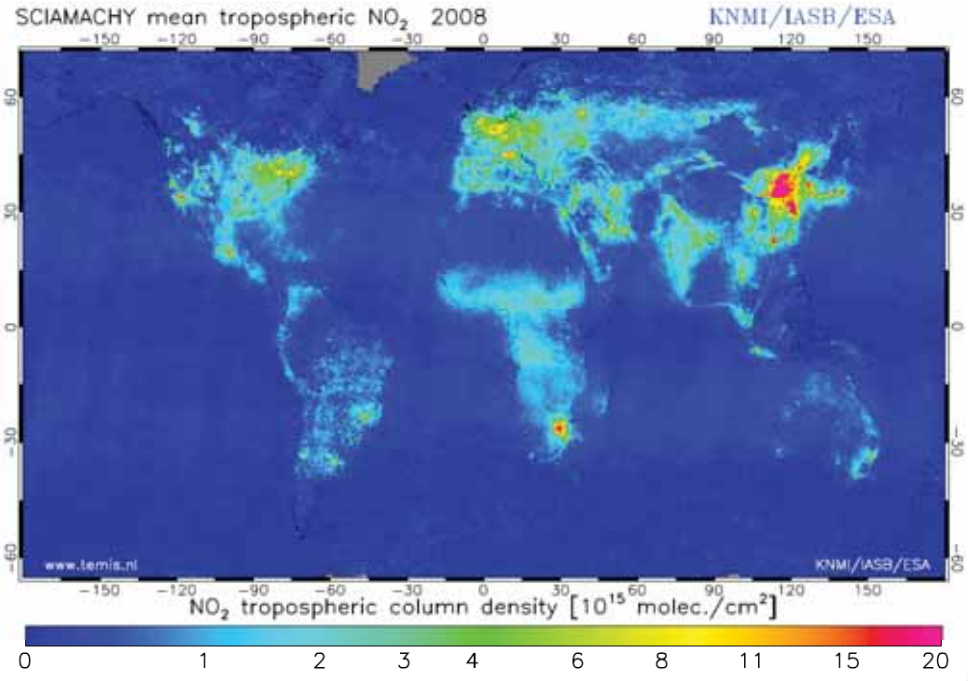

TEMPO: Pollution observed from GEO

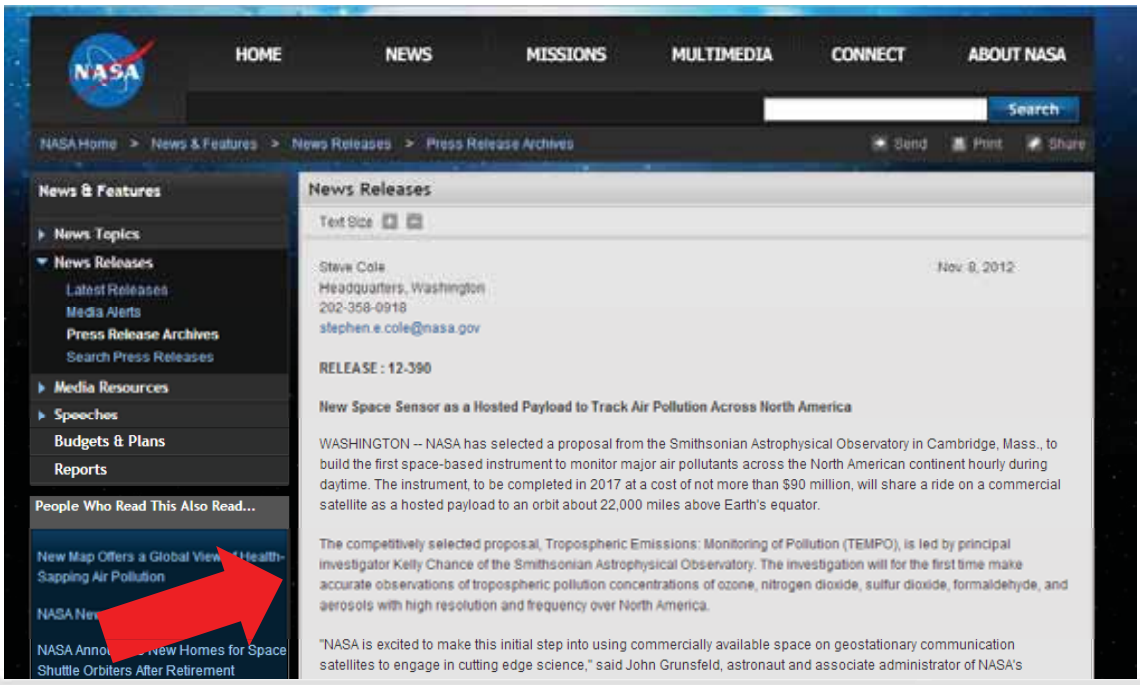

UV-visible absorption cross-sections

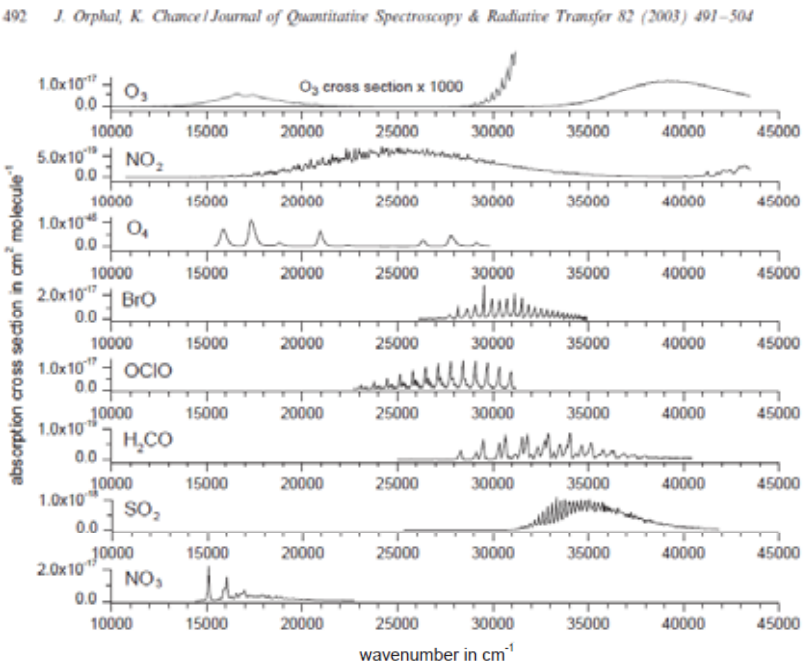

27 Prof. Dr. Johannes Orphal | 26.1.2012

Again laboratory spectroscopy:

J. P. Burrows, A. Dehn, B. Deters, S. Himmelmann, A. Richter, S. Voigt, and J. Orphal, „Atmospheric remote-sensing reference data from GOME: 1. **Temperature-dependent** absorption cross sections of NO_2 in the **231–794 nm range**“, *JQSRT* 60, 1025-1031, 1998.

J. P. Burrows, A. Richter, A. Dehn, B. Deters, S. Himmelmann, S. Voigt, and J. Orphal, „Atmospheric remote-sensing reference data from GOME: 2. **Temperature-dependent** absorption cross sections of O_3 in the **231–794 nm range**“, *JQSRT* 61, 509-517, 1999.

S. Voigt, J. Orphal, K. Bogumil, and J. P. Burrows, „The temperature dependence (203-293 K) of the absorption cross-sections of O_3 in the 230–850 nm region measured by Fourier-transform spectroscopy“, *J. Photochem. Photobiol. A* 143, 1-9, 2001.

S. Voigt, J. Orphal, and J. P. Burrows, „The temperature- and pressure-dependence of the absorption cross-sections of NO_2 in the 250–800 nm region measured by Fourier-transform spectroscopy“, *J. Photochem. Photobiol. A* 149, 1-7, 2002.

Again laboratory spectroscopy:

J. P. Burrows, A. Dehn, B. Deters, S. Himmelmann, A. Richter, S. Voigt, and J. Orphal, „Atmospheric remote-sensing reference data from GOME: 1. **Temperature-dependent** absorption cross sections of NO_2 in the **231–794 nm range**“, *JQSRT* 60, 1025-1031, 1998.

J. P. Burrows, A. Richter, A. Dehn, B. Deters, S. Himmelmann, S. Voigt, and J. Orphal, „Atmospheric remote-sensing reference data from GOME: 2. **Temperature-dependent** absorption cross sections of O_3 in the **231–794 nm range**“, *JQSRT* 61, 509-517, 1999.

S. Voigt, J. Orphal, K. Bogumil, and J. P. Burrows, „The temperature dependence (203-293 K) of the absorption cross-sections of O_3 in the 230–850 nm region measured **by Fourier-transform spectroscopy**“, *J. Photochem. Photobiol. A* 143, 1-9, 2001.

S. Voigt, J. Orphal, and J. P. Burrows, „The temperature- and pressure-dependence of the absorption cross-sections of NO_2 in the 250–800 nm region measured **by Fourier-transform spectroscopy**“, *J. Photochem. Photobiol. A* 149, 1-7, 2002.

Again laboratory spectroscopy:

J. P. Burrows, A. Dehn, B. Deters, S. Himmelmann, A. Richter, S. Voigt, and J. Orphal, „Atmospheric remote-sensing reference data from GOME: 1. **Temperature-dependent** absorption cross sections of NO_2 in the **231–794 nm range**“, *JQSRT* 60, 1025-1031, 1998.

J. P. Burrows, A. Richter, A. Dehn, B. Deters, S. Himmelmann, S. Voigt, and J. Orphal, „Atmospheric remote-sensing reference data from GOME: 2. **Temperature-dependent** absorption cross sections of O_3 in the **231–794 nm range**“, *JQSRT* 61, 509-517, 1999.

S. Voigt, J. Orphal, K. Bogumil, and J. P. Burrows, „The temperature dependence (203-293 K) of the absorption cross-sections of O_3 in the 230–850 nm region measured **by Fourier-transform spectroscopy**“, *J. Photochem. Photobiol. A* 143, 1-9, 2001.

S. Voigt, J. Orphal, and J. P. Burrows, „The temperature- and pressure-dependence of the absorption cross-sections of NO_2 in the 250–800 nm region measured **by Fourier-transform spectroscopy**“, *J. Photochem. Photobiol. A* 149, 1-7, 2002.

Similar efforts for, e.g., OClO, BrO, OBrO, IO, OIO, NO_3, HONO, H_2CO … all this takes TIME !

UV-visible absorption cross-sections

Available online at www.sciencedirect.com
SCIENCE DIRECT®
ELSEVIER
Journal of Photochemistry and Photobiology A: Chemistry 157 (2003) 185–209
Journal of Photochemistry and Photobiology A: Chemistry
www.elsevier.com/locate/jphotochem

A critical review of the absorption cross-sections of O_3 and NO_2 in the ultraviolet and visible☆

J. Orphal*
Laboratoire de Photophysique Moléculaire, CNRS, Bât. 350, Centre d'Orsay, Orsay 91405 Cedex, France

Received 10 July 2002; received in revised form 19 September 2002; accepted 19 September 2002

Abstract

The available laboratory measurements of UV-Vis (240–790 nm) absorption cross-sections of O_3 and NO_2 are critically reviewed taking into account the variation of the cross-sections with temperature (in the 200–300 K range) and with total pressure (< 1 atm).
© 2003 Elsevier Science B.V. All rights reserved.

Keywords: Absorption; Cross-section; Review; Ozone; O_3; NO_2

1. Introduction

The changing atmosphere of the Earth is a subject of great public and political interest [1–6]. Three topics are currently of major concern: (1) the destruction of the stratospheric

concentrations using the full spectral information in the 240–790 nm region. Besides the improved accuracy for the O_3 measurements that results from this broad spectral coverage at medium resolution (including O_3 profile retrieval), it is possible to detect many other species of atmospheric rel-

$BrONO_2$: 15 years from laboratory to detection

Orsay
N° d'ordre: 3510

UNIVERSITE DE PARIS-SUD
U.F.R. SCIENTIFIQUE D'ORSAY

THESE DE DOCTORAT

(Spécialité: Lasers et Matière)

présentée pour obtenir le grade de

DOCTEUR EN SCIENCES DE L'UNIVERSITE PARIS-XI

par

JOHANNES ORPHAL

Sujet

Spectroscopie Infrarouge à Haute Résolution
de Molécules Instables d'Intérêt Atmosphérique:
$ClONO_2$, $ClNO_2$ et $BrONO_2$

Soutenue le 12.1.1995 à 11h00
devant la Commission d'Examen

M. R.-J. Champeau
M. J. Demaison (Rapporteur)
M. J.-M. Flaud
M. G. Mégie
Mme M. Morillon-Chapey
M. M. Winnewisser (Rapporteur)

Figure 4-3: Synthèse de $ClONO_2$ par la réaction de Cl_2O et N_2O_5

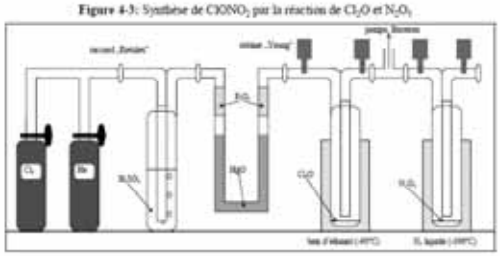

Figure 4-6: Synthèse de $BrONO_2$ à partir de $ClONO_2$

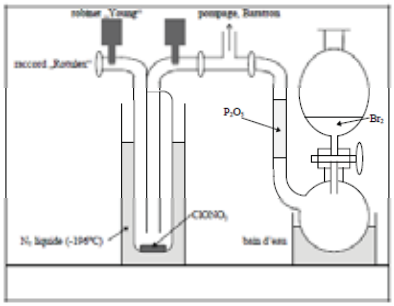

$BrONO_2$: 15 years from laboratory to detection

Chemical Physics Letters 458 (2008) 44–47

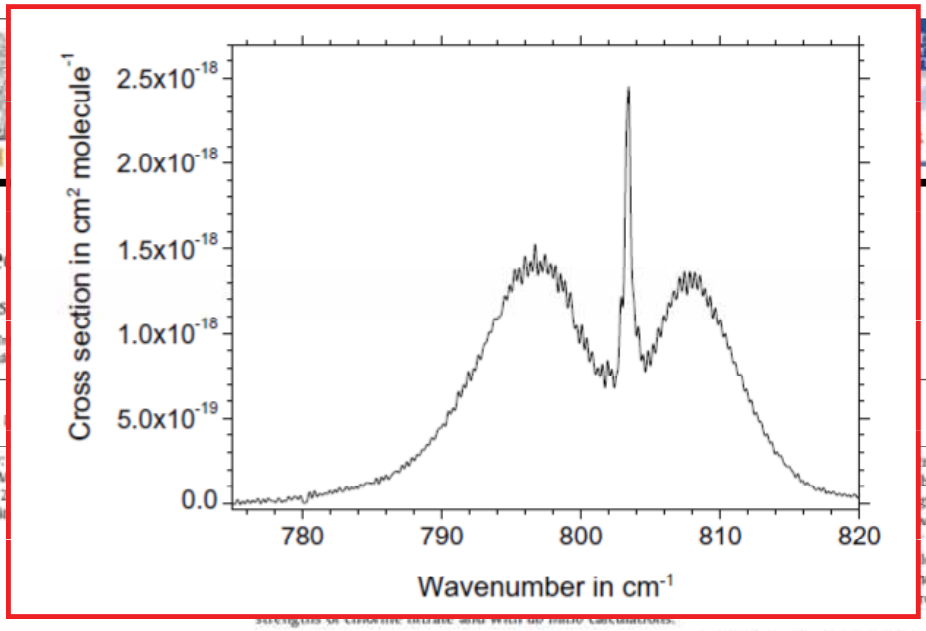

© 2008 Elsevier B.V. All rights reserved.

MIPAS: First detection of atmospheric $BrONO_2$

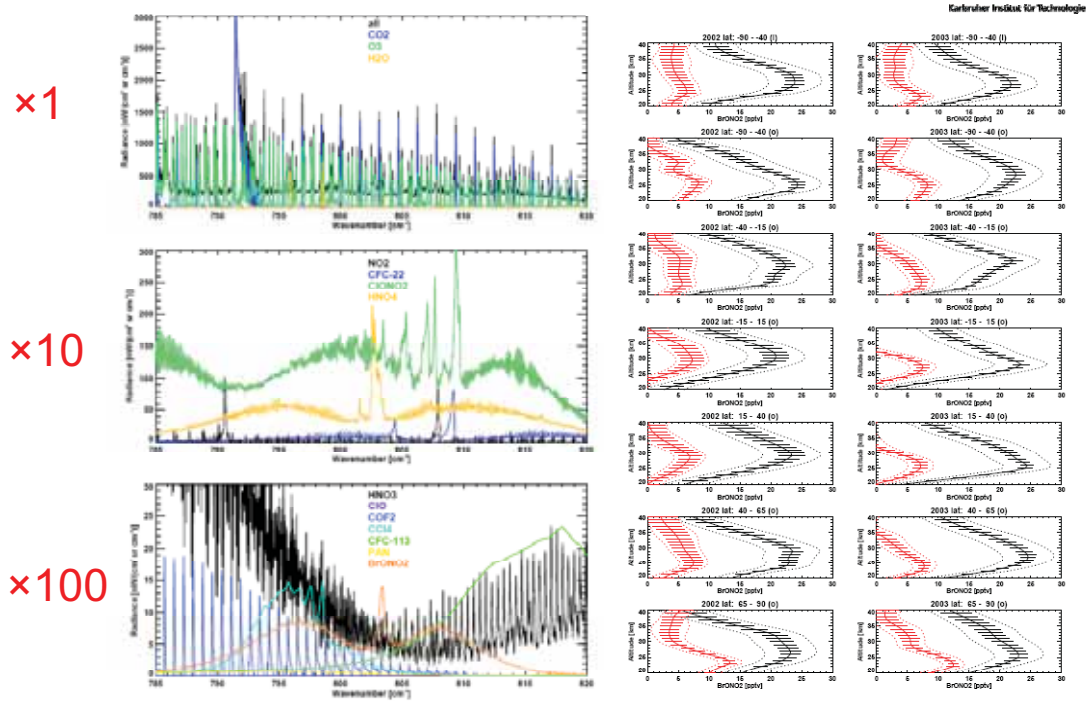

MIPAS: First detection of atmospheric $BrONO_2$

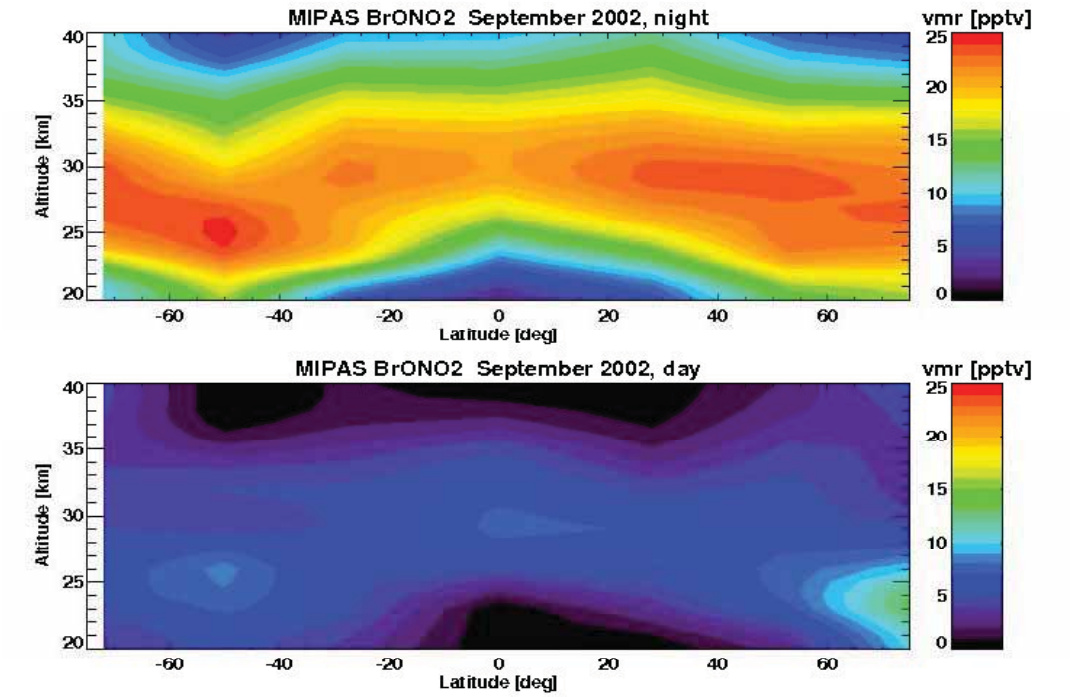

35 09.01.2013 Prof. Dr. Johannes Orphal Institut für Meteorologie und Klimaforschung (IMK)

MIPAS: First detection of atmospheric $BrONO_2$

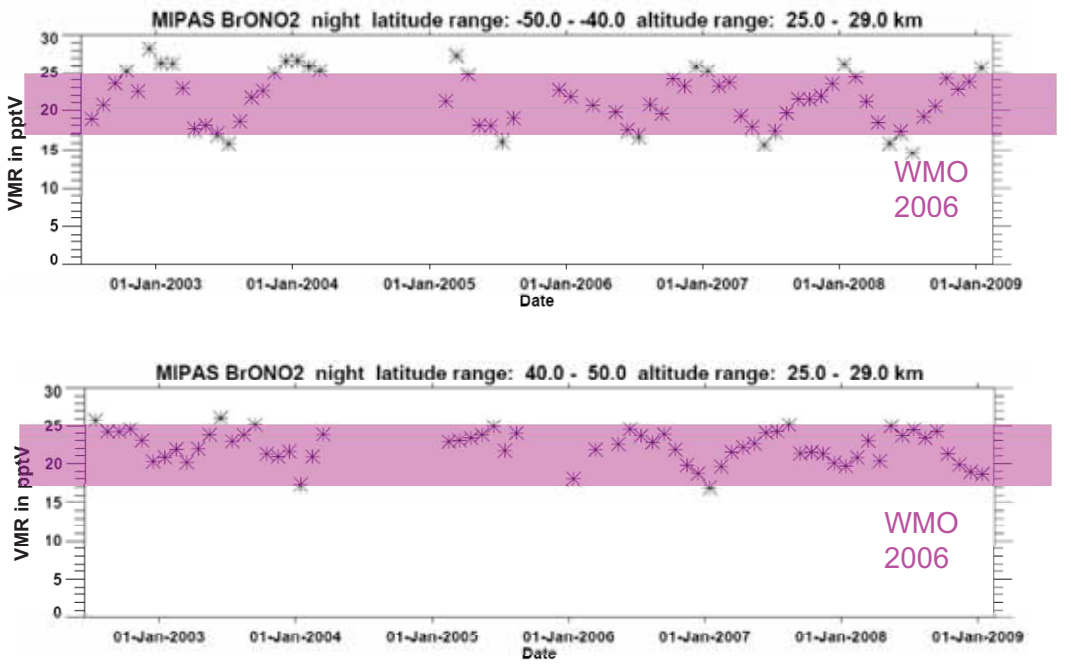

36 09.01.2013 Prof. Dr. Johannes Orphal Institut für Meteorologie und Klimaforschung (IMK)

MIPAS: First detection of atmospheric $BrONO_2$

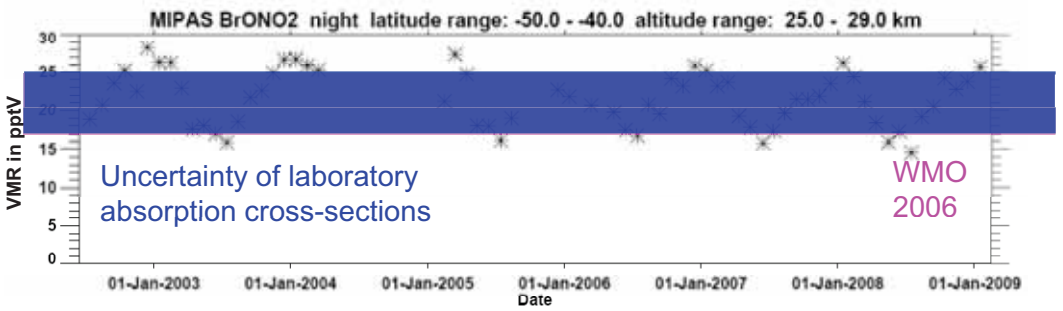

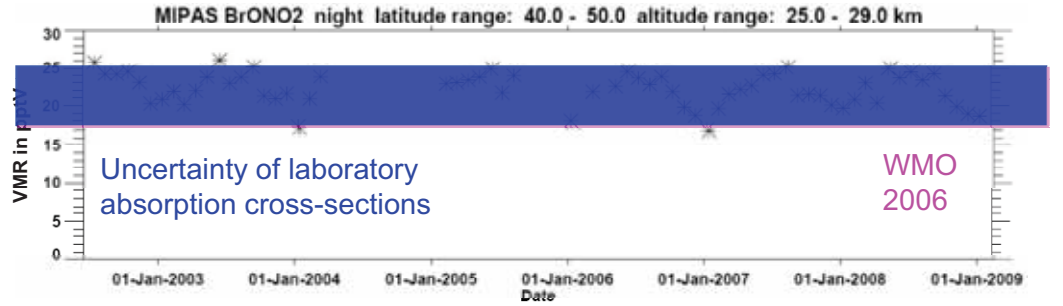

37 09.01.2013 Prof. Dr. Johannes Orphal Institut für Meteorologie und Klimaforschung (IMK)

Infrared line parameters: CF_4

Simulation of the spectrum of a pure (N_2, O_2, CF_4) atmosphere as seen by MIPAS

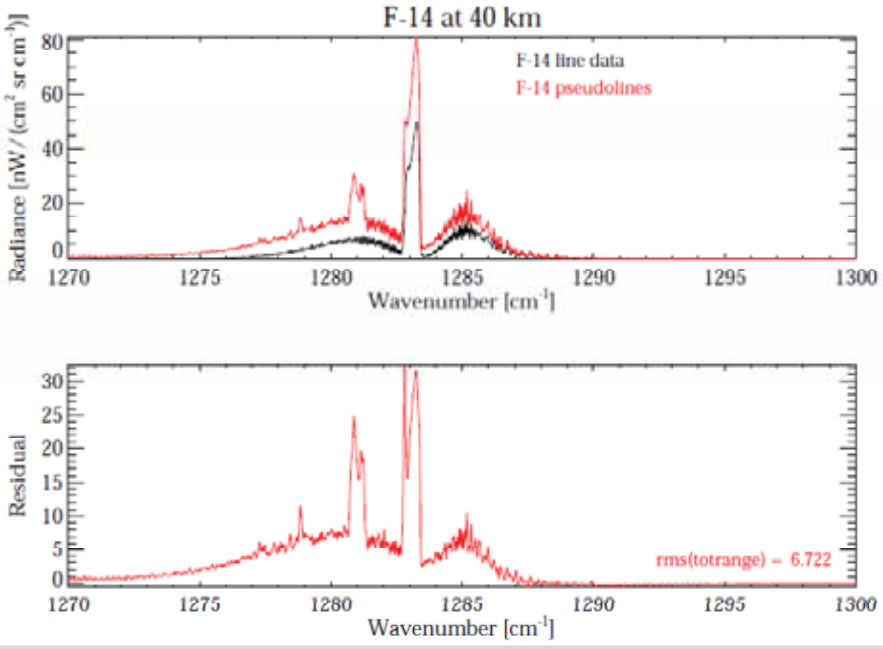

38 09.01.2013 Prof. Dr. Johannes Orphal Institut für Meteorologie und Klimaforschung (IMK)

Infrared line parameters: CF_4

CF_4 vertical profile retrievals from MIPAS along one orbit

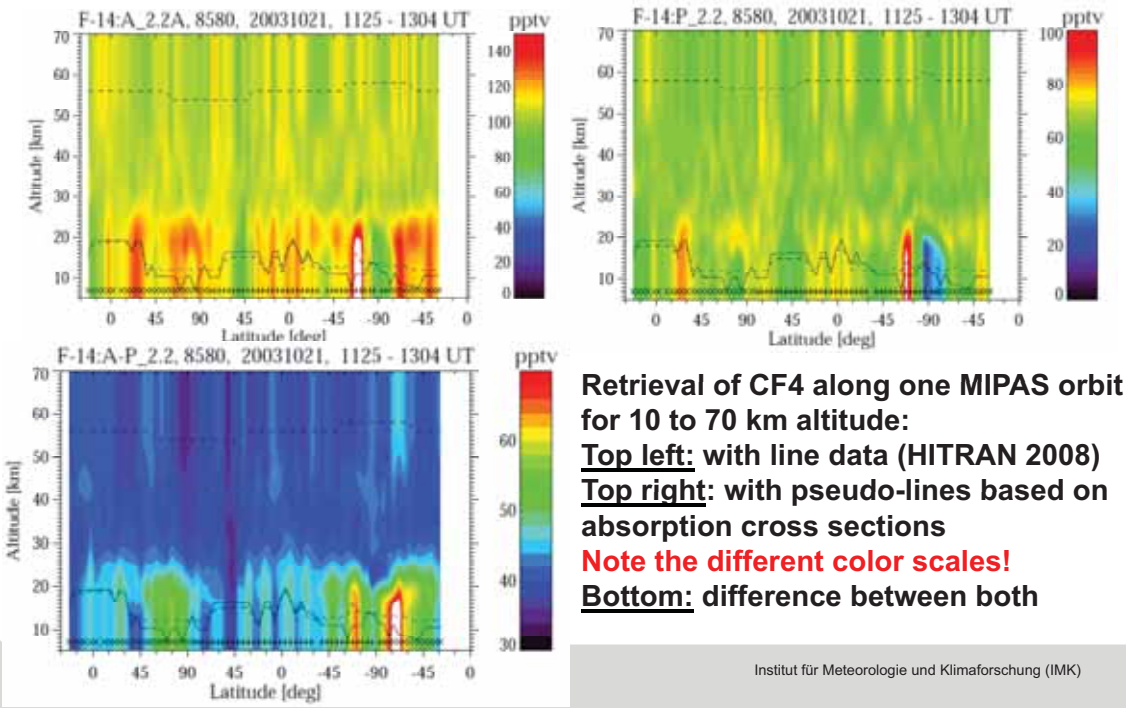

Retrieval of CF4 along one MIPAS orbit for 10 to 70 km altitude:
Top left: with line data (HITRAN 2008)
Top right: with pseudo-lines based on absorption cross sections
Note the different color scales!
Bottom: difference between both

Institut für Meteorologie und Klimaforschung (IMK)

Infrared line parameters: CF_4

Analysis of CF_4 atmospheric profiles with various spectroscopic data sets

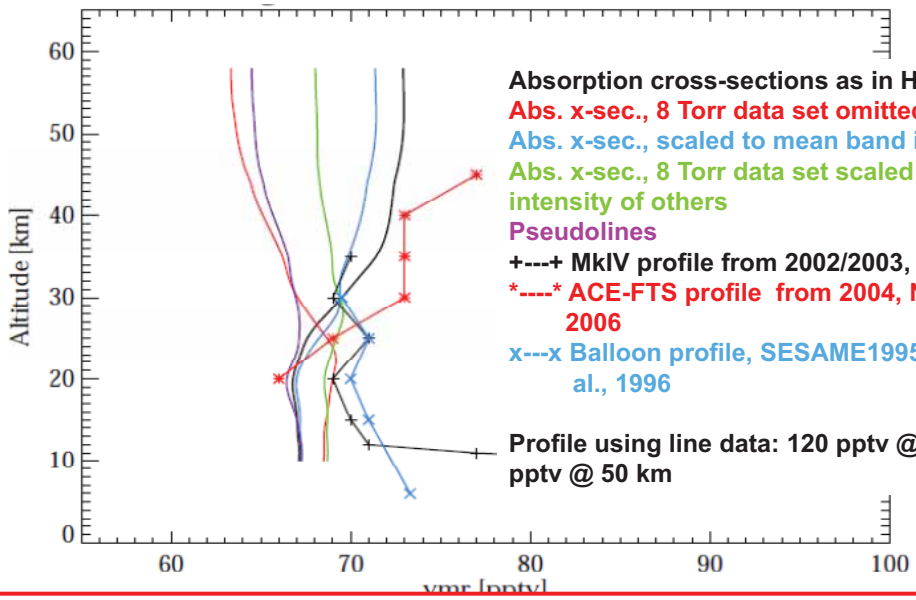

Absorption cross-sections as in HITRAN2004
Abs. x-sec., 8 Torr data set omitted
Abs. x-sec., scaled to mean band intensity
Abs. x-sec., 8 Torr data set scaled to mean band intensity of others
Pseudolines
+---+ MkIV profile from 2002/2003, Toon et al.
***----* ACE-FTS profile from 2004, Nassar et al., 2006**
x---x Balloon profile, SESAME1995, Harnisch et al., 1996

Profile using line data: 120 pptv @ 20 km to 100 pptv @ 50 km

Profiles vary by 10 pptv in the upper stratosphere depending on spectroscopy, However: we need an accuracy in the profile shape of about 1% (= 0.7 pptv) !

Water cycle from isotopes: HDO, $H_2{}^{18}O$

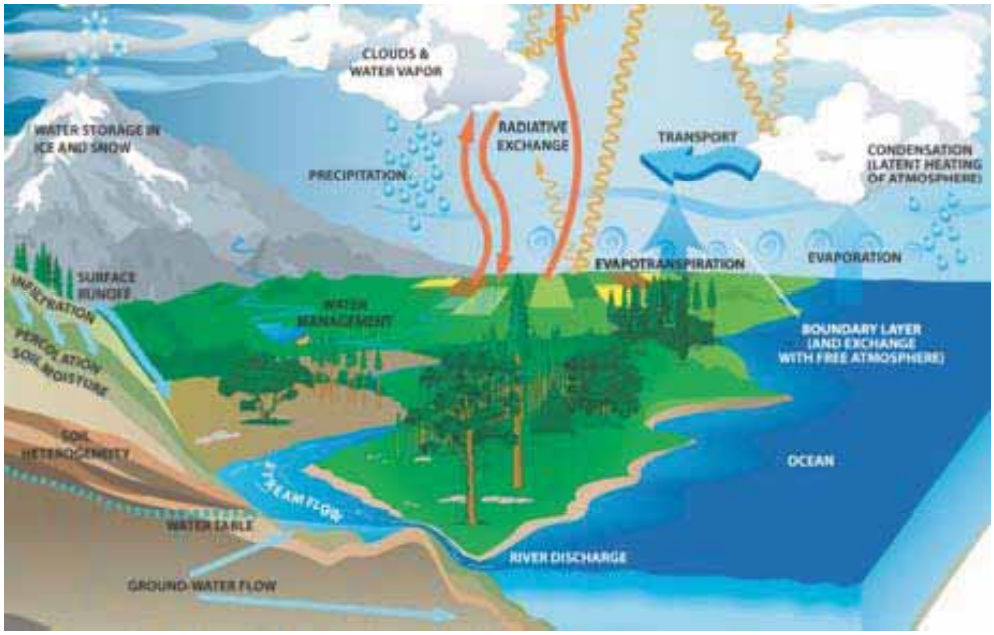

Water cycle from isotopes: HDO, $H_2{}^{18}O$

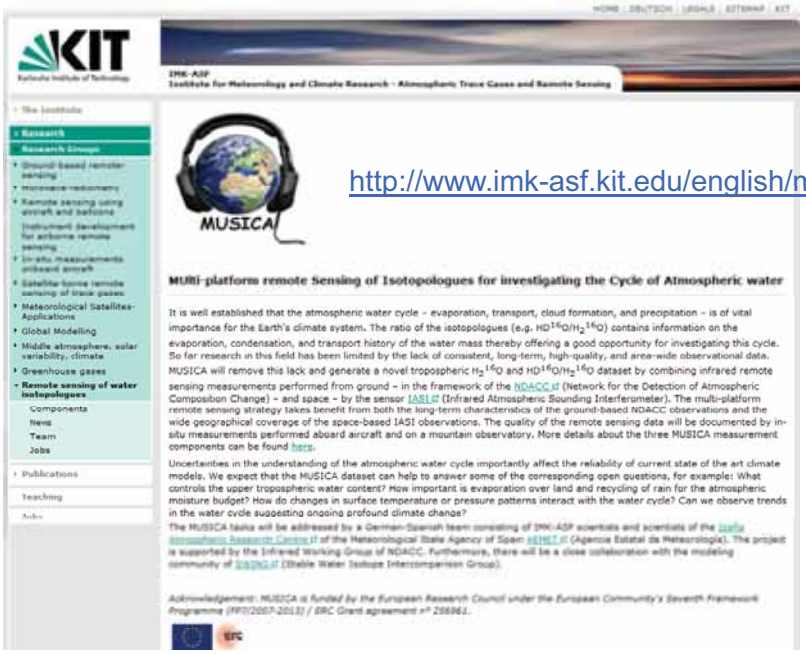

http://www.imk-asf.kit.edu/english/musica.php

Water cycle from isotopes: HDO, $H_2{}^{18}O$

ARTICLES
PUBLISHED ONLINE: 28 MARCH 2010 | DOI: 10.1038/NGEO822
nature geoscience

Tropical dehydration processes constrained by the seasonality of stratospheric deuterated water

Jörg Steinwagner[1], Stephan Fueglistaler[2]*, Gabriele Stiller[3], Thomas von Clarmann[3], Michael Kiefer[3], Peter-Paul Borsboom[1], Aarnout van Delden[1] and Thomas Röckmann[1†]

Stratospheric water vapour affects Earth's radiation budget. In addition, it has a key role in stratospheric chemistry and in processes that permit ozone depletion. Air largely enters the stratosphere in the tropics, but the processes that bring water through the cold tropopause into the stratosphere are not well understood. Here we present a 19-month record of non-deuterated (H_2O) and deuterated (HDO) water in the tropical stratosphere, collected through remote-sensing measurements with the Michelson Interferometer for Passive Atmospheric Sounding. Our data show a clear seasonal cycle in the isotopic composition that propagates upward in the tropical stratosphere, and is most likely created in the tropical tropopause layer. In addition, we find that the slope of the HDO-H_2O correlation of water entering the stratosphere in the tropics is close to, but slightly steeper than the slope expected from Rayleigh fractionation. We propose that gradual dehydration of air by cirrus clouds that are formed *in situ*, together with a seasonally varying contribution from the evaporation of convectively lofted ice, provides the most plausible explanation for our measurements. We conclude that potential changes in the water budget of the tropical tropopause layer and the stratosphere should be detectable in isotopic measurements.

Water cycle from isotopes: HDO, $H_2{}^{18}O$

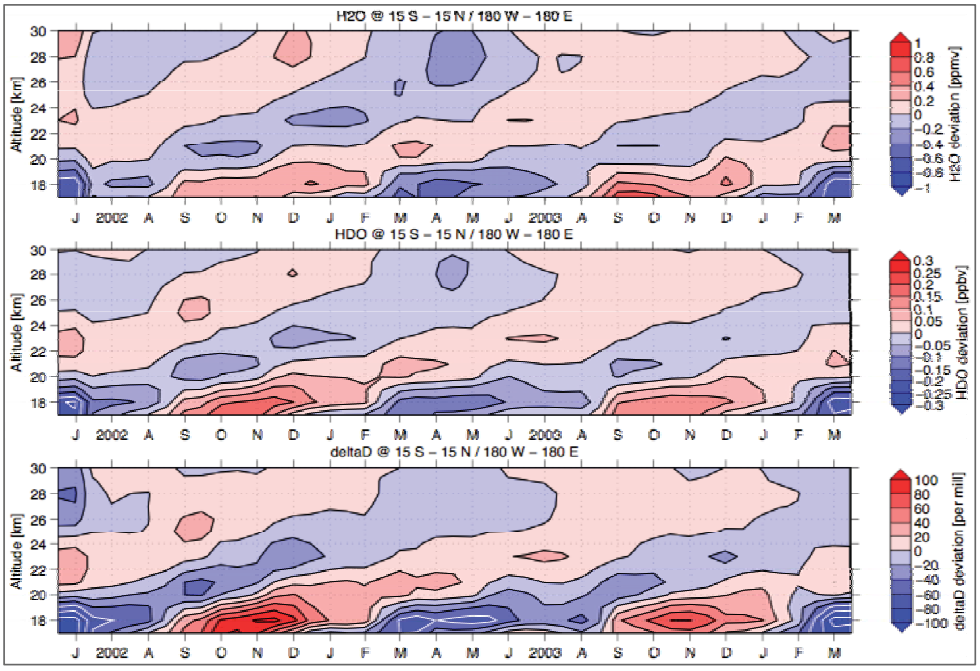

Infrared line parameters: $H_2{}^{18}O$

- Fit of MIPAS balloon spectra (38 km, one of 10 microwindows)

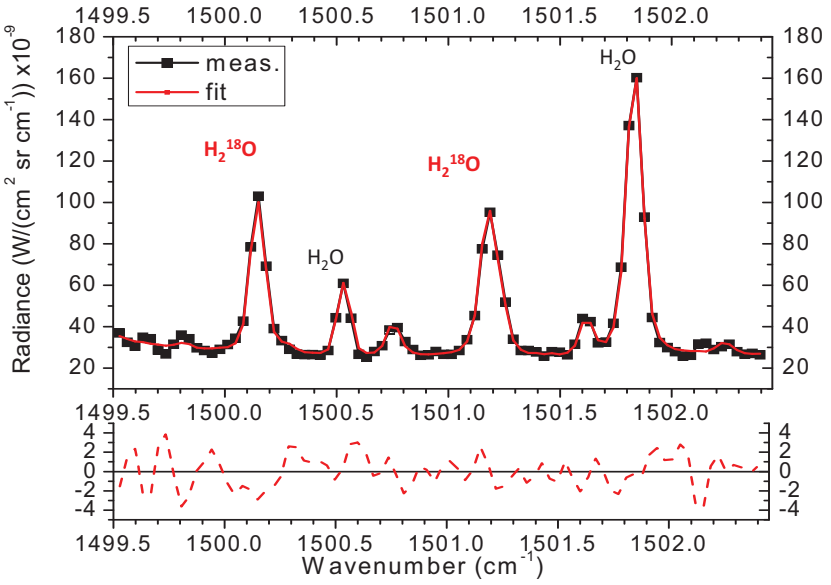

Infrared line parameters: $H_2{}^{18}O$

- Atmospheric profiles of 14.06.2005, Teresina, Brazil

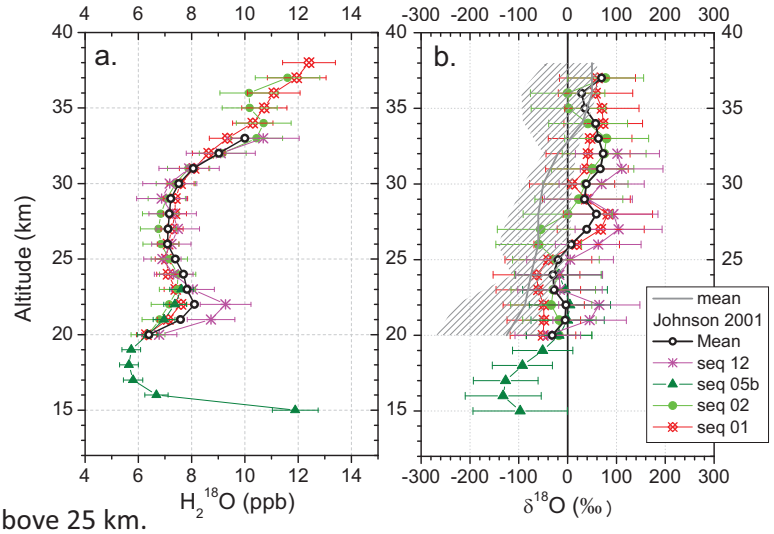

Shaded area : range of values observed by FIRS (Johnson et al, 2001)

$\delta^{18}O$>0 above 25 km.

Previous studies (Rinsland et al, 1991; Dinelli et al, 1991, Johnson et al, 2001) show slightly negative $\delta^{18}O$ in the mid-stratosphere

O_3: Consistency of IR and UV-visible

Atmos. Meas. Tech., 4, 535–546, 2011
www.atmos-meas-tech.net/4/535/2011/
doi:10.5194/amt-4-535-2011

Comparison of ground-based FTIR and Brewer O_3 total column with data from two different IASI algorithms and from OMI and GOME-2 satellite instruments

C. Vlatte[1], M. Schneider[2,3], A. Redondas[3], F. Hase[2], M. Eremenko[1], P. Chelin[1], J.-M. Flaud[1], T. Blumenstock[2], and J. Orphal[2]

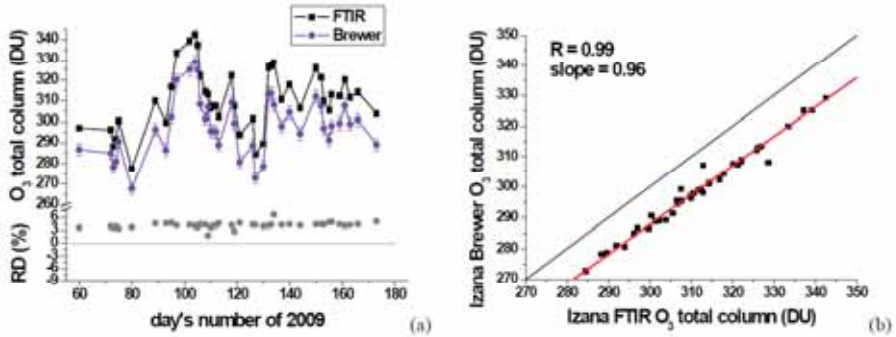

Fig. 4. Ground-based comparison of O_3 total columns. **(a)** Time series of O_3 total column derived from FTIR at Izaña (black) and from Brewer (dark blue) measurements. Relative errors and relative differences (RD % in gray) are plotted. **(b)** O_3 total column derived from Brewer measurement as a function of the FTIR O_3 measurements. Red line is a linear fit with zero y-intercept.

Requirements:

- accurate reference data (incl. uncertainties)
- expert evaluation of this data by the „users“
- establish priorities (traceability is not an issue !)
- currently known deficiencies from satellites:
  - consistency in different spectral regions
  - data on unstable species and isotopes
  - „exotic“ line shape models („non-Voigt“)
  - temperature-dependence of broadening

Requirements:

- accurate reference data (incl. uncertainties)
- expert evaluation of this data by the „users“
- establish priorities (traceability is not an issue !)
- currently known deficiencies from satellites:
  - consistency in different spectral regions
  - data on unstable species and isotopes
  - „exotic“ line shape models („non-Voigt“)
  - temperature-dependence of broadening
- **laboratory spectroscopy (already in danger!)**

"Efficient use of laboratory and theoretical spectroscopic data in HITRAN"

Dr. Iouli E. Gordon

Atomic and Molecular Physics Division,
Harvard-Smithsonian Center for Astrophysics

Dr. Iouli E. Gordon

Atomic and Molecular Physics Division, Harvard-Smithsonian Center for Astrophysics
60 Garden Street, 02138 Cambridge, MA, USA
Phone: +1 6174962259
E-mail: igordon@cfa.harvard.edu

Education and Professional Experience

since 2008	Physicist, Smithsonian Astrophysical Observatory, Atomic and Molecular Physics Division, Cambridge MA, USA
2006-2008	PostDoc, Atomic and Molecular Physics Division, Harvard-Smithsonian Center for Astrophysics, USA
2006	PhD, Department of Physics, University of Waterloo, Canada
2001	MSc, Department of Physics, University of Toronto, Canada
1999	Diploma, Department of Molecular and Biological Physics, Moscow Institute of Physics and Technology (MIPT), Russia

Activities, Honors and Awards

- Reviewer: Journal of Quantitative Spectroscopy and Radiative Transfer; Journal of Molecular Spectroscopy, Journal of Geophysical Research; Review of Scientific Instruments, Journal of Chemical Physics, Philosophical Transactions A, Aerosol Science & Technology, Geophysical Research Letters, Molecular Physics
- Guest editor for two JQSRT special issues, 2010 and 2012/2013
- Member of International HITRAN advisory committee
- External NASA proposal review: Mars Fundamental Research and Outer Planets Research Programs (2009 and 2012)
- Member of the Fellowship Selection Committee at the Harvard-Smithsonian Center for Astrophysics
- Member of American Geophysical Union

Efficient use of laboratory and theoretical spectroscopic data in HITRAN

Iouli E. Gordon, Laurence S. Rothman

Atomic and Molecular Physics Division, Harvard-Smithsonian Center for Astrophysics

The HITRAN database is a compilation of spectroscopic line parameters that are being used in a wide variety of applications that include remote sensing of the atmosphere, astrophysics, industry, etc. The database is a carefully selected amalgamation of theoretically and experimentally determined spectral parameters. In this talk a brief introduction to the database, its current and future structure and formalism will be given. The pros and cons of theoretical and experimental data and how these data are being combined into high-accuracy reference line lists will be explained using a few examples.

Efficient use of laboratory and theoretical spectroscopic data in HITRAN

Iouli Gordon and
Laurence Rothman

Eumetrispec meeting, November 16th, 2012

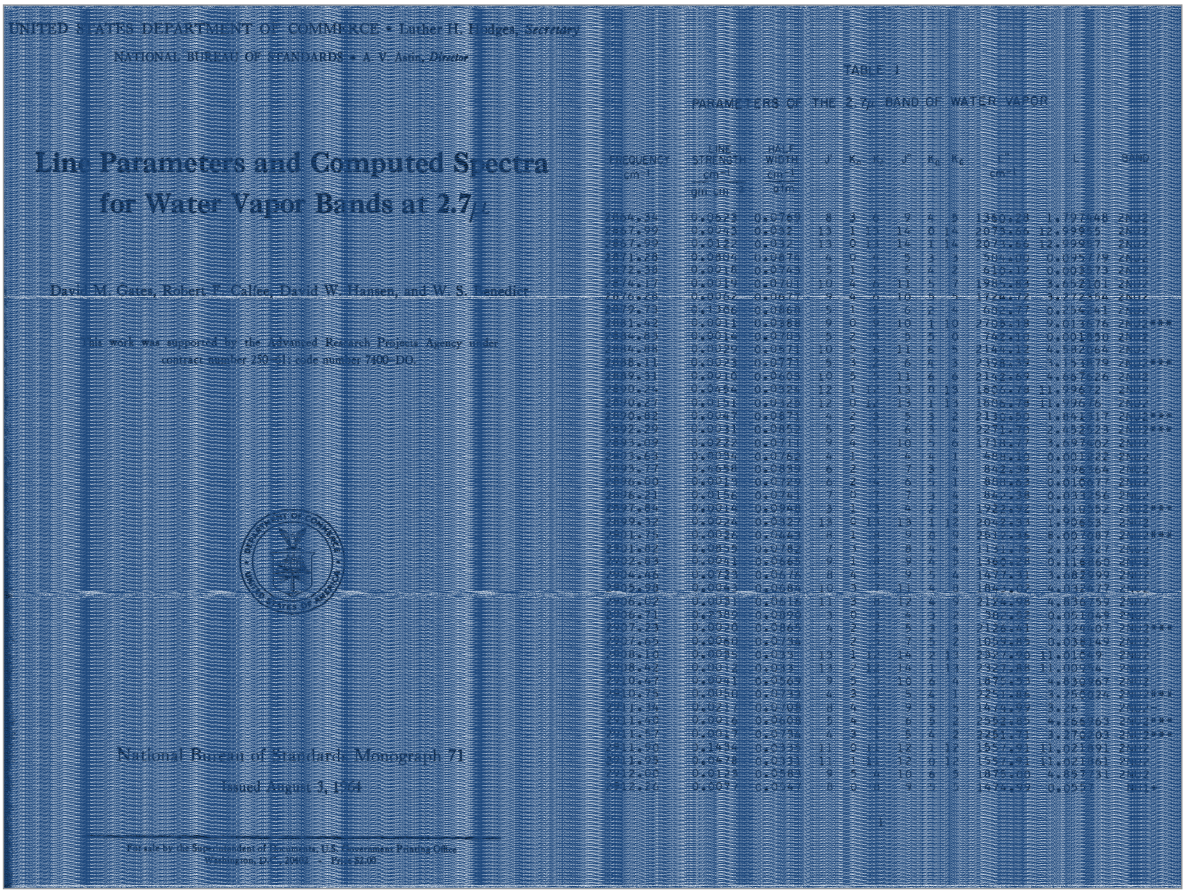
UNITED STATES DEPARTMENT OF COMMERCE • Luther H. Hodges, *Secretary*
NATIONAL BUREAU OF STANDARDS • A. V. Astin, *Director*

Line Parameters and Computed Spectra for Water Vapor Bands at 2.7 μ

David M. Gates, Robert F. Calfee, David W. Hansen, and W. S. Benedict

This work was supported by the Advanced Research Projects Agency of the contract number 150-61; code number 7400-DO.

National Bureau of Standards Monograph 71
Issued August 3, 1964

For sale by the Superintendent of Documents, U.S. Government Printing Office
Washington, D.C., 20402 — Price $1.00

TABLE 1
PARAMETERS OF THE 2.7 μ BAND OF WATER VAPOR

The Atmosphere as "Filter"

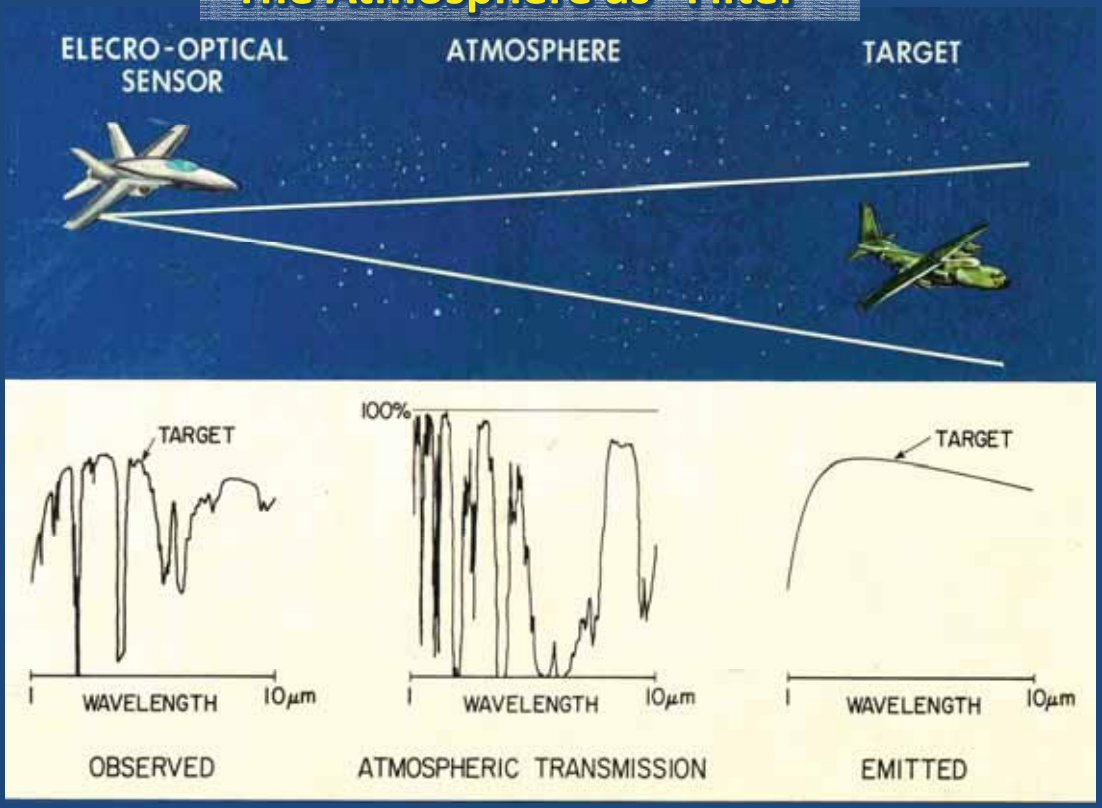

Schematic of Fundamental Spectroscopic Parameters of a Line Transition in HITRAN (the Dotted Line Refers to a Perturbed Transition)

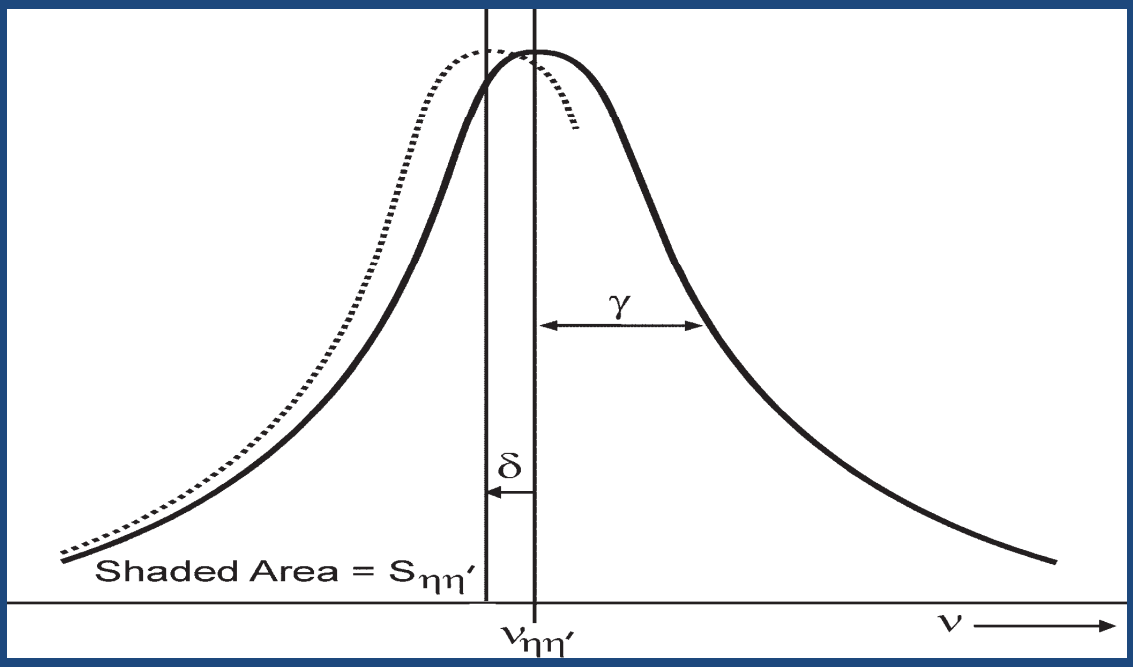

Molecular Absorption

$$S(T) = \frac{I_a g'}{Q_{tot}(T)} \frac{A_{21}}{8\pi c \nu_0^2} e^{-\frac{hcE''}{k_B T}} \left(1 - e^{-\frac{hc\nu_0}{k_B T}}\right)$$

Partition Sum:

$$Q(T) = \sum_{\eta} g_{\eta} \exp(-c_2 E_{\eta}/T)$$

Temperature dependence of halfwidth:

$$\gamma_{air}(p_{ref}, T) = \gamma_{air}(p_{ref}, T_{ref}) (T_{ref}/T)^n$$

HITRAN Line-by-line Parameters

Parameter	Field size	Definition
Mol	I2	Molecule number
Iso	I1	Isotopologue no.(1 = most abundant, 2 = second most abundant, …)
ν_{if}	F12.6	Transition wavenumber in vacuum [cm^{-1}]
S_{if}	E10.3	Intensity [cm^{-1}/(molecule·cm^{-2}) @ 296K]
A_{if}	E10.3	Einstein *A*-coefficient [s^{-1}]
γ_{air}	F5.4	Air-broadened half-width (HWHM) [cm^{-1}/atm @ 296K]
γ_{self}	F5.3	Self-broadened half-width (HWHM) [cm^{-1}/atm @ 296K]
E"	F10.4	Lower-state energy [cm^{-1}]
n_{air}	F4.2	Temperature-dependence coefficient of γ_{air}
δ_{air}	F8.6	Air pressure-induced shift [cm^{-1}/atm @ 296K]
v', v"	2A15	Upper and Lower "global" quanta
q', q"	2A15	Upper and Lower "local" quanta
ierr	6I1	Uncertainty indices for ν_{if}, S_{if}, γ_{air}, γ_{self}, n_{air}, δ_{air}
iref	6I2	Reference pointers for ν_{if}, S_{if}, γ_{air}, γ_{self}, n_{air}, δ_{air}
*	A1	Flag for line-coupling algorithm
g', g"	2F7.1	Upper and Lower statistical weights

M	I	ν_{if}	S_{if}	A_{if}	γ_{air}	γ_{self}	E''	n_{air}	δ_{air}	v'	v''	q'	q''	I_{err}	I_{ref}	*	g'	g''
31	1191.536600	1.221E-25	8.456E-01	.08050	.103	2224.58670	.710	.000000		3 0 0	1 0 1	13 4 10	12 4 9	0055501412	5 2 3	0	27.0	25.0
31	1191.559730	9.141E-23	1.223E-01	.07440	.083	570.24100	.79	-.000700		1 0 0	0 0 0	22 12 10	21 11 11	0065501412	4 2 2	1	45.0	43.0
31	1191.560490	3.286E-24	4.306E-02	.06820	.085	1221.74800	.76	-.000700		1 0 0	0 0 0	54 4 50	53 3 51	0042201412	8 2 1	1	109.0	107.0
31	1191.576700	1.740E-25	9.534E-01	.07930	.105	2191.07900	.710	.000000		3 0 0	1 0 1	14 1 13	13 1 12	0055501412	5 2 3	0	29.0	27.0
31	1191.583300	5.135E-24	5.479E-01	.07130	.095	1559.09810	.780	.000000		2 0 0	0 0 1	34 4 30	33 4 29	0055501412	5 2 3	0	69.0	67.0
31	1191.590060	7.477E-25	3.205E-03	.07420	.083	800.46830	.79	-.000700		1 0 0	0 0 0	21 15 7	21 14 8	0062501412	4 2 2	1	43.0	43.0
31	1191.606000	9.058E-25	6.492E-01	.07410	.081	1888.74110	.740	.000000		2 0 0	0 0 1	25 14 12	24 14 11	0052501412	5 2 3	0	51.0	49.0
31	1191.650000	1.798E-24	1.070E-01	.07180	.080	1399.67390	.800	.000000		1 1 0	0 1 0	28 12 16	27 11 17	0065501412	6 2 4	0	57.0	55.0
31	1191.655340	4.199E-24	1.582E-02	.06910	.088	941.28630	.76	-.000700		1 0 0	0 0 0	48 3 45	47 2 46	0045201412	8 2 1	1	97.0	95.0
31	1191.666010	7.104E-25	2.932E-03	.07460	.083	782.82530	.78	-.000700		1 0 0	0 0 0	20 15 5	20 14 6	0062501412	4 2 2	1	41.0	41.0
31	1191.690560	1.191E-25	2.024E-04	.07010	.086	750.26340	.85	-.000700		0 0 1	0 0 0	42 7 36	41 3 39	0065501412	4 2 2	1	85.0	83.0
31	1191.693400	5.846E-24	6.379E-01	.07150	.095	1557.62900	.780	.000000		2 0 0	0 0 1	33 5 29	32 5 28	0055501412	5 2 3	0	67.0	65.0
31	1191.695800	8.856E-25	2.380E-01	.07330	.084	1702.43590	.750	.000000		2 0 0	0 0 1	27 11 17	26 11 16	0055501412	5 2 3	0	55.0	53.0
31	1191.716620	3.443E-25	4.110E-04	.08050	.085	441.68660	.71	-.000700		0 0 1	0 0 0	13 13 0	12 11 1	0062501412	4 2 2	1	27.0	25.0
31	1191.720900	1.644E-24	8.796E-01	.07080	.079	1872.03620	.810	.000000		2 0 0	1 0 0	31 12 20	30 11 19	0065501412	6 2 4	0	63.0	61.0
31	1191.738120	6.547E-25	2.618E-03	.07500	.083	766.02150	.78	-.000700		1 0 0	0 0 0	19 15 5	19 14 6	0062501412	4 2 2	1	39.0	39.0
31	1191.753500	1.154E-24	1.231E-01	.06750	.095	1558.92790	.810	.000000		2 0 0	1 0 0	34 4 30	33 1 33	0065501412	6 2 4	0	69.0	67.0
31	1191.754400	1.856E-25	6.107E-02	.07000	.072	1838.42200	.850	.000000		0 1 1	0 1 0	43 13 30	42 11 31	0052501412	5 2 3	0	87.0	85.0
31	1191.757300	1.481E-25	4.379E-01	.07130	.095	2242.41580	.780	.000000		2 1 0	0 1 1	34 4 30	33 4 29	0055501412	5 2 3	0	69.0	67.0
31	1191.777300	2.433E-25	1.268E-02	.07740	.084	1283.46300	.720	.000000		0 1 1	0 1 0	18 14 5	17 12 6	0052501412	5 2 3	0	37.0	35.0
31	1191.777600	1.385E-25	4.200E-01	.07150	.095	2241.58450	.780	.000000		2 1 0	0 1 1	33 5 29	32 5 28	0055501412	5 2 3	0	67.0	65.0
31	1191.779300	1.635E-25	9.310E-01	.07980	.104	2198.93040	.710	.000000		3 0 0	1 0 1	14 2 12	13 2 11	0055501412	5 2 3	0	29.0	27.0
31	1191.806430	5.781E-25	2.255E-03	.07550	.084	750.05690	.78	-.000700		1 0 0	0 0 0	18 15 3	18 14 4	0062501412	4 2 2	1	37.0	37.0
31	1191.812310	1.064E-23	2.681E-01	.06820	.078	1356.11950	.76	-.000700		1 0 0	0 0 0	54 8 46	53 7 47	0042201412	8 2 1	1	109.0	107.0
31	1191.821500	1.865E-25	2.639E-01	.06800	.076	2192.28980	.760	.000000		1 1 0	0 1 0	56 9 47	55 8 48	0042201412	8 2 1	0	113.0	111.0
31	1191.870960	4.775E-25	1.829E-03	.07590	.084	734.93160	.78	-.000700		1 0 0	0 0 0	17 15 3	17 14 4	0062501412	4 2 2	1	35.0	35.0
31	1191.878000	1.587E-24	1.030E-01	.07340	.082	1386.35470	.790	.000000		1 1 0	0 1 0	24 13 11	23 12 12	0062501412	6 2 4	0	49.0	47.0
31	1191.897760	3.910E-23	2.080E-01	.06960	.080	994.48680	.84	-.000700		1 0 0	0 0 0	44 9 35	43 8 36	0065501412	4 2 2	1	89.0	87.0
31	1191.899500	1.760E-25	9.370E-01	.07780	.105	2185.03910	.710	.000000		3 0 0	1 0 1	14 0 14	13 0 13	0055501412	5 2 3	0	29.0	27.0
31	1191.911140	7.063E-23	1.452E-01	.07000	.083	752.30310	.82	-.000700		1 0 0	0 0 0	35 10 26	34 9 25	0065501412	4 2 2	1	71.0	69.0
31	1191.911700	1.327E-25	2.929E-01	.07630	.083	2075.14120	.720	.000000		2 0 0	0 0 1	20 17 3	19 17 2	0052501412	5 2 3	0	41.0	39.0
31	1191.924600	7.404E-25	2.118E-01	.06950	.076	1823.27600	.760	.000000		1 1 0	0 1 0	46 10 36	45 9 37	0045201412	8 2 1	0	93.0	91.0
31	1191.927300	2.212E-25	8.249E-02	.07540	.083	1709.31960	.780	.000000		2 0 0	1 0 0	20 13 7	19 12 8	0062501412	6 2 4	0	41.0	39.0
31	1191.931000	1.538E-24	1.628E-01	.06970	.079	1574.54930	.820	.000000		1 1 0	0 1 0	37 11 27	36 10 26	0065501412	6 2 4	0	75.0	73.0
31	1191.931740	3.500E-25	1.327E-03	.07640	.084	720.64590	.78	-.000700		1 0 0	0 0 0	16 15 1	16 14 2	0062501412	4 2 2	1	33.0	33.0
31	1191.947660	6.167E-23	1.020E-01	.07940	.085	523.44390	.77	-.000700		1 0 0	0 0 0	14 13 1	13 12 2	0062501412	4 2 2	1	29.0	27.0
31	1191.973400	9.904E-26	7.854E-01	.08050	.102	2252.30490	.710	.000000		3 0 0	1 0 1	13 5 9	12 5 8	0055501412	5 2 3	0	27.0	25.0

Molecule Number	Molecule	Isotopologue (AFGL notation)	Fractional Abundance	Spectral Coverage (cm^{-1})	Number of lines	Total number
1	H_2O	161	0.9973	0 – 25233	37432	69201
		181	$1.999\ 10^{-3}$	0 – 14519	9753	
		171	$3.719\ 10^{-4}$	10 – 14473	6992	
		162	$3.107\ 10^{-4}$	0 – 22708	13238	
		182	$6.230\ 10^{-7}$	0 – 3825	1611	
		172	$1.158\ 10^{-7}$	1234 – 1599	175	
2	CO_2	626	0.9842	352 – 12785	128170	314919
		636	$1.106\ 10^{-2}$	438 – 12463	49777	
		628	$3.947\ 10^{-3}$	0 – 11423	79958	
		627	$7.339\ 10^{-4}$	0 – 8271	19264	
		638	$4.434\ 10^{-5}$	489 – 6745	26737	
		637	$8.246\ 10^{-6}$	583 – 6769	2953	
		828	$3.957\ 10^{-6}$	491 – 8161	7118	
		827	$1.472\ 10^{-6}$	626 – 5047	821	
		838	$4.446\ 10^{-8}$	4599 – 4888	121	
3	O_3	666	0.9929	0 – 5787	249456	409686
		668	$3.982\ 10^{-3}$	0 – 2768	44302	
		686	$1.991\ 10^{-3}$	1 – 2740	18887	
		667	$7.405\ 10^{-4}$	0 – 2122	65106	
		676	$3.702\ 10^{-4}$	0 – 2101	31935	
4	N_2O	446	0.9903	0 – 7797	33074	47843
		456	$3.641\ 10^{-3}$	5 – 5086	4222	
		546	$3.641\ 10^{-3}$	4 – 4704	4592	
		448	$1.986\ 10^{-3}$	542 – 4672	4250	
		447	$3.693\ 10^{-4}$	550 – 4430	1705	
5	CO	26	0.9865	3 – 8465	917	4477
		36	$1.108\ 10^{-2}$	3 – 6279	780	
		28	$1.978\ 10^{-3}$	3 – 6267	760	
		27	$3.679\ 10^{-4}$	3 – 6339	728	
		38	$2.222\ 10^{-5}$	3 – 6124	712	
		37	$4.133\ 10^{-6}$	1807 – 6197	580	
6	CH_4	211	0.9883	0 – 9200	212061	290091
		311	$1.110\ 10^{-2}$	0 – 6070	28793	
		212	$6.158\ 10^{-4}$	7 – 6511	45024	
		312	$6.918\ 10^{-6}$	959 – 1695	4213	
7	O_2	66	0.9953	0 – 15928	1431	6428
		68	$3.991\ 10^{-3}$	1 – 15852	671	
		67	$7.422\ 10^{-4}$	0 – 14537	4326	

Molecule Number	Molecule	Isotopologue (AFGL notation)	Fractional Abundance	Spectral Coverage (cm^{-1})	Number of lines	Total number
8	NO	46 56 48	0.9940 $3.654\ 10^{-3}$ $1.993\ 10^{-3}$	0 – 9274 1609 – 2061 1602 – 2039	103701 699 679	105079
9	SO_2	626 646	0.9457 $4.195\ 10^{-2}$	0 – 4093 2463 – 2497	57963 287	58250
10	NO_2	646	0.9916	0 – 3075	104223	104223
11	NH_3	446 456	0.9959 $3.661\ 10^{-3}$	0 – 5295 0 – 5180	27994 1090	29084
12	HNO_3	146	0.9891	0 – 1770	487254	487254
13	OH	61 81 62	0.9975 $2.000\ 10^{-3}$ $1.554\ 10^{-4}$	0 – 19268 0 – 329 0 – 332	30769 295 912	31976
14	HF	19	0.9998	41 – 11536	107	107
15	HCl	15 17	0.7576 0.2422	20 – 13459 20 – 10995	324 289	613
16	HBr	19 11	0.5068 0.4931	16 – 9759 16 – 9758	651 642	1293
17	HI	17	0.9998	12 – 8488	806	806
18	ClO	56 76	0.7559 0.2417	0 – 1208 0 – 1200	5721 5780	11501
19	OCS	622 624 632 623 822	0.9374 $4.158\ 10^{-2}$ $1.053\ 10^{-2}$ $7.399\ 10^{-3}$ $1.880\ 10^{-3}$	0 – 4200 0 – 4166 0 – 4056 509 – 4164 0 – 4046	15618 6087 3123 2788 1626	29242
20	H_2CO	126 136 128	0.9862 $1.108\ 10^{-2}$ $1.978\ 10^{-3}$	0 – 3100 0 – 73 0 – 48	36120 563 367	37050
21	HOCl	165 167	0.7558 0.2417	1 – 3800 1 – 3800	8877 7399	16276
22	N_2	44	0.9927	1992 – 2626	120	120
23	HCN	124 134 125	0.9851 $1.107\ 10^{-2}$ $3.622\ 10^{-3}$	0 – 3424 2 – 3405 2 – 3420	2955 652 646	4253
24	CH_3Cl	215 217	0.7489 0.2395	0 – 3173 0 – 3162	100279 95892	196171
25	H_2O_2	1661	0.9950	0 – 1731	126983	126983
26	C_2H_2	1221 1231	0.9776 $2.197\ 10^{-2}$	604 – 9890 613 – 6589	11055 285	11340
27	C_2H_6	1221	0.9770	706 – 3001	22402	22402
28	PH_3	1111	0.9995	770 – 3602	20099	20099

Molecule Number	Molecule	Isotopologue (AFGL notation)	Fractional Abundance	Spectral Coverage (cm^{-1})	Number of lines	Total number
29	COF_2	269	0.9865	725 – 2002	70601	70601
30	SF_6	29	0.9502	580 – 996	2889065	2889065
31	H_2S	121 141 131	0.9499 $4.214\ 10^{-2}$ $7.498\ 10^{-3}$	2 – 4257 5 – 4172 5 – 4099	12330 4894 3564	20788
32	HCOOH	126	0.9839	10 – 1890	62684	62684
33	HO_2	166	0.9951	0 – 3676	38804	38804
34	O	6	0.9976	68 – 159	2	2
35	$ClONO_2$	5646 7646	0.7496 0.2397	763 – 798 765 – 791	21988 10211	32199
36	NO^+	46	0.9940	1634 – 2531	1206	1206
37	HOBr	169 161	0.5056 0.4919	0 – 316 0 – 316	2177 2181	4358
38	C_2H_4	221 231	0.9773 $2.196\ 10^{-2}$	701 – 3243 2947 – 3181	18097 281	18378
39	CH_3OH	2161	0.9859	0 – 1408	19897	19897
40	CH_3Br	219 211	0.5010 0.4874	794 – 1706 796 – 1697	18692 18219	36911
41	CH_3CN	2124	0.9739	890 – 946	3572	3572
42	CF_4	29	0.9889	594 – 1313	60033	60033

5 695 215 transitions
(2 713 918 in main folder)

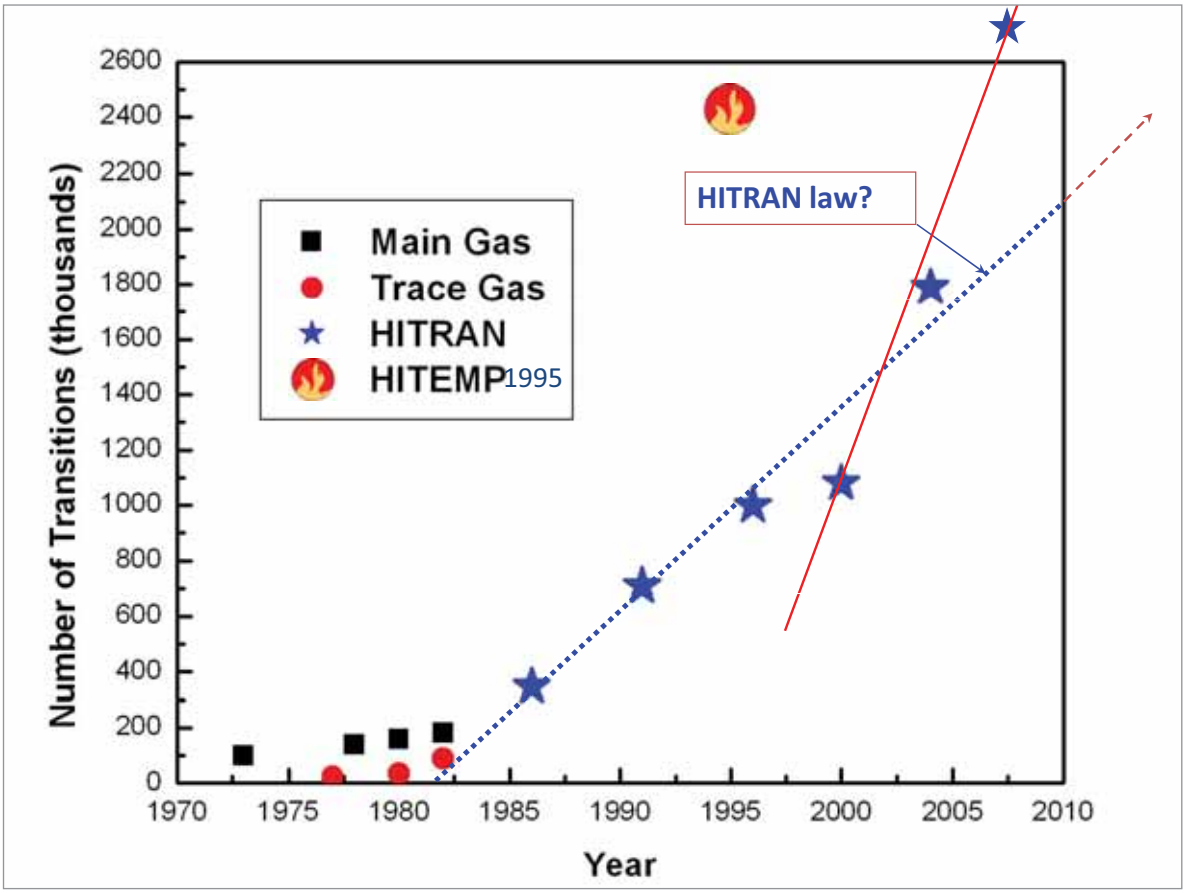

Cross-sections

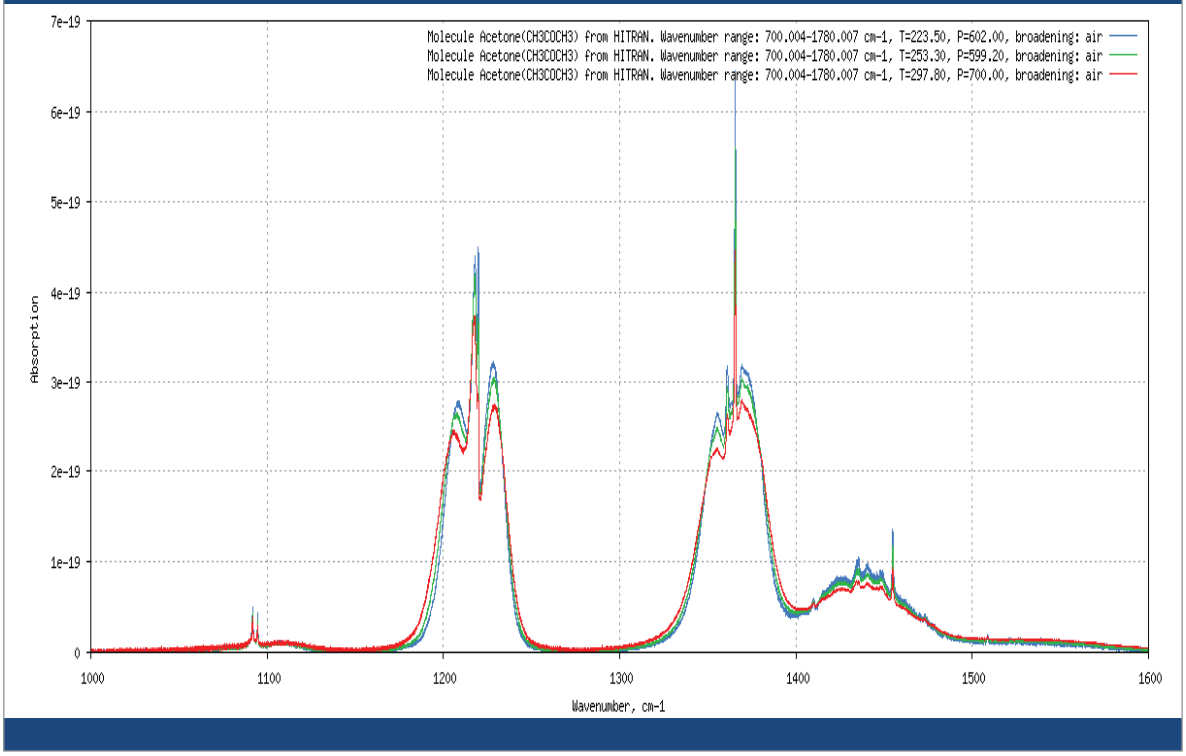

Collision Induced Absorption (CIA)

CIA system	Spectral range (cm^{-1})	Temperature range (K)	Number of sets	Band(s)
N_2–N_2	0.02 – 554	40 – 400	10	Roto-translational
	2000 – 2698	228 – 272	5	Fundamental
	1850 – 3000	300 – 362	5	Fundamental
N_2–H_2	0.02 – 1886	40 – 400	10	Roto-translational
N_2–CH_4	0.02 – 1379	40 – 400	10	Roto-translational
H_2–H_2	0.02 – 2400[a] 2400[b]	40 – 400	10	Roto-translational
	20 – 10000	200 – 3000	113	Roto-translational, Fundamental, 1st overtone
H_2–He	0.02 – 2400[a] 2400[b]	40 – 400	10	Roto-translational
	20 – 20000	200 – 9900	334	Roto-translational, Fundamental, 1st to 4th overtone
H_2–CH_4	0.02 – 1946[a] 1946[b]	40 – 400	10	Roto-translational
H_2–H	100 – 10000	1000 – 2500	4	Roto-translational, Fundamental, 1st overtone
He–H	50 – 11000	1500 – 10000	10	Roto-translational
O_2–O_2	1150 – 1950	193 – 353	15	Fundamental
	7450 – 8487	253 – 296	3	$a^1\Delta_g \leftarrow X^3\Sigma_g^-$ (0–0)
	9001 – 9997	296	1	$a^1\Delta_g \leftarrow X^3\Sigma_g^-$ (1–0)
	12600 – 13839	200 – 300[c]	1	A Band
	14996 – 29790	294	1	$a^1\Delta_g \rightarrow a^1\Delta_g$, $b^1\Sigma_g^+ \rightarrow a^1\Delta_g$, and $b^1\Sigma_g^+ \rightarrow b^1\Sigma_g^-$
O_2–N_2	7500 – 8600	200 – 295	7	$a^1\Delta_g \leftarrow X^3\Sigma_g^-$ (0–0)
	9000 – 10000	200 – 295	5	$a^1\Delta_g \leftarrow X^3\Sigma_g^-$ (1–0)
	12600 – 13839	200 – 300[c]	1	A Band
O_2–CO_2	12600 – 13839	200 – 300[c]	1	A Band
CO_2–CO_2	1 – 250	200 – 800	7	Roto-translational
CH_4–CH_4	0.02 – 990	40 – 400	10	Roto-translational
CH_4–Ar	1 – 697	70 – 296	5	Roto-translational

Systems highlighted in orange are provided in the main folder, while systems highlighted in green are provided in the alternate folder.
[a] refers to the "equilibrium" data
[b] refers to the "normal" data
[c] in this specific case, data between 200 and 300 K are the same and the temperature chosen for HITRAN is 296 K (room-temperature)

HITRAN on the Web

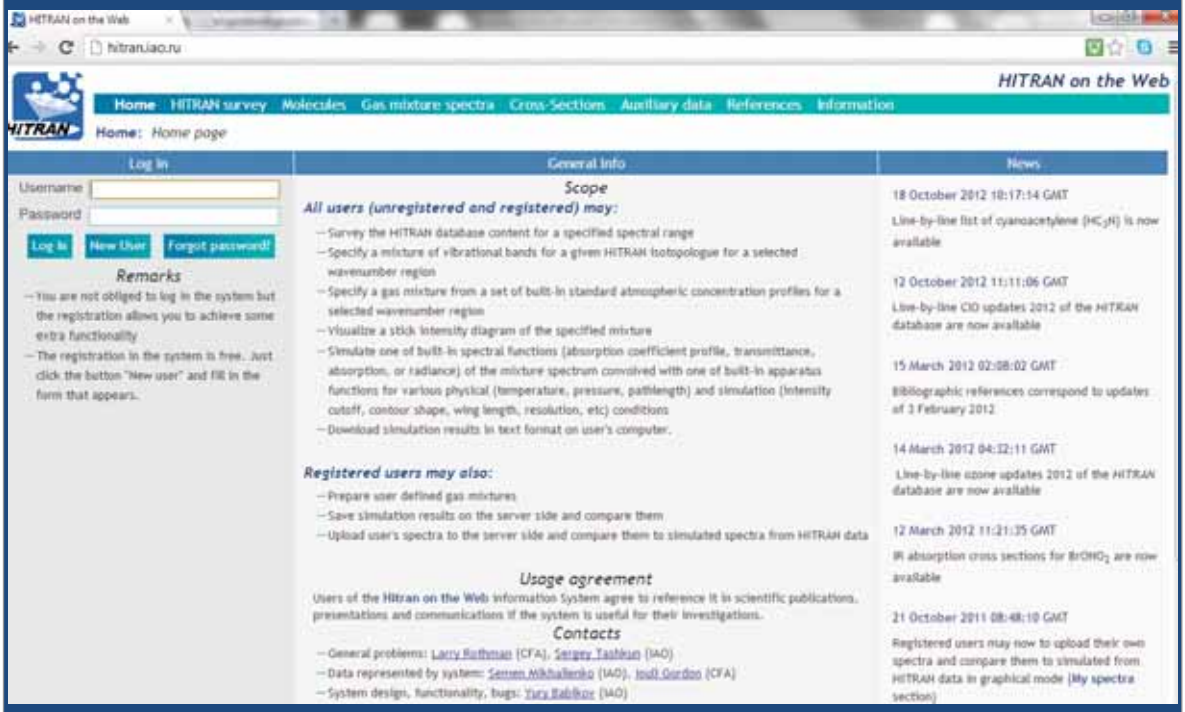

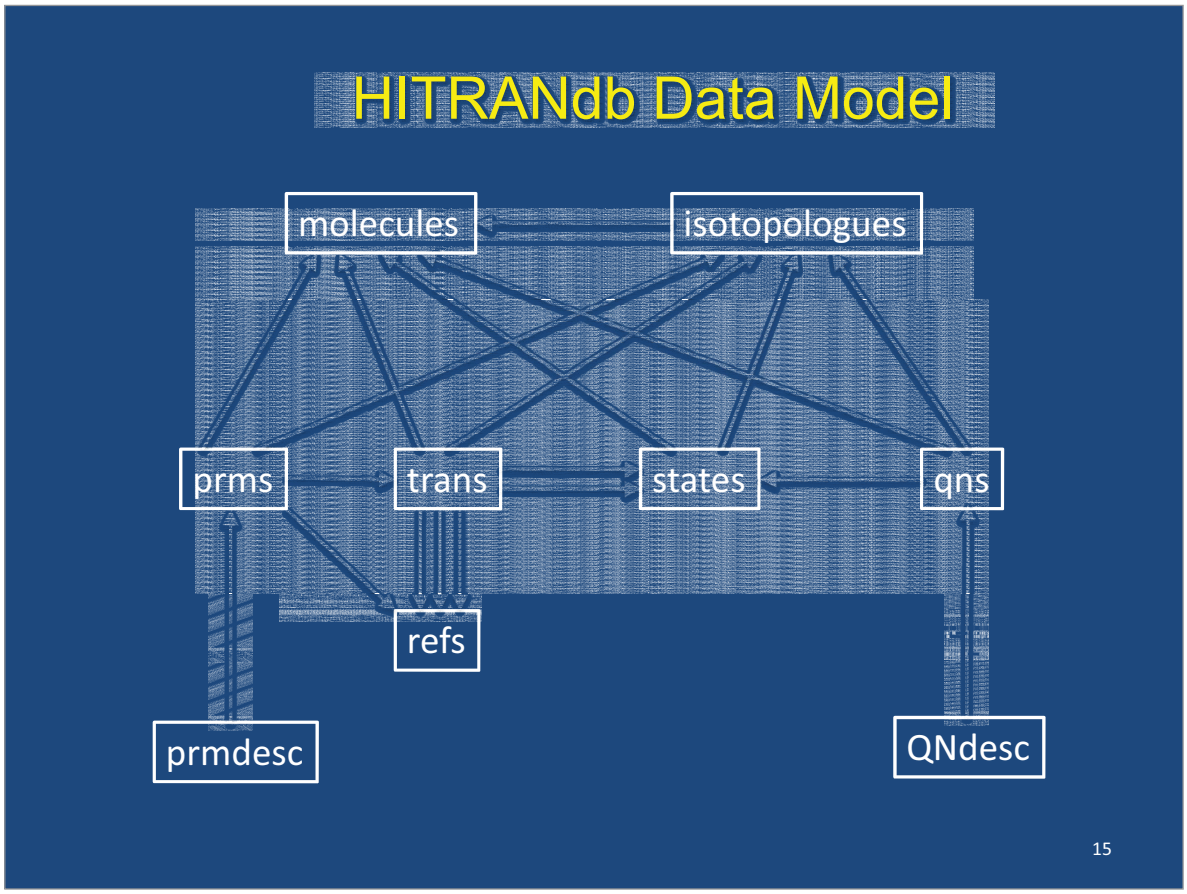
HITRANdb Data Model
molecules
isotopologues
prms
trans
states
qns
refs
prmdesc
QNdesc
15

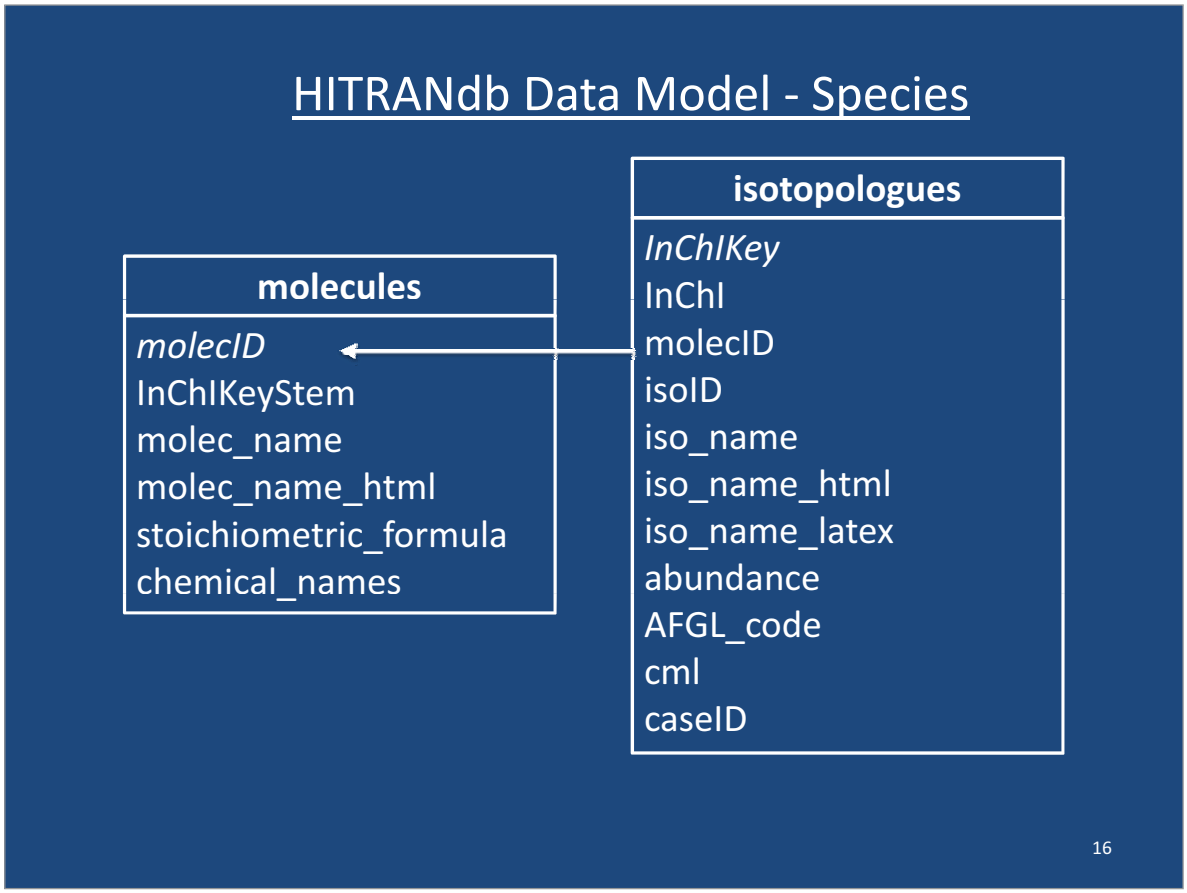
HITRANdb Data Model - Species
molecules
molecID
InChIKeyStem
molec_name
molec_name_html
stoichiometric_formula
chemical_names
isotopologues
InChIKey
InChI
molecID
isoID
iso_name
iso_name_html
iso_name_latex
abundance
AFGL_code
cml
caseID
16

HITRANdb Data Model – Transitions and States

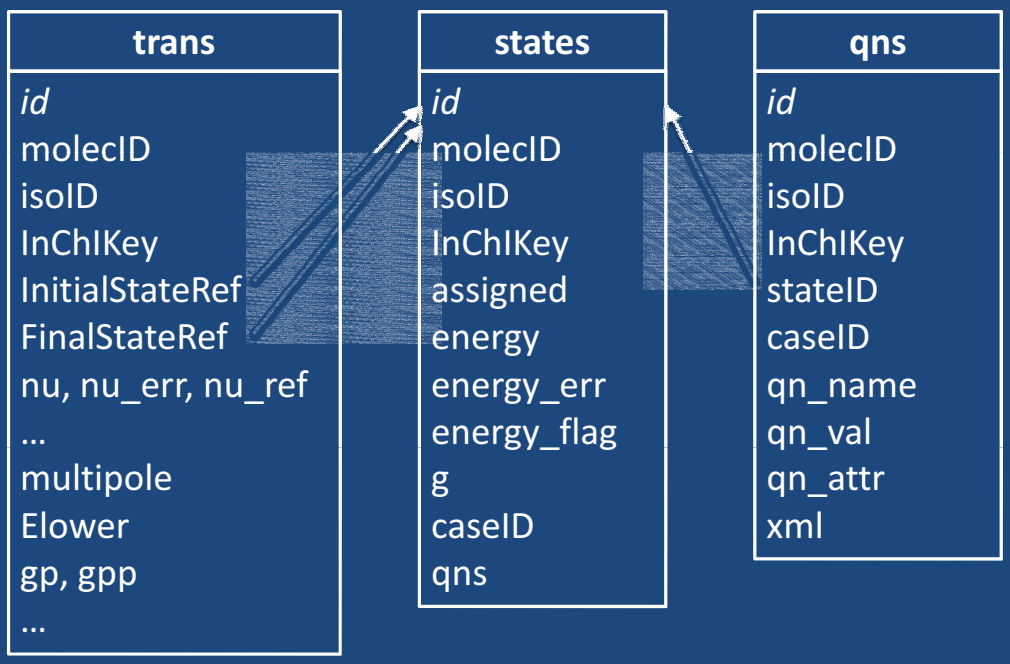

17

HITRANdb Data Model – Line Parameters

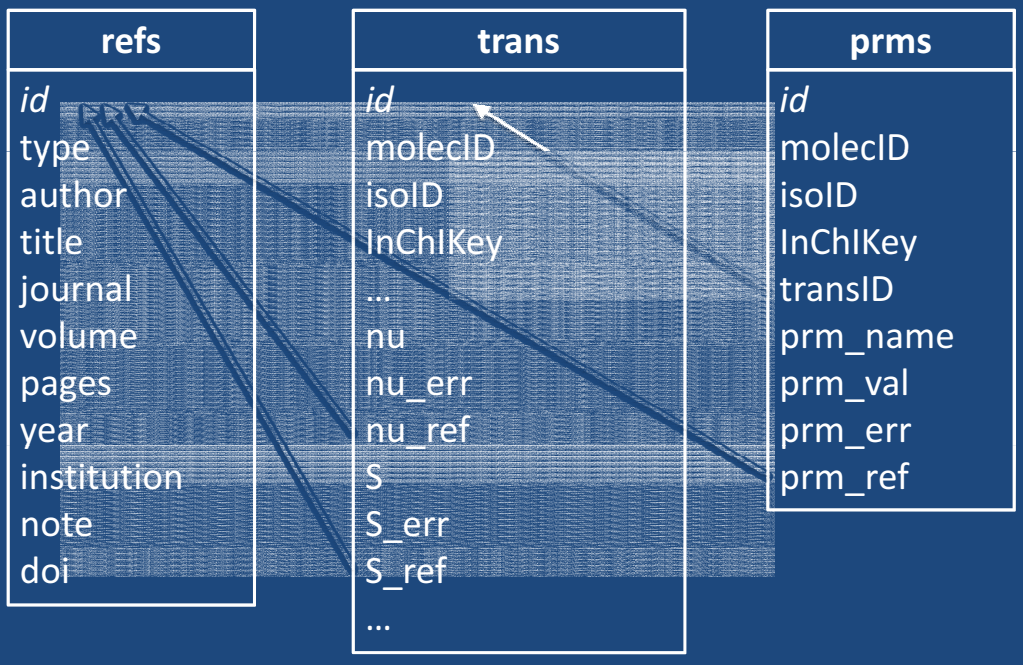

18

History of citations to HITRAN

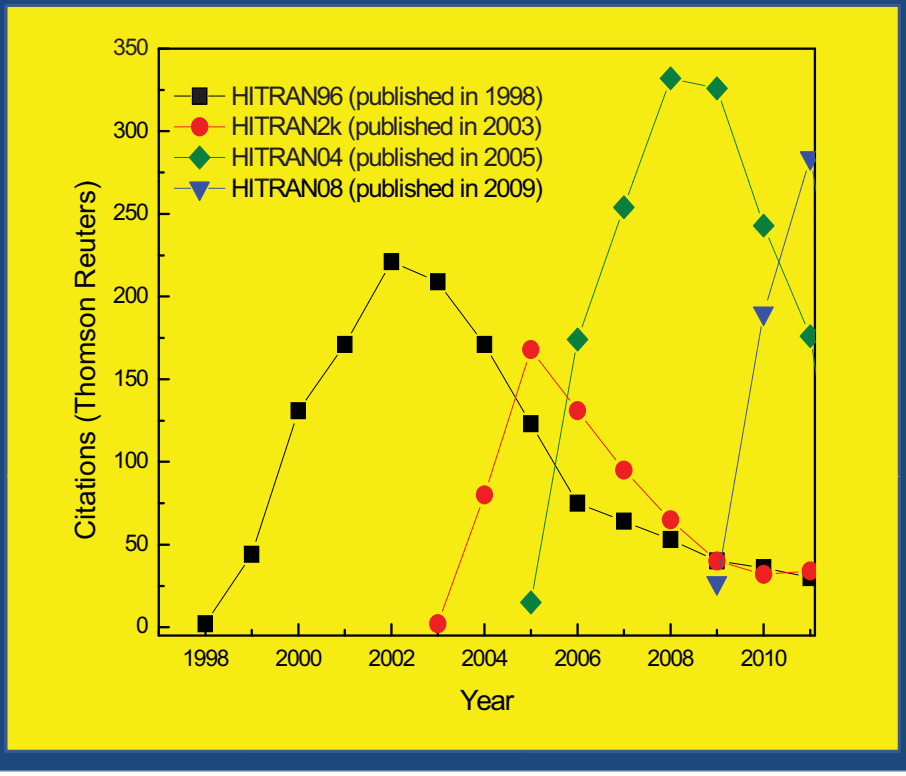

Applications of HITRAN

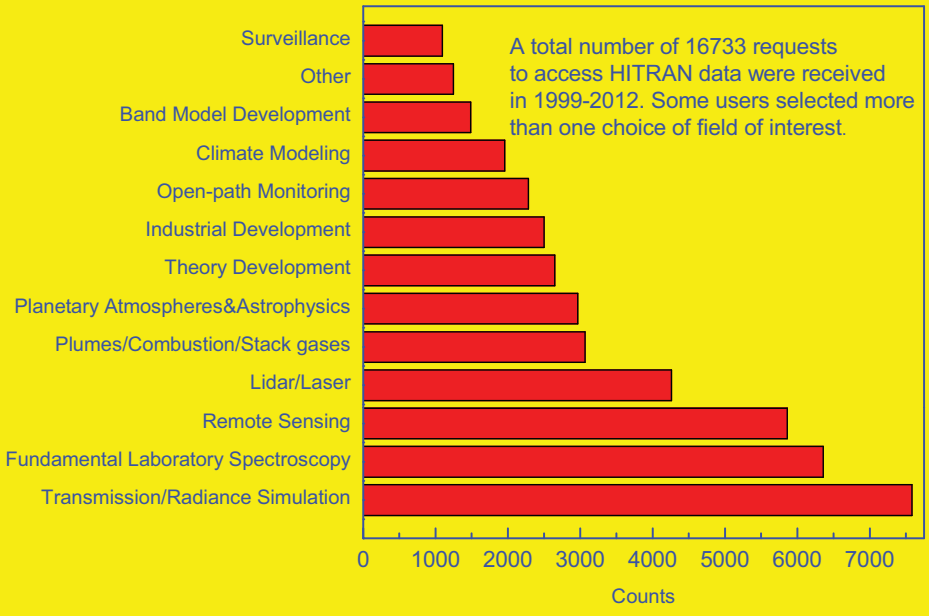

Pros and Cons of Experimental Data

- Advantages
  - Low uncertainty in determining parameters of relatively strong unblended lines
  - Direct observation of perturbations which often hard to account for with theoretical methods
- Disadvantages
  - Large uncertainty in determining parameters of weak or saturated lines
  - Sensitivity to impurities and congested spectra
  - Difficulties in controlling the conditions
  - Difficulties in covering large spectral and dynamic ranges simultaneously

Intercomparison of experimental measurements of water lines air-broadening in different laboratories

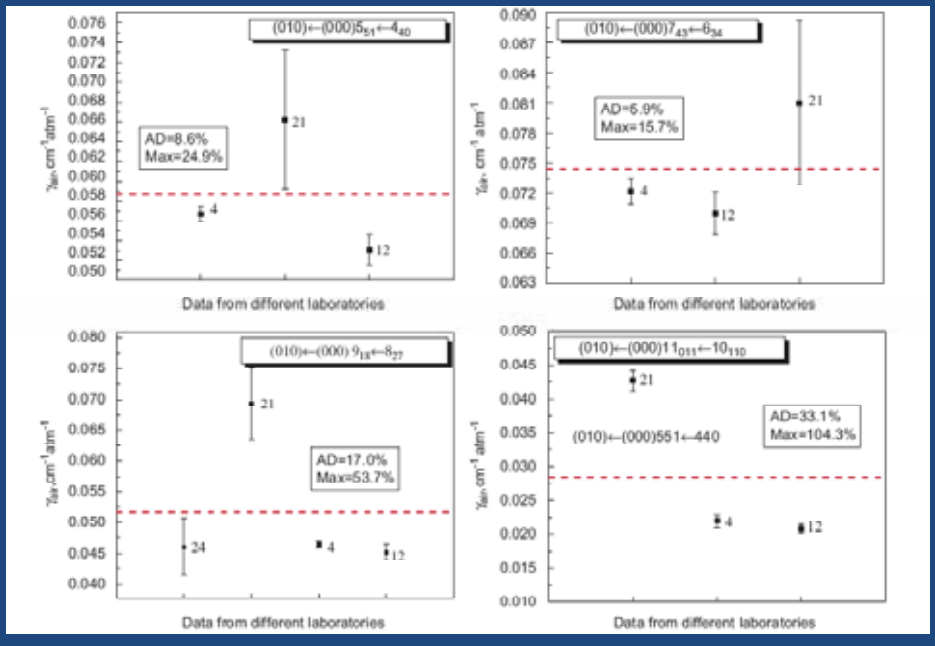

Intercomparison of experimental data

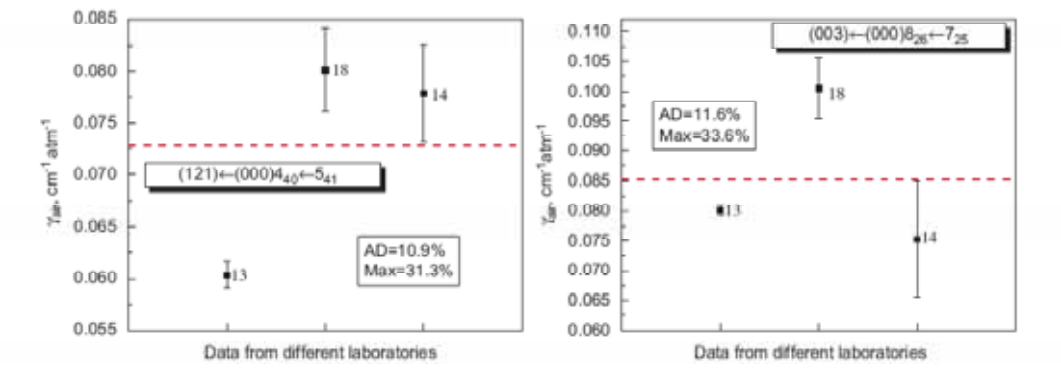

Gordon *et al*, *JQSRT* **108** (2007) 389–402

Pros and Cons of Theoretical and Semi-Empirical Data

- Advantages
  - Completeness, i.e. prediction of parameters that could not be measured by experiment
  - Can be easily adjusted to match high quality experiments
- Disadvantages
  - Rarely can compete with experimental uncertainty
  - Sometimes the model is oversimplified
  - Semi-empirical methods often lead to large errors when used for extrapolating the data

CO_2 data assembly for HITRAN2008 in the operational region of GOSAT and OCO-2 satellites

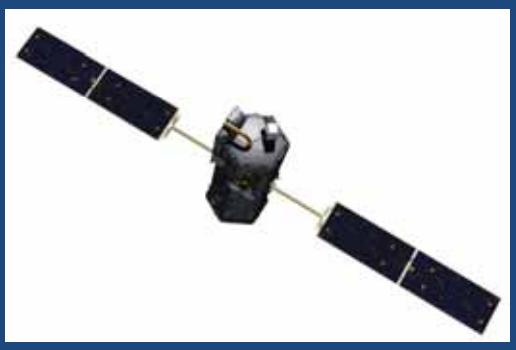

Sources for CO_2 data (4300-7000 cm^{-1})

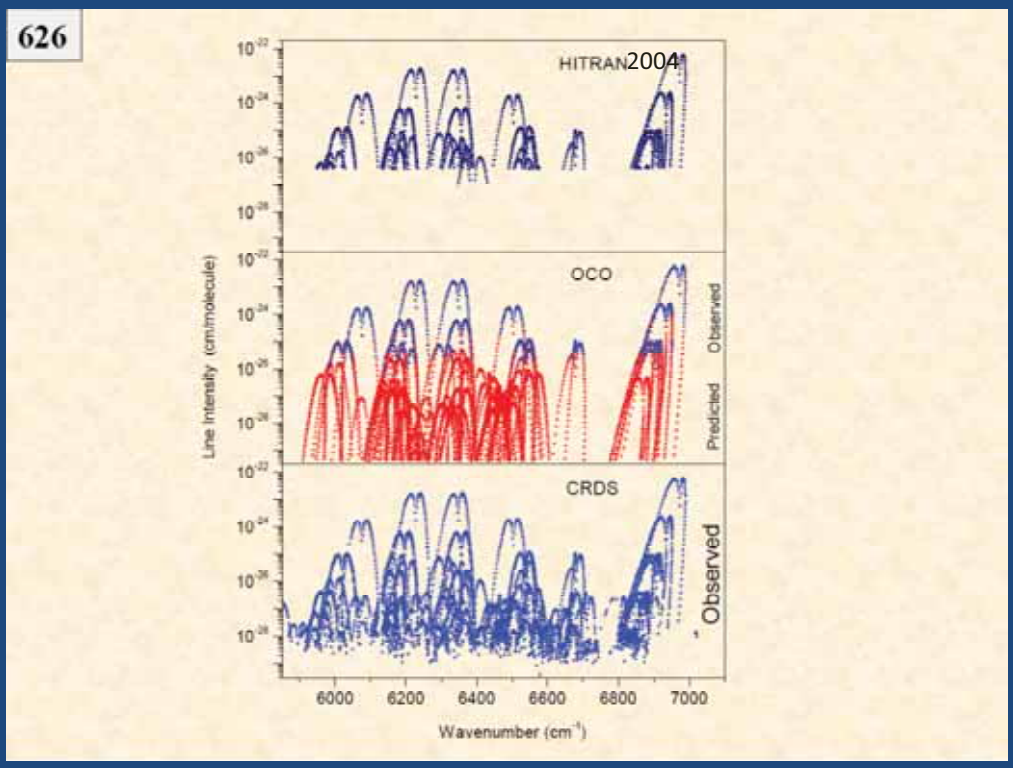

Assessment of Sources for CO_2 data (4300-7000 cm^{-1})

	Pros	*Cons*
JPL-OCO (FTS experiments)	• Very accurate observations for the strongest bands • Pressure shifts and self and air broadening coefficients	•Incomplete < 10^{-26} cm^{-1}/(molecule cm^{-2}) •Extrapolations down to **$4x10^{-30}$** cm^{-1}/(molecule cm^{-2}) show large deviations •Traceability
CRDS (Grenoble)	• Nearly complete above **$5x10^{-29}$** cm^{-1}/(molecule cm^{-2})	•Typical accuracy **$1x10^{-3}$** cm^{-1} • Limited spectral rane
CDSD (Effective Hamiltonian Calculations)	• Complete (at least for 626, 636 and 628) • Excellent predictive abilities for positions and intensities	•Interpolyad coupling •Cannot reproduce JPL accuracy

Algorithm for CO_2 assembly in HITRAN (4300-7000 cm^{-1})

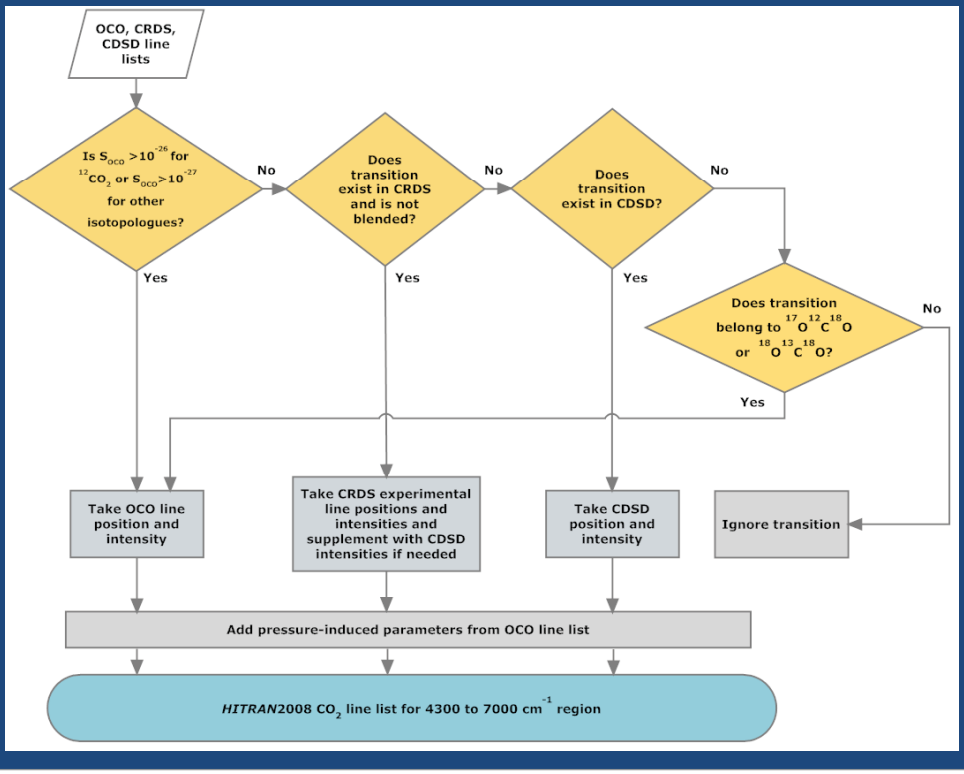

Traditional method of constructing semi-empirical DMF for diatomic molecules

Step 1:

Herman-Wallis fitting of the measurements in the individual vibrational bands

$$S = I_a \frac{8\pi^3}{3hc} e^{-c_2 E''/T_0}\left(1 - e^{-c_2 \nu/T_0}\right) g_i g_s |m| \boldsymbol{R}_{12} \times 10^{-36}$$

$$|\langle \upsilon J' | M(x) | 0 J'' \rangle|^2 = |R_{\upsilon 0}(0)|^2 (1 + C_\upsilon m + D_\upsilon m^2 + \ldots),$$

Herman-Wallis fitting

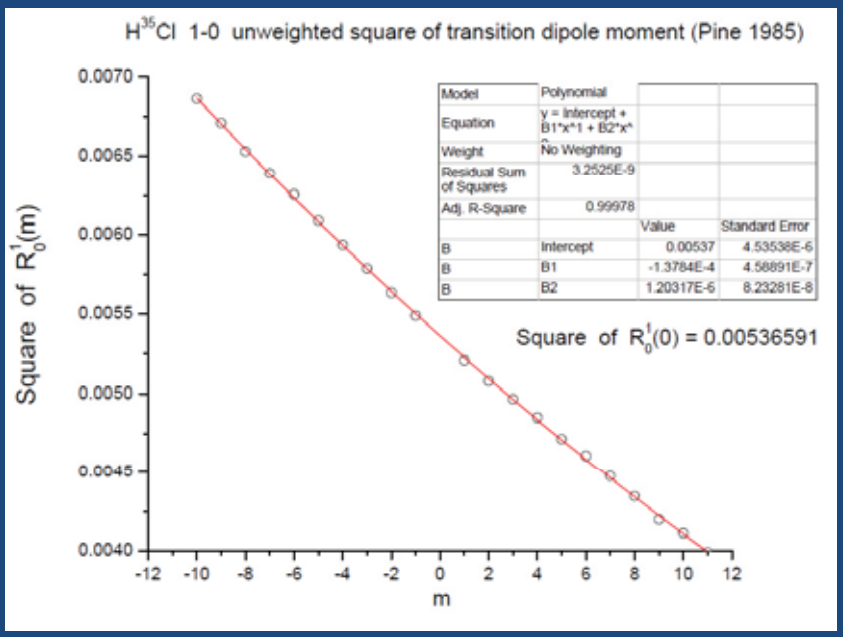

$$|\langle \upsilon J' | M(x) | 0 J'' \rangle|^2 = |R_{\upsilon 0}(0)|^2 (1 + C_\upsilon m + D_\upsilon m^2 + \ldots),$$

Traditional method

Step 1:

Herman-Wallis fitting of the measurements in the individual vibrational bands

Step 2:

Rotationless squares of the transition dipoles are fitted to the polynomial expressions

$$M(r) = \sum_i M_i x^i, \quad x = \frac{r - r_e}{r_e}$$

$$\langle vJ' | M(x) | 0J'' \rangle = \sum_{i=1}^{n} M_i \langle vJ' | x^i | 0J'' \rangle \ , \ J'=J''=0$$

Disadvantages of the traditional method and suggested alternatives

- Disregard of the rotational information
- Dependence on the amount of data within the same vibrational band
- Disregard of the experimental uncertainties

Kiriyama F, Rao BS, Nangia VK. Electric dipole moment function of $H^{35}Cl$. JQSRT 2001;69:35-40, suggested to fit all of the intensities to DMF.

$$\langle vJ' | M(x) | 0J'' \rangle = \sum_{i=1}^{n} M_i \langle vJ' | x^i | 0J'' \rangle$$

Flaws in Kiriyama et al. approach

- Still carried out the Hermann-Wallis fit to "smooth" experimental data
- Dependence on the amount and relative quality of the data within the same vibrational band
- Disregarded the experimental uncertainties
- Incorrect treatment of isotopic abundance when treating experimental data from Pine et al (1-0) and Toth et al (2-0)

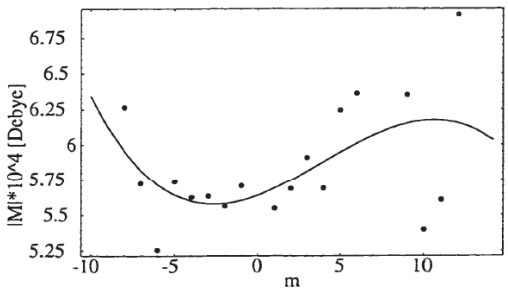

Figure 8. Matrix Elements and the Best Fit Polynomial (3rd order fit) in the 3-0 Band of HCl Using Line Strengths Measured by Ogilvie and Lee. [26].

Proposed approach

- Calculate expectation values using RKR or empirical potential
- Do a least squares fit to obtain M_i coefficients. Every ro-vibrational measurement is included with appropriate weight

$$\langle vJ'|M(x)|0J''\rangle = \sum_{i=1}^{n} M_i \langle vJ'|x^i|0J''\rangle$$

Input parameters

1-0

- Pine AS, Fried A, Elkins JW, J Mol Spectrosc 1985;109:30-45.

2-0

- a) Toth RA, Hunt RH, Plyler EK, J Mol Spectrosc 1970;35:110-26.
  b) De Rosa M, Nardini C, Piccolo C, Corsi C, D'Amato F, Appl Phys B: Lasers Opt 2001;72:245-8.
  c) Ortwein P, Woiwode W, Wagner S, Gisi M, Ebert V. , Appl Phys B: Lasers Opt 2010;100:341-7.

3-0

- a) Ogilvie JF, Lee Y-P, Chem Phys Lett 1989;159:239-43.
  b) Stanton AC, Silver JA, Appl Opt 1988;27:5009-15.

4-0 to 7-0

- a) Gelfand J, Zughul M, Rabitz H, Han CJ, JQSRT 1981;26:303-5.
  b) Reddy KV, J Mol Spectrosc 1980;82:127-37.

Obtained dipole moment function

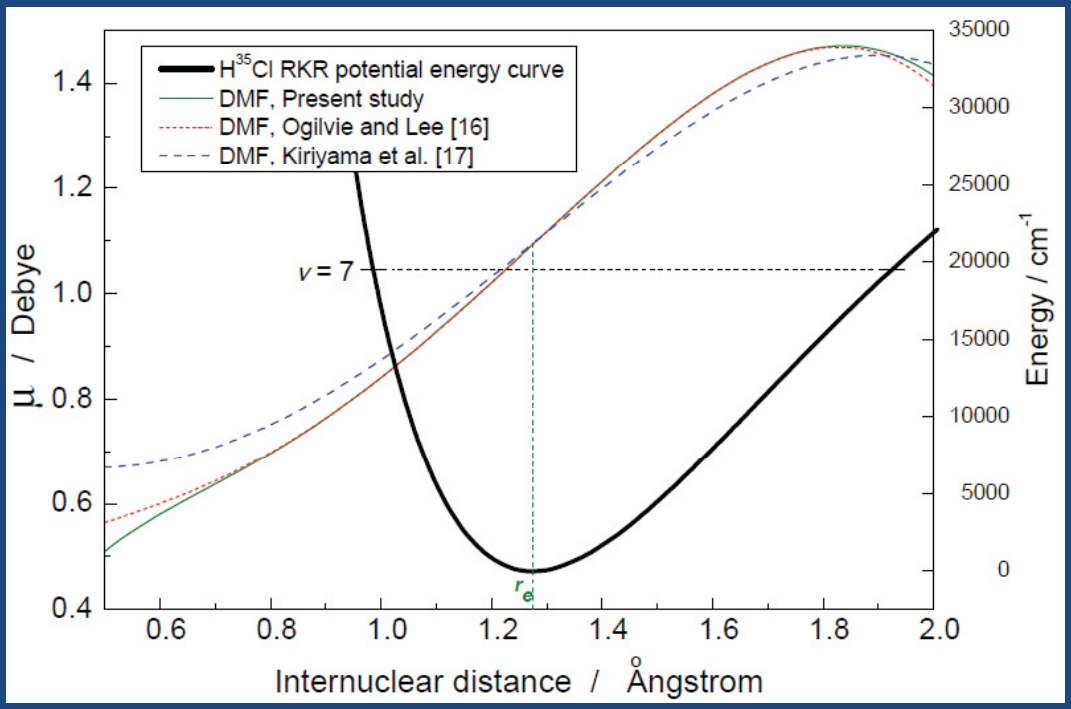

2-0 HCl line intensities

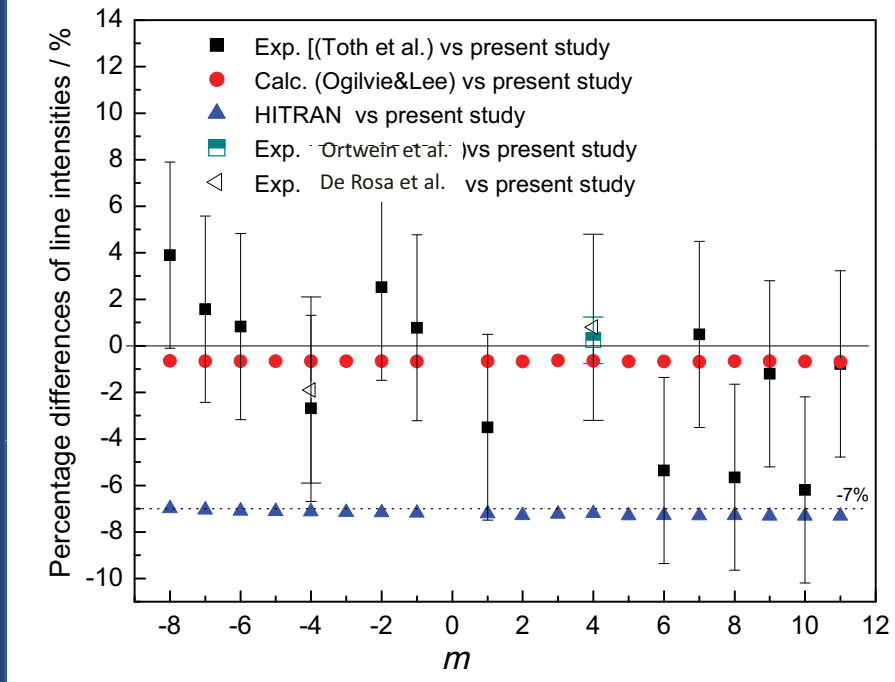

3-0 HCl line intensities

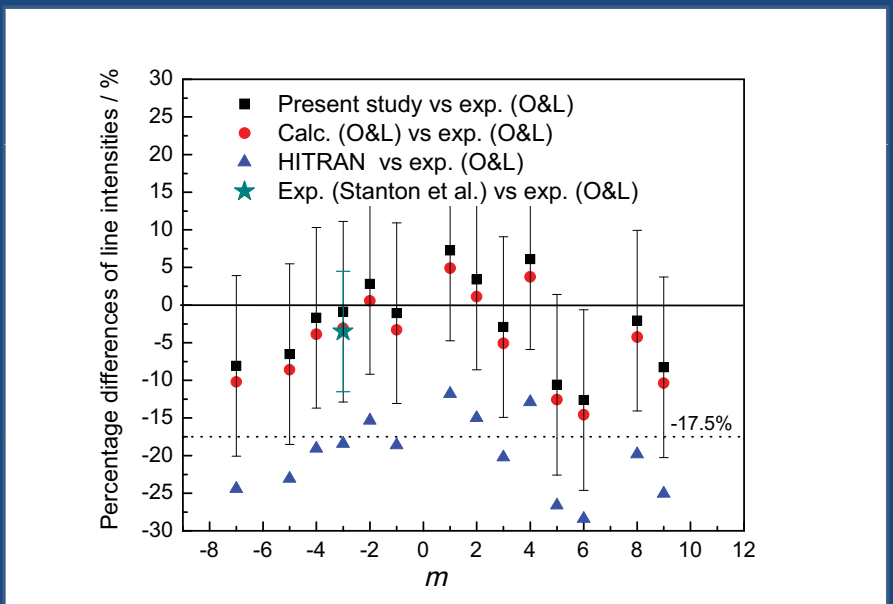

O&L- Ogilvie JF, Lee Y-P, Chem Phys Lett 1989;159:239-43.

5-0 HCl line intensities

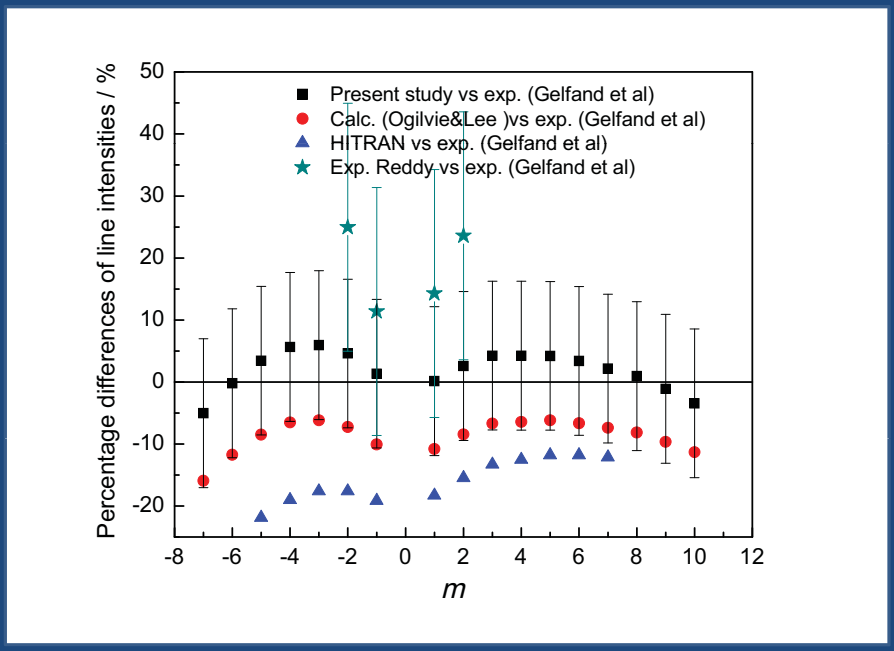

The general plan for H_2O

- Release intensity cut off and add missing lines. When no reliable measurements are available use line positions calculated from empirical energy levels and use ab initio intensities. There will be no unassigned lines.
- In certain regions intensities will be replaced with ab initio values (after rigorous evaluation).
- Update ν_2 band-region with semi-empirical intensities, Coudert et al and line shape parameters Birk and Wagner.
- Broadening parameters and their temperature dependences will be re-evaluated after corrections to CRB calculations by Gamache et al will be made.
- Line shifts for HDO lines will be added [Jenouvrier *et al*, *JQSRT* ***105, 326-355 (2007)***]
- Isotopologues line lists from semi-empirical/ab initio work of Tennyson et al.

40

The general plan for Carbon Dioxide (CO_2)

- Replace old DND calculations. Replace with validated new experimental values or with CDSD calculations.
- Include newest experimental results. Many new measurements predominantly from groups in Paris and China, analyzed in Tomsk.
- Multispectrum fit. Evaluate applicability of work of Benner et al for OCO-2 mission.
- Line-shape parameters. Change broadening parameters for J > 50 (Lamouroux et al, *JQSRT* (2012)); Use algorithm developed by Hartmann et al, *JQSRT* (2009) for unmeasured shifts; extend line-mixing work of Lamouroux et al, *JQSRT* (2010) to entire carbon-dioxide line list.

Methane (CH_4)

Many, many recent theoretical and experimental works by the groups at Grenoble, Reims, Dijon, Tomsk, JPL, NASA Langley...

- 1.26 - 1.71 µm region. Extensive cavity ring down experiments by Campargue et al.
- 2 µm region. For example, octad region FTS work of Daumont et al (Reims group).
- Deuterated species. Nikitin et al. Grenoble, Reims, Tomsk, JPL
- Line-shape parameters. New broadening parameters by Smith et al, *JQSRT* (2010 and 2011).

Improvements of Parameters for O_2

- A-, B-, and γ-Bands ($b\ ^1\Sigma_g^+$ level)
  - Positions and intensities of transitions
  - Self- and air-broadened half widths
  - Pressure shifts
  - Isotopologues ($^{16}O^{18}O$, $^{16}O^{17}O$)
  - Introduce line mixing
- Singlet-Delta bands ($a\ ^1\Delta_g$ level)
  - Positions and intensities of transitions
  - Self- and air-broadened half widths
  - Pressure shifts
  - Quadrupole transitions
- Microwave lines ($X\ ^3\Sigma_g^-$ ground state)
  - Positions
  - Intensities of high-rotational transitions
  - Self- and air-broadened half widths
  - Isotopologues ($^{16}O^{18}O$, $^{16}O^{17}O$)

Improvements and Enhancements to the Compilation being considered

- More temperature-pressure sets of cross-sections (IR and UV)
- Improved database structure (VAMDC paradigm)
- Additional high-temperature parameters (for HITEMP)
- Molecules for astrophysics applications
- Refined line-shape parameters
- Additional line-mixing algorithms
- More Collision-Induced Absorption bands

44

Acknowledgements

- HITRAN advisory committee
- Other contributors and users who validate the data
- NASA funding

"The GEISA Spectroscopic Database for Atmospheric Remote Sensing: Content Description and Critical Evaluation"

Johannes Orphal on behalf of N. Jacquinet-Husson

Ecole Polytechnique

The GEISA Spectroscopic Database for Atmospheric Remote Sensing: Content Description and Critical Evaluation

Nicole Jacquinet-Husson, Cherif Boutammine, Raymond Armante, Laurent Crepeau, Alain Chedin, Noelle Scott, Cyril Crevoisier, Virginie Capelle

Laboratoire de Météorologie Dynamique (LMD), Ecole Polytechnique, 91128 Palaiseau, France

For the remote sensing of planetary atmospheres from satellite spectra measurements, an essential prerequisite is the availability of a high accuracy forward radiative transfer modeling. Related to the strong impact of the quality of the reference spectroscopic information on the research in direct and inverse planetary radiative transfer, there is an acute and constant demand for validated, operational and interactive public spectroscopic databases. In this context, the ARA group at LMD (http://ara.abct.lmd.polytechnique.fr) develops and maintains, for over three decades, GEISA1 (Gestion et Etude des Informations Spectroscopiques Atmosphériques: Management and Study of Atmospheric Spectroscopic Information), a computer accessible database system. GEISA, in its latest edition, comprises three independent sub-databases devoted respectively to: line parameters (50 molecules involved, including 111 isotopes, for a total of 3 794 426 entries, in the spectral range from 10^{-6} to 35 877.031 cm^{-1}), infrared and ultraviolet absorption cross-sections, microphysical and optical properties of atmospheric aerosols. It is used on-line by more than 300 laboratories working in the domains of atmospheric physics, astronomy and astrophysics, and planetology.

The role of molecular spectroscopy in modern atmospheric research has entered a new phase with the launches of highly sophisticated spectroscopic instruments, like IASI on Metop-A (since October 2006) and Metop-B (since September 2012) (http://www.eumetsat.int/Home/Main/Satellites/Metop/index.htm?l=en). In this context, GEISA is the reference basis for the validation of the level-1 IASI (http://smsc.cnes.fr/IASI/index.htm) data (http://smsc.cnes.fr/IASI/index.htm), using the 4A radiative transfer model2 (4A/LMD; 4A/OP co-developed by LMD and Noveltis- http://www.noveltis.fr/, with the support of CNES). Consequently, GEISA/IASI spectroscopic database has been initiated since 1997. It is a sub-set, within the 599-3001 cm-1 spectral range, of the whole GEISA.

The summarized content and access of each of the three sections of the GEISA and GEISA/IASI 2011 editions will be presented. The quality requirements for spectroscopic line parameters will be specified with a specific emphasis for detailed assessment of the line parameter differences between GEISA and HITRAN.

GEISA is freely accessible from the CNRS/CNES/IPSL atmospheric chemistry data center Ether (http://www.pole-ether.fr/) and used on-line by more than 300 laboratories working in the domains of atmospheric physics, astronomy and astrophysics, and planetology.

[1] N. Jacquinet-Husson, L. Crepeau, R. Armante, C. Boutammine, A. Chedin, N. A. Scott, C. Crevoisier, V. Capelle, C. Boone, N. Poulet-Crovisier, A. Barbe, A. Campargue, D. Chris Benner, Y. Benilan, B. Bezard, V. Boudon, L. R. Brown, L. H. Coudert, A. Coustenis, V. Dana, V. M. Devi, S. Fally, A. Fayt, J.-M. Flaud, A. Goldman, M. Herman, G. J. Harris, D. Jacquemart, A. Jolly, I. Kleiner, A. Kleinböhl, F. Kwabia-Tchana, N. Lavrentieva, N. Lacome, Li-Hong Xu, O. M. Lyulin, J.-Y. Mandin, A. Maki, S. Mikhailenko, C.E. Miller, T. Mishina, N. Moazzen-Ahmadi, H. S. P. Müller, A. Nikitin, J. Orphal, V. Perevalov, A. Perrin, D. T. Petkie, A. Predoi-Cross, C. P. Rinsland, J. J. Remedios, M. Rotger, M. A. H. Smith, K. Sung, S. Tashkun, J. Tennyson, R. A. Toth, A.-C. Vandaele, J. Vander Auwera, J. Quant. Spectrosc. Radiat. Transf.,112, 2395, 2011.
[2] N. A. Scott, A. Chedin, J. Appl. Meteor., 20,556, 1981.

The GEISA Spectroscopic Database for Atmospheric Remote Sensing: Content Description and Critical Evaluation

http://ara.abct.lmd.polytechnique.fr

Presentation by J. Orphal on behalf of

N. Jacquinet-Husson,
Ch. Boutammine,
R. Armante, L.Crépeau,
A. Chédin, N.A. Scott,
C. Crevoisier, V. Capelle

Laboratoire de Météorologie Dynamique
Atmospheric Radiation Analysis Group/ABC(t)
Ecole Polytechnique
91128 Palaiseau, France

GEISA: Gestion et Etude des Informations Spectroscopiques Atmosphériques ; Management and Study of Atmospheric Spectroscopic Information

OUTLINE

[1] GEISA System General Overview

[2] Summary of Differences for Molecular Species Cataloged in the Line Parameter Portion of GEISA-09 and HITRAN 2008

[3] Critical Evaluation of Spectroscopic Parameter Differences an Example: *H_2O GEISA-11 and HITRAN-08 comparison*

[4] GEISA System Comprehensive Interactive Free distribution

[1] GEISA-11 SYSTEM GENERAL CONTEXT

- GEISA is a computer-accessible Spectroscopic Database designed for accurate forward atmospheric radiative transfer calculations using a line-by-line (atmospheric) layer-by-layer approach.

spectral range 10^{-6} – 35,877 cm^{-1}
10^{10} – 0.28 µm

GEISA: Gestion et Etude des Informations Spectroscopiques Atmosphériques ;
Management and Study of Atmospheric Spectroscopic Information

[1] FROM SATELLITE OBSERVATIONS TO CLIMATE VARIABILITY AND EVOLUTION ANALYSIS: a long process based on RadiativeTransfer

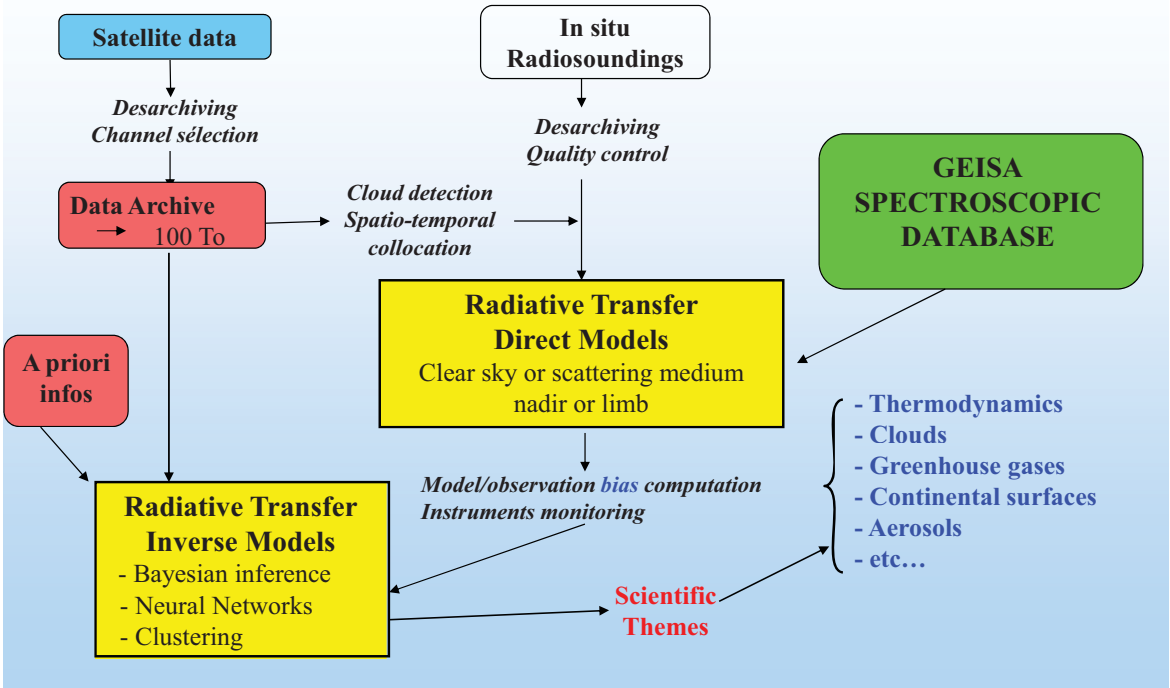

Courtesy A. Chédin, Trattoria/CNES
23 April 2008

[1] GEISA-2011 System Overall Description

spectral range 10^{-6} - 35,877 cm^{-1} *(1010 - 0.28 µm)*

MANAGEMENT SOFTWARES and DISTRIBUTION http://www.pole-ether.fr

Three SUB-DATABASES

- Line parameters sub-database
  - 50 molecules (111 isotopic species)
  - 3,794,426 entries in the spectral range 10^{-6} and 35,877 cm^{-1}
  - ➢ Major permanent constituants of EARTH atmosphere : O_2, H_2O, CO_2 …
  - ➢ Trace molecules in EARTH atmosphere : NO, SO_2, NO_2, NH_3, HNO_3, OH,HF, HCl, HBr, HI, ClO, OCS, H_2CO, PH_3 ,..
  - ➢ Molecules in atmospheres of JUPITER, SATURN, URANUS,TITAN etc.: C_6H_6, CH_3D, C_2H_2, C_2H_4, GeH_4, HCN, C_3H_8, C_3H_4

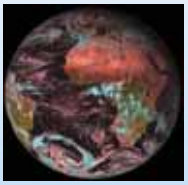

(MSG-2 25/01/06)
EARTH

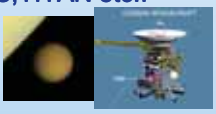

(CASSINI-HUYGENS 29/01/06 TITAN)

- Absorption cross-sections sub-database
  - IR: 39 molecular species (mainly CFC's)
  - UV/Visible : 17 molecular species
- Microphysical and optical properties of atmospheric Aerosols sub-database

GEISA 2013 UPDATE UNDERWAY

EUMETRISPEC workshop on traceable spectral reference for atmospheric monitoring , PTB, Braunschweig, Germany, 14-16 November 2012

[1] GEISA-11 Line Parameters Sub-database Evolution since 1978

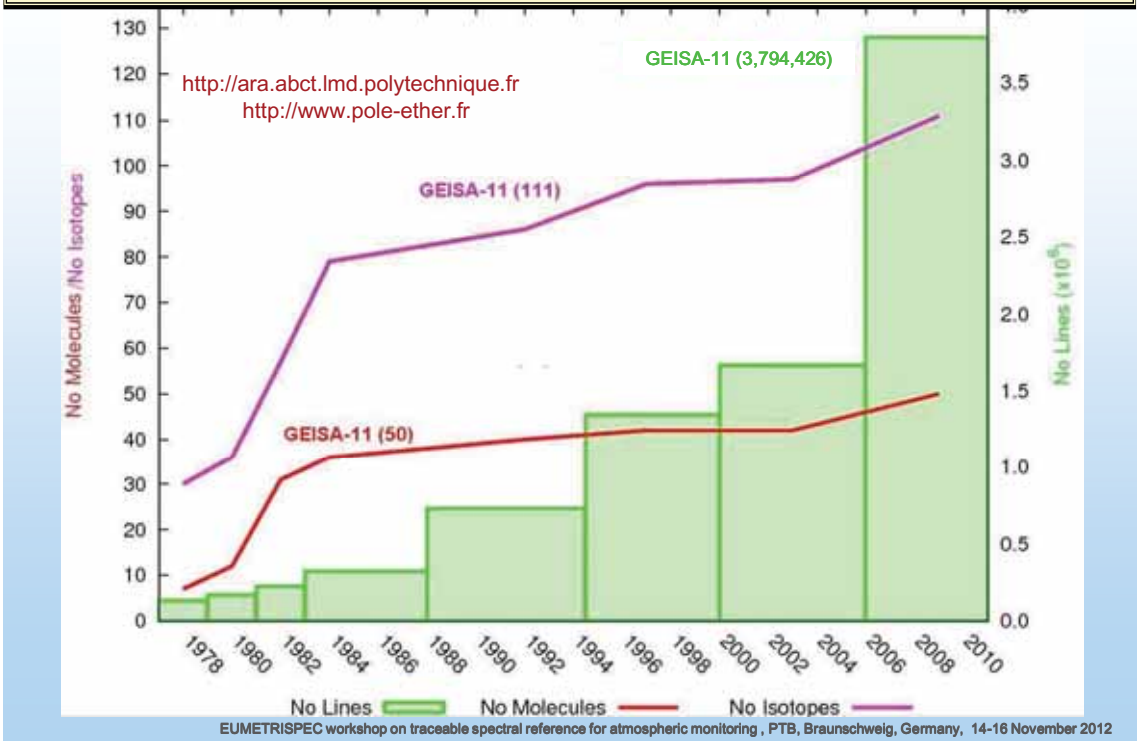

EUMETRISPEC workshop on traceable spectral reference for atmospheric monitoring , PTB, Braunschweig, Germany, 14-16 November 2012

[1] GEISA-11: Line Parameters Sub-database Content

Mole	Spectral range (cm^{-1})	# lines
H_2O	0.007 – 25,232.004	67,504
CO_2	5.891 – 12,784.053	413,524
O_3	0.0263 - 6395.379	389,378
N_2O	0.838 – 7,796.633	50,633
CO	3.414 – 8,464.882	13,515
CH_4	0.001 – 9,199.284	240, 858
O_2	0.000 – 15,927.230	6,428
NO	0.000 - 9273.214	105,079
SO_2	0.0174 – 4,092.948	68,728
NO_2	0.498 – 3,074.152	104,223
NH_3	0.058 – 5,294.501	29,082
PH_3	17.805 - 3601.652	20,364
HNO_3	0.0119 – 1,769.982	669,988
OH	0.005 – 35,877.031	42,866
HF	41.111 – 11,535.570	107
HCl	20.240 – 13,457.841	533

Mole	Spectral range (cm^{-1})	# lines
HBr	16.232 – 9,758.564	1,294
HI	12.509 – 8,487.305	806
ClO	0.015 – 1,207.639	7,230
OCS	0.381 – 4,199.671	33,809
H_2CO	0.000 – 3,099.958	37,050
C_2H_6	706.601501 - 961.145	28,439
CH_3D	7.760 – 6,510.326	49,237
C_2H_2	604.774 – 9,889.038	11,340
C_2H_4	701.203 – 3,242.172	18,378
GeH4	1,937.371 – 2,224.570	824
HCN	0.006 – 17,581.010	81,889
C_3H_8	700.015 - 799.930	8,983
C_2N_2	203.955 – 2,181.690	2,577
C_4H_2	191.635 - 730.235	119,480
HC_3N	463.604 - 759.989	179,347
HOCl	0.0236 – 3,799.682	17,862

Mole	Spectral range (cm^{-1})	# lines
N_2	1,992.628 – 2,625.497	120
CH_3Cl	674.143 – 3,172.927	18,344
H_2O_2	0.043 – 1,730.371	126,983
H_2S	2.985 – 4,256.547	20,788
HCOOH	10.018 – 1,889.334	62,684
COF2	725.005 – 2,001.348	70,904
SF_6	588.488 - 975.788	92,398
C_3H_4	288.913 - 673.479	19,001
HO_2	0.173 – 3,675.819	38,804
$ClONO_2$	0.636 - 797.741	356,899
CH_3Br	794.403 – 1,705.612	36,911
CH_3OH	0.019 – 1,407.206	19,897
NO+	1,634.831 – 2,530.462	1,206
HNC	0.217 – 4,814.904	5,619
C_6H_6	642.427 - 705.262	9,797
C_2HD	416.785 – 3,421.864	15,512
CF_4	594.581 – 1,312.648	60,033
CH_3CN	890.052 – 1,650.000	17,172

50 Molecules 111 isotopes
Total # lines 3,794,426

EUMETRISPEC workshop on traceable spectral reference for atmospheric monitoring , PTB, Braunschweig, Germany, 14-16 November 2012

Archived Spectroscopic Line Parameters
(GEISA specific field of line format)

- **A** Wavenumber (cm^{-1}) of the line
- **B** Intensity of the line in (cm^{-1}/(molecule.cm^{-2})
- **C** Air broadening pressure halfwidth (HWHM)(*) ($cm^{-1}atm^{-1}$)
- **D** Energy of the lower transition level (cm^{-1})
- **E** Transition quantum identifications for the lower and upper state of the transition
- **F** Temperature dependence coefficient n of the air broadening HWHM
- **G** Identification code for isotope as in GEISA
- **I** Identification code for molecule as in GEISA
- **J** Internal GEISA code for the data identification
- **K** Molecule number in HITRAN
- **L** Isotope number (1=most abundant. 2= second…etc) in HITRAN
- **M** Einstein A-coefficient (s^{-1}).
- **N** Self broadening pressure HWHM ($cm^{-1}atm^{-1}$) (for water)
- **O** Air pressure shift of the line transition ($cm^{-1}atm^{-1}$)
- **R** Temperature dependence coefficient n of the air pressure shift
- **A'** Estimated accuracy (cm^{-1}) on the line position
- **B'** Estimated accuracy on the intensity of the line in (cm^{-1}/(molecule.cm^{-2})
- **C'** Estimated accuracy on the air collision HWHM ($cm^{-1}atm^{-1}$)
- **F'** Estimated accuracy on the temperature dependence coefficient n of the air broadening HWHM
- **O'** Estimated accuracy on the air pressure shift of the line transition ($cm^{-1}atm^{-1}$)
- **R'** Estimated accuracy on the temperature dependence coefficient n of the air pressure shift
- **N'** Estimated accuracy on the self HWHM
- **T** Self pressure shift of the line transition ($cm^{-1}atm^{-1}$)
- **T'** Estimated accuracy on the self pressure shift of the line transition ($cm^{-1}atm^{-1}$)
- **U** Temperature dependence coefficient n of the self pressure shift
- **U'** Estimated accuracy on the temperature dependence coefficient n of the self pressure shift broadened HWHM ($cm^{-1}atm^{-1}$)
- **S** Temperature dependence coefficient n of the self broadening HWHM
- **S'** Estimated accuracy on the temperature dependence coefficient n of the self- broadening

NEW
Since GEISA-09
Standardized parameter missing values

For each line parameter effective accuracy value information

(*) HWHM: *line half-width at half-maximum*

EUMETRISPEC workshop on traceable spectral reference for atmospheric monitoring , PTB, Braunschweig, Germany, 14-16 November 2012

[3] GEISA and IASI Atmospheric Sounding

IASI
On Metop-A (19/10/2006)
On Metop-B (17/09/2012)

3 Spectral Bands

[1] 645 -1210 cm^{-1}
15.50 – 8.26 μm

[2] 1210 - 2000 cm^{-1}
8.26 – 5.0μm

[3] 2000 - 2760 cm^{-1}
5.0 – 3.62μm

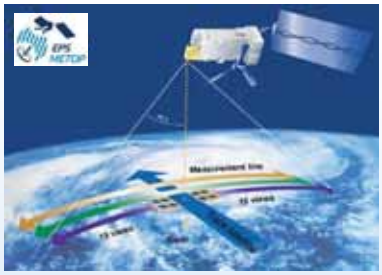

EUMETSAT

Reference Basis for
IASI Level 1 Cal/Val activities @ CNES and @ LMD

cnes

- **GEISA/IASI (599-3001 cm^{-1}) used as the reference spectroscopic database:** ***20 GEISA selected molecules for operational meteorology and trace gas retrievals; 6 IR cross-sections including PANS; associated aerosol components GEISA sub-database.***

- **Validation achieved using 4A/OP line by line Radiative Transfer Model** [Scott & Chédin, J.Appl.Met (1981); 4A/LMD http://ara.abct.lmd.polytechnique.fr;
4A/OP co-developed by LMD and Noveltis with the support of CNES (2006)]

EUMETRISPEC workshop on traceable spectral reference for atmospheric monitoring , PTB, Braunschweig, Germany, 14-16 November 2012

42 co-auteurs
16 laboratoires

ELSEVIER

Journal of Quantitative Spectroscopy & Radiative Transfer 95 (2005) 429–467

The 2003 edition of the GEISA/IASI spectr

53 co-auteurs
27 Laboratoires

ELSEVIER

Journal of Quantitative Spectroscopy & Radiative Transfer 109 (2008) 1043–1059

Journal of Quantitative Spectroscopy & Radiative Transfer

www.elsevier.com/locate/jqsrt

The GEISA spectroscopic database: Current and future archive for Earth and planetary atmosphere studies

N. Jacquinet-Husson[a,*], N.A. Scott[a], A. Chédin[a], L. Crépeau[a], R. Armante[a], V. Capelle[a], J. Orphal[b], A. Coustenis[c], C. Boonne[d], N. Poulet-Crovisier[d], A. Barbe[e], M. Birk[f], L.R. Brown[g], C. Camy-Peyret[h], C. Claveau[h], K. Chance[i], N. Christidis[j],

59 co-auteurs
26 laboratoires

Journal of Quantitative Spectroscopy & Radiative Transfer 112 (2011) 2395–2445

Contents lists available at ScienceDirect

Journal of Quantitative Spectroscopy & Radiative Transfer

journal homepage: www.elsevier.com/locate/jqsrt

ELSEVIER

UPDATED IN 2011

The 2009 edition of the GEISA spectroscopic database

N. Jacquinet-Husson[a,*], L. Crepeau[a], R. Armante[a], C. Boutammine[a], A. Chédin[a], N.A. Scott[a], C. Crevoisier[a], V. Capelle[a], C. Boonne[d], N. Poulet-Crovisier[d], A. Barbe[c], A. Campargue[d], D. Chris Benner[e], Y. Benilan[r], B. Bézard[g], V. Boudon[n], L.R. Brown[i], L.H. Coudert[f], A. Coustenis[g], V. Dana[j], V.M. Devi[e], S. Fally[k], A. Fayt[l], J.-M. Flaud[f], A. Goldman[m], M. Herman[n], G.J. Harris[o], D. Jacquemart[p], A. Jolly[f], I. Kleiner[f], A. Kleinböhl[l], F. Kwabia-Tchana[p], N. Lavrentieva[q], N. Lacome[p], Li-Hong Xu[r], O.M. Lyulin[q], J.-Y. Mandin[j], A. Maki[s], S. Mikhailenko[q], C.E. Miller[t], T. Mishina[q], N. Moazzen-Ahmadi[r], H.S.P. Müller[u], A. Nikitin[q], J. Orphal[v], V. Perevalov[q], A. Perrin[f], D.T. Petkie[w], A. Predoi-Cross[x], C.P. Rinsland[y], J.J. Remedios[z], M. Rotger[c], M.A.H. Smith[y], K. Sung[i], S. Tashkun[q], J. Tennyson[o], R.A. Toth[i], A.-C. Vandaele[k], J. Vander Auwera[n]

Atmospheric Radiation Analysis
Laboratoire de Météorologie Dynamique/CNRS/IPSL

[2] Summary of Differences for Molecular Species Cataloged in the Line Parameter Portion of GEISA-09 and HITRAN 2008

From Table-3 in

N. Jacquinet-Husson et al. / Journal of Quantitative Spectroscopy & Radiative Transfer 112 (2011) 2395–2445

The 2009 edition of the GEISA spectroscopic database

[2-a] Summary of differences for molecular species cataloged in the line parameter portion of GEISA-09 (G) and HITRAN 2008 (H)

Mol.	Mol ID		# bands		# isot		# lines		Spectral coverage (cm^{-1})			
	G	H	G	H	G	H	G	H	Minimum wavenumber (cm^{-1})		Maximum wavenumber (cm^{-1})	
									G	H	G	H
H_2O	1	1	245	373	6	6	67,789	69,201	0.007	0.007	25,232.004	25,232.004
CO_2	2	2	3747	2832	9	9	413,619	314,919	5.891	0.736	12,784.052	12,784.052
O_3	3	3	162	218	5	5	389,378	409,686	0.026	0.026	6395.379	5786.118
N_2O	4	4	369	351	8	5	50,633	47,843	0.838	0.838	7796.633	7796.633
CO	5	5	104	47	6	6	13,515	4477	3.414	3.462	8464.882	8464.881
→ CH_4	6	6	138(§)	138	2	2(§)	240,991(§)	240,854(§)	0.001	0.001	9155.326	9155.326
O_2	7	7	19	19	3	3	6428	6428	0.000	0.000	15,927.230	15,927.230
NO	8	8	293	293	3	3	105,079	105,079	0.000	0.000	9273.214	9273.214
SO_2	9	9	17	13	2	2	68,728	58,250	0.017	0.017	4092.948	4092.948
NO_2	10	10	11	11	1	1	104,223	104,223	0.498	0.498	3074.153	3074.153
NH_3	11	11	78	78	2	2	29,082	29,084	0.058	0.058	5293.578	5293.578
PH_3	12	28	19	18	1	1	20,423	20,099	17.805	770.877	3600.701	3600.701
HNO_3	13	12	26	18	1	1	669,988	487,254	0.012	0.012	1769.982	1769.982

CH_3D considered as an individual molecule in GEISA; but as an isotopologue of CH_4 in HITRAN

For HITRAN, column 9, sub-column "H", includes:
for CH_4 (Mol. "6"), total # lines of isotopologues numbered "1" and "2"

[2-b] Summary of differences for molecular species cataloged in the line parameter portion of GEISA-09 (G) and HITRAN 2008 (H)

Mol.	Mol ID		# bands		# isot		# lines		Spectral coverage (cm^{-1})			
	G	H	G	H	G	H	G	H	Minimum wavenumber (cm^{-1})		Maximum wavenumber (cm^{-1})	
									G	H	G	H
OH	14	13	245	221	3	3	42,866	31,976	0.005	0.003	35,877.030	19,267.804
HF	15	14	6	6	1	1	107	107	41.111	41.111	11,535.570	11,535.570
HCl	16	15	17	17	2	2	533	613	20.240	20.240	13,457.841	13,458.024
HBr	17	16	16	16	2	2	1293	1293	16.232	16.231	9758.312	9758.312
HI	18	17	9	9	1	1	806	806	12.509	12.509	8487.305	8487.305
ClO	19	18	12	16	2	2	7230	11,501	0.015	0.015	1207.639	1207.639
OCS	20	19	192	164	6	5	33,809	29,361	0.381	0.381	4199.671	4199.671
H_2CO	21	20	17	17	3	3	37,050	37,050	0.000	0.000	3099.958	3099.958
C_2H_6	22	27	6	6	2	2	28,439	28,439	706.601	706.601	3000.486	3000.486
CH_3D(s)	23	(s)	26	26	2	2(s)	49,237(s)	49,237(s)	7.760	7.760	6510.326	6510.326
C_2H_2	24	26	118	118	2	2	11,340	11,340	604.774	604.774	9889.038	9889.038
C_2H_4	25	38	12	12	2	2	18,378	18,378	701.203	701.203	3177.173	3177.173
GeH_4	26	*ABS*	1	*ABS*	1	*ABS*	824	*ABS*	1937.371	*ABS*	2224.570	*ABS*
HCN	27	23	775	30	4	3	82,042	4253	0.006	0.015	17,581.009	3423.927
C_3H_8	28	*ABS*	1	*ABS*	1	*ABS*	8983	*ABS*	700.015	*ABS*	799.930	*ABS*
C_2N_2	29	*ABS*	7	*ABS*	1	*ABS*	2577	*ABS*	203.955	*ABS*	2181.690	*ABS*
C_4H_2	30	*ABS*	1509	*ABS*	1	*ABS*	119,480	*ABS*	191.635	*ABS*	730.2352	*ABS*
HC_3N	31	*ABS*	3302	*ABS*	1	*ABS*	179,347	*ABS*	463.604	*ABS*	755.696	*ABS*
HOCl	32	21	6	8	2	2	17,862	16,276	0.024	1.081	3799.682	3799.682
N_2	33	22	1	1	1	1	120	120	1992.628	1992.628	2625.497	2625.497
CH_3Cl	34	24	14	83	2	2	18,344	196,171	674.143	0.873	3172.927	3172.927
H_2O_2	35	25	130	130	1	1	126,983	126,983	0.043	0.043	1730.371	1730.371

ABS stands for a molecular species not included in the actual database (HITRAN or GEISA)

For HITRAN, column9, sub-column "H", includes:for CH_3D (Mol. "23"), total # lines of CH_4 isotopologues numbered "3" and "4"

EUMETRISPEC workshop on traceable spectral reference for atmospheric monitoring , PTB, Braunschweig, Germany, 14-16 November 2012

[2-c] Summary of differences for molecular species cataloged in the line parameter portion of GEISA-09 (G) and HITRAN 2008 (H)

Mol.	Mol ID		# bands		# isot		# lines		Spectral coverage (cm^{-1})			
	G	H	G	H	G	H	G	H	Minimum wavenumber (cm^{-1})		Maximum wavenumber (cm^{-1})	
									G	H	G	H
H_2S	36	31	30	30	3	3	20,788	20,788	2.985	2.985	4256.546	4256.547
HCOOH	37	32	8	8	1	1	62,684	62,684	10.018	10.018	1889.334	1889.334
COF_2	38	29	7	7	1	1	83,750	70,601	725.005	725.005	2001.348	2001.348
SF_6(*)	39	30	6	3	1	1	92,398	2,889,065(*)	588.488	580.000	975.788	996.000
C_3H_4	40	*ABS*	22	*ABS*	1	*ABS*	19,001	*ABS*	288.912	*ABS*	673.479	*ABS*
HO_2	41	33	4	4	1	1	38,804	38,804	0.173	0.173	3675.818	3675.818
$ClONO_2$(*)	42	35	7	3	2	2	356,899	32,199(*)	0.636	763.641	797.741	797.741
CH_3Br	43	40	6	6	2	2	36,911	36,911	794.403	794.403	1705.612	1705.612
CH_3OH	44	39	16	16	1	1	19,897	19,897	0.019	0.019	1407.205	1407.205
NO^+	45	36	6	6	1	1	1206	1206	1634.831	1634.831	2530.462	2530.462
HNC	46	*ABS*	84	*ABS*	1	*ABS*	5619	*ABS*	0.217	*ABS*	4814.904	*ABS*
C_6H_6	47	*ABS*	1	*ABS*	1	*ABS*	9797	*ABS*	642.427	*ABS*	705.262	*ABS*
C_2HD	48	*ABS*	348	*ABS*	1	*ABS*	15,512	*ABS*	416.785	*ABS*	3385.564	*ABS*
CF_4	49	42	5	5	1	1	60,033	60,033	594.581	594.581	1312.647	1312.647
CH_3CN	50	41	2	2	1	1	17,172	3572	890.052	890.052	1650.000	945.655
O	*ABS*	34	*ABS*	1	*ABS*	1	*ABS*	2	*ABS*	68.716	*ABS*	158.303
HOBr	*ABS*	37	*ABS*	1	*ABS*	2	*ABS*	4358	*ABS*	0.155	*ABS*	315.908

ABS stands for a molecular species not included in the actual database (HITRAN or GEISA)

(*) Molecule included in HITRAN 2008 supplemental line list.

EUMETRISPEC workshop on traceable spectral reference for atmospheric monitoring , PTB, Braunschweig, Germany, 14-16 November 2012

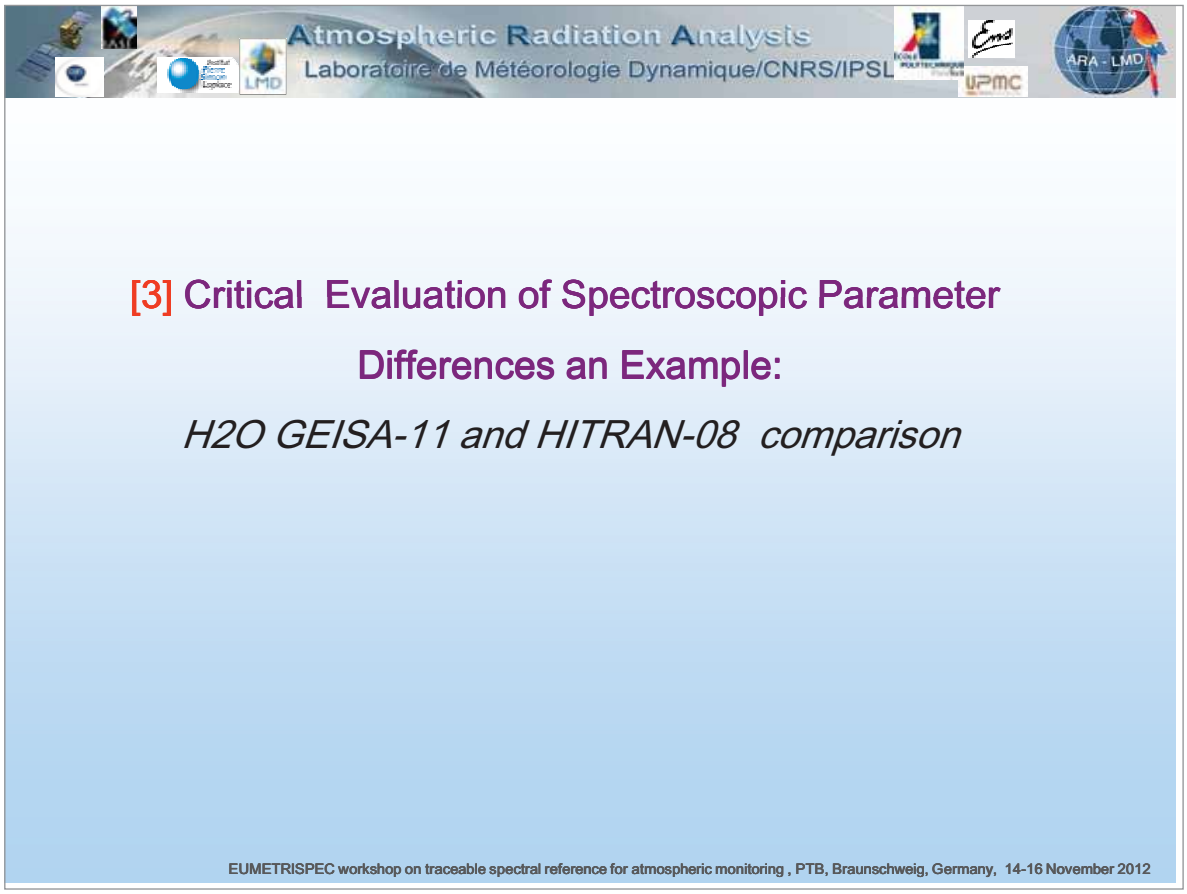

[3] Critical Evaluation of Spectroscopic Parameter Differences

Evaluation of the impact of H_2O spectroscopic archive on IASI radiative transfer modelling

❖ **Radiative transfer simulations with ARA/ABC(t)/LMD radiative transfer models in their lalest versions**

➢**STRANSAC;** line-by-line and layer-by-layer model
[N.A. Scott, 1974, JQSRT, 14, 691-707]

➢**4A** (**A**utomatized **A**tmospheric **A**bsorption **A**tlas); fast and accurate line-by-line radiative transfer model
[N.A. Scott and A. Chédin, 1981, J. Appl. Meteor., 20, n° 7, 802-812; Tournier et al. 1995; Chéruy et al. 1995]

❖**Selected Spectroscopic Databases**

GEISA [Jacquinet-Husson N. et al. JQSRT 112 (2011) 2395-2445] Revision 2011 of this reference

HITRAN [Rothman L.S. et al. JQSRT 110 (2009) 533-572] it its latest revision

Differences in spectroscopic parameters archives and subsequent IASI radiative transfer modelling, in terms of Brightness Temperature (K) differences Δ BT (K)

EUMETRISPEC workshop on traceable spectral reference for atmospheric monitoring , PTB, Braunschweig, Germany, 14-16 November 2012

[3-a] Quantitative comparison between H_2O intensity values in GEISA-11 and HITRAN-08

- spectral range 1400 – 2100 cm^{-1}
- 5626 transitions with common quantum identification in both databases (intensity values larger than 10^{-23} cm-1/(molecule cm^{-2}))
- 8% of the strong lines (intensities greater or equal 10^{-20} cm^{-1}/(molecule cm^{-2})) exhibit differences greater that 5%.

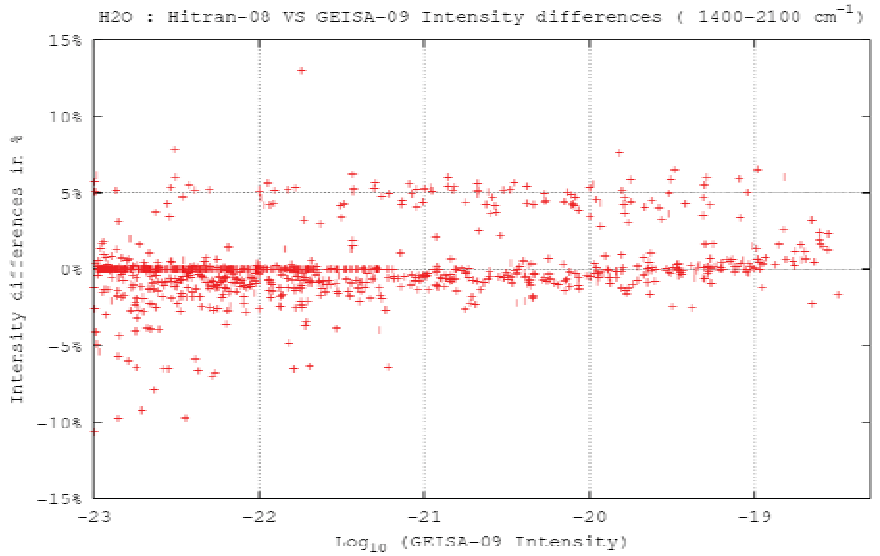

N. Jacquinet-Husson et al.
DOI 10.1016/j.jqsrt.2011.06.004

EUMETRISPEC workshop on traceable spectral reference for atmospheric monitoring , PTB, Braunschweig, Germany, 14-16 November 2012

[3-b] H_2O Spectroscopy Differences Illustration

IASI brightness temperature BT (K) simulation with GEISA

Differences in BT(K) using GEISA or HITRAN

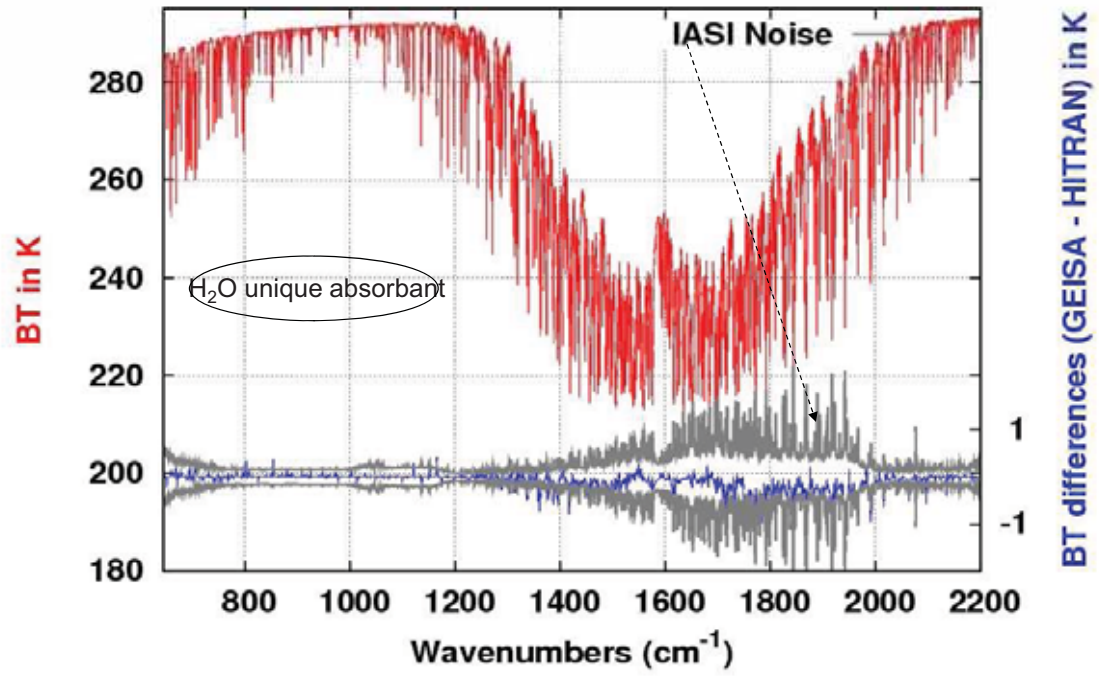

[3-c] Evaluation of spectroscopic parameters individual impact on IASI BT modelling differences

IASI Band 1 *(15.50 – 8.26 µm)* **Intensity impact evaluation**

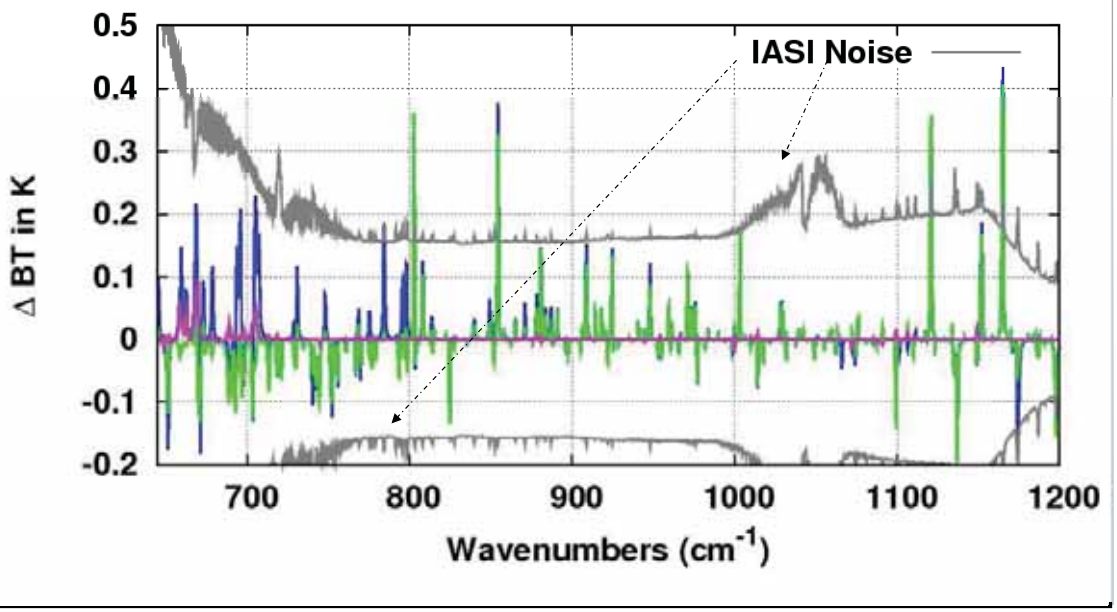

$TB_G - TB_H$ $TB_G - TB_{G\ with\ H\ intensities}$ $TB_G - TB_{G\ with\ H\ HWHM}$

[3-d] Evaluation of spectroscopic parameters individual impact on IASI BT modelling differences

IASI Band 3 *(15.50 – 8.26 µm)* **HWHM impact evaluation**

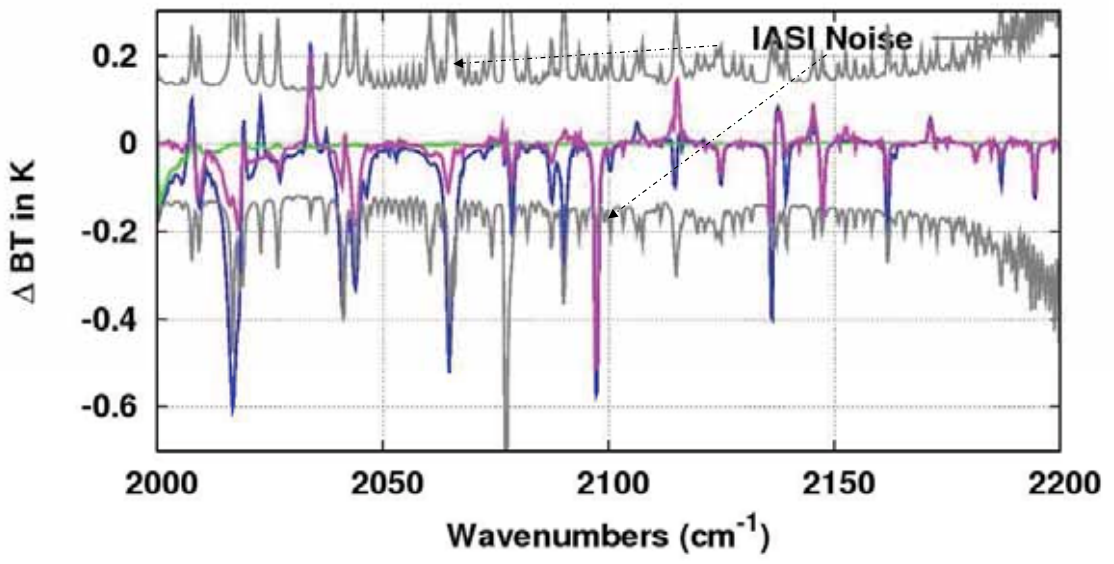

$TB_G - TB_H$ $TB_G - TB_{G\ with\ H\ intensities}$ $TB_G - TB_{G\ with\ H\ HWHM}$

[3-e] H_2O Spectroscopy Differences Illustration

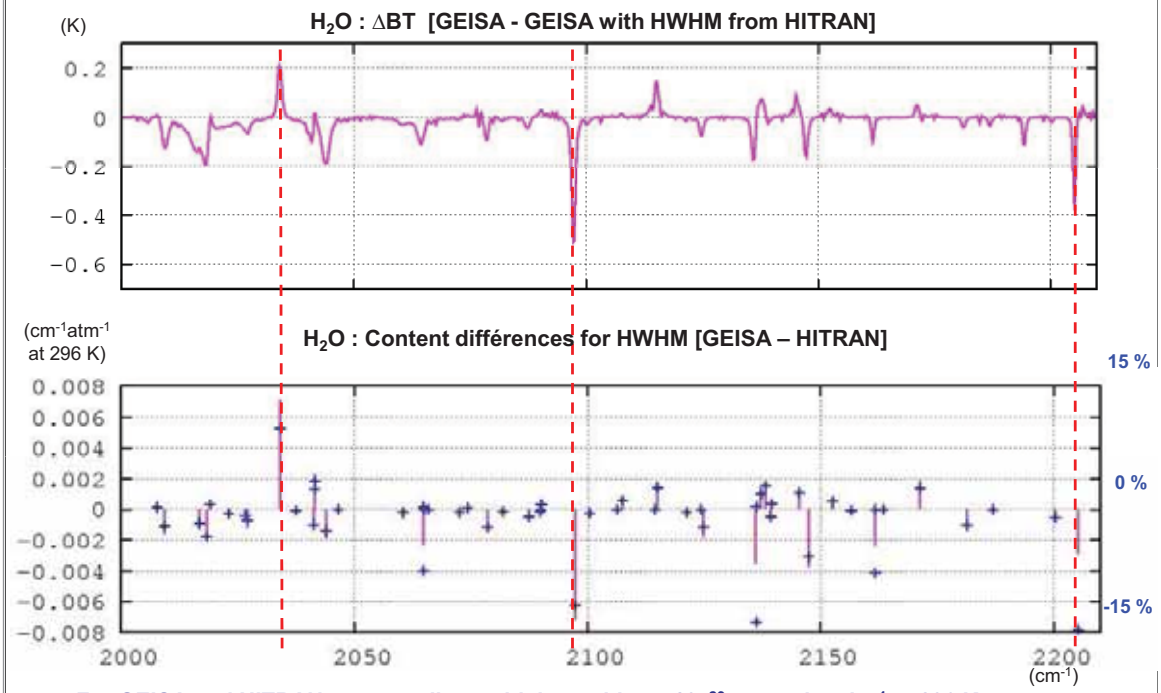

For GEISA and HITRAN common lines with intensities > 10^{-23} cm molecule $^{-1}$ at 296 K

[3-f] H_2O Spectroscopy Differences Illustration

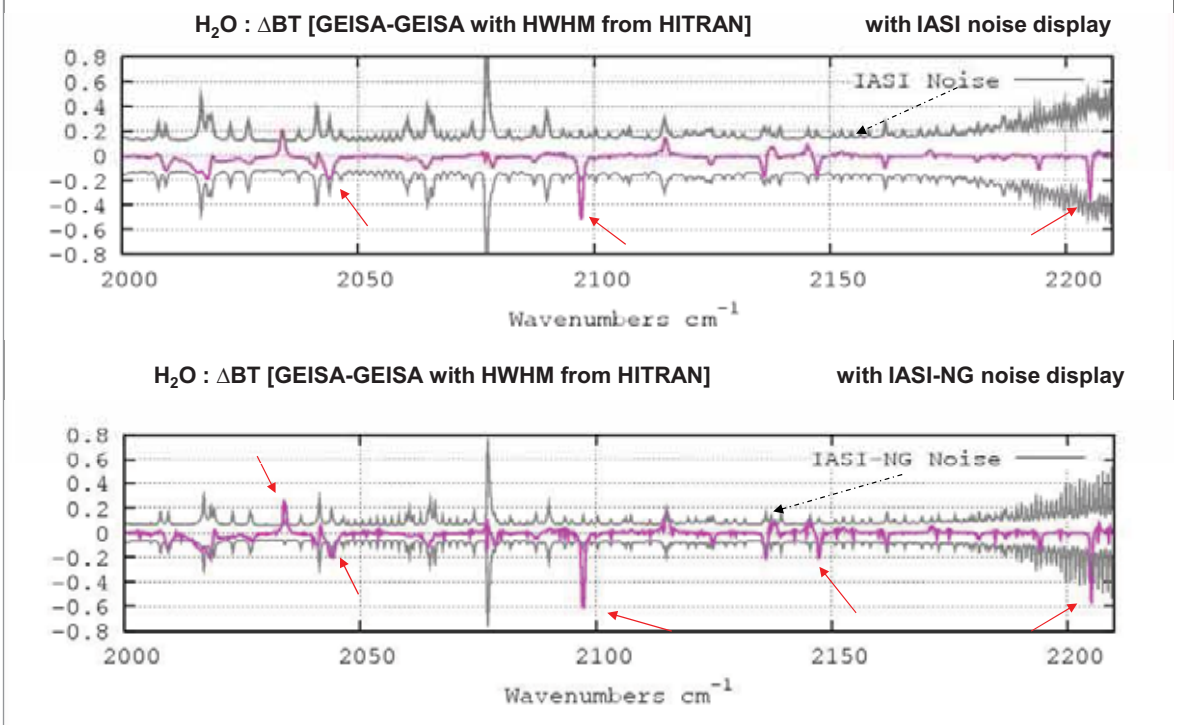

For IASI-NG: Spectral Resolution X 2 and Noise divided by 2 comparing with IASI

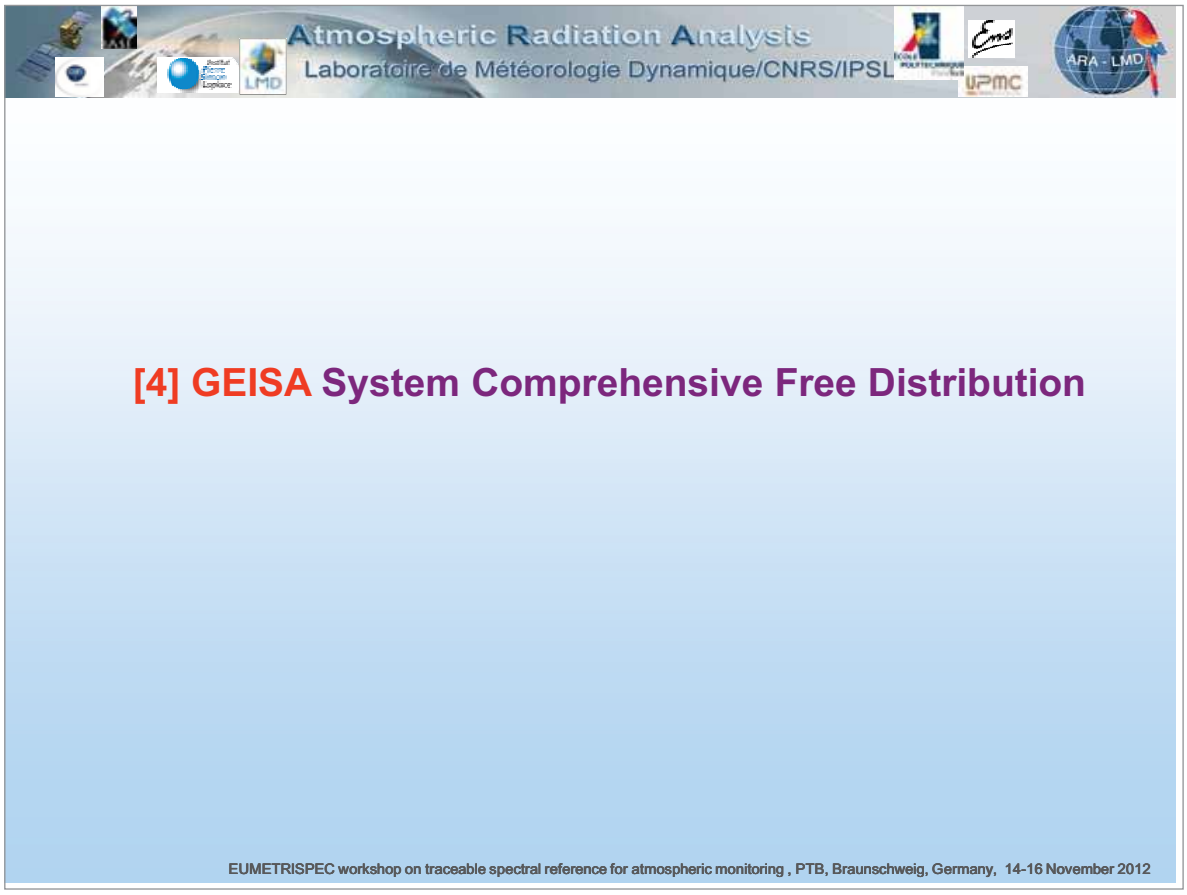
Atmospheric Radiation Analysis
Laboratoire de Météorologie Dynamique/CNRS/IPSL
ARA - LMD
[4] GEISA System Comprehensive Free Distribution
EUMETRISPEC workshop on traceable spectral reference for atmospheric monitoring , PTB, Braunschweig, Germany, 14-16 November 2012


[4] GEISA SYSTEM COMPREHENSIVE DISTRIBUTION
Ether
Atmospheric Chemistry
Data Centre
(No login no password)
http://www.pole-ether.fr
Home
News
Project call
Atmospheric Data
Satellites
Balloons
NDACC
ECCAD
IASI
GOSAT
IAGOS
Field Campaigns
Daily Modelisation and Forecast
Spectroscopic data and Kinetics
GEISA
Kinetics

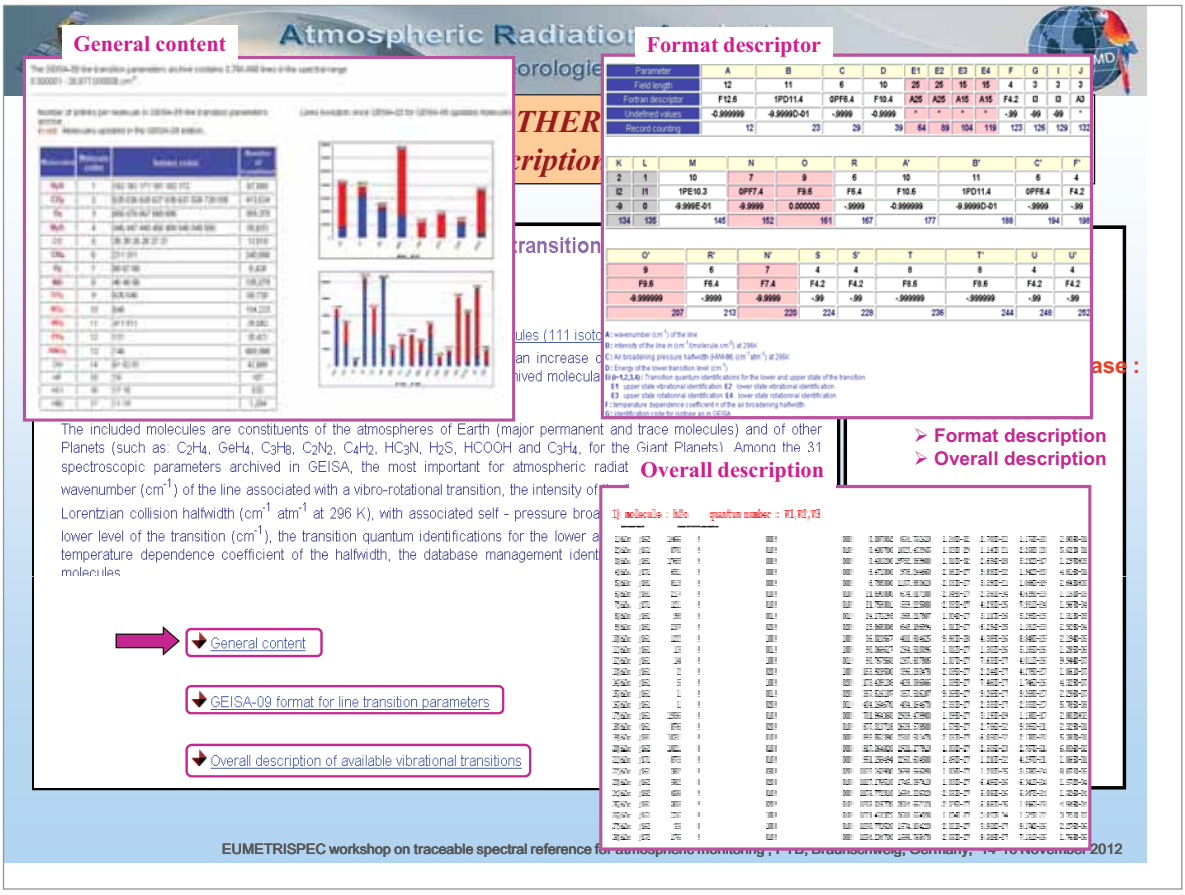
General content
Format descriptor
Overall description
Format description
Overall description
General content
GEISA-09 format for line transition parameters
Overall description of available vibrational transitions
EUMETRISPEC workshop on traceable spectral reference


Atmospheric Radiation Analysis
Laboratoire de Météorologie Dynamique/CNRS/IPSL
Thanks to J. Orphal for this Presentation
ACKNOWLEDGMENTS
to
CNES, CNRS/INSU and EUMETSAT
for their Encouragements and Supports
THANK YOU FOR YOUR ATTENTION
EUMETRISPEC workshop on traceable spectral reference for atmospheric monitoring , PTB, Braunschweig, Germany, 14-16 November 2012

"FT-based high resolution lab spectroscopy for atmospheric line data measurements"

Dr. Manfred Birk

Institut für Methodik der Fernerkundung,
Deutsches Zentrum für Luft- und Raumfahrt

Dr. Manfred Birk

Institut für Methodik der Fernerkundung, Deutsches Zentrum für Luft- und Raumfahrt
Münchner Str. 20, 82230 Wessling, Germany
Phone: +49 8153283084
E-mail: manfred.birk@dlr.de

Research

FT spectroscopy; FT technology; Space borne FT remote sensing; Optical design; FT level 1 processing; THz heterodyne technology and remote sensing; Background in atmospheric modelling and retrieval

Education and Professional Experience

since 2002	PI of international project TELIS (Terahertz and Submillimeter limb sounder), Design, construction and application of a 3 channel heterodyne balloon-borne spectrometer for measurement of stratospheric species together with MIPAS-B from IMK/FZK. Three successful flights in March 2009, January 2010, and April 2011 from Kiruna, Sweden
since 1990	Scientific project manager and project scientist, Deutsches Zentrum für Luft- und Raumfahrt e.V. (DLR), Institute for Optoelectronics (from 2000: Remote Sensing Technology Institute), Wessling, Germany, Main field of work: Improvement of the spectroscopic database of atmospheric trace gases by Fourier-transform spectrometry
1988	Ph.D. (Dr. rer. nat.) in Chemistry, Justus-Liebig-University of Gießen, Germany
1988-1990	NRC postdoctoral fellowship at JPL/NASA in Pasadena, California Institute of Technology, USA
1982-1988	Research Associate at Institute of Molecular Spectroscopy, Justus-Liebig-University of Gießen, Germany

Activities, Honors and Awards

- ISORAC, ISORAC-2, AEROJET, AEROJET 2, AEROPROFILE, SESAME, PIRAMHYD, ACE, etc.
- Member of ACVT for MIPAS/Envisat, Member of QWG for MIPAS/Envisat phase E, Task: improvement and characterisation of level 1 product
- Member of HITRAN scientific advisory committee
- Thesis adviser for 8 PhD theses since 1990

FT-based high resolution lab spectroscopy for atmospheric line data measurements

Manfred Birk and Georg Wagner

The Remote Sensing Technology Institute, German Aerospace Center

The DLR spectroscopy group has carried out high resolution Fourier-Transform spectroscopy of atmospheric species since 1990. The work started in the far-infrared, was extended to the near-infrared and is recently expanded up to the UV region. The measurement of spectroscopic data with small and defined error margins was always the main target. The Fourier-Transform instrument including measurement conditions were optimized and sample cells and gas handling equipment built. Numerous software tools for retrieval and quality assessment were developed. The most recent development in hardware will be presented including a completely refurbished coolable multireflection cell (base length 80 cm, absorption path >100 m) and a four window coolable short cell, both capable of measurements from FIR to UV with excellent temperature homogeneity. Methods and hardware have been made for generating defined water/air and ozone/air mixtures including transport/flow into the sample cell. Species covered over the years are OH, HO_2, H_2O, CO, NO, NO_2, O_3, ClO, ClOOCl, BrO, CO_2, $ClONO_2$ and N_2O_5. In most cases the resulting absorption cross sections and line parameters are included in the HITRAN database. Recent results on intercomparisons of water line strengths with ab initio and other experimental sources will be discussed. Finally, it will be explained why quantitative spectroscopy is science and cannot completely be standardized.

FT-based high resolution lab spectroscopy for atmospheric line data measurements

Manfred Birk, Georg Wagner

Remote Sensing Technology Institute (IMF)

Deutsches Zentrum für Luft- und Raumfahrt (DLR)

Background

- Group established in 1990
- Emphasis on quantitative spectroscopy of atmospheric trace gases to support atmospheric remote sensing
- Initial focus on far infrared but soon extended to mid and near infrared, UV since 2010
- Participation in several EU-, ESA-, nationally-funded projects
- Member of HITRAN scientific advisory committee

Infrastructure

- Bruker IFS120 HR Fourier-Transform spectrometer, replaced by new IFS125 HR in August 2010, extension to UV (250 nm)
- Coolable (190K), heatable (950K) cells, 130 m multireflection cell
- Lab equipment for production/handling of stable/unstable species

Short absorption path cell

- 25 cm absorption path
- Coolable to 195 K
- High temperature homogeneity (<0.1 K)

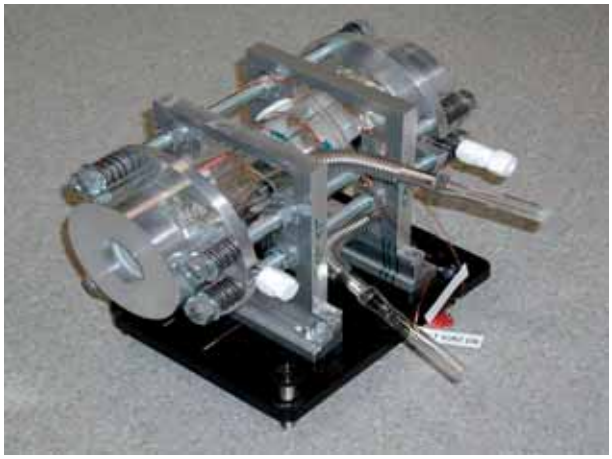

New short absorption path cell

- 20 cm absorption path
- Coolable to 190 K
- Two window pairs allowing UV+MIR, MIR+FIR, UV+FIR quasisimultaneously
- High temperature homogeneity (<0.1 K)
- Path length accuracy 0.1% - requires raytracing!

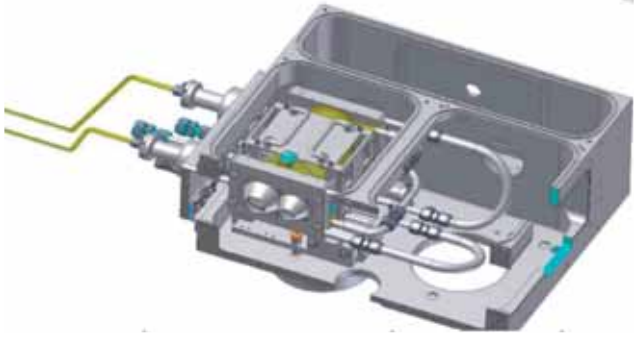

Multifreflection cell

- Designed at DLR 1991, refurbished 2012
- 80 cm baselength, up to 130 m absorption path
- Coolable down to 190 K
- Equipped for flow experiments with unstable species

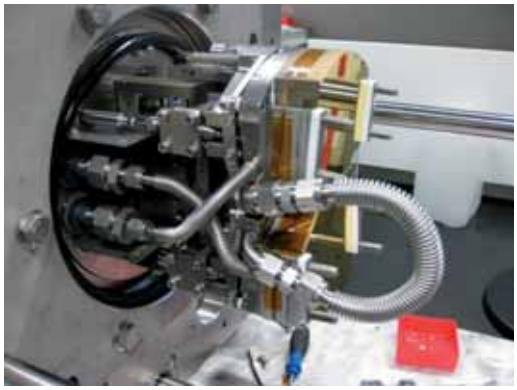

DLR

Improved detector design for thermal IR

- Adaptable detector FOV to reduce background photon noise
- Coolable optical filter
- Photoconductive MCT with 700 cm^{-1} cut-on @ 45 K

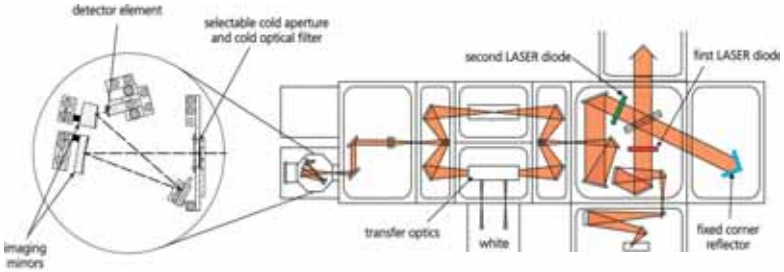

Intercomparison standard Bruker MCT – DLR design

- optical band pass filter, varying central wavenumber
- detector @ 45 K
- 200 cm filter bandwidth
- 1 mm and 2 mm Bruker entrance aperture
- no absorber- and 90% absorption-setup

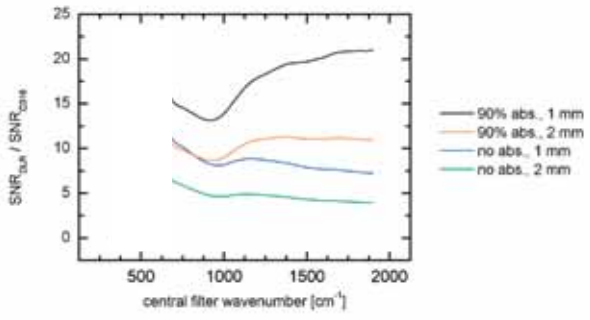

DLR

Output of spectroscopic work:

Absorption cross sections (ACS) or line-by-line (LBL) data

$$t = \exp\left(-\alpha\left(T,P,\sigma\right)\cdot l\cdot N\right)$$

t	transmittance of homogeneous sample	σ	wavenumber
$\alpha()$	absorption cross section	l	absorption path
T	temperature	N	number density
P	pressure		

$$\alpha = \sum_i S_i \cdot f\left(T,P,\sigma-\sigma_{0i}+\sigma_{si},\gamma_i,n_i\right)$$

i	line index	σ_{si}	pressure shift
S_i	linestrength	γ_i	pressure broadening
$f()$	monochromatic line profile⇒ convolution pressure broadening and Doppler profiles	n_i	temperature exponent
σ_{0i}	line position		

Line-by-line vs. absorption cross sections

Results	σ_0, γ, n, S, shift	$\alpha(\sigma,T,p)$
FTS resolution	$\leq \gamma_{min}$	$\leq 0.25\ \gamma_{min}$
Baseline	less critical	critical
Temperatures	≥2 for γ, n; 1 for σ_0, S	several
Pressures	≥2 for γ, shift	several
Line density	low	-
Analysis effort	depends on line density	low
Molecules	e.g. CO, NO, H_2O	e.g. HFCs, CFCs
Interpolation	-	Polynomial in T, p
Extrapolation	+	-
Redundancy capability	high	low

Line parameter retrieval

- **Input:** Transmittance spectra
- Spectrum cut in microwindows
- Line model: Convolution of instrumental lineshape and monochromatic transmittance
- Least-squares fit to match model to experiment
- **Output:** Line parameters, baseline and/or ILS parameter

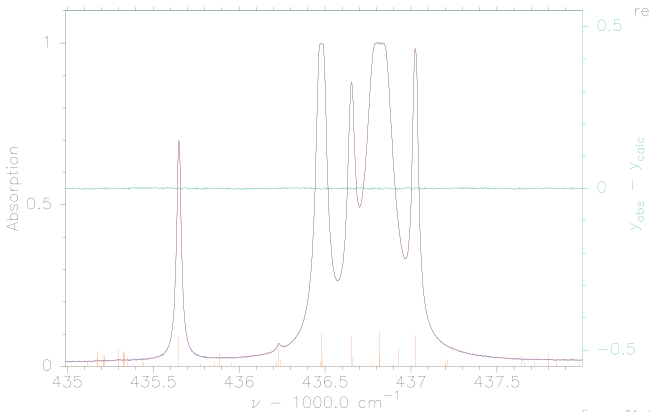

Line parameter retrieval codes at DLR

FitMAS (Fit Molecular Absorption Spectra)
- Single spectrum fit
- Voigt, Galatry, Rautian
- ILS: sinc x box, sinc
- Automatic microwindow and fit parameter selection by independent code

IDL line fitting code
- Single spectrum fit
- Voigt, Galatry, speed-dependent Voigt
- ILS: sinc x box
- Improved microwindow and fit parameter selection
- Only application sofar: 1 µm band of water

Multispectrum fitting code
- Under development

Line parameter retrieval codes and utilities at DLR

Linestrength averaging

- Averages linestrengths from several measurements
- Routines for validation of data product accuracy (VDPA)

Pressure broadening fitting

- Fits γ_{air}, n_{air}, γ_{self}, n_{self} from Lorentzian half widths of several measurements
- Automatic fit parameter and measurement selection
- Routines for VDPA

Line position and pressure-induced shift fitting

- Fits line positions, shifts, and temperature dependence from line positions of several measurements
- Automatic fit parameter and measurement selection
- Routines for VDPA

Temperature/number density fitting

- Fits average gas temperature and number density from linestrengths of single measurement using reference linestrengths

DLR

Spectroscopic database work at DLR

Species	FIR	MIR	Purpose/application	Remark
O_3	S, **g**(T)	**s**, S, **g**(T), **a**(T,p)	database improvedment	
$ClONO_2$		**a**(T,p)	database improvement, MIPAS	difficult synthesis
N_2O_5		**a**(T,p),	database improvement, MIPAS	
OH/HO_2	**s**		new methodology	extremely unstable
BrO	**s**, **g**(T)		database improvement, MASTER/SOPRANO	extremely unstable
ClO	**s**, **g**(T)	**s**, S	database improvement, MASTER/SOPRANO	unstable
ClOOCl	**s**	**a**(T,p)	remote sensing MIPAS	sample preparation difficult
HOCl	**s**		FIR database	
CO	S, **g**(T)	S, **g**(T)	error characterisation, high temperature database, Q/A	<1% radiometric accuracy
CO_2		**a**(T,p)	high temperature database	
H_2O		**s**, S, **g**(T), MIR+NIR	high temperature database improvement, climate, MIPAS, IASI, WALES	sample preparation difficult
NO		**s**, S, **g**(T)	high temperature database, engine emissions	
NO_2		**a**(T,p)	high temperature database, engine emissions	

Parameters in HITRAN, some also in GEISA

DLR

CO FIR measurement was important milestone for linestrength measurement

- There is no linestrength standard for rovibrational transitions
- Pure rotational linestrengths can be calculated from permanent electric dipole moment
- First experimental proof for 1% accurate linestrengths: Measurement of CO FIR linestrengths in cooperation with Steacie Institute for Molecular Sciences, NRC Canada
- Publication: Manfred Birk, Dieter Hausamann, Georg Wagner, John W. Johns, „Determination of line strengths by Fourier-transform spectroscopy“, Appl. Opt. 35, 2971-2985 (1996)

Status of spectroscopic databases

The spectroscopic database has significantly improved over the last years, however, the accuracy is sometimes not sufficient for the increasing needs of remote sensing

What is the reason for the lack in accuracy?

- Numerous systematic error sources, partially hidden and hard to quantify

Error categories

- Instrumental errors
- Sample errors
- Line parameter retrieval errors
- Data reduction model errors

Instrumental error sources

	Affecting:
Detector non-linearity	S
Phase errors (single-sided interferograms)	σ,δ
Sample/instrument thermal emission	S,γ
Instrumental lineshape knowledge	σ,γ,δ
Multipassing of radiation	ghosts, S
Insufficient beamsplitter wedge	S
Source instability	σ,γ,δ,S
Channeling, especially when variable in time	σ,γ,δ,S
Microphonics	σ,γ,δ,S
Temporal instrumental lineshape instability	γ,δ
Sampling jitter	ghosts, S
Scanner velocity instability	ghosts, S
Atmospheric absorption in beam path through instrument	γ,S,δ
Reference laser instability	ghosts, σ,γ,S,δ

Further instrument design specific error sources

Instrumental error sources - Non-linearity

30% absorption line

+1% transmittance offset

⇒ -1.1% linestrength error

⇒ ± 0% line width error

Fit residuals mostly unaffected

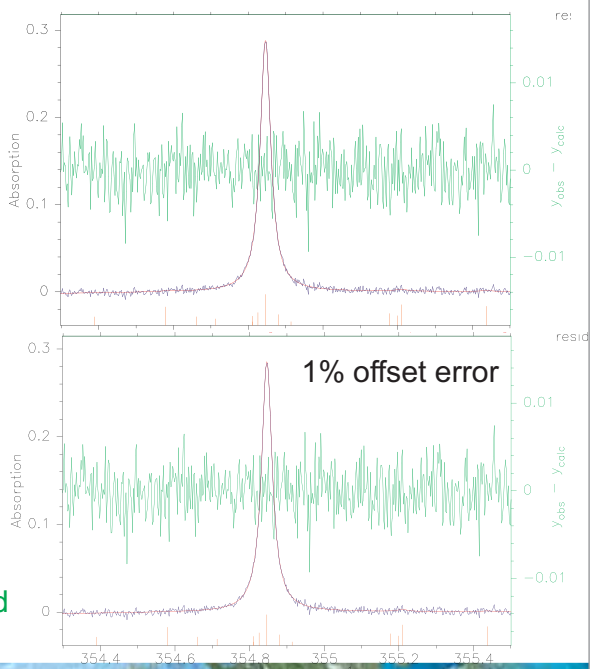

Fit residuals 10x expanded

Instrumental error sources - Non-linearity

95% absorption line

+1% transmittance offset
⇒ -2.4% linestrength error
⇒ +2% line width error

Fit residuals mostly unaffected

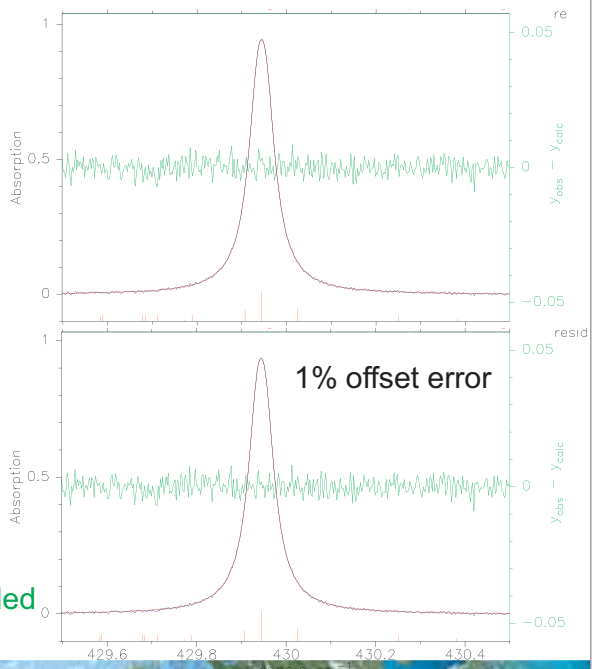

Fit residuals 10x expanded

Instrumental error sources - Channeling

Modelled impact

Period 2x, 4x linewidth

Amplitude 0.5x p-p noise

Channeling phase 0°,
90° wrt line symmetry

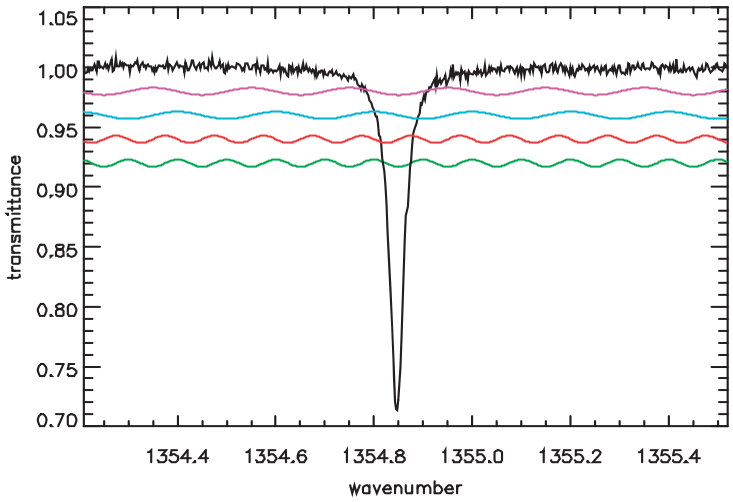

Instrumental error sources - Channeling

σ	Period	
Phase	$2b_L$	$4b_L$
0°	5e-5(8e-5)	3e-5(8e-5)
90°	**2e-4(8e-5)**	**2e-4(8e-5)**

S	Period	
Phase	$2b_L$	$4b_L$
0°	0.2%(0.3σ)	**1.4%(2σ)**
90°	0.1%(0.1σ)	0.03%(0σ)

γ	Period	
Phase	$2b_L$	$4b_L$
0°	**1.5%(2σ)**	0.3%(0.3σ)
90°	0.5%(0.5σ)	0%(0σ)

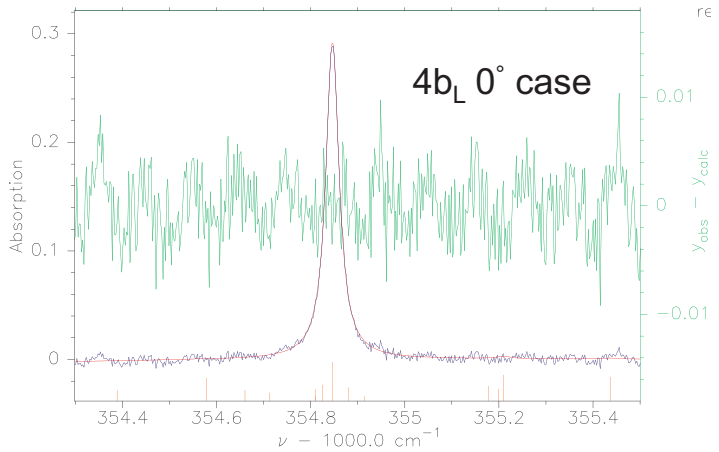

Error propagation hard to predict !!

Errors for line position, line shift, linestrength, line broadening

Sample errors

	Affecting:
Number density	S
Absorption path	S
Inhomogeneous sample distribution	S,γ
Inhomogeneous temperature distribution	γ,S,δ
Drifting sample amount	γ,S
Multipassing	S
Gas temperature knowledge	S,γ,δ
Drifting gas temperature	S,γ,δ
Total pressure	γ,δ

Sample errors - Temperature inhomogeneity

Impact on pressure-broadened line width

- Water spectra modelled: 0.65x233K + 0.35x253K
- Linefit, differences to input data
- Parameterisation of differences wrt E_{lower} and **temperature exponent**
- Plot of percentage line width error for 0.65xT + 0.35x(T+40K)
- Errors 1% to -3%
- **Undefined temperature gradient ⇒ undefined results**

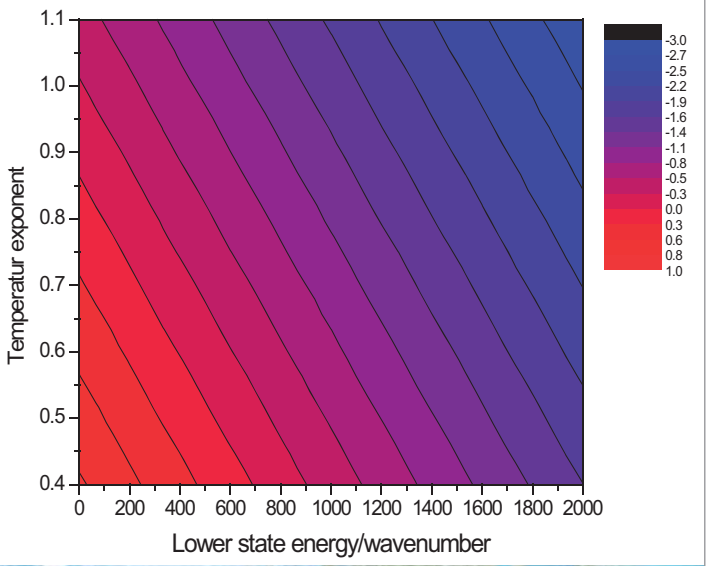

Line parameter retrieval errors

- Inadequate ILS model and parameters
- Blending
- **Inadequate monochromatic line model (non-Voigt line profile)**
- Faulty statistical errors due to correlation
- Bad prediction of weak „grass“ lines
- Inadequate microwindow width
- Bad temperature conversion of linestrengths

Defined error bars

- Numerous error sources affect line parameters
- Many errors can be reduced by
  - Instrument design and experimental setup
  - Measurement strategy
  - Dedicated correction methods
- Some remaining errors can be quantified and propagated into error bars of line parameters

But this is not sufficient to obtain defined error bars since

- Many error sources and their propagation cannot be sufficiently quantified
- Error sources may show complex non-additive interaction

Procedures for validation of data product accuracy (VDPA) required!

Redundancy

- VDPA requires redundancy!
- Redundancy does NOT mean simple measurement duplication!

Background: Data reduction from measurement specific parameters (e.g. linestrengths, Lorentzian half widths) derived by single spectra line parameter fitting, error-weighted Jacobi matrix *A*

Mathematical definition:
The contribution C_{ij} of each measurement *i* to a parameter *j* is given by

$$C = A^T \left(A A^T \right)^{-1}$$

The redundancy R_j is

$$R_j = \sum_i \frac{C_{ij}}{C_{i,\max}}$$

Example: Histogram of redundancy parameters and number of measurements in water ν_2 line width analysis fits.

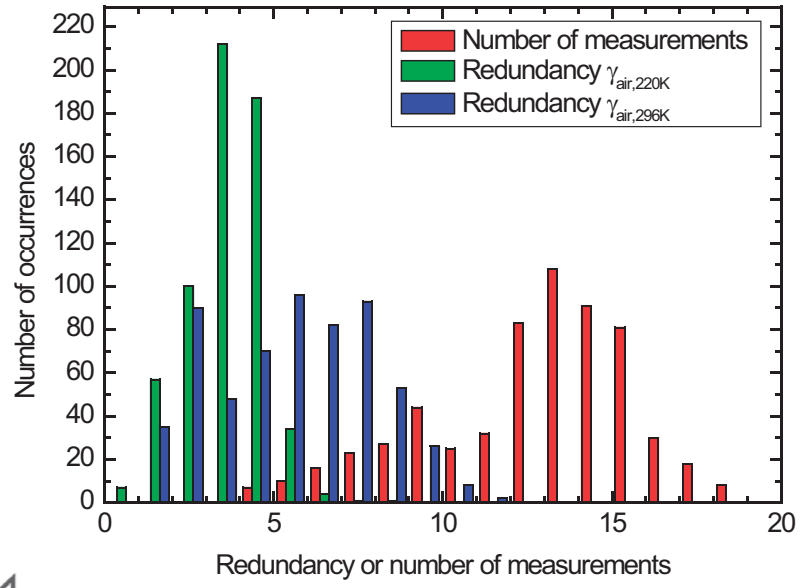

Validation of data product accuracy

- Generic: χ^2 test – all data reductions
- Generic: fits for different opacity ranges
- Generic: fits for different measurement conditions, e.g. total pressure for pressure broadening
- Generic: Averaged/binned residuals of fits or residuals as function of E_{lower}, σ, opacity, S, γ: „File cuts“

• Number density/temperature fit	S
• Quantum mechanical fit	S, σ
• Polynomial fit in quantum numbers for well-behaved molecules	γ
• Linestrength assessment	γ
• Model original laboratory spectra	all
• Model other laboratory spectra	all
• Retrieve atmospheric spectra, check residuals/results	all

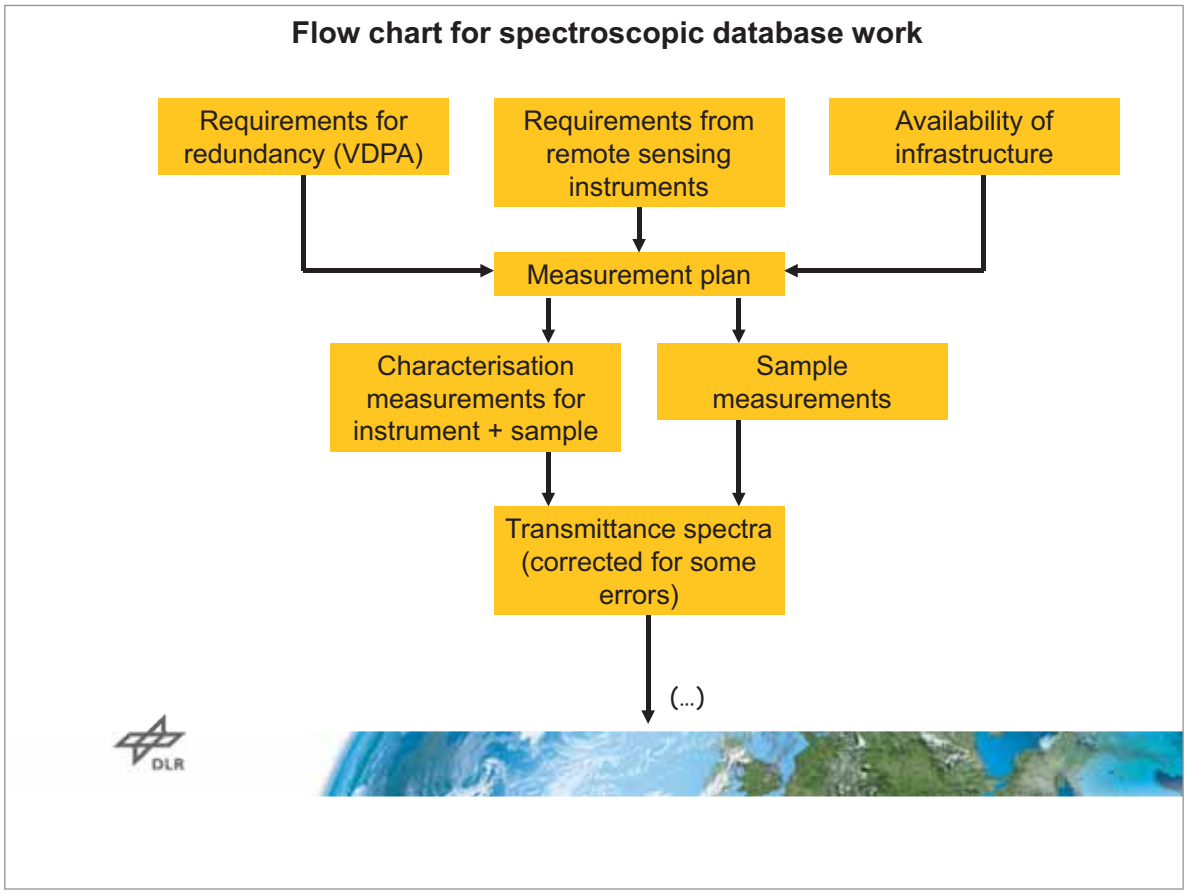
Flow chart for spectroscopic database work
Requirements for redundancy (VDPA)
Requirements from remote sensing instruments
Availability of infrastructure
Measurement plan
Characterisation measurements for instrument + sample
Sample measurements
Transmittance spectra (corrected for some errors)
(...)
DLR

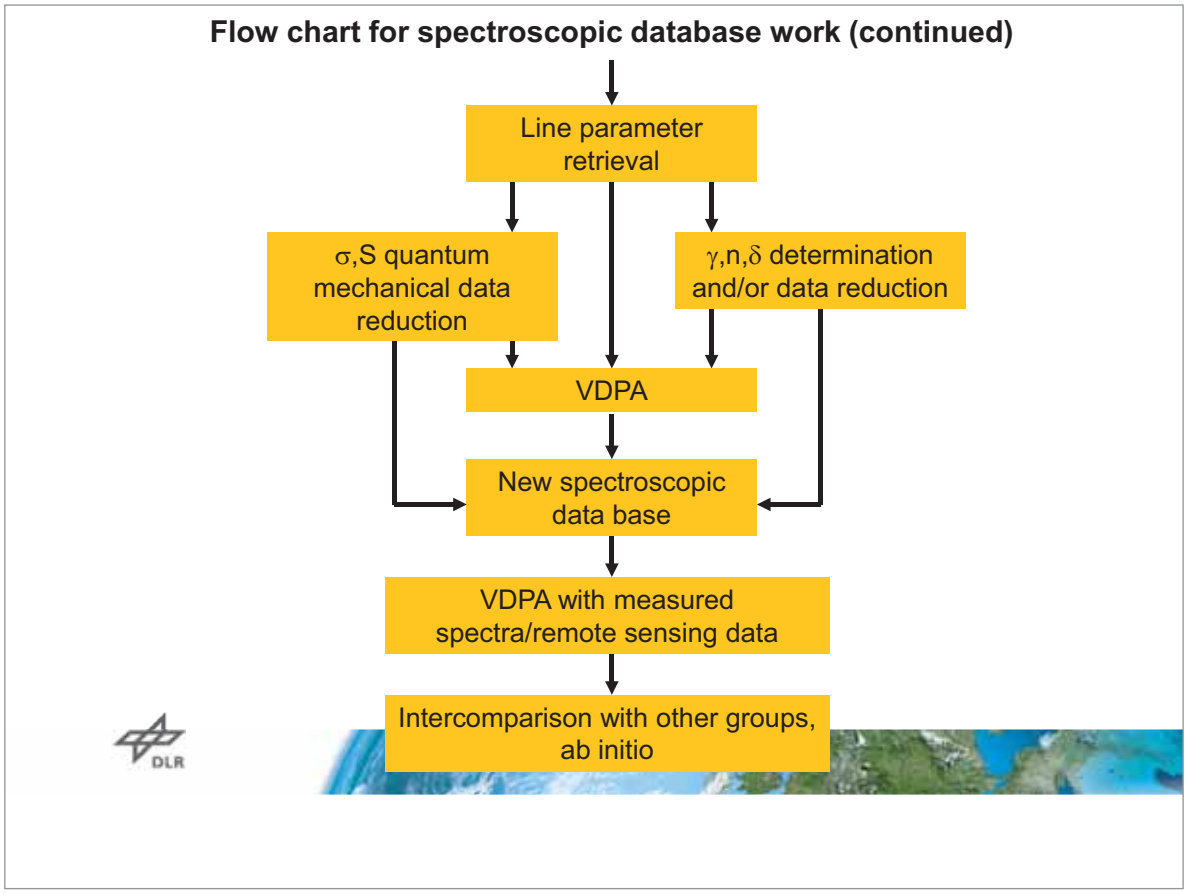
Flow chart for spectroscopic database work (continued)
Line parameter retrieval
σ,S quantum mechanical data reduction
γ,n,δ determination and/or data reduction
VDPA
New spectroscopic data base
VDPA with measured spectra/remote sensing data
Intercomparison with other groups, ab initio
DLR

Example: Water spectroscopy at DLR

ν_2 Region (1200 - 1800 cm^{-1}) for MIPAS/ENVISAT

- 52 measurements, 0.0009 - 5 mb H_2O, 0 - 1000 mb air, 207 - 316 K, 0.16 - 85 m
- Voigt profile for line fitting
- Linestrength analysis in cooperation with Laurent Coudert (quantum mechanics)
- Line broadening analysis
- Pressure induced line shifts and temperature dependence (not yet published)

1 µm Region (10000 - 11000 cm^{-1}) for WALES

- 17 measurements, 0.1 - 16 mb H_2O, 0 - 1000 mb air, 230 - 318 K, 85 m
- Speed-dependent Voigt profile for line fitting
- Spectroscopic database with linestrengths, pressure broadening parameters, line shifts (not yet published)

Water is among the most difficult species for spectroscopic investigations:

- Water adsorption to and desorption from walls changes composition of mixtures uncontrollably
- Pressure broadening parameter varies by more than 1 order of magnitude: Requires high resolution and hence sensitive detector
- Atmospheric column amounts hard/impossible to achieve in the laboratory – Example: limb sounding relevant linestrength range 10^{-19} - $2x10^{-25}$ $cm^{-1}cm^2molecule^{-1}$, >6 orders of magnitude: Requires multireflection cell and sensitive detector

Solution of adsorption problem

Development of equipment and procedures for generation of water/air mixtures in absorption cell with defined number densities:

- 800 l stainless steel mixing chamber (high volume/surface ratio, only minor water adsorption) equipped with magnetic stirrer
- Generation of mixtures by subsequent filling of water and air with absolute pressure measurement
- Establish pressure-controlled flows of mixture (or pure water vapor) through absorption cell. Check for proper conditioning (stable H_2O partial pressure) spectroscopically.

Experimental setup - White cell - pure water ν_2

- 10 measurements
- 0.2, 1.0, 5.0 mb pure water
- Ambient temperature, 273 K, 330 K
- Spectral resolution 0.0027 cm^{-1}
- Spectral range 1250 - 1750 cm^{-1}
- Flow 20, 40, 80 sccm

Target: Linestrength

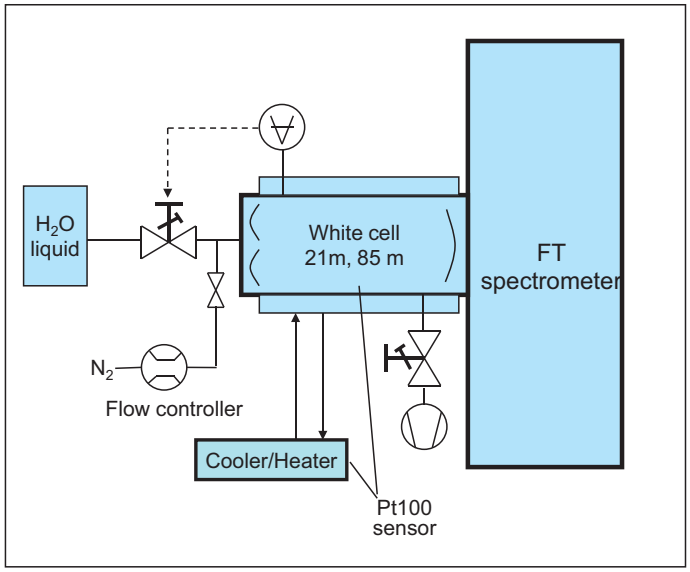

Experimental setup - White cell - water+air ν_2

Target: pressure broadening

- 37 measurements
- 0.05, 0.2, 1.0, 5.0 mb water
- 50, 100, 200 mb air
- 207, 233, 243, 258, 273, 296, 317 K
- Spectral resolution 0.0027 cm^{-1}
- Spectral range 1250 - 1750 cm^{-1}

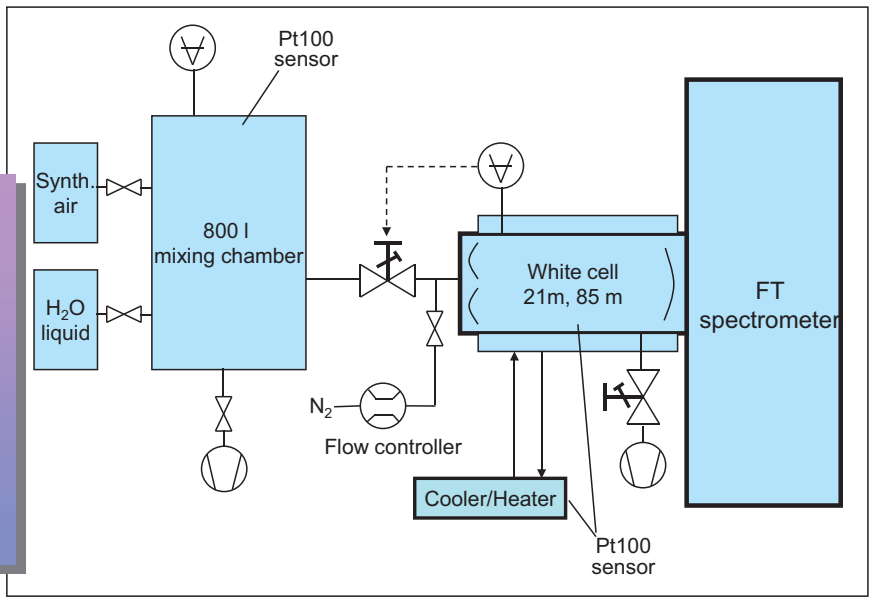

Excerpt of 200 mb total pressure, room temperature spectra with different column amount

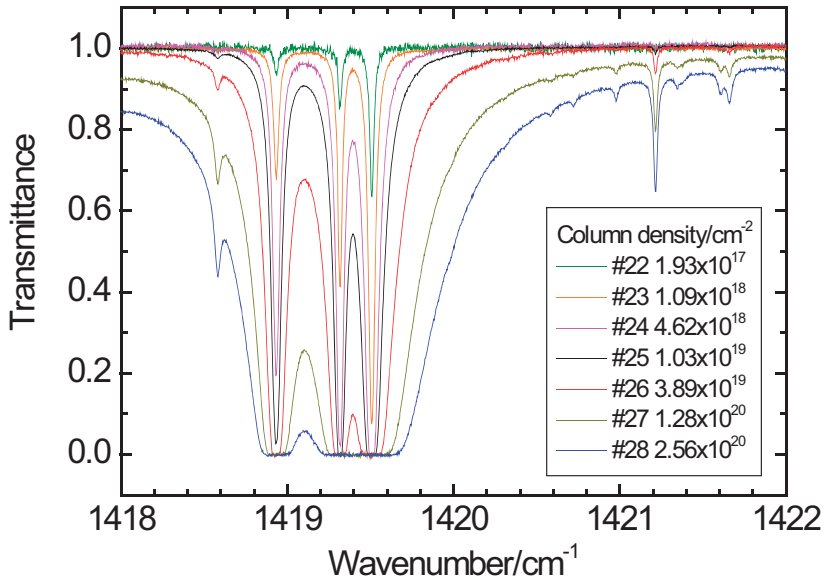

DLR

Measurements for γ: Number density/temperature fit

Test of method for defined water air mixtures

T_{bath}/°C	T_{bath}/K	T_{mirror}/K	P_{tot}/mb	P_{H2O}/mb	VMR	Absorpt. path/m	T_{fit}/K	$P_{H2O-fit}/P_{H2O}$
44.15	317.29	313.43	50.51	0.04947	9.8e-4	20	316.256(83)	1.00535(72)
44.15	317.29	313.40	201.1	0.04936	2.5e-4	20	316.484(57)	0.99252(29)
44.15	317.29	313.48	50.51	0.2016	4.0e-3	20	316.085(59)	0.99802(68)
44.15	317.29	308.3-311.5	50.37	1.0050	2.0e-2	85	315.645(75)	0.99611(132)
44.15	317.29	312.58	50.44	2.534	5.0e-2	78	315.348(100)	0.99776(209)
44.15	317.29	313.11	200.7	0.2043	1.0e-3	78	316.131(45)	1.00739(55)
44.15	317.29	313.18	200.7	1.1597	5.8e-3	78	315.779(42)	0.99305(66)
44.15	317.29	313.27	200.7	2.505	1.2e-2	78	315.655(50)	0.99309(85)
21.45	294.59	295.36	50.37	0.2020	4.0e-3	78	293.756(88)	1.00400(146)
24.15	297.29	297.35	200.7	0.2017	1.0e-3	20	297.185(34)	0.99310(33)
24.15	297.29	297.50	200.7	0.2022	1.0e-3	78	297.307(41)	1.00344(56)
0.1	273.24	279.35	199.7	2.500	1.3e-2	85	274.595(46)	1.00047(111)

DLR

Linestrength intercomparison in 1 µm region

- NIST: cavity ringdown by Daniel Lisak and Joseph T. Hodges
- HIT: HITRAN 2008, mainly experimental data by Robert A. Toth
- Excellent agreement DLR-NIST, mostly <1%
- HITRAN 2008 shows bias and large scatter

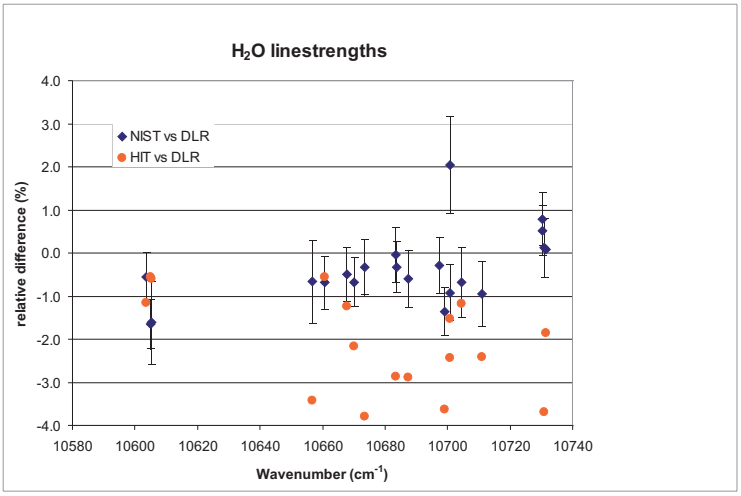

DLR

Linestrength intercomparison in 1 µm region

- Lodi: ab initio calculations by J. Tennyson's group
- Good agreement for 2 0 1 ← 0 0 0 and 0 0 3 ← 0 0 0 with occasional outliers
- Entire subbands shifted: 1 2 1 ← 0 0 0, 3 0 0 ← 0 0 0, 1 0 2 ← 0 0 0 up to 8%

Average differences

1 2 1 ← 0 0 0 4.1%
2 0 1 ← 0 0 0 0.0%
3 0 0 ← 0 0 0 4.0%
1 0 2 ← 0 0 0 -7.6%
0 0 3 ← 0 0 0 -0.1%

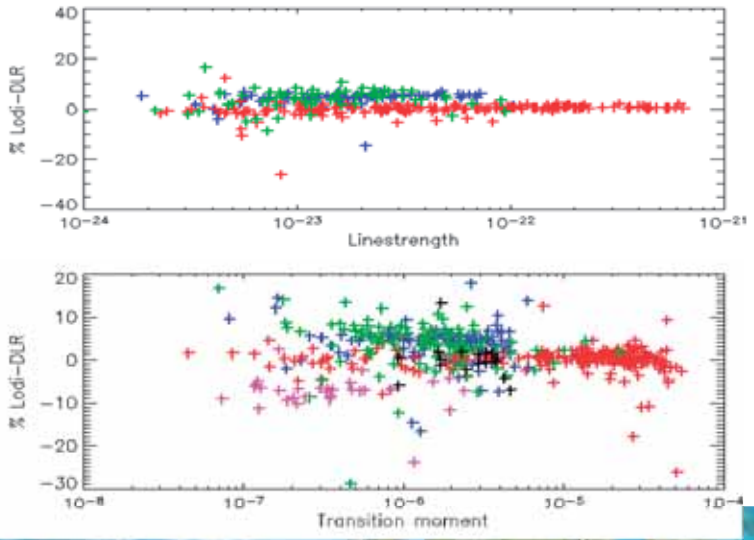

DLR

$H_2{}^{16}O$ linestrength intercomparison in ν_2 region

- HIT04: HITRAN 2004, mainly experimental data by Robert A. Toth
- Lodi: ab initio calculations

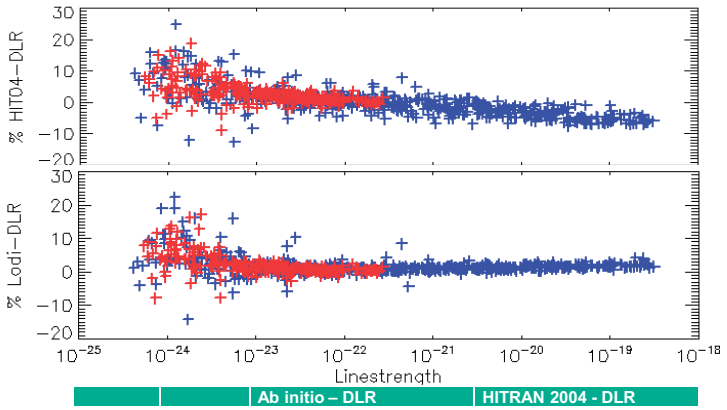

		Ab initio – DLR			HITRAN 2004 - DLR		
lg(Smin)	lg(Smax)	%Δ	%uncΔ	ndata	%Δ	%uncΔ	ndata
-24.5	-24.0	3.66	0.80	23	5.90	0.79	24
-24.0	-23.5	4.23	0.23	77	5.46	0.24	75
-23.5	-23.0	2.12	0.10	94	3.56	0.10	95
-23.0	-22.5	1.19	0.04	105	1.87	0.04	106
-22.5	-22.0	0.76	0.02	109	0.91	0.02	108
-22.0	-21.5	0.74	0.02	72	0.27	0.02	73
-21.5	-21.0	0.85	0.02	50	-1.52	0.01	53
-21.0	-20.5	1.13	0.02	52	-2.63	0.01	50
-20.5	-20.0	1.14	0.02	51	-2.73	0.02	50
-20.0	-19.5	1.62	0.02	51	-3.80	0.01	51
-19.5	-19.0	1.74	0.01	53	-5.79	0.01	55

$H_2{}^{18}O$ linestrength intercomparison in ν_2 region

- HIT04: HITRAN 2004, mainly experimental data by Robert A. Toth
- Lodi: ab initio calculations

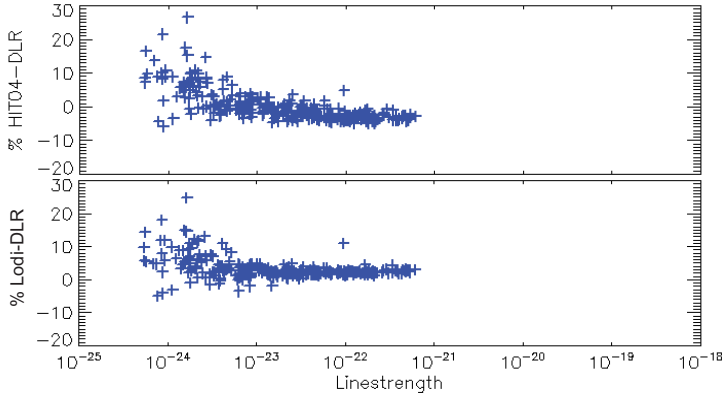

		Ab initio - DLR			HITRAN 2004 - DLR		
lg(Smin)	lg(Smax)	%Δ	%uncΔ	ndata	%Δ	%uncΔ	ndata
-24.5	-24.0	2.84	1.09	12	4.04	1.14	11
-24.0	-23.5	3.82	0.32	44	3.27	0.32	45
-23.5	-23.0	1.00	0.13	53	-1.20	0.13	53
-23.0	-22.5	0.28	0.06	50	-3.30	0.06	53
-22.5	-22.0	0.16	0.03	53	-4.75	0.03	55
-22.0	-21.5	0.27	0.02	47	-5.11	0.02	42
-21.5	-21.0	0.63	0.03	17	-5.43	0.03	17

$H_2{}^{16}O$ linestrength intercomparison in ν_2 region

Binned averages of single measurements vs. ab initio – measurements show inconsistencies ($\Delta = S_{ab\ initio} - S_{DLR}$)

			S: $10^{-24.5}$ – 10^{-24}			S: 10^{-24} – $10^{-23.5}$			S: $10^{-23.5}$ – 10^{-23}			S: 10^{-23} – $10^{-22.5}$		
p_{H2O}/mb	p_{tot}/mb	l/m	%Δ	%uncΔ	ndata	%Δ	%uncΔ	ndata	%Δ	%uncΔ	ndata	%Δ	%uncΔ	ndata
0.2000	0.2007	0.249	-	-	0	-	-	0	-	-	0	-	-	0
1.0007	1.0007	0.249	-	-	0	-	-	0	-	-	0	-	-	0
4.972	4.972	0.249	-	-	0	-	-	0	-	-	0	-15.67	4.19	16
0.2000	0.2007	20.990	-	-	0	-	-	0	-10.88	2.30	36	-0.03	0.63	98
1.0086	1.0086	20.990	-	-	0	-9.75	1.46	67	-1.39	0.83	90	0.60	0.27	101
4.950	4.950	20.990	-4.48	1.52	54	2.33	0.76	80	1.89	0.27	87	1.61	0.10	95
0.2000	0.2007	85.020	-	-	0	-	-	0	-0.68	0.66	72	0.38	0.21	104
1.0016	1.0016	85.020	-12.63	2.02	45	-0.54	1.07	82	0.32	0.37	92	0.36	0.14	97
4.952	4.952	85.020	1.20	1.10	54	1.76	0.37	68	1.31	0.16	72	1.11	0.11	70
0.2051	50.37	78.620	-	-	0	-	-	0	-2.06	1.60	24	-0.89	0.49	94
2.5061	50.49	20.990	-5.19	3.54	18	6.45	0.84	71	3.29	0.45	80	1.45	0.17	87
1.0049	50.39	85.020	-	-	0	-0.91	1.55	30	2.22	0.58	83	2.22	0.25	93
4.9626	49.83	20.990	8.89	1.60	44	8.50	0.69	75	2.81	0.30	76	1.15	0.11	81
2.5185	99.95	20.990	-	-	0	2.44	1.22	56	3.79	0.48	73	1.23	0.21	86
5.0295	100.57	20.990	2.45	2.45	19	5.70	0.64	67	4.40	0.33	68	0.78	0.12	72
0.0209	199.4	20.990	-	-	0	-	-	0	-	-	0	-	-	0
0.0239	199.4	78.620	-	-	0	-	-	0	-	-	0	-	-	0
0.2020	200.7	20.990	-	-	0	-	-	0	-	-	0	2.84	1.44	19
0.2050	200.7	78.620	-	-	0	-	-	0	-	-	0	2.27	0.62	36
2.5197	200.4	20.990	-	-	0	0.77	2.01	19	3.23	0.62	67	1.92	0.24	81
5.0134	199.6	20.990	-	-	0	4.81	0.90	51	5.58	0.41	61	1.19	0.18	71
2.5120	400.3	20.990	-	-	0	-	-	0	0.41	0.95	31	2.53	0.31	71
5.0250	399.9	20.990	-	-	0	4.04	1.68	12	2.87	0.53	49	2.49	0.24	59
2.8594	501.8	0.161	-	-	0	-	-	0	-	-	0	-	-	0
5.5612	1000.6	0.161	-	-	0	-	-	0	-	-	0	-	-	0

H_2O linestrength intercomparison in ν_2 region

After removal of 6 measurements consistent results

$H_2{}^{16}O$		All data			Data without selected air-broadened measurements		
lg(Smin)	lg(Smax)	%Δ	%uncΔ	ndata	%Δ	%uncΔ	ndata
-24.5	-24.0	3.66	0.80	23	0.41	1.26	12
-24.0	-23.5	4.23	0.23	77	1.61	0.30	66
-23.5	-23.0	2.12	0.10	94	1.34	0.11	94
-23.0	-22.5	1.19	0.04	105	1.19	0.05	105
-22.5	-22.0	0.76	0.02	109	0.97	0.03	109
-22.0	-21.5	0.74	0.02	72	1.08	0.03	71
-21.5	-21.0	0.85	0.02	50	1.03	0.02	50
-21.0	-20.5	1.13	0.02	52	1.15	0.01	52
-20.5	-20.0	1.14	0.02	51	1.12	0.02	51
-20.0	-19.5	1.62	0.02	51	1.60	0.02	51
-19.5	-19.0	1.74	0.01	53	1.71	0.01	53

$H_2{}^{18}O$		All data			Data without selected air-broadened measurements		
lg(Smin)	lg(Smax)	%Δ	%uncΔ	ndata	%Δ	%uncΔ	ndata
-24.5	-24.0	2.84	1.09	12	-	-	<11
-24.0	-23.5	3.82	0.32	44	-0.10	0.41	40
-23.5	-23.0	1.00	0.13	53	0.51	0.15	52
-23.0	-22.5	0.28	0.06	50	0.18	0.08	50
-22.5	-22.0	0.16	0.03	53	0.08	0.05	53
-22.0	-21.5	0.27	0.02	47	0.25	0.04	46
-21.5	-21.0	0.63	0.03	17	0.78	0.05	17

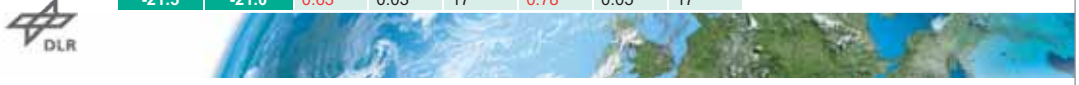

IASI retrieval improvement in H_2O ν_2 region using DLR linestrength and pressure broadening

Red: residuals DLR, pink: residuals HITRAN 2008

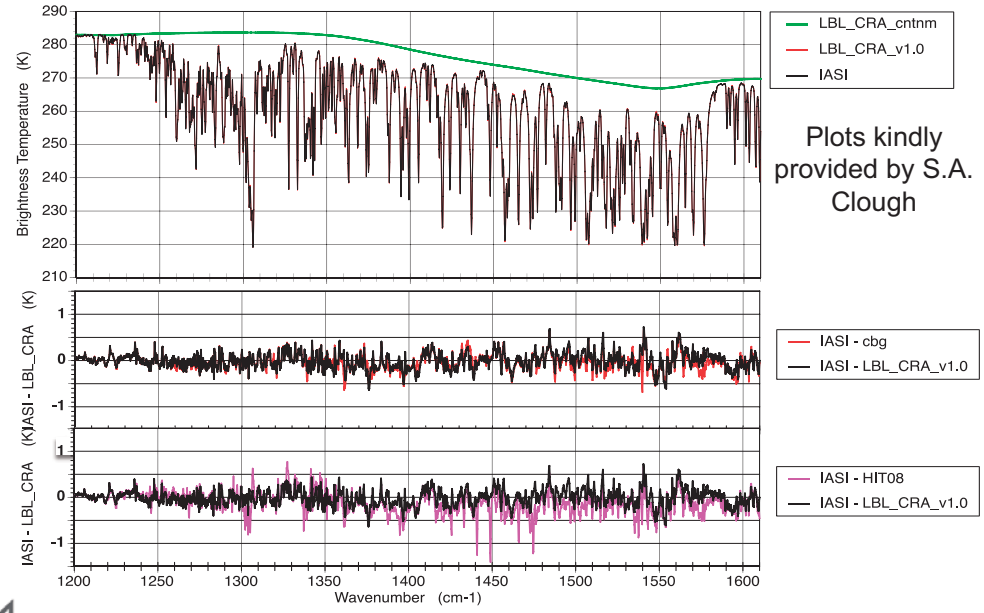

Plots kindly provided by S.A. Clough

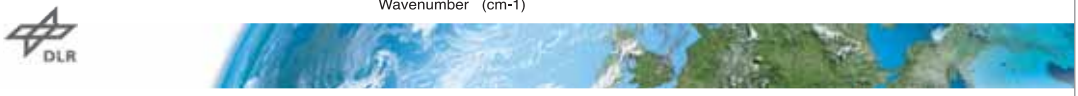

Conclusion

- Experimental set-up and measurement parameters CAN be designed/selected to minimise systematic errors
  - ➢ Standardised methods can be developed, e.g. how to build gas cells and other equipment, how to make a measurement plan including appropriate measurement parameters and characterisation measurements
- Redundancy is a key to identify remaining systematic errors, i.e. lines should be measured at different experimental conditions: opacity, line width, mixing ratio, instrumental parameters
- Analysis algorithms can be partly standardised: e.g. multispectrum fitting, line model, instrumental lineshape model, VDPA

⇒ **Standardisation helps, but …**

Conclusion (continued)

- Current problems in spectroscopic database are not solvable by primary standards, e.g.:
  - The gas temperature and its homogeneity in the gas cell is relevant
  - For the absorption path in a gas cell the mean length of the rays between the windows is relevant
  - For gas mixtures the mixing ratio in the gas cell is relevant
  - Traceable pressure sensors, temperature sensors, and CNC machines with adequate accuracy are commercially available

A scientific approach is required

since

- Accuracy requirements from remote sensing + molecule + spectral region give a large variety and complexity of spectroscopic tasks
- Most spectroscopic tasks have specific issues which cannot be standardised

"Absorption/emission spectra from first principles: Towards large-scale production of line lists for molecules of atmospheric importance"

Dr. Sergey N. Yurchenko

Department of Physics and Astronomy, University College London

Dr. Sergey N. Yurchenko

Department of Physics and Astronomy, University College London
Gower Street, WC1E 6BT London, UK
Phone: +44 02076790172
E-mail: s.yurchenko@ucl.ac.uk

Education and Professional Experience

since 2011	Principal Research Associate, Department of Physics & Astronomy, University College London, UK
2007-2011	Wissenschaftlicher Mitarbeier (Researcher), Theory group (Prof. G. Seifert), Technical University of Dresden (TU Dresden), Germany
2004-2006	Theoretical Chemistry Group (Prof. W. Thiel), Max-Planck-Institut für Kohlenforschung, Mülheim an der Ruhr, Germany
2002-2004	Researcher, Theory and Computational Group (Dr. Ph. Bunker), Steacie Institute for Molecular Sciences, National Research Council of Canada, Ottawa, Canada
2000-2001	Wissenschaftlicher Mitarbeier, Theoretical Chemistry Group (Prof. P. Jensen), Bergische Universität, Wuppertal, Germany
1998-2000	Senior Teacher, Optics and Spectroscopy Department (Prof. Yu. S. Makushkin), Tomsk State University, Russia
1998	Ph.D. (Molecular Spectroscopy), Tomsk State University, Russia, Thesis Title: Analysis of dynamic properties of small molecules using methods of the ro-vibration spectroscopy
1996-1997	Teaching Assistant, Optics and Spectroscopy Department, Tomsk State University, Russia
1992-1995	PhD Fellowship, Tomsk State University, Russia
1985-1992	Diploma with Honors, Department of Physics, Tomsk State University, Russia, Title: Spectroscopic approach to the reconstruction of temperature distributions in axisymmetric gas ows

Activities, Honors and Awards

- Visiting Scientists at University of Huelva, Spain, 2008
- Visiting Scientists at University College London, Great Britain, 2006-2010
- Max Planck Fellowship held at Max-Planck-Institut für Kohlenforschung, Mülheim an der Ruhr, Germany, 2004
- NSERC Fellowship held at Steacie Institute for Molecular Sciences, National Research Council of Canada, Ottawa, 2003-2004
- Visiting Scientists at University of Science and Technology of China, Hefei, China, 1996
- Tomsk State University Award for the Best Scientific Work Among Young Researchers on Physics, November of 1996

Absorption/emission spectra from first principles: Towards large-scale production of line lists for molecules of atmospheric importance

Sergei. N. Yurchenko

Department of Physics and Astronomy, University College London

Most of the modern observations of the processes and phenomena taking place in our atmosphere or in the atmospheres of other astrophysical objects are based on fundamental atomic and molecular data, necessary to interpret these observations. Variational nuclear motion calculations, combined with high accuracy *ab initio* electronic structure computations, are making a significant impact on high-resolution spectroscopy as well as astrophysics and atmospheric physics. This work is important for spectral analysis and particularly for dipole transition intensities, which are often very difficult to measure reliably but are essential inputs for many applications such as modeling of radiative transport and remote sensing. Very extended libraries of molecular spectroscopic parameters (positions, intensities, and assignments) are required for spectral characterization, spectral simulation and as input of atmospheric models for the Earth as well as for different astrophysical bodies (cool stars, planets, and planetary discs) at a broad range of temperatures. Demands for extended line lists covering many millions of transitions are best met with high quality theoretical models. We are using first principles quantum mechanical methods and empirical tuning based on laboratory spectroscopic data and making extensive use of state-of-the-art computing. These and other aspects of the line list production will be discussed with reference to the importance of the high-resolution laboratory measurements.

ExoMol

UCL

Absorption/emission spectra from first principles: Towards large scale production of line lists for molecules of atmospheric and *astrophysical* importance

Sergey N. Yurchenko

Jonathan Tennyson and Exomol group

Physics and Astronomy Department

University College London

erc

Hot ammonia: Emission (T = 900 K) spectrum

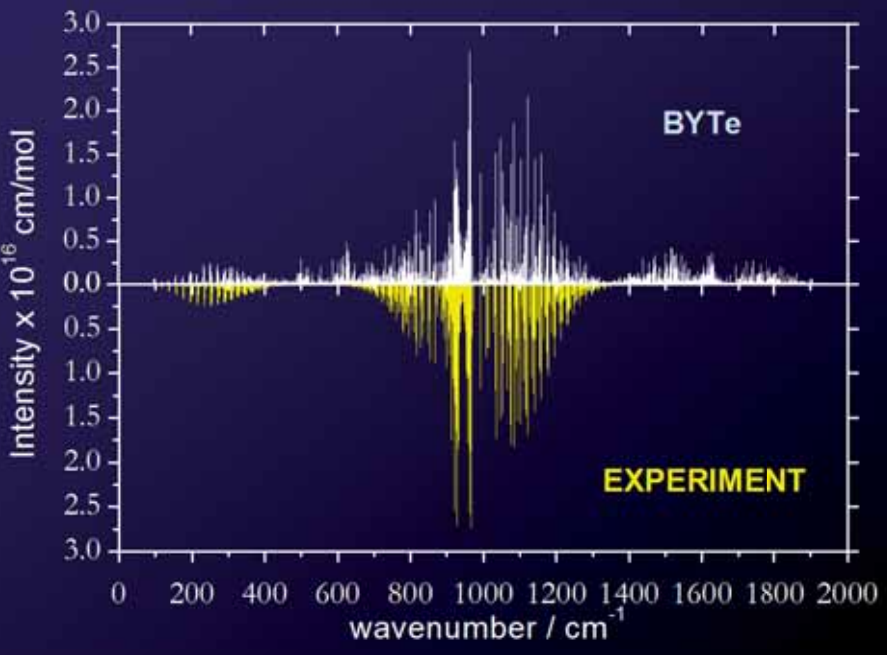

BYTe: S.N. Yurchenko, R.J. Barber, J. Tennyson, MNRAS 413, 1828 (2011).
Experiment: Sh. Yu et al., J. Chem. Phys. 133, 174317 (2010).


ExoMol
Molecular Line Lists for Exoplanet Atmospheres

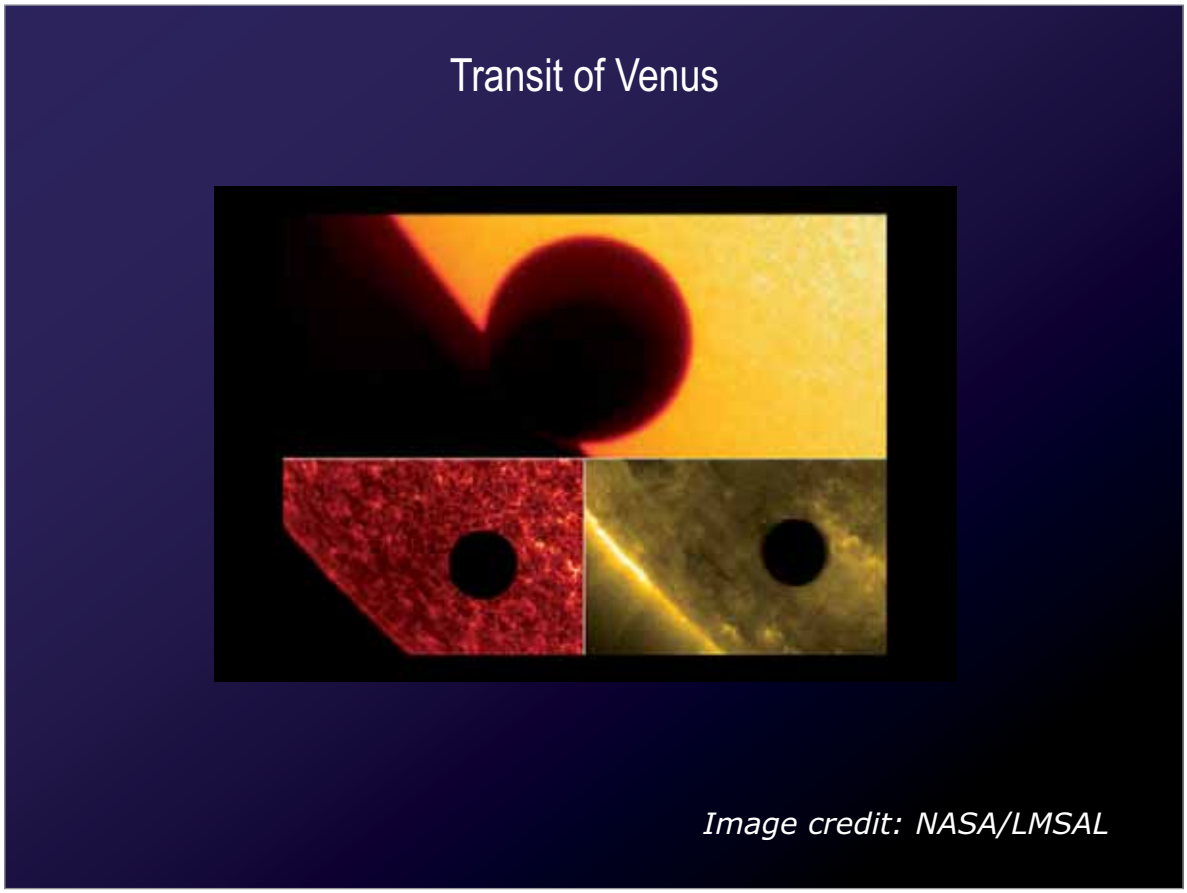
Transit of Venus
Image credit: NASA/LMSAL

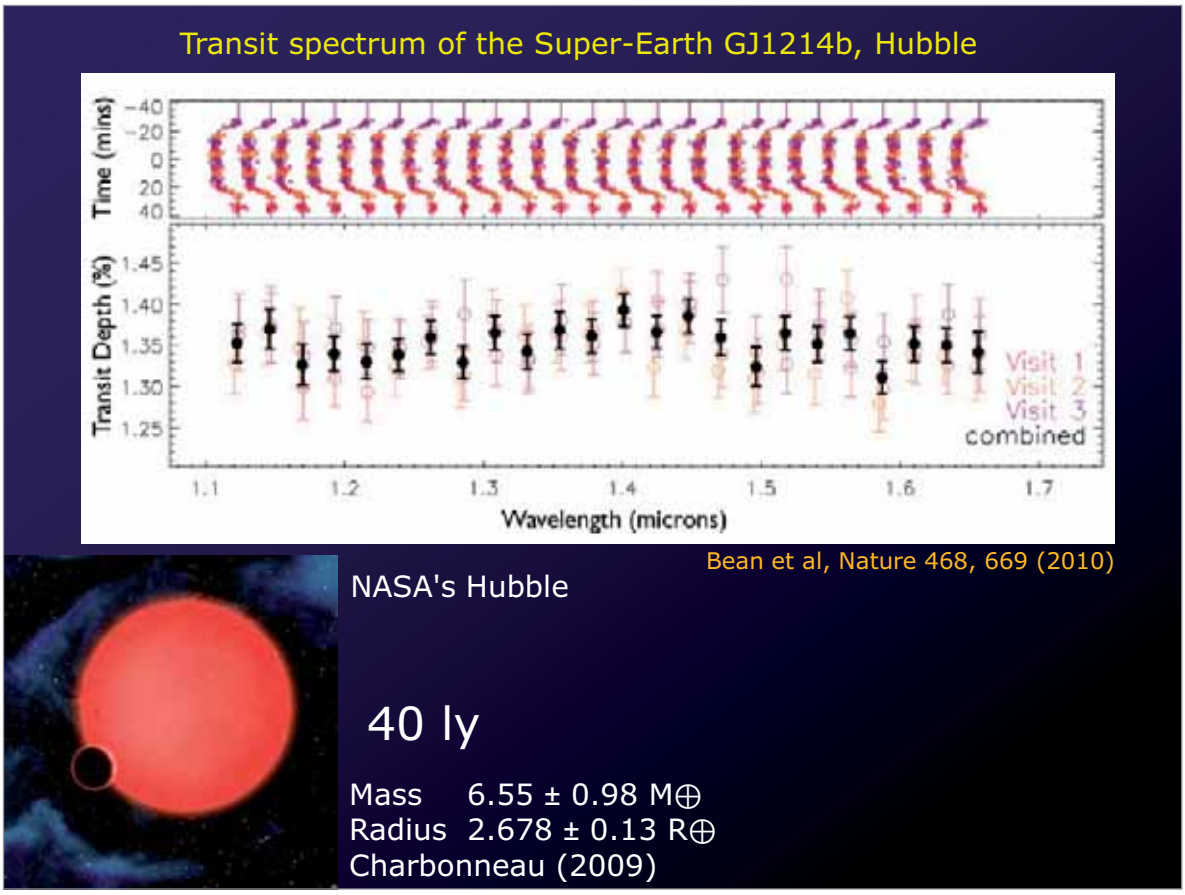
Transit spectrum of the Super-Earth GJ1214b, Hubble
Time (mins)
Transit Depth (%)
Wavelength (microns)
Visit 1
Visit 2
Visit 3
combined
Bean et al, Nature 468, 669 (2010)
NASA's Hubble
40 ly
Mass 6.55 ± 0.98 M⊕
Radius 2.678 ± 0.13 R⊕
Charbonneau (2009)

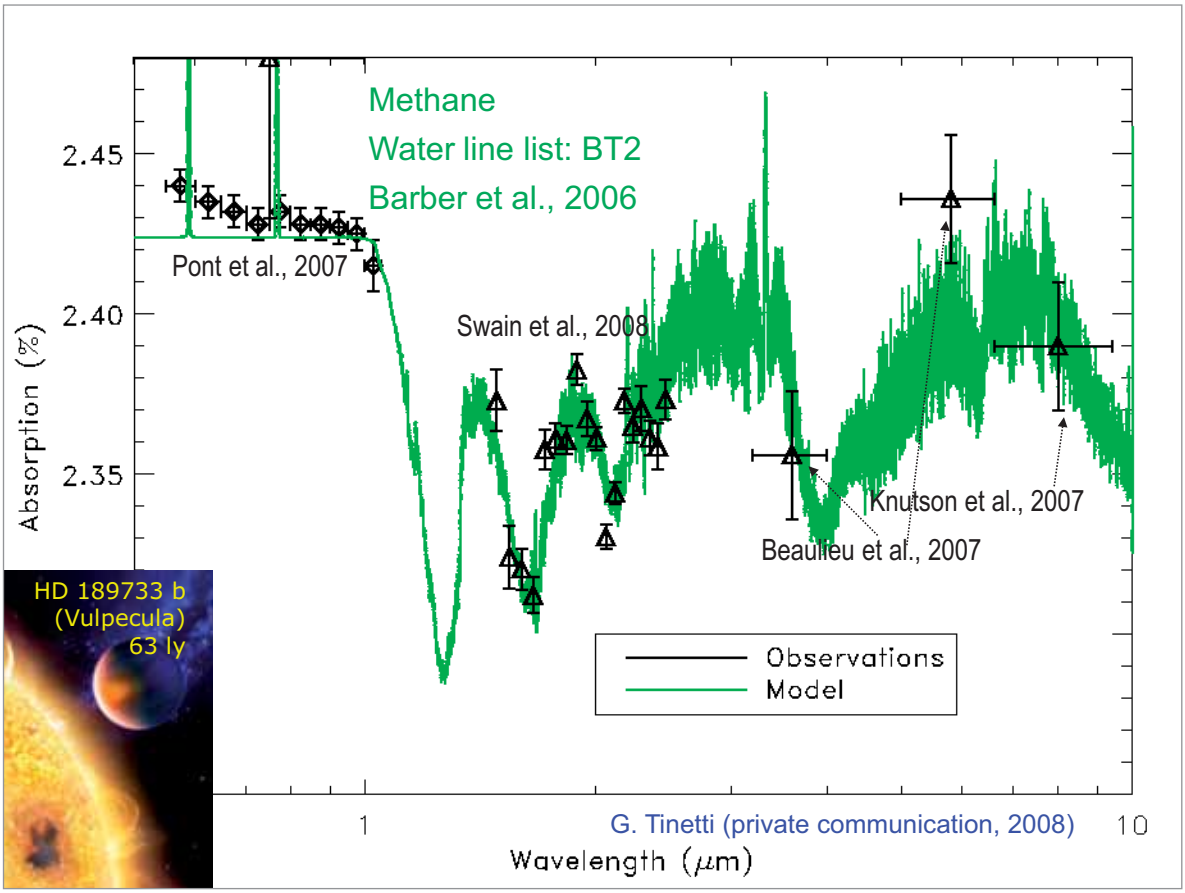
Methane
Water line list: BT2
Barber et al., 2006
Pont et al., 2007
Swain et al., 2008
Knutson et al., 2007
Beaulieu et al., 2007
Absorption (%)
Observations
Model
HD 189733 b
(Vulpecula)
63 ly
G. Tinetti (private communication, 2008)
Wavelength (μm)

Transit spectrum of the super-Earth GJ1214b

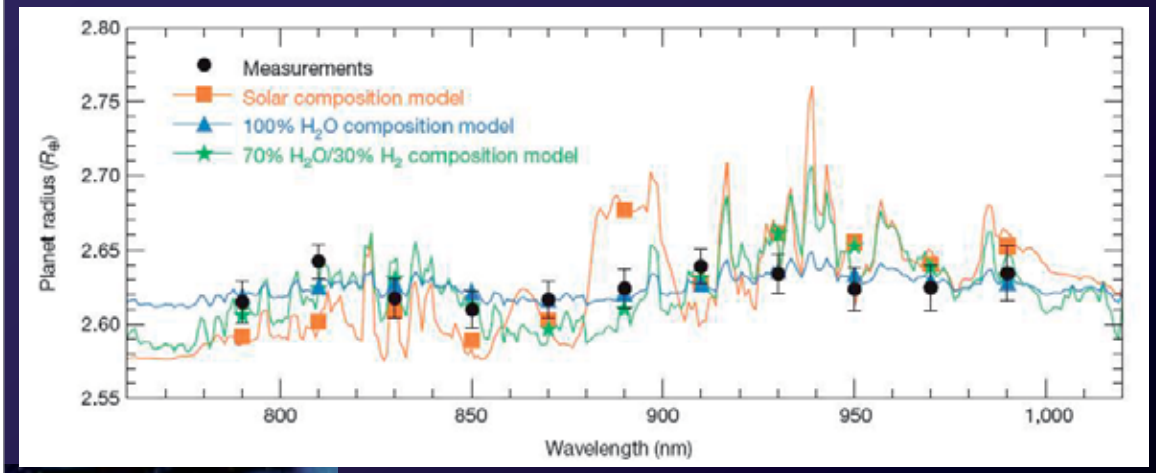

NASA's Hubble

40 ly

Mass 6.55 ± 0.98 M⊕
Radius 2.678 ± 0.13 R⊕
Charbonneau (2009)

ExoMol "PERIODIC" TABLE

Molecular line lists for exoplanet & other atmospheres

Primordial	Terrestrial Planets (Oxidising)			Giant-Planets & Cool Stars						
H_2									H_2	Already available
LiH	OH						TiO	CO	CO_2	
HeH^+	NO						CN	CH	HCN	
H_3^+	O_3	CO_2	HDO	H_2O	NH_3	CaH	BeH	MgH	HNC	
H_2D^+	O_2	HOOH	HNO_3	H_2S	VO	FeH	AlH	C_3	C_2H_2	ExoMol
	SO_3	H_2CO	PH_3	SO_2	YO	AlO	SiH	HCl	C_2H_4	
				CH_4	NiH	TiH	SiH	KCl	C_2H_6	
				HNO_3	CrH	SiO	HF	NaCl	C_3H_8	
					C_2					

www.exomol.com

Other known sources of hot line lists

- UCL: H_2O, H_3^+, HDO, HCN/HNC,HD^+,HeH^+
- HITEMP (HITRAN?): CO,OH, NO,H_2O,CO_2
- P. Bernath's data (http://bernath.uwaterloo.ca/XY, e.g.XY=FeH)

  FeH, CrH, TiH, ...
- Kurucz's CDs, http://kurucz.harvard.edu/

  FeH, H_2, H_2O, H_2, SiH, TiO (Schwenke) ...
- SCAN data by Uffe Jørgensen

  CH, CN, C_2, C_3,TiO, and H_2O, ...
- UGAMOP (University of Georgia)

  H_2, H_2^+, HD, HeH^+,LiH, MgH, CaH, LiCl, H ...
- ...

J. Tennyson AND S. N. Yurchenko, MNRAS, 425, 21 (2012)

Method: from "first-principles"

Our approach: from "first-principles"

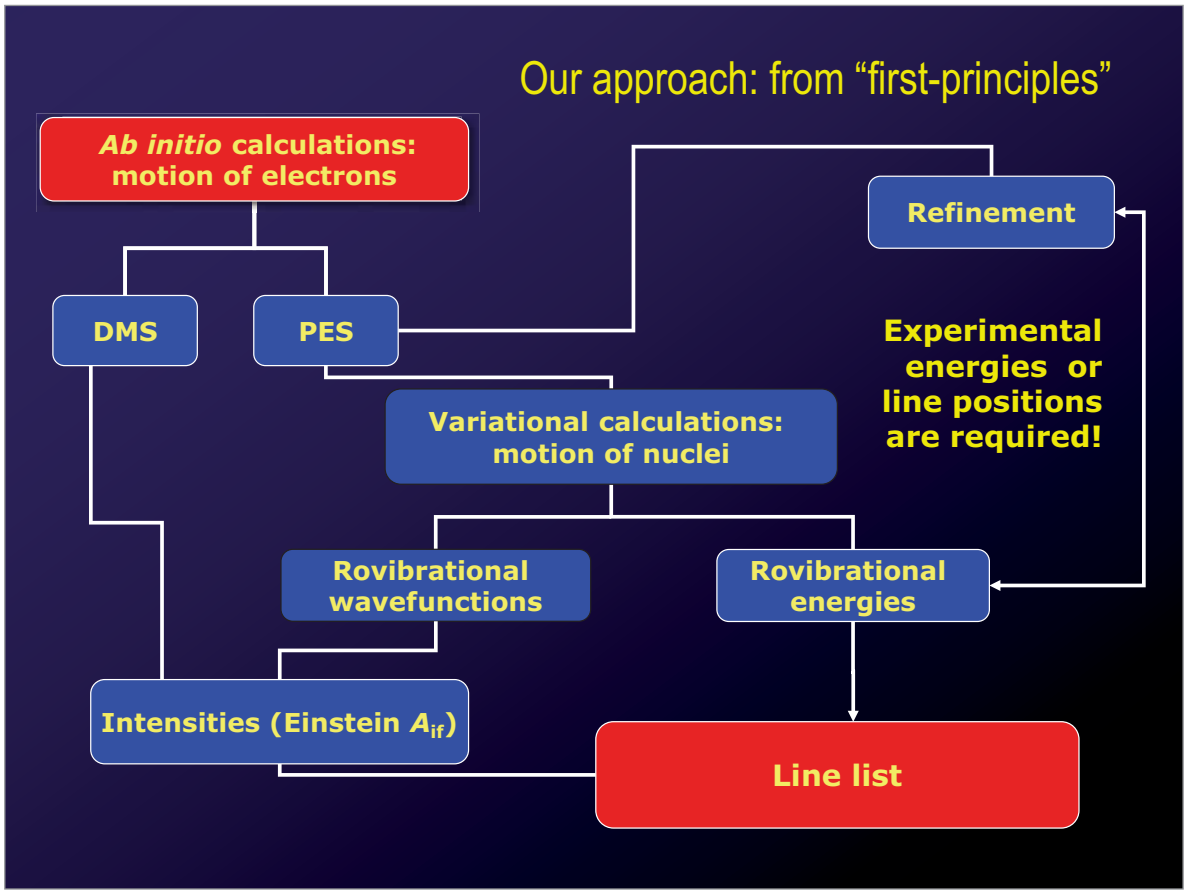

MgH

Potential energy curve

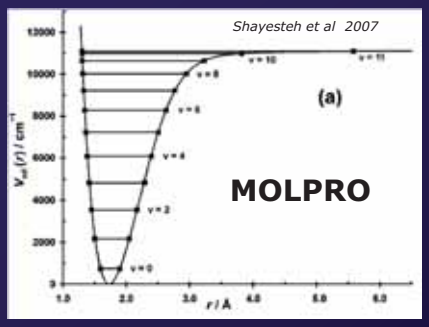

Dipole moment curve

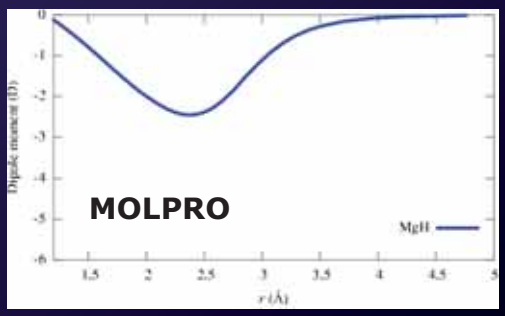

Solve for the motion of the nuclei

LEVEL 8.0
R. Le Roy,
Waterloo, Canada

Line list: 6690 lines, N_{max}=60

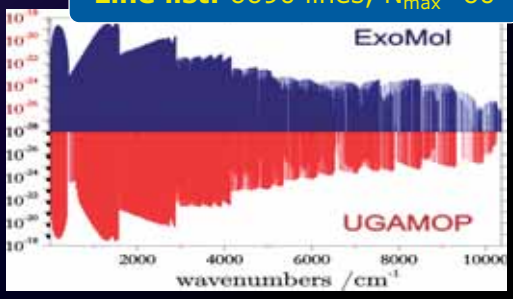

B. Yadin et al. MNRAS (2012)

Line list (in progress): C_2

Potential energy

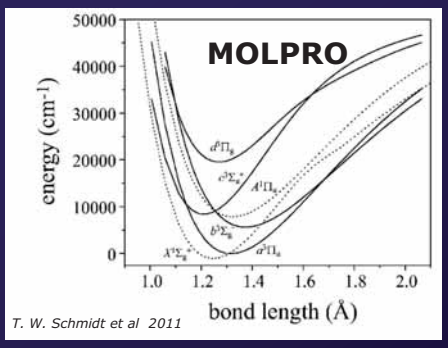

Spin-Orbit coupling

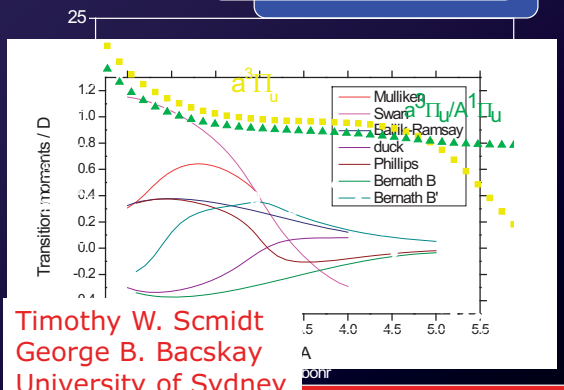

Timothy W. Scmidt
George B. Bacskay
University of Sydney

Solve for the motion of the nuclei

Line list: in progress

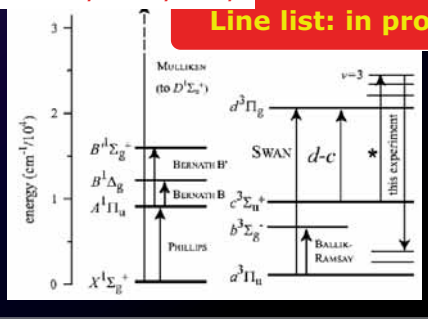

~~**LEVEL 8.0**~~

Our program *duo*

István Szabó, Eötvös University

Line list (in progress): AlO

Potential energy

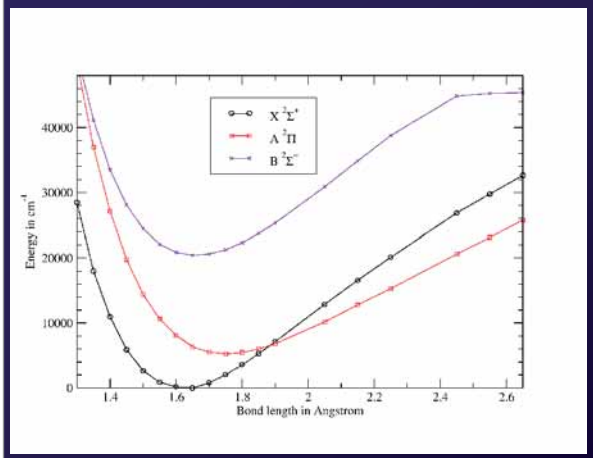

Line list

M.D. Saksena et al.
J. of Molec. Spectrosc. **247**, 47 (2008)

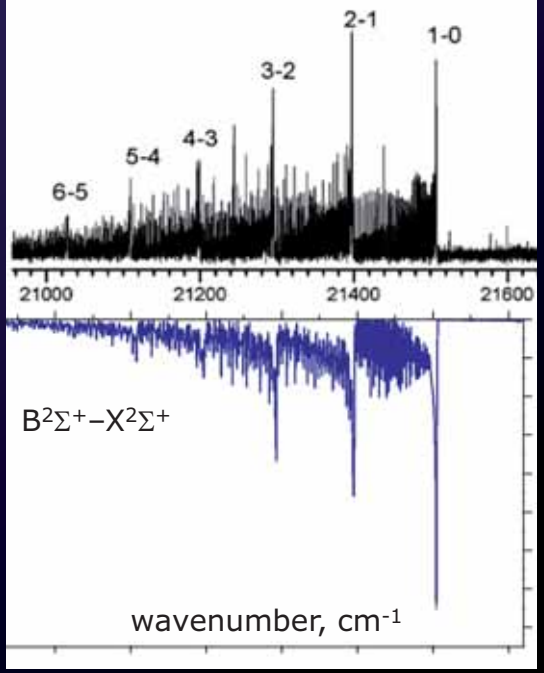

Andrei Patrascu

FeO

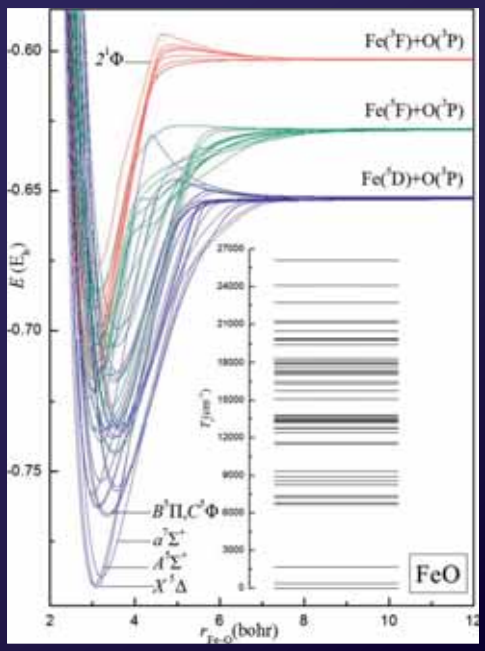

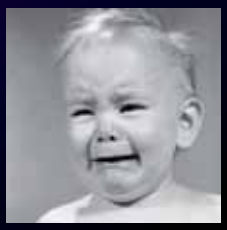

Sakellaris, et al. J. Chem. Phys. **134**, 234308 (2011)

Methane: in progress

Potential energy

9D surface
130 000
geometries

MOLPRO
CCSD(T)-f12/QZ

Ab initio
10 electrons
Ground
electronic state

Dipole moment

Three 9D surfaces
130 000
geometries

MOLPRO
CCSD(T)-f12/TZ

Solve for the motion of the nuclei

~~**LEVEL 8.0**~~
TROVE
Yurchenko, Thiel, Jensen, JMS **245**, 126 (2007)

Line list:

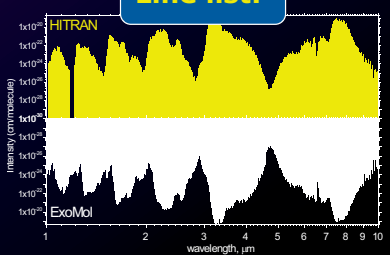

Billions of transitions

METHOD: TROVE

S. Yurchenko, W. Thiel, and P. Jensen

Andrey Yachmenev (Karlsruhe),
Roman Ovsyannikov (N. Novgorod)

TROVE: S.N. Yurchenko, W. Thiel, and P. Jensen, J. Mol. Spectrosc. 245, 126 (2007).

TROVE: Theoretical ROVibrational Energies

- Variational calculations
- Not exact kinetic energy operator
- OpenMP parallelization
- For a general molecule of arbitrary structure, arbitrary basis sets or coordinates
- FBR method (not a DVR)

Black-box program

- Intensity simulations
- Automatic symmetrization
- Lanczos diagonalization (large matrices)
- Automatic labeling of the levels
- Optimized for high *J*
- For a large amplitude motion (only one)
- Vibrational contraction of the basis set
- **Basis sets:**
  Harmonic oscillator
  Morse oscillator
  "Numerov-Cooley" solutions

TROVE: S.N. Yurchenko, W. Thiel, and P. Jensen, J. Mol. Spectrosc. 245, 126 (2007).

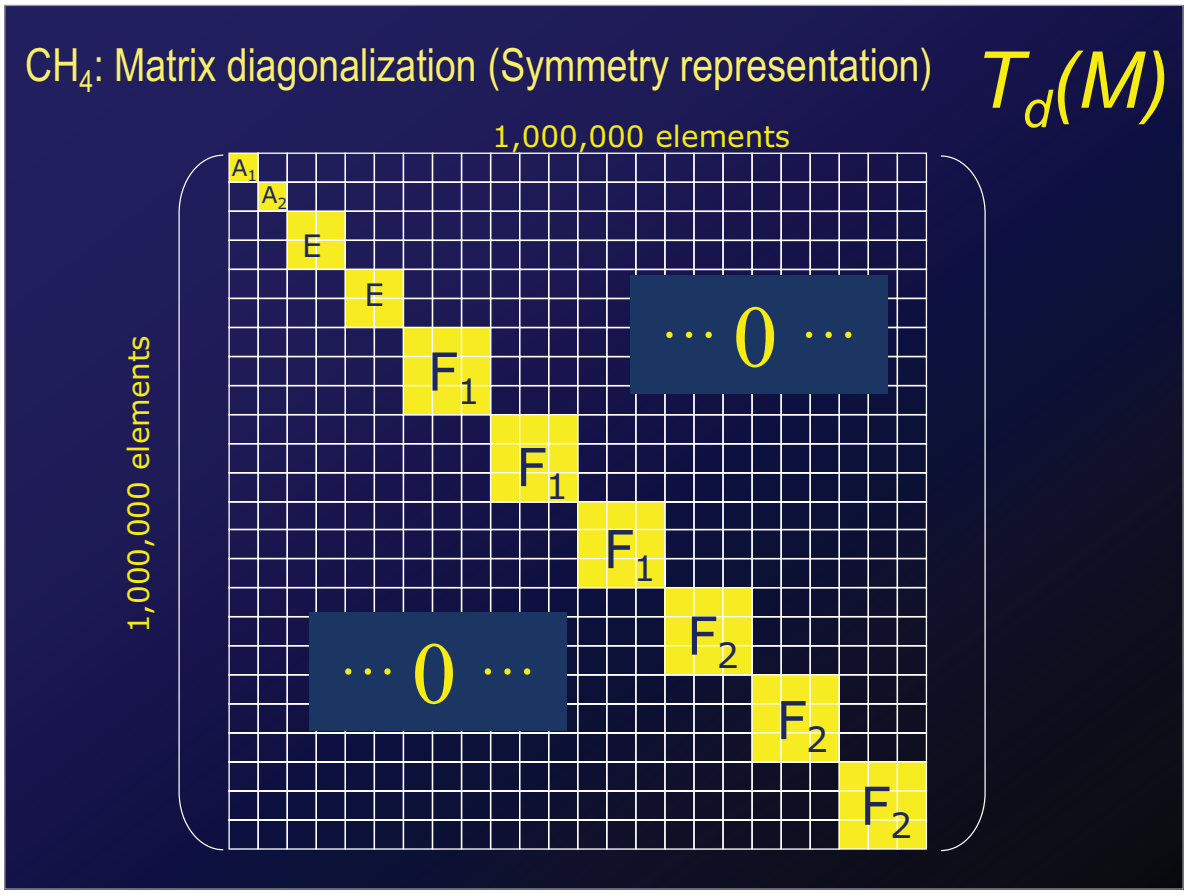
CH4: Matrix diagonalization (Symmetry representation)
Td(M)
1,000,000 elements
1,000,000 elements
A1
A2
E
E
F1
F1
F1
F2
F2
F2
… 0 …
… 0 …

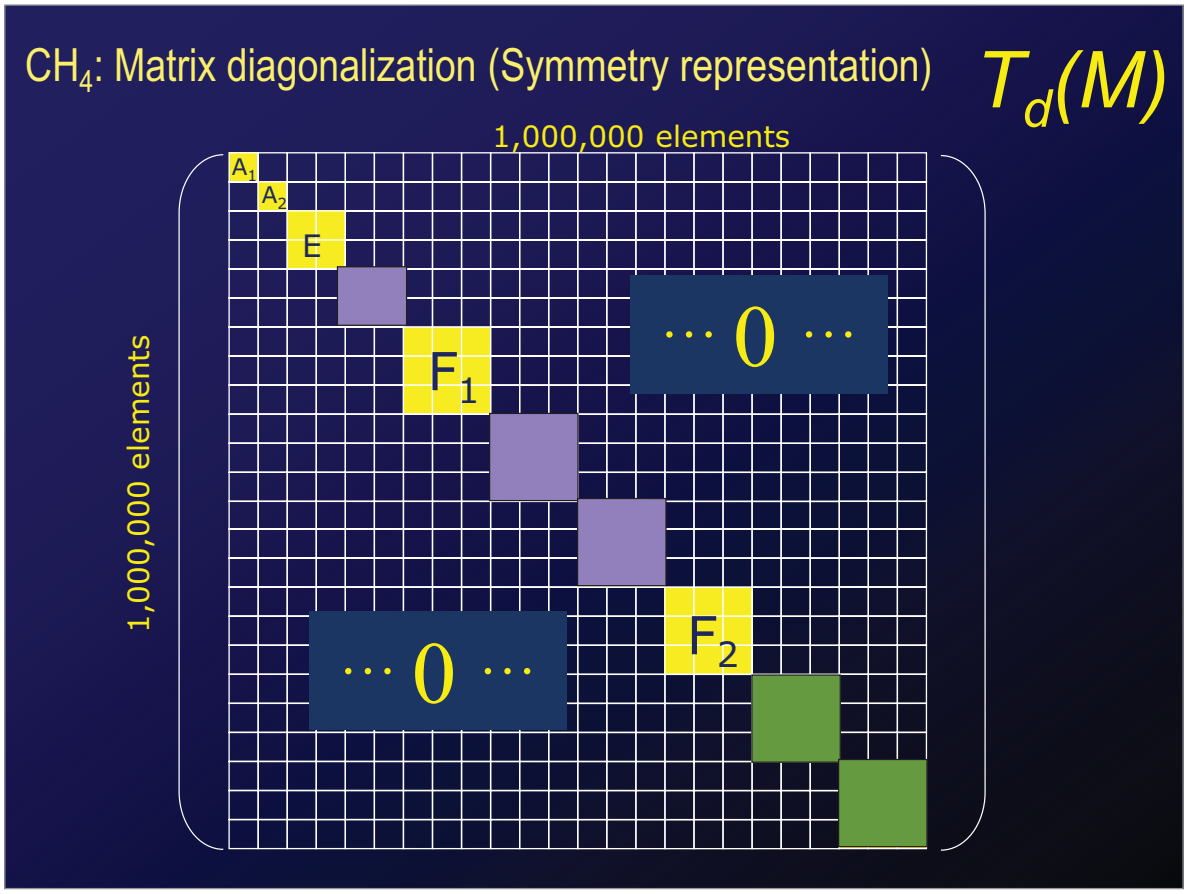
CH4: Matrix diagonalization (Symmetry representation)
Td(M)
1,000,000 elements
1,000,000 elements
A1
A2
E
F1
F2
… 0 …
… 0 …

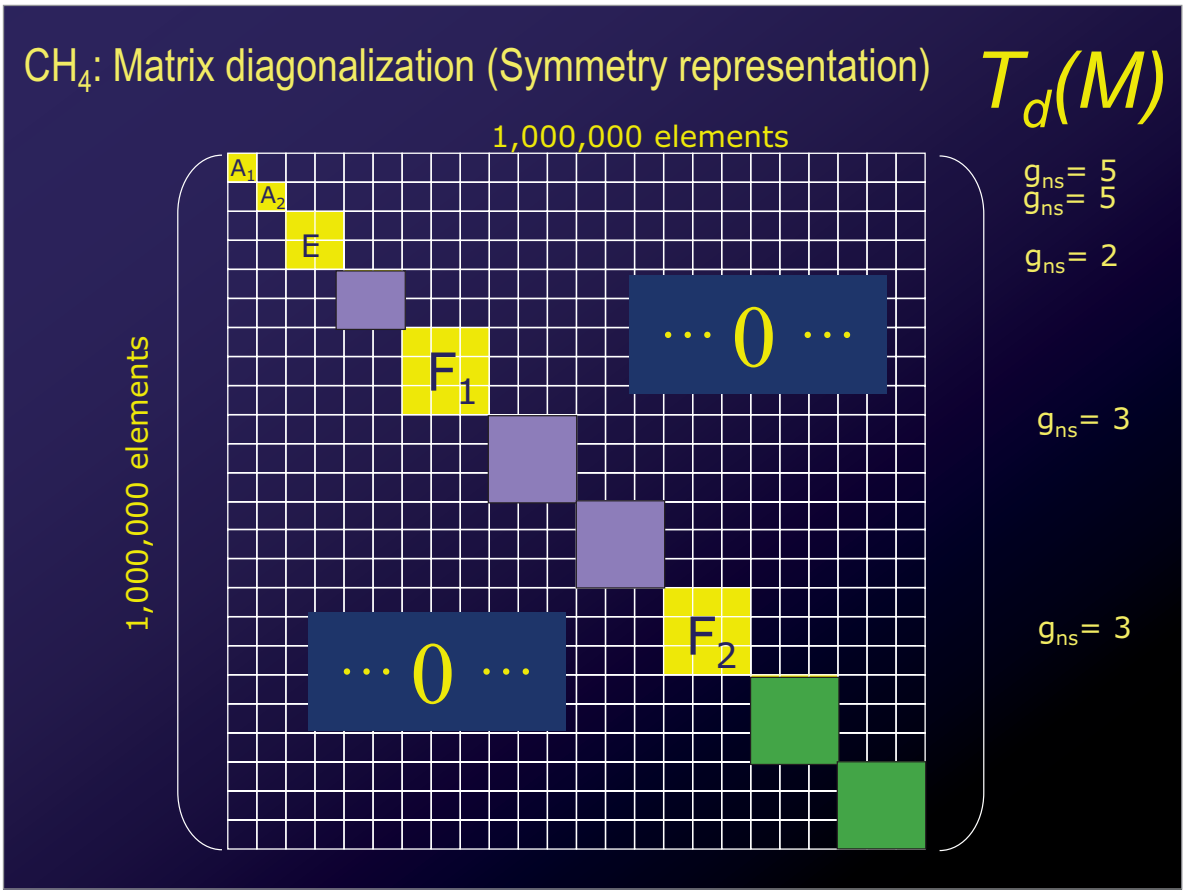

Theoretical line lists:
Completeness

Completeness: Absorption of ammonia (T=300 K)

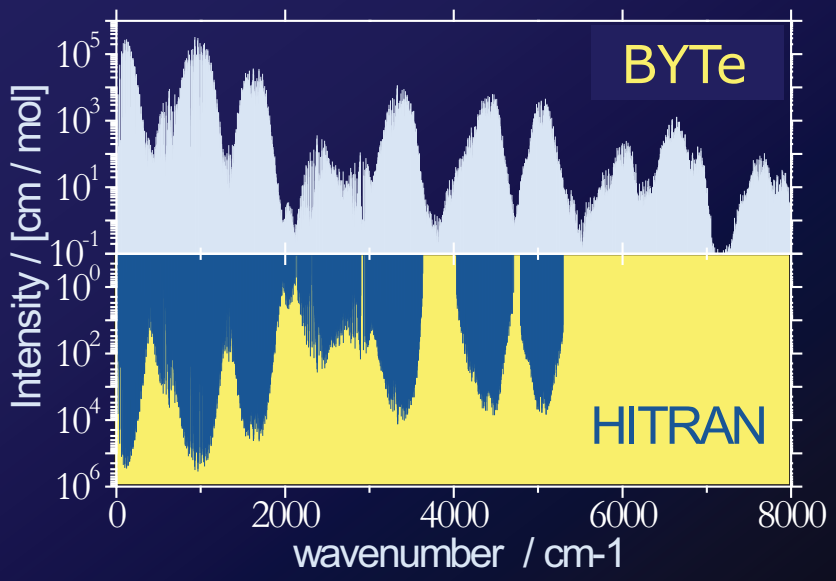

Less than 30,000 NH_3 lines are known experimentally: our list contains 1.1 billion lines, or about 40,000 times as many!

Completeness: Absorption of phosphine (T=300 K)

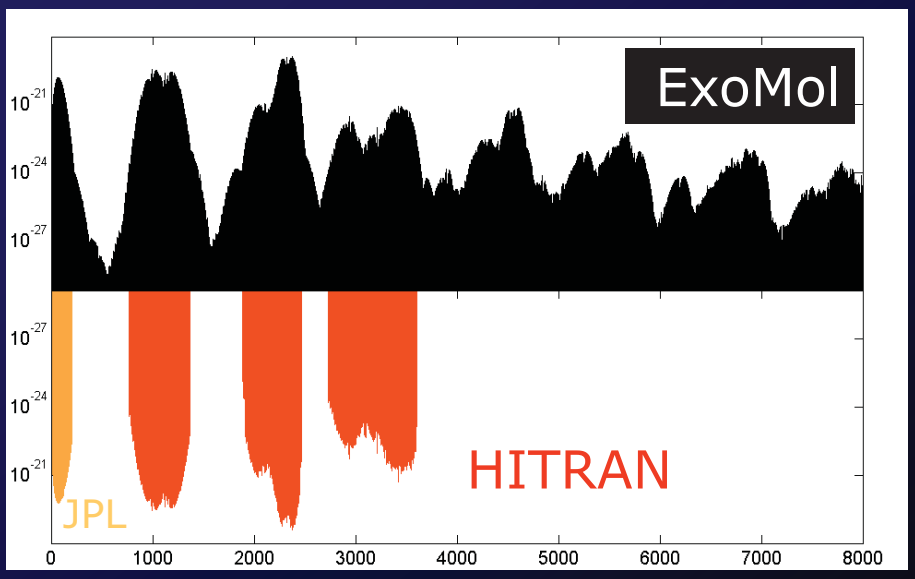

Clara Sousa Silva

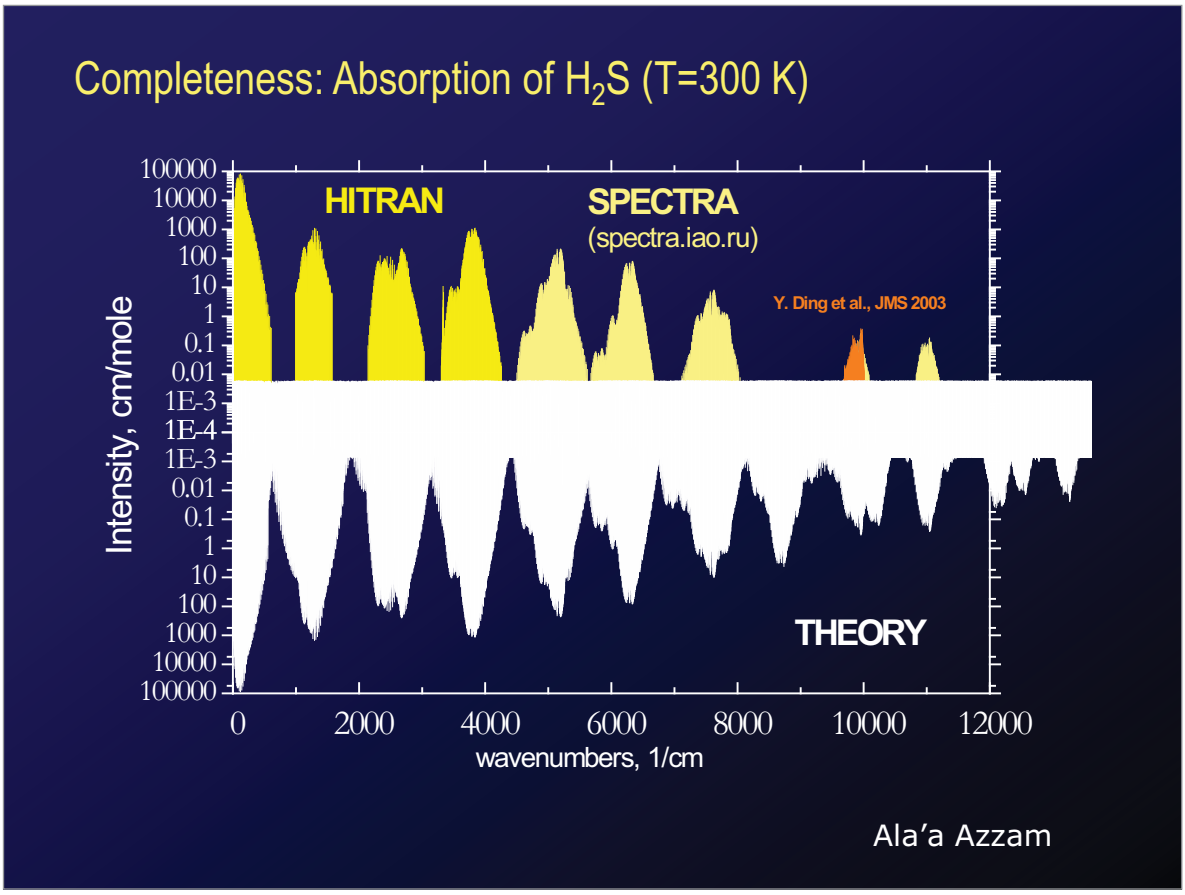
Completeness: Absorption of H_2S (T=300 K)
HITRAN
SPECTRA
(spectra.iao.ru)
Y. Ding et al., JMS 2003
THEORY
Intensity, cm/mole
100000
10000
1000
100
10
1
0.1
0.01
1E-3
1E-4
1E-3
0.01
0.1
1
10
100
1000
10000
100000
0
2000
4000
6000
8000
10000
12000
wavenumbers, 1/cm
Ala'a Azzam

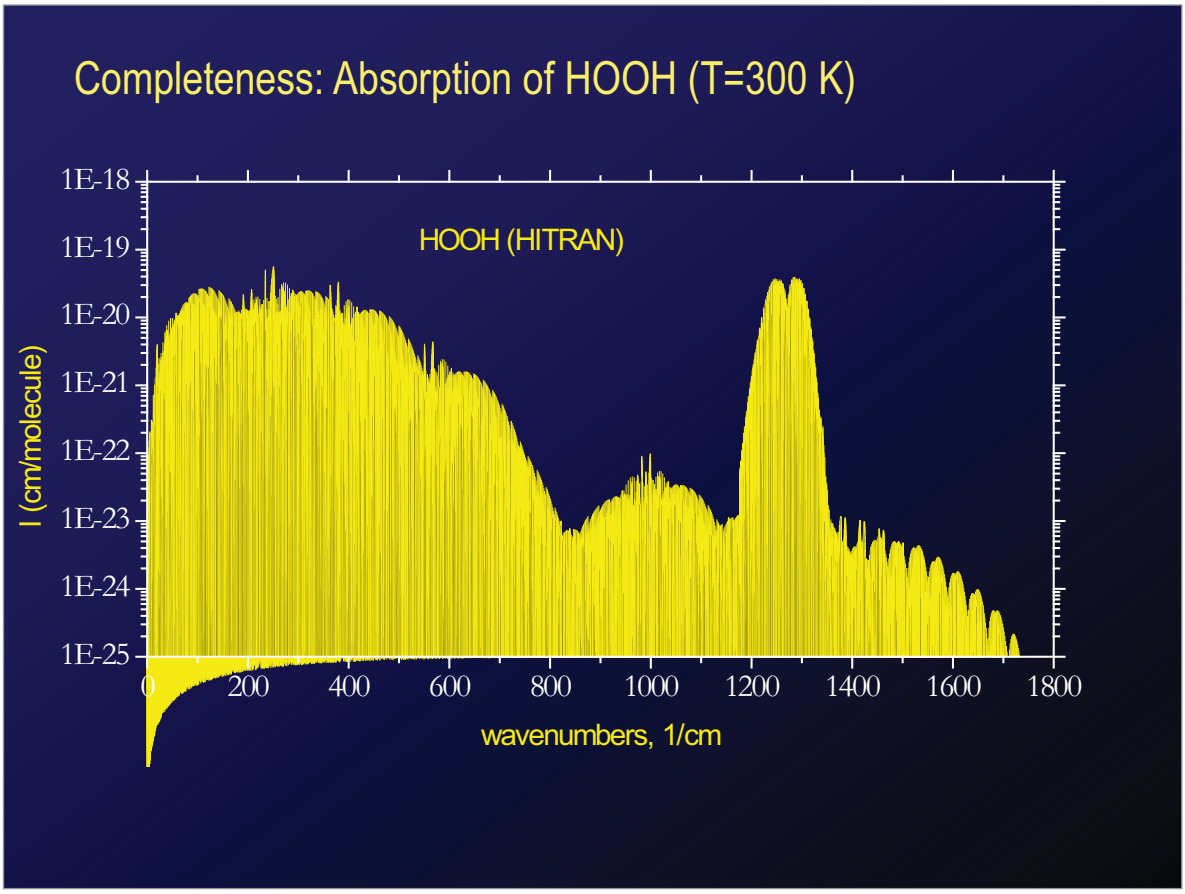
Completeness: Absorption of HOOH (T=300 K)
HOOH (HITRAN)
I (cm/molecule)
1E-18
1E-19
1E-20
1E-21
1E-22
1E-23
1E-24
1E-25
0
200
400
600
800
1000
1200
1400
1600
1800
wavenumbers, 1/cm

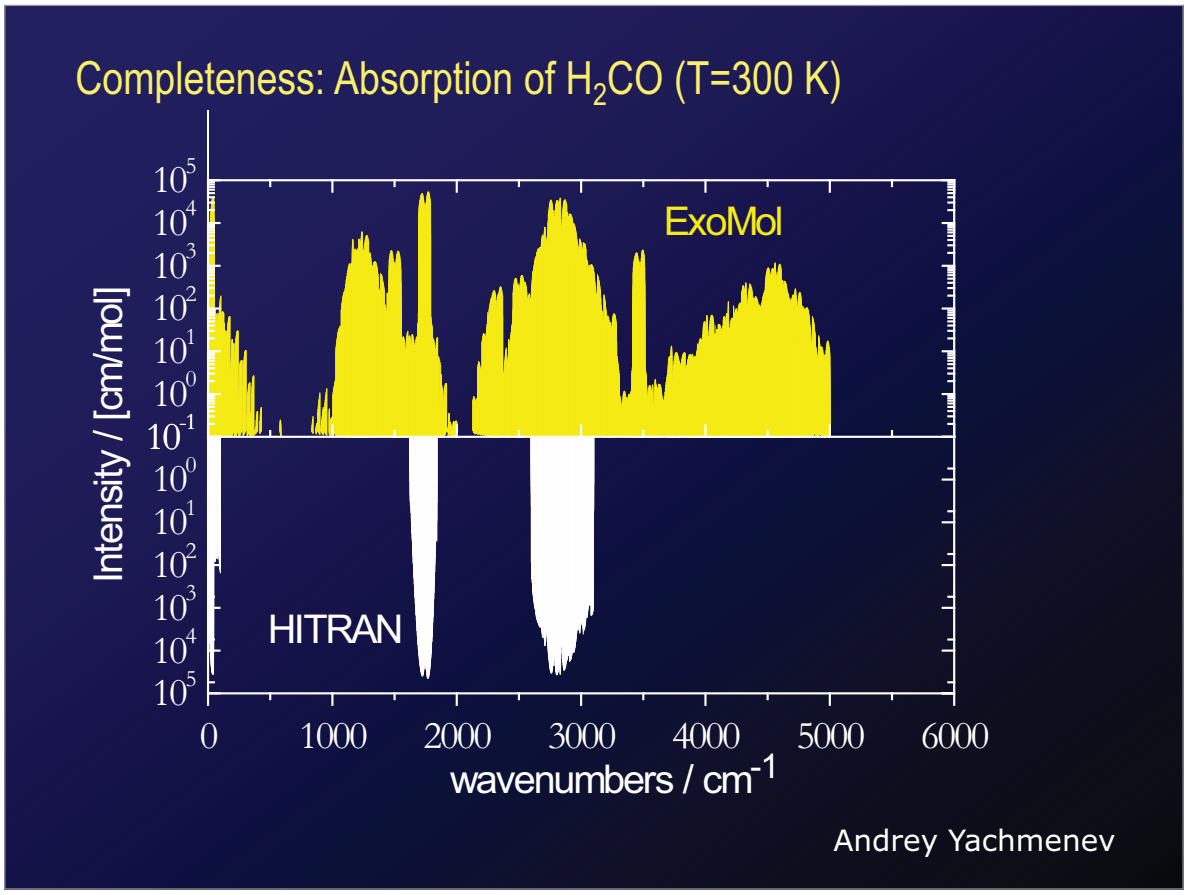
Completeness: Absorption of H_2CO (T=300 K)
ExoMol
HITRAN
Intensity / [cm/mol]
wavenumbers / cm^{-1}
Andrey Yachmenev

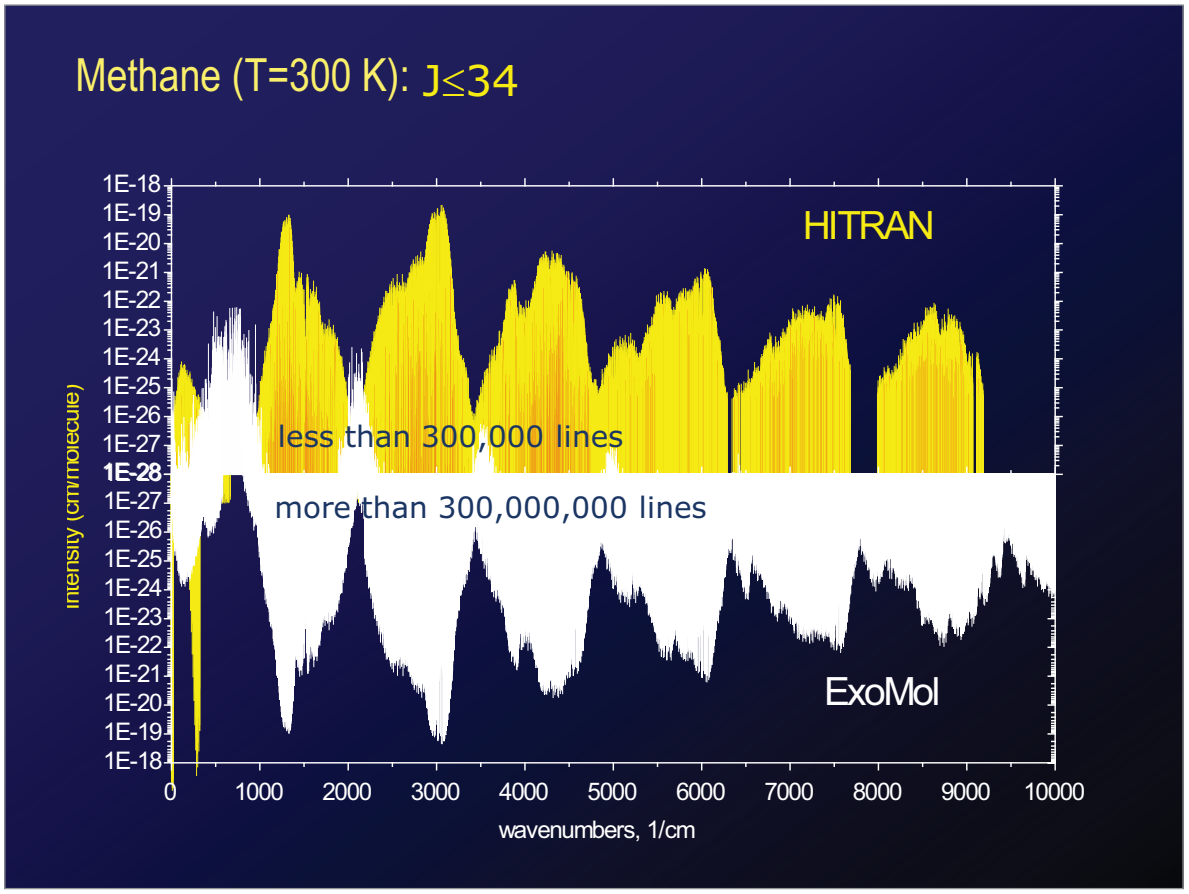
Methane (T=300 K): J≤34
HITRAN
less than 300,000 lines
more than 300,000,000 lines
ExoMol
Intensity (cm/molecule)
wavenumbers, 1/cm

CH_4 opacity at 1000 K

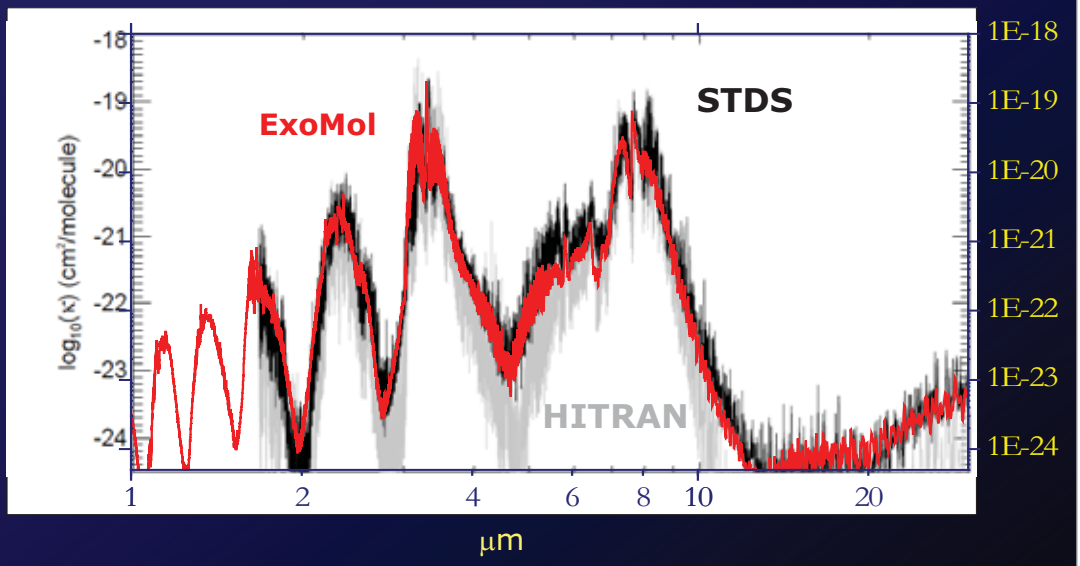

SO_3 (T=300 K)

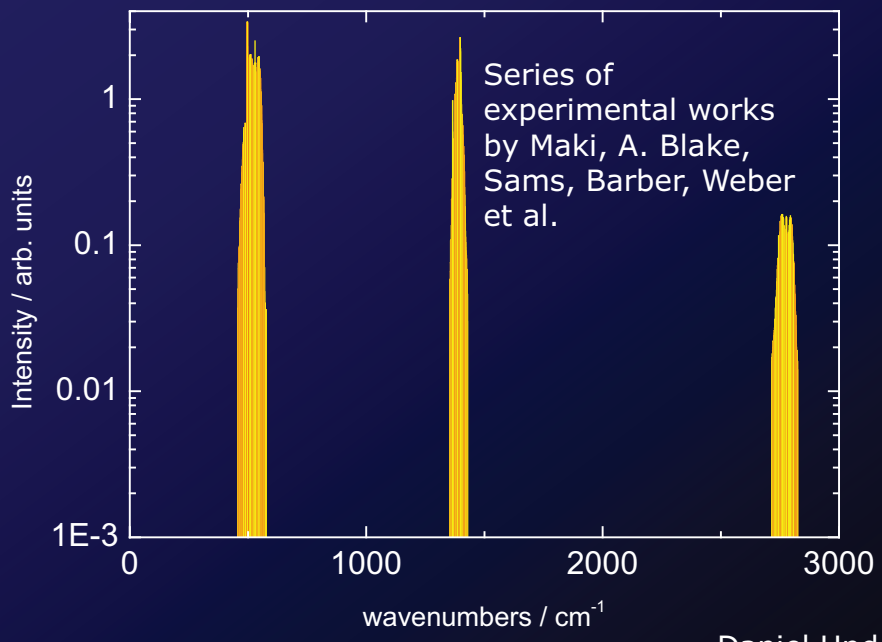

Daniel Underwood
Alexander Fateev

Absorption (T=300K) spectrum of NH_3: Accuracy

S.N. Yurchenko, R.J. Barber, A. Yachmenev, W. Thiel, P. Jensen, J. Tennyson, *J.Phys.Chem. A*, **113**, 11845 (2009).

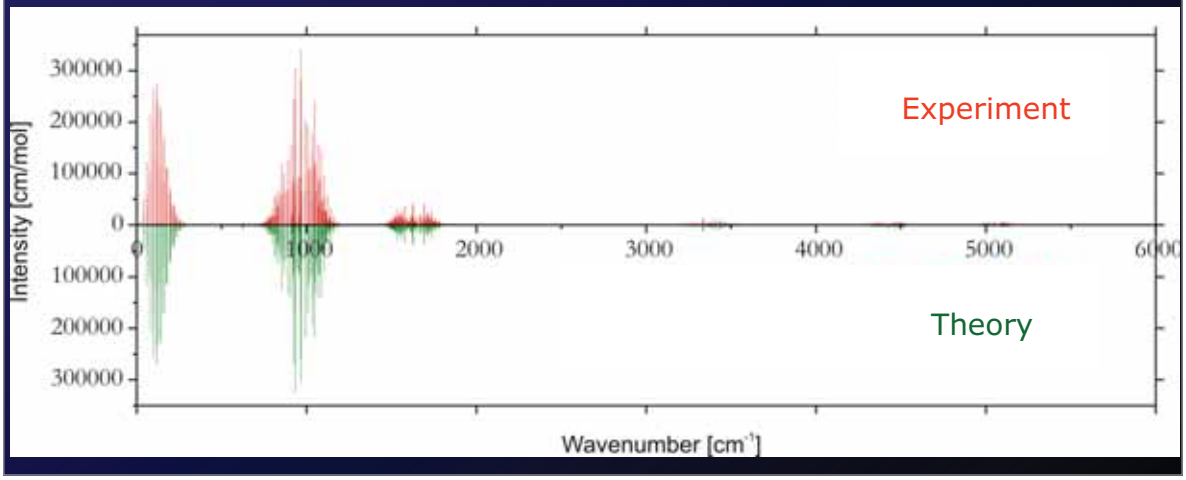

Absorption (T=300K) spectrum of NH_3: Accuracy

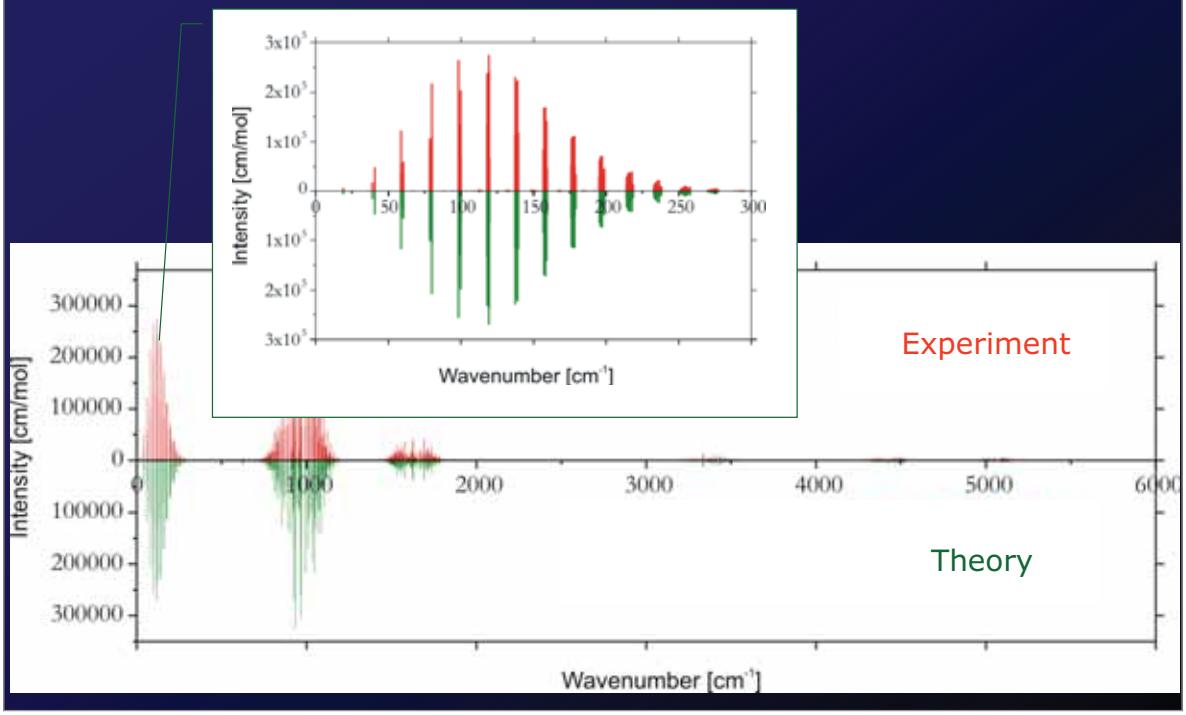

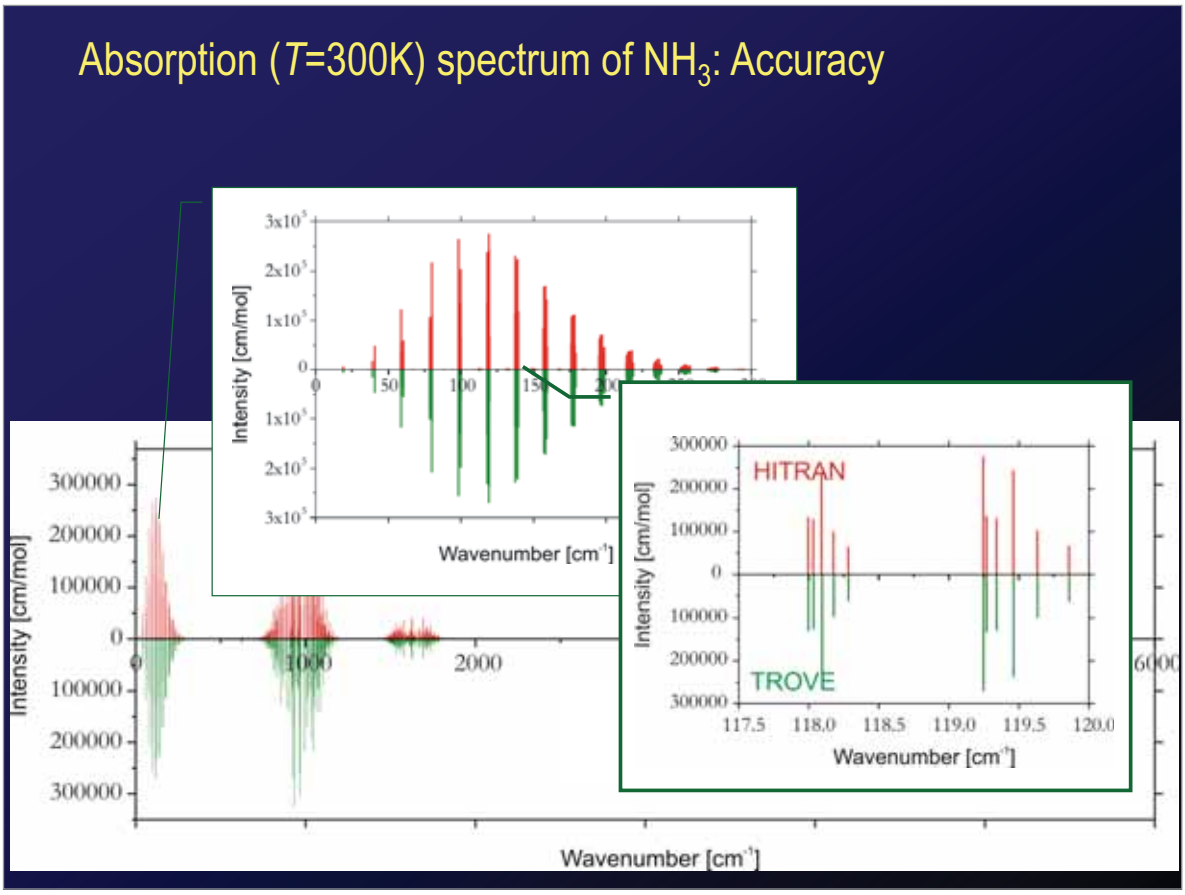
Absorption (T=300K) spectrum of NH3: Accuracy
Intensity [cm/mol]
Wavenumber [cm-1]
HITRAN
TROVE

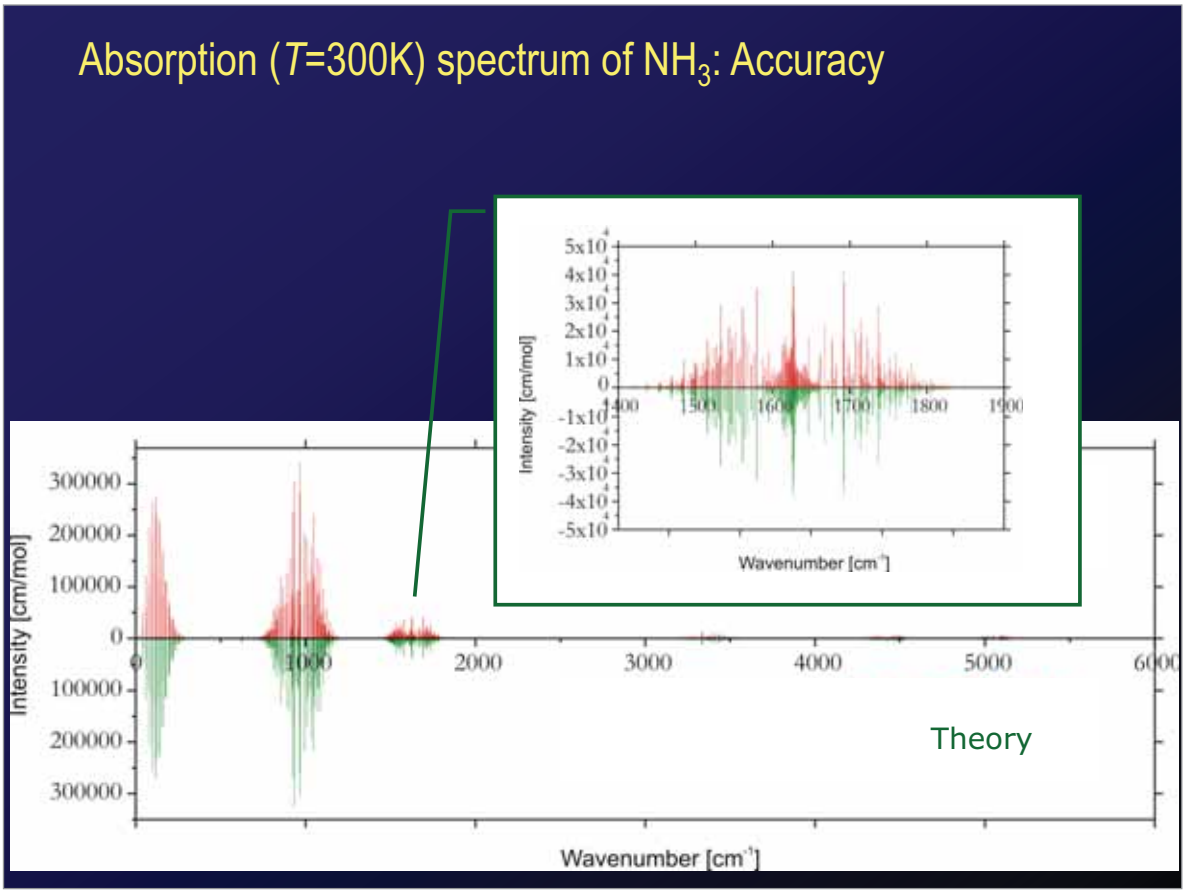
Absorption (T=300K) spectrum of NH3: Accuracy
Intensity [cm/mol]
Wavenumber [cm-1]
Theory

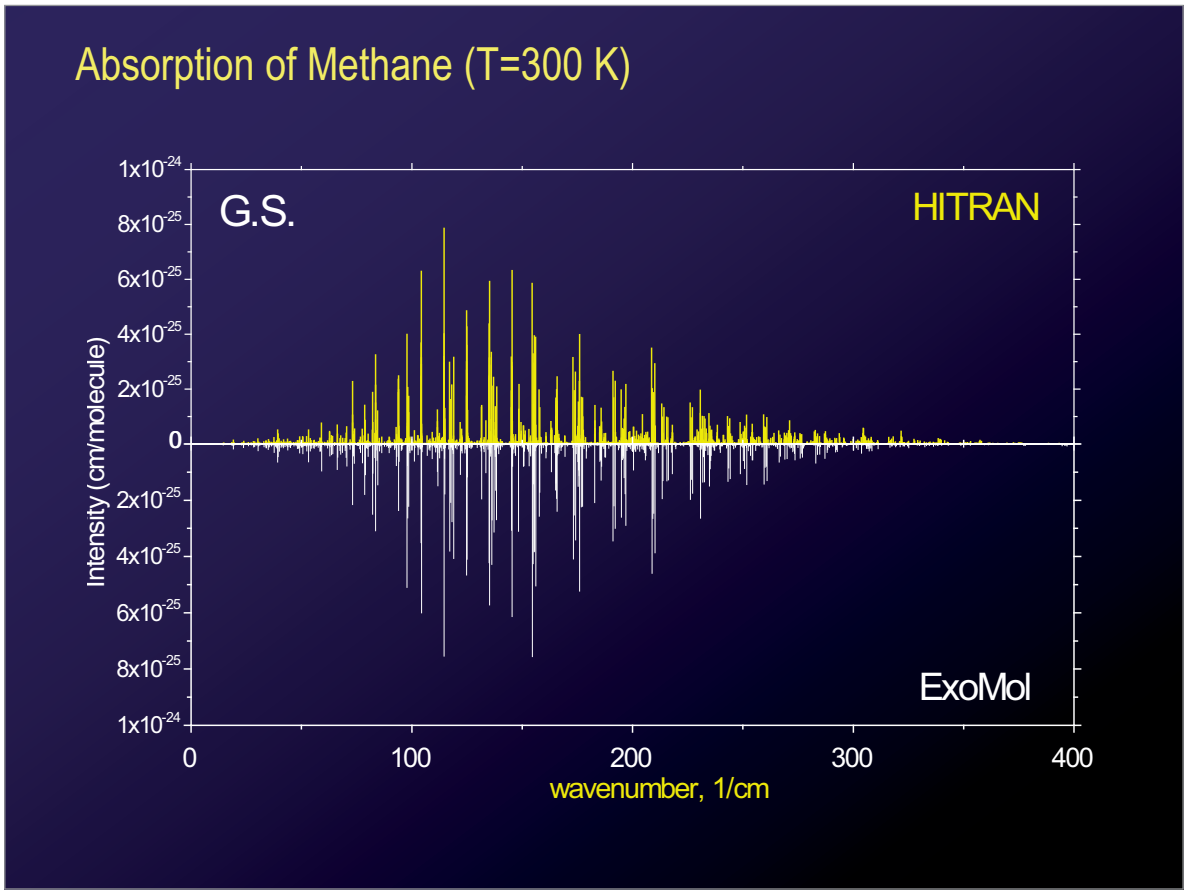
Absorption of Methane (T=300 K)
G.S.
HITRAN
ExoMol
Intensity (cm/molecule)
1x10-24
8x10-25
6x10-25
4x10-25
2x10-25
0
2x10-25
4x10-25
6x10-25
8x10-25
1x10-24
0
100
200
300
400
wavenumber, 1/cm

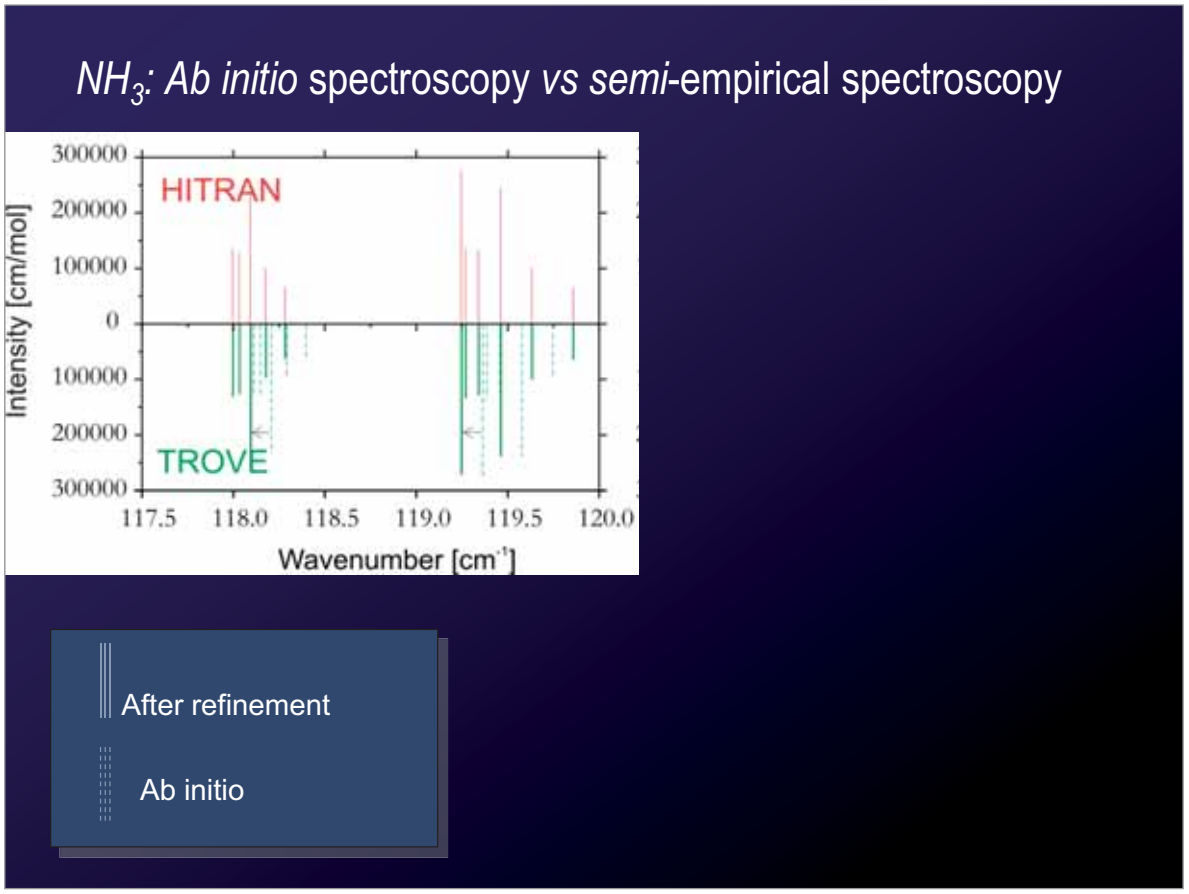
NH3: Ab initio spectroscopy vs semi-empirical spectroscopy
HITRAN
TROVE
Intensity [cm/mol]
300000
200000
100000
0
100000
200000
300000
117.5
118.0
118.5
119.0
119.5
120.0
Wavenumber [cm-1]
After refinement
Ab initio

CH_4: Refinement of the equilibrium parameters

J	Symmetry	obs	"ab initio"	obs-calc	Refined r_e	obs-calc
0	A1	0.00000	0.00000	0.00000	0.00000	0.00000
1	F1	10.48165	10.48191	-0.00026	10.48164	0.00001
2	E	31.44212	31.44290	-0.00078	31.44211	0.00001
2	F2	31.44239	31.44316	-0.00077	31.44237	0.00002
3	A2	62.87817	62.87973	-0.00156	62.87815	0.00002
3	F1	62.87578	62.87734	-0.00156	62.87576	0.00002
3	F2	62.87684	62.87840	-0.00156	62.87682	0.00002
4	A1	104.77284	104.77548	-0.00263	104.77283	0.00001
4	E	104.77603	104.77866	-0.00263	104.77602	0.00001
4	F1	104.77470	104.77733	-0.00263	104.77469	0.00001
4	F2	104.78001	104.78263	-0.00262	104.77999	0.00002
5	E	157.13719	157.14116	-0.00397	157.13721	-0.00001
5	F1	157.12434	157.12833	-0.00399	157.12437	-0.00003
5	F1	157.13892	157.14289	-0.00397	157.13893	-0.00001
5	F2	157.12793	157.13191	-0.00398	157.12795	-0.00002

Absorption of Methane (T=300 K): after a band shift

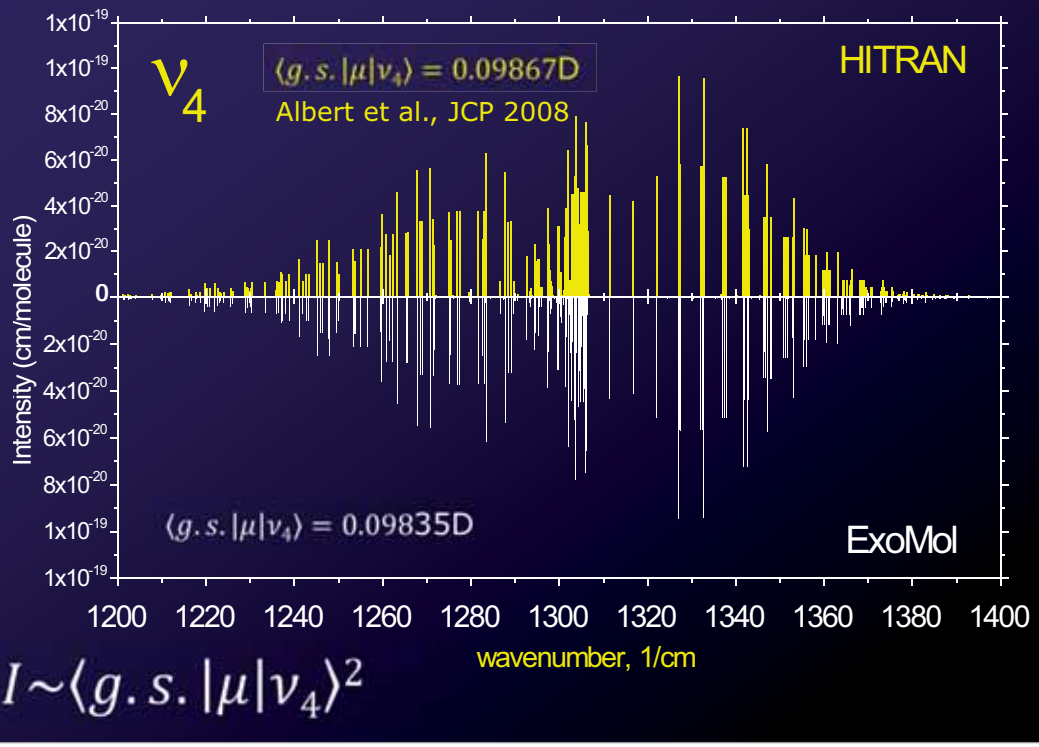

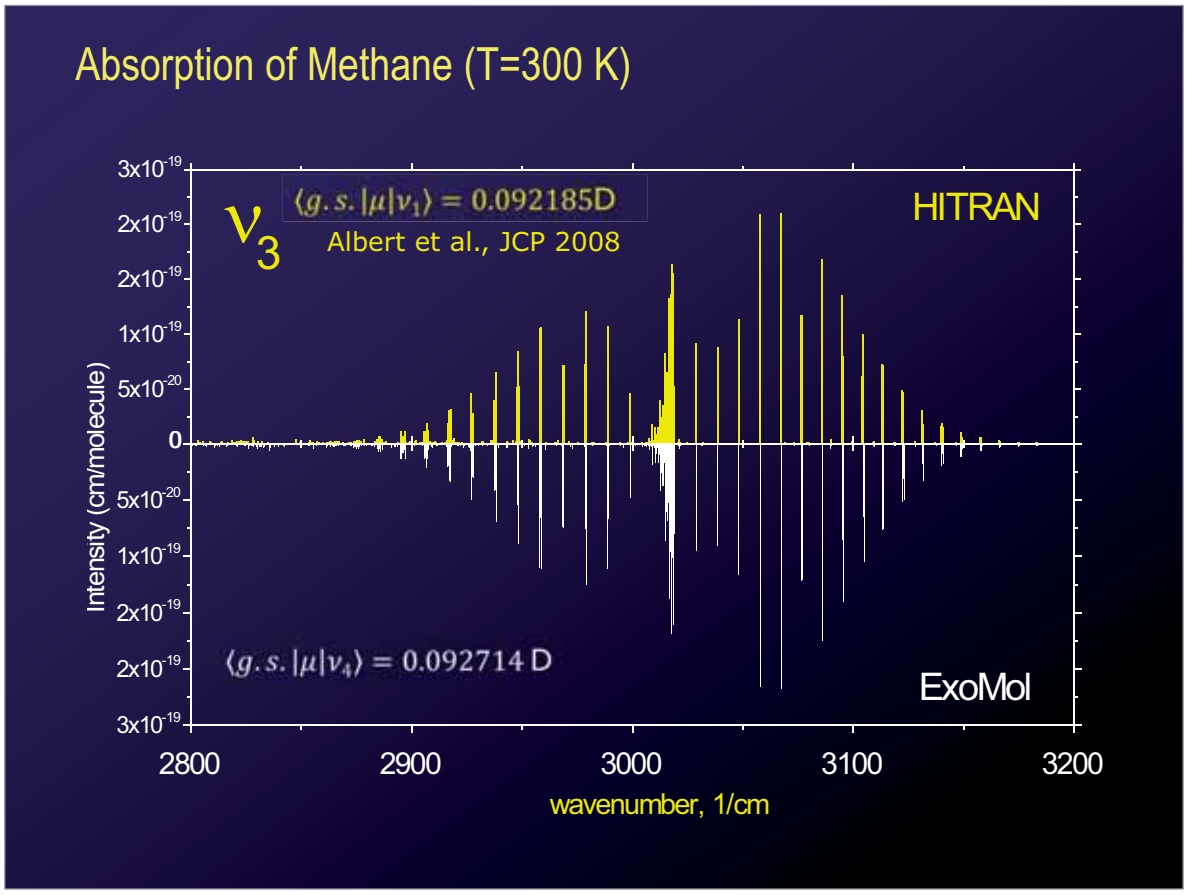
Absorption of Methane (T=300 K)
ν_3
$\langle g.s.|\mu|\nu_1\rangle = 0.092185$D
Albert et al., JCP 2008
HITRAN
$\langle g.s.|\mu|\nu_4\rangle = 0.092714$ D
ExoMol
Intensity (cm/molecule)
3x10-19
2x10-19
2x10-19
1x10-19
5x10-20
0
5x10-20
1x10-19
2x10-19
2x10-19
3x10-19
2800
2900
3000
3100
3200
wavenumber, 1/cm

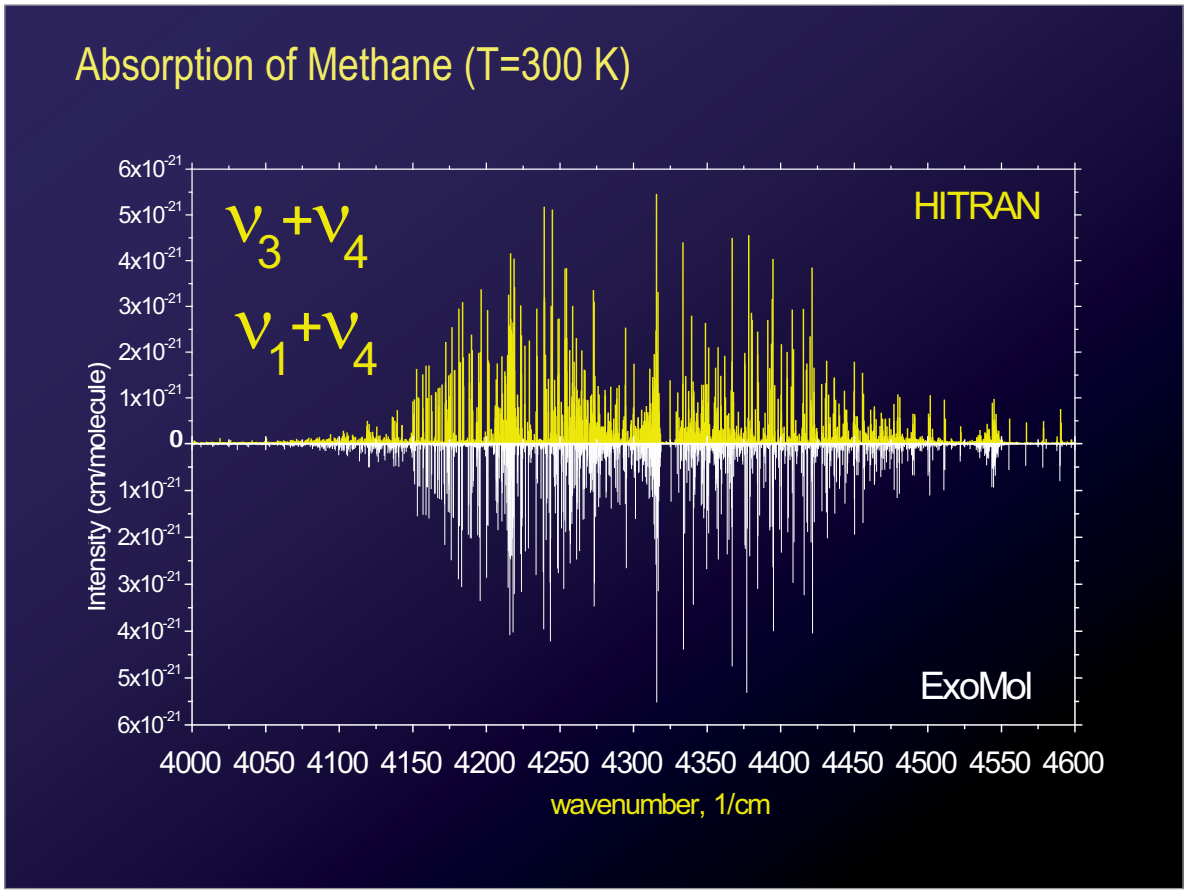
Absorption of Methane (T=300 K)
$\nu_3+\nu_4$
$\nu_1+\nu_4$
HITRAN
ExoMol
Intensity (cm/molecule)
6x10-21
5x10-21
4x10-21
3x10-21
2x10-21
1x10-21
0
1x10-21
2x10-21
3x10-21
4x10-21
5x10-21
6x10-21
4000 4050 4100 4150 4200 4250 4300 4350 4400 4450 4500 4550 4600
wavenumber, 1/cm

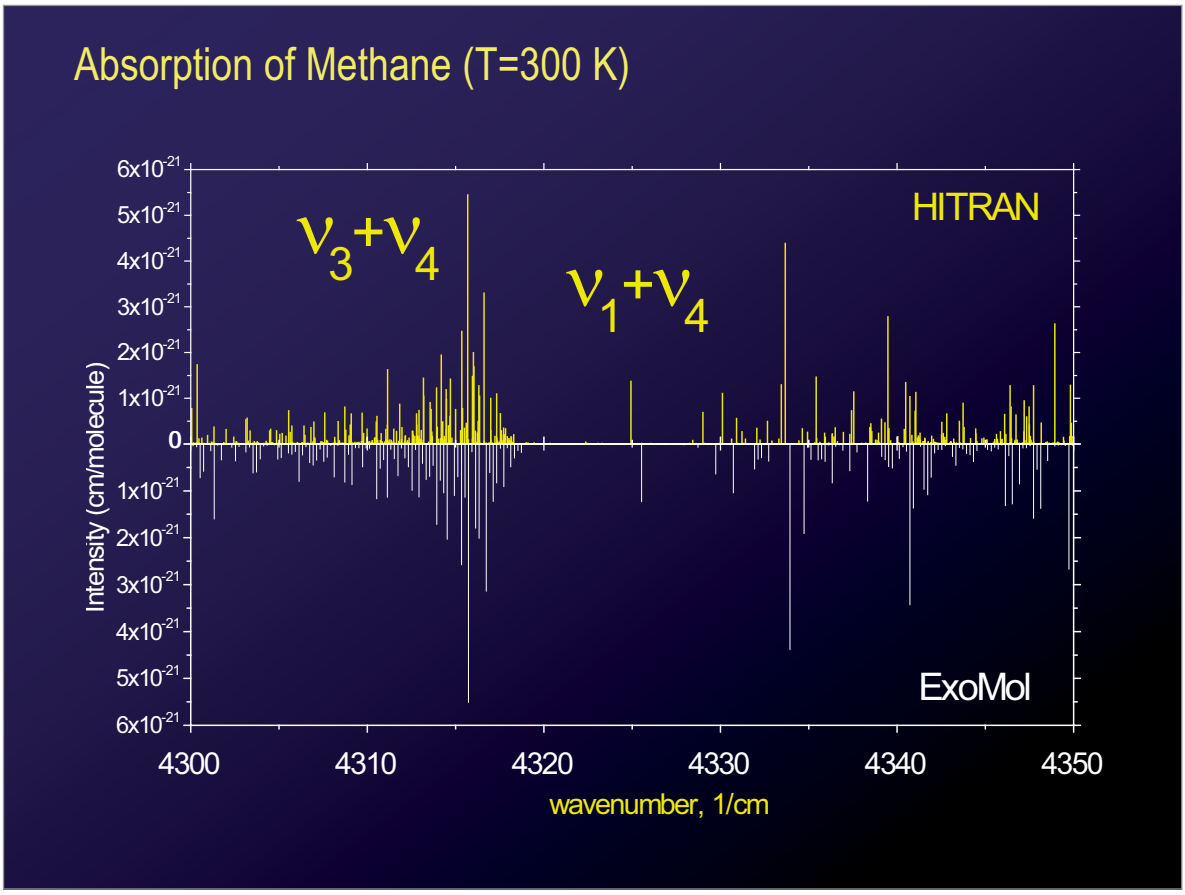
Absorption of Methane (T=300 K)
HITRAN
ExoMol
$\nu_3+\nu_4$
$\nu_1+\nu_4$
Intensity (cm/molecule)
wavenumber, 1/cm

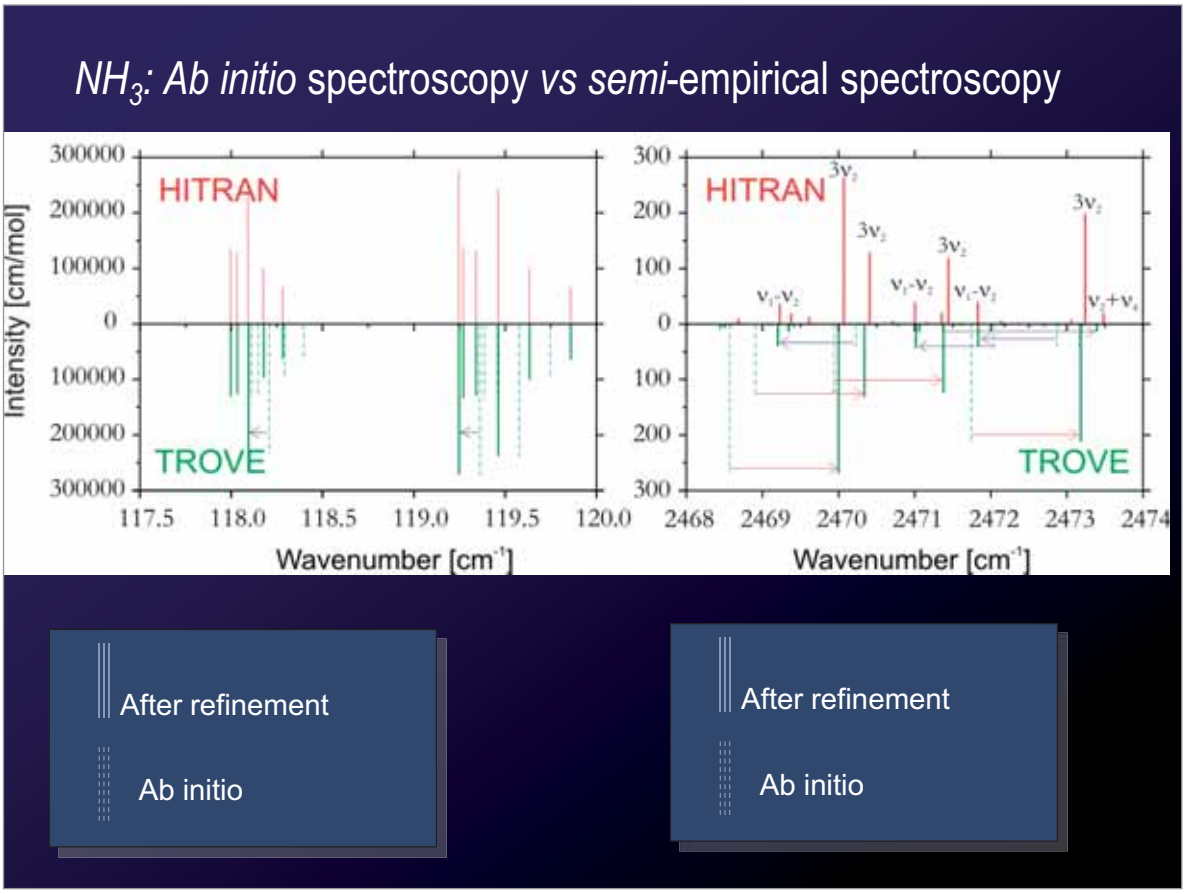
NH_3: *Ab initio* spectroscopy *vs semi*-empirical spectroscopy
HITRAN
TROVE
Intensity [cm/mol]
Wavenumber [cm^{-1}]
After refinement
Ab initio

Obtaining 'spectroscopic' PES

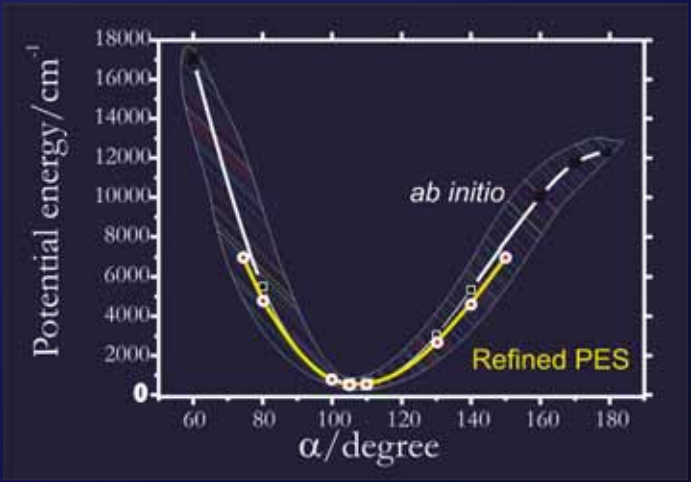

NH_3 spectrum: Empirical refinement of

Equilibrium constants

Potential energy surface

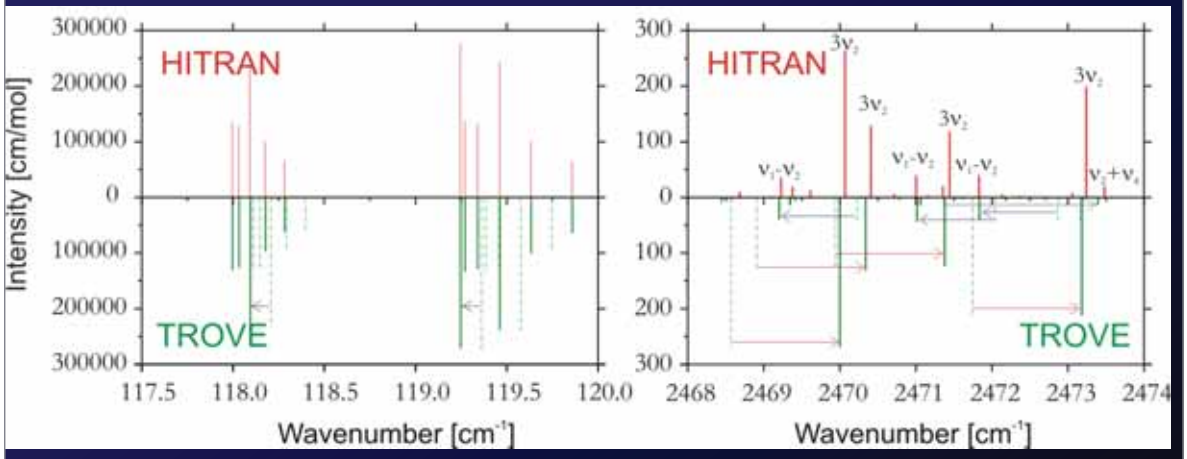

Still not perfect!

J=0 contraction

$$H = H_{\text{vib}} + H_{\text{rot-vib}}$$

Using the *J*=0 eigenfunctions as a basis set for *J*>0

$$H_{\text{vib}}\phi_n = E_n^{\text{vib}}\phi_n$$

$$\langle \phi_n | H | \phi_m \rangle = E_n^{\text{vib}}\delta_{n,m} + \langle \phi_n | H_{\text{rot-vib}} | \phi_m \rangle$$

Band center adjustment

$$H = H_{\text{vib}} + H_{\text{rot-vib}}$$

$$H_{\text{vib}}\phi_n = E_n^{\text{vib}}\phi_n$$

$$\langle \phi_n | H | \phi_m \rangle = E_n^{\text{vib}}\delta_{n,m} + \langle \phi_n | H_{\text{rot-vib}} | \phi_m \rangle$$

$$E_n^{\text{vib}} \leftarrow E_n^{\text{Obs.}}$$

Final tuning:
We substitute the band centers
by the experimental values

Empirical band center correction

HOOH: non-rigid molecule

Hunt et al, J.Chem.Phys. **42**, 1931 (1965)

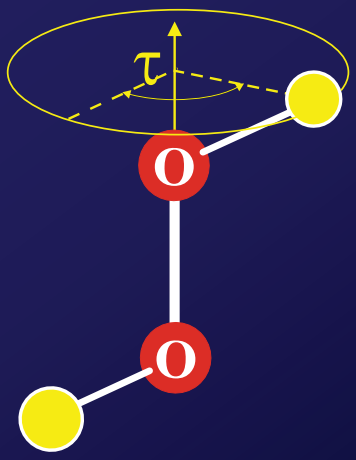

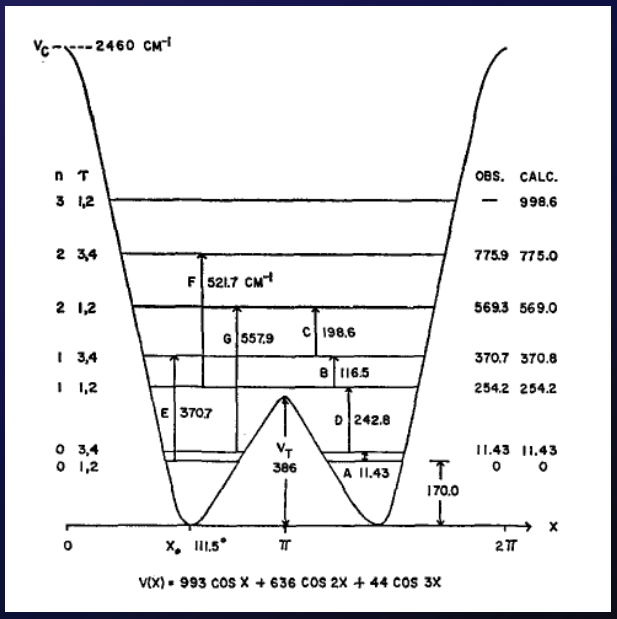

New highly accurate ab initio PES
Paweł Małyszek, and Jacek Koput, J. Comp. Chem. 2012

HOOH: accuracy of our calculations

Dr. Oleg Polyansky

J	Ka	Kc	Obs	Calc	Obs-Calc	Obs	Calc	Obs-Calc
1	0	1	1.712	1.712	0.000	256.255	256.255	0.000
1	1	1	10.907	10.907	0.000	265.427	265.427	0.000
1	1	0	10.943	10.943	0.000	265.474	265.475	0.001
3	0	3	10.268	10.268	0.000	264.777	264.777	0.000
3	1	3	19.374	19.374	0.000	273.830	273.831	-0.001
3	1	2	19.589	19.589	0.000	274.119	274.117	0.002
3	2	2	47.115	47.115	0.000	301.555	301.556	0.001
3	2	1	47.115	47.115	0.000	301.556	301.557	0.001
3	3	1	93.155	93.155	0.000	347.509	347.512	0.003
3	3	0	93.155	93.155	0.000	347.509	347.512	0.003
5	0	5	25.667	25.666	0.000	280.113	280.112	0.001
5	1	5	34.613	34.613	0.000	288.954	288.954	0.000
5	1	4	35.151	35.150	0.001	289.671	289.671	0.000
5	2	4	62.513	62.513	0.000	316.893	316.893	0.000
5	2	3	62.517	62.517	0.000	316.899	316.899	0.000
5	3	3	108.551	108.551	0.000	362.845	362.847	0.002
5	3	2	108.551	108.551	0.000	362.845	362.847	0.002
5	4	2	172.968	172.968	0.000	427.143	427.146	0.003
5	4	1	172.968	172.968	0.000	427.143	427.146	0.003
5	5	1	255.733	255.733	0.000	509.757	509.764	0.007
5	5	0	255.733	255.733	0.000	509.757	509.764	0.007

HOOH: accuracy of our calculations, high *J*

Dr. Oleg Polyansky

J	Ka	Kc	Obs	Calc	Obs-Calc	Obs	Calc	Obs-Calc
30	0	30	789.577	789.581	-0.004	1038.983	1038.925	0.058
30	1	30	793.053	793.065	-0.012	1041.540	1041.481	0.039
30	1	29	809.594	809.565	0.029	1063.053	1063.007	0.046
30	2	29	829.292	829.282	0.010	1080.396	1080.345	0.051
30	2	28	832.547	832.521	0.026	1086.079	1086.036	0.043
30	3	28	876.030	876.017	0.013	1127.862	1127.815	0.047
30	3	27	876.191	876.174	0.017	1128.304	1128.262	0.042
30	4	27	940.027	940.015	0.012	1191.838	1191.794	0.044
30	4	26	940.029	940.013	0.016	1191.850	1191.807	0.043
30	5	26	1022.323	1022.311	0.012	1274.332	1274.293	0.039
30	5	25	1022.324	1022.312	0.012	1274.332	1274.293	0.039
30	6	25	1122.848	1122.837	0.011	1371.047	1371.024	0.023
30	6	24	1122.849	1122.838	0.011	1371.047	1371.024	0.023
30	7	24	1241.304	1241.294	0.010	1491.957	1491.933	0.024
30	7	23	1241.304	1241.294	0.010	1491.957	1491.933	0.024
30	8	23	1381.938	1381.916	0.022	1628.749	1628.731	0.018
30	9	21	1534.588	1534.578	0.010	1782.735	1782.739	-0.004
30	10	21	1707.358	1707.349	0.009	1958.577	1958.558	0.019
30	11	19	1898.169	1898.159	0.010	2148.182	2148.186	-0.004

Theoretical line lists:
Modeling temperature effects

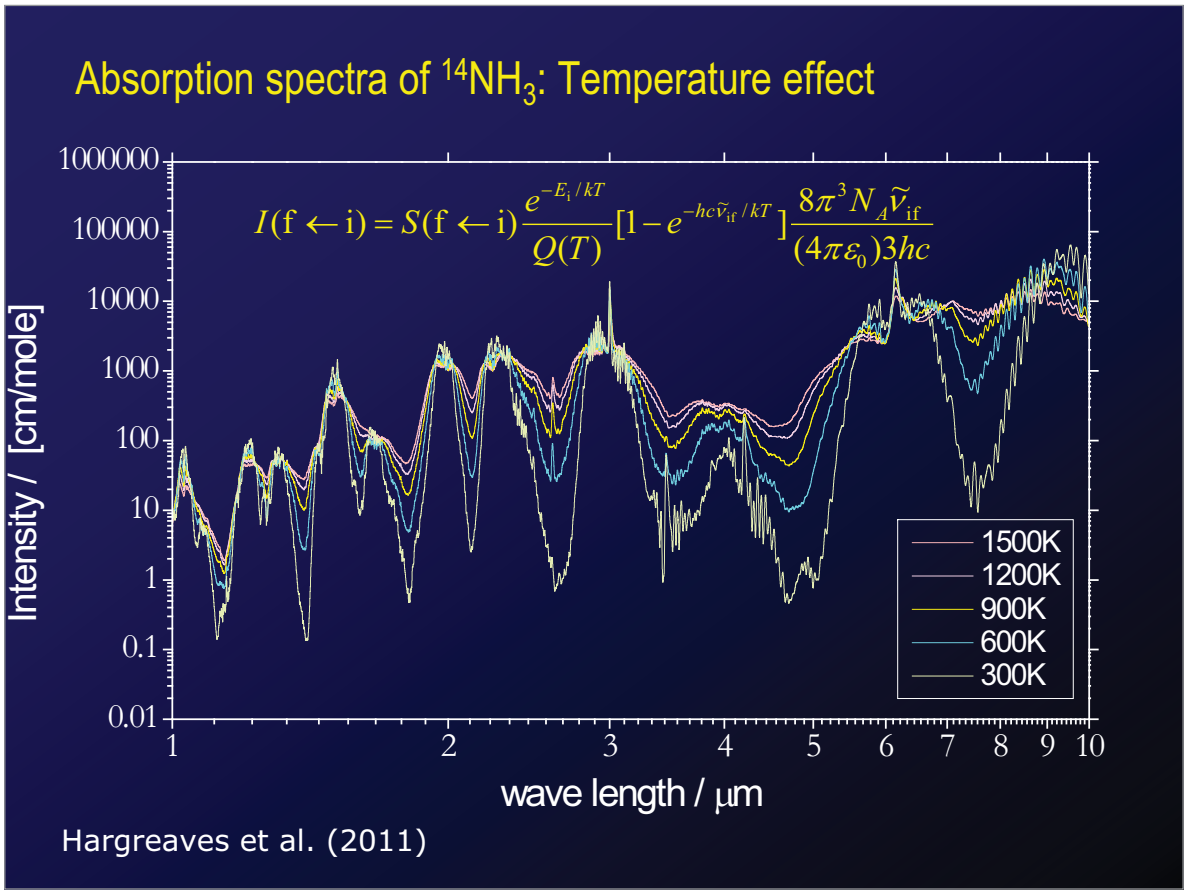
Absorption spectra of $^{14}NH_3$: Temperature effect
$I(\mathrm{f} \leftarrow \mathrm{i}) = S(\mathrm{f} \leftarrow \mathrm{i}) \frac{e^{-E_i/kT}}{Q(T)} [1 - e^{-hc\tilde{\nu}_{if}/kT}] \frac{8\pi^3 N_A \tilde{\nu}_{if}}{(4\pi\varepsilon_0)3hc}$
Intensity / [cm/mole]
1000000
100000
10000
1000
100
10
1
0.1
0.01
1
2
3
4
5
6
7
8
9
10
wave length / μm
1500K
1200K
900K
600K
300K
Hargreaves et al. (2011)

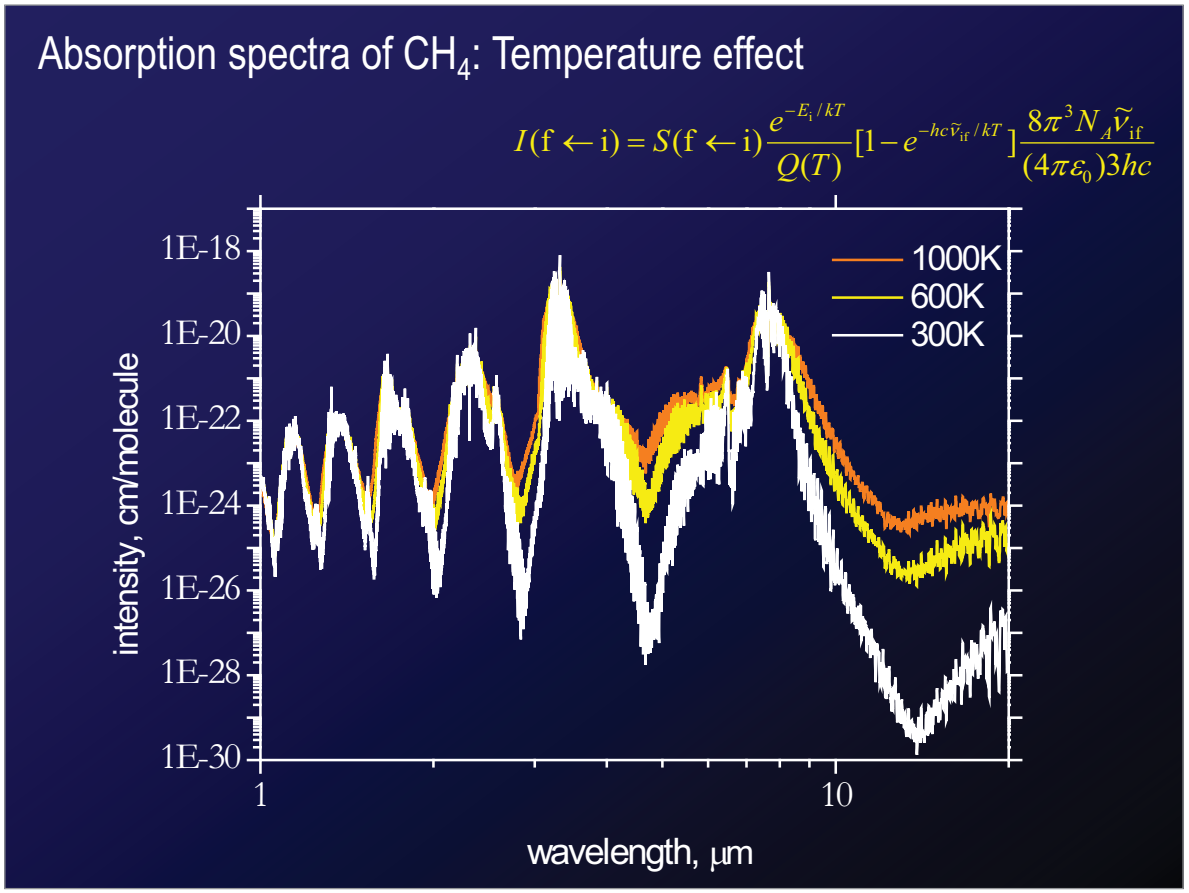
Absorption spectra of CH_4: Temperature effect
$I(\mathrm{f} \leftarrow \mathrm{i}) = S(\mathrm{f} \leftarrow \mathrm{i}) \frac{e^{-E_i/kT}}{Q(T)} [1 - e^{-hc\tilde{\nu}_{if}/kT}] \frac{8\pi^3 N_A \tilde{\nu}_{if}}{(4\pi\varepsilon_0)3hc}$
intensity, cm/molecule
1E-18
1E-20
1E-22
1E-24
1E-26
1E-28
1E-30
1
10
wavelength, μm
1000K
600K
300K

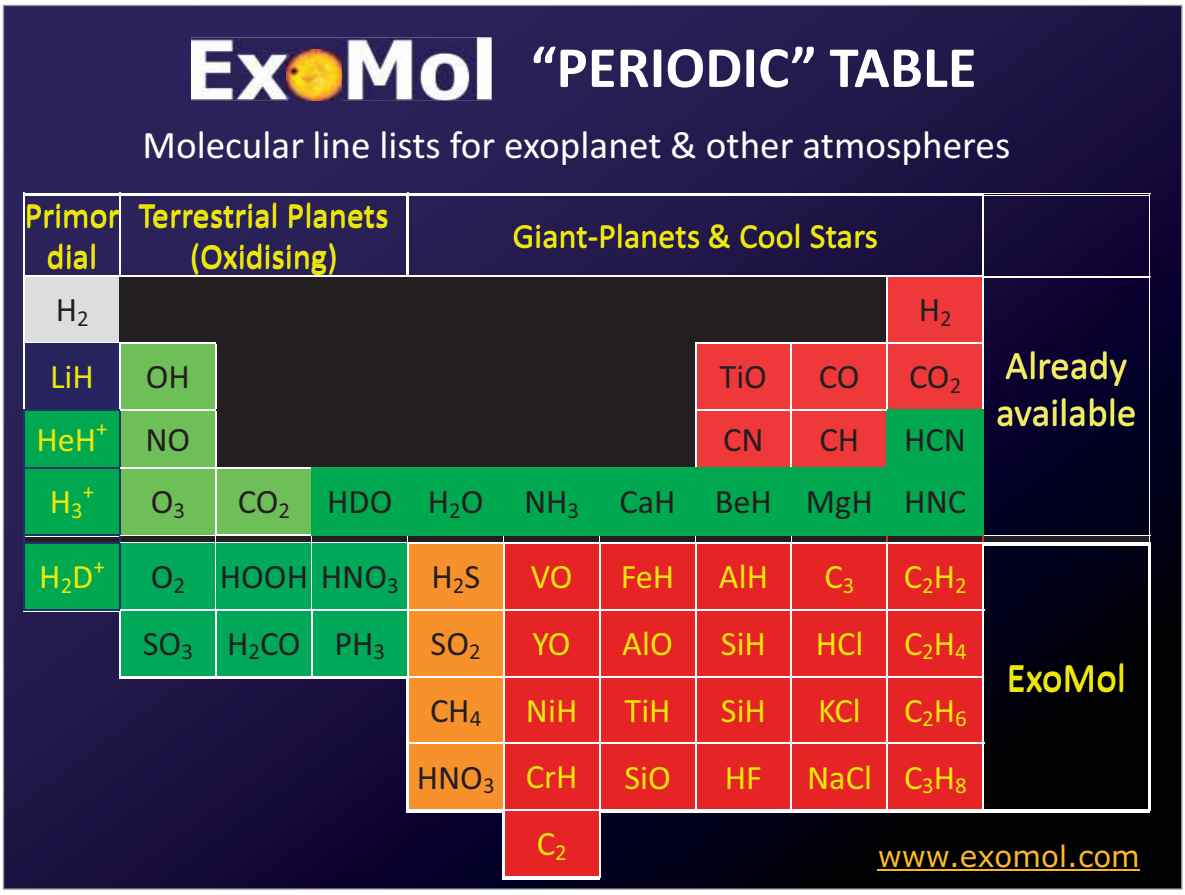
ExoMol "PERIODIC" TABLE
Molecular line lists for exoplanet & other atmospheres
Primordial
Terrestrial Planets (Oxidising)
Giant-Planets & Cool Stars
Already available
ExoMol
www.exomol.com

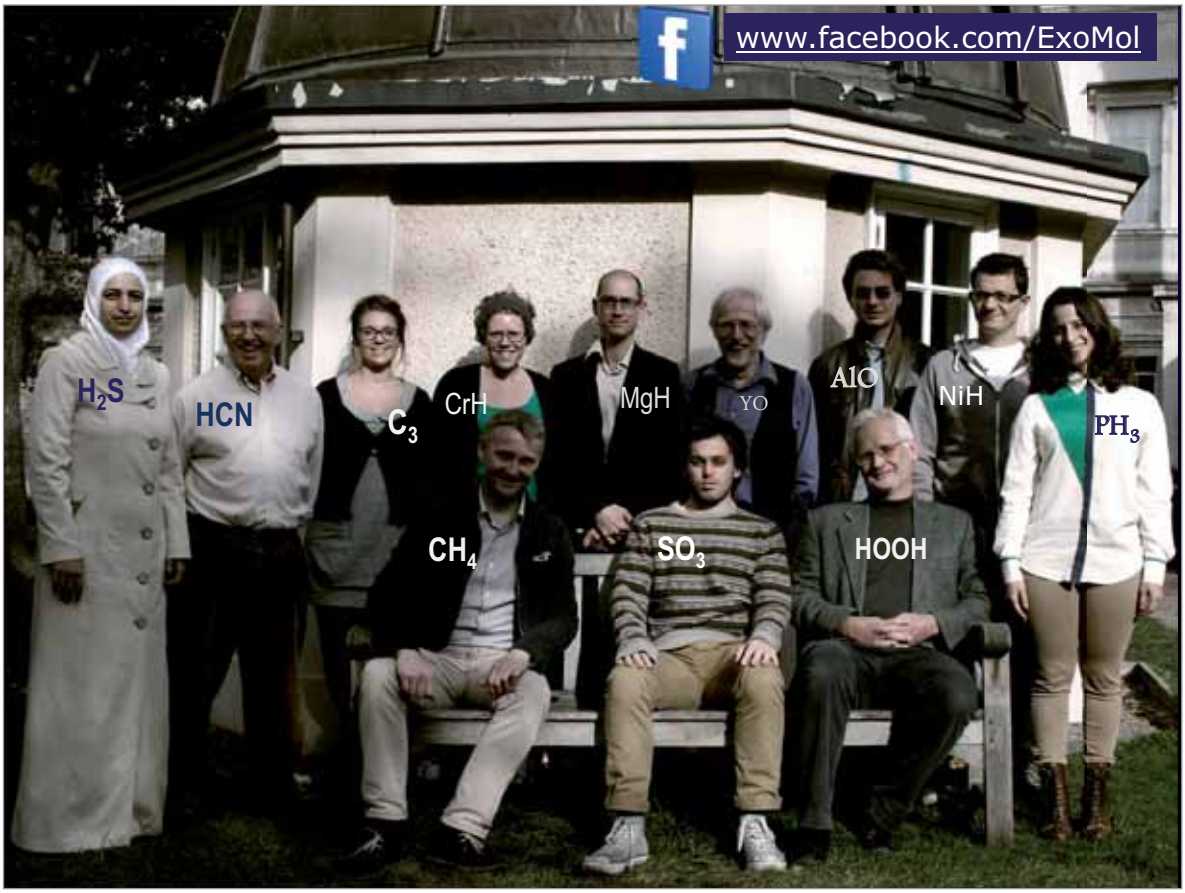
www.facebook.com/ExoMol
H2S
HCN
C3
CrH
MgH
YO
AlO
NiH
PH3
CH4
SO3
HOOH

"The role of refined line shape models and line mixing for the extraction of high accuracy spectral line data: Status and need for experimental validation"

Prof. Dr. Ha Tran

Laboratoire Interuniversitaire des Systèmes Atmosphériques,
Université Paris-Est Créteil

Prof. Dr. Ha Tran

Laboratoire Interuniversitaire des Systèmes Atmosphériques, Université Paris-Est Créteil
Université Paris-Est Créteil , 94010 Créteil Cedex, France
Tel: +33 145176558
Email: ha.tran@lisa.u-pec.fr

Research

Molecular Spectroscopy; FIR, IR, NIR Spectroscopy; Intermolecular Collisions and impact on the line‐shape; Molecular Dynamic Simulations; Atmospheric spectra analysis; Green House Gases Remote Sensing

Education and Professional Experience

2004	Ph. D. Thesis at the Universite de Franche‐Comte Supervisors: Bruno Lavorel (Research Director, CNRS), Pierre Joubert (Professor)
2001	Master of Research at the Universite de Franche‐Comte

Activities, Honors and Awards

- Supervisor of two Ph. D. Thesis and several Master Thesis
- Member of the French comity Comite Scientifique du colloque JSM (Journees de Spectroscopie Moleculaire)
- Member of the IUPAC water spectroscopy task group
- Reviewer of Journal of Quantitative Spectroscopy and Radiative Transfer, Molecular Physics, Canadian Journal of Physics, Journal of Chemical Physics
- Young Scientist Award in Quantitative Spectroscopy, Elsevier, 2009

The role of refined line shape models and line mixing for the extraction of high accuracy spectral line data: Status and need for experimental validation

H. Tran, J.-M. Hartmann

Laboratoire Interuniversitaire des Systemes Atmospheriques, Universite Paris-Est Creteil

It is well known that Voigt profiles do not well describe the measured absorption shapes of molecular gases. For an isolated optical transition (line), this is due to the neglect of the intermolecular collision-induced velocity changes and of the speed dependences of the collisional parameters. For closely spaced lines, in addition to these effects, collisional line interferences due to population transfers may also have significant effects. The resulting spectral shapes can then be significantly different from the addition of individual line contributions with Voigt profiles. Examples of the influence of these non-Voigt effects on the extraction of spectral line parameters from laboratory-measured spectra as-well-as on atmospheric measurements will be shown. Some existing empirical more refined line-shape models and examples of their application will be presented. Recent theoretical lineshape models developed in our group will be detailed. In contrast with empirical models widely used ([1] and references therein) where model parameters are adjusted to measured spectra, our ab initio approaches are directly based on independent classical molecular dynamics simulations. Very good agreement is obtained between high signal-to-noise ratio measurements and our predictions[2-4]. The latter are then used as a benchmark to choose the "proper" simplified line-shape model to fit measured spectra. Futures works and experimental needs for proper determinations of line parameters will be also discussed.

[1] J.-M. Hartmann, C. Boulet, D. Robert, Amsterdam: Elservier, 2008.
[2] N. H. Ngo, H. Tran, R. R. Gamache, J. Chem. Phys., 136, 154310, 2012.
[3] N. H. Ngo, H. Tran, R. R. Gamache, D. Bermejo, J.-L. Domenech, J. Chem. Phys., 137, 064302, 2012.
[4] J.-M. Hartmann, H. Tran, N. H. Ngo, et al., Phys. Rev. A, submitted, 2012.

The role of refined line shape models and line mixing for the extraction of high accuracy spectral line data: Status and need for experimental validation

H. Tran, J.-M. Hartmann, N. H. Ngo, R. R. Gamache…
LISA, CNRS UMR 7583,
University Paris-Est Créteil and Paris Diderot, France

ha.tran@lisa.u-pec.fr

1

Isolated transitions

2

The Voigt profile

Voigt profile $\Phi^{\text{Voigt}}(\sigma-\sigma_{fi}) = \Phi^{\text{Doppler}}(\sigma-\sigma_{fi}) \otimes \Phi^{\text{Lorentz}}(\sigma-\sigma_{fi})$

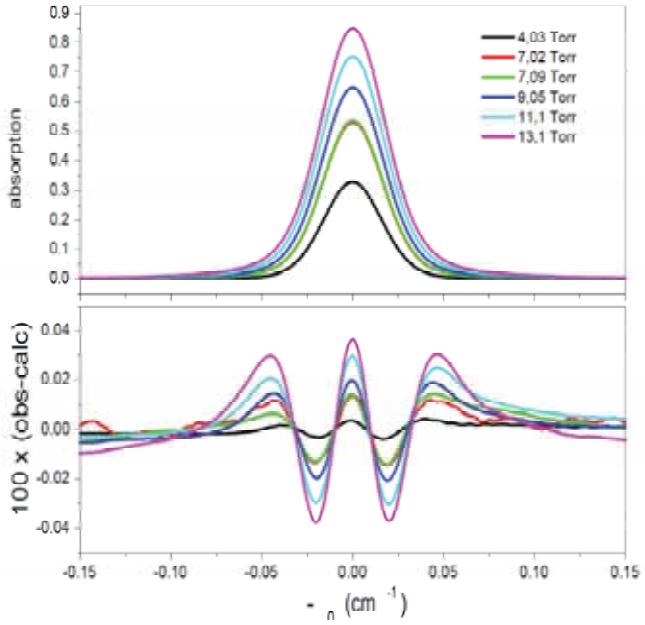

Voigt fits of diode laser measurement of pure H2O absorption by line near 816 nm

Voigt fit leaves important residuals with a W shape characteristic of a narrowed profile

3

Problems with the Voigt profile

It neglects:

1. The velocity changes induced by collisions.
   The detailed balance: $f(\vec{v} \to \vec{v}') \times f_{MB}(\vec{v}) = f(\vec{v}' \to \vec{v}) \times f_{MB}(\vec{v}')$
   → change from v to v' < v is more probable than that from v to v' > v.
   → reduction of the Doppler broadening → Dicke narrowing effect

2. The speed-dependences of the collisional width Γ(v) and shift Δ(v) of the line.
   This also (in general) leads to a narrowed line

4

Simple and widely used non-Voigt approaches

- For the velocity changes effect: The Galatry (soft collisions) and Rautian (or Nelkin-Ghatak, hard collisions) line-shapes. Introducing a parameter ν_{VC} (or β) - the velocity changing collisions frequency.

- For the speed dependences of the line-width and shift: The speed-dependent Voigt profile, assuming a simple quadratic dependence on the absolute speed or polynomial dependence on the relative speed

$$\Gamma(v) = \Gamma_0 + \Gamma_2[(v/\bar{v})^2 - 3/2] \quad \text{or} \quad \Gamma(v_r) = A\, v_r^{\,p}$$

5

Influence of non-Voigt effects on atmospheric retrievals

In situ absorption spectrum of tropospheric H_2O recorded by balloonborne diode laser and its fits using the Voit profile and the Hard Collision profile

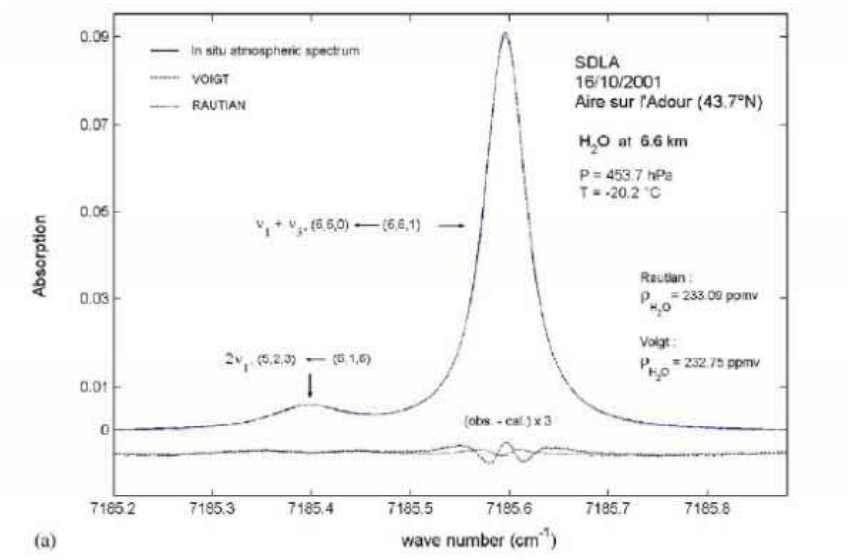

*Durry et al, JQSRT **94**, 387,2005*

6

Influence of non-Voigt effects on atmospheric retrievals

HF profile retrieved from ground-based absorption FTIR measurements (Jungfraujoch station) in the (1-0) R(1) micro-window by using the Voigt profile and the Soft Collision model, compared with the HALOE (Halogen Occultation Experiment) profiles smoothed.

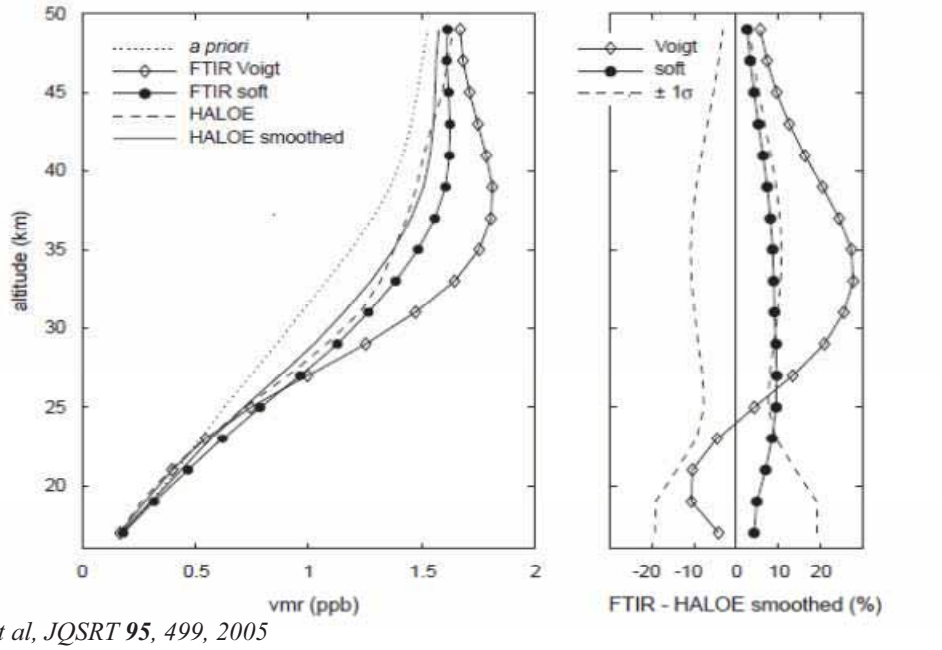

7

*Barret et al, JQSRT **95**, 499, 2005*

Influence of non-Voigt effects on line parameters determination

(Diode laser) Measured absorption of pure H_2O (left) and H_2O in air (right) and their differences with those adjusted using the VP, HC, and SDVP

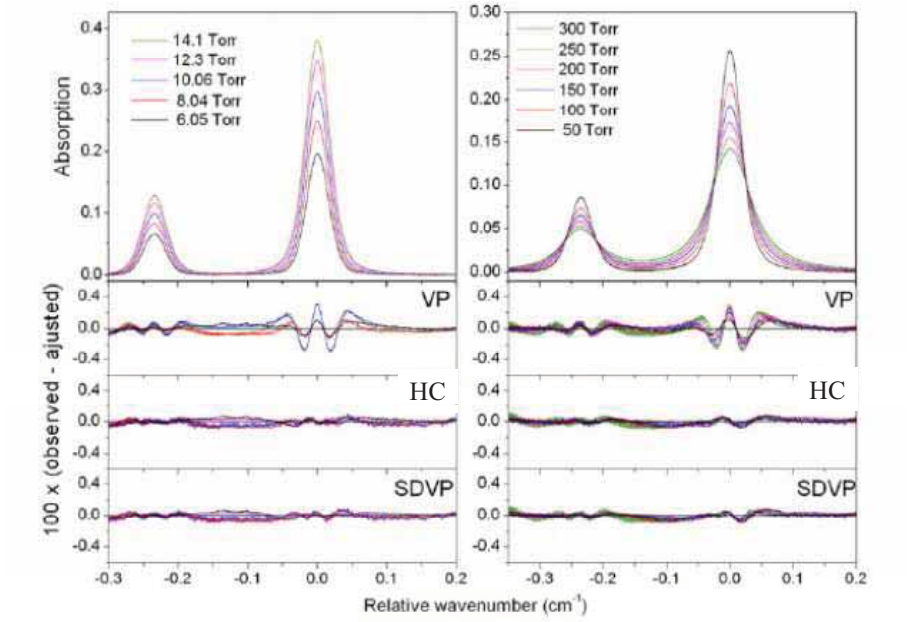

8

*Ngo et al, JQSRT **113**, 873, 2012*

Influence of non-Voigt effects on line parameters

Ratios of the self-broadening coefficients and intensity obtained by the HC (o) and SDVP (▪) to those obtained by the VP, for 13 H_2O lines in the near-infrared.

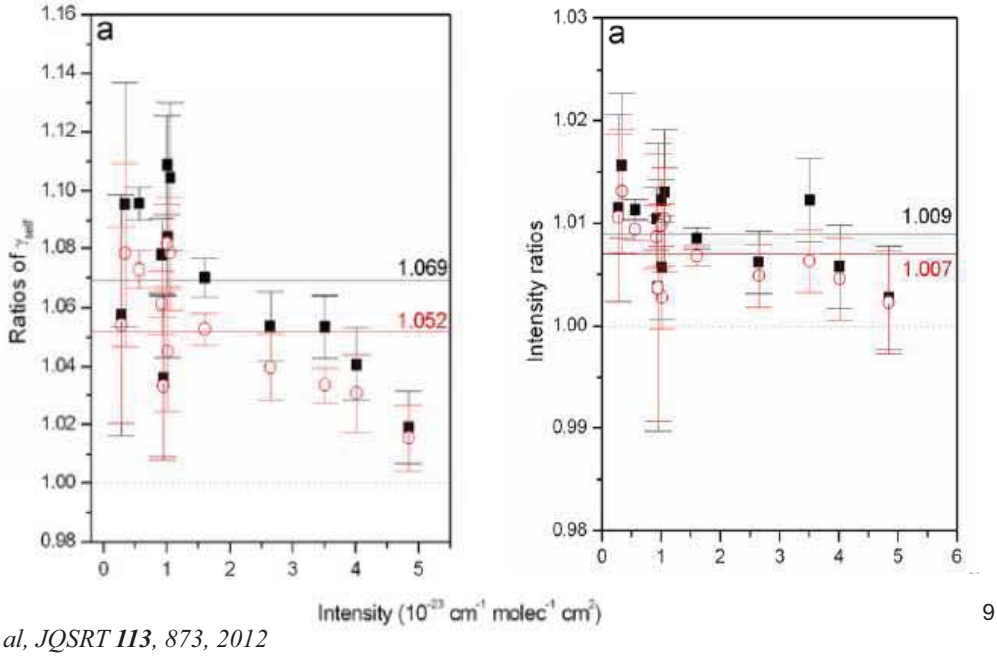

9

*Ngo et al, JQSRT **113**, 873, 2012*

Remaining problems with these simplified non-Voigt approaches

Dependence of ν_{VC} on pressure

Relaxation of the 317.2 GHz line of O_3 in collision with O_2 at 240 K.

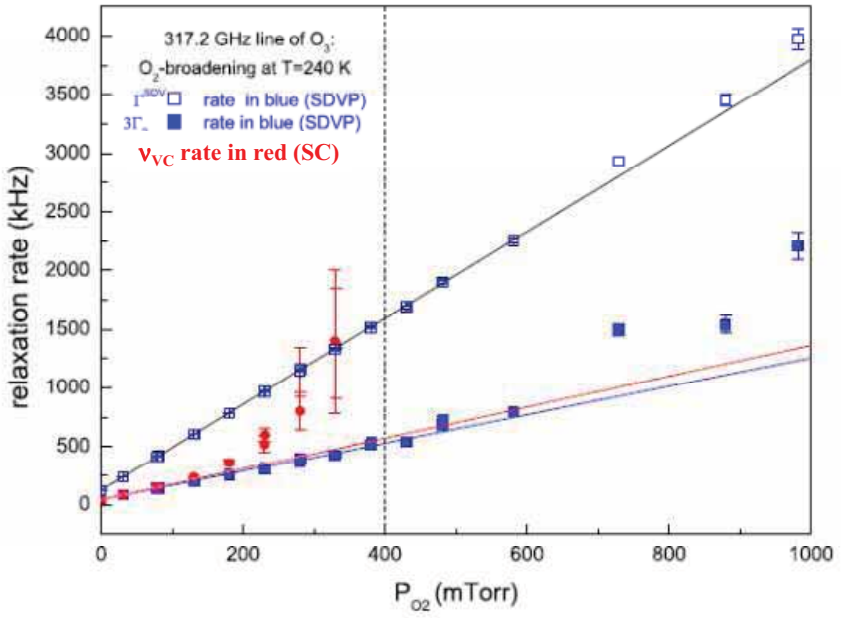

10

*Rohart et al, J Mol Spectrosc **251**, 282, 2008*

Remaining problems with these simplified non-Voigt approaches

H_2O/N_2, $2\nu_1+\nu_3$ $4_{04} \leftarrow 3_{03}$ line

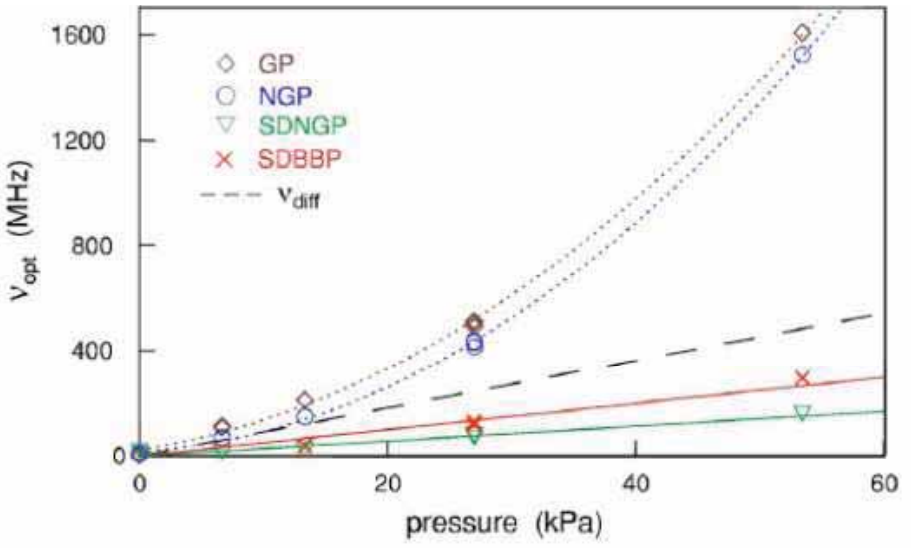

11

Lisak et al, Phys Rev A ***73****, 102507, 2006*

<u>Our approach</u>: Try to fix as much parameters as possible with values derived from independent calculations.

Starting from an input reliable inter-molecular potential

1- Carry Classical Molecular Dynamics Simulations to get the velocity changes collision-kernels $f(\vec{v} \rightarrow \vec{v}')$ (ie the frequency at which the velocity changes from $\vec{v}$ to $\vec{v}'$)

2- Carry semi-classical calculations of the broadening and shifting coefficients vs the relative speed v_r from which the dependence on the absolute speed is easily derived

12

Classical molecular dynamic simulations (CMDS)

• Compute the time evolution of the system using the classical equations, for molecule i:

$$m\dot{\vec{v}}_i = \vec{f}_i \quad and \quad I\dot{\vec{\omega}}_i = \vec{\tau}_i$$

where the force f and torque τ are computed from the potential gradient summed over all nearby collision partners $\sum_{j\neq i} \vec{\nabla} V_{i,j}$

→ This provides the c.o.m. positions and velocities as well as the orientations and angular velocity of all molecules at all times

Velocity changes by using MDS

• Directly deduced the kernels by looking at the molecules with given velocity at time zero that have other velocity at time t: H_2-H_2, H_2-Ar

• Assume a velocity changing model and deduce its parameters from proper velocity auto-correlation functions by CMDS: H_2O-H_2O, H_2O-N_2

13

Velocity changing by the Keilson and Storer model

$$f_{KS}(\vec{v} \to \vec{v}') = \nu_{VC} \times (1-\alpha^2)^{-3/2} \times f_{MB}\left(\frac{\vec{v}' - \alpha\vec{v}}{\sqrt{1-\alpha^2}}\right)$$

α : memory parameter

2 limits

$\alpha = 0 \Rightarrow \quad f(\vec{v} \to \vec{v}') = \nu_{VC} f_{MB}(\vec{v}') \longrightarrow$ ***Hard collision model***

$\alpha = 1 \Rightarrow \quad f(\vec{v} \to \vec{v}') = \nu_{VC} \delta(\vec{v}, \vec{v}') \longrightarrow$ ***Soft collision model***

→ KS more realistic than these two extreme cases and more suitable for intermediate cases

14

The KS model: Determination of model parameters

With KS model, the expressions of the time auto-correlation functions of the velocity and of the kinetic energy are analytical.

$$\Phi_{\vec{v}}(t) \propto \exp[-\nu_{VC}(1-\alpha)t]$$

$$\Phi_{E}(t) \propto \exp[-\nu_{VC}(1-\alpha^2)t]$$

$\rightarrow \nu_{VC}$ and α can be directly derived from the MDS results for these to auto-correlation functions

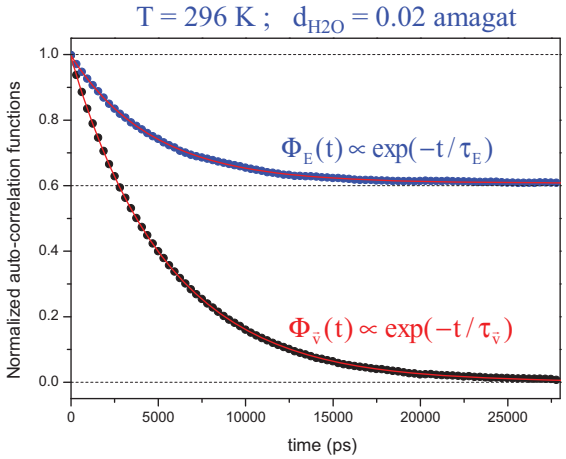

Results at 296 K and 1 atm

H_2O-H_2O :
$\nu_{VC} = 0.054$ cm^{-1}
$\alpha = 0.17$

H_2O-N_2 :
$\nu_{VC} = 0.023$ cm^{-1}
$\alpha = 0.13$

15

CMDS results: Correlation between velocity- and state-changing collisions?

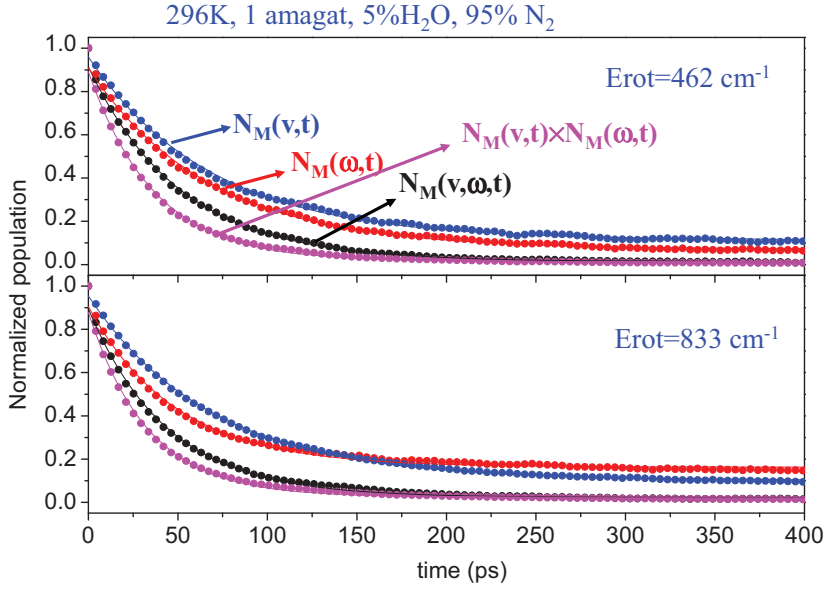

Conclusion: There is a partial correlation between velocity- and rotational state-changing collisions and the magnitude of this correlation depends on the considered line

16

Speed-dependent broadening and shifting

$\gamma(v_r)$ and $\delta(v_r)$ calculated, versus the relative (H_2O-perturber) speed v_r with the CRB semi-classical model

Then averaging over the Boltzmann distribution of the perturber velocities v_p gives $\gamma(v)$ and $\delta(v)$ vs the absolute speed v of the H_2O molecule

Pure H_2O, 296 K $6_{0\,6} \leftarrow 5_{0\,5}$ line, $2\nu_1+\nu_2+\nu_3$ band

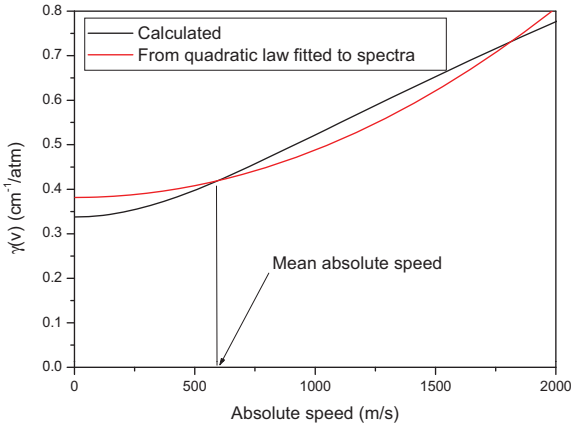

17

Model-experiment comparison

With the model (ν_{VC}, α, correlation from MDS) and SD from semi-classical (fixed inputs) we compute the line shape.
Then we fit the calculated spectra (as the measured ones) by Voigt profiles and look at the residuals.

Pure H_2O, 296K, $2\nu_1+\nu_2+\nu_3$ band: — measured, — calculated

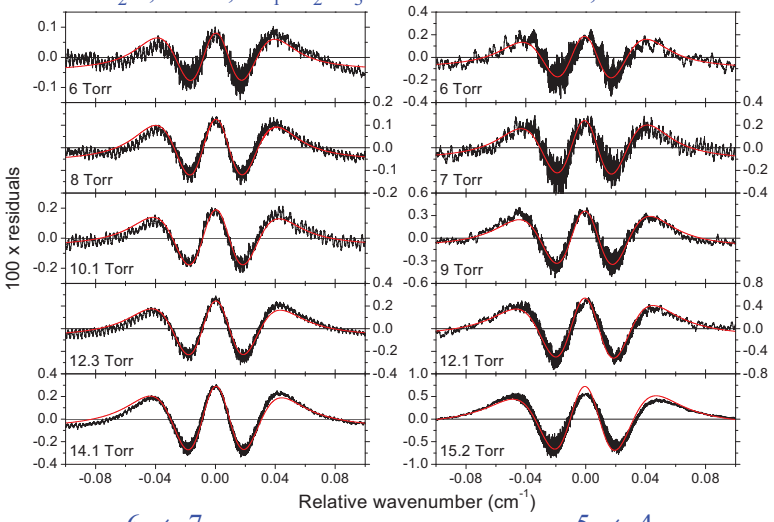

$6_{06} \leftarrow 7_{07}$ $5_{15} \leftarrow 4_{14}$

18

Ngo et al, J Chem Phys ***136****, 154310, 2012*

Model-experiment comparison

H_2O/N_2, 296K, ν_3, $11_{111} \leftarrow 10_{110}$, $11_{011} \leftarrow 10_{010}$ doublet

H_2O/air, 296K, $2\nu_1+\nu_2+\nu_3$, $5_{15} \leftarrow 4_{14}$ line

— measured, — calculated

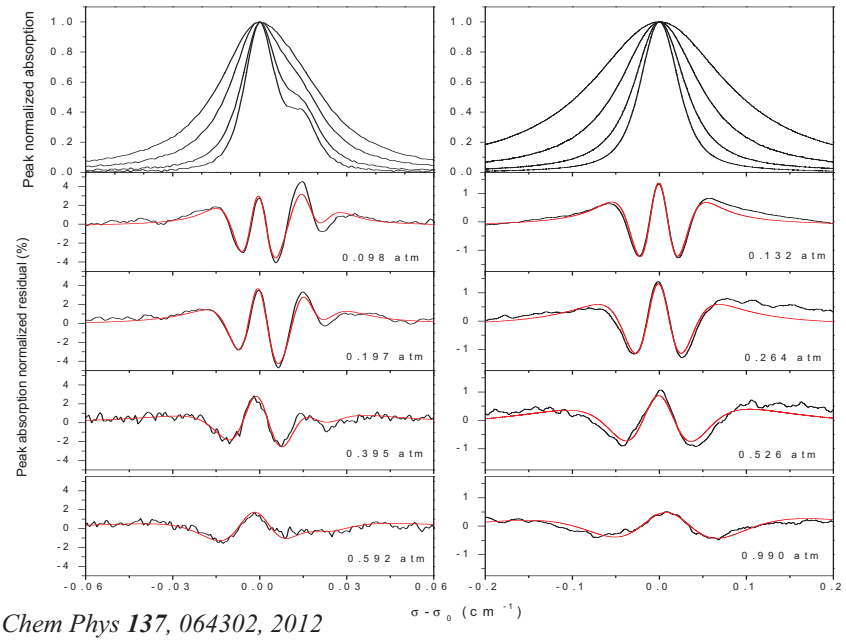

19

Ngo et al, J Chem Phys ***137****, 064302, 2012*

Model-experiment comparison

H_2O/N_2, ν_3 band lines

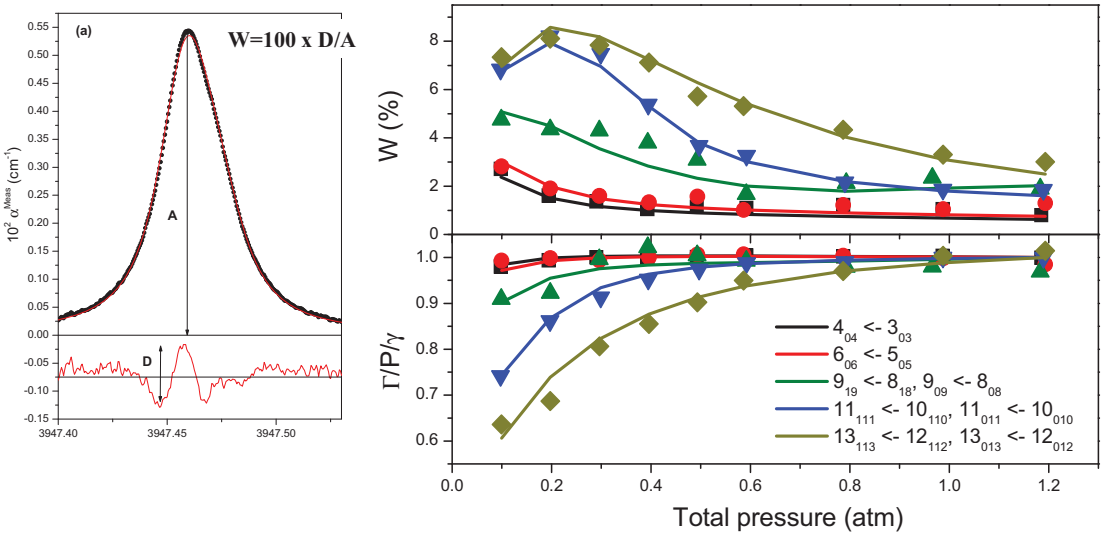

Measured (full symbols) and pCSDKS-calculated (lines) spectra with Voigt profiles.

20

Ngo et al, J Chem Phys ***137****, 064302, 2012*

Influence of different contributions on the line-shape

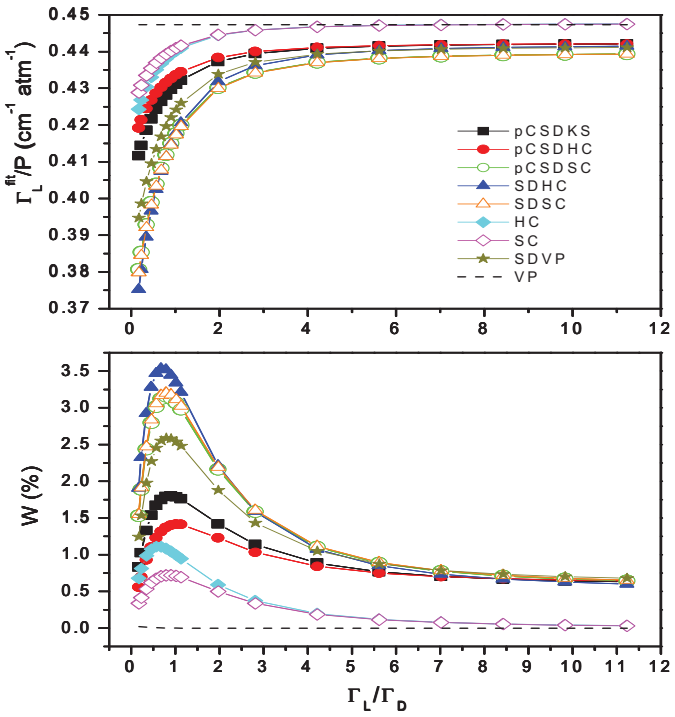

21

Tran et al, J Chem Phys, submitted

CO_2: *Ab initio* line-shape calculations by CMDS

- The classical rotational angular momentum is requantized, and the Doppler term is introduced.

$$\Phi(\omega,t) = \left\langle e^{-i\vec{k}(\omega).\vec{q}(t)}\vec{d}(t).\vec{d}(0)e^{+i\vec{k}(\omega).\vec{q}(0)} \right\rangle$$

$$F(\omega) = \mathrm{Re}\left\{ \frac{1}{2\pi}\int_{-\infty}^{+\infty}\Phi(\omega,t)e^{-i\omega t}dt \right\}$$

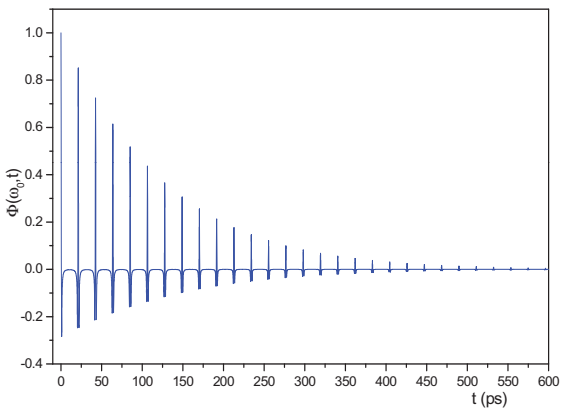

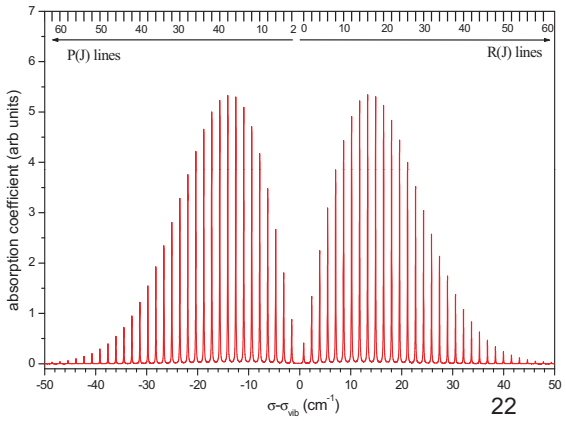

22

Hartmann et al, Phys Rev A, submitted

CO_2: Model-experiment comparison

Voigt-fits residuals for the P(14) line of the $\nu_1+5\nu_3$ band, • measured, — calculated

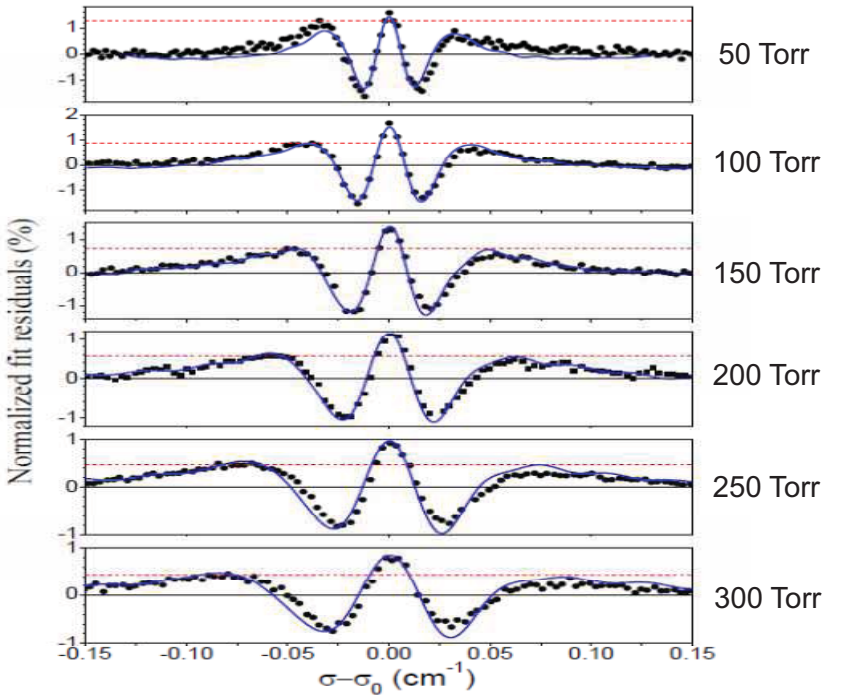

23

Hartmann et al, Phys Rev A, submitted

CO_2: Model-experiment comparison

Observed (symbols) and calculated (lines) broadening coefficient and fit residual amplitude

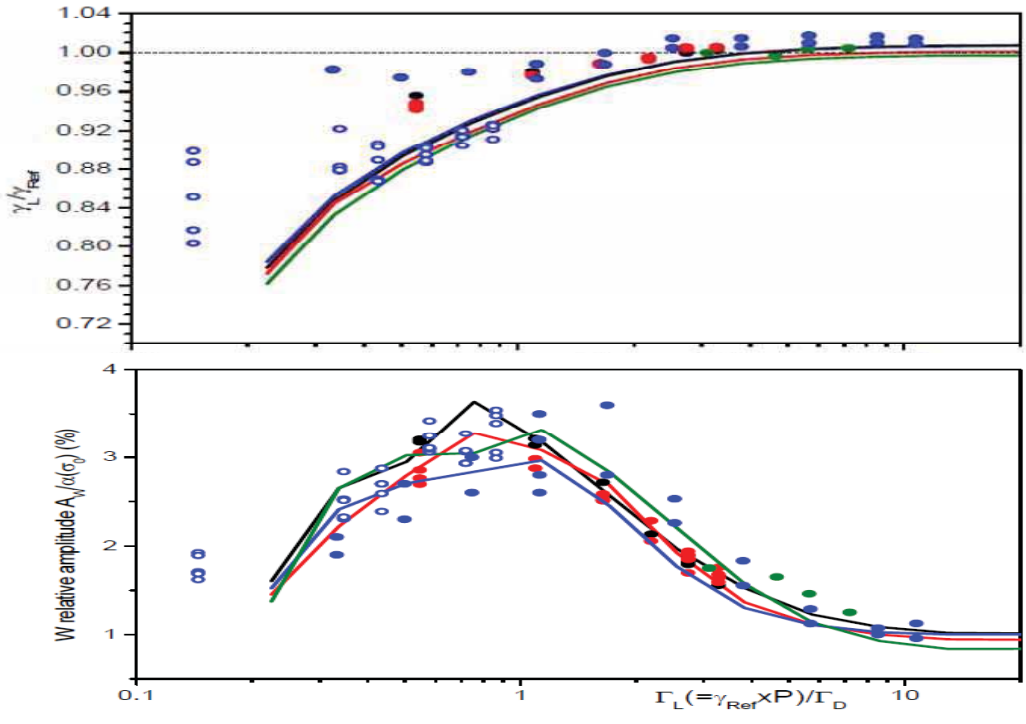

Conclusions, future studies

1. Molecular Dynamics Simulations appear as interesting tools to model line shapes without use of phenomenological approaches.

2. CMDS spectra can be used as a benchmark in order to choose or to build up a simplified approach suitable for practical applications such as atmospheric spectra predictions.

3. For H_2O, it was shown that the pCSDHC is the most suitable for line-shape modeling.

4. Studies of other radiating molecules (CO_2, CH_4, O_2), other perturbers from light to heavy ones for which the speed dependences and velocity changes are expected to be very different -> a common model?

25

Non isolated lines. Collisional line-mixing

26

Introduction

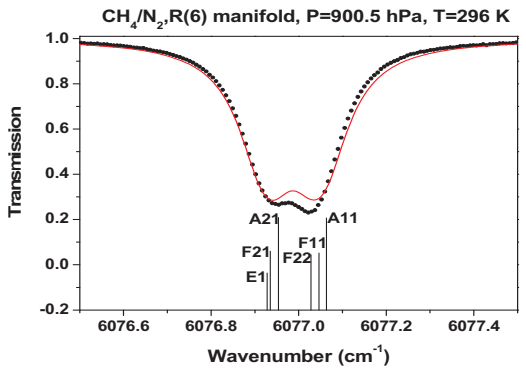

In some cases, for closely spaced lines, the Voigt profile fails when P increases. It predicts shapes that are too broad.

Collisions induce transfers of populations between the levels of the two lines that lead to transfers of intensity between the lines.

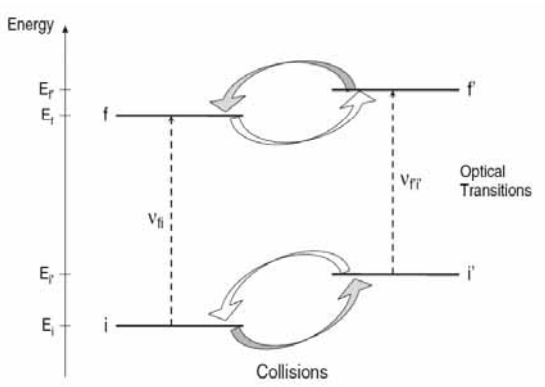

Introduction

Need to know the « relaxation matrix W» whose off-diagonal elements represent the couplings between the lines, the diagonal ones being Γ and Δ.

For moderate line overlapping, a first order perturbation approach is possible. Then we only need to know one line-coupling parameter (Y, related to the W matrix elements) per line

$$Y_k = 2\sum_{\ell \neq k} \frac{d_\ell}{d_k} \frac{\mathbf{W}_{k\ell}}{\sigma_k - \sigma_\ell}$$

28

Laboratory studies

Measurements: increasing number of measurements for various absorbing species, pure or diluted in various mixture
- Generally limited to the Y's (limits in pressure)
- Efforts still needed for the T dependence
- Almost nothing on H_2O

Calculations: various models, more or less based on parameters adjusted on measured spectra
- Fitting and scaling laws
- Semi-classical approaches from intermolecular potential
- Fully quantal approaches (simple systems)

Generally lead to agreement with measurements within better than 5%

Available data:
- CO_2, O_2, CH_4, NH_3, CH_3Cl, …
- A lot on Raman Q branches
- H_2O missing

29

Influence on retrievals. Vmrs soundings

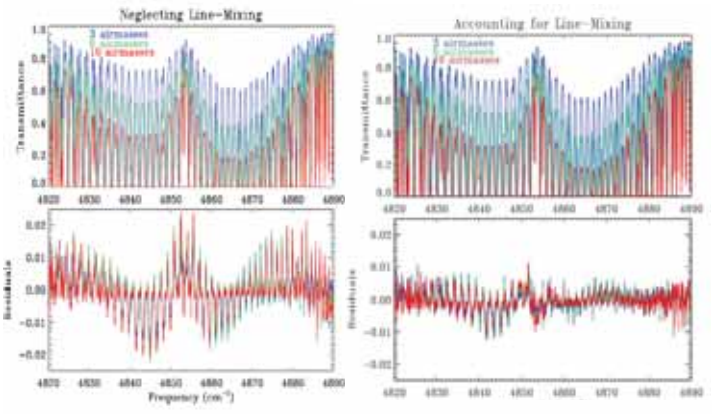

← Fits of a ground based transmission spectra in the region of the 2 $\nu_1+\nu_3$ band of CO_2

Significant errors (10%) on the CO_4 atmospheric amount. Sinks and sources !!!

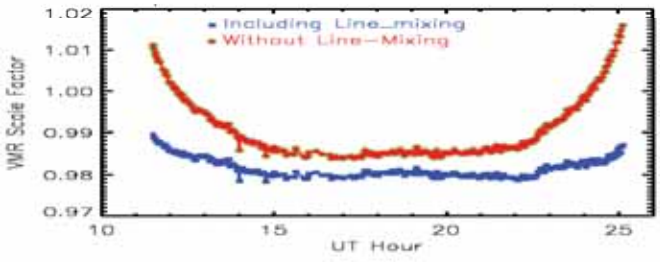

Hartmann et al, ACP, 9, 7303, 2009

Influences of line-mixing on line parameters determination

CH_4/air, $2\nu_3$ band

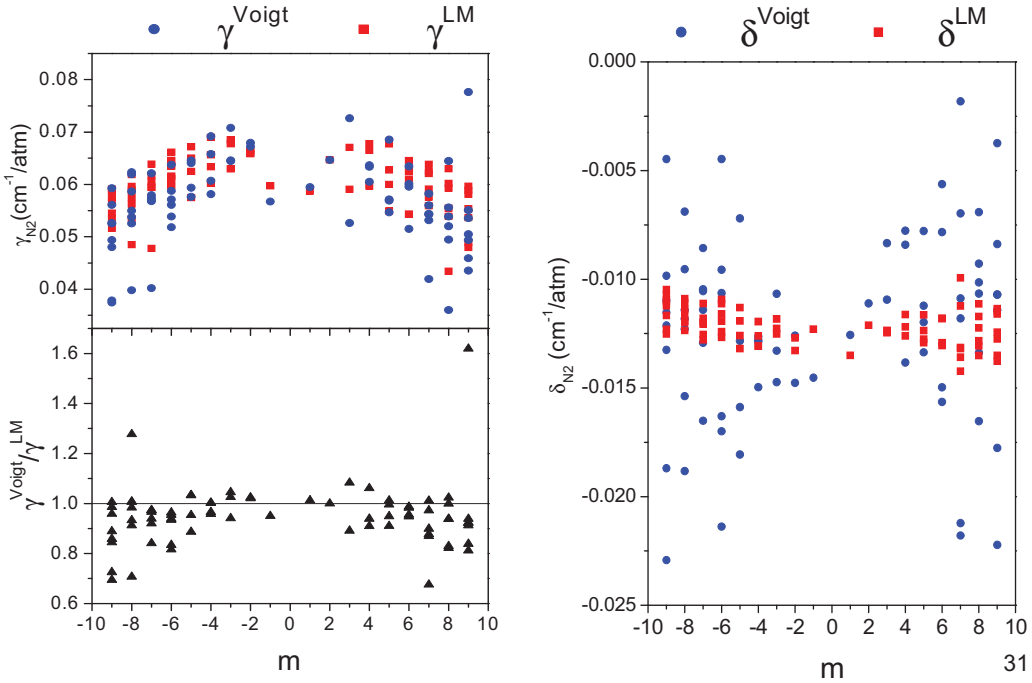

31

*Tran et al, JQSRT, **111**, 1344, 2010*

Conclusion

- Large progresses on knowledge and modeling of collisional effects on molecular spectra from laboratory studies
- Increasing evidences of influence for remote sensing
- Becoming a key issue for high precision soundings (OCO, ACE, …)
- Widely used Voigt isolated line profile progressively abandoned

Remaining problems

- Many laboratory experimental and theoretical studies still to be made
  large range of pressure
  very long paths

- A lot to be made for remote sensing
  Standardized data for spectral shapes
  Include more collisional shape parameters in database
  Develop efficient computing routines

32

"Cavity ring-down spectroscopy for high-precision molecular line parameters"

Daniel Lisak

Institute of Physics, Nicolaus Copernicus University in Torun

Prof. Dr. Daniel Lisak

Instytut Fizyki , Uniwersytet Mikołaja Kopernika
Grudziądzka 5/7, 87-100 Torun, Poland
Phone: +48 609768516
E-mail: dlisak@fizyka.umk.pl

Research

The main research activity is related to atomic and molecular spectroscopy, particularly spectral line shapes investigations. It includes study of such effects as collisional broadening and shifting of lines, dependence of collisional parameters on velocity of molecules, Dicke narrowing. The recent experimental work devoted to H_2O, O_2 and CO_2 spectra is based on frequency-stabilized cavity ring-down spectroscopy (CRDS). Spectrometer constructed at NIST was used for optical hygrometry with a primary humidity standard as a gas source. These experiment allowed to quantify systematical errors of trace water vapor measurement associated with line shape models. Investigations of O_2 and CO_2 spectra were motivated by application to remote sensing of atmosphere composition and improvement of spectroscopic databases. It is focused on spectral line shapes and transition frequencies measured with the optical frequency comb. The most recent research done at NCU is focused of the limits of precision and accuracy of CRDS method.

Education and Professional Experience

2012	2-months research trip to the National Institute of Advanced Industrial Science and Technology AIST, National Metrology Institute of Japan NMIJ, Tsukuba, Japan, working in the group of Dr. Hisashi Abe
2005 – 2008	Postdoctoral research associate - (19 months) in the National Institute of Standards and Technology - NIST, Process Measurements Division (Gaithersburg, MD, USA). Working in a group of Dr. Joseph T. Hodges
since 2004	Assistant Professor in the Department of Atomic, Molecular and Optical Physics of the Institute of Physics, NCU
2003	1.5-month research trip to the Universita di Napoli "Federico II", Dipartimento di Scienze Fisiche (Naples, Italy), working in the group of Prof. Antonio Sasso
2002 – 2004	Assistant in the Department of Gas Phase Spectroscopy of the Institute of Physics, NCU
2003	Nicolaus Copernicus University in Torun, Doctor of Physics
1998	Nicolaus Copernicus University (NCU) in Torun, Master of Physics

Cavity ring-down spectroscopy for high-precision molecular line parameters

Daniel Lisak

Institute of Physics, Nicolaus Copernicus University in Torun

Cavity ring-down spectroscopy (CRDS) is one of the most sensitive of laser spectroscopic techniques, which allows for investigation of weak molecular spectra with very high resolution and precision[1]. The frequency-stabilized CRDS (FS-CRDS) technique, first developed at NIST, Gaithersburg MD[2,3], and further improved at NIST and at UMK Torun, Poland[4-9] will be presented with technical details. The ring-down cavity is actively length-stabilized to the reference HeNe laser to eliminate any temperature-induced drift of the resonant frequencies and the probe laser is mode-matched and locked to the TEM_{00} mode. Single-mode excitation of the cavity enables to achieve high-quality exponential decay signals and eliminate systematic errors of the measured absorption coefficients. In the most recent configuration the probe laser is Pound-Drever-Hall locked to the ring-down cavity[5,6]. It was demonstrated that spectra with extremely high signal-to-noise ratio (SNR) of over 2×10^5 can be achieved[8]. The frequency axis of measured spectra is determined by direct comparison of the probe laser frequency to the optical frequency comb (OFC) at each point of the measured spectrum. This approach enables to determine molecular transition frequencies with relative uncertainties 10^{-9}[9].

FS-CRDS spectrometer was used to low-uncertainty measurements of line intensities, collisional parameters and line frequencies of molecules of atmospheric interest, such as oxygen, water vapor, carbon dioxide. Particular attention was paid to the influence of the line spectral line shape model on systematic errors of determined line parameters. Such physical effects as Dicke-narrowing and the speed-dependence of collisional broadening and shifting have to be taken into account in data analysis in order to reduce uncertainties of line parameters below 1 percent, as required in many modern applications.

[1] D.A. Long, A. Cygan, R.D. van Zee, M. Okumura, C.E. Miller, D. Lisak, J.T. Hodges, Chem. Phys. Lett., 536, 1, 2012.
[2] J. T. Hodges, H. P. Layer, W. W. Miller, G. E. Scace, Rev. Sci. Instrum., 75, 849, 2004.
[3] J. T. Hodges, R. Ciurylo, Rev. Sci. Instrum., 76, 023112, 2005.
[4] D. Lisak, P. Maslowski, A. Cygan, K. Bielska, S. Wojtewicz, M. Piwinski, J. T. Hodges, R. S. Trawinski, R. Ciurylo, Phys. Rev. A., 81, 042504, 2010.
[5] A. Cygan, D. Lisak, P. Masłowski, K. Bielska, S. Wojtewicz, J. Domyslawska, R. S. Trawinski, R. Ciurylo, H. Abe, J. T. Hodges, Rev. Sci. Instrum., 82, 063107, 2011.
[6] A. Cygan, D. Lisak, S. Wojtewicz, J. Domyslawska, R. S. Trawinski, R. Ciurylo, Meas. Sci. Technol., 22, 115303, 2011.
[7] S. Wojtewicz, D. Lisak, A. Cygan, J. Domyslawska, R. S. Trawinski, R. Ciurylo, Phys. Rev. A, 84, 032511, 2011.
[8] A. Cygan, D. Lisak,S. Wojtewicz, J. Domyslawska, J. T. Hodges, R. S. Trawinski, R. Ciurylo, Phys. Rev. A., 85, 022508, 2012.
J. Domyslawska, S. Wojtewicz, D. Lisak, A. Cygan, F. Ozimek, K. Stec, Cz. Radzewicz, R. S. Trawinski, R. Ciurylo, J. Chem. Phys., 136, 024201, 2012.

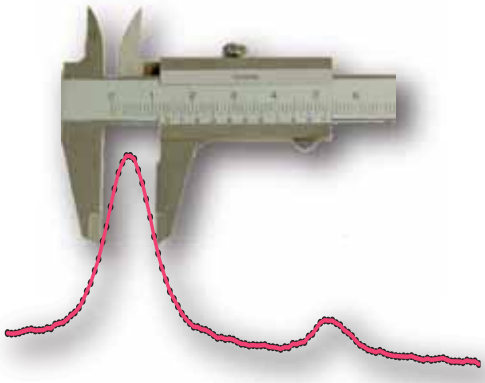

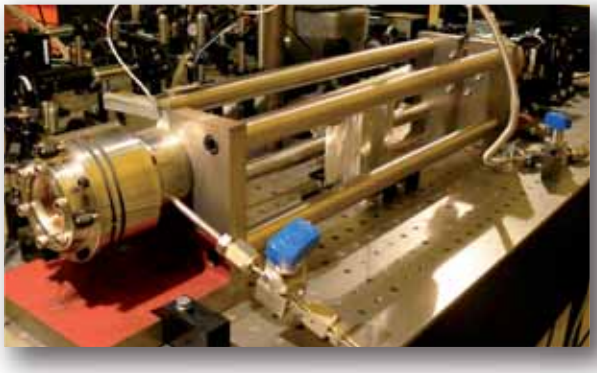

Cavity ring-down spectroscopy for high-precision molecular line parameters

Daniel Lisak

Instytut Fizyki, Uniwersytet Mikołaja Kopernika
Toruń, Poland

Outline

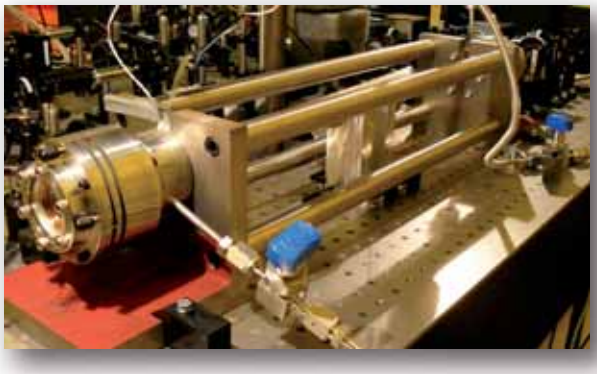

- **Principles of CRDS**
- **Frequency-stabilized CRDS**
- **Experimental realization**
- **Spectral line shapes and line intensity**
- **Low-uncertainty data**
- **Conclusions**

Cavity ring-down spectroscopy - CRDS

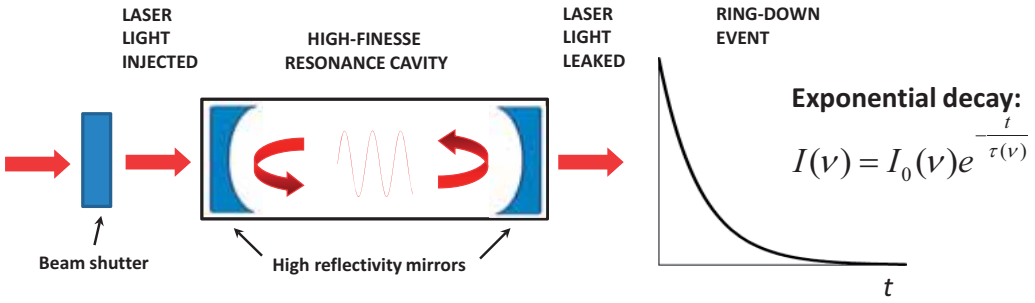

Exponential decay:

$$I(\nu) = I_0(\nu) e^{-\frac{t}{\tau(\nu)}}$$

Decay time

$$\tau(\nu) = \frac{L}{c(1 - R + \alpha(\nu)L)}$$

$$[c\tau(\nu_q)]^{-1} = \alpha_{bg}(\nu_q) + \alpha_{\text{abs}}(\nu_q)$$

$$= \alpha_{bg}(\nu_q) + nc \sum_i S_i g_i(\nu_q - \nu_i),$$

- high sensitivity
- high spectral resolution
- insensitive to laser power fluctuations

Multi-exponential decay → limitation of sensitivity

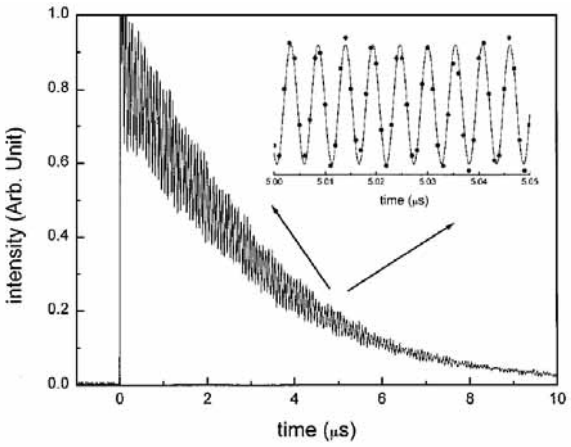

Pulsed laser
FSR=1.12 GHz

Beat note of two modes
Separated by 187 MHz

J. T. Hodges et al., *J. Chem. Phys.* **105**, 10278 (1996)

MM-CRDS → *Multi-Mode CRDS*

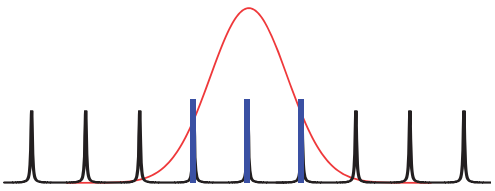

SM-CRDS → *Single-Mode CRDS*

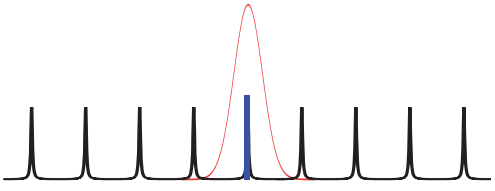

Single-exponential decay→ increase of sensitivity and accuracy

Frequency-stabilized cavity ring-down spectroscopy FS-CRDS

Vibrations and thermal drift of cavity resonances

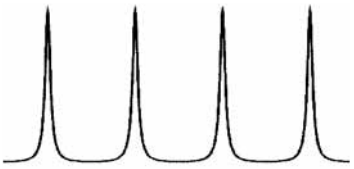

J. T. Hodges, D. Lisak, *Appl. Phys. B* **85**, 375 (2006)

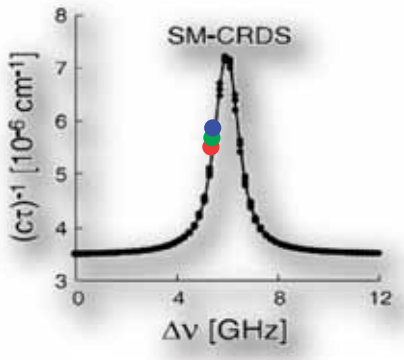

FS-CRDS * → *Frequency-Stabilized CRDS*

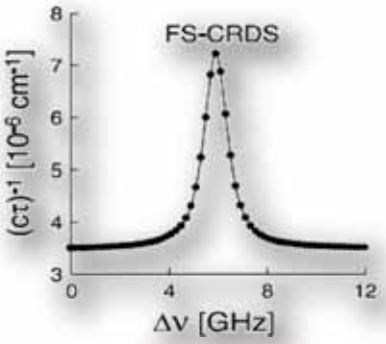

Active stabilization of the optical path length in the cavity

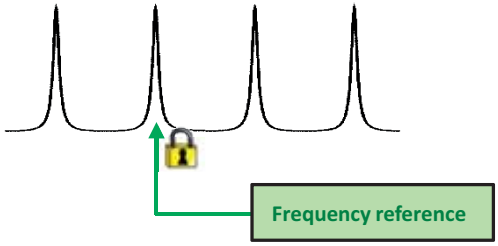

* Hodges, Layer, Miller, Scace, *Rev. Sci. Instrum.* **75**, 849 (2004).

Laser lock to the cavity

low-bandwidth lock

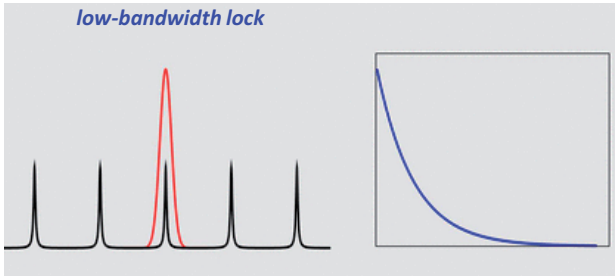

FS-CRDS

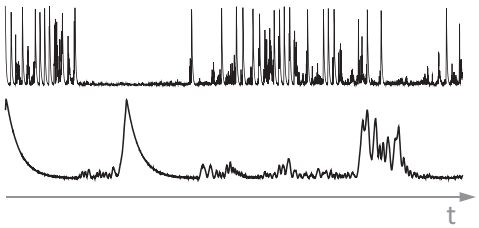

high-bandwidth Pound-Drever-Hall lock

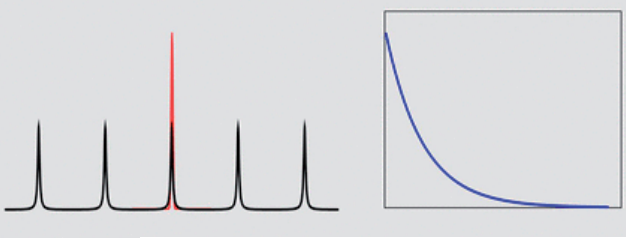

PDH-locked FS-CRDS

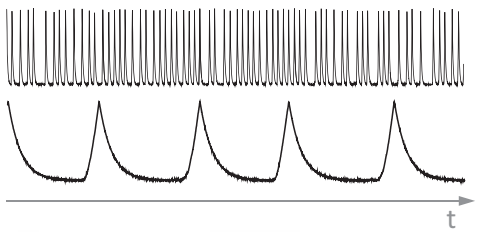

Increase of repetition rate→ faster signal averaging → increase of precision

optical feedback lock (Grenoble) Morville et al., *Appl. Phys. B* **80**, 027 (2005)

Experimental setup of PDH-locked FS-CRDS

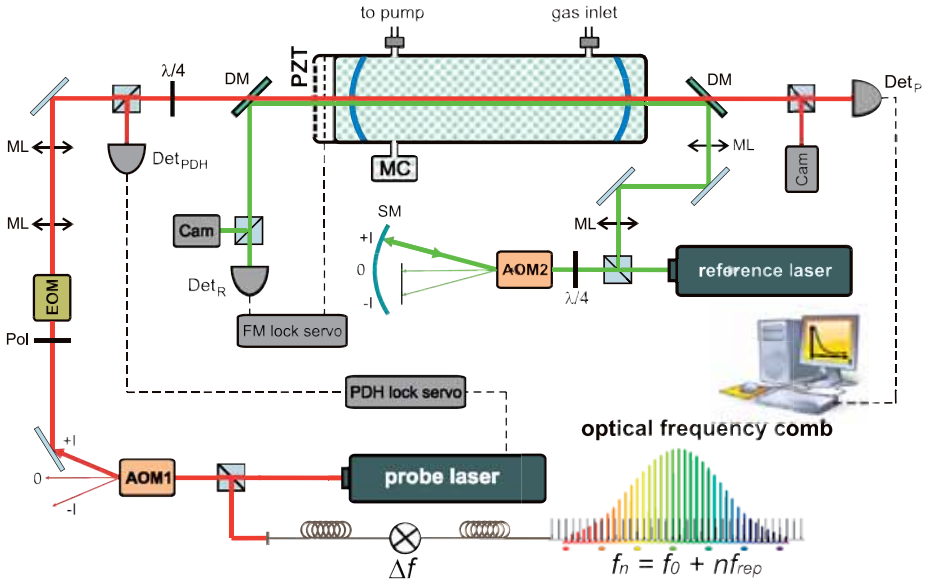

resolution ≈ 1 MHz to 10 kHz
depending on the recerence laser

3000 decays in 0.2 s, f_{rep} = 15 kHz

detection limit MDAL = 2 x 10^{-10} cm^{-1}
(7.5 x 10^{-11} cm^{-1} $Hz^{-1/2}$)

Experimental setup of PDH-locked FS-CRDS

Laser scan with a step FSR ≈ 204 MHz

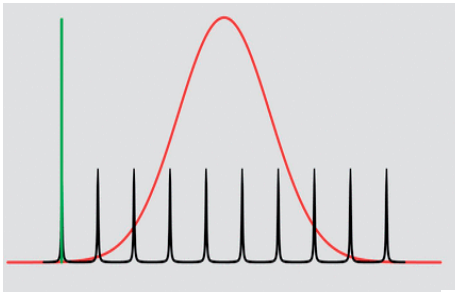

Laser scan with decreased step – by tuning the reference laser

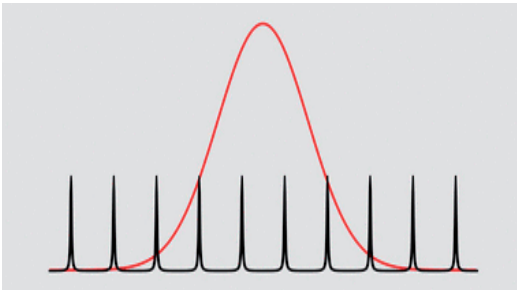

resolution ≈ 1 MHz to 10 kHz
depending on the recerence laser

3000 decays in 0.2 s, f_{rep} = 15 kHz

detection limit MDAL = 2 x 10^{-10} cm^{-1}
(7.5 x 10^{-11} cm^{-1} $Hz^{-1/2}$)

Spectral line shape and line intensity

4 lines of H_2O near 7156.817 cm^{-1} broadened by N_2

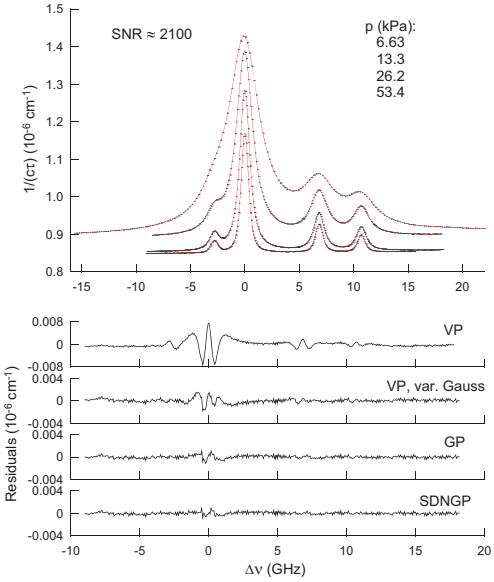

D. Lisak, J. T. Hodges, Appl. Phys. B, **88**, 317-325 (2007)

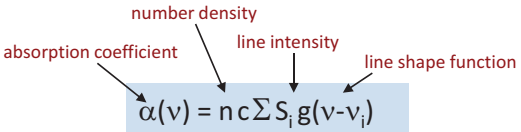

Pressure dependence of the fractional difference in the fitted area ΔA_B (relative to SDNGP line shape model)

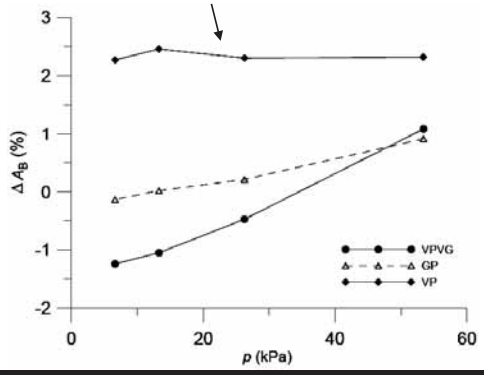

Spectral line shape models

Speed-dependence functions for van der Waals interaction

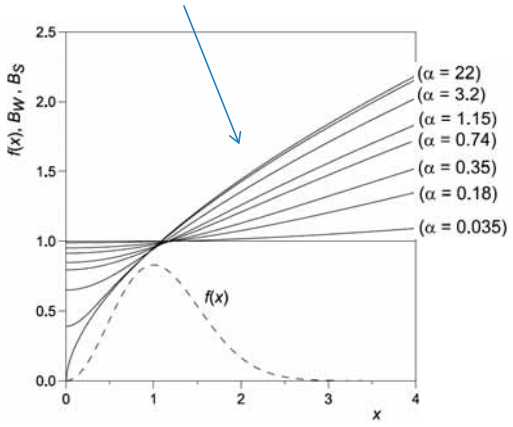

$f(x)$ – Maxwell distribution of velocities
α –perturber to absorber mass ratio

Semi-classical line shape models:

- Free motion of absorber, pressure (collisional) and Doppler broadening statistically independent – **Voigt profile (VP)**
- Dependence of collisional width and shift on absorber velocity – **Speed-dependent Voigt profile (SDVP)**

  $B_W(x) = \Gamma(xv_{m_A})/\Gamma$, $B_S(x) = \Delta(xv_{m_A})/\Delta$,

  where $x = v_A / v_{m_A}$; v_A is the absorber speed and v_{m_A} is the most probable absorber speed.

  Quadratic speed-dependence model:

  $B_W(x) = 1 + a_W(x^2 - 3/2)$ and $B_S(x) = 1 + a_S(x^2 - 3/2)$
- Velocity-changing collisions (Dicke narrowing)

  ν_{opt} – frequency of velocity-changing collisions (optical collisions)

  - soft collision model – **Galatry profile (GP)**
  - hard collision model – **Nelkin-Ghatak profile (NGP)** (or Rautian profile)
    billiard-ball model – (**BBP**)

Spectral line shape and line intensity

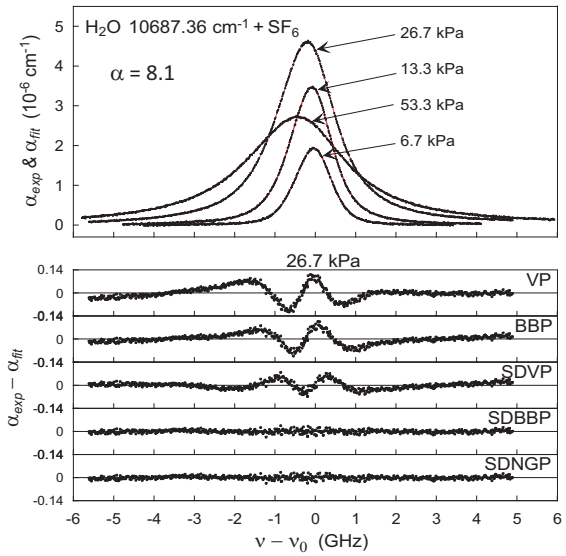

High mass ratio of SF_6 to H_2O (α=8.1) and high pressure shifting of line leads to strong asymmetry caused by the speed-dependent effects

Systematic error of line intensity determination caused by simplified line shape model

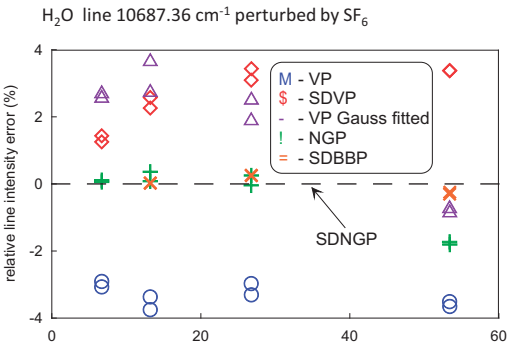

Spectral line shape and line intensity

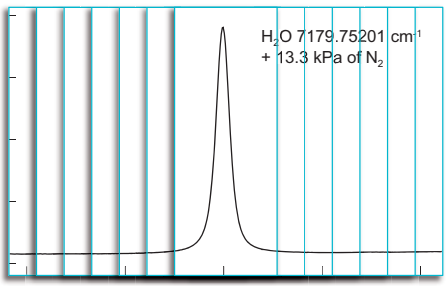

D. Lisak, D. K. Havey and J. T. Hodges, Phys. Rev. A **79**, 052507 (2009)

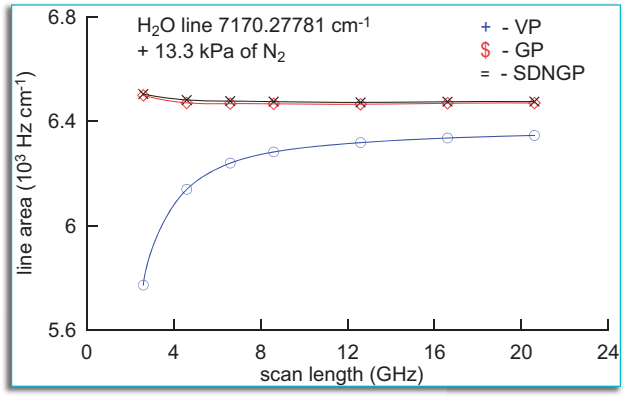

VP fit underestimates line area by 2% do 11%, depending on scan length

System for H_2O spectra (1.39 um)

NIST primary standard humidity generator

sample generation

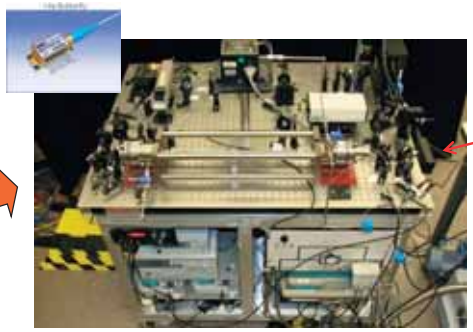

FS-CRDS built at NIST (USA)

Portable FS-CRDS system

chilled-mirror hygrometer

H_2O spectrum

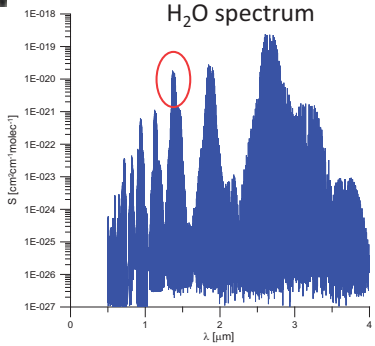

Uncertainty of H_2O line intensities

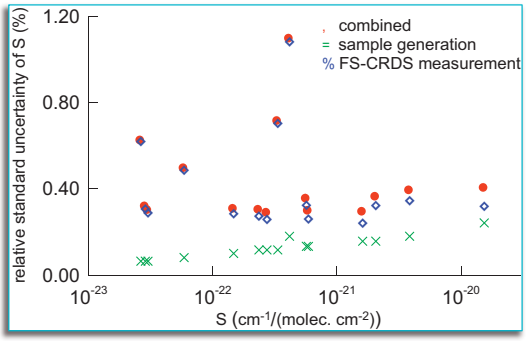

In most cases
u(S)/S < 0.4%

For the strongest line relative contribution of sample generation and CRDS measurements are comparable

D. Lisak, D. K. Havey and J. T. Hodges, *Phys. Rev. A* **79**, 052507 (2009)

Line intensity measurements

H_2O lines near **940 nm** measured by FS-CRDS compared to other data

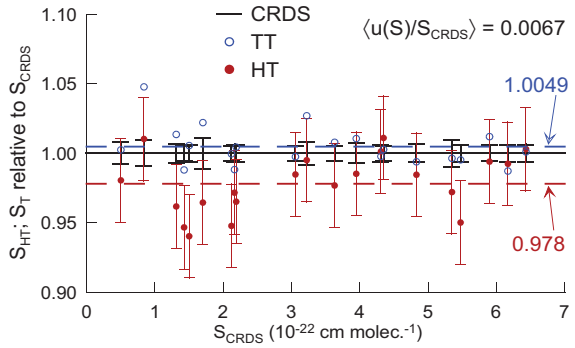

[HT] L.S. Rothman, et al., J. Quantum Spectrosc. Radiat. Transf. **96**, 139 (2004)
[TT] R. Tolchenov, J. Tennyson, JQSRT **109**, 559 (2008)

H_2O lines near **1.39 µm** measured by FS-CRDS compared to other data

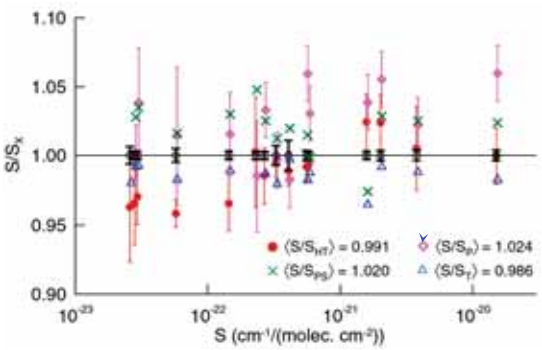

[P] B. Parvitte, V. Zéninari, I. Pouchet, and G. Durryet, JQSRT **75**, 493 (2002).
[PS] H. Partridge and D. W. Schwenke, J. Chem. Phys. **106**, 4618 (1997).
[T] J. Tennyson, private communication.

D. Lisak, J. T. Hodges, J. Molec. Spectrosc., **249**, 6–13 (2008)

Saturation spectroscopy

- decrease of relative line positions uncertainty by up to 3 orders of magnitude

- decrease of line area (~intensity) uncertainty by an order of magnitude

~ 1 MHz-wide Lamb dips

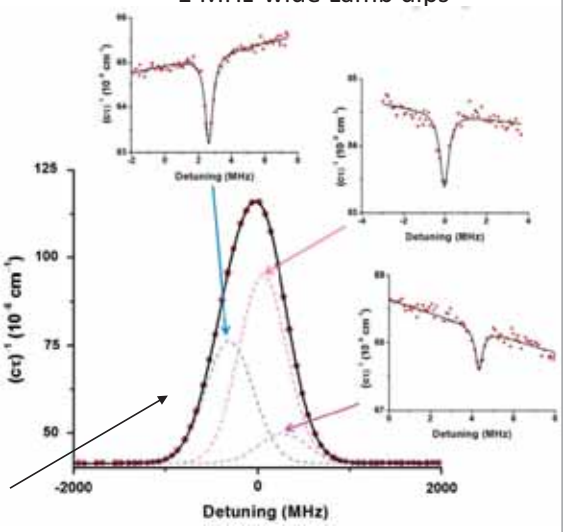

	Δf from Lamb dips		Δf from lineshape fits		
parametr	value	uncertainty	value	uncertainty	uncert. ratio
area1	35217	206	35888	2025	**9.8**
area2	22854	161	23119	532	**3.3**
area3	5552	305	4622	3094	**10.1**
delta f 1-2	-366.338	0.014	-369	8.8	**620**
delta f 1-3	217.376	0.019	225	29.1	**1518**

D. Lisak, J. T. Hodges, Appl. Phys. B, **88**, 317-325 (2007)

X STL, Świnoujście 2012

PDH-locked FS-CRDS, limits of precision

Oxygen ($^{16}O_2$) B-band R7Q8 line at 933 Pa

with 1000 spectra averaging the
quality of the fit (QF) is about 80 000

$$QF = (\alpha_{max} - \alpha_{min})/S_R$$

signal-to-noise ratio = 220 000

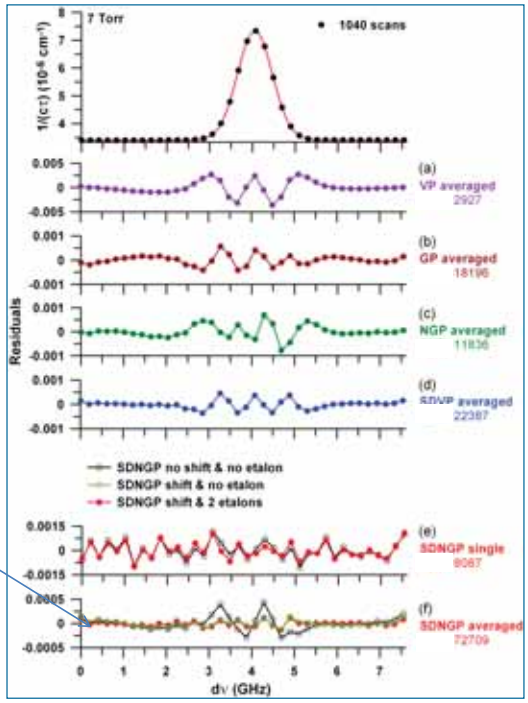

A. Cygan, et al, Phys. Rev. A **85**, 022508 (2012)

Linearity of detection system

linearity of AD converter

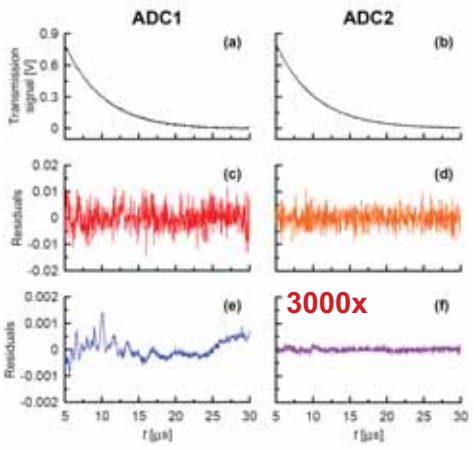

fit window

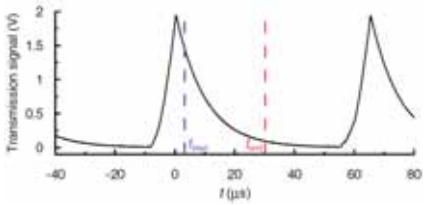

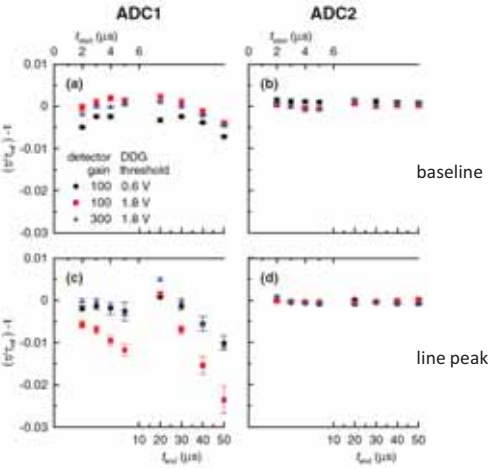

S. Wójtewicz, et al, *Phys. Rev. A* 84, 032511 (2011).

Oxygen B-band spectra

Oxygen B-band, transitions frequencies & pressure shifting

$u(\nu_0)$ = 1.1 MHz

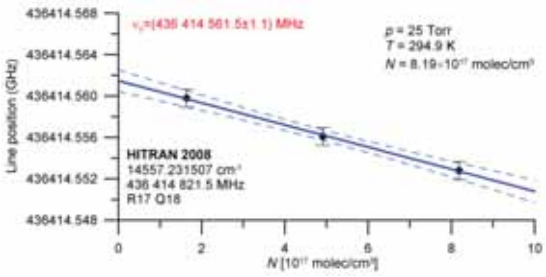

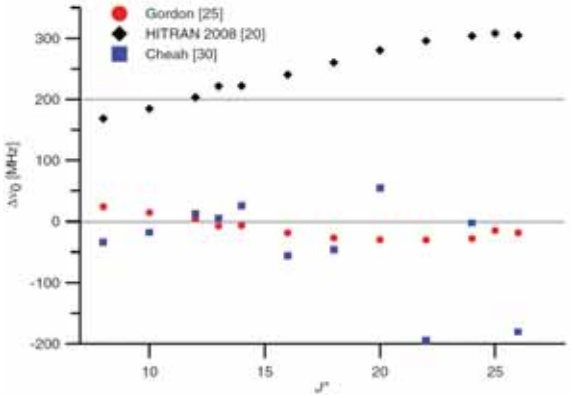

J. Domysławska, et al., *J. Chem. Phys.* **136**, 024201 (2012).

[25] Gordon, et al. JQSRT **112**, 2310 (2011)
[20] Rothman, et al. JQSRT **110**, 533 (2009)
[30] Cheah et al. JQSRT **64**, 467 (2000)

Conclusions

SNR evolution (2010 – 2012)

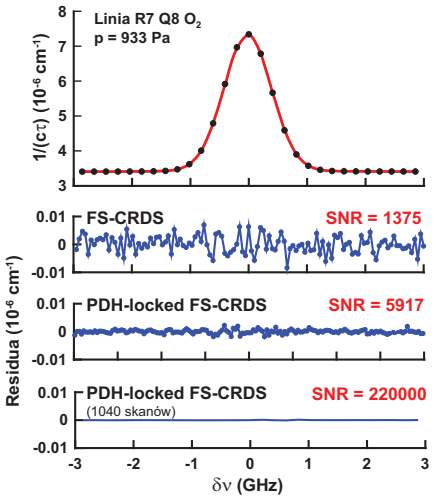

- **FS-CRDS properties:**
  - Is based on time and frequency measurements with well determined uncertainties
  - High dynamic range: SNR > 200 000
  - High spectral resolution: Δf < 50 kHz demonstrated
  - High precision of measurements: σ_S / S < 0.2 %
- **Allow for measurement of very week spectral lines:**
  - Line intensity, collisional broadening and shifting, subtle line-shape effects
  - Line shifting and precise line positions of weak lines – reference to OFC
- **Low-uncertainty determination of spectral line area (line intensity) requires knowledge of line shape function**

FS-CRDS, recent papers

1. D. Lisak, P. Masłowski, A. Cygan, K. Bielska, S. Wójtewicz, M. Piwiński, J. T. Hodges, R. S. Trawiński, R. Ciuryło, *"Line shapes and intensities of self-broadened O_2 $b^1\Sigma_g^+$ (v=1) ← $X^3\Sigma_g^-$ (v=0) band transitions measured by cavity ring-down spectroscopy",* Phys. Rev. A **81**, 042504 (2010).
2. A. Cygan, D. Lisak, P. Masłowski, K. Bielska1 S. Wójtewicz, J. Domysławska, R. S. Trawiński, R. Ciuryło, H. Abe, J. T. Hodges, *"Pound-Drever-Hall-locked, frequency-stabilized cavity ring-down spectrometer",* Rev. Sci. Instrum. **82**, 063107 (2011).
3. D. Long, K. Bielska, D. Lisak, D. K. Havey, M. Okumura, C. E. Miller, J. T. Hodges, *"The air-broadened, near-infrared CO_2 line shape in the spectrally isolated regime: Evidence of simultaneous Dicke narrowing and speed dependence"*, J. Chem. Phys. **135**, 064308 (2011).
4. S. Wójtewicz, D. Lisak, A. Cygan, J. Domysławska, R. S. Trawiński, R. Ciuryło, *"Line-shape study of self-broadened O_2 transitions measured by Pound-Drever-Hall-locked frequency-stabilized cavity ring-down spectroscopy"*, Phys. Rev. A **84**, 032511 (2011).
5. A. Cygan, D. Lisak, S. Wójtewicz, J. Domysławska, R. S. Trawiński, R. Ciuryło, *"Active control of the Pound–Drever–Hall error signal offset in high-repetition-rate cavity ring-down spectroscopy"*, Meas. Sci. Technol. **22**, 115303 (2011).
6. A. Cygan, D. Lisak, S. Wójtewicz, J. Domysławska, J. T. Hodges, R. Trawiński, R. Ciuryło, *" High signal-to-noise ratio laser technique for accurate measurements of spectral line parameters", Phys. Rev. A. **85,** 022508 (2012)*
7. J. Domysławska, S. Wójtewicz, D. Lisak, A. Cygan, F. Ozimek, K. Stec, Cz. Radzewicz, R. S. Trawiński, R. Ciuryło, *"Cavity ring-down spectroscopy of the oxygen B-band with absolute frequency reference to the optical frequency comb"*, J. Chem. Phys. **136**, 024201 (2012).

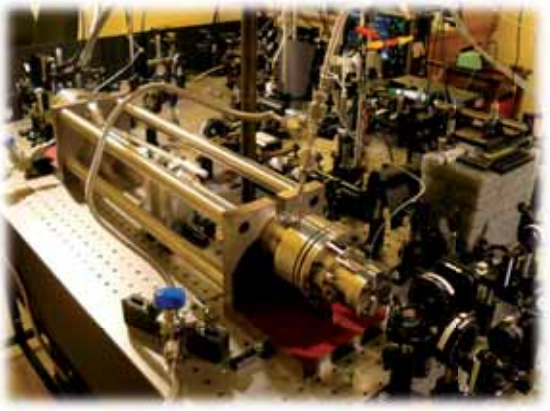

"Primary Reference Gas Mixtures: Preparation & Analysis"

Stefan Persijn

Dutch Metrology Institute, Van Swinden Laboratory (VSL)

Primary Reference Gas Mixtures: Preparation & Analysis

Stefan Persijn (VSL)
Mirka Valková (SMU)

EUMETRISPEC Stakeholder Workshop
15-16 November 2012

Dutch Metrology Institute

VSL (Van Swinden Laboratory) – Dutch Metrology Institute

Jan Hendrik van Swinden
"The meter" (1799)

National measurement standards
- Maintenance, Development
- Assure international traceability

Main Departments
- Calibration and Reference materials
- Customized Applied Metrology
- Research and Development

Metrological services (industrial metrology)
- Calibrations, Traceability
- Consultancy, R&D
- Training (Metrology college)
- Interlaboratory comparisons

Private company with a public task
- 97 employees; Turnover 13,2 M€ ; 35% from 'market'
- Website: http://www.vsl.nl

Dutch Metrology Institute

Pag.

Overview of mixture preparation

Static mixture preparation
- Root of metrological traceability chain in gas analysis
- 'Stable' components

Dynamic preparation
- Very low amount–of–substance fraction levels
- 'Unstable' components

Dutch Metrology Institute

Pag. 3

Primary realisation of mole

A primary realisation (PSM) of the amount fraction in a static gas mixture involves:

- accurate weighing (incl. buoyancy correction) of pure parent gases (or liquids) in a clean high pressure cylinder
- impurity analysis of the parent gases/liquids
- Analytical verification of the composition against a coherent set of primary standards
- Stability testing

Problems: low amount fractions (nmol/mol) for reactive gases, sorption on cylinder wall, isotopic variation

Dutch Metrology Institute

Pag.

Equipment for the gravimetric preparation


filling station


automatic balance for 5-liter cylinders

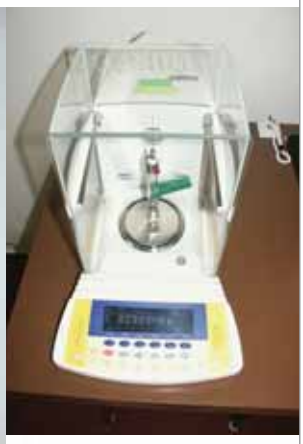
analytical balance for weighing liquids

Typical relative uncertainty of gravimetric preparation

- The uncertainty of the calculated mole fraction is affected by the uncertainties of:

  -weighted masses parent gases: 0.002 – 0.1 % rel.,

  - the parent gas composition: 0.0001 – 0.005 %rel.,

  -molar masses of components: 0.0003 – 0.006 %rel.

- Standard uncertainty from one differential weighing on automatic balance is 6 mg. It demands that ideal mass of added gas is at least 20 g.

- The pure component, under the laboratory conditions in a liquid state, is inserted into the vial with septum cap. Through this cap it is possible to take it into the syringe. Filling to the cylinder is realised by the injection through heated sample loop

Validation of composition

Standard for comparing gas mixtures: ISO 6143

Dutch Metrology Institute

Pag. 7

PRMs

environmental monitoring, law enforcement, custody transfer,….

PRMs

- CO, CO_2, O_2, C_3H_8, CH_4, SO_2, NO, NO_2, N_2O, H_2S, BTEX, medical diagnostics, natural gas, ethanol, SF_6, NH_3, H_2O, VOC (30 components), automotive, coke oven, refinery gas, sulfurs (H_2S, COS, CH_3SH, C_2H_5SH, $(CH_3)_2S$), biogas, stack gas, LPG and Liquid butane

Soon:

- HCl, S-free odorants, siloxanes

Key comparison: example for CO_2 in air

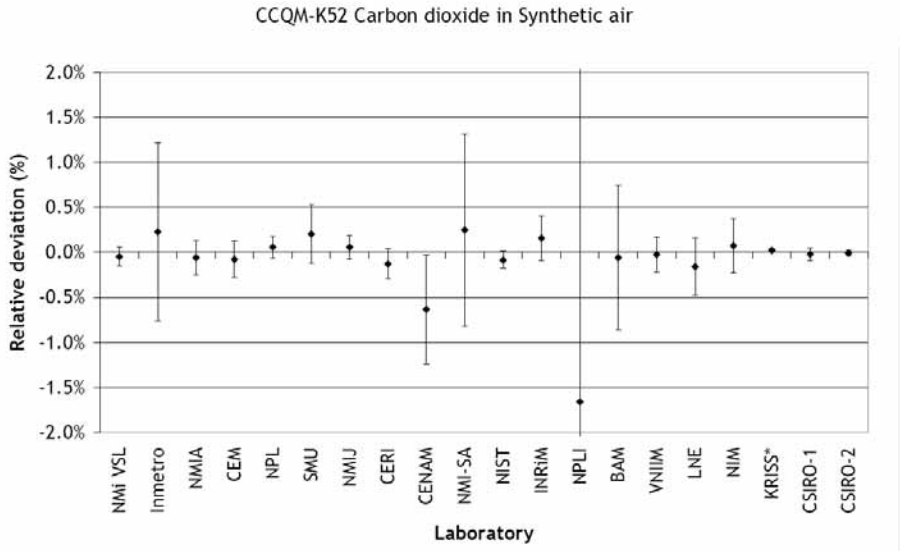

Figure 1: Relative deviation from the reference value with uncertainties stated by the laboratories (k=2)

Dutch Metrology Institute

Pag.

Nominal amount of substance fraction: 360 μmol/mol

NO comparison

Year	Amount of Substance Fraction (ppm) NIST		Amount of Substance Fraction (ppm) VSL		Relative Bias (%)
1995	A	60100	G	60036	0.11
	A	998.4	G	997.74	0.07
	A	101.2	G	101.12	0.08
2000	G	3271.0 ± 6.5	A	3274 ± 11	-0.09
	G	485.8 ± 1.0	A	486.6 ± 1.7	-0.16
	G	45.60 ± 0.09	A	45.53 ± 0.29	0.15
2003	A	0.496 ± 0.006	G	0.500 ± 0.005	-0.8

VSL-NIST Memorandum of Cooperation
Bilateral Comparisons
Declaration of Equivalence

10

Dutch Metrology Institute

Pag. VSL - Technology Chemistry

Example use of mixtures for spectroscopic studies

Molecular Physics
Vol. 109, No. 4, 20 February 2011, 535–542

Taylor & Francis

RESEARCH ARTICLE

The effect of collisions with nitrogen on absorption by oxygen in the A-band using cavity ring-down spectroscopy.

Frans R. Spiering[a]*, Maria B. Kiseleva[ab], Nikolay N. Filippov[b], Bas van Lieshout[a], Adriaan M.H. van der Veen[c] and Wim J. van der Zande[a]

[a]*Department of Molecular and Biophysics, Institute for Molecules and Materials, Radboud Universiteit, AJ 6525 Nijmegen, The Netherlands;* [b]*Institute of Physics, St. Petersburg University, St. Petersburg-Petrodvoretz, 198904, Russia;* [c]*VSL, 2600 AR Delft, The Netherlands*

(*Received 12 August 2010; final version received 15 October 2010*)

This paper reports on the effect of collisions between nitrogen and oxygen on absorption in the A-band near 760 nm under atmospheric conditions relevant for satellite retrieval studies. We use pulsed laser cavity ring-down spectroscopy with a narrow bandwidth laser and use pressure scans to increase the accuracy of the measured oxygen extinction coefficients. We use the so-called Adjustable Branch Coupling model to describe line mixing in the magnetic allowed A-band dipole absorption and we retrieve the collision induced absorption spectrum due to N_2–O_2 collisions.

Table 1. The mixing ratios of the gas mixtures used for determination of the CIA in O_2N_2 mixtures.

	vol.% O_2	vol.% N_2	
Mixture 1	54 ± 1	46 ± 1	←'home made'
Mixture 2	20.97 ± 0.03	79.03 ± 0.03	←Supplied by VSL
Mixture 3	29.989 ± 0.002	70.011 ± 0.002	←Supplied by VSL

Collision-induced absorption has quadratic dependence on O_2 amount of substance !

Dutch Metrology Institute

Pag.

Dynamic methods

Preparation of gas mixtures by mixing of known (mass) flows of calibration compound(s) and complementary gas, usually nitrogen or air

Dutch Metrology Institute

Pag. 12

Dynamic generation of formaldehyde

ISO 6145-8

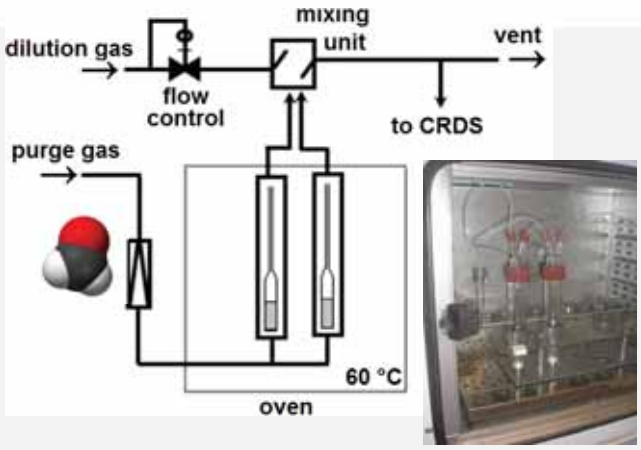

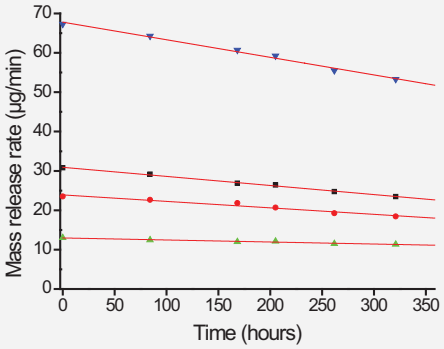

Solid paraformaldehyde kept in oven at 60 °C. Stream of N_2 purge gas, then further diluted

Paraformaldehyde mass release rate

Dutch Metrology Institute Pag.

Comparison measurements with Hitran 2004

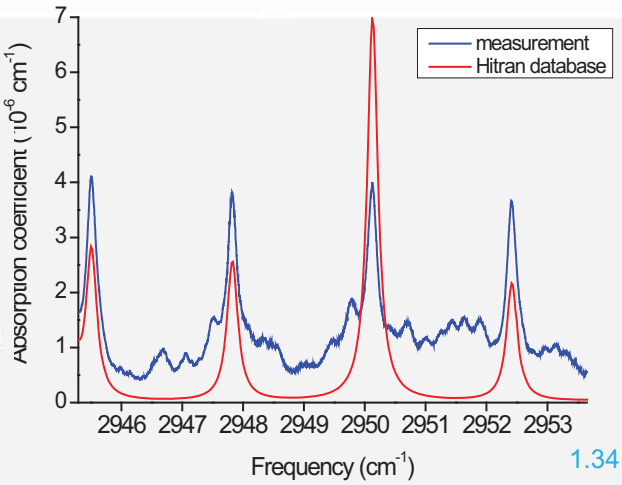

1.34 µmol/mol

Hitran 2004 is incomplete and incorrect (most peaks ~30% too low). Several studies are based on these Hitran data.

Dutch Metrology Institute Pag.

Comparison with Hitran 2008 & PNNL

1.34 µmol/mol

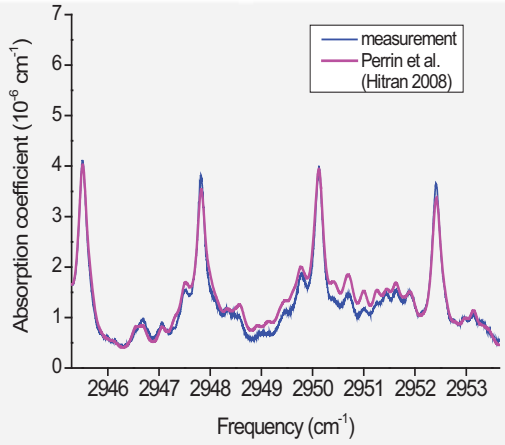

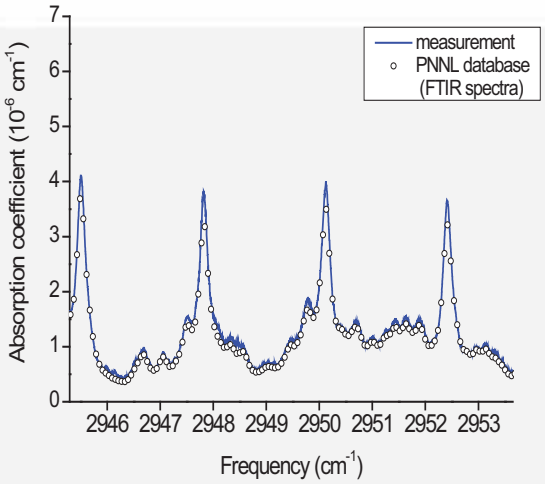

Hitran 2008 (work of Perrin et al): major improvement

Agreement with PNNL good

Dutch Metrology Institute

Pag.

Comparison with Hitran 2008 & PNNL

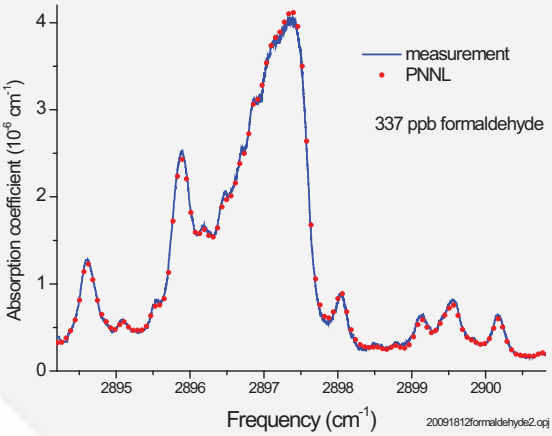

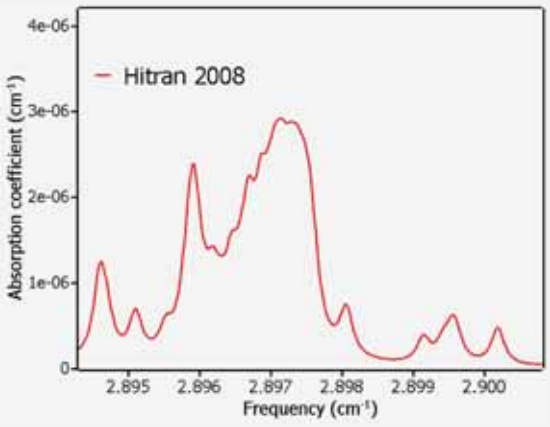

For certain regions Hitran data for formaldehyde still requires improvements

Dutch Metrology Institute

Pag.

Gases in spectroscopic studies

Prepare gases yourself for spectroscopic measurements is not trivial. For example for formaldehyde (CH_2O):

-generated from paraformaldehyde: water formed

-generated from trioxane: residual trioxane left, carbon monoxide,…

Measuring gas mixtures instead of pure compounds might be beneficial as it may reduce:

— polymerization
— reactions
— number of absorption cells (i.e, different path lengths) needed.

Dutch Metrology Institute

Pag.

Thank you for your attention

VSL
Thijsseweg 11
2629 JA Delft
Postbus 654
2600 AR Delft

T 015 269 15 00
F 015 261 29 71
E info@vsl.nl
I www.vsl.nl

Dutch Metrology Institute

"EUMETRISPEC Work Package 1: Generating traceable spectral line data"

Jean-Jacques Zondy

Laboratoire National de Métrologie et d'Essais (LNE)

WP 1: Generating traceable spectral line data

JRP ENV06 EUMETRISPEC
Spectral Reference Data for Atmospheric Monitoring

Month12-Meeting & Stakeholder Workshop, PTB, 2012-11-14/16

Spectral Reference Data for Environmental Monitoring (FP7/EURAMET)

J.-J. Zondy, LNE; M. Cadoret, Cnam
O. Werhan, V. Ebert, PTB
M. Vainio, MIKES
J. Petersen, DFM
S. Persijn, VSL

Outline

- ✓ Goals of WP1: Traceable laser-based spectroscopic measurements at satellite facilities (SF) in support/validation of CF-FTIR
- ✓ Overview of SF laser equipments and some past/recent spectroscopic measurements/data

Aims of WP1:

• creating a (initial) set of traceable (to national standards) spectral absorption line data (from near infrared to mid infrared) for stakeholders' needs

• data to be included in the pre-cursor data store for the Molecular Line Database (MLDB) and in HITRAN/GEISA (though data may be truncated)

• determination of line data depending on atmospheric conditions by means of
  - PTB's central facility (CF-FTIR, WP2) and
  - high-resolution laser instrumentation at CNAM, DFM, LNE, MIKES, and VSL

• measurements according to measurement protocols and traceability strategies delivered by WP3

Spectral data to be measured

• providing measurement results on spectral line data for named species according to measurement protocols delivered by WP3:

  - line position ν_0 and (air) pressure shift $d\nu_0/dp$ (acc. 10^{-5} cm^{-1} to 10^{-6} cm^{-1})
  - line strength $S_0|_{296K}$ (10^{-3} relative accuracy)
  - air broadening coefficients γ_{air} (10^{-3} relative) and *T*-dependence (10^{-2} relative)
  - spectral range λ: 0.7 – 10µm (all intrumentation combined)
  - Temperature range: 220/240 => 300 K (CF)
  - Pressure range: 10 hPa – 1100 hPa

• by SF as and at anchor points to CF and to report into the pre-MLDB

• by CF-FTS in broader ranges to populate the pre-MLDB

forms the backbone of the whole JRP, iteration with WP3, entangled structure

Molecules and Spectral ranges

SF (line position, linestrength, pressure dependence at T=296 K:

Molecule	Spectral Range	Tool	JRP-Partner
CH_4	3150 to 3500 cm^{-1} & 2940 to 3125 cm^{-1}	(fs-comb/OPO)	MIKES & LNE/CNAM
N_2O	2175 to 3525 cm^{-1}	(fs-comb/OPO) + QCL	MIKES & VSL
CO_2	~ 4810 cm^{-1} and ~ 6250 cm^{-1}	DL	DFM
HCl	2900 to 3100 cm^{-1}	OPO	VSL & CNAM/LNE
H_2O	6950 to 7250 cm^{-1}	DL	DFM
O_2	~7810 cm^{-1}	DL	DFM
HNO_3	3520 to 3580 cm^{-1}	OPO	VSL

CF (pressure broadened linewidth vs Temperature):

Molecules	Spectral Range	Thermal range	Pressure range	Tool	JRP-Partner
CH_4	2900 to 3500 cm-1	220-300K	10 - 1100 hPa	FTIR	PTB & SMU
N_2O	2100 to 3600 cm-1	220-300K	10 - 1100 hPa	FTIR	PTB & SMU
CO_2	2300 to 6300 cm-1	220-300K	10 - 1100 hPa	FTIR	PTB & SMU
H_2O	3600 to 7250 cm-1	250-300K	10 - 1100 hPa	FTIR	PTB & SMU
HCl	2700 to 3000 cm-1	296 K	10 - 1100 hPa	FTIR	PTB & SMU

Laser absorption spectrometry: equipment & techniques

Table 2 shows the equipment at each of the JRP-Partner's and the spectral ranges they are able to cover:

JRP-Partner	Spectral range covered	Instrumentation used:	Instrument group
CNAM/LNE	3 µm to 4 µm (MIR)	OPO= optical parametric oscillator	Satellite Facility (SF)
DFM	1.27 µm to 2 µm (NIR)	DL = diode laser	Satellite Facility (SF)
MIKES	3.2 µm to 4 µm (MIR)	OPO= optical parametric oscillator /fsec comb	Satellite Facility (SF)
VSL	2.7 µm to 3.5 µm (MIR)	OPO= optical parametric oscillator	Satellite Facility (SF)
VSL	Around 4.6 µm (MIR)	QCL=quantum cascade laser	Satellite Facility (SF)
PTB	0.7 µm to 10 µm (NIR to MIR	FT-IR = Fourier Transform infrared spectrometer	Central Facility (CF)

Equipment at SFs:

- ❑ Tunable near-IR semi-conductor diode lasers (TDL, λ<2µm) – DFM
  - TDLS/multipass cells
- ❑ MIR Quantum cascade lasers (QCLs, λ ~4-5µm) - VSL, PTB
  - TQCLS/multipass cells
- ❑ Widely tunable MIR cw OPOs (2.8 – 4.3µm) – VSL, MIKES, LNE/Cnam
  - OPO-CRDS
  - OPO-single-pass/multipass cells, saturated absorption spectroscopy
- ❑ Optical Frequency Combs based on fs mode-locked lasers (Ti:Sa, Er:fiber)
  - OFC-assisted high-resolution sub-Doppler spectroscopy using OPOs (absolute line positions, hyperfine structure)

Absolute-frequency measurements of CH_4 and N_2O line centers

- Purpose: Determine absolute frequencies of the positions of selected absorption lines of methane (CH_4) and nitrous oxide (N_2O), as well as their pressure shifts.
- Measurement range is from 2.85 to 3.45 µm (2900 to 3500 cm^{-1})
- Expected accuracy of the line position measurements is ± 5 – 100 kHz ($<10^{-8}$ relative acc. for OFC-assisted measurements)
- The measurements will be done at MIKES (CH_4 and NO_2) and LNE (CH_4) using cw OPOs referenced to a frequency comb.
- The measured data will be used as anchor points to validate the FTIR data of the central facility.

MIKES

Absolute-frequency measurements of CH_4 and N_2O line centers (referenced to an OFC)

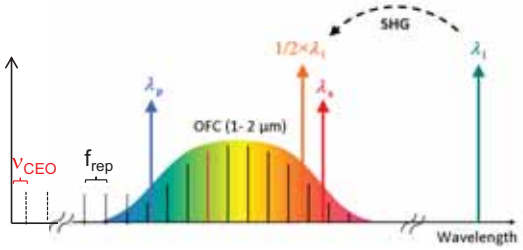

MIR idler locked to saturation dip and measured with near-IR OFC after SHG stage

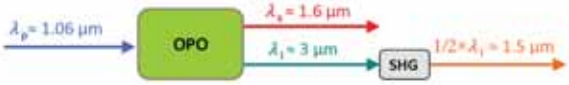

Er:fibre fs mode-locked Optical Frequency Comb

• bridges optical domain to µ-wave time standards

$$\nu_N = \nu_{CEO} + N*f_{rep}$$

optical ← RF ↓ RF

Locked to Cs clock or H-maser

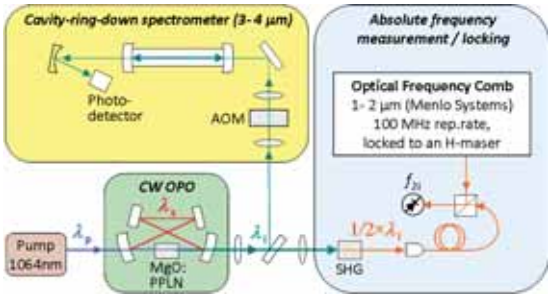

MIKES

Absolute-frequency measurements of CH_4 and N_2O line centers

- Current status of the work
  - Test measurements done with the first version of the setup, which was based on a Ti:sapphire-laser frequency comb (see below).
  - New version of the setup, based on an Er-laser frequency comb, built but not tested yet. (OPO pump laser failed, new one ordered).
  - First results (measurements of CH_4 lines) are expected in Jan-13

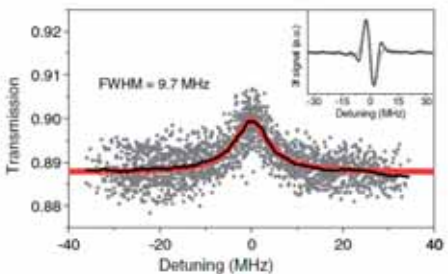

Example of a sub-Doppler spectrum (Lamb dip) of the $F^{(2)}_2$ P(7) ν_3 transition of $^{12}CH_4$, measured with the first version of the experimental setup [using a Ti:sapphire-laser OFC, *Opt. Lett.* **36**, 4122-4124 (2011)].

MIKES

Locking the OPO to an Optical Frequency Comb (OFC)

➢An OFC is a grid of millions of phase-locked equally-spaced longitudinal modes of a mode-locked Er:fibre fs laser . The spacing is set by the repetition rate f_r =250 MHz of the laser pulses. Each comb absolute frequency (referenced to a time standard) is $f_N = f_{ceo} + N*f_r$

➢ By referencing the pump *and* signal waves frequencies to the nearest respective comb tooth, one can deduce the absolute frequency of the idler: $\nu_i = \nu_p - \nu_s = (N_p-N_s)*f_r+\Delta_p+\Delta_s$

OFC (collaboration LNE-CNR/INO, Italy – De Rosa/De Natale)

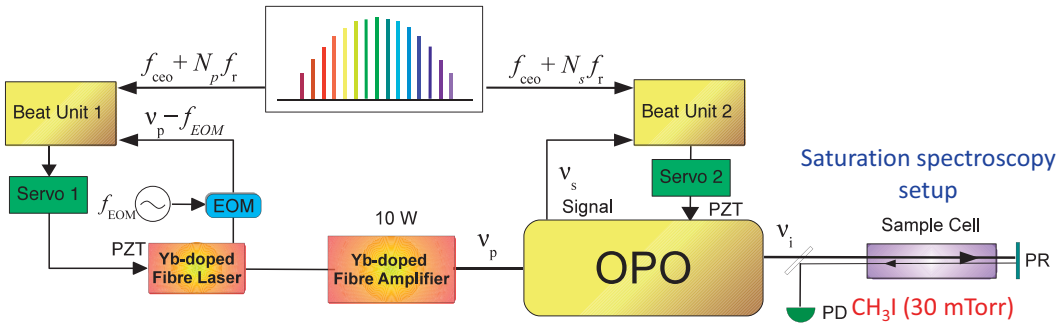

The comb/signal beatnote Δ_s is used to control the OPO cavity kength and the comb/pump beatnote Δ_p is fed back to the pump frequency . Hence the OFC absolute stability and accuracy are transfered to the idler frequency (drift cancellation).

LNE INO-CNR Laboratoire Commun de Métrologie LNE-Cnam le cnam

Doppler & sub-Doppler spectroscopy of CH_3I

Doppler lines of CH_3I near 3.4 µm (signal-wave cavity-stabilized OPO)

Ricciardi et al, Mol. Phys. ***110****, 2103 (2012)*

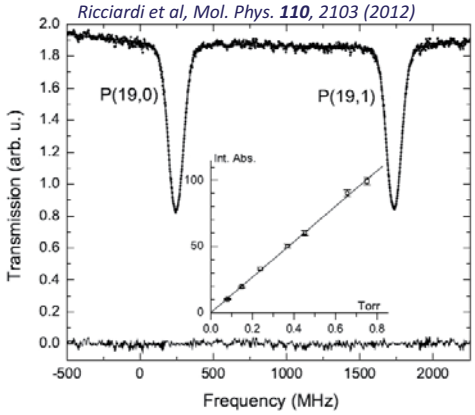

➢ Line strength measurements

P(19,0):

$S = (2.74 \pm 0.04) \times 10^{-21}$ cm/molecule

P(19,1) :

$S = (2.76 \pm 0.04) \times 10^{-21}$ cm/molecule

Inset: Doppler-broadened profile with small Lamb dip at the center.

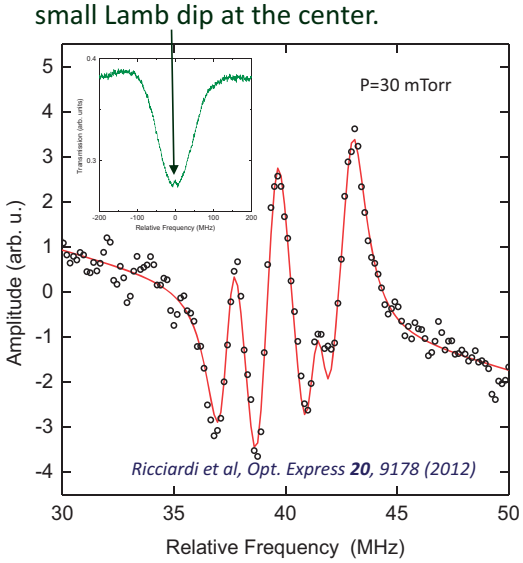

Lockin absorption signal of the hyperfine structure (6 components) of the ν_1 P(18,3) rovibrational transition of CH_3I:

LNE — INO-CNR — Laboratoire Commun de Métrologie LNE-Cnam — le cnam

Spectroscopy on CO_2 in N_2 at 2 µm

+ DFM

1. 40 m and 200 m multi pass cell absorption spectrometers have been setup.
2. Negotiating with a commercial CRDS vendor on acquiring/loaning a system for comparison measurements.
3. Investigating CO_2 adsorption effects.

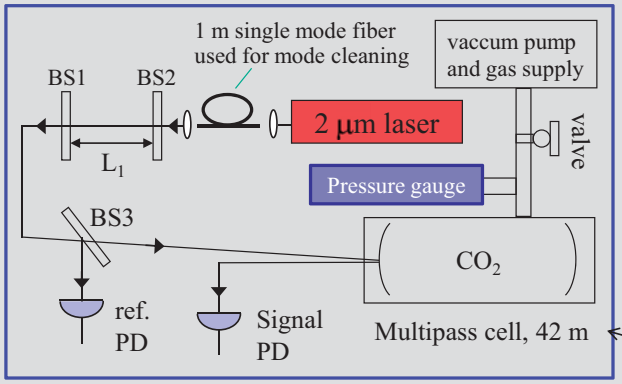

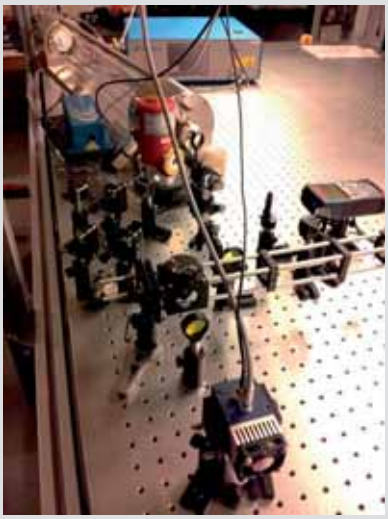

BS1, BS2: removable interferometer for obtaining a frequency scale

12 03/12/2012

CO_2 adsorption in the measurement cell

40 m multipass cell filled with 300 hPa certified mixture of 1000 ppm CO_2 in N_2.
Graphs show changes in pressure and spectroscopically measured concentration.

Where does the CO_2 go?

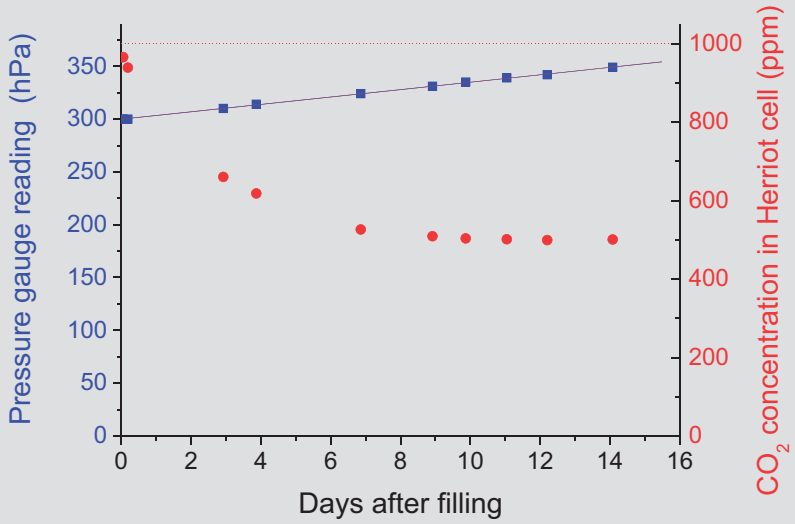

13 03/12/2012

CH_4 line strengths: 3450-3500 cm^{-1} region

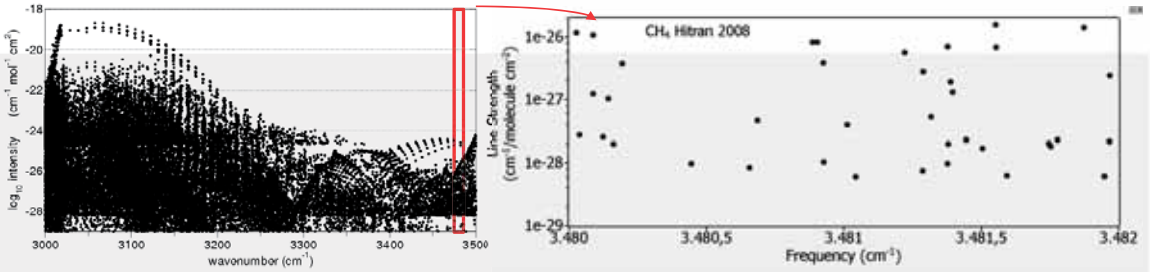

Weak CH_4 lines in the 3450-3500 cm^{-1} region will be measured using OPO-based CRDS (operating range 2850-3710 cm^{-1})

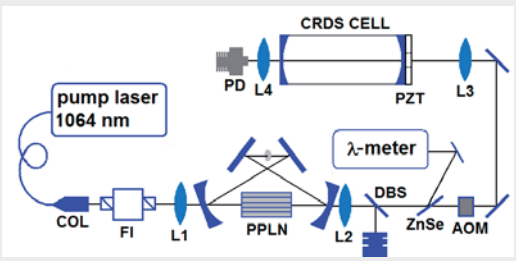

CH_4 line strengths: 3450-3500 cm^{-1} region

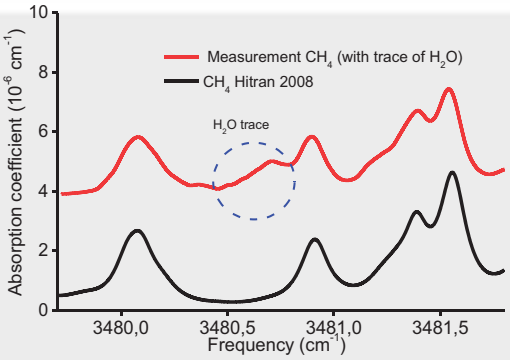

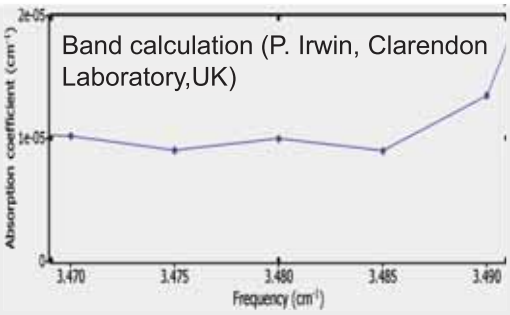

An offset is visible due to contributions from distant methane lines. This offset is however ~3x lower than predicted by CH_4 band calculations (often used for planetary observations)

Measurements at low pressures are planned to measure individual line strengths (awaits availability mirrors with higher R later this year)

Dutch Metrology Institute

Conclusions and prospects

✓ The consortium of SF is equipped with suitable cw tunable laser sources and spectroscopic equipments to produce traceable and accurate spectroscopic data sets from the NIR to MIR up to 4.5 μm for anchoring and validating the CF-FTIR facility.

✓ Intercomparision of measured data within SF will be conducted to validate accuracy and identify potential bias effects

✓ possible extension of measurements to deeper MIR (5 – 12 μm) using DFG laser sources

Thank you for your attention!

EUMETRISPEC

Spectral Reference Data for Environmental Monitoring (FP7/EURAMET)

EUMETRISPEC Work Package 2: "Setup, characterization and validation of the central facility FTIR spectrometer for traceable spectral data measurement"

Jens Brunzendorf

Physikalisch-Technische Bundesanstalt (PTB)

EUMETRISPEC Work Package 2

"Setup, characterization and validation
of the **central facility FTIR spectrometer**
for traceable spectral data measurement"

**Jens Brunzendorf, Volker Ebert,
Anne Rausch, Anton Serdykov,
Olav Werhahn, Viktor Werwein**

PTB Braunschweig

EMRP
European Metrology Research Programme
Programme of EURAMET
The EMRP is jointly funded by the EMRP participating countries within EURAMET and the European Union

EUMETRISPEC Stakeholder Workshop, 2012-11-15/16

Key Tasks

T2.1 **Setting up the core of the FT-IR spectrometer hardware**
Who? → mainly PTB

T2.2 **Develop/setup /characterize surrounding spectroscopic infrastructure of the CF**
Who? → PTB, DFM, LNE, MIKES, SMU, VSL

T2.3 **Traceably validate the CF by intercomparing CF spectral data (the reference data sets) with traceable reference spectral data collected by the top-performing laser instruments at the Satellite facilities (SFs)**
Who? → PTB, CNAM, DFM, LNE, MIKES, SMU, VSL

Human resources: 7 person-years, 78% PTB

T2.1. FT-IR target performance

- **Spectral resolution** (Target uncertainty better 10^{-5} **relative** across spectral range)
- Characterized nonlinearity of the **transmission axis**
  (Target uncertainty: linearity better than 10^{-1} in three investigated wavelength ranges (NIR/SWMIR/LWMIR)
- Wavelength accuracy **(wavelength axis)**
  (Target uncertainty: relative accuracy 10^{-5})
- Characterization of **instrumental line shape function** of the CF
  (in three investigated wavelength ranges)

- Traceable measurement of cell **pressure** ≈1 hPa to ≈1100 hPa
  (Target uncertainty 10^{-3} relative)
- Traceable measurement of cell **temperature** 220 K to 320 K
  (Target uncertainty **100mK**)
- Traceable **absorption length** measurement
  (Target uncertainty 10^{-3} relative)

T2.2. Develop/setup and characterize the surrounding spectroscopic infrastructure of the CF

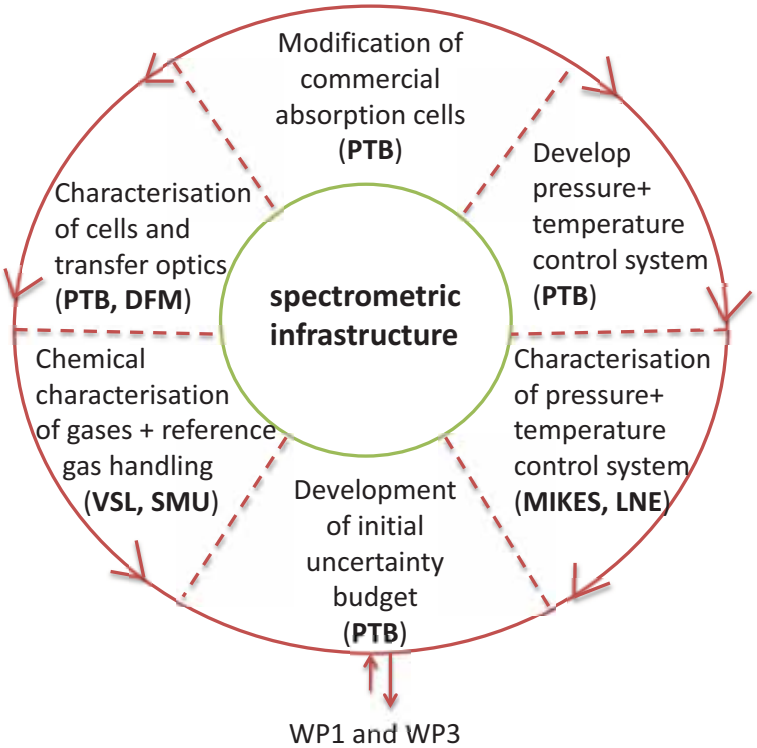

T2.3. Traceably validate the CF by intercomparing CF spectral data with traceable reference spectral data collected by the top-performing laser instruments at the Satellite facilities (PTB, CNMA, DFM, LNE, MIKES, SMU, VSL)

Spectral windows:
- 1µm – 2µm (NIR)
- 2 µm – 3 µm (SW MIR)
- 3 µm – 10 µm (LW MIR)

Preliminary intercomparison 1 will be used to optimize the CF's spectrometer & data evaluation

Independent intercomparison with independent set of data will be used to characterize the CF performance & to evaluate the final uncertainty budget

T2.3. Intercomparing CF spectral data with spectral data collected by the satellite facilities

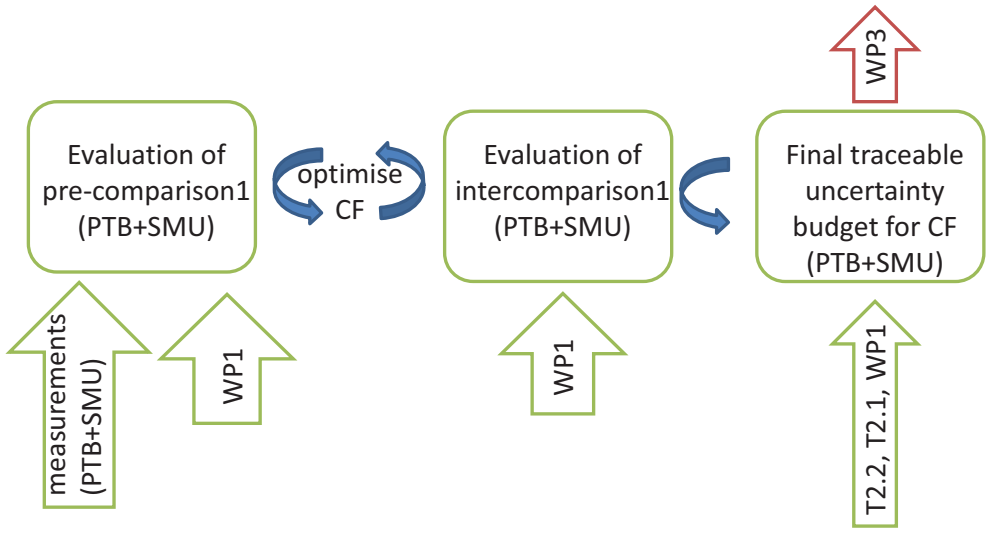

WHERE ARE WE NOW?

FTIR-Spectrometer (core facility)

Bruker IFS 125HR spectrometer

Commercial high-resolution Fourier-Transform-Infrared-Spectrometer (FTIR)

Wavelength range: 0.7-14 µm

max. optical path difference 481 cm

Detectors: InSb, MCT, InGaAs, Si

Beam splitter: KBr, CaF_2, Quartz

Vacuum quality (empty FTS, no gas cell installed)

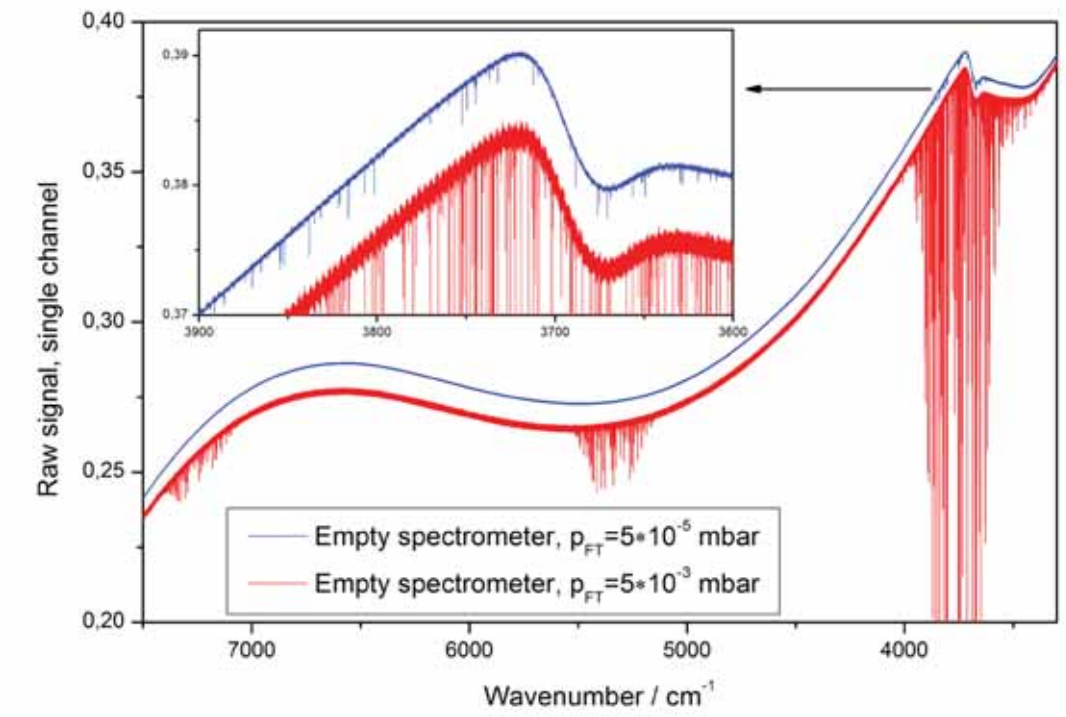

A good vacuum is essential for high-quality H_2O, CO_2, … measurements

The way to a good vacuum

1. Good pumps

2. air-tight instrument

- typical leakage rate of a Bruker IFS 125HR: 0.5 … 1 mbar/day
- Our FTS: initial leakage rate 0.7 mbar/day
- Now: 0.1 mbar/day
- Key task: find & eliminate all leaks (includes careful handling & cleaning ☺)

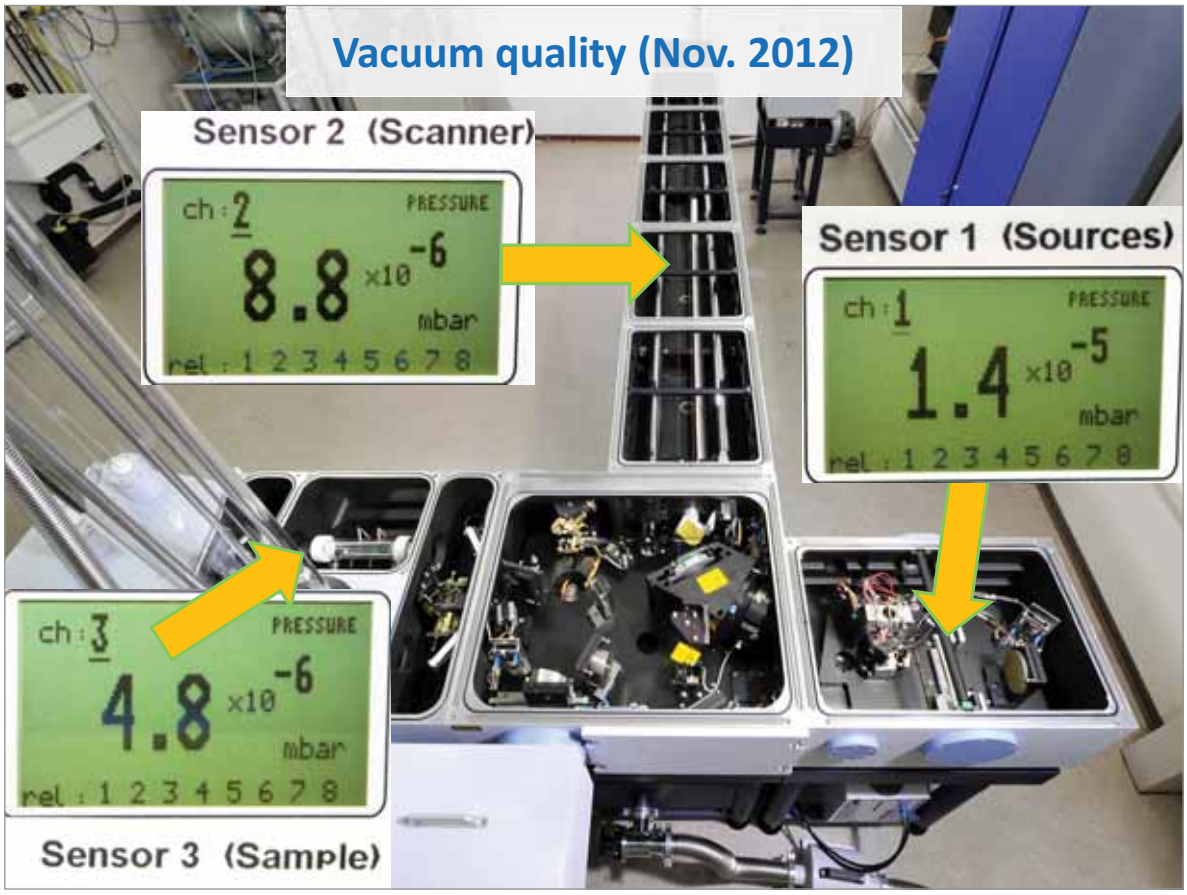
Vacuum quality (Nov. 2012)
Sensor 2 (Scanner)
ch : 2
PRESSURE
8.8 x10 -6
mbar
rel : 1 2 3 4 5 6 7 8
Sensor 1 (Sources)
ch : 1
PRESSURE
1.4 x10 -5
mbar
rel : 1 2 3 4 5 6 7 8
ch : 3
PRESSURE
4.8 x10 -6
mbar
rel : 1 2 3 4 5 6 7 8
Sensor 3 (Sample)

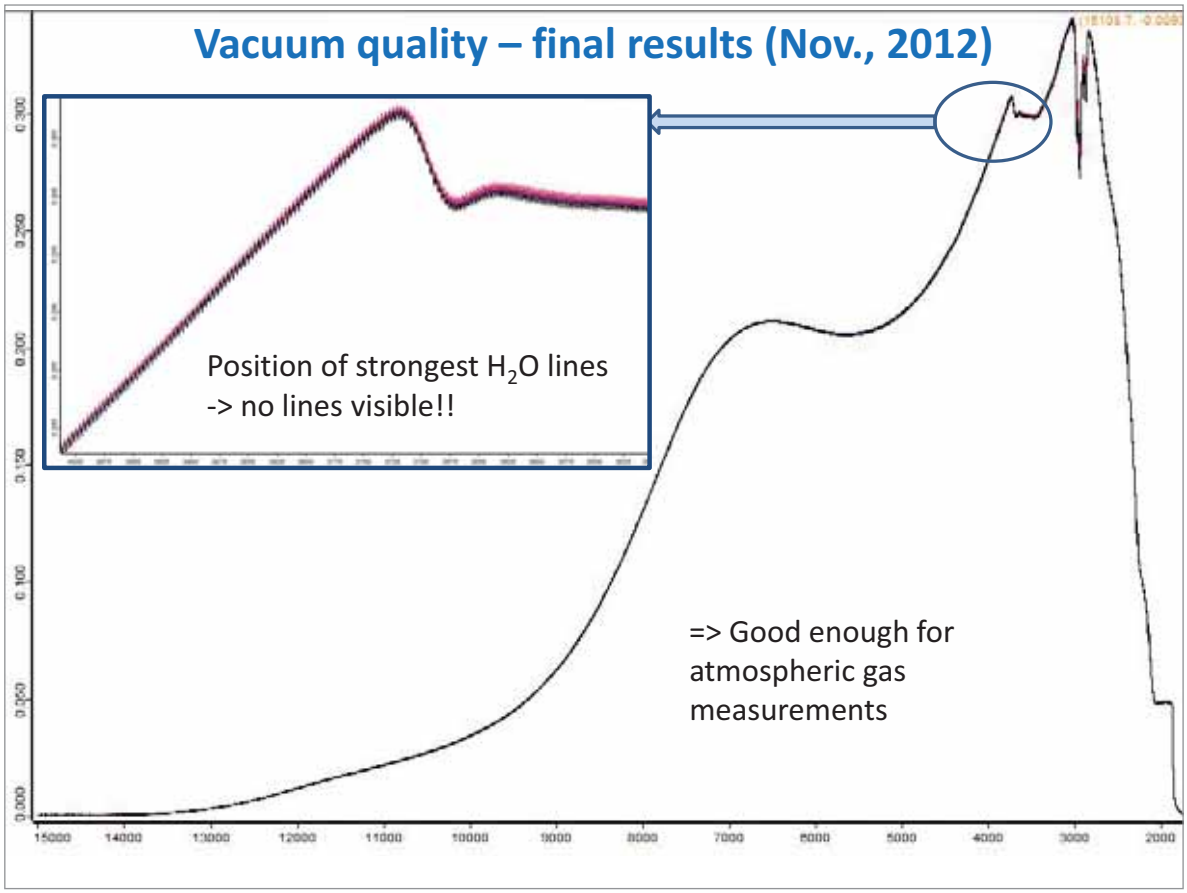
Vacuum quality – final results (Nov., 2012)
Position of strongest H_2O lines
-> no lines visible!!
=> Good enough for
atmospheric gas
measurements
15000
14000
13000
12000
11000
10000
9000
8000
7000
6000
5000
4000
3000
2000

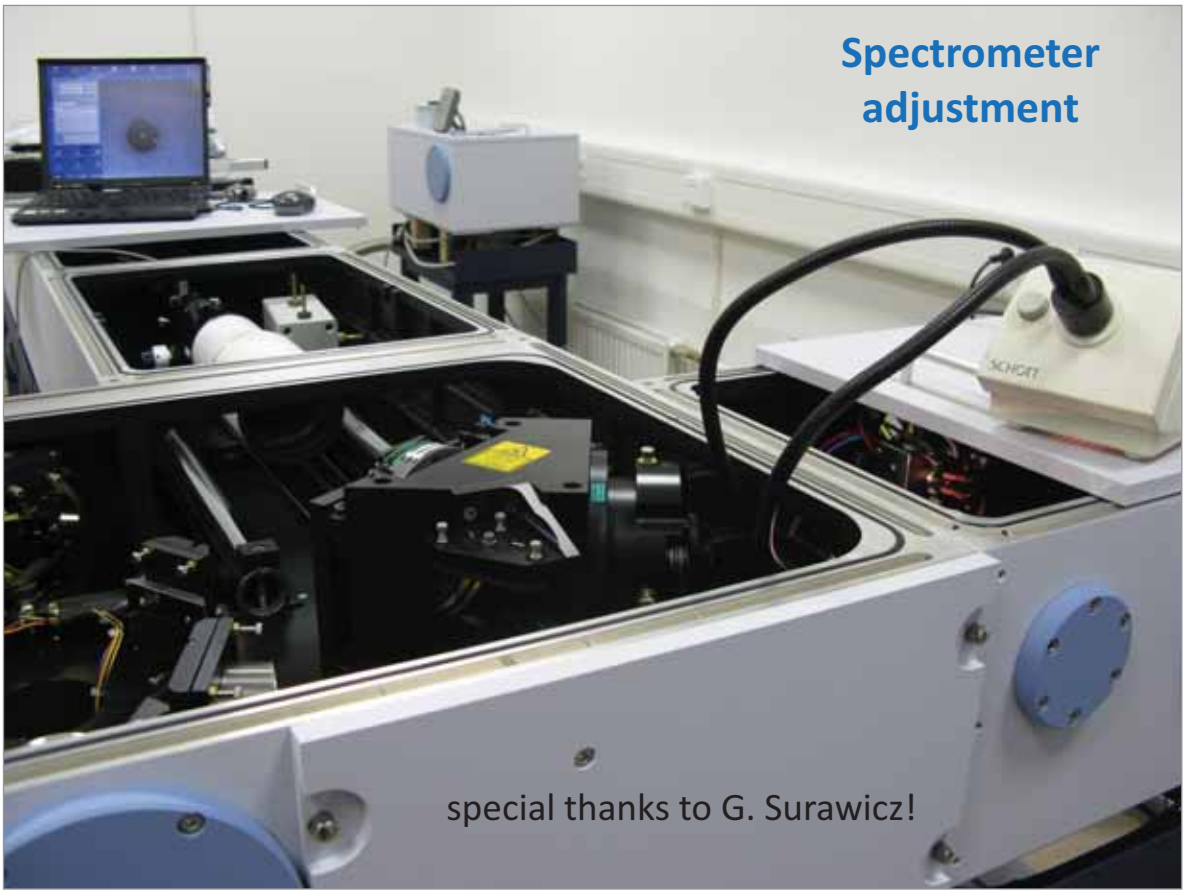

Accurate spectrometer adjustment

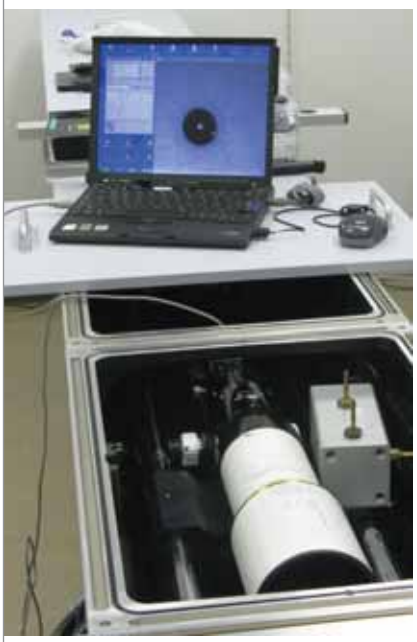

Optical abberations deteriorate the instrumental resolution & line shape

=> Optical fine-tuning together with Bruker

1. Further minimization of astigmatism
   - careful re-alignment of the optical components
   - improved symmetry of spectral lines
2. Better collimation of the beam in the interferometer compartment

Resolution test

CO_2 lines, 20 cm gas cell, 1.8 mbar pressure, aperture 1.5 mm, maximum resolution: 0.0015 cm^{-1}

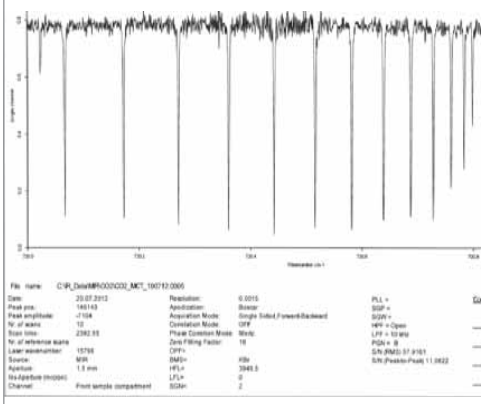

Wellenzahl	Absolute	Intensität	Relative Intensität	Breite	Gefunden,
720.06640	0.954		0.865	0.00155	68.484467
720.17227	0.988		0.909	0.00167	71.361847
720.27024	1.095		1.025	0.00154	80.740761
720.36016	1.214		1.148	0.00152	89.968269
720.44212	1.327		1.258	0.00131	99.511696
720.51581	1.156		1.078	0.00164	85.178139
720.58129	1.193		1.109	0.00159	87.375008
720.63828	1.014		0.923	0.00187	73.148102
720.68713	0.963		0.871	0.00182	68.945831
720.72750	1.013		0.921	0.00151	73.015411
720.75934	0.676		0.580	0.00186	45.909748
720.78277	0.559		0.462	0.00183	36.571781
720.79768	0.366		0.266	0.00190	21.092960

- Measured FWHM line widths are 0.0016 cm^{-1} (48 MHz)
  - Smaller than the requested FT resolution: 0.002 cm^{-1} (60 MHz)
  - Close to the true value of 0.0014 cm^{-1}
  - Conclusion: Instrumental line broadening (ILS) well below 0.002 cm^{-1}

=> Resolution $\Delta\nu/\nu = 2 \cdot 10^{-6}$ => test passed

TCCON performance tests (see also: Frank Hase, linefit)

TCCON is a network of ground-based Fourier Transform Spectrometers recording direct solar spectra in the near-infrared spectral region. From these spectra, accurate and precise column-averaged abundance of CO_2, CH_4, N_2O, HF, CO, H_2O, and HDO are retrieved.

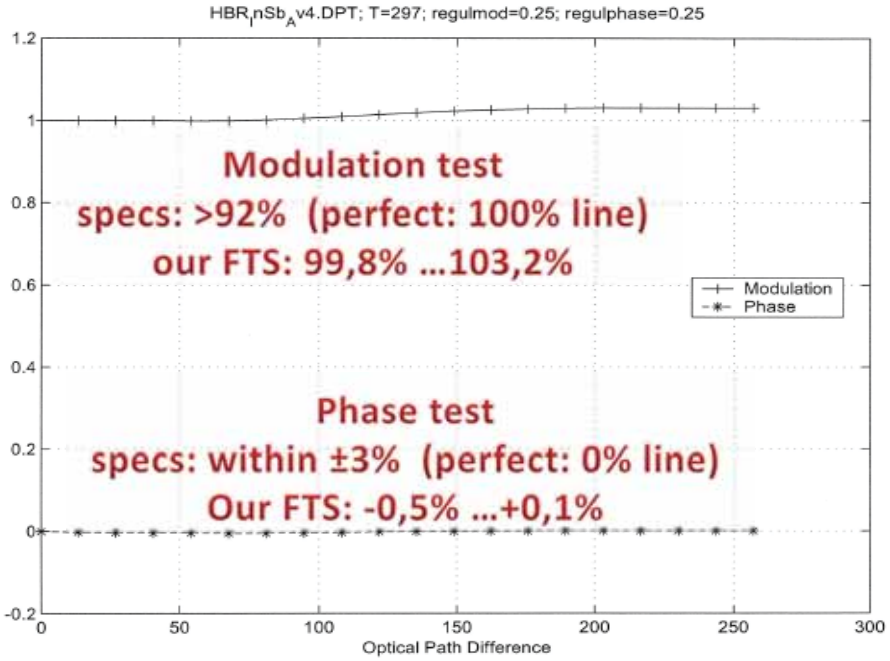

Spectrometric Infrastructure

20 cm single-pass gas cell

Stainless steel cylinder with sapphire-windows, 3 connection ports compatible to ISO KF 16

Spectrometric Infrastructure

3.2-40 m multi-pass gas cell

- **Modification of the commercial multipass-cell:**
  - 3.2-40 m optical path length
  - max. 1050 hPa
  - Glass cylinder with KBr-windows and gold-coated mirrors
  - Sealed adapter for the IFS 125HR with transfer optics
  - 3 connection ports (1x ISO KF 16, 2x Swagelok 6 mm)
  - In progress:
    - Incorporation of pressure and temperature sensors
    - Temperature stabilization

Spectrometric Infrastructure

Sensors and other Components

- **Pressure** sensor**:**
  - Paroscientific 6000-23A (0 hPa to 1585 hPa; uncertainty <0,01% of full scale)
    - ➢ ***Calibration by MIKES***
- **Temperature** sensor**:**
  - PT100-thermocouples (DIN EN 60751:2009-05; 100 K to 1100 K)
    - ➢ ***Calibration by LNE***
- **Optical path length** of the cells:
    - ➢ **Calibration by DFM**
- **Cooling** liquid cryostat:
  - Julabo FPW90-SL **(180 K to 370 K)**
- **Vacuum system** for absorption cells:
  - Turbo pumping station Pfeiffer HiCube Classic 80 MVP 070 (vacuum <1E-7 hPa)
    - ➢ handling of non corrosive gases
  - Diaphragm pump Vacuubrand MD 12C Vario-B (vacuum 2 hPa)
    - ➢ handling of corrosive gases

Central Spectroscopic Facility (CF)

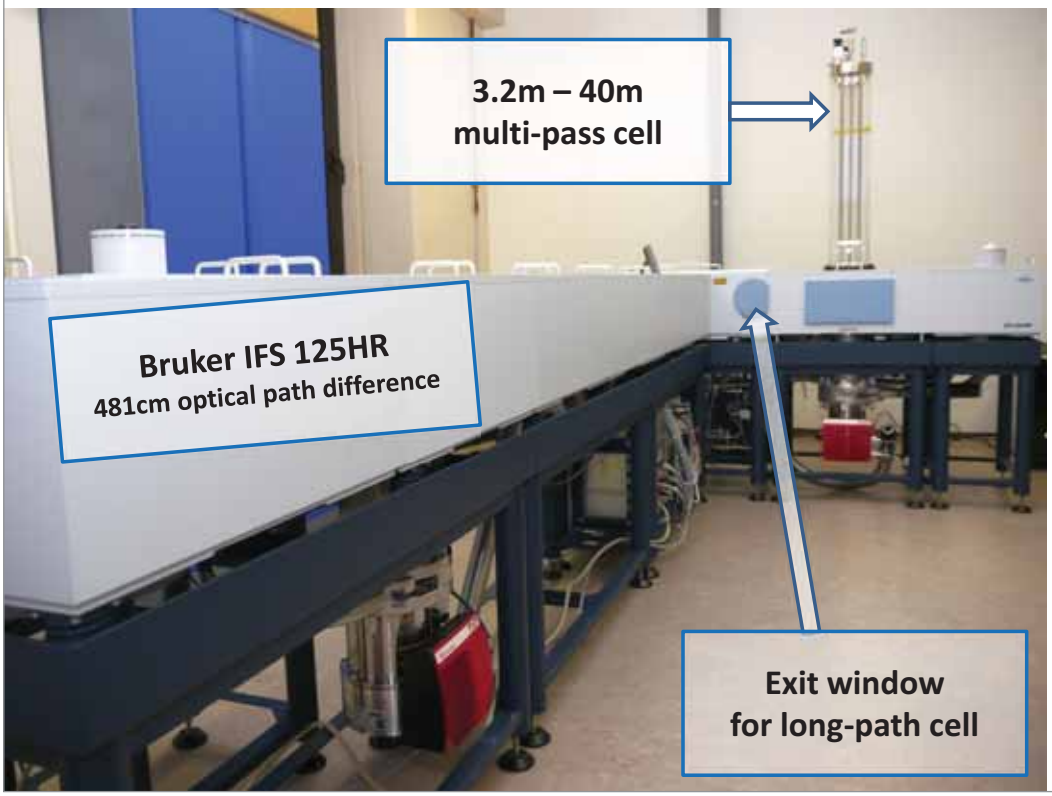

Thank you for your attention

ENV06-PTB-Team

	Volker Ebert	
Jens Brunzendorf	Oliver Ott	Anne Rausch
Anton Serdykov	Olav Werhahn	Viktor Werwein

You are kindly invited to a lab tour tomorrow 11:45

"EUMETRISPEC Work Package 3: Procedures for generating traceable spectral absorption data, to support atmospheric monitoring"

Jan C. Petersen

Danish Fundamental Metrology (DFM)

WP 3: Procedures for generating traceable spectral absorption data, to support atmospheric monitoring

JRP ENV06 EUMETRISPEC
Spectral Reference Data for Atmospheric Monitoring

Stakeholder Workshop, PTB, 2012-11-15/16

Spectral Reference Data for Environmental Monitoring (FP7/EURAMET)

Outline

- ✓ Goals of WP3
- ✓ Aim of WP3
- ✓ WP3 Tasks: 3.1 – 3.5
- ✓ Overview of

Goal of WP3: Develop measurement procedures and data analysis protocols to support the collection of traceable high quality reference spectral data, and their related uncertainties.

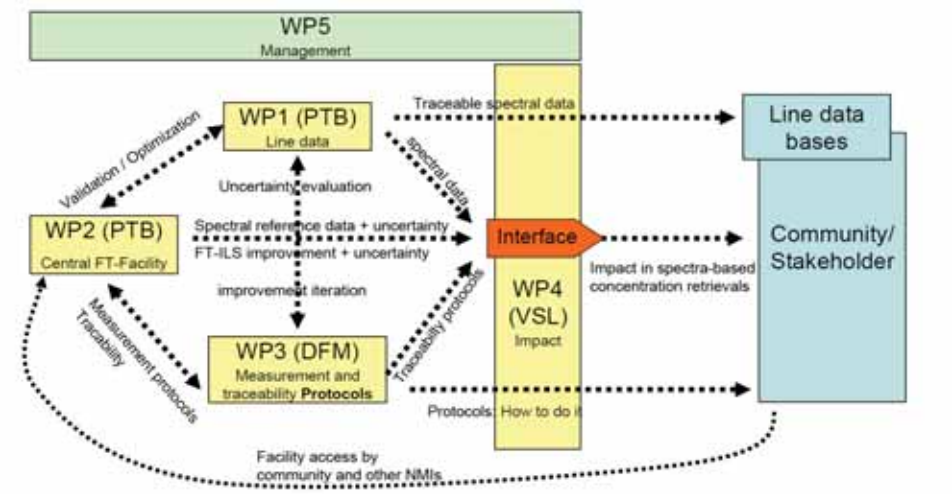

Aims of WP3:

I. Ensure that researchers (from this JRP-Consortium and beyond) generate high quality data with accurately established uncertainties.

II. To improve the quality of data on spectroscopic databases.

III. To ensure data from many sources can be analysed in a uniform and compatible way.

WP3 Tasks

Task 3.1: Procedure 3: An overview of requirements when establishing molecular line reference data for atmospheric monitoring.

- The procedure will describing the general boundary conditions and measurement data required to generate traceable molecular line reference data.
- Guidance about generating spectral absorption data, gathering related environmental data (required to establish the uncertainty budget)
- Provide an overview of the equations and models that can be used for data correction, data processing, and data retrieval.

WP3 Tasks

Task 3.2: Procedures for collecting spectral absorption data from the CF and molecular line reference data from the SFs

- Agree on and document common procedures for collection of spectral absorption data by the JRP-Partners.
- The procedures agreed on will be used by all JRP-Participants during the project.
- The procedures will form the basis of Good Practice Guides that will be made available to the stakeholder community (particularly organisations using the CF).

Suggested Good Practice Guides aimed at stakeholders:

"How to retrieve molecular line reference data from experimental (raw) FTS datasets"

"Ensuring comparability of spectral data using FTS and HRLS spectrometric techniques"

WP3 Tasks

Task 3.3: Good Practice Guide 3: "Assessing uncertainty budgets for spectral absorption measurements and molecular line reference data".

- Provide a common procedure for estimating, combining and reporting uncertainties of spectral absorption data, in full agreement with GUM.
- The procedure will be documented in a Good Practice Guide, and associated spreadsheet template.
- Two reports will describe the influence of various parameters on spectral data quality from the SF and CF respectively.

All parameters having an influence on the uncertainty of the spectral reference data will be assessed (from SF and CF)

the overall measurement uncertainties will be estimated from actual measurements.

WP3 Tasks

At least data related to the following parameters will be generated in order to determine how much these parameters affect the uncertainty of the spectral absorption data: pressure broadening coefficient, line shape, path length, uncertainty due to using coherent/ incoherent light sources, line position, base line variation, FT transmission nonlinearity, gas temperature, gas pressure, line strength and gas contamination.

A report on how to make traceable measurements of the parameters and how the parameter influences the spectral data quality will be made.

Reports that will be generated:

"The effect of various influence parameters on spectral absorption data quality for the SF".

"The effect of various influence parameters ……. for the CF"

"Assessing uncertainty budgets for spectral absorption measurements and molecular line reference data".

Spreadsheet for uncertainty incl. instructions :

Spreadsheets for: line-fitting and uncertainty budget calculations
Including Instructions and Documentation.

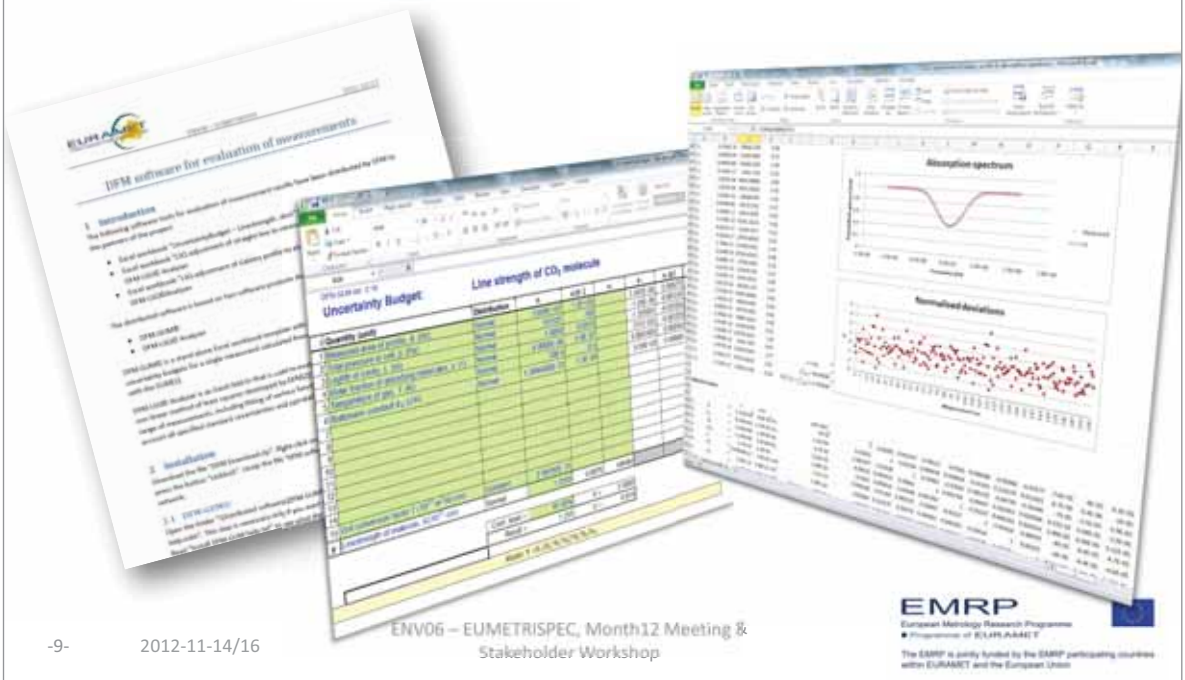

WP3 Tasks

Task 3.4: Development of Intercomparison protocols

- Provide intercomparison protocols for comparing measurements of molecular reference data from CF and SF for a few selected molecular species.
- The protocols will describe the measurement method, analysis of results, data formats, and calculation of uncertainty budget.
- All participants of the intercomparisons are expected to follow the protocols.
  - *Two types of intercomparisons are planned: molecular line data and mole fraction. (Both based on circulated gas samples prepared using standard techniques).*
  - *Each satellite facility will participate in at least one intercomparison.*
  - *The comparisons will at least include CO2, CH4, N2O and HBr (or HCl).*
  - *The intercomparison results will be used to validate JRP-Partner capabilities, to optimise procedures being developed, and to generate traceable molecular line reference data and uncertainties.*

WP3 Tasks

Task 3.5: Intercomparisons

- Two round robin intercomparisons of all JRP-Partners' measurement capabilities will be realised in orderr to validate all JRP-Partners' capabilities, and identify possible improvements.
- The mole-fraction intercomparison also seeks to demonstrate the added value of traceable molecular reference line data.

Important outcome of WP3:

a) Procedures for collecting traceable spectral absorption data (Draft finished)

b) Three Inter-comparison protocols (Finished)

c) Three Good Practice Guides

d) Iterations with the WP1 and WP2 to ensure robustness and practicality.

e) Uncertainty budget spread-sheet according to GUM

Tasks and deliverables

Present time

deliverable	Task description	lead
3.1.1	Draft overview procedure 3	DFM
3.1.2	Procedure 3 "An overview ...for atmospheric monitoring"	DFM
3.2.1	Draft procedures 4/5/6: CDRS / TDLRS / DFS to generate data	DFM
3.2.2	Draft procedure 7: Using CF to generate traceable data	PTB
3.2.3	Good Practice Guide: calculate data from experimental FTS data	PTB
3.2.4	Good Practice Guide: Ensuring comparability of FTS and HRLS data	PTB
3.2.5	4 updated procedures 4/5/6/7	PTB
3.3.1	Report: influences on spectral absorption data quality (for SF)	DFM
3.3.2	Report: influences on spectral absorption data quality (for CF)	DFM
3.3.3	Uncertainty budget template(s)/ spreadsheet	DFM
3.3.4	Draft GRP: Assessing uncertainty budgets for JRP partners	DFM
3.3.5	GPG: Assessing uncertainty budgets for spectroscopic meas	DFM
3.4.1	Intercomparison 1: protocol	DFM
3.4.2	Intercomparison 2: protocol	DFM
3.4.3	Intercomparison 3: protocol	VSL
3.5.1	Report:intercomparison 2 of molecular lines	SMU
3.5.2	Report: intercomparison 3 of measured mole-fraction	VSL

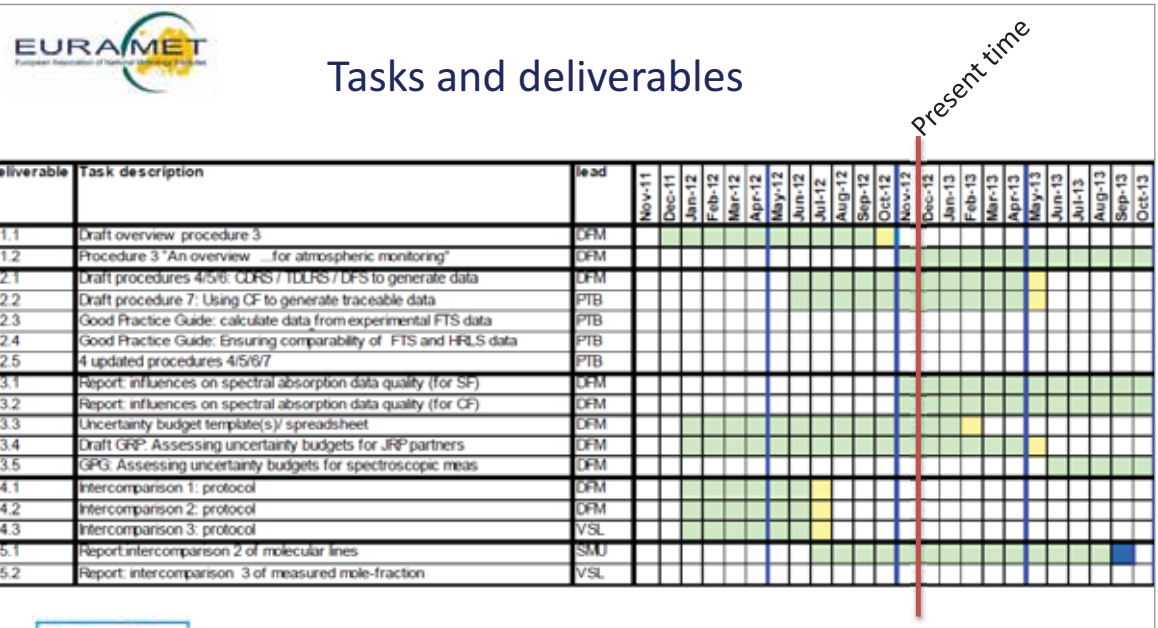

-13- 2012-11-14/16 ENV06 – EUMETRISPEC, Month12 Meeting & Stakeholder Workshop

Thank you for your attention!

Spectral Reference Data for Environmental Monitoring (FP7/EURAMET)

-14- 2012-11-14/16 ENV06 – EUMETRISPEC, Month12 Meeting & Stakeholder Workshop

PART 2: POSTERS

CONTENTS: PART B - POSTER SESSION

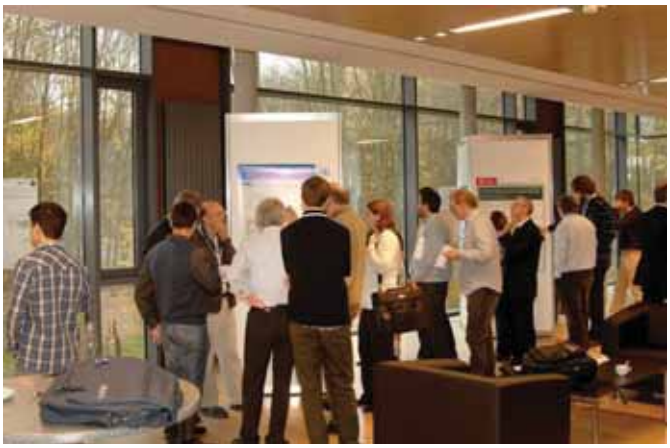

T. Forsting, I. Vespoli, C. Maul ***"Teaching an old dog new tricks: Quantum state selective detection of molecular chlorine by high-resolution cavity ring-down spectroscopy"***	**Poster 10**
J. Hald, L. Nielsen, J. C. Petersen **"*Towards Accurate Determination of Molecular Line Strength - Exemplified by Acetylene*"**	**Poster 11**
G. Leggett, T. Gardiner, R. Robinson **"*The Identification and Quantification of Greenhouse Gas Point Source Emissions Using Cavity Ring-Down Spectroscopy, Complementary to Other Techniques*"**	**Poster 12**
A. Nikitin, L. Brown, K. Sung, M. A Smith, A. Mantz, X. Thomas, L. Regalia, L. Daumont, R. Kochanov, M. Rey, V.G Tyuterev **"*New measurements and analyses of line positions and intensities of CH_3D in the infrared*"**	**Poster 13**
J. Nwaboh, A. Pogány, O. Werhahn, V. Ebert ***"Line strengths and collisional broadening coefficients of CO_2 (@2 µm) and H_2O (@2.7 µm), traceability and uncertainty assessment"***	**Poster 14**
A. Pogany, J. Nwaboh, O. Werhahn, V. Ebert **"*Towards traceability in CO2 line strength measurements at 2.7 µm using tunable diode laser absorption spectroscopy*"**	**Poster 15**
K. Schäfer, R. Harig, T. Blumenstock, N. Höfert, K. Weber **"*Development of a VDI guideline for passive FTIR measurements in the atmosphere*"**	**Poster 16**
E. Starikova, V. Tyuterev , A. Barbe , M.-R. De Backer, X. Thomas, S. A. Taskhun ***"Analysis of the FTS spectrum of $^{16}O_3$ in the range 3300 cm^{-1}: First example of new theoretical modelling for polyad of strongly coupled (220)/(121)/(022) states"***	**Poster 17**
M. Vainio, J. Peltola, M. Merimaa **"*Absolute-frequency measurements of CH_4 and N_2O line centers in the mid-infrared*"**	**Poster 18**
J. Vander Auwera, M. Herman, B. Amyay, K. Didriche, T. Foldes, D. Golebiowski, M. Tudorie, A. Fayt **"*Infrared line parameters for constituents of planetary and stellar atmospheres*"**	**Poster 19**
S. Wagner, P. Ortwein, V. Ebert **"*Spectroscopic Line Data for High Temperature Process Diagnostics in Complex Chemical Matrixes*"**	**Poster 20**
S. Welzel, J. Röpcke, R. Engeln **„ *Mid-IR Chemical Sensing Applied to Reactive Non-Equilibrium Environments*"**	**Poster 21**

High-Resolution IR Spectroscopy of $^{13}CH_4$: The Pentad and the Octad

[a]Sieghard Albert, [a,b]Sigurd Bauerecker, [c]Vincent Boudon, [c]Jean-Paul Champion, [a]Hans-Martin Niederer, [a]Martin Quack

[a]ETH Zürich, Wolfgang-Pauli-Strasse 10, CH-8093 Zürich, Switzerland
[b]TU Braunschweig, Hans-Sommer-Strasse 10, D-38106 Braunschweig, Germany
[c]Laboratoire Interdisciplinaire Carnot de Bourgogne, UMR 6303 CNRS-Université de Bourgogne 9 Avenue Alain Savary, BP 47 870, F-21078 DIJON Cedex, FRANCE

Besides many applications ranging from astrophysics to atmospheric pollution and combustion engines methane is also of fundamental importance for understanding molecular quantum dynamics, potential hypersurfaces and fundamental symmetries including parity violation [1,2]. In this context spectroscopic studies of methane are important. We have carried out new high resolution measurements of infrared spectra of methane and its isotopomers $^{12}CH_4$ [3], $^{13}CH_4$ [4,5], $^{12}CH_3D$ [6], $^{12}CH_2D_2$ [7], $^{12}CHD_3$ [6] and $^{12}CD_4$ [8]. The spectra have been taken in the range 900-12000 cm^{-1} at low temperature (80K) and at room temperature (293K) using the Zürich prototype Bruker 125 spectrometer (ZP 2001) in combination with a low temperature cooling cell [9]. Low temperature, giving rise to reduced Doppler widths (by a factor of 1.9) and very high resolution (0.0027 cm^{-1} for spectra in the region around 3000 cm^1), made it possible to determine line positions very accurately, *i.e.* for $^{13}CH_4$ better than 10^{-4} cm^{-1} around 3000 cm^{-1}. We have studied $^{13}CH_4$ spectra in its pentad region [4,5] (2250-3250 cm^{-1}). Now we are analyzing the octad region (3800-4750 cm^{-1}), recently analyzed for the isotopomer $^{12}CH_4$ [3]. An initial analysis of this region counting 8 levels is presented in [5,10] and compared to the work on $^{12}CH_4$ [3]. The complex interacting system is analyzed using an effective Hamiltonian theory described in [11]. A closely similar version of the present work has been presented in ref. [12] previously.

[1] R. Marquardt and M. Quack, *J. Chem. Phys*., **1998**, *109*, 10628; R. Marquardt and M. Quack, *J. Phys. Chem. A.*, **2004**, *108*, 3166.

[2] M. Quack, Angew. Chem. Int. Ed. Engl., **1989**, *28*, 571 – 586 and: M. Quack, *Fundamental Symmetries and Symmetry Violations from High Resolution Spectroscopy*, in *Handbook of High Resolution Spectroscopy*, Vol. 1, pp. 659 – 722, M. Quack and F. Merkt (eds.), Wiley, **2011**.

High-Resolution IR Spectroscopy of $^{13}CH_4$: The Pentad and the Octad

S. Albert, H. M. Niederer, M. Quack
V. Boudon, J. P. Champion
S. Bauerecker

ETH Eidgenössische Technische Hochschule Zürich Swiss Federal Institute of Technology Zurich

UNIVERSITÉ DE BOURGOGNE

TECHNISCHE UNIVERSITÄT CAROLO-WILHELMINA ZU BRAUNSCHWEIG

Introduction

There has been renewed interest in the spectroscopy of methane because of new developments in high resolution spectroscopy. We may mention as examples the studies of intramolecular vibrational redistribution [1,2] or recent work on constructing accurate potential hypersurfaces using the methane molecule as an important prototype [3-5]. We have taken new high resolution infrared spectra of methane and its isotopomers $^{12}CH_3D$, $^{12}CH_2D_2$, $^{12}CHD_4$, $^{13}CH_4$ and $^{12}CD_4$ in the range 900-12000 cm^{-1} at low temperature (80 K) and at room temperature using the Zürich prototype Bruker 125 spectrometer (ZP 2001) in combination with a low temperature cooling cell [6]. Low temperature, giving rise to a reduced Doppler full width at half maximum (factor of 1.91) and very high resolution (0.0027 cm^{-1} for spectra in the region around 3000 cm^{-1}), made it possible to determine line positions better than 10^{-4} cm^{-1}. We have studied $^{13}CH_4$ spectra in its pentad region [7,8] (2250-3250 cm^{-1}). Now we are climbing up the polyad ladder into the octad region counting 8 levels (3800-4750 cm^{-1}) [8,9]. The octad was recently analyzed for the isotopomer $^{12}CH_4$ [10]. The complex interacting system is analyzed using the effective Hamiltonian approach elaborated in Dijon [11,12], implemented in the XTDS program package [13] and freely available at http://icb.u-bourgogne.fr/omr/SMA/SHTDS/XTDS.html .

Polyad Scheme for $^{13}CH_4$

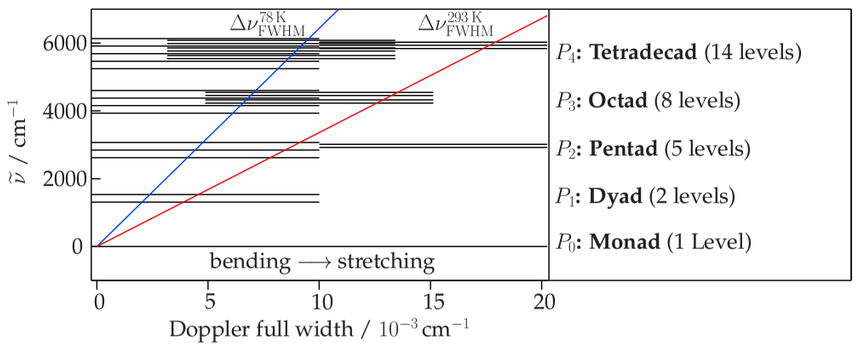

Figure 1: *The vibrational levels on the left are positioned according to their stretching and bending character. Straight line diagonals denote the Doppler full widths at half maximum of transitions in the 0-6500 cm^{-1} region at 78 K and 293 K, respectively. On the right the polyad nomenclature.*

Survey of the Experimental Studies

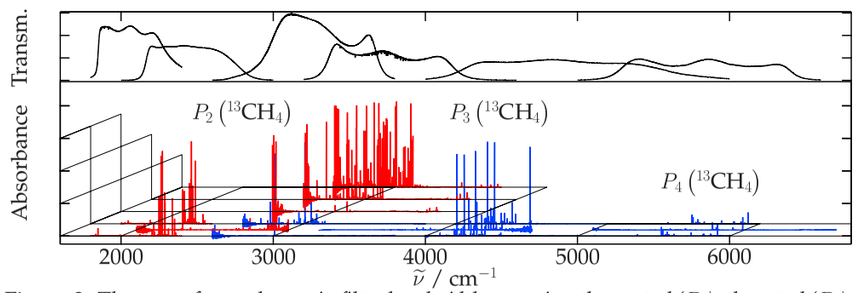

Figure 2: *The upper frame shows six filter bandwidths covering the pentad (P_2), the octad (P_3) and the tetradecad (P_4) region of $^{13}CH_4$. In the lower frame a selection of the recorded spectra is shown. Red and blue lines correspond to spectra recorded at room temperature and 78 K, respectively.*

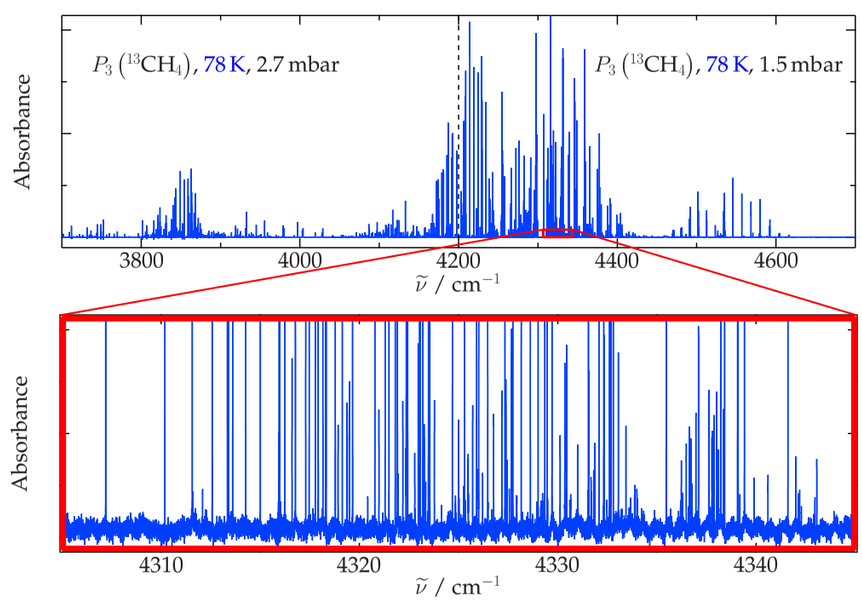

Figure 3: *Complex spectra can be simplified by cooling the sample gas. Hot bands appear attenuated and complex polyad patterns can be more easily analyzed. The widths of the rotation-vibration bands decrease approximately proportionally with temperature, cf. Figure 2. In addition, the Doppler width of a single spectral line narrows with the square root of the temperature, cf. Figure 5.*

Experimental Setup

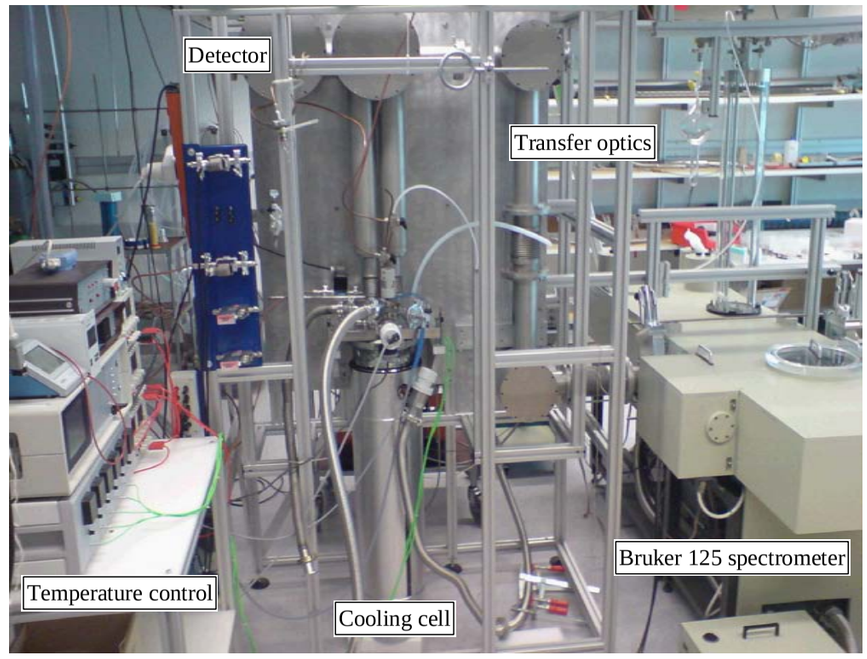

Figure 4: *Collisional cooling system combined with the Zürich Prototype Bruker IFS 125 HR (ZP 2001) interferometric Fourier transform infrared (FTIR) spectrometer. The setup allows experiments covering many extraterrestrial basic conditions. E.g. experiments at similar conditions as they are observed in the methane containing atmosphere of Saturn's largest moon Titan [14]. The cell is connected via an evacuated transfer optics chamber to the external parallel port of the Bruker spectrometer. The temperature and pressure can be adjusted independently between 4 and 400 K and between 0.01 and 3000 mbar. A multiple-pulse injection system allows the generation of molecular nanoparticles, core-shell structured particles and other nanocomposites [6].*

Experiment versus Simulation

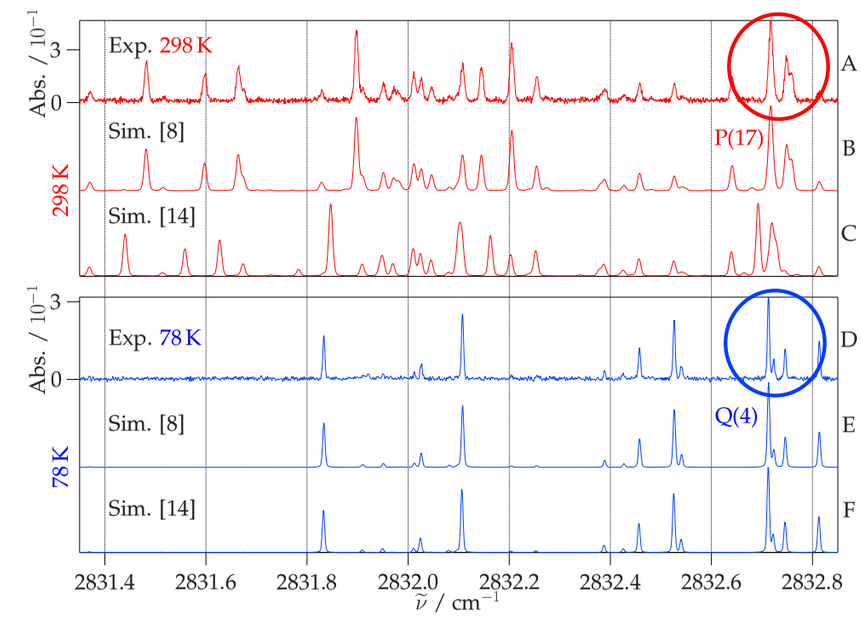

Figure 5: *Detail of two IR spectra of $^{13}CH_4$ recorded at room temperature (frame A) and at 78 K (frame D). Due to simplification and higher resolution, transitions could be distinguished and assigned with very high confidence (e.g. transitions around 2832.7 cm^{-1}). The simulations using parameters according to [15] (frames C and F) reproduce rotationally low lying levels about as well as the simulations from the present work [7,8] (frames B and E). However, rotationally highly excited states are only correctly reproduced in the new simulation (frame B).*

References

[1] M. Lewerenz and M. Quack, *J. Chem. Phys.*, **1988**, *88*, 5408.
[2] M. Quack, *Ann. Rev. Phys. Chem.*, **1990**, *41*, 839.
[3] R. Marquardt and M. Quack, *J. Phys. Chem. A*, **2004**, *108*, 3166.
[4] R. Marquardt and M. Quack, *J. Chem. Phys.*, **1998**, *109*, 10628.
[5] H. Hollenstein, R. Marquardt, M. Quack and M. A. Suhm, *J. Chem. Phys.*, **1994**, *101*.
[6] S. Albert, S. Bauerecker, M. Quack and S. Steinlin, *Mol. Phys*, **2007**, *105*, 541.
[7] H. M. Niederer, S. Albert, S. Bauerecker, V. Boudon, J. P. Champion and M. Quack, *Chimia*, **2008**, *62*, 273.
[8] H. M. Niederer, *Ph.D. Thesis*, **2011**, Eidgenössische Technische Hochschule Zürich, Diss. ETH Nr. 19829.
[9] T. Carrington, H. M. Niederer, X. G. Wang, S. Albert, S. Bauerecker, V. Boudon, and M. Quack, *J. Mol. Spectrosc.*, **2012**, (in preparation).
[10] S. Albert, S. Bauerecker, V. Boudon, L. R. Brown, J. P. Champion, M. Loëte, A. Nikitin and M. Quack, *Chem. Phys.*, **2009**, *356*, 131.
[11] J. P. Champion, M. Loëte and G. Pierre in *Spectroscopy of the Earth's Atmosphere and Interstellar Medium*, edited by K. N. Rao and A. Weber, **1992**, Academic Press, San Diego.
[12] A. Frank and P. van Isacker, *Algebraic Methods in Molecular and Nuclear Structure Physics*, **1994**, John Wiley & Sons, New York.
[13] C. Wenger, V. Boudon, M. Rotger, M. Sanzharov, and J. P. Champion, *J. Mol. Spectrosc.*, **2008**, *251*, 102.
[14] C. A. Griffith, P. Penteado, P. Rannou, R. Brown, V. Boudon, K. H. Baines, R. Clark, P. Drossart, B. Buratti, C. P. McKay, P. Nicholson, A. Coustenis, A. Negrao, R. Jaumann, *Science*, **2006**, *313*, 1620.
[15] J. M. Jouvard, B. Lavorel, J. P. Champion and L. R. Brown, *J. Mol. Spectrosc.*, **1991**, *150*, 201.

Acknowledgements: Sincere thanks are given to the Université de Bourgogne for co-financing study visits. Our work is supported financially by ETH Zürich and the Swiss National Science Foundation.

IMPLEMENTATION OF S&MPO OZONE INFORMATION SYSTEM FOR THE VIRTUAL ATOMIC AND MOLECULAR DATA CENTER (VAMDC)

Yurii L. Babikov[1], Semen N. Mikhailenko[1], Alain Barbe[2] and Vladimir G. Tyuterev[2]

[1] Institute of Atmospheric Optics, SB RAS, 634055 TOMSK, Russia
[2] Groupe de Spectrométrie Moléculaire Atmosphérique, UMR 6089,
Université de Reims Champagne Ardenne, Moulin de la Housse,
BP 1039 - 51687 REIMS Cedex 2 France

IMPLEMENTATION OF S&MPO OZONE INFORMATION SYSTEM FOR THE VIRTUAL ATOMIC AND MOLECULAR DATA CENTER (VAMDC)

Yurii L. Babikov*, Semen N. Mikhailenko*, Alain Barbe[#] and Vladimir G. Tyuterev[#],,

[#]Groupe de Spectrométrie Moléculaire Atmosphérique, UMR 6089, Université de Reims Champagne Ardenne, Moulin de la Housse, BP 1039 - 51687 REIMS Cedex 2 France

** Institute of Atmospheric Optics, SB RAS, 634055 TOMSK, Russia*

The S&MPO information system has been developed with **contributions of**

Contributors	*(main involvement)*
J.M.Flaud	analysis and predictions for 005/311 band system
A.Campargue	experimental CRDS spectra
S.Kassi	experimental CRDS spectra
D.Mondelain	experimental CRDS spectra
C.Janssen	experimental intensity data
J.Malicet	experimental UV data
D.Daumont	experimental UV data
M.R. De Backer	absolute intensity measurements, spectra analysis, Dobson spectrometry
E.Starikova	isotopic spectra analysis
J.J.Plateaux	code for primary data reduction (MULTIFIT) and server administration
S.A.Tashkun	code for spectra calculation (GIP), optimization of codes for global calculations
X.Thomas	instrumental and software support of FTS and spectra recording
P.Von Der Heyden	instrumental support of FTS, optical and mechanical systems, ozone generation
L.Regalia	primary data reduction and Multifit code
T.Cours	wavefunction plots from global models
R.Gamache	line width and partition function calculations

What is S&MPO ?

S&MPO is the abbreviation of
"**Spectroscopy and Molecular Properties of Ozone**".

➢**S&MPO** is an **interactive** graphical information system accessible via Internet.
➢**S&MPO** contains Information, Data and a Software written in PHP JavaScript, C++.
➢**S&MPO** can be **accessible** from any computer and a graphical display should be independent on an operation system
➢**S&MPO** is essentially based on **experimental and theoretical** joint research of two laboratories GSMA (Reims, France) and LTS (Tomsk, Russia), complemented with results of larger collaborations (LSP, Grenoble) and with information available in spectroscopic literature.

How is S&MPO distinguished from existing spectroscopic databases like HITRAN, GEISA, TDS etc…

S&MPO is concerned with the **ozone molecule** and its **isotopomers** which is the only one known for the complexity of its spectra and electronic structure as well as for its particularly important role in advanced fundamental and applied research in Molecular Physics and Quantum Chemistry. Most of other spectroscopic databases are dealing with all types of molecules involved specifically in atmospheric applications.

Molecular Properties

Compared to other spectroscopic databases S&MPO is enhanced with information on molecular properties. It includes 3D and contour plots for accurate potential energy surface in the electronic ground state and for full vibrational wavefunctions with a coordinate choice on user's request, global **predictions of vibrational levels** for its isotopic species, **dipole moment surfaces**, centrifugal distortion, transition moments parameters, references etc.

Modeling versus Compilation + Experimental spectra

S&MPO contains Fundamental Spectroscopic Data (Energies - Transition Moments - Spectroscopic Constants) recovered from Comprehensive Modeling and Simultaneous Fitting of experimental spectra. Particular attention is paid to Interpretation, Validation, Precision Estimation to allow reliable extrapolations of Laboratory Measurements. Ro-vibrational energy levels and mixing coefficients for each resonance group, simulated spectra together with band statistics, accuracy estimations are provided on user's request.

Interactive access via Internet

S&MPO has more extended and flexible operation-system-independent interface which should allow a real-time treatment of user requests in graphical or numerical forms.

A current European project "Virtual Atomic and Molecular Data Center" (VAMDC) [1] aims to build a documented, exible and interoperable environment-based interface to the existing data in the eld. This is covering the development and deployment of the infrastructure and the development of interfaces to the existing atomic and molecular databases as well as providing a forum for training potential users and dissemination of expertise across the research communities in atmospheric and planetary applications, astrophysics, plasma, laser and chemical physics. In this presentation the internet accessible information system "Spectroscopy and Molecular Properties of Ozone" (SMPO) system [2], developped jointly by the University of Reims and the Institute of Atmpospheric Optics of Tomsk, as well as the implementation of interactive access to this system via VAMDC services currently in progress (WP4/WP5) are overwieved. The SMPO contains various types of data for ozone isotopologues, including Hamiltonian and dipole moment parameters, transitions probabilities, rovibrational energy leves as well as other information on molecular properties. The web information system provides to the user interactive tools for data selection, comparison, spectra simulation a complete list of references, including ab initio calculations and analyses of high-resolution spectra [3, 4, 5]
The support of VAMDC EC project is acknowledged.

Relation with

VIRTUAL ATOMIC AND MOLECULAR DATA CENTER (VAMDC)

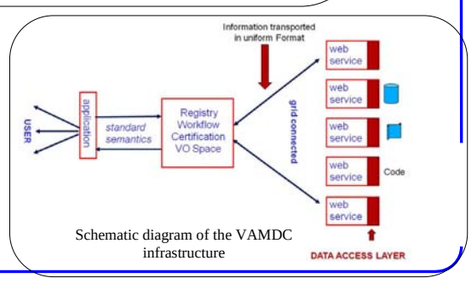

Schematic diagram of the VAMDC infrastructure

GLOBAL

EGS Structure and Spectroscopic constants

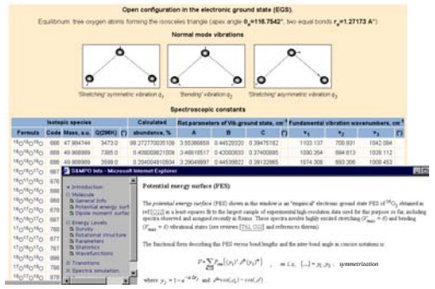

Potential energy surface (PES) versus bond lengths (angle = 116.75°)

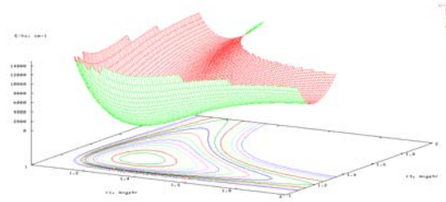

A 'bend-stretch' cut though the P.E.S. (r_3 = 1.2717 Å)

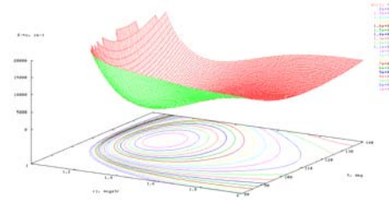

Wavefunction of A_1 vibrational state (500)

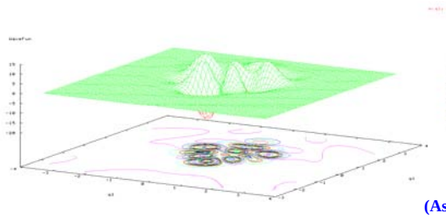

Wavefunction of B_1 vibrational state (005)

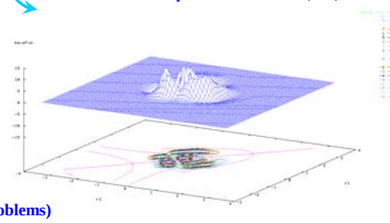

(Assignment problems)

Vibrational levels of $^{16}O_3$

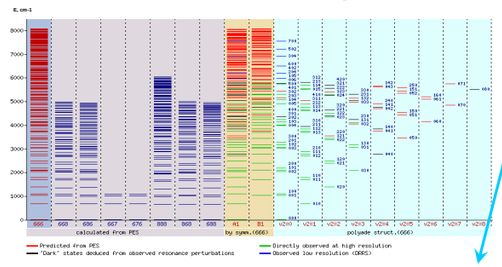

Example of accuracy achieved in global variational calculation of vibrational band centres for $^{16}O_3$

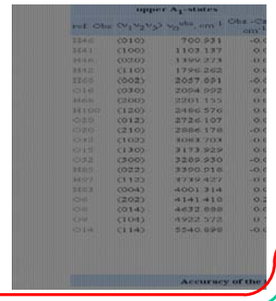

***Note** : The table includes all (000)–(v1v2v3) bands directly observed so far in high resolution spectra. Columns 2 gives conventional normal mode quantum numbers $v_1v_2v_3$ as assigned in the analyses of the experimental spectra (references are given in Column 1). Column 3 gives observed band centres ν_0 (=upper state term values). Calculations are performed with the PES of [4]*

HIGH RESOLUTION

Rotational structure of $^{16}O_3$ (nonad)

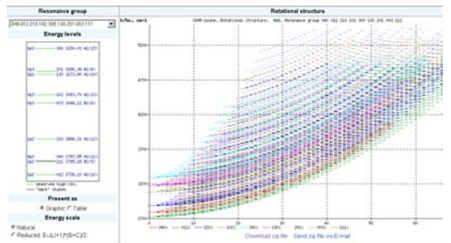

Atlas : example of $^{16}O_3$ bands included in the banks

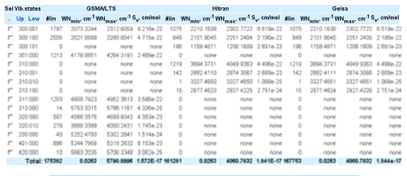

Final agreement Obs. – Calc. around 2329.5 cm^{-1}

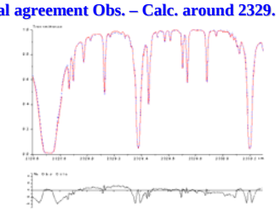

Calculated sticks spectrum of $^{16}O_3$ from GSMA / LTS

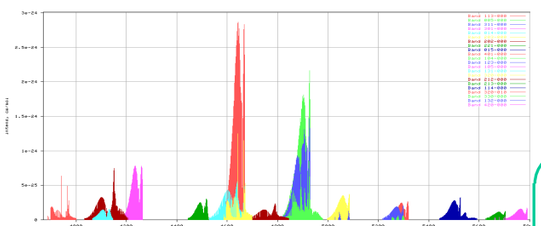

Example of experimental spectrum : general survey

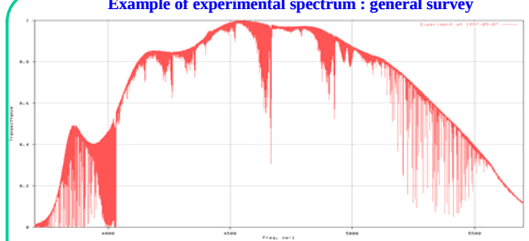

The $\nu_1+\nu_2+3\nu_3$ region : observed (a), calculated (b) transmittances and sticks (c). General survey

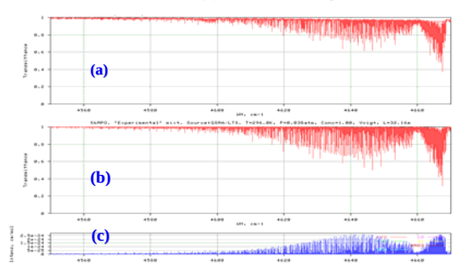

Example of statistics for line intensities of $^{16}O_3$

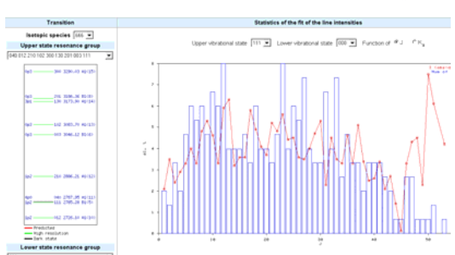

References:

S&MPO includes references on the following topics:

- ***O** Original studies of the SMPO team*
- ***H** High-resolution IR,MW spectra/analysis/data reduction*
- ***L** Low-resolution spectra/ broadening*
- ***T** Theoretical background/ ro-vibrational models*
- ***E** Electronic structure, transitions/ab initio/UV*
- ***P** Potential/Dipole/Global calculations*
- ***C** Chemistry/Dissociation/Kinetics*
- ***A** Atmospheric measurements/applications*
- ***D** Databases/information systems in spectroscopy*

Refs Poster:
1. M.L. Dubernet et al, JQSRT, 111, 2151-2159 (2010).
2. S.N. Mikhailenko, Yu.L. Babikov, Vl.G. Tyuterev, A. Barbe, Journal of Computational Technologies 7, 64-70 (2002.
3. S.N. Mikhailenko, A. Barbe, Vl.G. Tyuterev and A. Chichery Atmos. Ocean. Opt., 12(9), 771{785 (1999)
4. A. Campargue, M.-R. De Backer-Barilly, A. Barbe, Vl.G. Tyuterev and S. Kassi, Chem.Chem. Phys., 10, 2925{2946 (2008).
5. E. Starikova, A.Barbe, Vl.G. Tyuterev, M-R De Backer-Barilly, S. Kassi, A. Campargue, J. Mol. Spectrosc. , 257, 40-56 (2009).

TOWARDS SI-TRACEABLE REFERENCE LINE-BY-LINE SPECTRAL DATA USING A MODIFIED BRUKER IFS125HR SPECTROMETER

J. Brunzendorf, A. Serdyukov, O. Werhahn, V. Werwein, A. Rausch, V. Ebert

Physikalisch-Technische Bundesanstalt, Bundesallee 100, 38116 Braunschweig, Germany

Towards SI-traceable reference line-by-line spectral data using a modified Bruker IFS125HR spectrometer

J. Brunzendorf, A. Serdyukov, O. Werhahn, V. Werwein, A. Rausch, V. Ebert
Corresponding author: Jens.Brunzendorf@PTB.de Project coordinator: Volker.Ebert@PTB.de

MOTIVATION

Spectral reference line data are fundamental for spectroscopic instruments and atmospheric models

Measurements and simulations are only of limited value if the uncertainties of the results are unknown or ill defined.

Spectroscopic data reductions and numerical simulations often require spectroscopic input data which are frequently taken from the large line-by-line data bases like HITRAN and GEISA. These data bases are comprehensive compilations of the available spectroscopic data which adhere to the data quality rules set by the database managers.

The demand for a higher accuracy in data retrievals requires well defined uncertainties in the spectroscopic data. Unfortunately, uncertainty assessments are typically not standardized in the papers and are thus often not comparable, neither do they follow metrological principles of quantifying and stating the uncertainties. Finally, it is not that unusual that uncertainties are not provided at all or in an inconsistent way.

Summary:

No traceable line by line database available

OBJECTIVES

Traceability:
Traceability means that the measurement results can be traced back in an unbroken chain to the primary standards of the SI units.
This typically requires a chain of calibrated instruments that are well-characterized. The advantage is that the uncertainties of the measurements are comparably low and - more important - a full uncertainty budget can be derived, which is a prerequisite for reliable measurements.

Our objectives are:
Setup European spectroscopic infrastructure
for traceable line data measurements
* Central high-resolution FT-IR spectrometer facility (NIR to MIR, 0,002cm^{-1} resolution)
* Development of special traceable measurement cells and infrastructure
* Setup of reference gas handling facility
* Traceability of all measurands including $p, T, L, X_i, X_{isotopes}$

As the PTB runs the national primary standards for the realization and dissemination of the legal units of the SI we have direct access to all reference standards needed for accurate and traceable measurements.

Our aim: Provide accurate traceable line data for selected molecules with atmospheric relevance (H_2O, CO_2, CH_4, N_2O, ...) in the Range 0...1 bar, 180...320 K.

PROJECT: EUMETRISPEC

EUMETRISPEC: European Metrology Project
"Spectral reference data for atmospheric monitoring"
www.eumetrispec.org

Coordinator:
Physikalisch-Technische Bundesanstalt (PTB)

Funded Partners:
Conservatoire national des arts et metiers (France)
Dansk Fundamental Metrologi (Denmark)
Laboratoire national de métrologie et d'essais (France)
Mittatekniikan Keskus (Finland)
Slovenský Metrologický Ústav (Slovakia)
Dutch Metrology Institute VSL B.V. (Netherlands)

Funds:
4 M€ total eligible costs, 275 person-months, end of 2011-2014

Collaborators:
Radboud Universiteit Nijmegen (Reg host)
Rice University
National Physical Laboratory
University of Wollongong
Deutsches Zentrum für Luft- und Raumfahrt

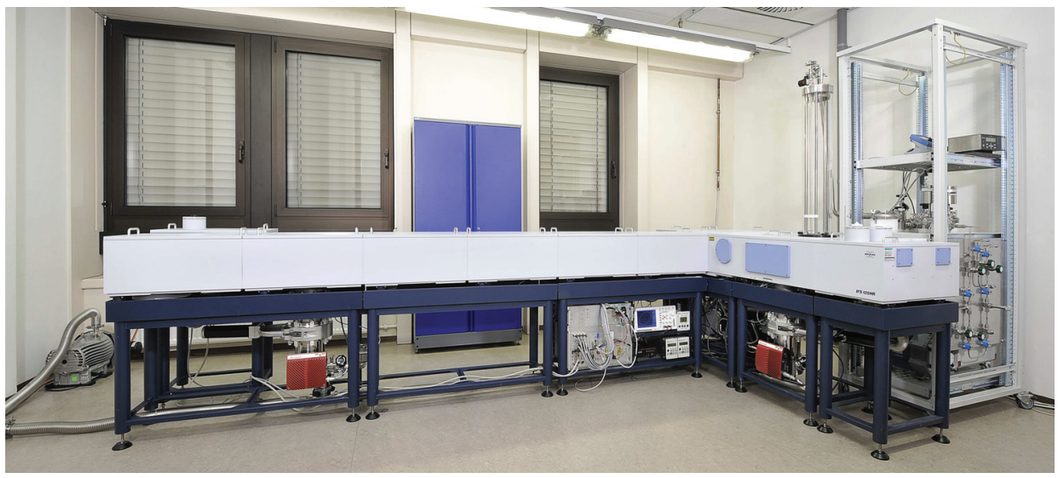

TECHNICAL DATA

Spectrometer type:	Bruker IFS125HR with 6 scanner compartments
Location:	PTB Braunschweig
Optical path difference:	up to 481 cm
Spectral range:	<1000 cm^{-1} ... >10000 cm^{-1}
Spectral resolution: (without deconvolution)	better than 0.002 cm^{-1} (measured values: 0.0013 cm^{-1} ... 0.0019 cm^{-1})
Pressure in FT:	final pressure 10^{-5} mbar leakage rate 0.1 mbar/day

FT VACUUM SYSTEM

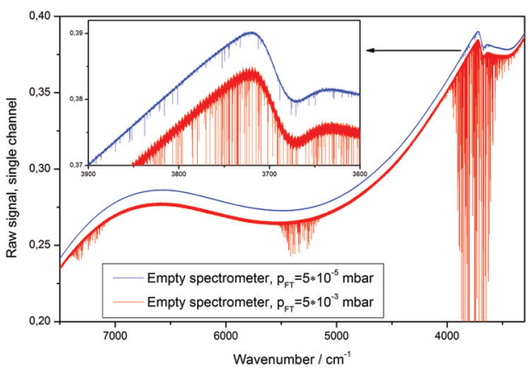

Influence of FT vacuum quality on the background signal
red: empty FT spectrum, pressure in FT: 5*10^{-3} mbar (typical FT vacuum)
blue: empty FT spectrum, pressure in FT: 5*10^{-5} mbar (our FT after one day of pumping)

The ultimate pressure in our FT is 1*10^{-5} mbar.

The good vacuum almost eliminates the disturbances of the atmospheric absorption lines of CO_2 and H_2O.

CO_2 SAMPLE SPECTRUM

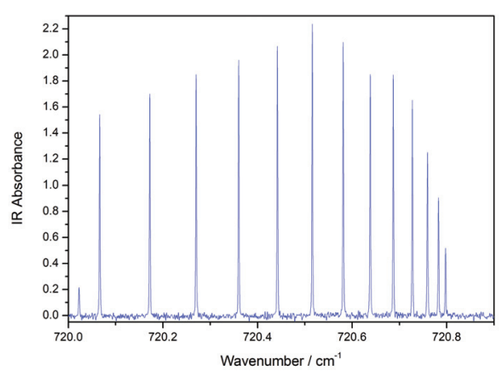

Sample spectrum of Co_2 in 20 cm gas cell, 1.8mbar
(whole spectrum covers 500 cm^{-1} ... 10000 cm^{-1})
KBr beamsplitter, MCT detector
nominal resolution: 0.002 cm^{-1}, aperture 1.7 mm
ten scans (30min measuring time)

measured linewidth (=720.638 cm^{-1}): FWHM = 0.0016 cm^{-1}
(calculated CO_2 linewidth (without ILS): FWHM = 0.0014 cm^{-1})

The experimentally determined resolution of the FT is better than the targeted value of FWHM = 0.002 cm^{-1}.

TCCON PERFORMANCE TESTS

TCCON is a network of ground-based Fourier Transform Spectrometers recording direct solar spectra in the near-infrared spectral region. From these spectra, accurate and precise column-averaged abundances of CO_2, CH_4, N_2O, HF, CO, H_2O, and HDO are retrieved.

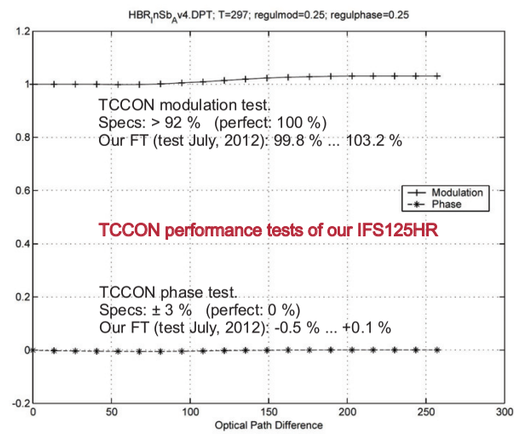

The performance of our FT spectrometer is well within the TCCON specifications, abberations are neglectable

EMRP European Metrology Research Programme Programme of EURAMET
The EMRP is jointly funded by the EMRP participating countries within EURAMET and the European Union

Towards a Traceable TLDAS Hygrometer for airborne applications

B. Buchholz[1,2], N. Böse[2], V. Ebert[1,2]*
[1] *Center of Smart Interfaces, Technische Universität Darmstadt, Germany*
[2] *Physikalisch Technische Bundesanstalt Braunschweig, Germany*
**corresponding author: volker.ebert@ptb.de*

In-situ water vapor measurements are absolutely necessary for improving our understanding of the processes in the atmosphere, because water vapor by itself is the most important greenhouse gas and is frequently used as correction value for many other gas analytical measurements principles. Over the past decades many different hygrometers types have been developed. Nevertheless, even under static conditions the deviations of the best instruments are in the ± 10 % range [1]. In extrapolation to in-flight environments with its aggravating effects like sampling artifacts, vibrations, thermal impacts etc. these deviations may increase significantly and make a precise instrument comparison and a correct interpretation of the atmospheric water vapor signatures very difficult.

From our perspective one of the biggest issue for theses deviations is the different calibration quality, especially if it is done by online calibration in the lower ppmv range during flight, or before and after flights with the expectations, that theses calibration are also valid in the different airborne conditions during flight. In order to avoid such complications it seems a logical step to develop calibration-free or self-calibrating instruments and to validate them on a metrological level via intercomparison with a primary humidity standard.

SEALDH (Selective Extractive Airborne Laser Diode Hygrometer) is a new, absolute TDLAS (Tunable Diode Laser Absorption Spectroscopy) hygrometer at wavelength of 1370 nm, which uses an advanced multi-line spectroscopic fitting process for calibration-free evaluation of the tunable diode laser absorption signal, TDLAS [2]. The compact (19 ” 4 HU) form factor is especially designed for extractive airborne applications and the internal optical white cell with its 1.5 m optical path length allows a dynamic range from about 30 to 30000 ppmv. The prototype has already been validated in a blind intercomparison campaign [3]. The time resolution of the SEAL hygrometer is directly limited by the flow through the internal absorption cell with a volume of 300 ccm. Depending on the inlet system of the aircraft, this results at a flow of 8 slm and a pressure of 200 hPa with the assumption of a bulk flow to an exchange time of 0.45 sec. The optical sample frequency can be adapted within a wide range to the particular application requirements of the flight. Typically a sampling frequency of 140 Hz is used. This results in a maximum time resolution of about 7 msec. Averaging data for 2.1 sec we achieve an excellent precision of 33 ppbv, i.e. a band width and path length normalized precision of 72 ppbv·m·$(Hz)^{-1/2}$.

The fast measurements, its excellent precision, high validated accuracy, and absolute, calibration-free multi-line evaluation in combination with the compact, robust setup allows airborne measurements in the range of the troposphere up to the lower stratosphere.

[1] D. Fahey and R. Gao, “Summary of the AquaVIT Water Vapor Intercomparison: Static Experiments,” *source: https://aquavit. icg. kfa-juelich. de/WhitePape*, no. October, 2009.

[2] V. Ebert and J. Wolfrum, “Absorption spectroscopy,” in *OPTICAL MEASUREMENTS-Techniques and Applications, ed. F. Mayinger*, Springer, 1994, pp. 273–312.

[3] B. Buchholz, B. Kühnreich, H. G. J. Smit, and V. Ebert, “Validation of an extractive, airborne, compact TDL spectrometer for atmospheric humidity sensing by blind intercomparison,” *Applied Physics B*, Sep. 2012. online first DOI 10.1007/s00340-012-5143-1

EUMETRISPECs Stakeholder Workshop 15.-16. November 2012

Towards a Traceable TLDAS Hygrometer for airborne applications

B. Buchholz[1,2], N. Böse[1] , V. Ebert[1,2]

[1]Physikalisch-Technische Bundesanstalt, Bundesallee 100, 38116 Braunschweig;
[2]CSI TU Darmstadt, Petersenstraße 32, 64287 Darmstadt;
corresponding author: volker.ebert@ptb.de

Motivation

Scientific background

- Water vapor is the key greenhouse gas
- Water vapor concentration is needed as a correction value for many other measurement principles
- Water vapor is an important tracer for atmospheric exchange processes

Sate of the art airborne influenced issues

- Data quality is difficult to quantify in flight operation, since typically calibration conditions are different
- Pre and post calibration are done for many instruments to get the best possible performance
- Waste of measurement time for in-flight calibrations

Experimental approach

- Calibration-free, long term stable **T**unable **D**iode **L**aser **A**bsorption **S**pectroscopy hygrometry to avoid any calibration problems
- Instrument validation at PTB primary H_2O standards

Setup & H_2O - Spectroscopy

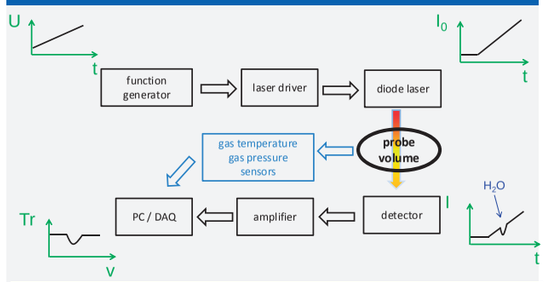

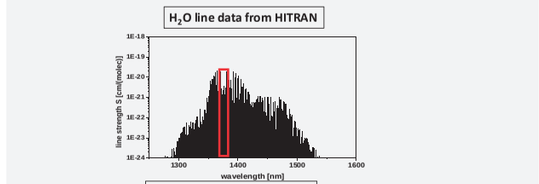

TDLAS Principle

Extended Lambert-Beer-law[1,2]

$$I(\lambda) = E(t) + I_0(\lambda) \cdot Tr(t) \cdot exp[-S(T) \cdot g(\lambda - \lambda_0) \cdot N \cdot L]$$

with ideal gas law:

$$c = \frac{k_B \cdot T}{S(T) \cdot L \cdot p} \int ln\left(\frac{I(\nu) - E(t)}{I_0(\nu) \cdot Tr(t)}\right) \frac{d\nu}{dt} dt$$

- pressure and temperature from measurements
- absorption length from mechanical design
- $d\nu/dt$ from laser characterization
- $I(\nu)$, $I_0(\nu)$, $E(t)$ and $Tr(t)$ from raw signal

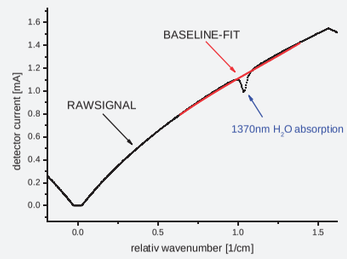

[1] Ebert et al., Proc. Comb. Inst. 28-1 (2000)
[2] Schlosser et al., Proc. Comb. Inst. 29-1 (2002) 353-360

Instrument: SEALDH

Selective **E**xtractive **A**irborne **L**aser **D**iode **H**ygrometer at 1.4 µm

SEALDH-I and SEALDH-II have performed very well on several flight campaigns in 2011 and 2012

LEARJET 35 A
image: enviscope GmbH

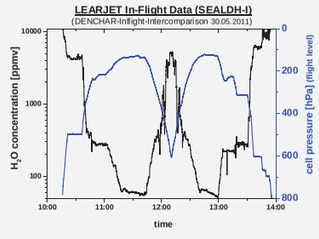

SEALDH-I Performance: Accuracy

SEALDH-I Validation at PTB national primary H_2O standard
(two pressure generator)

Processed single shot signal
transmission, baseline, offset corrected

Performance
OD_{peak} = 7.23E-2
OD_{noise} = 2.96E-4 (1σ)

⇨ SNR = 244 (1σ)
with: $C_{absolut}$ = 600 ppmv
⇨ C_{noise} = 2.45 ppmv

frequency of individual measurements: 140 Hz
optical path length: 1.50 m
⇩
$C_{precision}$ = 310 ppbv · m · $Hz^{-1/2}$

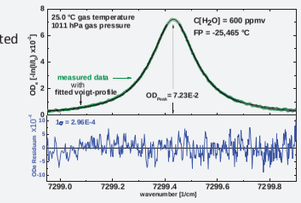

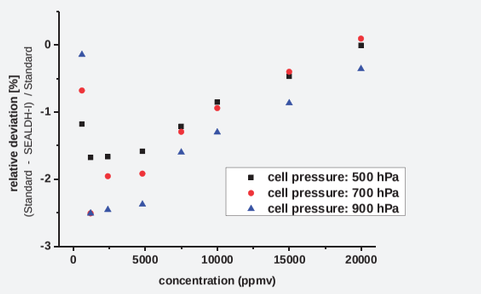

SEALDH-I Performance: Precision

SEALDH-I : system stability

Allan-Variance $\sigma^2(\tau) = \frac{1}{2}\left\langle(\overline{y}_{n+1} - \overline{y}_n)^2\right\rangle$

τ is the observation period
$\overline{y}_n$ is the fractional concentration average over the observation time

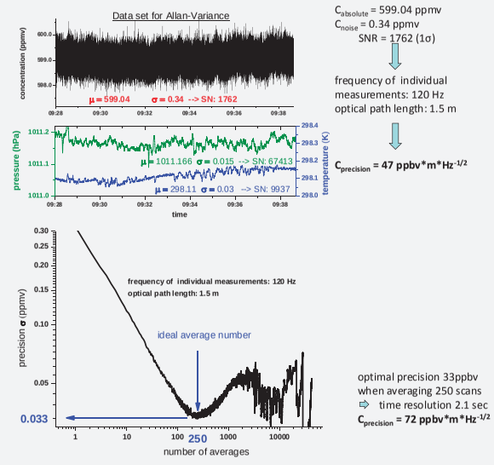

$C_{absolute}$ = 599.04 ppmv
C_{noise} = 0.34 ppmv
SNR = 1762 (1σ)
⇩
frequency of individual measurements: 120 Hz
optical path length: 1.5 m
⇩
$C_{precision}$ = 47 ppbv*$Hz^{-1/2}$

optimal precision 33ppbv when averaging 250 scans
⇨ time resolution 2.1 sec
$C_{precision}$ = 72 ppbv*$Hz^{-1/2}$

Line data: Broadening Coefficient

Improved broadening coefficient from HITRAN is needed to allow:

- validation of dynamic laser tuning determination
- validation of overall fitting process at different water vapor ratios e.g. transmissions or detector nonlinearity

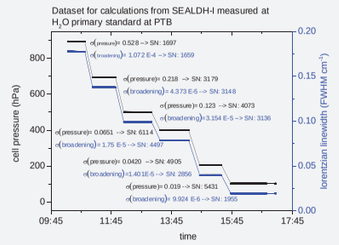

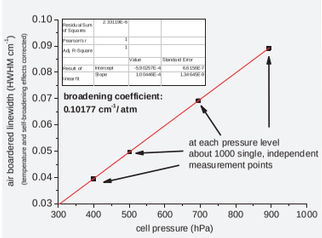

	air broadening coefficient (cm^{-1}/atm)	deviation from HITRAN
Hitran	(+/- 2 %) 0.1032	
SEALDH-I 600 ppmv	(+/- 2.5 %) 0.1077	4.3%
SEALDH-II	(+/- 2.5 %)	
600 ppmv	0,10121	1.9%
2500 ppmv	0,10039	2.7%
8000 ppmv	0,10061	2.5 %

Line data: Pressure Shift

THE SEALDH instruments provide a long-term spectrally stabilized, modulated light beam with about $\Delta\nu = 8 * 10^{-5}\ cm^{-1}$ (1 σ) spectral noise.

Lower spectral noise after Voigt-profile fit (shown above):
Every single complete absorption scan contains 2000 samples with 16-bit ADC resolution

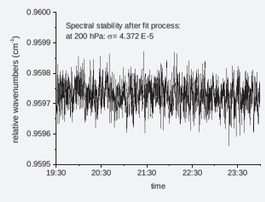

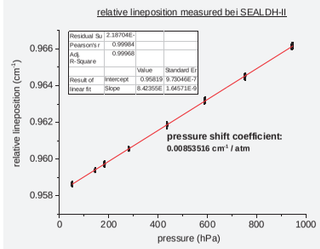

Comparison:
HITRAN:
0.00878 cm^{-1}/atm
(20 % uncertainty)

SEALDH-II:
0.008535 cm^{-1}/atm
(2 % uncertainty)

relative deviation from HITRAN:
2.7 %

Conclusion

- ✓ The SEALDH instruments represent a major improvement toward traceable airborne laser hygrometry
- ✓ The SEALDH instruments offer high precision, high accuracy, calibration freeness and long-term stability
- ✓ Solid validation at the national primary H_2O standard of PTB
- ✓ Measurements of high quality line data

Outlook

Future activities

- ✓ Further validation and line shape studies to improve instrument performance
- ✓ Improvement of the fit process
- ✓ More flight campaigns for endurance testing
- ✓ Long-term operation to validate the stability of the SEALDH instruments
- ✓ Optimized, standardized uncertainty analysis
- ✓ Traceability to metrological H_2O standard

Parts of this work have been funded by the EURFAR Project (European Facility for Airborne Research EUFAR, Grant No 227159) and the HAI Project (Deutsche Forschungsgemeinschaft, DFG , FKZ EB 235/3-1 and EB 235/3-2) within the HALO-SPP 1294

The WKMC empirical line lists (5852-7919 cm^{-1}) for methane between 80 K and 296 K

A. Campargue, O. Leshchishina, L. Wang, D. Mondelain, S. Kassi

Université Grenoble 1/CNRS, UMR5588 LIPhy, Grenoble, F-38041, France
Alain.Campargue@ujf-grenoble.fr

The methane line list included in the last version of the HITRAN and GEISA databases, is insufficient to fulfil important needs for planetary and atmospheric sciences for three main reasons: *(i)* it lacks in sensitivity especially in the transparency windows, *(ii)* except for a few strong lines, it does not provide lower state energy levels necessary to calculate the temperature dependence of the line intensities, *(iii)* transitions due to the CH_3D and $^{13}CH_4$ isotopologues are not systematically identified.
During the five last years, we have constructed empirical line lists for methane at room temperature and at 80 K from spectra recorded by *(i)* differential absorption spectroscopy (DAS) in the high energy part of the tetradecad (5852-6195 cm^{-1}) and in the icosad (6717-7589 cm^{-1}) *(ii)* high sensitivity CW-Cavity Ring Down Spectroscopy (CRDS) in the 1.58 μm and 1.28 μm transparency windows (6165-6750 cm^{-1} and 7541-7919 cm^{-1}, respectively). We have recently assembled the global line lists for methane in natural isotopic abundance, covering the spectral region from 5854 to 7919 cm^{-1} [1, 2].

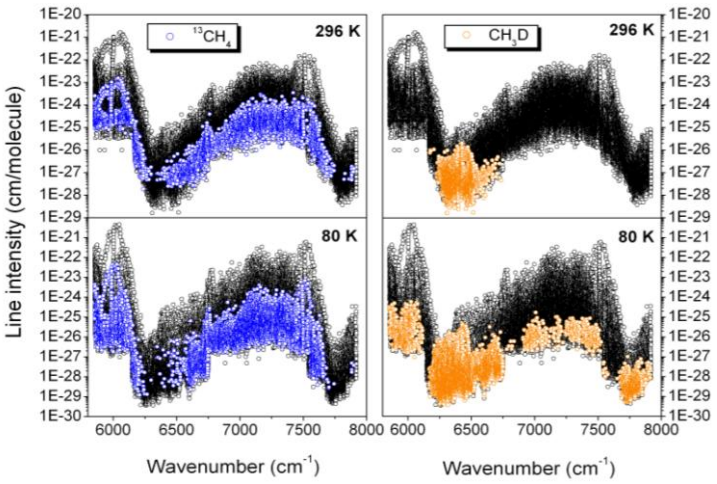

Fig. 1: The WKMC empirical line lists for methane at 80 K and 296 K showing the lines of $^{13}CH_4$ and CH_3D in "natural" methane.

These WKMC (for Wang, Kassi, Mondelain, Campargue) empirical lists include about 43000 and 46420 lines at 80±3 K and 296±3 K, respectively. The "two temperature method" provided lower state energy values, E_{emp}, for about 24000 transitions. The obtained data sets allow us to account for most of the temperature dependence of the absorption over the considered region. The WKMC list at 80 K has been successfully applied in a large range of temperature conditions existing on Titan [1], Uranus, Pluto, Saturn and Jupiter.

[1] A. Campargue, L. Wang, S. Kassi, D. Mondelain, B. Bézard, E. Lellouch, A. Coustenis, C. de Bergh, M. Hirtzig, P. Drossart. Icarus. **219**, 110-128 (2012).
[2] A. Campargue, O. Leshchishina, L. Wang, D. Mondelain, S. Kassi, A.V. Nikitin, JQSRT **113**,1855-73 (2012).

The WKMC empirical lists (5852 -7919 cm^{-1}) for methane between 80 K and 296 K.

Alain Campargue, Le Wang, O. Leshchishina, Didier Mondelain and Samir Kassi
Université Grenoble 1/CNRS, UMR5588 LIPhy, Grenoble, F-38041, France

The methane line list included in the last version of the HITRAN and GEISA databases, is insufficient to fulfill important needs for planetary and atmospheric sciences for three main reasons: (*i*) it lacks in sensitivity especially in the transparency windows, (*ii*) except for a few strong lines, it does not provide lower state energy levels necessary to calculate the temperature dependence of the line intensities, (*iii*) transitions due to the CH_3D and $^{13}CH_4$ isotopologues are not systematically identified.
During the five last years [1-13], we have constructed empirical line lists for methane at room temperature and at 80 K from spectra recorded by (*i*) differential absorption spectroscopy (DAS) in the high energy part of the tetradecad (5852-6195 cm^{-1}) and in the icosad (6717-7589 cm^{-1}) (ii) high sensitivity CW-Cavity Ring Down Spectroscopy (CRDS) in the 1.58 mm and 1.28 mm transparency windows (6165-6750 cm^{-1} and 7541-7919 cm^{-1}, respectively). We have recently assembled the global line lists for methane in natural isotopic abundance, covering the spectral region from 5854 to 7919 cm^{-1} [1, 2]. By comparison with DAS spectra of highly enriched $^{13}CH_4$ and CH_3D, recorded in the same temperature conditions, transitions of $^{13}CH_4$ and CH_3D present in "natural" isotopic abundance were identified.
These WKMC (for Wang, Kassi, Mondelain, Campargue) empirical lists include about 43000 and 46420 lines at 80±3 K and 296±3 K, respectively. The "two temperature method" provided lower state energy values, E_{emp}, for about 24000 transitions. The obtained data sets allow us to account for most of the temperature dependence of the absorption over the considered region.
The WKMC list at 80 K has been successfully applied in a large range of temperature conditions existing on Titan [1], Uranus, Pluto, Saturn and Jupiter.

CRDS and DAS at 80K

An original cryogenic cell

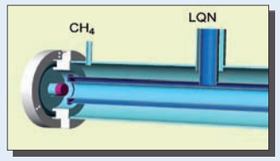

Our cold cell has **no insulating jacket**. It consists in a long hollow cylinder filled with liquid nitrogen (deep blue) and held by its single filling tube inside a cylindrical tank kept at room temperature. The gas (light blue), free to go in or out the cryostat, has shown to stabilize at a temperature of about 80K in the cryostat.

There is no **extra windows** and the cryostat thermal stress doesn't perturb the highly critical optical alignment as the wall temperature was found to stabilize around 7 °C within 20 min. A small dry nitrogen flow kept the mirrors free of water condensation.

The CW-CRDS@80K spectrometer

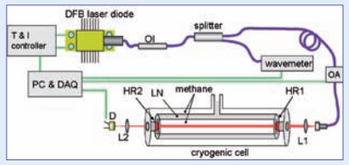

The fibered DFB laser diode is protected from back reflections by an optical isolator (OI). A splitter sends 10% of the light to a wavemeter and 90%, through an optoacoustic modulator (OA), to the CRDS cavity made of two mirrors (HR1, HR2). L1 modematches the laser to the cavity, L2 focuses the signal on an InGaAs photodiode (D).

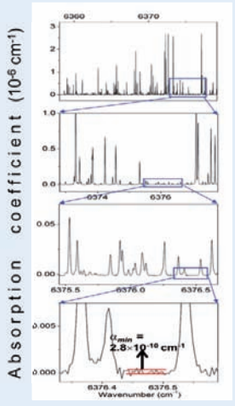

Very high accuracy and sensitivity

The left hand side Fig. shows part of the CW-CRDS spectrum of methane recorded at 80 K in the 1.58 µm transparency window. The noise equivalent absorption could be estimated to α_{min}~1.2×10^{-10} cm^{-1} (lower panel).
Three successive enlargements illustrate the high dynamics of the CW-CRDS spectrometer allowing for the measurement of **absorption coefficient** differing by **four orders of magnitude**.
Our LNT and RT CRD spectrometers reach the same level of sensitivity, dynamics, resolution, calibration and data acquisition speed.

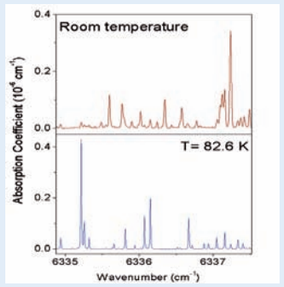

The cooling from RT down 81 K leads to a dramatic change in the appearance of the methane spectra as illustrated on the above Fig. corresponding to the highest transparency spectral section of the 1.58 µm window.
In general, the reduction by a factor of 2 of the Doppler line width reveals a number of multiplets which are strongly blended at room temperature.

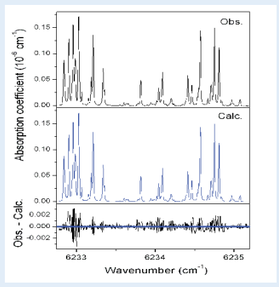

An example of simulation of the CH_4 spectrum recorded at LNT near 6234 cm^{-1}.
Upper panel: Experimental spectrum at LNT (P = 10 Torr),
Middle panel: Simulated spectrum resulting from the line fitting procedure (a Voigt profile was affected to each line),
Lower panel: Residuals between the simulated and experimental spectra.

The WKMC line lists at 80 K and 296 K

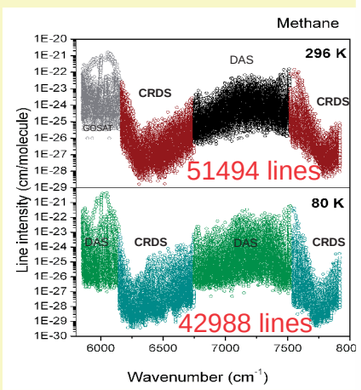

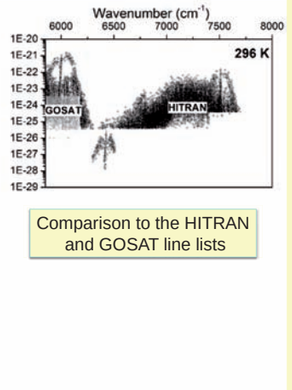

Comparison to the HITRAN and GOSAT line lists

Identification of the $^{13}CH_4$ and CH_3D transitions

By comparison with DAS spectra of highly enriched $^{13}CH_4$ and CH_3D, recorded in the same temperature conditions, transitions of $^{13}CH_4$and CH_3D present in "natural" isotopic abundance were identified.

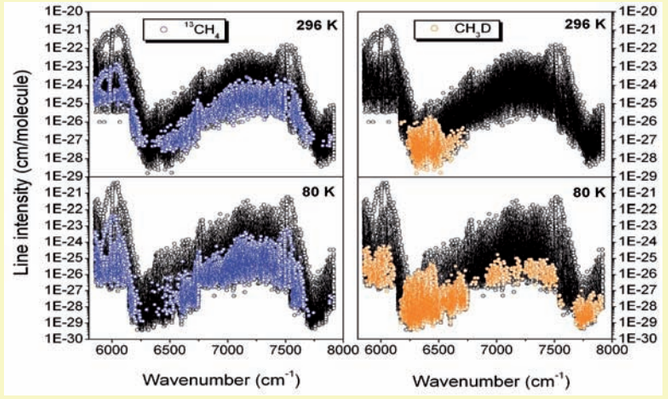

CH_3D in the 1.58 µm window

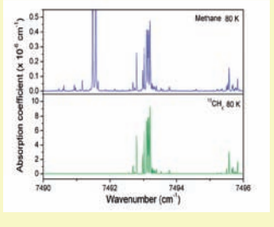

Identification of the $^{13}CH_4$ lines in the spectrum of "natural" methane at 80 K by comparison of the methane and $^{13}CH_4$ spectra near 7493 cm^{-1}. The two spectra were recorded at 80 K with a pressure of 6.0 Torr and 1.0 Torr, respectively. The chosen interval shows the Q branch of the $\nu_2 + 2\nu_3$ band of $^{13}CH_4$.

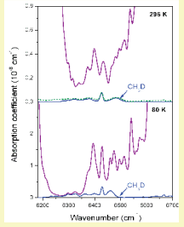

Low resolution simulations (P = 1.0 Torr) obtained from the complete line list (purple) and limited to the CH_3D lines (blue) showing the fraction of the absorption due to CH_3D in natural abundance between 6150 and 6750 cm^{-1}. The CH_3D contribution has been highlighted in blue.

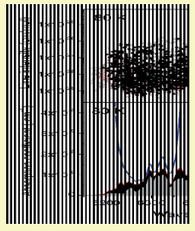

In order to determine the temperature dependence of the CH_3D absorption in the 1.58 µm region, the lower state energy levels were obtained by applying the two temperature method to DAS spectra of pure CH_3D [11]. The empirical values were transferred in the WKMC list at 80 K allowing to account for the T dependence of the methane absorption in the region.

Experimental determination of the lower state energy

The "two temperature" method consists in deriving the low energy values of the transitions from the ratio of their intensities measured at 296 K and 80 K :

$$S_T(T) = AT^{-3/2} \times \exp(-E/kT)$$

$$-\ln\left(\frac{S_{w_n}(T)}{S_{w_n}(T_0)}\right) = \frac{3}{2}\ln\left(\frac{T}{T_0}\right) + E\left[\frac{1}{kT} - \frac{1}{kT_0}\right]$$

for CH_4 species $E = BJ(J+1)$

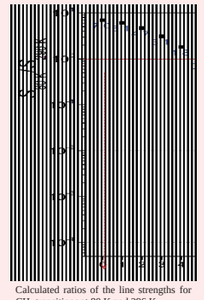

Calculated ratios of the line strengths for CH_4 transitions at 80 K and 296 K.
Note the considerable decrease of the J>10 intensities at 80 K.

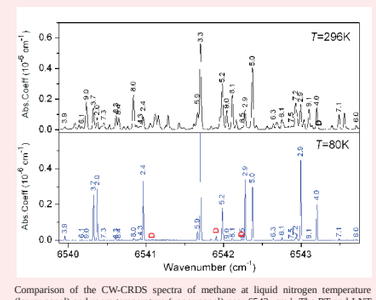

Comparison of the CW-CRDS spectra of methane at liquid nitrogen temperature (lower panel) and room temperature (upper panel) near 6542 cm^{-1}. The RT and LNT spectra were recorded with pressures of 10.0 and 1.0 Torr, respectively. The few CH_3D transitions observed in the region are marked with "D". The empirical J values obtained from the temperature variation of the line intensities are indicated for the CH_4 isotopologue.

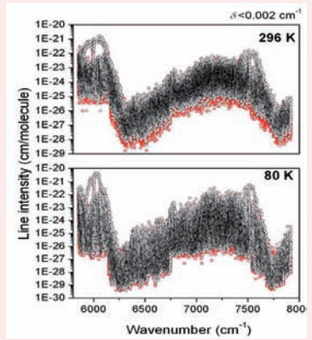

Overview of the empirical line lists of methane between 5834 and 7919 cm^{-1}, at 296 K (upper panel) and 80 K (lower panel). The black circles (plotted last) highlight the transitions in common in the two lists for which it was possible to derive the empirical lower state energy (δ < 0.002 cm^{-1})

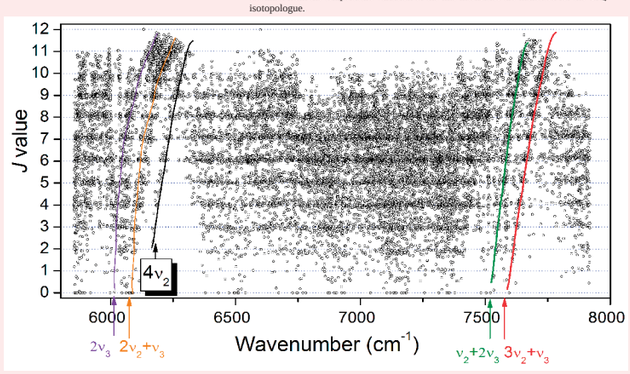

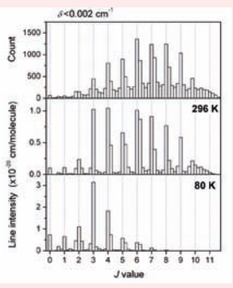

Histograms of the empirical J values determined for the CH_4 transitions (step interval of 0.2). The upper panel is relative to the number of lines. In the two lower panels, the corresponding line intensities at 296 K and 80 K were added for each step interval. Note that the contrast between integers and non integers is more pronounced in terms of intensities than in terms of number of lines.

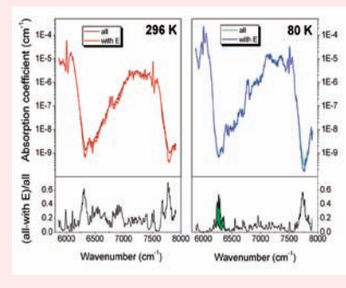

Part of the methane absorption at 80 K for which the temperature dependence has been derived The upper panels show low resolution simulations (FWHM= 10.0 cm^{-1}) of the methane spectrum at 1 Torr for all the lines or only those with with lower state energy derived by the "two temperature" method. The lower panels show the relative differences.

Conclusion

The sensitivity, accuracy and completeness (isotopologue identification, temperature dependence) of the WKMC line lists represent an important breakthrough for the spectroscopy of methane in the near infrared.

The WKMC has become the reference list for planetary applications (Titan Uranus, Pluto, Saturn and Jupiter) .

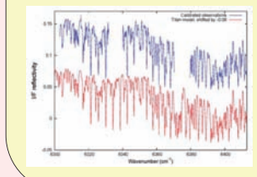

Example of agreement between the spectrum of Titan (July 28 2010 , CRIRES-ESO VLT 8.2 m telescope) and a simulation based on the WKMC list at 80 K (Campargue et al. Icarus 2012)

Acknowledgments:
This work is part of the ANR project "CH4@Titan" (ref: BLAN08-2_321467) which is a joint effort among four French groups (ICB-Dijon, GSMA-Reims, LIPhy-Grenoble and LESIA-Meudon) to model the NIR methane opacity. The support from the Programme National de Planétologie is also acknowledged.

1. A. Campargue, L. Wang, S. Kassi, D. Mondelain, B. Bézard, E. Lellouch, A. Coustenis, C. de Bergh, M. Hirtzig, P. Drossart. Icarus. 219, 110-128 (2012).
2. A. Campargue, O. Leshchishina, L. Wang, D. Mondelain, S. Kassi, A.V. Nikitin, JQSRT in press http://dx.doi.org/10.1016/j.jqsrt.2012.05.011.
3 S. Kassi, B. Gao, D. Romanini, A. Campargue, Phys. Chem. Chem. Phys. 10 (2008) 4410.
4. B. Gao, S. Kassi, A. Campargue, J. Mol. Spectrosc. 253 (2009) 55.
5. L. Wang, S. Kassi, A. Campargue, J. Quant. Spectrosc. Radiat. Transfer. 111 (2010) 1130
6. E. Sciamma-O'Brien, S. Kassi, B. Gao, A. Campargue, J. Quant. Spectrosc. Radiat. Transfer. 110 (2009) 951.
7. A. Campargue, Le Wang, S. Kassi, M. Mašát, O. Votava, J. Quant. Spectrosc. Radiat. Transfer. 111 (2010) 1141.
8. O. Votava, M. Mašát,P. Pracna, S. Kassi, A. Campargue, Phys. Chem. Chem. Phys. 12 (2010) 3145.
9. S. Kassi, D. Romanini, A. Campargue, Chem. Phys. Lett. 477 (2009) 17.
10. L. Wang, S. Kassi, A. W. Liu, S. M. Hu, A. Campargue, J. Mol. Spectrosc. 261 (2010) 41-52.
11. A. Campargue, L. Wang, A. W. Liu, S. M. Hu, S. Kassi. Chem. Phys. 373(2010) 203–10.
12. D. Mondelain S. Kassi L.Wang , A. Campargue, Phys Chem Chem Phys.17 (2011) 7985-96.
13. Y. Liu, D. Mondelain, S. Kassi, A. Campargue, J. Quant. Spectrosc. Radiat. Transfer. 112 (2011)2683-97.
14. de Bergh C, Courtin R, Bézard B, Coustenis C, Lellouch E, Hirtzig M, Rannou P, Drossart P, Campargue A, Kassi S, Wang L, Boudon V, Nikitin A, Tyuterev V. Plan Space Sci 61 (2012) 85-99.

Quantitative spectroscopy in the mid-infrared region by comb-referencing quantum cascade lasers

Antonio Castrillo and Livio Gianfrani

Dipartimento di Matematica e Fisica, Seconda Università di Napoli, Caserta, Italy

Marco Marangoni and Paolo Laporta

Dipartimento di Fisica, Politecnico di Milano, Milano, Italy

Gianluca Galzerano

Istituto di Fotonica e Nanotecnologie del CNR, Milano, Italy

Atmospheric and planetary science communities make a daily use of molecular spectroscopic parameters, such as center frequencies and intensity factors of vibration-rotation lines in the infrared portion of the electromagnetic spectrum. Most data are taken from the HITRAN database, which is widely recognized as a good compendium made of a proper combination of laboratory measurements and quantum mechanical calculations. Even though refined in the course of the years, its level of accuracy remains insufficient for some specific applications, including atmospheric monitoring for the study of climate changes and for the validation of climate models, where high-quality and traceable spectroscopic parameters are needed, at least for those molecules contributing to the greenhouse effect.

The past 12 years have witnessed the advent of an extremely fine spectroscopic tool, the optical frequency comb synthesizer (OFCS). Based upon mode-locked femtosecond lasers, an OFCS provides hundreds of thousands of sharp, equally spaced, spectral components, distributed across hundreds of nanometers. The main motivation for its invention was to provide a direct and phase-coherent link between optical and microwave domains, thus allowing for precision measurements of optical frequencies. As a result, the field of frequency metrology has received a tremendous impulse in the last decade. Nowadays, the OFCS technology is finding an increasing number of new applications in different research fields, either in the near-infrared (NIR) or in the mid-infrared (MIR).

In the framework of molecular spectroscopy, frequency combs have been so far mostly applied to the determination of line-center frequencies with extreme accuracy: in such measurements the frequency comb typically acts as a rigid ruler to count the frequency of a continuous-wave (cw) laser that has been tightly locked to a sub-Doppler absorption feature.

In this work, we show how traceable and accurate spectroscopic data can be retrieved in the mid-infrared (MIR) region by taking the advantage of a referencing scheme allowing a quantum-cascade-laser (QCL) to be phase-locked to a NIR frequency comb [1, 2]. Tuning the comb repetition rate allows the QCL to be scanned across a given absorption line with a highly accurate, absolute, and repeatable frequency axis, so as to obtain absorption spectra with the highest metrological qualities.

We demonstrate the concept of determining the line-centre frequency, line strength, pressure shift, and pressure broadening coefficients for molecules of strong atmospheric interest (such as carbon dioxide), in the so-called fingerprint region [3]. In this respect, we benefit from the fact that widely tunable QCLs are commercially available in the whole 3-12 μm spectral range. The proposed methodology has thus the potential of being a standardized procedure with the highest metrological qualities, capable of solving the inconsistency problem of the currently available molecular databases.

Quantitative spectroscopy in the mid-infrared region by comb-referencing quantum cascade lasers

A. Castrillo,[1] G. Galzerano,[3] P. Laporta,[2] M. Marangoni,[2] and L. Gianfrani[2]

(1) Dipartimento di Matematica e Fisica, Seconda Università degli Studi di Napoli, Caserta, Italy
(2) Dipartimento di Fisica, Politecnico di Milano, Milano, Italy
(3) Istituto di Fotonica e Nanotecnologie del CNR, Milano, Italy

Atmospheric and planetary science communities make a daily use of molecular spectroscopic parameters, such as center frequencies and intensity factors of vibration-rotation lines in the infrared portion of the electromagnetic spectrum. Most data are taken from the HITRAN database, which is widely recognized as a good compendium made of a proper combination of laboratory measurements and quantum mechanical calculations. Even though refined in the course of the years, its level of accuracy remains insufficient for some specific applications, including atmospheric monitoring for the study of climate changes and for the validation of climate models, where high-quality and traceable spectroscopic parameters are needed, at least for those molecules contributing to the greenhouse effect. The past 12 years have witnessed the advent of an extremely fine spectroscopic tool, the optical frequency comb synthesizer (OFCS). Based upon mode-locked femtosecond lasers, an OFCS provides hundreds of thousands of sharp, equally spaced, spectral components, distributed across hundreds of nanometers. The main motivation for their invention was to provide a direct and phase-coherent link between optical and microwave domains, thus allowing for precision measurements of optical frequencies. As a result, the field of frequency metrology has received a tremendous impulse in the last decade. Nowadays, the OFCS technology is finding an increasing number of new applications in different research fields, either in the near-infrared (NIR) or in the mid-infrared (MIR). In the framework of molecular spectroscopy, frequency combs have been mostly applied , so far, to the determination of line-center frequencies with extreme accuracy: in such measurements the frequency comb typically acts as a rigid ruler to count the frequency of a continuous-wave (cw) laser that has been tightly locked to a sub-Doppler absorption feature.

In this work, we show how traceable and accurate spectroscopic data can be retrieved in the mid-infrared (MIR) region by taking the advantage of a referencing scheme allowing a quantum-cascade-laser (QCL) to be phase-locked to a NIR frequency comb. Tuning the comb repetition rate allows the QCL to be scanned across a given absorption line with a highly accurate, absolute, and repeatable frequency axis, so as to obtain absorption spectra with the highest metrological qualities. We demonstrate the concept of determining the line-centre frequency, line strength, pressure shift, and pressure broadening coefficients for molecules of strong atmospheric interest, in the so-called fingerprint region. In this respect, we benefit from the fact that widely tunable QCLs are commercially available in the whole 3-12 μm spectral range. The proposed methodology has thus the potential of being a standardized procedure with the highest metrological qualities, capable of solving the inconsistency problem of the currently available molecular databases.

[1] D. Gatti, A. Gambetta, A. Castrillo, G. Galzerano, P. Laporta, L. Gianfrani, and M. Marangoni, Opt. Express **19**, 17520-17527 (2011).
[2] A. Gambetta, D. Gatti, A. Castrillo, G. Galzerano, P. Laporta, L. Gianfrani, and M. Marangoni, Appl. Phys. Lett. 99, 251107 (2011).
[3] A. Castrillo, A. Gambetta, D. Gatti, G. Galzerano, P. Laporta, M. Marangoni, L. Gianfrani, Appl. Phys. B, DOI 10.1007/s00340-012-5013-x (2012).
[4] A. Gambetta, D. Gatti, A. Castrillo, N. Coluccelli, G. Galzerano, P. Laporta, L. Gianfrani, M. Marangoni, Appl. Phys. B, DOI 10.1007/s00340-012-4947-3 (2012).
[5] A. Mills, D. Gatti, J. Jiang, C. Mohr, W. Mefford, I. Hartl, M. Fermann, L. Gianfrani, M. Marangoni, Opt. Letters 37, 4083 (2012).

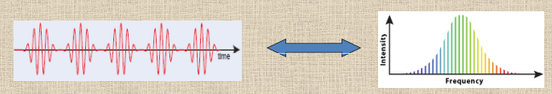

Overview of a typical experimental setup

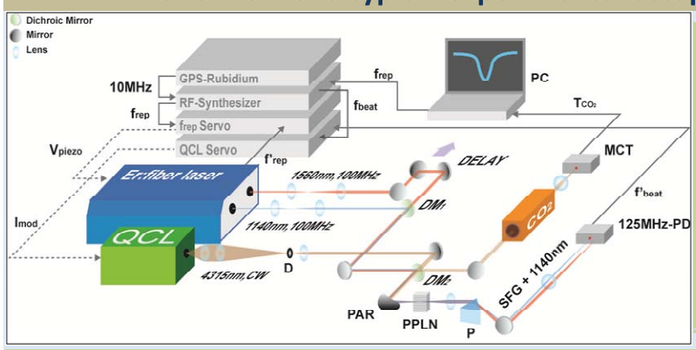

Optical frequency combs are modelocked lasers providing a train of ultra-short pulses (~ 10 fs) at a repetition rate in the RF region. In the frequency domain, this is equivalent to hundreds of thousands of sharp modes evenly distributed across hundreds of nanometers. The frequency of each mode is determined by :

$$\nu_m = m\, f_r + f_0$$

m being an integer number, f_r the repetition rate, and f_0 the carrier-envelope offset frequency.

The experimental apparatus used to obtain referencing of the QCL to the comb is particularly compact. The QCL is a cw liquid-nitrogen cooled DFB laser, driven by a commercially-available power supply, providing single longitudinal mode operation and an optical power up to 20 mW, with a threshold of 90 mA and a slope of 170 μW/mA. It can be tuned around 4.33 μm by roughly 120 GHz with a sensitivity of ~370 MHz/mA. After proper beams spatial and temporal matching, the two outputs of the Er:fiber laser are collinearly recombined with each other and then with the QCL by means of dichroic mirrors. The three beams are focused in a 4-mm long PPLN crystal providing the up-conversion of the QCL to the 1.14 μm spectral region used for the beating (power levels inside the crystals amount to 770 μW for the QCL and 150 mW for the 1.55-μm comb). The spectrum of the sum-frequency beam spans roughly 10 nm and it overlaps with the spectrum of the SC when tuned to the same 1.14 μm central wavelength. After spectral filtering of the broader SC, the beating-note between the two signals (50 μW for the SC and 5 nW for the sum frequency) is extracted by a 125 MHz InGaAs detector. Such scheme allows the QCL frequency to be directly referred to the repetition frequency of the comb without any contribution from the carrier-envelope-offset frequency.

Comb-referencing of DFB QC lasers

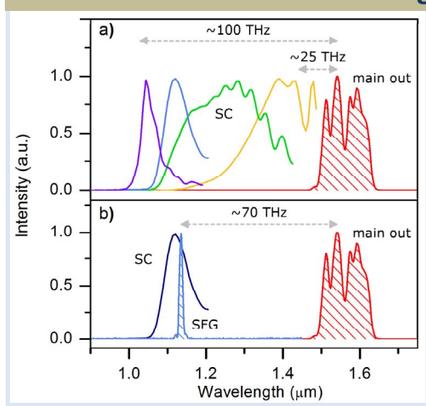

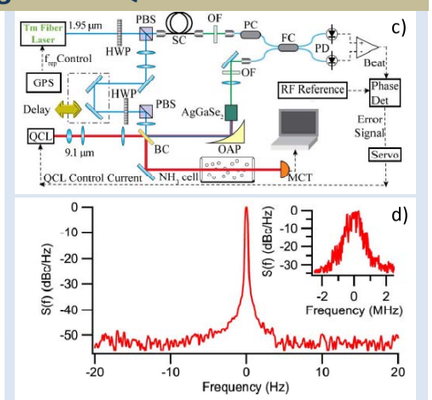

(a) Examples of phase-coherent spectra from a dual-branch Er-fiber laser: main output at 1.55 μm (red line) and SC output (coloured lines at shorter wavelengths), together with their frequency difference (horizontal arrows and corresponding labels). (b) Spectrum (light blue) resulting from SFG between QCL (not reported in the figure) and main oscillator output (red line), together with the SC spectrum used for the beating (dark blue), as situated 70 THz far apart the main Erbium output. (c) Example of another powerful apparatus, based upon a Tm-fiber laser frequency comb, developed in collaboration with scientists from IMRA. (d) Electrical spectrum of the beat-note between comb and QCL. Main panel: phase-locked conditions, 0.3 Hz resolution bandwidth. Inset: free-running beating, 300 kHz resolution bandwidth, 10 MHz span, 25 ms sweep.

Frequency-comb-assisted spectroscopy

CO_2 spectrum at 4.3 μm

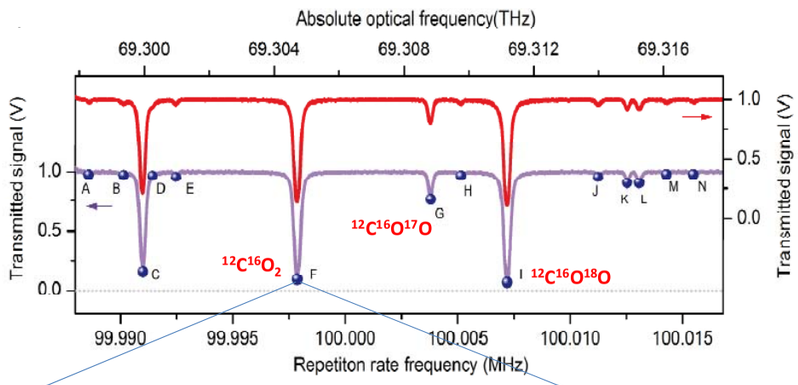

Tuning of the comb repetition rate allows the QCL to be scanned across a given region with a highly-accurate, absolute and repeatable frequency axis, so as to obtain absorption spectra with the highest metrological qualities. The figure on the left shows examples of CO_2 absorption spectra (from a gas cell filled at 7.3 Torr), covering a frequency range of 20 GHz. The scanning time was about 7 minutes. To obtain absolute frequencies, both the 15-MHz frequency offset and the repetition-rate of the Erbium laser were referred to a GPS-disciplined Rb oscillator.

ref.	transition	isotopologue	HITRAN (cm^{-1})	CAFS (cm^{-1})
A	Q 6f	$^{12}C^{16}O_2$	2311.541	2311.5429(3)
B	Q 5e	$^{12}C^{16}O_2$	2311.577	2311.5777(2)
C	P 18e	$^{12}C^{16}O_2$	2311.597	2311.597204(8)
D	Q 4f	$^{12}C^{16}O_2$	2311.607	2311.6071(1)
F	Q 3e	$^{12}C^{16}O_2$	2311.631	2311.6314(2)
F	P 15f	$^{12}C^{16}O_2$	2311.756	2311.756144(8)
G	P 33e	$^{16}O^{12}C^{17}O$	2311.893	2311.89299(3)
H	P 15e	$^{12}C^{16}O_2$	2311.924	2311.9244(2)
I	P 25e	$^{16}O^{12}C^{18}O$	2311.971	2311.971789(7)
J	P 4f	$^{12}C^{16}O_2$	2312.065	2312.0644(1)
K	P 10f	$^{16}O^{12}C^{18}O$	2312.095	2312.09542(8)
L	P 10e	$^{16}O^{12}C^{18}O$	2312.107	2312.10781(8)
M	P 19f	$^{16}O^{12}C^{17}O$	2312.135	2312.1348(3)
N	P 19e	$^{16}O^{12}C^{17}O$	2312.163	2312.1638(4)

Line fitting

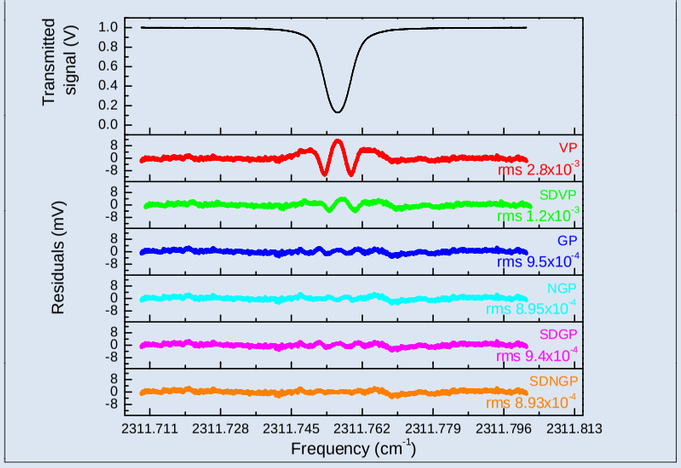

Absolute linestrength determination

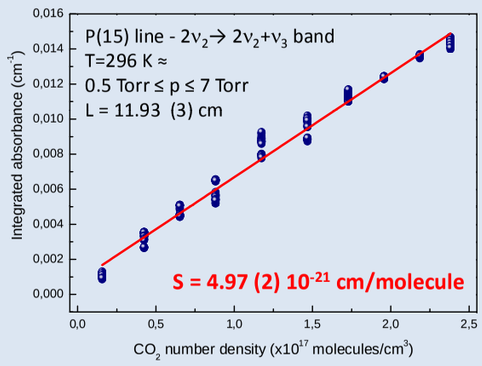

Measured spectroscopic parameters:

- Linestrength	4.97 (2) 10^{-21} cm/molecule
- Self-broadening coefficient	0.1026 (7) cm^{-1}/atm
- Pressure-shift coefficient	-4.53 (19) 10^{-6} cm^{-1}/Torr
- Line-center frequency (at zero pressure)	2311.7561434 (10) cm^{-1}

NH_3 spectrum at 9.1 μm

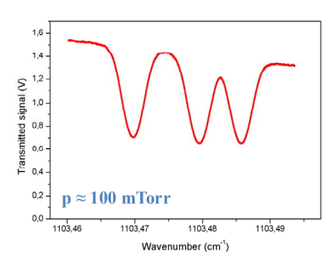

Example of multiple-line fitting

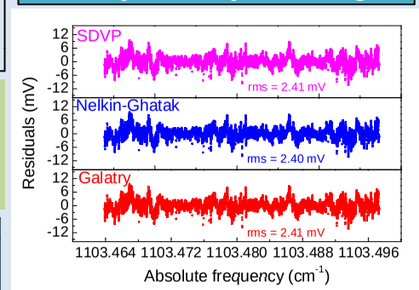

In conclusion, a simple and effective scheme to refer the frequency of a MIR QCL to a NIR comb is demonstrated and shown to be suitable for highly-accurate and traceable determinations of spectroscopic parameters in gaseous samples. The results here reported for a single CO_2 line around 4.3 μm are likely to be extended to any absorption line of the so-called fingerprint region of any molecule of atmospheric interest, since widely tunable QCLs are commercially available in the whole 3-12 μm spectral range.
We are presently doing, in collaboration with people from IMRA (Martin Fermann, Ingmar Hartl and co-workers) a similar experiment on NH_3 lines of the ν_2 band, using a QCL at 9.1 μm and a Tm-fiber laser frequency comb. In this case, SFG NIR radiation is produced in an $AgGaSe_2$ crystal.

Frontier Sources for High-Resolution Spectroscopy

M. De Rosa, G. Gagliardi, P. Maddaloni, P. Malara, S. Mosca, I. Ricciardi, A. Rocco,
CNR–INO, Istituto Nazionale di Ottica, Napoli (Italy)
S. Borri, S. Bartalini, P. Cancio, I. Galli, G. Giusfredi, D. Mazzotti, P. De Natale
CNR–INO, Istituto Nazionale di Ottica, Firenze (Italy)

Atomic and molecular spectroscopy continues to play a major role in the understanding of Nature and represents a test bench for fundamental physical theories, from the microscopic world to the cosmic scale. Accurate measurements of transition parameters demand for increasingly stable and spectrally pure laser sources. We present an overview of different laser sources and spectroscopic techniques, developed in our labs, aimed to accurate measurements on molecular transitions, falling in the infrared region. We developed different sources, based on difference frequency generation [1,2] and optical parametric oscillation [3] in nonlinear crystals, which can cover the spectral range between 2.7 and 4.5 μm. At longer wavelengths, we investigated the ultimate performances of quantum cascade lasers [4,5], which are more and more proving to be reliable sources for high-resolution spectroscopy. All these sources have been used in combination with optical frequency synthesizers, for frequency stabilization and absolute frequency determination. Finally, high-sensitivity techniques have been developed for quantitative measurement of gas concentration [6,7].

References

[1] P. Maddaloni et al., J. Chem. Phys. **133**, 154317 (2010).
[2] I. Galli et al., Optics letters **35**, 3616 (2010).
[3] I. Ricciardi et al., Optics Express **20**, 9178 (2012).
[4] S. Borri et al., Optics Express **16**, 11637 (2008).
[5] F. Cappelli et al., Optics Letters **37**, 4811 (2012).
[6] G. Giusfredi et al., Phys. Rev. Lett. **104**, 110801 (2010).
[7] I. Galli et al., Phys. Rev. Lett. **107**, 270802 (2011).

Frontier Sources for High-Resolution Spectroscopy

INO
Istituto Nazionale di Ottica

M. De Rosa, G. Gagliardi, P. Maddaloni, P. Malara, S. Mosca, I. Ricciardi, A. Rocco — CNR-INO, Napoli (Italy)
S. Bartalini, S. Borri, P. Cancio, I. Galli, G. Giusfredi, D. Mazzotti, P. De Natale — CNR-INO, Firenze (Italy)

We present an overview of different laser sources and spectroscopic techniques, developed in our labs, aimed to accurate measurements on molecular transitions, falling in the infrared region. We developed different sources, based on difference frequency generation and optical parametric oscillation in nonlinear crystals, which can cover the spectral range between 2.7 and 4.5 μm. At longer wavelengths, we investigated the ultimate performances of quantum cascade lasers, which are more and more proving to be reliable sources for high-resolution spectroscopy. All these sources have been used in combination with optical frequency synthesizers, for frequency stabilization and absolute frequency determination. Finally, high-sensitivity techniques have been developed for quantitative measurement of gas concentration.

Comb-referenced DFG

A 3-μm continuous-wave difference-frequency source is directly referenced to an optical frequency comb covering the 1 – 2 μm octave.

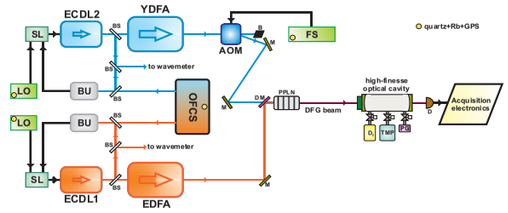

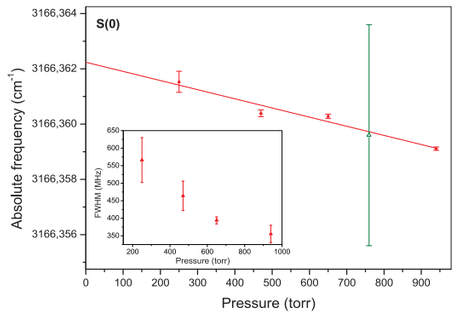

We revisited the fundamental rovibrational band of D_2 by cavity ring-down spectroscopy. The S(0) and S(1) transitions in the fundamental band have been recalibrated in an absolute way in terms of position, pressure shift, and line strength, improving the accuracy in the line-center frequency by more than one order of magnitude

Maddaloni et al., J. Chem. Phys. **133**, 154317 (2010)

Intracavity DFG

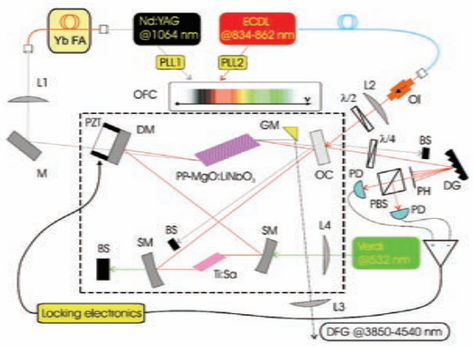

Following a scheme proposed by Cummings et al. [Appl. Opt. **41**, 7583 (2002)], we demonstrated up to 30 mW at 4510 nm by putting the nonlinear crystal inside the cavity of a Ti:sapphire laser.

Galli et al., Opt. Lett. 35, 3616 (2010)

30 mW cw power @ 4.5 mm with 10 Hz linewidth

Comb-referenced OPO

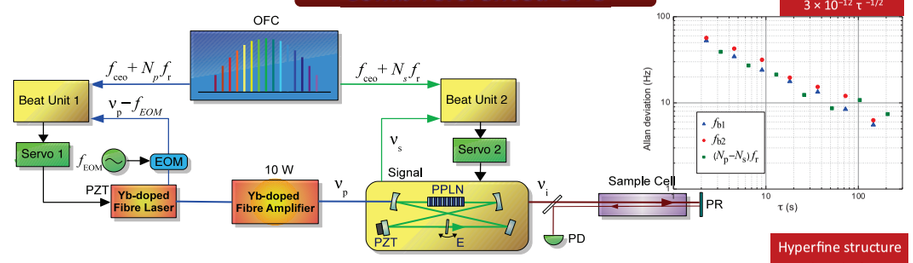

Ricciardi et al., Opt. Express **20**, 9178 (2012)

A singly-resonant optical parametric oscillator, emitting more than 1 W in the region between 2.7 and 4.2 μm, has been frequency-referenced by locking both the pump and the signal frequencies to the frequency comb generated by a NIR fs mode-locked fibre laser, linked to the caesium primary standard.

We carried out saturation spectroscopy of the ν_1 band rovibrational transitions of CH_3I, resolving their electronic quadrupole hyperfine structure

Pump: $\nu_p = f_{ceo} + N_p f_r + f_{b1} + f_{EOM}$
Signal: $\nu_s = f_{ceo} + N_s f_r + f_{b2}$
Idler: $\nu_i = \nu_p - \nu_s = (N_p - N_s)\, f_r + f_{b1} - f_{b2} + f_{EOM}$

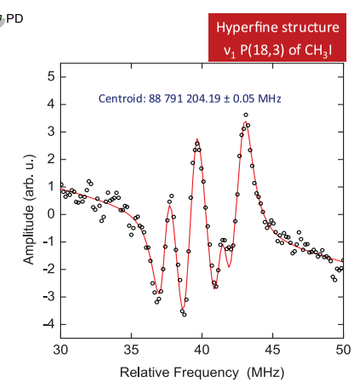

SCAR: Saturated-absorption Cavity Ring-down

We propose a new spectroscopic technique, saturated-absorption cavity ring-down (SCAR), very effective in identifying and decoupling any variation of the empty-cavity decay rate, improving the CRD sensitivity

Giusfredi et al., Phys. Rev. Lett. 104, 110801 (2010)

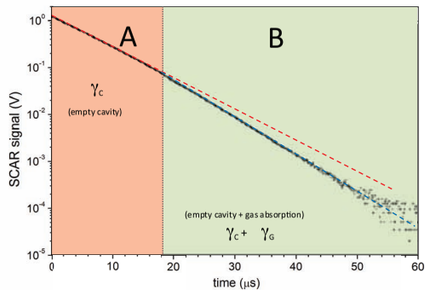

Radiocarbon Detection

The ultimate sensitivity of this technique has been exploited by detecting the elusive radiocarbon molecule ($^{14}C^{16}O_2$) at concentrations down to 43 parts per quadrillion (ppq).

Galli et al., Phys. Rev. Lett. 107, 270802 (2011)

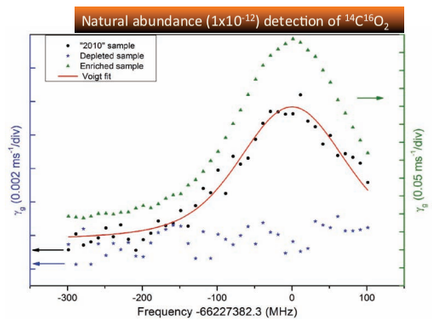

A smart DFG link to Comb

The pump and signal lasers of a DFG coherent source have been frequency linked by means of an optical frequency-comb synthesizer, according to a scheme proposed by Telle et al.[Appl. Phys. B **74**, 1 (2002)]. The OFC acts as a mere frequency transfer, without adding extranoise.
The DFG source achieves a 10-Hz intrinsic linewidth, is tunable from 4 to 4.5 μm with a presettable absolute frequency and, when coupled to a high-finesse cavity, can provide a short-term absorption sensitivity of $1.3 \cdot 10^{-11}$ cm^{-1} Hz$^{-1/2}$.

Galli et al., Opt. Express **17**, 9582 (2009)

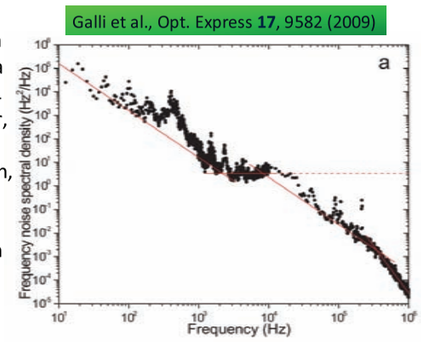

Linking a QCL to a near-IR Comb

A metrological link between a quantum cascade laser and a Ti:sapphire optical frequency comb synthesizer has been carried out by up-conversion of the MIR radiation in PPLN.

The QCL frequency has been stabilized to the Lamb-dip center of a CO_2 ro-vibrational transition and its absolute frequency counted with a kHz-level precision and an overall uncertainty of 75 kHz.

Borri et al., Opt. Express 16, 11645 (2008)

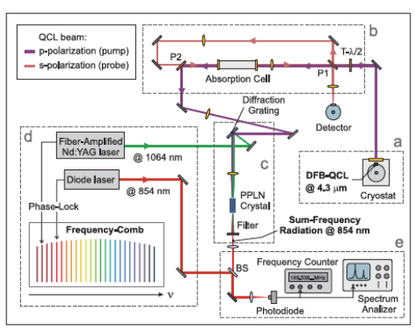

Sub-Doppler spectroscopy
$^{12}CO_2$ (01^11-01^10) P(30)

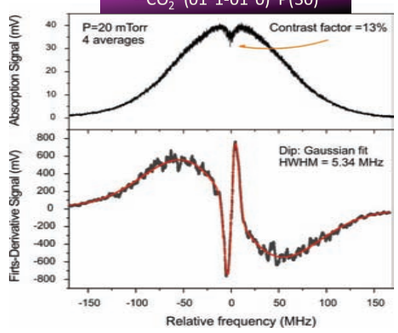

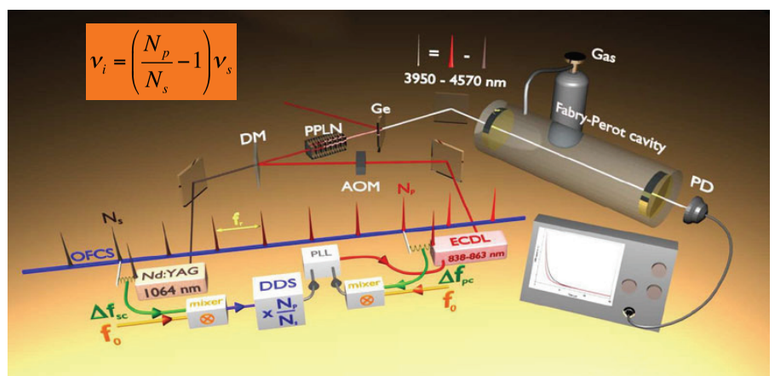

LINE PARAMETERS OF THE HCl ABSORPTION BAND IN THE FIRST OVERTONE AT UP TO 10 BAR

V. Ebert[1,2,3], M. Gisi[2], P. Ortwein[1,2], A. Serdyukov[1], S. Wagner[2,3], W. Woiwode[2]

[1] Physikalisch-Technische Bundesanstalt, Bundesallee 100, 38116 Braunschweig, Germany
[2] Physical Chemistry Institute (PCI), Universität Heidelberg, INF253, 69120 Heidelberg, Germany
[3] Center of Smart Interfaces, Technische Universität Darmstadt, Petersenstraße 32, 64287 Darmstadt, Germany

EUMETRISPEC Stakeholder Workshop, Braunschweig, Germany, 15-16 November 2012

LINE PARAMETERS OF THE HCl ABSORPTION BAND IN THE FIRST OVERTONE AT UP TO 10 BAR

V. Ebert[1,2,3], M. Gisi[2], P. Ortwein[1,2], A. Serdyukov[1], S. Wagner[2,3], W. Woiwode[2]

[1] *Physikalisch-Technische Bundesanstalt, Bundesallee 100, 38116 Braunschweig, Germany volker.ebert@ptb.de*

[2] *Physical Chemistry Institute (PCI), Universität Heidelberg, INF253, 69120 Heidelberg, Germany, www.gasanalysis.org*

[3] *Center of Smart Interfaces, Technische Universität Darmstadt, Petersenstraße 32, 64287 Darmstadt, Germany*

MOTIVATION

⇨The detection of HCl plays an important role in many issues of atmospheric chemistry as well as in combustion and gasification processes

⇨The $H^{35}Cl$ R(3) line in the first overtone region provides good spectroscopic characteristics for the detection of HCl at atmospheric conditions as well as in high temperature processes

⇨A sensitive measurement of the volumetric content of HCl especially in gasification processes with high process temperatures and pressures requires a precise knowledge of the spectroscopic line parameters

⇨In particular self and foreign broadening coefficients with other species are of great interest. In the reference database HITRAN 2008 only self and air broadening coefficients of HCl are given

⇨Due to the discrepancy of the values for the pressure broadening coefficients and line strength between HITRAN 2008 and other authors a precise investigation of these parameters was performed

⇨Using a vertical cavity surface emitting laser (VCSEL) at 1.74µm with a wide current tuning range of 10 cm-1 a highly sensitive TDLAS spectrometer was developed to realize an analysis of the $H^{35}Cl$ R(3) absorption line even under high pressures

TDLAS-MEASUREMENT PRINCIPLE

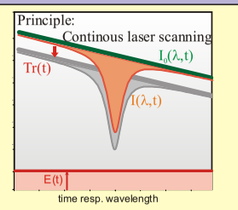

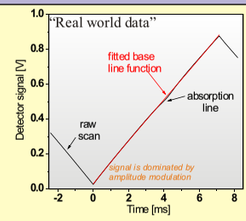

$$I(\lambda,t) = I_0(\lambda,t)\cdot Tr(t)\cdot \exp[-S(T)\cdot\phi_{line}\cdot N\cdot L] + E(t)$$

$$\Rightarrow N = \frac{-1}{S(T)\cdot L}\int \ln\left(\frac{I(\lambda,t)-E(t)}{I_0(\lambda)\cdot Tr(t)}\right)\frac{\delta\lambda}{\delta t}\,dt \Rightarrow$$

Absolute number densities
Self calibrating
Laser characterisation
Fitting process / Transm + emiss. Correction
Absorption length measurement
Line strength and temperature dependence

$$c_{H_2O} = \frac{p_{H_2O}}{p} = \frac{nk\cdot T}{p}$$

Temperature
Pressure → Pressure broad. coefficient γ^0 → Line width

Experimental Setup:
⇨The laser beam (10.4 Hz or 139.8 Hz modulation frequency) is transmitted through a 24.5±0.1 cm long high pressure cell (pressure determined with Omega PAA33X-V-30 0-30 bar, cell temperature with type K thermoelement), captured by a photodiode (InGaAs ext.)
⇨The resulting signal is digitized with an fast A/D-converter (NI-PXI-5105 with 60 MS/s, 12 bit)

LASER CHARACTERIZATION (VCSEL)

⇨spectral integration requires transfer of the signal from time space to frequency space:

$$\frac{\partial\nu}{\partial t} \Leftrightarrow \frac{\partial\nu}{\partial I_{op.}}$$

⇨10cm air spaced etalon
⇨advanced fitting procedure

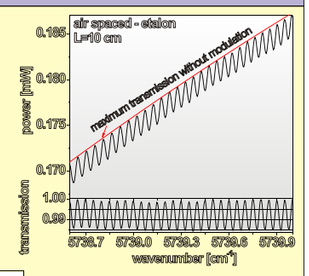

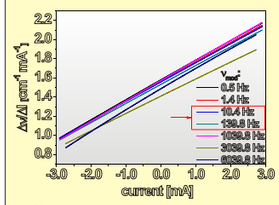

Dynamic wavelength tuning
⇨needed for abolute concentration
⇨wavelength tuning is nonlinear modulation frequency dependent
⇨sensitive to working point

Spectral axis validation
⇨needed for abolute concentration
⇨Doppler width [cm^{-1}]:
calculated: $1.994\cdot10^{-2}$
fit: $1.991\cdot10^{-2}$
⇨0.15% deviation
⇨very precise tuning measurement
⇨0.5% reproducibility

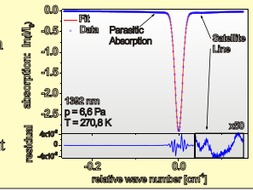

HCl LINE STRENGTH AND SELF BROADENING

⇨The line strength and the self broadening coefficient of the $H^{35}Cl$ R(3) absorption line was determined with pure HCl in a pressure range of 10 to 1000mbar at room temperature.

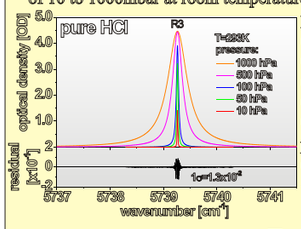

Line strength of $H^{35}Cl$ R(3)
⇨pure HCl (checked with FTIR)
⇨ν_{mod}: 10.4 Hz
⇨Voigt line shape model
⇨offset corrected10 scan average
⇨$S(T_0)$ can be calculated by l, T, p, c_{HCl} and integrated absorption
⇨$S(T_0)$=12.53(11)·10^{-21} $cm^{-2}/(cm^{-2}\cdot molec)$

Self broadening of $H^{35}Cl$ R(3)
⇨Gauß width linked to gas temperature
⇨Lorentz width floating
⇨pressure dependence of Lorentz width delivers γ^0_{HCl} by (with s=0.5):

$$\gamma_L = \gamma^0_{HCl}\, p\left(\frac{T_0}{T}\right)^s$$

⇨offset 56 (11) MHz describes laser line width
⇨γ^0_{HCl}=0.021787 (61) cm^{-1}/atm

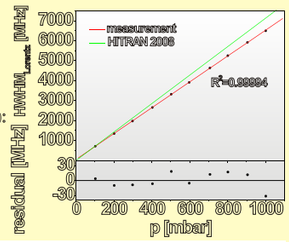

	S_0 [10^{-21} $cm^{-1}/(cm^{-2}\cdot molec)$]	γ^0_{HCl} [cm^{-1} atm^{-1}]
our measurement	12.53 (11)	0.21787 (61) (0-1000mbar)
DeRosa et al. [1]	12.6	0.2171 (0-150mbar)
HITRAN 2008	11.60	0.241 (1-0 band only!)

HCl FOREIGN BROADENING: HE/AR

Foreign broadening HCl + He
⇨offset corrected 25 scan average
⇨3rd order polynom background fit
⇨Voigt multiline fit (HCl R3-R5)
⇨Gauß width linked to gas temp.
⇨Lorentz width floating
Optical resolution (1σ):
⇨$5.6\cdot10^{-4}$ OD ⇨S/N 1000
⇨pressure dependence of Lorentz width delivers γ^0_{He} by (with s=0.5):

$$\gamma_C = \gamma^0_{HCl}\, p_{HCl}\left(\frac{T_0}{T}\right)^s + \gamma^0_{He}\, p_{He}\left(\frac{T_0}{T}\right)^s$$

⇨offset: 29 (2) MHz
⇨γ^0_{He}=0.02113 (1) cm^{-1}/atm (296K)
⇨γ^0_{He}=0.0221 cm^{-1}/atm ($lit^{[1]}$) (0-1000 mbar)
⇨deviation $\gamma^0_{He}/\gamma^0_{He}(lit^{[1]})$: 4.4%
⇨first high pressure data!

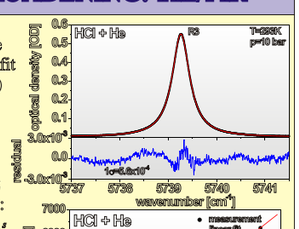

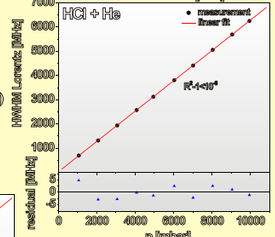

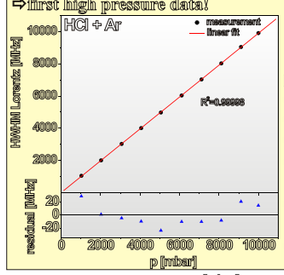

Foreign broadening HCl + Ar
⇨same measurement principle
⇨offset: -4 (12) MHz
⇨γ^0_{Ar}=0.03349 (6) cm^{-1}/atm (296K)
⇨γ^0_{Ar}=0.0342 cm^{-1}/atm ($lit^{[1]}$) (0-900 mbar)
⇨γ^0_{Ar}=0.0372 cm^{-1}/atm ($lit^{[2]}$) (FTIR, 10-50 bar)
⇨deviation $\gamma^0_{Ar}/\gamma^0_{Ar}(lit^{[2]})$: 10%

HCl FOREIGN BROADENING: O_2 AND N_2

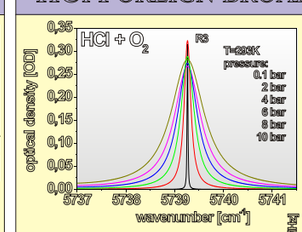

Foreign broadening HCl + O_2

⇨Voigt line fits from 0.1 to 10 bar

⇨offset: 4 (7) MHz
⇨γ^0_{O2}=0.03978 (6) cm^{-1}/atm (296K)
⇨γ^0_{O2}=0.0401 cm^{-1}/atm ($lit^{[1]}$) (0-840 mbar)
⇨deviation $\gamma^0_{O2}/\gamma^0_{O2}(lit^{[1]})$: 0.8%
⇨first high pressure data!

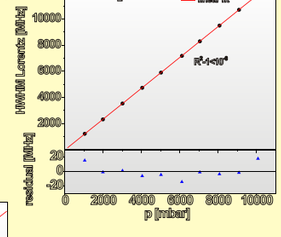

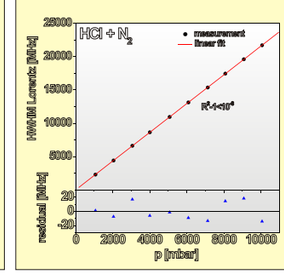

⇨offset: 9 (9) MHz
⇨γ^0_{N2}=0.07292 (5) cm^{-1}/atm (296K)
⇨γ^0_{N2}=0.0753 cm^{-1}/atm ($lit^{[1]}$) (0-470 mbar)
⇨deviation $\gamma^0_{N2}/\gamma^0_{N2}(lit^{[1]})$: 3.2%
⇨first high pressure data!

MULTILINE FIT AND ANALYSIS OF HCl DATA MEASURED WITH FTIR

FTIR data at different pressures

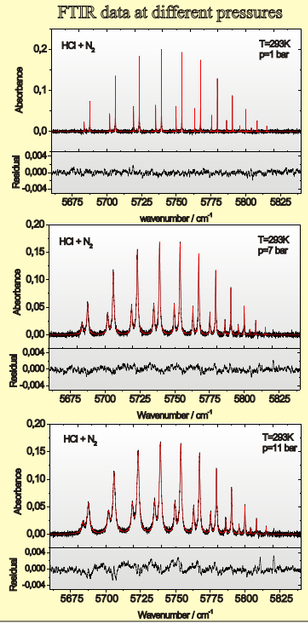

⇨Bruker Vertex 80
⇨fiber coupled measruement in a 24.5±0.1 cm long high pressure cell
⇨resolution 0.075cm-1
⇨simultaneous detection of whole bands
Optical resolution (1σ):
⇨$2.3\cdot10^{-3}$ OD ⇨S/N 75

Comparison FTIR vs laser-measurements:
⇨foreign broadening for the whole HCl R-branch (2-0)
⇨very good agreement between FTIR and 1.74µm VCSEL
⇨deviation γ^0_{N2}(VCSEL)/γ^0_{N2}(FTIR): 0.2%

Comparison FTIR vs literature for R(3) line:
⇨γ^0_{N2}=0.07306 (16) cm^{-1}/atm (296K)
⇨γ^0_{N2}=0.0753 cm^{-1}/atm ($lit^{[1]}$) (0-470 mbar)
⇨Deviation $\gamma^0_{N2}/\gamma^0_{N2}(lit^{[1]})$: 3%

HCl R-branch (2-0) FTIR vs HITRAN

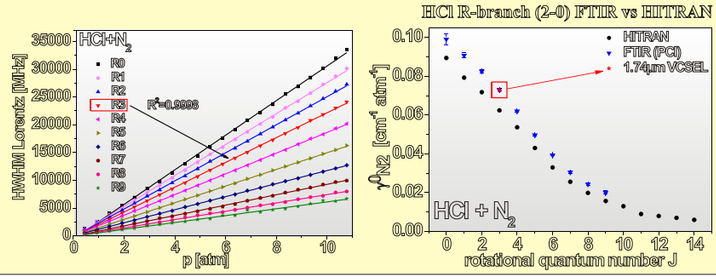

CONCLUSION AND OUTLOOK

Summary of the results:

	this paper	*De Rosa et al*
γ^0_{N2} [cm^{-1}/atm]	0.07292 (5)	0.07530 (60)
pressure range [MPa]	0.01 - 1	0.01 - 0.047
relative error [%]	0.07	0.8
relative deviation to this paper [%]	-	3.2
γ^0_{He} [cm^{-1}/atm]	0.02113 (1)	0.02210 (40)
pressure range [MPa]	0.01 - 1	0.026 – 0.1
relative error [%]	0.05	1.8
relative deviation to this paper [%]	-	4.4
γ^0_{O2} [cm^{-1}/atm]	0.03978 (6)	0.04010 (40)
pressure range [MPa]	0.01 - 1	0.023 – 0.084
relative error [%]	0.15	1
relative deviation to this paper [%]	-	0.8

H_2O linedata at 1370mm (low temperature study)

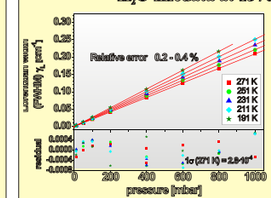

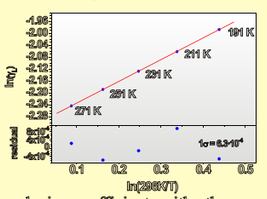

Further measurements of foreign broadening coefficients with other species such as CO, CO_2, H_2 and CH_4 are planed. Also a application of the HCl spectrometer in a high pressure gasification process.

[1] M. de Rosa et al. *Appl. Phys. B 72*, 245-248 (2001)
[2] C. Boulet et al. *J. Chem. Phys. 120*, 11053 (2004)

High-resolution spectroscopy of gases for industrial applications

Alexander Fateev* **and Sønnik Clausen**

*) e-mail: alfa@kt.dtu.dk

Optical Diagnostics Group,
DTU Chemical Engineering, Frederiksborgvej 399, Roskilde, DK-4000, Denmark

Keywords: high-resolution spectroscopy, gas cells, databases

High-resolution spectroscopy of gases is a powerful technique which has various fundamental and practical applications: *in situ* simultaneous measurements of gas temperature and gas composition, radiative transfer modeling, validation of existing and developing of new databases and etc. Existing databases (e.g. HITRAN, HITEMP or CDSD) can normally be used for absorption spectra calculations at limited temperature/pressure ranges. Therefore experimental measurements of absorption/transmission spectra gases (e.g. CO_2, H_2O or SO_2) at high-resolution and elevated temperatures are essential both for analysis of complex experimental data and further development of the databases.

High-temperature gas cell facilities available at DTU Chemical Engineering are presented and described. The gas cells and high-resolution spectrometers allow us to perform high-quality reference measurements of gases relevant to, for example, atmospheric research, combustion and gasification. Some high-temperature, high-resolution IR/UV absorption/transmission measurements gases (e.g. CO_2, SO_2, SO_3 and phenol) are presented.

DTU Chemical Engineering
Department of Chemical and Biochemical Engineering

High-resolution spectroscopy of gases for industrial applications

Alexander Fateev and Sønnik Clausen

Optical Diagnostics Group, DTU Chemical Engineering, Frederiksborgvej 399, Roskilde, DK-4000, Denmark

Abstract

High-resolution spectroscopy of gases is a powerful technique which has various fundamental and practical applications: *in situ* simultaneous measurements of gas temperature and gas composition, radiative transfer modeling, validation of existing and developing of new databases and etc. Existing databases (e.g. HITRAN, HITEMP or CDSD) can normally be used for absorption spectra calculations at limited temperature/pressure ranges. Therefore experimental measurements of absorption/transmission spectra gases (e.g. CO_2, H_2O or SO_2) at high-resolution and elevated temperatures are essential both for analysis of complex experimental data and further development of the databases.

High-temperature gas cell facilities available at DTU Chemical Engineering are presented and described. The gas cells and high-resolution spectrometers allow us to perform high-quality reference measurements of gases relevant to, for example, atmospheric research, combustion and gasification. Some high-temperature, high-resolution IR/UV absorption/transmission measurements gases (e.g. CO_2, SO_2, SO_3 and phenol) are presented.

Gas cells with highly-uniform temperature profiles (+/-0.5C).

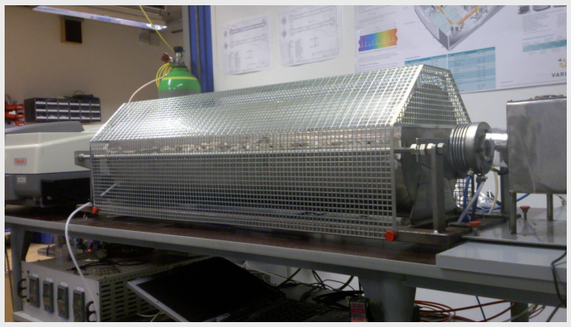


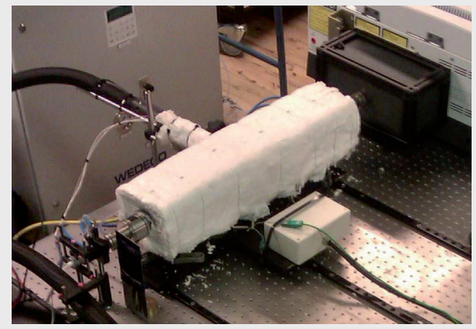

- 3-zones flow gas cells: from UV to IR;
- With/without internal (solid) windows;
- Highly-stable uniform T-profile (0.5C);
- T_{max} = 1600C L=33-53 cm P=1-4 bar

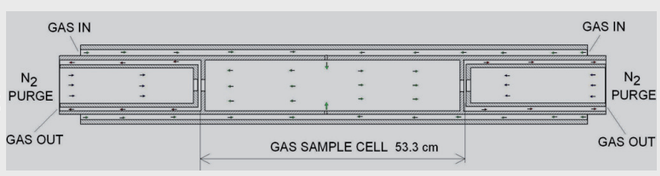

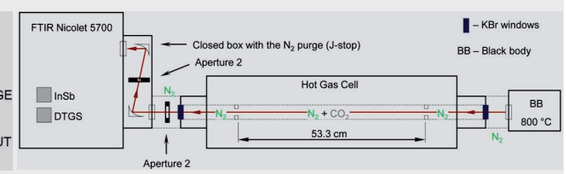

Examples: from database validation/development (e.g. SO_2/SO_3 DTU/UCL) to applications (combustion, gasification)

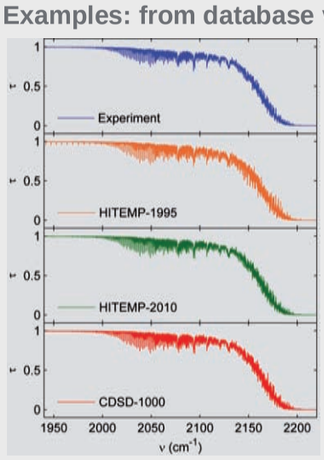

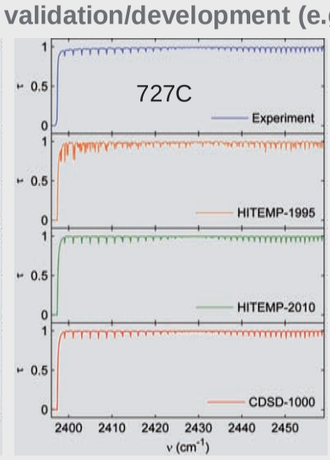

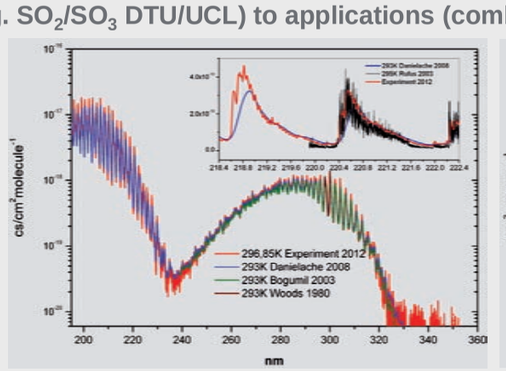

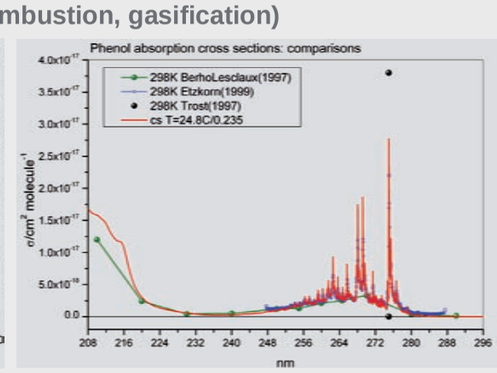

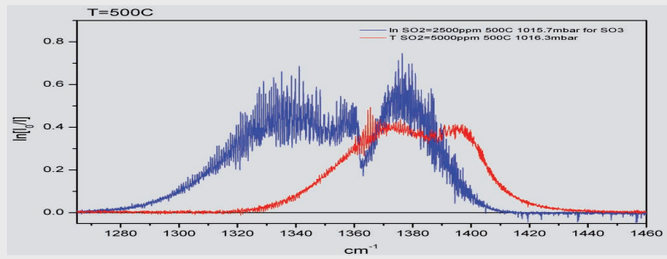

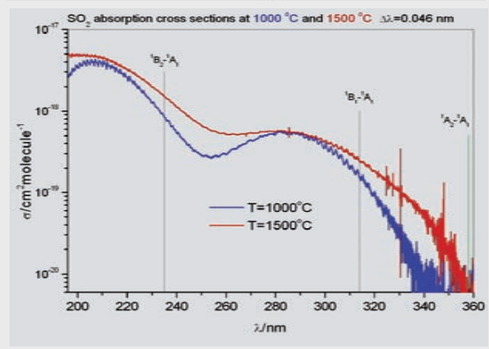

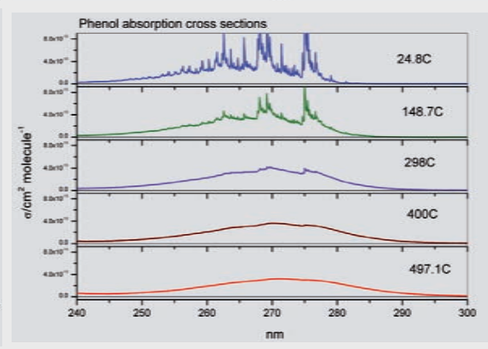

Acknowledgements: Energinet.dk, projects No. 2011-1-10622, 2010-1-10422

Quantum state selective detection of molecular chlorine by high-resolution cavity ring-down spectroscopy

Thomas Forsting, Ignacio Vespoli, and Christof Maul
Institut für Physikalische und Theoretische Chemie, TU Braunschweig,
Hans-Sommer-Str. 10, 38106 Braunschweig, GERMANY

State resolved detection of nascent products of chemical reactions and/or photodissociation provides valuable information about the dynamics of the underlying elementary processes. Molecular chlorine is of particular interest with respect to is role in atmospheric chemistry, however, detailed studies have remained scarce due to the lack of suitable optical detection methods.

The weak rovibrational bands in the visible absorption spectrum of molecular chlorine have been reexamined in the region of 485 – 505 nm at room temperature with the highest instrumental resolution yet known (0.001 nm). Due to the small absorption cross-sections of about 10^{-21} to 10^{-22} cm^2 in this region a method of very high sensitivity needs to be employed: Cavity Ring-Down (CRD) Spectroscopy. Absorption spectra are presented that were obtained via a Cavity Ring-Down cell with a XeCl excimer laser pumped dye-laser as pulsed light-source and a photo-multiplier tube as detector.

The resulting absorption spectrum shows rotationally resolved bands of the spin-forbidden transition $B^3\Pi(0_u^+) \leftarrow X^1\Sigma_g^+$. A rovibrational analysis of the observed bands is performed and takes into account that chorine occurs in three isotopomers $^{35}Cl_2$, $^{35}Cl^{37}Cl$ and $^{37}Cl_2$ with the natural abundances of 57.4 %, 36.7 % and 5.9 % respectively.

Altogether we present CRD Spectroscopy as a powerful and yet very easy method to obtain high resolution gas-phase absorption spectra of species with very low absorption cross-sections. The current detection limit is of the order of 10^{15} cm^{-3}. The results are a proof of concept as well as a preliminary stage to carry out chemical reactions with in situ detection of gaseous reaction products.

Technische Universität Braunschweig

Institut für Physikalische und Theoretische Chemie

Teaching an old dog new tricks: Quantum state selective detection of molecular chlorine by high-resolution cavity ring-down spectroscopy

Thomas Forsting, Ignacio Vespoli, Christof Maul
Technische Universität Braunschweig | Institut für Physikalische und Theoretische Chemie
t.forsting@tu-braunschweig.de | Telefon +49 (0) 531 391-5345

Introduction

State resolved detection of nascent products of chemical reactions and/or photodissociation provides valuable information about the dynamics of the underlying elementary processes. Due to the lack of suitable optical detection methods molecular elimination processes of the diatomic halogens have only rarely been studied.[1, 2] For chlorine in particular no such data exist up to date.

A promising candidate for state-specific detection of molecular chlorine as nascent photoproducts from an elementary chemical reaction is the (spin-forbidden) transition $B^3\Pi(o_u^+) \leftarrow X^1\Sigma_g^+$. Its weak, rovibrationally resolved bands lie in the visible range with absorption cross-sections of about 10^{-21} to 10^{-22} cm².[3]

Background Information

general principle of cavity ring-down (CRD) spectroscopy[4]:

highly sensitive | intensity indepedent | suitable for all type of molecules

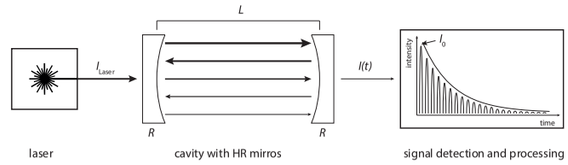

$I_0 = I_{Laser}\, T^2\, e^{-\alpha d}$ with: $T = 1 - R$ | $I(t) = I_0 \exp\left(-\frac{t\,c}{L}(1 - R + \alpha\, d)\right)$ | $\alpha(\nu) = \sigma(\nu)\,\frac{N}{V} = \frac{L}{d}\left(\frac{1}{c\,\tau(\nu)} - \frac{1}{c\,\tau_0(\nu)}\right)$

potential energy curves of chlorine [5]:

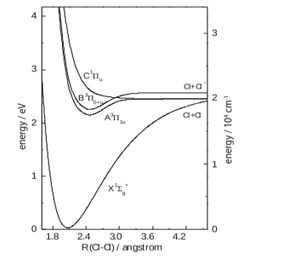

Experimental Setup and Results

general scheme of our CRD-setup:

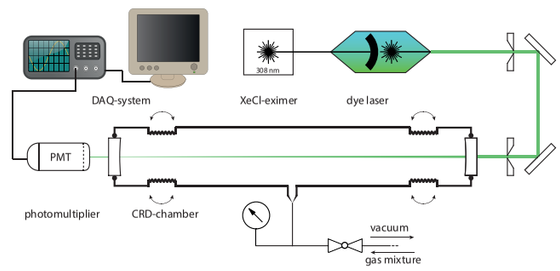

experimental parameters of the CRD-chamber:
temperature: T = r. t. (approx. 298 K)
gas mixture pressure: p = 10.5 mbar Cl_2 in He (1 atm)
mirror reflectivity R = 0.9998

fitted ring-down signal:

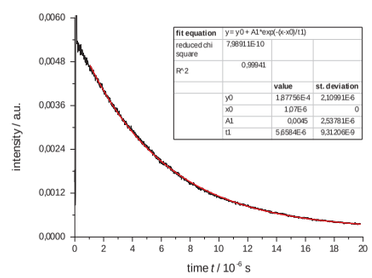

experimental parameters of the DAQ-system:
horizontal resolution: 600 MHz
vertical resolution: 8 bit
trigger frequency: 50 Hz

comparison of measured and simulated data:

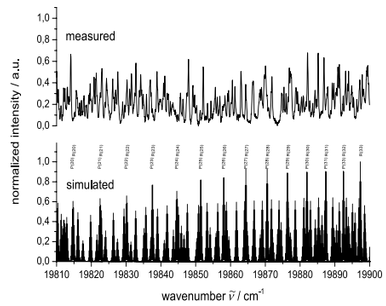

$B^3\Pi(o_u^+)\,(v' = 12) \leftarrow X^1\Sigma_g^+(v'' = 0)$

We present experimentally observed and simulated spectra both taking into account the natural abundance of the three isotopologues $^{35}Cl_2$, $^{35}Cl^{37}Cl$ and $^{37}Cl_2$ of 57.4 %, 36.7 % and 5.9 % respectively.

Simulation was carried out in PGOPHER[6] with spectroscopic constants taken from [7] and [8].

Peak assignment of measured data is still in progress.

Discussion and Conclusion

semi-empirical caculation of the complete absorption spectrum of Cl_2.[9]

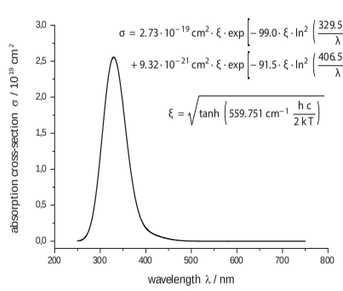

Cl_2-absorption spectrum with broadband technique (resolution: 0.04 nm)[9]

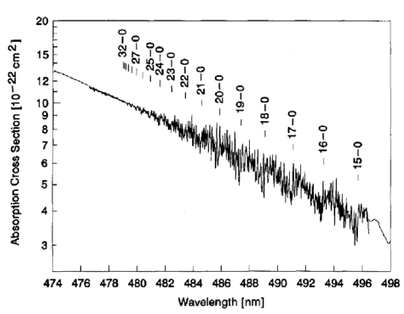

detail of our recorded spectrum with CRD spectroscopy (resolution: 0.001 nm)

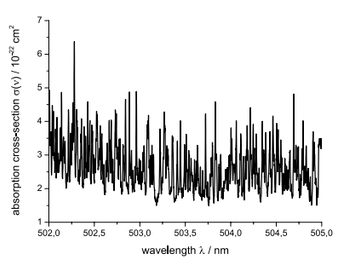

Cl_2-absorption spectrum with BBCEAS (broad band cavity enhanced absorption spectroscopy) (resolution: 0.36 nm)[3]

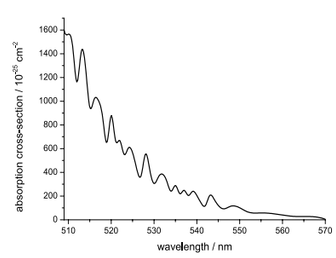

We show that CRD spectroscopy is a powerful and yet very easy method to obtain high resolution gas-phase absorption spectra of species with very low absorption cross-sections. The current detection limit is of the order of 10^{14} cm^{-3}. The results are a proof of concept and as well as a preliminary stage to carry out chemical reactions with in situ detection of gaseous reaction products and can compete with known absorption cross-sections while enhancing the spectral resolution about factor 40 compared to [9].

[1] P.-Y. Wei, Y.-P. Chang, Y.-S. Lee, W.-B. Lee, and K.-C. Lin, J. Chem. Phys. 126, 034311 (2007)
[2] S.-Y. Chen, P.-Y. Tsai, H.-C. Lin, C.-C. Wu, K.-C. Lin, B.J. Sun, and A.H.H. Chang, , J. Chem. Phys. 134, 034315 (2011)
[3] I.A.K. Young, C. Murray, C.M. Blaum, R.A. Cox, R.L. Jones, and F.D. Pope, Phys. Chem. Chem. Phys. 13, 15318 (2011)
[4] G. Berden, R. Engeln: Cavity ring-down spectroscopy. Techniques and applications. Chichester: Wiley (2009)
[5] D. Zhang, A. Abdel-hafiez, B. Zhang, Chem. Phys. Lett. 428, 49 (2006).
[6] Western, C. M.: PGOPHER. A Program for Simulating Rotational Structure. University of Bristol (2010) (http://pgopher.chm.bris.ac.uk)
[7] G. Herzberg, K. P. Huber: Constants of Diatomic Molecules. New York, London: Van Nostrand Reinhold (1979)
[8] J. A. Coxon, J. Mol. Spec. 82, 264 (1980)
[9] D. Maric, J. P. Burrows, R. Meller, and G. K. Moortgat, J. Photochem. Photobiol. A: Chem. 70, 205 (1993)

TOWARDS ACCURATE DETERMINATION OF MOLECULAR LINE STRENGTHS – EXEMPLIFIED BY ACETYLENE

J. Hald, L. Nielsen, and J. C. Petersen

Danish Fundamental Metrology, Matematiktorvet 307, DK-2800 Kongens Lyngby, Denmark

Towards Accurate Determination of Molecular Line Strengths – Exemplified by Acetylene

Danish Fundamental Metrology
www.dfm.dtu.dk

Jan Hald, Lars Nielsen, and Jan C. Petersen

Introduction:

- Accurate spectral line data are important for quantitative spectroscopic monitoring of climate and environment.
- The integrated line area is an essential parameter for determination of spectral line data.
- Two possible strategies: Numerical integration
  Line fitting
- Challenges in numerical integration:
  background/baseline variations and noise,
  finite integration limits.
- Challenges in line fitting:
  accuracy of semi-empirical models (e.g. unknown molecular perturbations)

Theory:

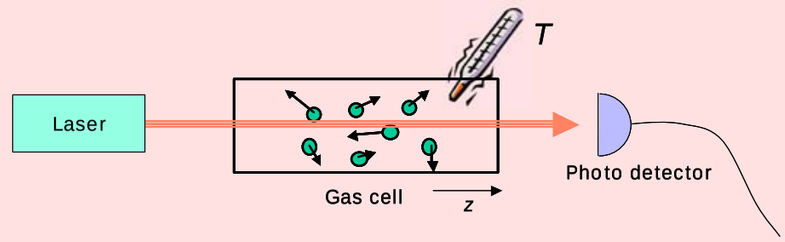

Maxwell velocity distribution:

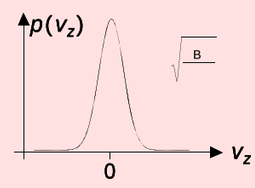

Laser transmission:

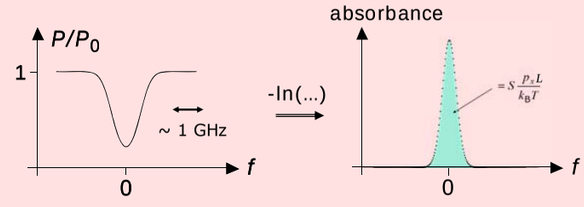

Experiment:

- Molecule: ^{13}C acetylene ($^{13}C_2H_2$) P(16) line at 1542.3837 nm.
- Master laser: fiber laser stabilized to $^{13}C_2H_2$ saturated absorption signal
- Slave laser: offset locked fiber laser. $u(f_i) < 1$ kHz ~ $4 \cdot 10^{-6}\ \Delta f_D$
- Active intensity stabilization. $u(P_i)/P_0 \sim 2 \cdot 10^{-5}$
- Preliminary experiments in a glass cell.
- Detector linearity is essential, first measurements indicate 10^{-5} or better.

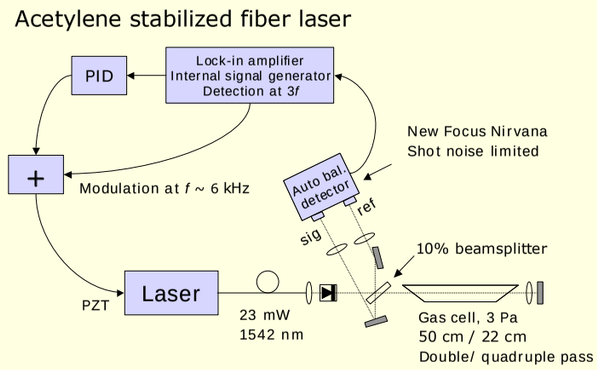

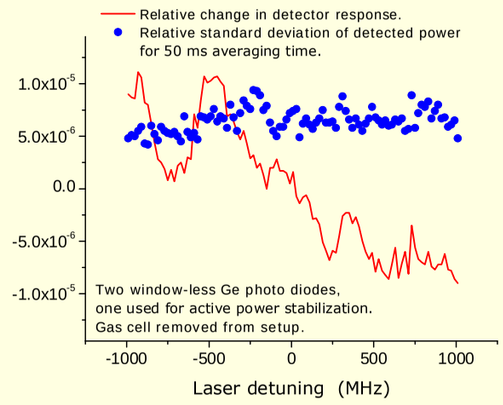

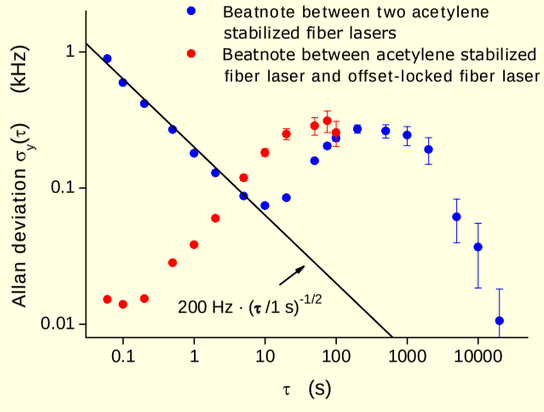

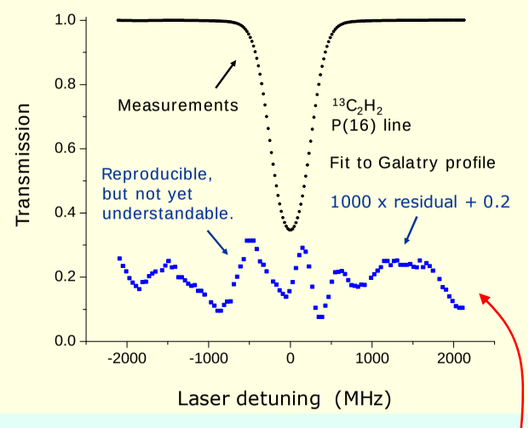

Analysis – derivation of line area:

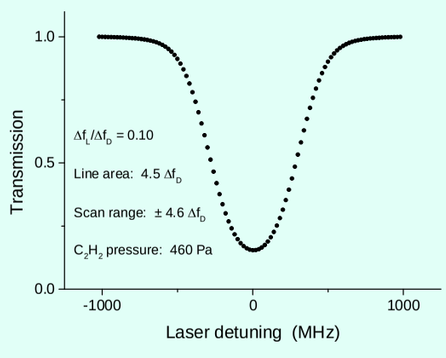

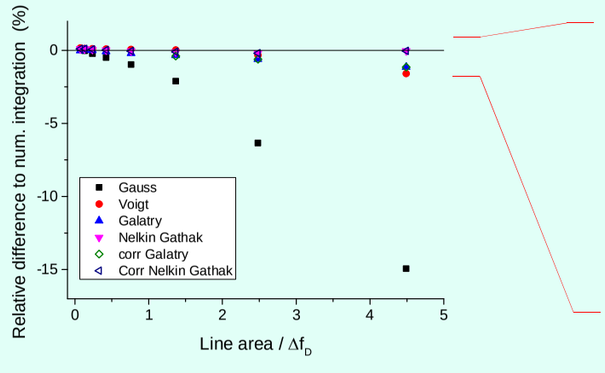

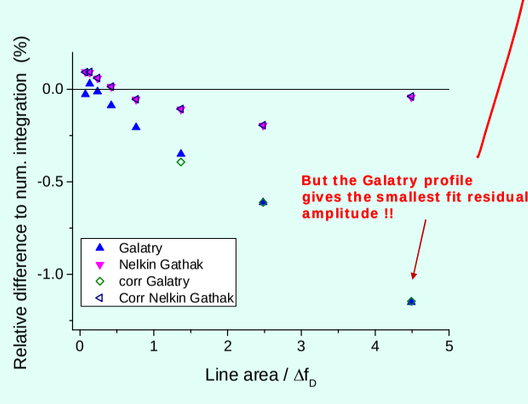

- Numerical integration is corrected for 'missing' area outside scan range using an estimate based on a Voigt model.
- Correction is 3.3 % at highest pressure (460 Pa) and scales close to linearly with pressure

The Identification and Quantification of Greenhouse Gas Point Source Emissions Using Cavity Ring-Down Spectroscopy, Complementary to Other Techniques

Graham Leggett[1], Tom Gardiner[2], Rod Robinson[2]

[1] Tiger Optics LLC, 250 Titus Avenue, Warrington, PA 18976-2426, USA
[2] National Physical Laboratory, Hampton Road, Teddington, Middlesex, TW11 0LW, United Kingdom

The provision of robust, accurate, stable, and mobile instrumentation for the determination of key greenhouse gases (GHGs) in ambient air is essential for assessing the emissions of these species from anthropogenic sources such as landfill sites, industrial processes, and agricultural facilities, for the purpose of process optimisation and carbon accounting activities. We report the details of a study where a commercial cavity ring-down spectroscopy (CRDS) based analyser (Tiger Optics Tiger-i 2000) has been developed to complement the measurement of point source emissions of greenhouse gases using more established techniques such as open-path FTIR and Differential Absorption LIDAR (DIAL). We give an introduction to the CRDS technique, its application to GHG measurements, and wider applications of the technique relevant to the environmental sector. We demonstrate that cavity ring-down spectroscopy provides a reliable, fast response, calibration-free, relatively low-cost option for the identification of point sources and the subsequent quantification of emitted greenhouse gases. We show how the technology provides the appropriate sensitivity in order to determine the output of gases at some distance from the emission source, and also the dynamic range to allow effective measurements of localised sources within the site of interest.

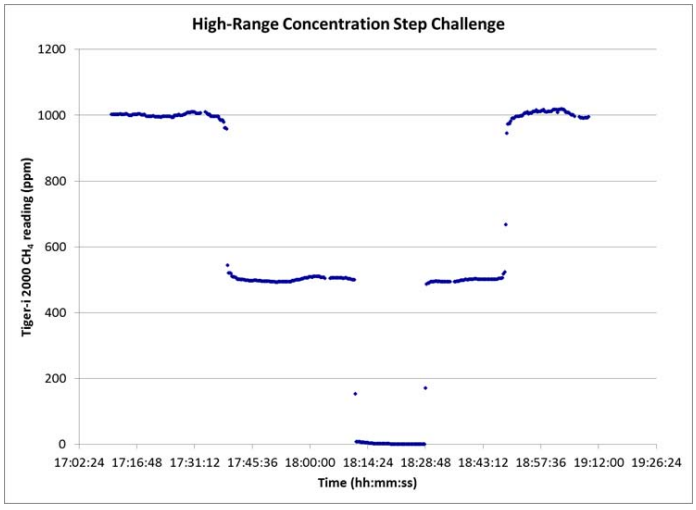

Figure 1. Tiger-i 2000 response to high concentration CH_4 intrusion.

The Identification and Quantification of Greenhouse Gas Point Source Emissions Using Cavity Ring-Down Spectroscopy, Complementary to Other Techniques

Graham Leggett - Tiger Optics
Tom Gardiner, Rod Robinson - National Physical Laboratory, UK

Greenhouse Gases – Focus on Methane

- GWP 21 times that of CO_2
- Atmospheric lifetime ~12 years
- CH_4 concentrations have more than doubled since pre-industrial times: 700 ppb > 1780 ppb
- More than half from anthropogenic sources
- Complex system of sources and sinks

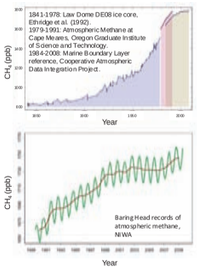

Sources of Atmospheric Methane

- Natural gas systems – Fugitive emissions
- Wetlands and landfill
  - Bacterial decomposition of organic materials under anaerobic conditions via fermentation and hydrogenotrophic methanogenesis
  - $H_3C\text{-}COOH \rightarrow CH_4 + CO_2$
  - $4H_2 + CO_2 \rightarrow CH_4 + 2H_2O$
- Mining
- Agriculture
  - Ruminant animals
  - Rice cultivation

National Physical Laboratory – Capabilities

NPL – Open-Path FTIR and DIAL

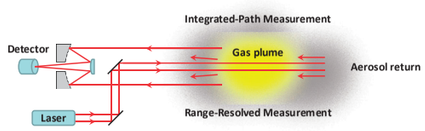

CW CRDS Technology

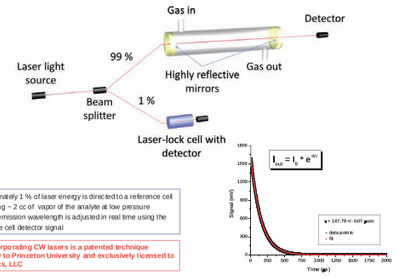

- Approximately 1 % of laser energy is directed to a reference cell containing ~ 2 cc of vapor of the analyte at low pressure
- Laser's emission wavelength is adjusted in real time using the reference cell detector signal

CRDS incorporating CW lasers is a patented technique proprietary to Princeton University and exclusively licensed to Tiger Optics, LLC

CW CRDS Technology

First Measurement: $\tau_{zero} = \dfrac{d}{c(1-R)}$

Second Measurement: $\tau(\nu) = \dfrac{d}{c(1-R+\sigma(\nu)Nd)}$

Calculate Concentration: $N = \dfrac{1}{c\,\sigma(\nu)}\left(\dfrac{1}{\tau(\nu)} - \dfrac{1}{\tau_{zero}}\right)$

Ringdown Time vs. Wavelength

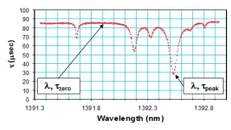

c-speed of light
d-cell length
R-reflectivity of mirror
N-molecular density (concentration)
σ-absorption cross section*
τ- ring-down time
n-laser frequency

*From NIST

Features and Benefits of CRDS Technology

- Accuracy traceable to the world's major national reference labs
- Specificity – no ozone or other interferences
- Sub-ppb detection capability
- No need for span calibrations
- No periodic sensor replacement/maintenance
- Fast speed of response
- Superior sensitivity
- Wide dynamic range
- Easy installation & simple operation

Available species

- HF
- HCN
- HCl
- H_2S
- H_2O
- N_2O
- NH_3
- PH_3
- AsH_3
- CO
- CO_2
- CH_4
- C_2H_2
- C_2H_4
- C_3H_6
- O_2

Features and Benefits of CRDS Technology

Linearity

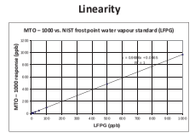

Speed of response

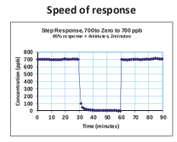

Sensitivity

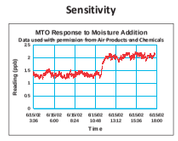

Long-term stability

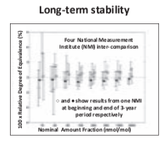

Methane Instrument Development

- Dynamic range 0 – 1000 ppm
- LDL ~10 ppb
- Sensitivity ~5 ppb
- Accuracy +/- 4 % or 1*LDL
- Operating temperature 10 °C – 40 °C
- Half standard rack width
- External sample pump

Tiger-i 2000

Methane Instrument Development

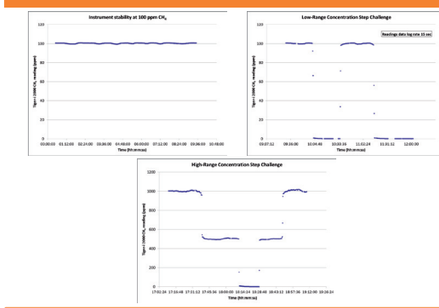

Future Work with NPL

- Laboratory validation work
  - Comparison with gravimetric gas standards
  - Tiger-i 2000 comparison with open-path FTIR using standard atmosphere generator
  - Nafion dryer performance
- Field studies
  - Tiger-i 2000 complementary to open-path FTIR and DIAL

NPL National Physical Laboratory

Tigeroptics

Acknowledgements

- I would like to thank my colleagues at Tiger Optics for the technical information contained in this presentation. This poster presents just a brief summary of the result of many years of development work, which continues with pace as we respond to customer demands and look forward to making our contribution to the improvement of our environment. Particular thanks to Lisa Bergson (CEO), Jerry Riddle (President), Yu Chen, Erika Coyne, Hongbing Chen, and the many others who have made their contribution to Tiger Optics' success.

- Email : gleggett@tigeroptics.com
- Telephone : +44 1865 522951
- Mobile: +44 7715 676751
- www.tigeroptics.com
- twitter.com/Tiger_Optics

- Thanks also to National Physical Laboratory, UK; Mr Tom Gardiner and Mr Rod Robinson.

www.npl.co.uk/environmental-measurement/

Tigeroptics

NEW MEASUREMENTS AND ANALYSES OF LINE POSITIONS AND INTENSITIES OF CH_3D IN THE INFRARED

A. Nikitin[1], L. Brown[2], K. Sung[2], M. A. Smith[4], A. Mantz[5], X. Thomas[3], L. Regalia[3], L. Daumont[3], R. Kochanov[3,1], M. Rey[3], and V. Tyuterev[3]

[1] Laboratory of Theoretical Spectroscopy, V.E. Zuev Institute of Atmospheric Optics, SB RAS, Academician Zuev square, 634021, Tomsk, Russia
[2] Jet Propulsion Laboratory, California Institute of Technology, 4800 Oak Grove Drive, Pasadena, CA 91109, USA
[3] Groupe de Spectrométrie Moléculaire et Atmosphérique, UMR CNRS 7331, Université de Reims Champagne Ardenne, Moulin de la Housse, BP 1039-51687 REIMS Cedex 2, France
[4] Science Directorate, NASA Langley Research Center, Hampton, VA 23681, USA
[5] Dept. of Physics, Astronomy and Geophysics, Connecticut College, 270 Mohegan Avenue, New London, CT 06320, USA

Recently a new study of $^{12}CH_3D$ line positions and intensities of strong and medium lines has been performed for the upper portion of the Enneadecad polyad between 4000 and 4550 cm^{-1}. For this, FTIR spectra were recorded with D-enriched methane samples: one at 80 K with a Bruker 125 IFS at 0.005 cm^{-1} resolution, 3.35 Torr with path length 0.2 m at the Jet Propulsion Laboratory in Pasadena and two others at 291 K with the McMath-Pierce FTS at 0.011 cm^{-1} resolution, 0.72 and 4.88 Torr with path length 2.39 m at the Kitt Peak National Observatory in Tucson. Line positions and intensities were retrieved by least square curve-fitting procedures and analyzed using the effective Hamiltonian and the effective Dipole moment expressed in terms of irreducible tensors operators adapted to symmetric top molecules. Combining the two temperature datasets confirmed the assumed quantum assignments and also demonstrated the relative accuracies to be better than ±0.0002 cm^{-1} for line positions and at least ±6% for ~1160 selected features. Including additional assignments from the room temperature spectra alone permitted 1362 line intensities of 12 bands (involving 23 vibrational symmetry components) to be reproduced with an RMS of 9%. Over 4085 selected positions for 12 bands were modeled to 0.008 cm^{-1}. In order to extend the knowledge of $^{12}CH_3D$ weak lines, new long path FTS measurements are recorded in Reims between 1850 and 9200 cm^{-1} at 290 K, 2.58 Torr with path lengths of 201, 302 and 1603 m. In this work we focus particularly on the full spectral range of this polyad (3300-4550 cm^{-1}). The aim is to complete the previous study by intensity measurements of lines corresponding to higher J transitions and to improve the modelling in the 3300-4000 cm^{-1} range using new theoretical predictions for band centers and resonance coupling parameters.

New measurements and analyses of line positions and intensities of CH_3D in the infrared

A. Nikitin[1], L. Brown[2], K. Sung[2], M. A. Smith[4], A. Mantz[5]
X. Thomas[3], L. Regalia[3], L. Daumont[3], R. Kochanov[3,1], M. Rey[3] and V. Tyuterev[3]

1. **Laboratory of Theoretical Spectroscopy,** V.E. Zuev Institute of Atmospheric Optics, SB RAS, Academician Zuev square, **634021, Tomsk, Russia**
2. **Jet Propulsion Laboratory,** California Institute of Technology, 4800 Oak Grove Drive, Pasadena, **CA 91109, USA**
3. **Groupe de Spectrométrie Moléculaire et Atmosphérique,** UMR CNRS 7331, Université de Reims Champagne Ardenne, Moulin de la Housse, **BP 1039-51687 REIMS Cedex 2, France**
4. **Science Directorate, NASA Langley Research Center,** Hampton, **VA 23681, USA**
5. **Dept. of Physics, Astronomy and Geophysics,** Connecticut College, 270 Mohegan Avenue, New London, **CT 06320, USA**

Abstract

Recently a new study of $^{12}CH_3D$ line positions and intensities of strong and medium lines has been performed for the upper portion of the Enneadecad polyad between 4000 and 4550 cm^{-1} [1]. For this, FTIR spectra were recorded with D-enriched methane samples: one at 80 K with a Bruker 125 IFS at 0.005 cm^{-1} resolution, 3.35 Torr with path length 0.2 m at the Jet Propulsion Laboratory in Pasadena and two others at 291 K with the McMath-Pierce FTS at 0.011 cm^{-1} resolution, 0.72 and 4.88 Torr with path length 2.39 m at the Kitt Peak National Observatory in Tucson. Line positions and intensities were retrieved by least square curve-fitting procedures and analyzed using the effective Hamiltonian and the effective Dipole moment expressed in terms of irreducible tensors operators adapted to symmetric top molecules. Combining the two temperature datasets confirmed the assumed quantum assignments and also demonstrated the relative accuracies to be better than ±0.0002 cm^{-1} for line positions and at least ±6% for ~1160 selected features. Including additional assignments from the room temperature spectra alone permitted 1362 line intensities of 12 bands (involving 23 vibrational symmetry components) to be reproduced with an RMS of 9%. Over 4085 selected positions for 12 bands were modeled to 0.008 cm^{-1} [1].

In order to extend the knowledge of $^{12}CH_3D$ weak lines, new long path FTS measurements are recorded in Reims between 1850 and 9200 cm^{-1} at 290 K, 2.58 Torr with path lengths of 201, 302 and 1603 m. In this work we focus particularly on the full spectral range of this polyad (3300-4550 cm^{-1}). The aim is to complete the previous study [1] by intensity measurements of lines corresponding to higher J transitions and to improve the modelling in the 3300-4000 cm^{-1} range using new theoretical predictions for band centers and resonance coupling parameters.

CH_3D Vibrational States: polyads

Focus of this study
Upper part = Polyad3
12 bands,
23 sub-vibs

Enneadecad
19 vib. States!
a) Nonad:
3 fundamentals
+ 6 (overtone &combo)
b) Triad:
3 fundamentals
a) Nikitin et al. 2002
b)Nikitin et al. 2006

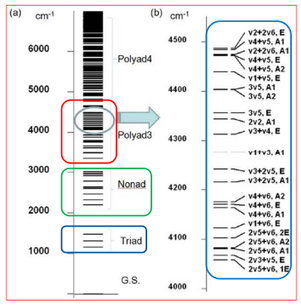

CH_3D Experimental Spectra

Table 1 Experimental conditions of the two FTIR laboratory spectra of CH_3D

Configurations/conditions	McMath Kitt Peak	Bruker125HR JPL
Light Source	Quartz-halogen	Tungsten lamp
Beam Splitter	CaF_2	CaF_2
Detector	InSb	InSb
Resolution (unapodized) (cm^{-1})	0.0118	0.005
Useable Band pass (cm^{-1})	1850 – 5500	3880 – 5000
Gas sample	CH_3D (^2D, 98%)	CH_3D (^2D, 99%)
Temperature (K)	291	80
Sample pressure (Torr)	0.72, 4.88	3.35
Gas absorption cell		
Path length (m)	2.39	0.2038
Cell windows	CaF2	ZnSe (wedged)
Vacuum box windows	(none: purged air path)	KBr (wedged)
Scanning time (hours)	1.1	3.5
Calibration standards & factor	CO [26] 1.00000020 (3)	H_2O [14] 0.999999842 (16)

Note: 1 atm = 760 Torr = 1013 hPa

CH_3D at 291 K and 80 K

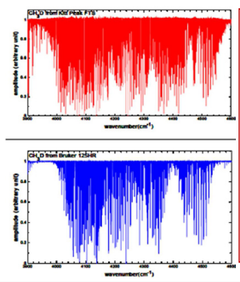

Kitt Peak FTS
2.4 m and 4.88 torr at 291 K
Used for Nonad (2002) and lower Enneadecad (2006)
Positions and intensities retrieved by Nikitin et al. With Reims-Tomsk software

JPL Bruker
0.204 m and 3.35 torr at 80 K
Positions and intensities retrieved by Brown with JPL software

Theoretical model

- A full six-order Effective Hamiltonian model up through the Polyad3 of CH3D accounting for the above resonance conditions contains **4310 symmetry-allowed terms**. In order to keep the number of adjusted parameters within reasonable bounds, the vibrationally off-diagonal terms are selected in a pragmatic.

This model can be called '*close neighbors Effective Hamiltonian*' because only diagonal parameters and interaction parameters among neighboring vibrational states within the polyads are adjusted, while all interaction parameters of distant vibrational states are set to zero.

- The effective ro-vibrational Hamiltonian adapted to the polyad structure of the CH3D molecule is expressed as:

$$H = H_{\{GS\}} + H_{\{Triad\}} + H_{\{Nonad\}} + H_{\{Polyad\ 3\}}$$

- Each group contains a series of terms identified by rotational, vibrational and symmetry indices according to the general nomenclature

$$t^{\Omega(K,kC)}_{n_1 n_2 n_3 n_4 n_5 n_6 m_1 m_2 m_3 m_4 m_5 m_6} T^{\Omega(K,kC)}_{n_1 n_2 n_3 n_4 n_5 n_6 m_1 m_2 m_3 m_4 m_5 m_6}$$

- **The Effective Hamiltonian of the Nonad augmented by diagonal terms of Polyad3 is used as the initial model**

The Enneadecad of CH_3D

Prior *Ennea* work
Nikitin 2006
3250 – 3700 cm^{-1}
for outer planets

Predicted upper state levels by extrapolating ro-vibrational constants from Triad and Nonad.

Ulenikov et al. 2010
(assigned positions of 33 *Ennea* sub-vibs)
Using cold data from Zurich FTS

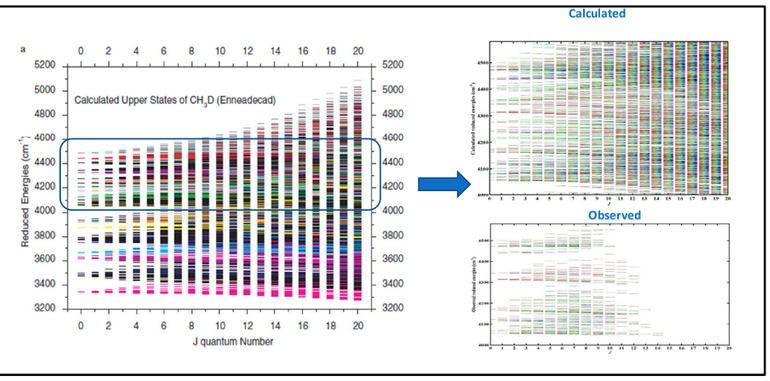

Modeling CH_3D Enneadecad intensities

Long path spectra @ room T, 2.5 torr with 200, 600 and 1600 m absorption path length (Reims 50 m cell).

TF:
max MOPD=3m

+

Long cell:
50 m base long

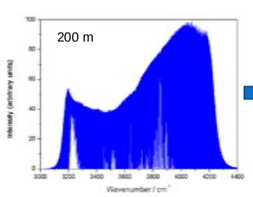

Predictions

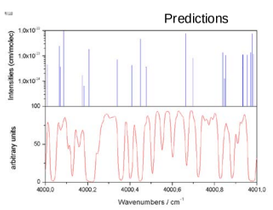

Obs/JPL.(top) & Calc. (bottom) CH_3D Log (intensity) vs cm^{-1}

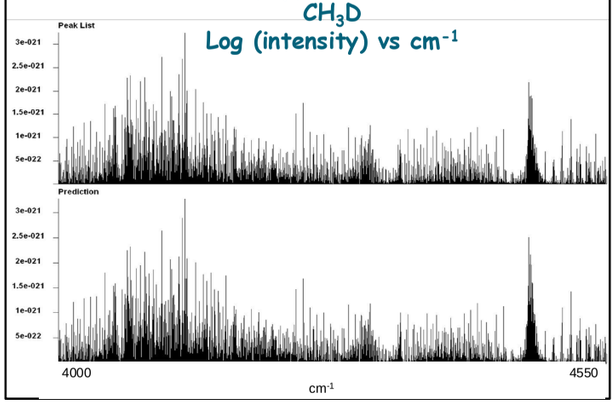

Lower Ennea: previous 2006 analysis

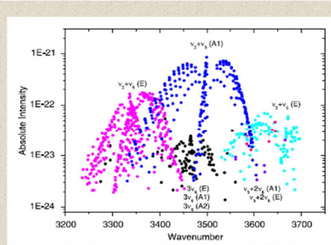

Lower Ennea: Nikitin et al. 2006 **measured and modeled 874 intensities of 6 bands**

New goal:
Measure more intensities and provide initial prediction for the Upper Ennea (Polyad3)

Upper Ennea: NEW 2012 analysis!

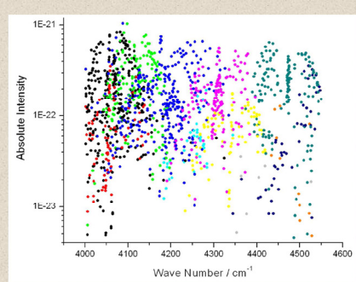

$(2v_5+v_6)$
$(2v_3+v_5)$
(v_1+v_6)
(v_4+v_6)
(v_3+2v_5)
(v_3+v_4)
$(2v_5)$
$(3v_5)$
(v_1+v_5)
(v_4+v_5)
(v_2+2v_6)

Average CH_3D intensities: (80 K-JPL) + (291 K Tomsk)

Obs Pos cm^{-1}	quanta* J'' C'' α''	J' C' α'	E'' cm^{-1}	E'obs(v+E'') cm^{-1}	S_{abs}(296 K) cm/molecule	Averaged %rms
4050.931106	2 E 1	1 E 28	24.649117	4075.580223	5.343E-23	.
4066.449698	1 E 1	1 E 28	9.130579	4075.580277	7.056E-23	.
4103.031972	2 A1 1	1 A2 19	23.279194	4126.311166	6.512E-23	.
4126.311111	0 A1 1	1 A2 19	0.000000	4126.311292	1.861E-22	2.1
4112.752281	6 E 1	5 E 127	164.240403	4276.992774	5.392E-23	0.3
4126.414250	5 E 1	5 E 127	150.578239	4276.992489	7.671E-23	2.0
4193.936614	4 E 2	5 E 127	83.056222	4276.992836	9.333E-23	3.6
4079.934893	6 E 4	5 E 127	197.057437	4276.992450	3.024E-22	0.5
4145.772883	7 A1 1	7 A2 87	229.404232	4375.177115	1.143E-22	.
4096.075326	8 A1 1	7 A2 87	279.101330	4375.177512	6.068E-23	1.9
4212.302061	8 A1 1	7 A2 87	162.875088	4375.177363	7.902E-23	2.0
4156.055376	9 E 2	9 E 213	354.230581	4510.286206	9.970E-23	0.2
4225.737777	8 E 2	9 E 213	284.548935	4510.286235	3.884E-23	2.9
4229.823556	8 E 1	9 E 213	280.462997	4510.286418	9.407E-23	1.8
4167.196358	13 A2 1	14 A1 115	704.460648	4871.657006	8.776E-23	.
4155.126082	13 E 3	14 E 232	726.049202	4881.175284	6.513E-23	.

Σ Line Strengths: 11 CH_3D bands

Vibrational Bands	Σ intensities calc at 296 K	#param Ω=0	#param Ω=1	# lines fitted
$2v_5+v_6$ E	2.1 E-20	1	0	83
$2v_5+v_6$ A_1, A_2, 1E, 2E	13.0 E-20	3	2	288
v_1+v_6 E	7.8 E-20	1	1	155
v_4+v_6 A_1, A_2, E	12.0 E-20	2	5	319
v_4+2v_5 A_1, E	1.1 E-20	2	4	41
v_3+v_5 E	5.9 E-20	1	2	161
$2v_5$ A_1	1.5 E-20	1	0	85
$3v_5$ A_1, A_2, E	0.7 E-20	1	0	8
v_4+v_5 E	1.7 E-20	1	2	44
v_4+v_5 A_1, A_2, E	8.6 E-20	2	3	167
v_2+2v_6 A_1, E	0.6 E-20	1	0	11

CH_3D Vibrational sublevels	Center obs (cm^{-1})	Number of fitted positions	St. Dev (10^{-3} cm^{-1})	# fitted intensities	St.Dev (%)
$2v_5+v_6$ 1E	4058.69288	399	1.05	215	7.3
$2v_3+v_5$ E	4067.85425	251	6.70	83	8.8
$2v_5+v_6$ A_1	4081.32898	114	7.57	21	12.7
$2v_5+v_6$ A_2		48	7.75	11	12.3
$2v_5+v_6$ 2E	4102.43880	175	7.39	41	11.5
v_1+v_6 E	4122.58929	290	1.08	155	9.1
v_4+v_6 A_1	4163.49100	237	5.55	90	9.3
v_4+v_6 E	4170.35959	439	6.11	201	6.7
v_4+v_6 A_2		109	6.73	28	9.2
v_3+2v_5 A_1	4215.28429	104	8.89	32	8.1
v_3+2v_5 E	4241.74412	190	6.53	9	14.2
v_1+v_3 A_1		0		0	
v_3+v_4 E	4313.42477	387	9.08	161	7.8
$2v_5$ A_1	4344.12459	178	4.93	85	6.8
$3v_5$ E	4356.88614	180	7.13	7	25.4
$3v_5$ A_2		0		0	
$3v_5$ A_1	4404.35936	25	8.52	1	6.6
v_4+v_5 E	4439.73017	253	8.68	44	13.3
v_4+v_5 A_2		104	1.54	14	19.0
v_1+v_5 E	4472.64849	352	7.73	140	10.5
v_2+2v_6 A_1		34	6.93	4	14.6
v_4+v_5 A_1	4484.82316	131	6.31	13	14.3
v_2+2v_5 E	4486.88302	85	9.16	7	14.9

LINE STRENGTHS AND COLLISIONAL BROADENING COEFFICIENTS OF CO_2 (@2 µm) AND H_2O (@2.7 µm), TRACEABILITY AND UNCERTAINTY ASSESSMENT

J. Nwaboh, A. Pogány, O. Werhahn, V. Ebert

Physikalisch-Technische Bundesanstalt, Bundesallee 100, 38116 Braunschweig, Germany

EUMETRISPEC Stakeholder Workshop, 14-16. November 2012, Braunschweig

Line strengths and collisional broadening coefficients of CO_2 (@2 µm) and H_2O (@2.7 µm), traceability and uncertainty assessment

EMRP
European Metrology Research Programme
Programme of EURAMET
The EMRP is jointly funded by the EMRP participating countries within EURAMET and the European Union

J. Nwaboh*, A. Pogány, O. Werhahn, V. Ebert
Corresponding author, e-mail: volker.ebert@ptb.de
Physikalisch-Technische Bundesanstalt, Bundesallee 100, 38116 Braunschweig (DE)

Introduction

-Line strengths and broadening coefficients are used as input parameters for climate change and radiation transfer models in atmospheric science.

-The line strengths of CO_2 and H_2O, for instance, are used to quantify molecular species in gas analysis application such as environmental monitoring and breath analysis [1].

-Up to now, the relative uncertainties of the majority of, e.g., CO_2 line data are in the 2–5% range [2].

-In some cases, line data uncertainties in literature are even larger than 10 %, undefined, or simply unreported.

-The application of metrological principles like the GUM [3] and the traceability of measured line data has been sparsely realized [4].

Experimental set-up

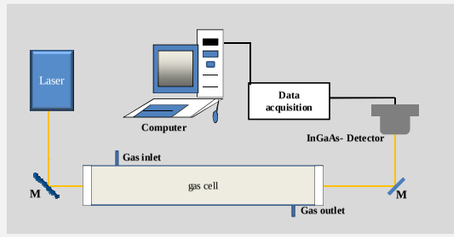

Light source
- DFB diode lasers: 2.004 µm (CO_2), 2.763 µm (H_2O)
- swept at 139 Hz in a spectral window of ~2 cm^{-1} across a molecular transitions by current modulation

Gas cell
- single pass gas cells (L = 0.2 m, L =0.05 m), total pressure (p) varied between 4-1000 hPa

Detector
-InGaAs photodiode (λ: 1.2 - 2.6 µm, d = 0.5 mm)
-InAs photodiode (λ: 1 - 3.4 µm, d = 1 mm)

Concept

From the Beer-Lambert law, the line strength S_T is given by,

$$S_T = \frac{A_{\mathrm{Line}} \cdot k_B \cdot T}{x_{\mathrm{species}} \cdot p \cdot L}$$ → Line strength at gas temperature T

$$\Rightarrow A_{Line} = S_T \cdot \chi,$$ ← Linear function of the line area (A_{Line}) vs χ

$$\text{where } \chi = \frac{x_{\mathrm{species}} \cdot p \cdot L}{(k_B \cdot T)}$$

k_B: Boltzmann constant
x_{Species}: amount fraction of gas species

-The variation in χ is mostly related to the variation in the total gas pressure.
-The value of the line strength is traceable if all input quantities such as the gas pressure and temperature are traceable.

Typical data, line strength derivation

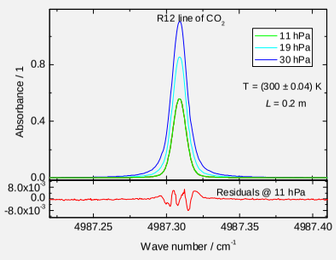

The absorption line is recorded at different pressures.

The line area is determined by fitting a Voigt profile to the measured data.

The derived line area is plotted as a function of χ and S_T (R(12)) is determined by means of a generalized linear regression.

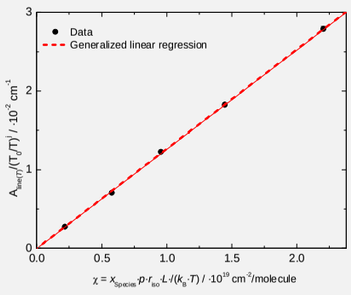

Self and air boadening coefficients

Model: $\Delta\tilde{\nu}_L = 2 \cdot p_{CO2} \cdot \gamma_{CO2} \left(\frac{T_0}{T}\right)^n + 2 \cdot p_{\mathrm{col.\ partner}} \cdot \gamma_{\mathrm{col.\ partner}} \left(\frac{T_0}{T}\right)^n$

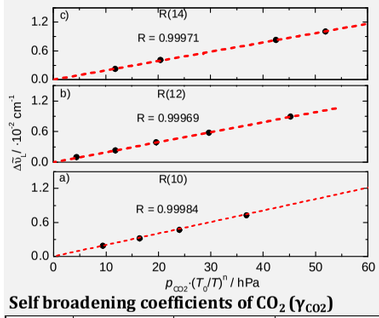

Plot of the lorentzian ($\Delta\nu_L$) line width as a function of the partial pressure of CO_2 (n =0.5).

Self broadening coefficients of CO_2 (γ_{CO2})

Line	Wave number / cm^{-1}	$\gamma_{CO2MEAS}$ / ·10^{-3} cm^{-1}/atm	$\gamma_{CO2HITRAN}$ [2] / ·10^{-3} cm^{-1}/atm	$\lvert E_n \rvert$
R10	4985.93	104.8 ± 0.4	109.0 ± 2.1	1.9
R12	4987.31	99.4 ± 1.9	105.0 ± 2.0	2.0
R14	4988.65	96.9 ± 2.2	103.0 ± 2.0	2.1

Air (0.79 γ_{N2} +0.21 γ_{O2}) broadening coefficients of CO_2 (γ_{air})

Line	Wave number / cm^{-1}	$\gamma_{airMeas}$ / 10^{-3} cm^{-1}/atm	$\gamma_{AirHITRAN}$ [2] / 10^{-3} cm^{-1}/atm	$\lvert E_n \rvert$
R10	4985.93	78.1 ± 2.4	79.9±1.5	0.6
R12	4987.31	77.7 ± 2.6	78.0±1.5	0.1
R14	4988.65	76.9 ± 4.4	76.5±1.5	0.1

Uncertainty assessment

Typical uncertainty contribution of the individual input parameters to the uncertainty of the measured line strength.
Example at 9.5 hPa pressure in case of R(10) line of CO_2 at 4985.93 cm^{-1}.

Quantity	Value	Standard uncertainty	Relative standard uncertainty / %	Relative contribution to the uncertainty of S_T / %
L	0.20 m	$2.5 \cdot 10^{-9}$ cm	$1.25 \cdot 10^{-6}$	0.0
T	299.39 K	0 .50 K	0.16	5.0
p	9.480 hPa	0.028 hPa	0.29	15.5
r_{iso}	1	$4.06 \cdot 10^{-3}$	0.41	29.3
A_{line}	0.00498 cm^{-1}	$26.5 \cdot 10^{-6}$ cm^{-1}	0.53	50.2
S_T	$1.10 \cdot 10^{-21}$ $cm^{-1}/(cm^{-2} \cdot molecule)$	$8.14 \cdot 10^{-24}$ $cm^{-1}/(cm^{-2} \cdot molecule)$	0.7	

Note: Only the most significant uncertaity contributions to the uncertainty of S_T are presented. Input quantities such as the Boltzmann and the Planck constant are omitted

Line strength results

Molec.	Line	Wave number	S This work(S_{dir}) U_{rel} ±1.6 % range	S HITRAN08 [2] U_{rel} ±1.9 % range	$\lvert E_n \rvert$ HITRAN 08 [2]	S Casa et al. [5] U_{rel} ±0.1 % range	$\lvert E_n \rvert$ Casa et al. [5]	S Toth et al. [6] U_{rel} ±1.0 % range	$\lvert E_n \rvert$ Toth et al [6]	S Regalia et al. [7] U_{rel} ±3.2 % range	$\lvert E_n \rvert$ Regalia et al. [7]	S Padilla et al. [8] U_{rel} ±1.0 % range	$\lvert E_n \rvert$ Padilla et al. [8]
CO_2	R10	4985.93	1.115 ± 0.012	1.127±0.021	0.5	1.1366±0.0012	1.7	1.119±0.008	0.3	-	-	-	-
CO_2	R12	4987.31	1.251 ± 0.017	1.222±0.023	0.9	1.2344±0.0014	0.9	1.222±0.012	0.9	1.23±0.04	0.5	1.255±0.0145	0.2
CO_2	R14	4988.65	1.293 ± 0.014	1.275±0.024	0.6	1.2889±0.0013	0.2	-	-	1.30±0.03	0.2	-	-
H_2O	423-522	3619.61	73.550 ± 1.41	83.51±15.03	0.6	-	-	-	-	-	-	.	-

Measured line strengths (S x 10^{-21} ·cm^{-1}/(cm^{-2}·molecule)). U_{rel} : expanded uncertainty, k=2.

Normalized error (E_n)

$$|E_n| = \left|\frac{D}{U(D)}\right| = \left|\frac{S - S_{dir}}{2\sqrt{u^2(x) + u^2(x_{ref})}}\right|$$

Where, S_{dir} and S are the line strengths of this work and from literature, respectively. The quantity $u(S)$ and $u(S_{dir})$ are the standard uncertainties of the line strengths. If $|E_n| < 1$, the two values (i.e., S_{dir} and S) agree with each other. For $|E_n| > 1$, the two values do not agree with each other.

Conclusions

-The guidelines of the GUM were followed while deriving the line parameters of CO_2 and H_2O.
-The relative standard uncertainties of the self and air broadening coefficients are in the ±1.1 % and ±2.8 % range, respectively.
-The relative standard uncertainties of all line strength figures are in ±0.8 % range.

References

[1] J. Nwaboh, O. Werhahn, P. Ortwein, D. Schiel, V. Ebert, *Meas. Sci. Technol. (2012), in press.*
[2] HITRAN2008, http://www.cfa.harvard.edu/HITRAN/, L. Rothman et al., *J. Quant. Spectrosc. Rad. Transf.* vol. 110, pp. 533 (2009).
[3] ISO Guide 98-3, Guide to the Expression of Uncertainty in Measurement, 1. International Organization for Standardization, Geneva 2008, ISBN 9267101889.
[4] L. S. Rothman, N. Jacquinet-Husson, C. Boulet, and A. M. Perrin, *C. R. Physique*, vol. 6, pp. 897-907, (2005).
[5] G. Casa, R. Wehr, A. Castrillo, E. Fasci, and L. Gianfrani, *J. Chem. Phys.*, vol. 130, pp. 184306, (2009).
[6] R. A. Toth, L. R. Brown, C. E. Miller, V. Malathy Devi, and D. Chris Benner, *J. Mol. Spectrosc.*, vol. 239, pp. 221, (2006).
[7] Régalia-Jarlot, V. Zeninari, B. Parvitte, A. Grossel, X. Thomas, P. von der Heyden, and G. Durry, *J. Quant. Spectrosc. Radiat. Transf.*, vol. 101, pp. 325, (2006).
[8] G. J. Padilla-Viquez, J. Koelliker-Delgado, O. Werhahn, K. Jousten, and D. Schiel, *IEEE Trans. Instr. Measur. J.*, vol. 56, pp. 529-533 (2007).

Acknowledgements

The authors acknowledge financial support and collaboration in iMERA-plus and EMRP projects Breath Analyis, MACPoll and GAS (ENG01). The EMRP is jointly funded by the EMRP participating countries within EURAMET and the European Union. The work received funding from the European Union Framework Programme, ERA-NET Plus, under the iMERA-Plus Project–Grant Agreement No. 217257.

Towards traceability in CO_2 spectroscopic line parameter measurements using tunable diode laser absorption spectroscopy

Andrea Pogany, Javis A. Nwaboh, Olav Werhahn, Volker Ebert

Physikalisch-Technische Bundesanstalt, Bundesallee 100, 38116 Braunschweig, Germany, andrea.pogany@ptb.de, javis.nwaboh@ptb.de, olav.werhahn@ptb.de, volker.ebert@ptb.de

Tunable diode laser absorption spectroscopy (TDLAS) is a measurement technique with exceptionally high spectral resolution in the range of 10^{-4} cm^{-1} and therefore is highly interesting for accurate measurements of molecular spectral line parameters, like line strengths or pressure broadening coefficients[1]. Based on such data TDLAS enables absolute measurements and traceability, which ensures reliability and comparability of results.

We are aiming at traceable line parameter measurements by means of TDLAS[2,3]. Such spectroscopic line parameters are frequently measured by Fourier-transform infrared spectroscopy (FTIR) or other broadband techniques to derive data for a whole multifold of lines. Results are collected in databases that are typically used for concentration determinations. A recent project, e.g., aims at traceable spectral line data for atmospheric monitoring using traceable FTIR spectroscopy[4]. FTIR provides extremely wide spectral coverage, however at the price of a limited spectral resolution of 10^{-2} to 10^{-3} cm^{-1}. TDLAS-based high resolution spectral anchor points are beneficial in order to validate and increase the reliability of FTIR measurements.

We have measured the strength of a number of CO_2 lines between 2 and 3 µm employing TDLAS. Traceability of the measured line strength values requires traceability of all input parameters, namely the gas temperature and pressure, the concentration and isotopic composition of the measured species in the gas sample, the optical path length, as well as the line area. Thus we discuss the question of traceability in case of each of these parameters. We present the retrieved line strength values together with an uncertainty assessment referring to the ISO-GUM, identifying critical parameters influencing the accuracy of the resulting line strength. Finally, we compare the measured line strength values to literature data. This work was initiated within the framework of the European project MACPoll[5], devoted to air pollutant and gas purity measurements.

References

[1] P. Ortwein, W. Woiwode, S. Wagner, M. Gisi, V. Ebert, Appl. Phys. B **100**, 341-347, 2010

[2] G. J. Padilla-Viquez, J. Koelliker-Delgado, O. Werhahn, K. Jousten, D. Schiel, IEEE Trans. on Instr. Meas. **56**, 529-533, 2007

[3] G. Wübbeler, G. J. Padilla-Viquez, K. Jousten, O. Werhahn, C. Elster, J. Chem. Phys. **135**, 204304, 2011

[4] EUMETRISPEC Spectral reference data for atmospheric monitoring, http://www.eumetrispec.org/emrp/eumetrispec-home.html

[5] Metrology for Chemical Pollutants in Air (MACPoll), http://www. macpoll.eu

Towards traceability in CO_2 line strength measurements at 2.7 µm using tunable diode laser absorption spectroscopy

EMRP
European Metrology Research Programme
Programme of EURAMET
The EMRP is jointly funded by the EMRP participating countries within EURAMET and the European Union

A. Pogány, J. Nwaboh, O. Werhahn, V. Ebert*
*Corresponding author, e-mail: volker.ebert@ptb.de
Physikalisch-Technische Bundesanstalt, Bundesallee 100, 38116 Braunschweig (DE)

Motivation

Traceability:
– links measurement results to a standard (SI units) through an unbroken chain of calibrations
→ ***guarantees reliability of the results***
– each step contains uncertainty assessment using the internationally accepted method (GUM [1])
→ ***ensures comparability of the results***

Traceable line parameters are necessary to achieve traceability in absolute concentration measurements.

Advantages of tunable diode laser absorption spectroscopy (TDLAS) in line strength measurements:

- ***absolute measurement***
- ***high spectral resolution with a relatively simple set-up***
- ***potential of traceability [2]***

Experimental set-up

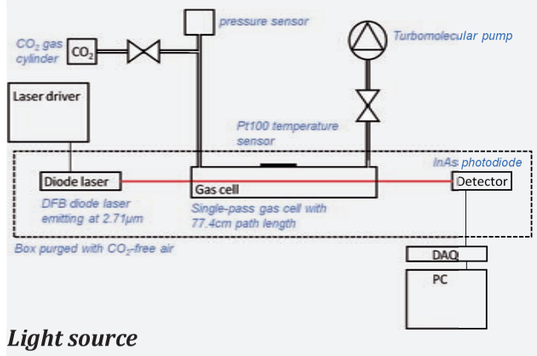

Light source
- DFB diode laser emitting at 2.715 µm
- swept at 139.8 Hz in a spectral window of ~1.5 cm^{-1} across the P36e line of the $\nu_1+\nu_3$ band of CO_2 at $\tilde{\nu}$=3682.77 cm^{-1} by current modulation

Gas cell
- Single pass cell (L = 0.774 m), total pressure varied between 0.15 and 0.5 hPa,

Detector
- InAs photodiode (λ: 1 – 3.4 µm, d = 1 mm)

Measurement method

Tunable
Diode
Laser
Absorption
Spectroscopy

Measurement of spectral absorbance

$$A(\tilde{\nu}) = -\ln\left(\frac{\Phi(\tilde{\nu})}{\Phi_0(\tilde{\nu})}\right)$$

Derivation of the line area

$$A_{\text{line}} = \int A(\tilde{\nu})\,d\tilde{\nu}$$

Input parameters measured during (p, T) or determined before the measurement (L, S)

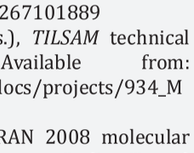

Calculation of the line strength

$$S_T = \frac{A_{\text{line}} \cdot k_B \cdot T}{x_{CO_2} \cdot L \cdot p \cdot r_{\text{iso}}}$$

A: absorbance
A_{line}: line area
x_{CO2}: CO_2 concentration
k_B: Boltzmann constant
T: temperature
S_T: line strength
L: path length of the cell
p: total pressure
r_{iso}: correction factor for isotopic composition

Typical measured data

The line area is determined by fitting a Voigt profile to the measured data.

Several measurements have been carried out at room temperature (294-296K), at different pressures between 0.15 and 0.5 hPa.

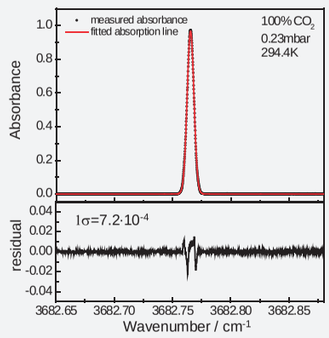

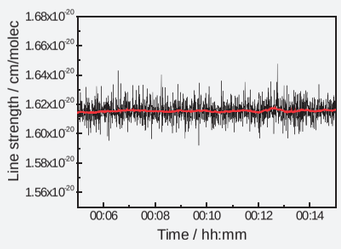

S=1.616·10⁻²⁰
σ=5.9·10⁻²³ (0.37% rel.)
can be further decreased by averaging, e.g. averaging 100 scans:
σ=1.1·10⁻²³ (0.07% rel.)

Results

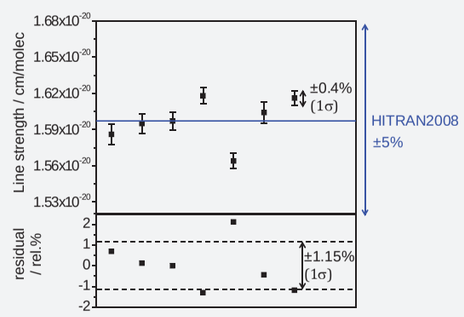

Measured data

S=1.597·10⁻²⁰ cm/molec
σ=1.9·10⁻²² cm/molec

HITRAN2008 database [3]

S_H=1.595 ·10⁻²⁰ cm/molec

Expanded uncertainty (coverage factor of 95%):
2σ=3.8·10⁻²² cm^{-1}/molec cm^{-2} (2.3% rel.)

2-5% relative

Uncertainty assessment

Typical uncertainty contribution of the individual input parameters to the uncertainty of the measured line strength.
Example at 0.33 hPa pressure.

Quantity	Value	Expanded uncertainty	Relative expanded uncertainty
T	296.05 K	0.48 K	0.16%
p	0.3398 hPa	0.0006 hPa	0.26%
L	0.774 m	0.002 m	0.26%
r_{iso}	1	0.0017	0.17%*
x_{CO2}	1	0.00005	0.005%*
A_{line}	0.01047 cm^{-1}	0.00021	2.3%*
S_0	**1.629·10⁻²⁰ cm^{-1}/molec·cm^{-2}**	**0.033·10⁻²⁰ cm^{-1}/molec·cm^{-2}**	**2.3%**

*estimated uncertainty

Traceability

Challenging, due to a number of influencing factors, e.g. detector linearity, determination of the wavenumber axis, fitting the line profile function.

Traceability has been achieved by using calibrated sensors

$$S_T = \frac{T \cdot k_B \cdot A_{\text{line}}}{p \cdot x_{CO_2} \cdot L \cdot r_{\text{iso}}}$$

Natural abundance of the isotopes [4] was supposed.

CO_2 concentration in the gas cylinder was not proved, as well as CO_2 concentration in the gas cell might change due to leakage.

Path length of single pass cells can be determined relatively easily. Traceability was achieved by calibration using a reference cell.

Conclusion and outlook

Results:

- Line strength of a CO_2 line at 2715.35 nm has been measured
- Traceability was achieved for: T, p, L
- The line area has the major contribution to the final uncertainty
- The measured line strength agrees with the value given in the HITRAN2008 database

Outlook:

- Decreasing uncertainty by identifying and eliminating systematic errors (statistical uncertainty of A_{line} is well below 1%)
- Traceability of r_{iso}, x and A_{line}
- Complete uncertainty assessment
- Comparison to FTIR measurements
- Application of the method to other lines, other analytes

References

[1] ISO Guide to the Expression of Uncertainty in Measurement, 1. International Organization for Standardization, Geneva 2008, ISBN 9267101889
[2] O. Werhahn, J. C. Petersen (eds.), *TILSAM* technical protocol V1_2010-09-29. Available from: http://www.euramet.org/fileadmin/docs/projects/934_METCHEM_Interim_Report.pdf
[3] L. S. Rothman et. al., "The HITRAN 2008 molecular spectroscopic database," J. Quant. Spectrosc. Radiat. Transf. 110(9-10), 533-572 (2009).
[4] M. Berglund, M.E. Wieser, Pure Appl. Chem., Vol. 83, No. 2, pp. 397–410, 2011

Acknowledgement

The authors acknowledge financial support and collaboration in iMERA-plus and EMRP projects Breath Analyis, MACPoll and GAS. The EMRP is jointly funded by the EMRP participating countries within EURAMET and the European Union. The work received funding from the European Union Framework Programme, ERA-NET Plus, under the iMERA-Plus Project–Grant Agreement No. 217257.

Development of a VDI guideline for passive FTIR measurements in the atmosphere

K. Schäfer*[1], R. Harig[2], T. Blumenstock[3], N. Höfert[4], K. Weber[5]
[1]Karlsruhe Institute of Technology, IMK-IFU, Kreuzeckbahnstr. 19, 82467 Garmisch-Partenkirchen (D)
e-mail: klaus.schaefer@kit.edu
[2]Bruker Optik GmbH, Remote Sensing and Gas Analysis, Rudolf-Plank-Str. 27, 76275 Ettlingen (D)
[3]Karlsruhe Institute of Technology, IMK-ASF, Hermann-von-Helmholtz-Platz 1, 76344 Eggenstein-Leopoldshafen (D)
[4]Verein Deutscher Ingenieure, Commission on Air Pollution Prevention of VDI und DIN, VDI-Platz 1, 40468 Düsseldorf (D)
[5]University of Applied Sciences Düsseldorf, Georg-Glock-Str. 19, 40474 Düsseldorf (D)

The passive FTIR technique is based on the original radiation of gases and aerosols in the atmosphere depending from their own temperature as well as the natural radiation sources as the sun. Such infrared radiation measurements can be applied for the determination of atmospheric composition, detection of air pollutants and calculation of emission source strengths. This remote sensing method offers some important advantages over the in situ techniques: low operational costs, ease of handling, online measurements, possibility of re-analysis without affecting the data source (measured spectra), no extractive sampling, thus avoiding any chemical changes which may occur within the probe and extraction system before reaching analytical equipment, avoids contamination of measurement equipment by dangerous substances and reduces risk of damage of exhaust emitters as e.g. turbines.
The determination of the spatial distribution of concentrations of compounds in the atmosphere is important for the detection of pollutants as well as harmful emissions and allows the validation of numerical simulations of physical and chemical processes. Originated by these motivations a VDI guideline for passive FTIR spectrometry is under development. The main content of this guideline is the following:

- Basics of the measurement technique
  Principles for the detection of gaseous clouds and exhaust composition, radiative transfer model, radiative temperature, noise equivalent column density and detection limits.
- Measurement systems
  Fourier transform spectroscopy, Michelson interferometers, measurement configurations, spectrometers with one detector element, scanning systems, scanning imaging systems, spectrometers with a detector array, measurement settings.
- Calibration
  Error sources, disturbances and limits of measurements, radiometric calibration, system calibration.

The guideline includes the following applications also:

- Remote sensing of gases at ambient temperature
  Basics, identification of gases, quantifications, application examples.
- Remote sensing of gases at high temperatures (smoke stacks, aircraft engine exhausts, flares)
  Basics, quantification of gas temperature, quantification of composition, application examples.
- Remote sensing of gases by means of solar radiation
  Basics, measurement performance, data analyses, application examples.

The number of the guideline is 4211 and the title is “Remote sensing – Atmospheric measurements using passive FTIR spectroscopy – Emission and ambient air measurements”. A first draft is available. The further work will incorporate the description of different application cases of the measurement methods. Future application of passive FTIR technique will depend from:

- Accuracy of spectral line data which influences the detection limits of this method for single compounds as well as the determination of interferences of mixtures of compounds and thus the accuracy of this method.
- Availability of spectral line data of compounds of gaseous emissions of anthropogenic and natural origin.
- Availability of spectral line data of such compounds at high temperatures which are important for certain emissions and combustion processes.

Karlsruhe Institute of Technology

Institute of Meteorology and Climate Research
Department Atmospheric Environmental Research
Kreuzeckbahnstraße 19
82467 Garmisch-Partenkirchen
Internetadresse: http://imk-ifu.kit.edu

Fachhochschule Düsseldorf
University of Applied Science

Development of a VDI guideline for passive FTIR measurements in the atmosphere

Klaus Schäfer[a], Roland Harig[b], Thomas Blumenstock[c], Norbert Höfert[d], Konradin Weber[e]

[a]Karlsruhe Institute of Technology, Institute of Meteorology and Climate Research, Department of Atmospheric Environmental Research (IMK-IFU), Garmisch-Partenkirchen, Germany
[b]Bruker Optik GmbH, Remote Sensing and Gas Analysis, Ettlingen, Germany
[c]Karlsruhe Institute of Technology, Institute of Meteorology and Climate Research, Department of Atmospheric Trace Gases and Remote Sensing (IMK-ASF), Eggenstein-Leopoldshafen, Germany
[d]Verein Deutscher Ingenieure, Commission on Air Pollution Prevention of VDI und DIN, Düsseldorf, Germany
[e]University of Applied Science Düsseldorf, Düsseldorf, Germany

Basis is either the **own radiation** of gases and aerosols in the atmosphere depending from their temperature or natural radiation sources as the **sun**. Such infrared radiation measurements can be applied for the determination of atmospheric composition, detection of air pollutants and calculation of emission source strengths.

Advantages in comparison to other measurement systems are:
- low operational costs,
- investigation of difficult accessible sites,
- online measurements,
- possibility of re-analysis without affecting the data source (measured spectra),
- no extractive sampling, thus avoiding any chemical changes which may occur within the probe and extraction system before reaching analytical equipment,
- avoids contamination of measurement equipment by dangerous substances, and
- reduces risk of damage of exhaust emitters as e.g. turbines.

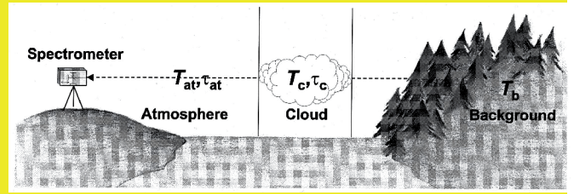

Main content of this guideline

- Basics of the **measurement technique**
  Principles for the detection of gaseous clouds and exhaust composition, radiative transfer model, radiative temperature, noise equivalent column density and detection limits
- **Measurement systems**
  Fourier transform spectroscopy, Michelson interferometers, measurement configurations, spectrometers with one detector element, scanning systems, scanning imaging systems, spectrometers with a detector array, measurement settings
- **Calibration**
  Error sources, disturbances and limits of measurements, radiometric calibration, system calibration
- **Applications**
  - **Remote sensing of gases at ambient temperature** (fires, chemical accidents, terrorist attacks, war)
    Basics, identification of gases, quantifications, application examples
  - **Remote sensing of gases at high temperatures** (smoke stacks, aircraft engine exhausts, flares)
    Basics, quantification of gas temperature, quantification of composition, application examples
  - **Remote sensing of gases by means of solar radiation** (composition of the atmosphere, diffuse sources)
    Basics, measurement performance, data analyses, application examples

Basics of the measurement techniques

- Described by a model in which the atmosphere is divided into plane-parallel homogeneous layers along the optical path.
- Real, i.e. measured instrumental line shape function (ILS) of FTIR spectrometers differs significantly from ideal, particularly if the instrument is optimized for high signal-to-noise ratio.
- Real ILS may be modelled by convolution of the ILS of the ideal FTIR spectrometer with a so-called inherent ILS describing the deviations.

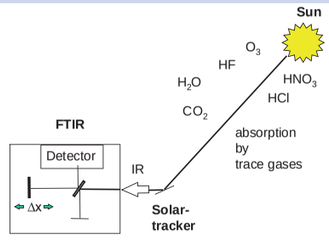

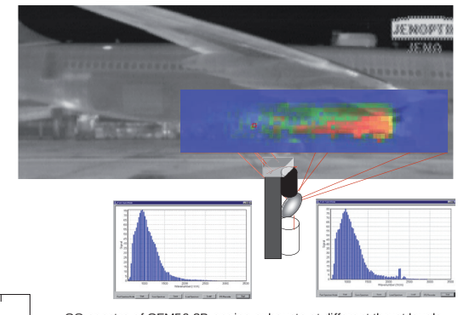

CO spectra of CFM56-3B engine exhausts at different thrust levels

Calibration

Real ILS determined by measurement of a spectrum of a well-known gas sample (CO) contained in a gas cell with black body as radiation source.
Determination of the ILS performed by minimization of difference between measured spectrum and spectrum calculated using a model.
Measured high-resolution spectrum is used for this method.
Best-fit parameters determined by the Levenberg-Marquardt method.
In order to quantify unknown samples, an analogous method with fixed ILS parameters is applied.

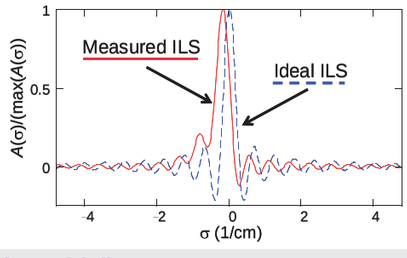

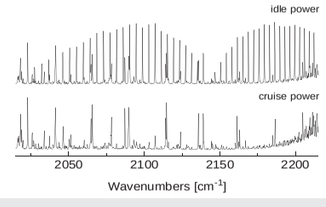

Status of the guideline

A draft is available for guideline VDI 4211 and the title is “Remote sensing – Atmospheric measurements using passive FTIR spectroscopy – Emission and ambient air measurements”. The further work will incorporate the description of different application cases of the measurement methods.

Outlook

Future application of passive FTIR technique will depend from:
- Accuracy of spectral line data which influences the detection limits of this method for single compounds as well as the determination of interferences of mixtures of compounds and thus the accuracy of this method.
- Availability of spectral line data of compounds of gaseous emissions of anthropogenic and natural origin.
- Availability of spectral line data of such compounds at high temperatures which are important for certain emissions and combustion processes.

References

Harig, R.: „Passive remote sensing of pollutant clouds by FTIR spectrometry: Signal-to-noise ratio as a function of spectral resolution“. Applied Optics 43, 23, 4603-4610, 2004.
Schäfer, K., J. Heland, D.H. Lister, C.W. Wilson, R.J. Howes, R.S. Falk, E. Lindermeir, M. Birk, G. Wagner, P. Haschberger, M. Bernard, O. Legras, , P. Wiesen, R. Kurtenbach, K.J. Brockmann, V. Kriesche, M. Hilton, G. Bishop, R. Clarke, J. Workman, M. Caola, R. Geatches, R. Burrows, J.D. Black, P. Hervé, J. Vally: “Non-intrusive optical measurements of aircraft engine exhaust emissions and comparison with standard intrusive techniques“. Applied Optics 39, 31, 441-455, 2000.
Hase, F., T. Blumenstock, C. Paton-Walsh: “Analysis of the instrumental line shape of high-resolution Fourier transform IR spectrometers with gas cell measurements and new retrieval software“. Applied Optics 38, 3417-3422, 1999.

ANALYSIS OF THE FTS SPECTRUM OF $^{16}O_3$ IN THE RANGE 3300-3600 cm^{-1}: FIRST EXAMPLE OF NEW THEORETICAL MODELLING FOR POLYAD OF STRONGLY COUPLED (220)/(121)/(022) STATES

Evgeniya Starikova[1,2], Vladimir Tyuterev[1], Alain Barbe[1],
Marie-Renée De Backer[1], Xavier Thomas[1], Sergei Tashkun[2]

[1] Groupe de Spectrométrie Moléculaire et Atmosphérique, UMR CNRS 7331,
Université de Reims Champagne Ardenne, Moulin de la Housse,
BP 1039 - 51687 REIMS Cedex 2, France
[2] Laboratory of Theoretical Spectroscopy of IAO SB RAN, av. 1,
Akademician Zuev square, 634021 TOMSK, Russia

EUMETRISPEC Workshop, November 2012, Braunschweig

Analysis of the FTS spectrum of $^{16}O_3$ in the range 3300-3600 cm^{-1}: First example of new theoretical modelling for polyad of strongly coupled (220)/(121)/(022) states

Evgeniya Starikova[1,2], Vladimir Tyuterev[1], Alain Barbe[1], Marie-Renée De Backer[1], Xavier Thomas[1], Sergei Tashkun[2]

1- Groupe de Spectrométrie Moléculaire et Atmosphérique, UMR CNRS 7331, Université de Reims Champagne Ardenne, Moulin de la Housse, BP 1039 - 51687 REIMS Cedex 2, France
2- Laboratory of Theoretical Spectroscopy of IAO SB RAN, av. 1, Akademician Zuev square, 634021 TOMSK, Russia

Abstract

The infrared spectrum of $^{16}O_3$ has been recorded anew in the ranges 3300-3600 cm^{-1} by the Fourier Transform Spectrometer of Reims [1], with an improved signal/noise ratio. In this spectral range the weak $2\nu_1+2\nu_2$ band is observed and assigned for the first time allowing to complete the triad of strongly interacting (220), (121), and (022) states [2]. To analyze this polyad of coupled states we applied for the first time a new theoretical approach. It is based on the determination of all resonance coupling parameters of the polyad effective Hamiltonian model via very accurate predictions from a molecular potential energy surface (PES), using high-order Contact Transformation (CT) method [3-6]. Diagonal triad state parameters were also computed via CT [5, 6] and served as initial values for a further optimisation during the fit to observed transitions. This mixed half theoretical / half empirical model (with 39 fitted and 77 theoretically constrained parameters) developed in this work for the first time allows an excellent description of 1897 line positions with the *rms* deviation ~0.001 cm^{-1} closed to the experimental precision.
Thanks to the improved S/N ratio of our spectrometer we were also able to observe for the first time two new hot bands: $\nu_2+4\nu_3-\nu_3$ and $\nu_1+\nu_2+3\nu_3-\nu_1$.

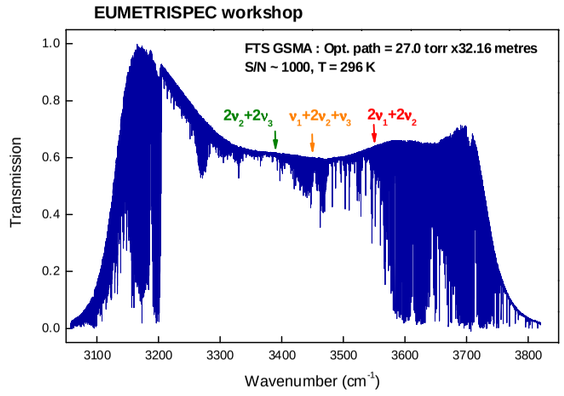

References:
[1] Régalia L. *Habilitation à Diriger des Recherches; Université de Reims* (2004)
[2] S. Bouazza, A. Barbe, S. Mikhailenko, J.J. Plateaux, *J. Mol. Spectrosc.* **166**, 365–371 (1994)
[3] Vl.G. Tyuterev, V.I. Perevalov, *Chem. Phys. Lett.* **74**, 494–502 (1980)
[4] Yu.S. Makushkin, Vl.G. Tyuterev, *Novosibirsk: Nauka*, 1–239 (1984)
[5] Vl.G. Tyuterev, S.A. Tashkun, H. Seghir, *SPIE*, **5311**, 164–75 (2004)
[6] Vl.G. Tyuterev, S.A. Tashkun, H. Seghir, *to be published*
[7] Perevalov VI, Tyuterev VlG. *Opt. and Spectrosc.* **52**, 644–50 (1982)
[8] Perevalov VI, Tyuterev VlG. *Russian Physics Journal* **2**, 179–82 (1982)
[9] Tyuterev Vl.G. Generating function approach to the formulation of effective rotation Hamiltonian. Simple closed form model describing strong centrifugal distortion in water type molecules. *J.Mol.Spectrosc.*,1992,151,p97-129
[10] Vl.G. Tyuterev, S. A. Tashkun, D.W. Schwenke, A. Barbe, Variational calculations of high-*J* rovibrational states of the ozone molecule from empirically determined isotopically invariant potential energy surface, *SPIE, Vol N° 5311, pp176-184 (2004)* [11] Watson JKG. *J Chem Phys* 46, 1935–49 (1967)
[12] Plateaux JJ, Régalia L, Boussin C, Barbe A. *JQSRT* **68**, 507–20 (2001)
[13] Mikhailenko SN, Babikov YuL, Tyuterev VlG, Barbe A. The databank of ozone spectroscopy on WEB (S&MPO). *J Comput. Technologies* **7**, 64–70 (2002) (Current state in www.ozone.univ-reims.fr and www.ozone.iao.ru)

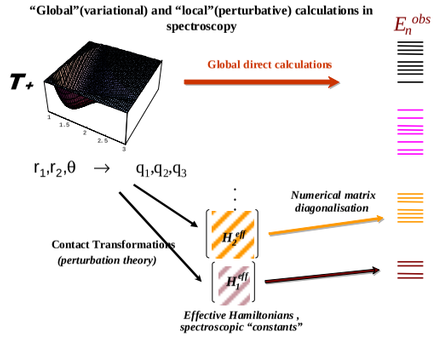

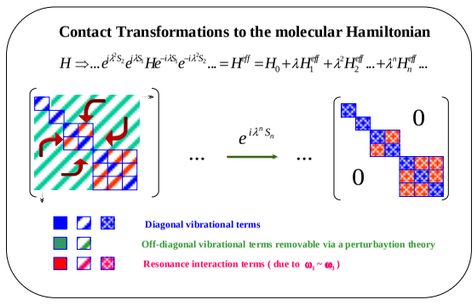

By fixing the resonance interaction parameters to the theoretical values we expect then avoiding well-known severe "co-linearity problems" of ambiguously defined empirically fitted parameters, which systematically occur for polyad spectroscopic models. Diagonal triad state parameters were also computed via CT [5, 6] and served as initial values for a further optimisation during the fit to observed transitions.

Mixed « theoretical / empirical » model

$$ {}^{eff}H^{triad} = \begin{bmatrix} H^{(022)} & Cor & Anh \\ & H^{(121)} & Cor \\ h.c. & & H^{(220)} \end{bmatrix} \quad (1) $$

$$ H^{cor} = \sum_{\substack{r \\ odd}} \sum_{l,m} C_{Lmr} \left(\mathbf{J}^2\right)^l \left\{ J_+^{\,r} \left(J_z + \tfrac{1}{2}\right)^m - (-1)^m \left(J_z + \tfrac{1}{2}\right)^m J_-^{\,r} \right\} \quad (2)\ [7] $$

$$ H^{anh} = \sum_{r,l,m} F_{LmR} \left(\mathbf{J}^2\right)^l \left\{ J_+^{\,2r} \left(J_z + r\right)^m + (-1)^m \left(J_z + r\right)^m J_-^{\,2r} \right\} \quad (3)\ [8] $$

$$ H^{(v_1 v_2 v_3)} = \sum_{lm} b_{Lm0}\, \mathbf{J}^{2l} J_z^m + \sum_{lm} b_{Lm2}\, \mathbf{J}^{2l} \{ J_+^{\,2} \left(J_z+1\right)^m + \left(J_z+1\right)^m J_-^{\,2} \} \quad (4)\ [9] $$

Triad diagonal parameters:
72 { 35 adjusted / 37 predicted

Resonance parameters:
19 { 1 adjusted (variation ~4%) / 18 predicted

In total, for four upper states:
61 parameters are fitted,
55parameters are fixed

rms = 0.001 cm^{-1} for 1897 transitions

Spectroscopic parameters (in cm^{-1}) of four upper vibration states {(022) / (121) / (220)} and (050) involved in the 3300-3600 cm^{-1} analyses

Parameters of diagonal vibration blocks:

Eq.(4)	(*)		(022)	(121)	(220)	(050)
b_{000}	E^{VV} (***)		3396.05905$_1$ (18)	3455.82462$_5$ (12)	3562.9268$_0$ (54)	3478.3334$_5$ (86) (**)
b_{020}	A-$(B+C)/2$		3.144534$_3$ (13)	3.1953284$_0$ (66)	3.25823$_6$ (13)	3.43013 [f]
b_{200}	$(B+C)/2$		0.40854643$_7$ (61)	0.40931420$_5$ (51)	0.4111397$_0$ (15)	0.4106824$_4$ (97)
b_{002}	$(B$-$C)'/4$		0.01284796$_2$ (23)	0.01303123$_0$ (22)	0.01313733$_0$ (64)	0.014071 [f]
b_{040}	Δ_K	$\times 10^3$	0.24759$_0$ (21)	0.26227$_0$ (12)	0.27408 [f]	0.345116 [f]
b_{220}	Δ_{JK}	$\times 10^5$	-0.1926$_1$ (18)	-0.1687$_4$ (15)	-0.19185 [f]	-0.135774 [f]
b_{400}	Δ_J	$\times 10^6$	0.47023$_5$ (54)	0.49279$_0$ (56)	0.47532$_0$ (81)	0.474813 [f]
b_{202}	δ_J	$\times 10^7$	0.8288$_0$ (13)	0.6663$_0$ (13)	0.5630$_0$ (54)	0.668 [f]
b_{022}	δ_K	$\times 10^5$	0.3512$_0$ (22)	0.4243$_0$ (25)	0.4586 [f]	0.694 [f]
b_{060}	H_K	$\times 10^7$	0.5985$_0$ (98)	0.6002$_8$ (81)	0.66169 [f]	1.006 [f]
b_{240}	H_{KJ}	$\times 10^8$	-0.214$_0$ (11)	-0.263$_9$ (11)	-0.2902 [f]	-0.3251 [f]
b_{420}	H_{JK}	$\times 10^9$	0.0375$_9$ (74)	-0.238$_7$ (11)	-0.00505 [f]	0.004972 [f]
b_{600}	H_J	$\times 10^{11}$	0.179$_7$ (14)	-0.147$_5$ (16)	0.01861 [f]	0.01426 [f]
b_{042}	h'_K	$\times 10^8$	0.4647 [f]	-0.863$_3$ (41)	0.2542 [f]	0.4272 [f]
b_{222}	h'_{JK}	$\times 10^{10}$	-0.2275 [f]	-0.2104 [f]	-0.1656 [f]	-0.262 [f]
b_{402}	h'_J	$\times 10^{12}$	0.1485 [f]	0.1742 [f]	0.1959 [f]	0.205 [f]
b_{080}	L_K	$\times 10^{10}$	-0.1634 [f]	-0.191$_5$ (16)	-0.1856 [f]	-0.2755 [f]
b_{260}	L_{KKJ}	$\times 10^{12}$	0.7710 [f]	0.8257 [f]	0.8758 [f]	0.1155 [f]
b_{440}	L_{JK}	$\times 10^{11}$	-0.0021 [f]	0.0680$_8$ (90)	-0.00197 [f]	-0.0036 [f]
b_{620}	L_{1JK}	$\times 10^{15}$	-0.4938 [f]	-0.5737 [f]	-0.5767 [f]	-0.720 [f]
b_{062}	P_K	$\times 10^{12}$	-0.3284 [f]	-0.2307 [f]	-0.2136 [f]	-0.599 [f]
b_{0100}	P_K	$\times 10^{14}$	0.2866 [f]	0.2868 [f]	0.2868 [f]	0.2879 [f]
b_{280}	P_{KKJ}	$\times 10^{15}$	-0.1760 [f]	-0.1801 [f]	-0.1798 [f]	-0.1964 [f]
b_{460}	P_{KJ}	$\times 10^{16}$	0.0276 [f]	0.0432 [f]	0.04217 [f]	0.1102 [f]

Resonance parameters:

Coriolis coupling parameters				Anharmonic coupling parameters	
Eq.(2)	(121) / (022)	(220) / (121)	(050) / (121)	Eq.(3)	(220) / (022)
C_{001}	-0.3415089 [f]	-0.3543214248 [f]		F_{000}	-29.7372 [f]
C_{011}	-0.0168540$_5$ (16)	-0.015974 [f]	-0.2672$_6$×10^{-3} (59)	F_{200}	-0.2354×10^{-3} [f]
C_{021}	-0.30150×10^{-3} [f]	-0.1915×10^{-6} [f]		F_{020}	0.2455×10^{-3} [f]
C_{201}	0.37845×10^{-6} [f]	0.17752×10^{-6} [f]		F_{002}	0.3625×10^{-4} [f]
C_{031}	-0.59021×10^{-6} [f]	-0.46858×10^{-6} [f]		F_{040}	-0.3709×10^{-4} [f]
C_{211}	-0.13806×10^{-6} [f]	-0.13799×10^{-6} [f]			
C_{041}	0.44199×10^{-8} [f]	0.6328×10^{-8} [f]			

[f] fixed to theoretical values predicted [6] from PES [10];
(*) Parameter notations: diagonal rotational terms have the same form as those in Watson A-reduction [11]; "primed" terms represent combinations of Watson off-diagonal centrifugal distortion constants.
(**) As only 2 transitions of $5\nu_2$ were observed, only 2 corresponding levels at J, K_a = 29, 5 and 32, 5 were derived. With this very limited experimental information the upper (050) state is considered as "dark" state (grey background). In this case a true uncertainty of the J = 0 level determination for (050) is estimated as ~0.7 cm^{-1} that is much larger than a pure statistical error quoted in parentheses.
(***) Due to off-diagonal anharmonic coupling terms (low panel), the diagonal vibrational matrix elements E^{VV} are different from the band centers.

Results

Range of observations compared with our previous work [2] in the 3300-3600 cm^{-1} interval

	Number of transitions	Number of upper state levels and range of observed quantum numbers (J, K_a)	
Band	**This work**	**This work**	**Ref [2]**
$\nu_1+2\nu_2+\nu_3$	1138	515 (50, 17)	335 (45, 14)
$2\nu_2+2\nu_3$	670	386 (56, 11)	177 (56, 9)
$2\nu_1+2\nu_2$	87	52 (43, 3)	0
$5\nu_2$	2	2 (31, 4)	0
TOTAL	1897	955	512

Parameters of the effective transition moment operator for the triad and for the hot bands obtained from the fit of observed intensities and calculated integrated band intensities, S_v, (in cm/molecule at 296K)

Band (center in cm^{-1})/ operator	Parameters (in Debye)	Value	Number of observed line intensities and range of quantum numbers (J, K_a)	rms deviation (%)
$2\nu_2+2\nu_3$ (3390.918)		S_v = 1.03×10^{-22}		
φ_x	d_1 (×10^3)	0.10520$_8$ (97)	251 (52, 11)	8.0
$\{\varphi_z, iJ_y\}$	d_5 (×10^5)	-0.4439$_3$ (21)		
$\nu_1+2\nu_2+\nu_3$ (3455.825)		S_v = 6.30×10^{-22}		
φ_z	d_1 (×10^3)	0.6924$_1$ (15)		
$\{\varphi_z, \mathbf{J}^2\}$	d_2 (×10^7)	0.1282$_8$ (88)	686 (49, 17)	6.0
$\{\varphi_z, J_z^2\}$	d_3 (×10^6)	0.3692$_8$ (94)		
$2\nu_1+2\nu_2$ (3568.07)		S_v = 1.75×10^{-23}		
φ_x	d_1 (×10^4)	0.275$_4$ (22)		
$\{\varphi_z, iJ_y\}$	d_5 (×10^5)	-0.3692$_5$ (41)	39 (44, 2)	21.4
TOTAL:			976	7.7
$\nu_2+4\nu_3-\nu_3$ (3590.804)		S_v = 1.17×10^{-22}		
φ_z	d_1 (×10^2)	0.3426$_1$ (40)		
$\{\varphi_z, \mathbf{J}^2\}$	d_2 (×10^6)	0.344$_1$ (34)	91 (40, 11)	13.2
$\{\varphi_z, J_z^2\}$	d_3 (×10^5)	0597$_5$ (49)		
$\nu_1+\nu_2+3\nu_3-\nu_1$ (3555.813)		S_v = 3.63×10^{-23}		
φ_z	d_1 (×10^2)	0.2801$_8$ (26)	38 (27, 7)	12.9
TOTAL			129	13.1

The cut-off for S_v calculations is 3× 10^{-27} cm/molecule at 296 K

Comparison between observed and calculated spectra

The $\nu_1+2\nu_2+\nu_3$ band as well as the $2\nu_2+2\nu_3$ band have been already observed and analysed, the results being collected in ref. [2]. The $2\nu_1+2\nu_2$ band observed here for the first time is very weak and hidden by a large number of hot bands of ozone, and first of all by many impurity lines of the CO_2 molecule (including its isotopologues).

976 observed line intensities of the bands under study, measured with the use of Multifit code [12], were fitted with the *rms* deviation of 7.7% that corresponds to an average error of absolute intensity determinations.
With the effective Hamiltonian and dipole moment parameters, a full list of transitions was created, with the intensity cut-off of 3×10^{-27} cm/molecule at 296 K and J and $K_{a\ max}$ corresponding to observed values. This list of 4620 transitions was used to generate synthetic spectra. An excellent agreement between observed and calculated spectra confirms again the validity of our model.

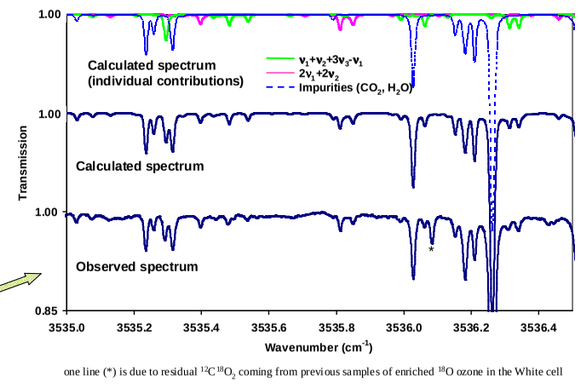

one line (*) is due to residual $^{12}C^{18}O_2$ coming from previous samples of enriched ^{18}O ozone in the White cell

Thanks to the improved S/N ratio of our spectrometer we were also able to observe for the first time two new hot bands: $\nu_2+4\nu_3-\nu_3$ and $\nu_1+\nu_2+3\nu_3-\nu_1$, which have the stretching dyad {(100)/(001)} as lower states. The upper and lower state effective Hamiltonian parameters for these bands have been determined from our previous analyses of corresponding cold bands as reported in S&MPO ([13] and references therein). As the agreement in line positions using these parameters was satisfactorily (differences between calculations and observations on the order of experimental accuracy), we only fitted the transition moment parameters for these two hot bands including 91 line intensities for $\nu_2+4\nu_3-\nu_3$ and 38 line intensities for $\nu_1+\nu_2+3\nu_3-\nu_1$.
A final calculation of all bands included in this spectral range along with transitions from CO_2 and H_2O (impurity gases in the sample) led to synthetic spectra in very good agreement with experimental observations.

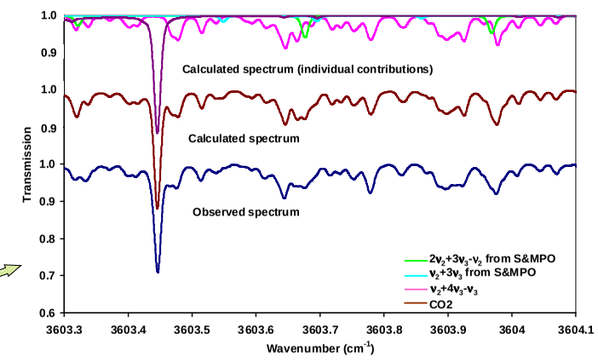

Absolute-frequency measurements of CH_4 and N_2O line centers in the mid-infrared

M. Vainio[1], J. Peltola[2], M. Merimaa[1]

[1] Centre for Metrology and Accreditation, P.O. Box 9, FIN-02151 Espoo, Finland
[2] Laboratory of Physical Chemistry, Department of Chemistry, P.O. Box 55, FIN-00014 University of Helsinki, Finland
email: markku.vainio@mikes.fi

We report a mid-infrared spectrometer that has been designed to accurately measure molecular spectroscopic data, in order to improve the quality of the existing spectroscopic databases. The spectrometer, which is schematically depicted in Fig. 1, is based on a wavelength-tunable continuous-wave optical parameter oscillator (cw OPO). The OPO can be used for high resolution spectroscopy between 3 and 4 µm mid-infrared wavelengths [1]. In the first version of our experimental setup, the frequency of the mid-infrared (idler) beam of the OPO was linked to an optical frequency comb through its near-infrared pump and signal beams [2]. We have recently improved the experimental setup so that the link to the frequency comb can be established by simply frequency doubling of the mid-infrared beam (Fig. 1).

The frequency-comb-referenced cw OPO can be used to accurately measure frequencies, linewidths, and pressure shifts of molecular absorption lines in the mid-infrared. In this work we focus on the spectroscopy of methane (CH_4) and nitrous oxide (N_2O) within the spectral range between 2.85 and 3.45 µm. In our upgraded setup we use cavity-ring-down spectroscopy, which is an extremely sensitive and accurate technique for absorption measurements and makes it possible to measure also the strength of the molecular absorption line under study.

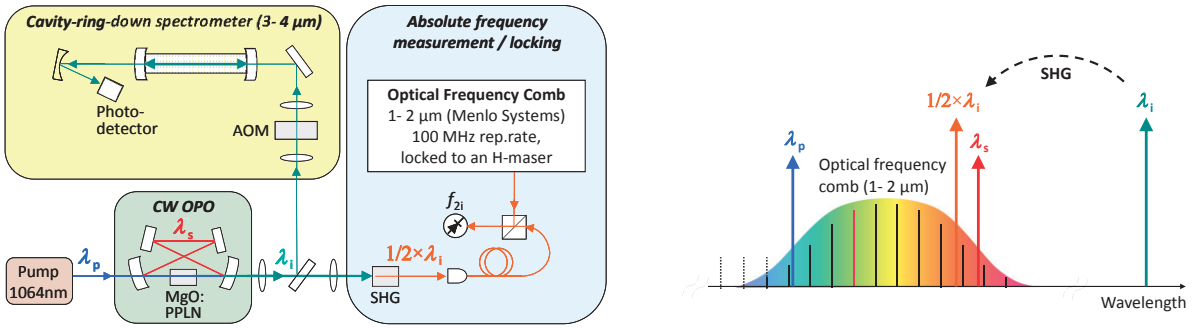

Fig. 1. The OPO is pumped at wavelength λ_p = 1064nm, and it produces two new wavelengths, λ_s ~ 1.6 µm and λ_i ~3 µm such that $1/\lambda_i = 1/\lambda_p - 1/\lambda_s$. The absolute frequency of the mid-infrared (λ_i) beam can be determined with a commercially available optical frequency comb after frequency doubling (SHG).

Acknowledgement: The research leading to these results has received funding from the European Union on the basis of Decision No 912/2009/EC.

References

[1] M. Vainio, J. Peltola, S. Persijn, F. J. M. Harren, and L. Halonen, *Opt. Express*, **16**, 11141 (2008).
[2] M. Vainio, M. Merimaa, and L. Halonen, *Opt. Lett*. **36**, 4122-4124 (2011).

Absolute-frequency measurements of CH_4 and N_2O line centers in the mid-infrared

Markku Vainio[1], Jari Peltola[2], Mikko Merimaa[1]
(1) Centre for Metrology and Accreditation (MIKES), Finland
(2) University of Helsinki, Finland

Objective

Absolute frequencies of the positions of selected absorption lines of methane (CH_4) and nitrous oxide (N_2O), as well as their shift with pressure will be measured at MIKES. The measured data will be used as anchor points to validate the FTIR data of the central facility (PTB). The measurements will be done within the mid-infrared (MIR) range between 2.85 and 3.45 µm (2900 to 3500 cm^{-1}) using a cw optical parametric oscillator (OPO). The OPO is linked to an optical frequency comb for absolute frequency scale.

Method

A cw OPO is used for high-resolution spectroscopy of CH_4 and N_2O. The OPO is pumped at 1.064 µm, and it produces two output beams - so-called signal and idler beams - at 1.5 µm and at 3 µm, respectively. The frequencies of these three beams fulfill the law of energy conservation: $\omega_{idler} = \omega_{pump} - \omega_{signal}$. Therefore, the absolute frequency ω_{idler} of the idler beam (which is used for spectroscopy in the MIR) can be determined by measuring the pump and signal frequencies using a commercially available optical frequency comb (OFC). Another possibility, which is used in this work, is to frequency double the MIR idler beam, after which its absolute frequency can be referenced to the OFC. The principle of this approach is illustrated below.

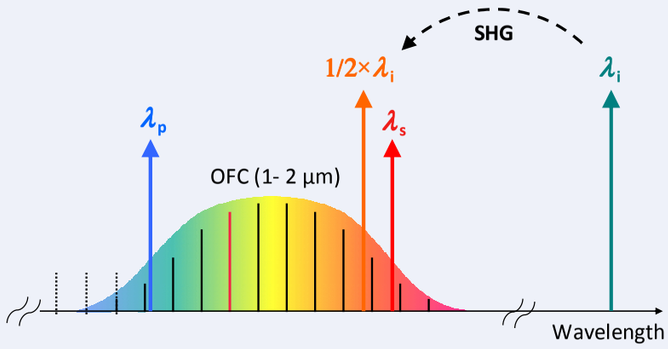

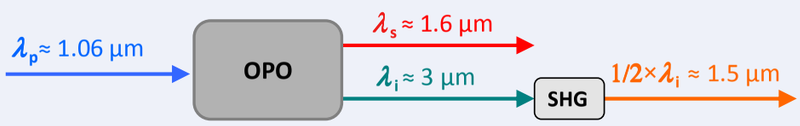

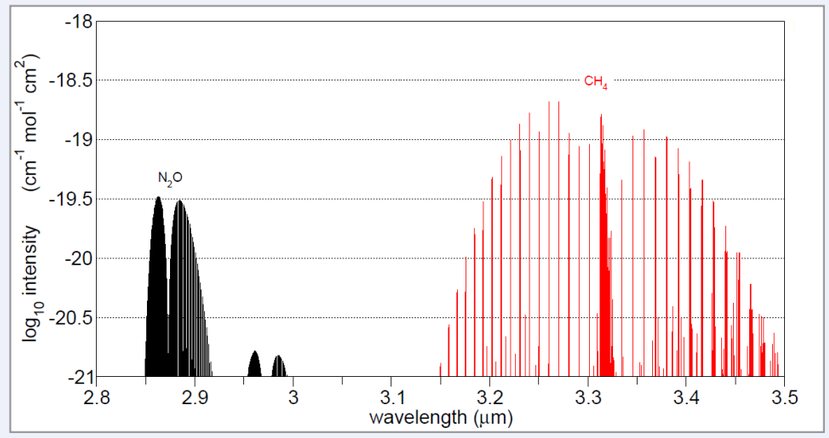

Spectral range and molecules to be covered/measured with the absolute-frequency spectroscopy setup.

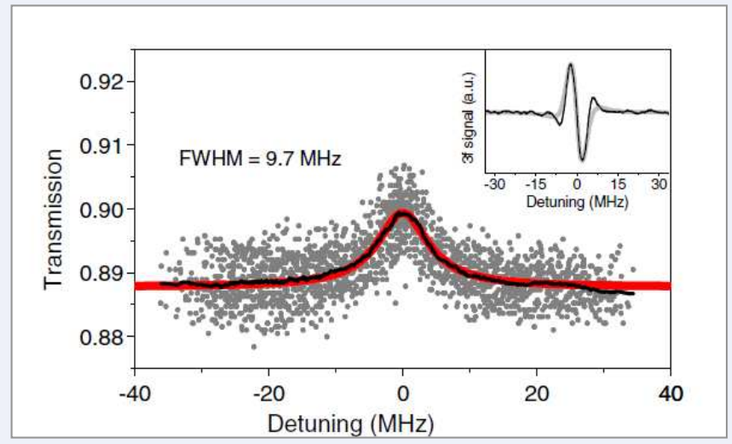

Example of a sub-Doppler spectrum (Lamb dip) of the $F^{(2)}_2$ P(7) ν_3 transition of $^{12}CH_4$, measured with the first version of the experimental setup [using a Ti:sapphire-laser OFC, *Opt. Lett.* **36**, 4122-4124 (2011)]. The inset shows an example of the respective signal when using wavelength modulation spectroscopy with 3*f* detection.

Experimental setup

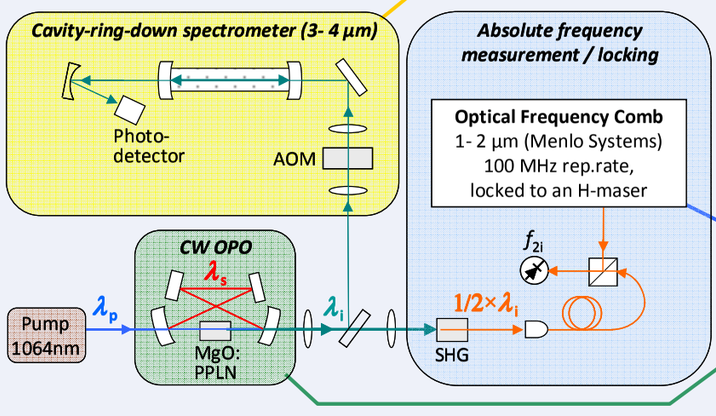

Schematic of the experimental setup. The OPO produces a wavelength-tunable MIR beam, which is used for high-resolution (sub-Doppler) spectroscopy of CH_4 and N_2O. The spectrometer is based on cavity-ring-down spectroscopy. The MIR beam is frequency-doubled (SHG), after which its frequency can be referenced to an optical frequency comb for absolute frequency scale. For more details, see M. Vainio *et al.* "Frequency-comb-referenced molecular spectroscopy in the mid-infrared region," *Opt. Lett.* **36**, 4122-4124 (2011).

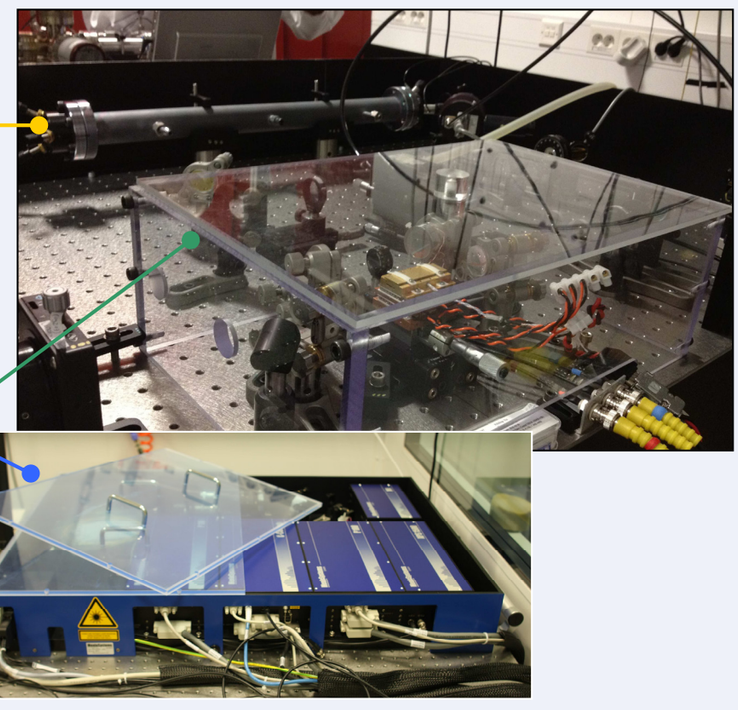

Infrared line parameters for constituents of planetary and stellar atmospheres

J. Vander Auwera,[a] M. Herman,[a] B. Amyay,[a] K. Didriche,[a] T. Foldes,[a]
D. Golebiowski,[a] M. Tudorie,[a] A. Fayt [b]

(a) Service de Chimie Quantique et Photophysique, C.P. 160/09, UniversitŽ Libre de Bruxelles (ULB), 50 avenue F.D. Roosevelt, B-1050 Brussels, Belgium

(b) Laboratoire de Spectroscopie MolŽculaire, UniversitŽ Catholique de Louvain (UCL), 2 chemin du cyclotron, bo"te L7.01.07, B-1348 Louvain-La-Neuve, Belgium

Relying on high resolution instrumental and methodological means, our activities aim to provide reference spectroscopic information required to quantitatively probe the composition of atmospheres and to study the internal structure of molecules. The common ground supporting these activities is the investigation of the energy, intensity and shape of spectral lines. Much of the reference spectroscopic information we obtained is included in the HITRAN and GEISA databases. After a brief description of our experimental means, a few examples of our recent research are presented.

Acknowledgments Financial support from the *Fonds de la Recherche Scientifique* (FRS-FNRS, Belgium), the *Action de Recherches ConcertŽes* of the *CommunautŽ fran•aise de Belgiqu*e, and the Belgian Federal Science Policy Office (Belspo) is gratefully acknowledged.

Infrared line parameters for constituents of planetary and stellar atmospheres

J. Vander Auwera,[a] M. Herman,[a] B. Amyay,[a] K. Didriche,[a] T. Foldes,[a] D. Golebiowski,[a] M. Tudorie,[a] A. Fayt [b]

(a) Service de Chimie Quantique et Photophysique C.P. 160/09, Université Libre de Bruxelles (ULB), 50 avenue F.D. Roosevelt, B-1050 Brussels, Belgium
(b) Laboratoire de Spectroscopie Moléculaire, Université Catholique de Louvain (UCL), 2 chemin du cyclotron, boîte L7.01.07, B-1348 Louvain-La-Neuve, Belgium

INTRODUCTION

Relying on high resolution instrumental and methodological means, our activities aim to provide reference spectroscopic information required to quantitatively probe the composition of atmospheres and to study the internal structure of molecules. The common ground supporting these activities is the investigation of the energy, intensity and shape of spectral lines. Much of the reference spectroscopic information we obtained is included in the HITRAN and GEISA databases. After a brief description of our experimental means, a few examples of our recent research are presented.

FOURIER TRANSFORM SPECTROSCOPY

Bruker IFS125HR Fourier transform spectrometer (MOPD = 716 cm), operated from the far infrared to the visible spectral ranges. It is equipped with various ancillary equipment, including thermostatic absorption cells (path lengths from 1.5 to 20 cm) and two multipass White-type cells (path lengths from 60 cm to 55 m).

CAVITY RING DOWN AND CAVITY ENHANCED ABSORPTION SPECTROSCOPY

The FANTASIO+ set-up (for "Fourier trANsform, Tunable diode and quadrupole mAss spectrometers interfaced to a Supersonic expansIOn") [1] is based on a CW-CRDS system centered around 1.5 µm. The 130 µs ring down time provides a 5 10^{-10} /cm sensitivity and the 1 MHz laser bandwith assures a minimum resolution of 10^{-4} cm^{-1}. The CRDS cavity is built around a supersonic expansion generated by two large turbomolecular pumps allowing the gaseous samples to be cooled down to 3 K and molecular van der Waals complexes to be formed [2].

A complementary CEAS probe technique, tunable from 3000 to 9000 cm^{-1}, is being developed [3]. It involves an optical parametric oscillator (OPO), pumped by a Ti:Sa femtosecond laser, coupled to a high finesse cavity and a (second) high resolution continuous scan Fourier transform interferometer.

SOFTWARE

Modeling and mono- or multi-spectrum fitting of high-resolution absorption spectra, using various line shape functions and including instrumental distortions.

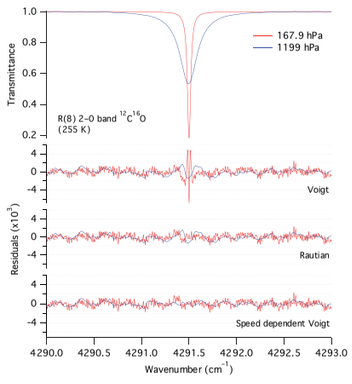

Least squares fits with different line shape functions of a line of $^{12}C^{16}O$ diluted in CO_2 at two different total pressures.

GLOBAL EFFECTIVE HAMILTONIAN

A global effective Hamiltonian model describing the vibration-rotation energy levels structure of acetylene in extreme details (see figures here below), up to 8900 cm^{-1}, has been built [4]. Using it, the total internal partition function of acetylene was calculated with high accuracy [5], and a database including line positions and intensities thus predicted and broadening coefficients from the literature is being created.

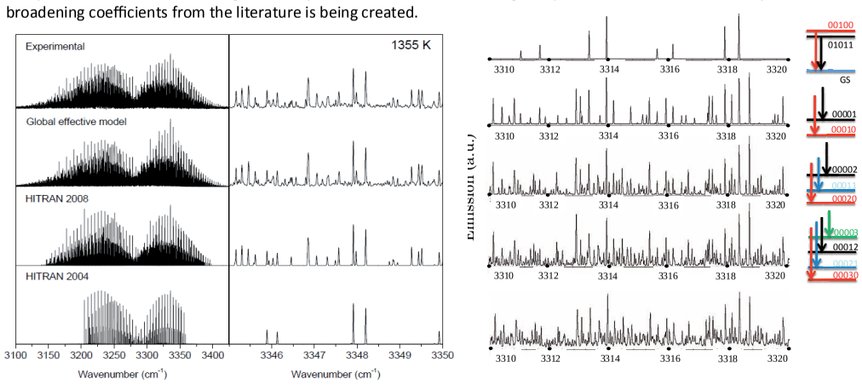

Spectrum of the ν_3 region of acetylene $^{12}C_2H_2$ at 1355 K: Observation (R. Georges, U. Rennes 1) and simulations using HITRAN 2008 and the global effective Hamiltonian [4].

PRESSURE INDUCED LINE BROADENING AND SHIFT

We measure broadening and shift coefficients of vibration-rotation lines of atmospheric trace gases [6,7]. As an example of such activities, recent measurements of CO_2 broadening and shift coefficients for the 1–0 band of several isotopologues of hydrogen chloride [6] are presented.

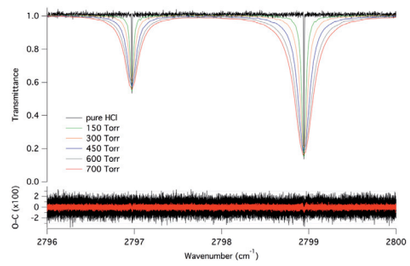

Multi-spectrum fit of the P(4) lines of $H^{35}Cl$ and $H^{37}Cl$ (Voigt profiles). Six out of the 231 observed spectra fitted are shown in the upper panel, one for each pressure used in the fit (each spectrum is the average of two interferograms). The best-fit residuals for the 231 fitted spectra are presented in the lower panel, in black for the pure HCl spectra and in red for the others.

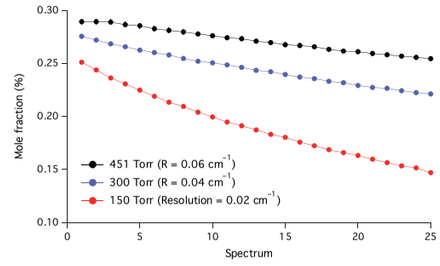

Because of the reactivity of hydrogen chloride, its amount in the cell decreased as the spectra were recorded. This evolution was measured and taken into account in the multi-spectrum analysis. The figure shows the mole fraction of HCl measured in each of the 25 spectra recorded successively for 3 of the samples analyzed.

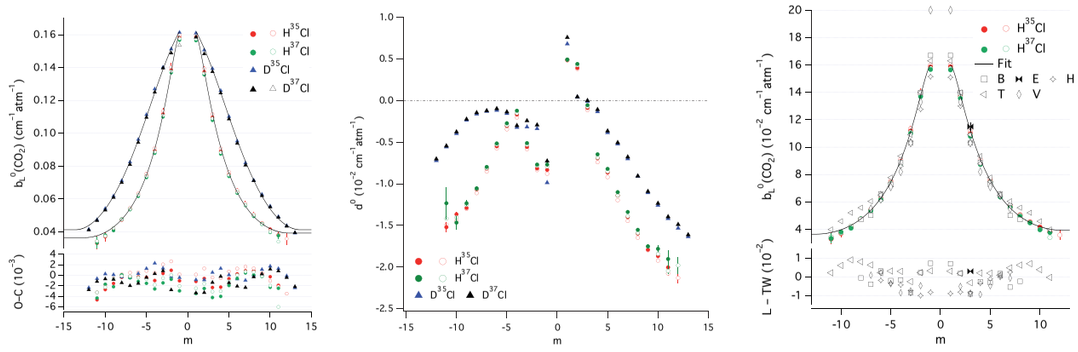

CO_2 broadening (left) and shift (middle) coefficients measured for the 1–0 band of several isotopologues of hydrogen chloride. For HCl, the filled and open circles correspond to measurements in HCl/CO_2 and $DCl/HCl/CO_2$ samples, respectively. Right: Comparison of the broadening coefficients measured in this and previous work. The filled and open circles, and curves are from this work, and "B", "E", "H", "T" and "V" are literature values (see [6] for details). The differences between values from the literature ("L") and calculated in this work ("TW") are shown in the lower panel (the two values at |m| = 1 from "V" are off-scale).

LINE INTENSITIES AND ABSORPTION CROSS SECTIONS

We measure absolute line intensities for chemically stable and unstable species, such as C_2H_2, OCS, $^{13}CO_2$, N_2O, C_2H_4, CH_4, HOCl and HCOOH (see for example [8-16]), and obtained the infrared absorption cross section of a few H(C)FCs [17]. As an example of these activities, line intensities measured for the ν_6 and ν_8 bands of formic acid near 9 µm are presented. They eventually led to a spectroscopic determination of the dissociation constant K_p of the formic acid dimer $(HCOOH)_2$ [15].

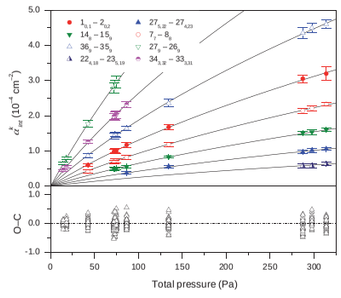

$$(HCOOH)_2 \rightleftharpoons 2\ HCOOH$$

Solid curves : Simultaneous fit of all the integrated absorption coefficients to the following expression to yield the absolute intensity S_k of the 72 lines measured and the dissociation constant of the dimer K_p :

$$\alpha_{int}^{k} = S_k \frac{-K_p + \sqrt{K_p^2 + 4K_p P_{tot}}}{2}$$

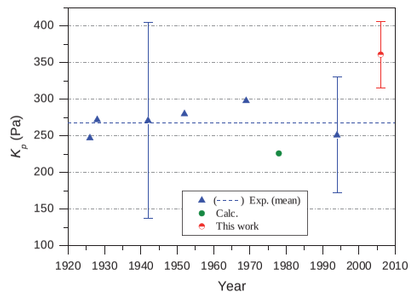

437 integrated absorption coefficients were measured for 72 lines of the ν_6 band of trans-$H^{12}C^{16}O^{16}OH$ in absorption spectra recorded at different total pressures P_{tot}. **Left**: Evolution with P_{tot} of the integrated absorption coefficients of eight of these lines [upper pane; the symbols represent the observed values and the error bars are the estimated precision (3σ) of measurement]; the residuals of the fit (10^{-5} cm^{-2}) are plotted for all the lines in the lower panel. **Right**: Comparison of the value of K_p determined spectroscopically in this work (red) with previous work.

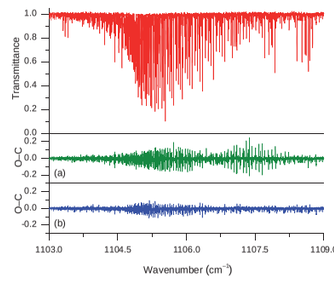

HITRAN 2004 **x 2**

This work

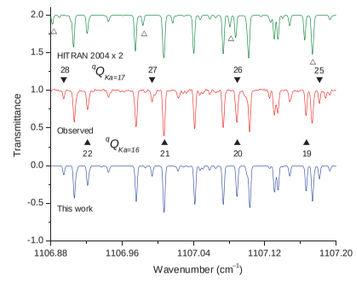

This work resulted in a significant improvement of the line intensities for HCOOH : the line intensities available in HITRAN 2004 were shown to be a factor of about 2 too small. The two figures compare the residuals obtained when using HITRAN 2004 and the linelist generated in this work [15] to calculate the observed spectrum of the Q branch of the ν_6 band (left) and part of its R branch.

REFERENCES

1. K. Didriche et al, Mol Phys 108 (2010) 2155.
2. K. Didriche et al, 2012 (in press).
3. X. de Ghellinck d'Elseghem Vaernewijck et al, Mol Phys 109 (2011) 2173.
4. B. Amyay et al, J Chem Phys 131 (2010) 114301.
5. B. Amyay et al, J Chem Phys 135 (2011) 234305.
6. M. Tudorie et al, J Quant Spectrosc Radiat Transfer 113 (2012) 1092.
7. M. Sanzharov et al, J Quant Spectrosc Radiat Transfer 113 (2012) 1874.
8. R. El Hachtouki and J. Vander Auwera, J Mol Spectrosc 216 (2002) 355.
9. J. Vander Auwera and A. Fayt, J Mol Struct780 (2006)134.
10. J. Vander Auwera et al, J Mol Spectrosc 235 (2006) 77.
11. L. Daumont et al, J Quant Spectrosc Radiat Transfer 104 (2007) 342.
12. M. Rotger et al, J Quant Spectrosc Radiat Transfer 109 (2008) 952.
13. J. Vander Auwera et al, J Mol Spectrosc 204 (2000) 36.
14. V. Boudon et al, J Quant Spectrosc Radiat Transfer 111 (2010) 1117.
15. J. Vander Auwera et al, J Chem Phys 126 (2007) 124311; A. Perrin and J. Vander Auwera, J Quant Spectrosc Radiat Transfer 108 (2007) 363.
16. A. Perrin et al, J Quant Spectrosc Radiat Transfer 110 (2009) 743.
17. J. Vander Auwera, J Quant Spectrosc Radiat Transfer 66 (2000) 143.

ACKNOWLEDGMENTS

Financial support from the *Fonds de la Recherche Scientifique* (FRS-FNRS, Belgium), the *Action de Recherches Concertées* of the *Communauté française de Belgiqu*e, and the Belgian Federal Science Policy Office (Belspo) is gratefully acknowledged.

SPECTROSCOPIC LINE DATA FOR HIGH TEMPERATURE PROCESS DIAGNOSTICS IN COMPLEX CHEMICAL MATRIXES

Steven Wagner[1,2], Pascal Ortwein[2], Volker Ebert[2,3]

[1] High Temperature Process Diagnostics, CSI, TU Darmstadt, Petersenstraße 32, 64287 Darmstadt, Germany;
[2] Physikalisch-Technische Bundesanstalt, Bundesallee 100, 38116 Braunschweig, Germany;
[3] Analytical Photonics Group, CSI, TU Darmstadt, Petersenstraße 32, 64287 Darmstadt, Germany

EUMETRISPEC workshop "Traceable Spectral Reference Data For Atmospheric Monitoring", November 15th to 16th 2012, Physikalisch-Technische Bundesanstalt, Braunschweig, Germany

Spectroscopic Line Data for High Temperature Process Diagnostics in Complex Chemical Matrixes

Steven Wagner[1,2], Pascal Ortwein[2], Volker Ebert[2,3]
wagner@csi.tu-darmstadt.de

[1] High Temperature Process Diagnostics, CSI, TU Darmstadt, Petersenstraße 32, 64287 Darmstadt, Germany;
[2] Physikalisch-Technische Bundesanstalt, Bundesallee 100, 38116 Braunschweig, Germany;
[3] Analytical Photonics Group, CSI, TU Darmstadt, Petersenstraße 32, 64287 Darmstadt, Germany

Motivation

Chemiluminescence as an indicator for heat release

BUT:
- poor quantitative understanding of CL
- CL species and reaction paths not included in standard flame reaction models

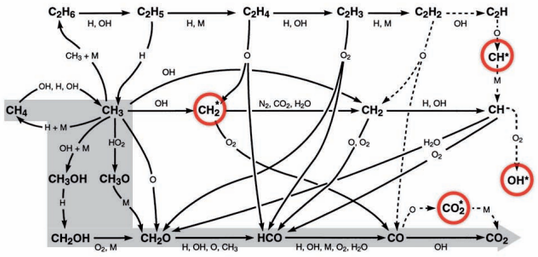

Approach:
- Improved flame chemistry models and CL modeling (DLR)
- TDLAS Model validation
- Species: CO, OH, C_2H_2, H_2O, temperature, CH_4
- Low dimensional model flame
  - stabilized flame
  - Easy experimental access
  - Homogeneous path

Counter Flow Burner

Tsuji-Burner*

- Laminar counterflow diffusion flame
- Non-premixed CH_4/air
- Strain variation possible
- Fuel variation possible
- Vertical translation

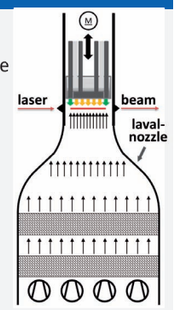

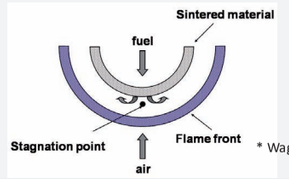

* Wagner et.al. APB 107-3 (2012)585-589
Wagner et.al. APB (2012) online

TDLAS Principle

Extended Lambert-Beer-law[1,2,3]

$$I(\lambda) = E(t) + I_0(\lambda) \cdot Tr(t) \cdot exp[-S(T) \cdot g(\lambda - \lambda_0) \cdot N \cdot L]$$

with ideal gas law:

$$c = \frac{k_B \cdot T}{S(T) \cdot L \cdot p} \int ln\left(\frac{I(\nu) - E(t)}{I_0(\nu) \cdot Tr(t)}\right) \frac{d\nu}{dt} dt$$

Database — Meas. — Absorption Line Area

Available Dataset, i.e. $CO+C_2H_2$

HITRAN-Statistics (2008 compilation w/o updates)

Uncertainty [%]	Line Strength [#]	Air Broadening [#]	Self Broadening [#]	Temperature Coefficiant [#]
Unreported or unavailable	431140	167679	452539	349336
Default or constant	20	86872	42243	397920
Average or estimate	15252	826529	927702	808756
20	786395	120175	466625	288828
10	589615	310157	66782	170612
5	638186	875423	685358	694488
2	246751	318400	67979	4029
1	5055	7447	4043	0
0	1555	1276	698	0

CO R20 (2ν) at 4324,4 cm^{-1} / 2313 nm

Name		Value	Index	Uncertainty	Unit Uncertainty
Line Position	ν	4324,41	4	≥ 10^{-4} und < 10^{-3}	cm^{-1}
Line Strength	S	3,302 x 10^{-22}	6	≥ 2 und < 5	%
Air Broadening$_{HWHM}$	γ_{air}	0,05	7	≥ 1 und < 2	%
Self Broadening$_{HWHM}$	γ_{self}	0,054	6	≥ 2 und < 5	%
Temperature coefficiant	n_{air}	0,67	2	estimated/averaged	%
Pressure Shift	δ_{air}	-0,00517	3	≥ 10^{-3} und < 10^{-2}	cm^{-1}

C_2H_2 P17e at 6512,99 cm^{-1} / 1535,4 nm

Name		Value	Index	Uncertainty	Unit Uncertainty
Line Position	ν	6512,99	4	≥ 10^{-4} und < 10^{-3}	cm^{-1}
Line Strength	S	6,665 x 10^{-21}	7	≥ 1 und < 2	%
Air Broadening$_{HWHM}$	γ_{air}	0,0733	6	≥ 2 und < 5	%
Self Broadening$_{HWHM}$	γ_{self}	0,132	6	≥ 2 und < 5	%
Temperature coefficiant	n_{air}	0,75	4	≥ 10 und < 20	%
Pressure Shift	δ_{air}	-0,001	2	≥ 0,01 und < 0,1	cm^{-1}

Collision Broadening – CO

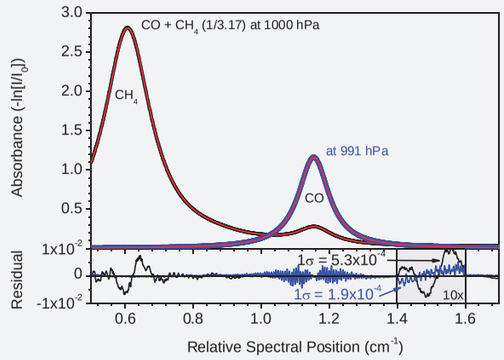

CO R20 (2ν) at 2313 nm
- 100 scan average (5sec)
- coupled 161 line Voigt shape fit

→ Fractional resolution – 1,9 x 10^{-4}
→ Signal-to-noise ratio – > 6000 (1σ)

Measurement of broadening coefficient:

$$\gamma_{CO} = \left(\gamma^0_{CO-CO} \cdot p_{CO} + \gamma^0_{CO-X} \cdot p_X\right) \cdot \left(\frac{T_0}{T}\right)^n$$

Collision Broadening – CO

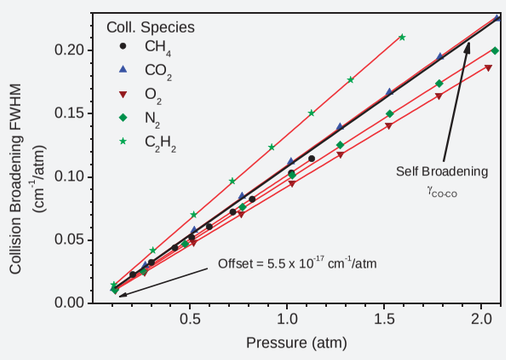

Species	Broadening Exp. FWHM (MHz/Pa)	Broadening Exp. FWHM (cm^{-1}/atm)	Fit R^2	Broadening Lit. FWHM (cm^{-1}/atm)	Δ Exp. (%)
CO – CO	0,03297(05)	0,11145(17)	0,99993	0,10680	4,2
CO – N_2	0,02933(10)	0,09913(34)	0,99975	0,09982	0,7
CO – O_2	0,02744(05)	0,09274(18)	0,99992	0,09120	1,7
CO – CO_2	0,03332(08)	0,11262(28)	0,99986	0,11760	4,4
CO – CH_4	0,03026(22)	0,10229(74)	0,99865	-	-
CO – C_2H_2	0,04211(13)	0,14232(44)	0,99979	-	-
Residual	0,0572(14)	0,1933(48)	-	[0,2200]	[13,8]

- R^2 - 0.9987 to 0.999
- Δ(Exp.-Lit) 0,7 to 4,4 %
- First measurements for CH_4 and C_2H_2

Collision Broadening – CO

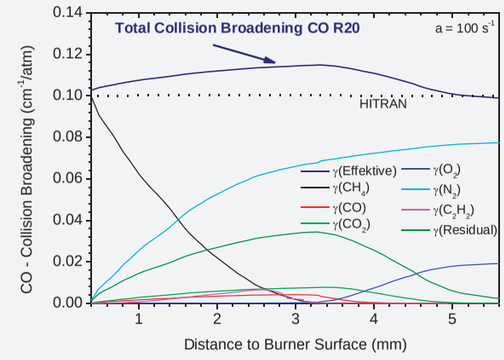

Matrix dependent collision broadening

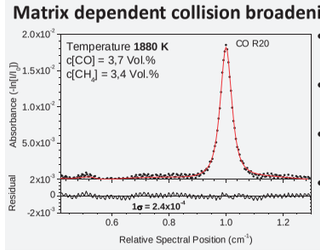

- Δ(HITRAN – Exp.) up to 15 %
- Calculated broadening with T_{CARS}, p and γ_{Exp}
- Constrained fit values on every position
- Stabilization of the line fit for in-flame CO-measurements

Collision Broadening – C_2H_2

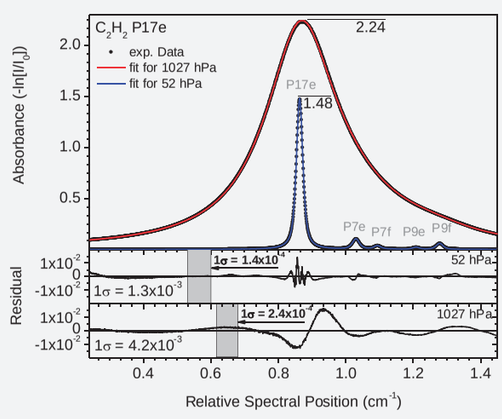

C_2H_2 P17 (2ν) at 1535.4 nm
- 100 scan average (5sec)
- coupled 7 line Voigt shape fit
- $\gamma_{Doppler}$ fixed to T_{exp}
- $\gamma_{Collision}$ fixed to T_{exp} and p_{exp}

Collision Broadening – C_2H_2

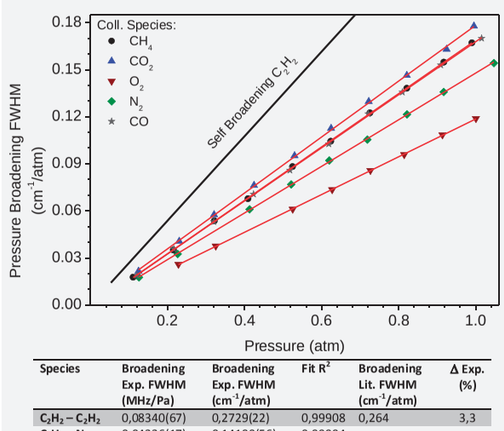

Species	Broadening Exp. FWHM (MHz/Pa)	Broadening Exp. FWHM (cm^{-1}/atm)	Fit R^2	Broadening Lit. FWHM (cm^{-1}/atm)	Δ Exp. (%)
C_2H_2 – C_2H_2	0,08340(67)	0,2729(22)	0,99908	0,264	3,3
C_2H_2 – N_2	0,04336(17)	0,14190(56)	0,99994	-	-
C_2H_2 – O_2	0,03409(12)	0,11155(40)	0,99993	-	-
C_2H_2 – Luft	0,04141(16)	0,13553(53)	-	0,1466(73)	8,2
C_2H_2 – CO_2	0,05116(32)	0,1674(10)	0,99967	new	-
C_2H_2 – CH_4	0,05020(12)	0,16428(38)	0,99995	new	-
C_2H_2 – CO	0,05067(19)	0,16582(61)	0,99988	new	-
Residual	0,097(09)	0,318(32)	-	new	-

- R^2 - 0.99908 to 0.99995
- Δ(Exp.-Lit) 3.3 to 8.2 %
- **First measurements for N_2, O_2, CO_2, CH_4 and CO**

Collision Broadening – C_2H_2

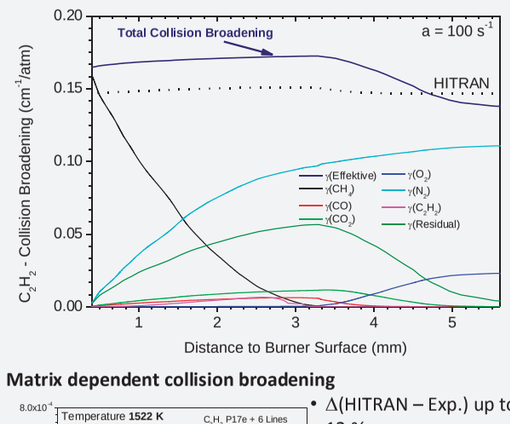

Matrix dependent collision broadening

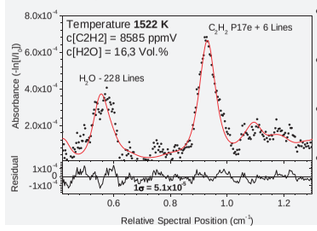

- Δ(HITRAN – Exp.) up to 12 %
- Calculated broadening with T_{CARS}, p and γ_{Exp}
- Constrained fit values on every position
- Stabilization of the line fit for in-flame C_2H_2-measurements

Challenges in Mid-Infrared Chemical Sensing Applied to Reactive Non-Equilibrium Environments

S. Welzel[1], J. Röpcke[2], R. Engeln[1]

[1] Eindhoven University of Technology, Applied Physics, P.O. Box 513, 5600 MB Eindhoven, The Netherlands
[2] INP Greifswald, Felix-Hausdorff-Str. 2, 17489 Greifswald, Germany

Chemical sensing in the mid-infrared (IR) spectral region (3 - 20 µm) is a versatile non-invasive and selective means to detect, monitor and quantify stable and transient molecules as well as free radicals in their electronic ground states. High resolution absorption cross section or line strength data are thereby essential for obtaining absolute number densities from relative intensity measurements.

Particularly in reactive and non-equilibrium environments, such as electrical gas discharges, additional challenges have to be considered that finally determine the accuracy of the results. Non-equilibrium conditions are frequently present in reactive plasmas used for materials and gas phase processing, such as surface modification, e.g. deposition and etching, and gas conversion. A few spectroscopic challenges that are highlighted in the contribution are summarised below:

- complex gas mixtures:
  - congested spectra
  - collisional partners (line-broadening) different from atmospheric mixtures
- non-equilibrium conditions ($T_g \sim T_{rot} < T_{vib} < T_e$)
- elevated gas temperatures (up to 1000 K and higher)
- gradients in temperatures and densities along the line-of-sight
- time-dependent quantities and short reaction time-scales (clearly below seconds)
  - time-dependent temperatures and hence line-strengths
  - convolution of changes in line-strengths and densities of species
  - limited sensitivity (accuracy) in highly time-resolved measurements

Opportunities to overcome some of these challenges enabled by the recent progress in mid-IR laser technology, e.g. the time-resolved detection of the absorption coefficient and a more localised measurement of quantities in inhomogeneous gas-phases, will be addressed [1,2]. Additionally, the application of (infrared) spectral databases during the analysis of (congested) Fourier-Transform (FT) IR spectra is discussed.

[1] J. Röpcke, P.B. Davies, N. Lang, A. Rousseau, S. Welzel, *J. Phys. D: Appl. Phys.* **45** (2012) 423001
[2] S. Welzel, F. Hempel, M. Hübner, N. Lang, P.B. Davies, J. Röpcke, *Sensors* **10**, (2010) 6861

Mid-IR Chemical Sensing Applied to Reactive Non-Equilibrium Environments

S. Welzel[1*], J. Röpcke[2], R. Engeln[1]

[1] Eindhoven University of Technology, Applied Physics, P.O. Box 513, 5600 MB Eindhoven, The Netherlands
[2] INP Greifswald, Felix-Hausdorff-Str. 2, 17489 Greifswald, Germany

*) ✉ s.welzel@tue.nl

Acknowledgements

J.J.L.M. Meulendijks, M.J.F. v.d. Sande, J.J.A. Zeebregts, R.F. Rumphorst (TU Eindhoven)

S. Glitsch, U. Macherius, S. Saß, F. Weichbrodt (INP Greifswald)

H. de Vries, S.A. Starostin, B. Korngold, R. v. Beijnen (FUJIFILM Manufacturing Europe B.V.)

Motivation & Challenges

Chemical sensing in the mid-infrared (IR) spectral region (3 - 20 µm) is a versatile non-invasive and selective means to detect, monitor and quantify stable and transient molecules as well as free radicals in their electronic ground states. High resolution absorption cross section or line strength data are thereby essential to obtain absolute number densities from relative intensity measurements.

Particularly in reactive and non-equilibrium environments, such as electrical gas discharges, the temperature dependence of spectral line data becomes an important parameter. Additionally, under these conditions several spectroscopic challenges have to be accounted for that determined the accuracy of the results:

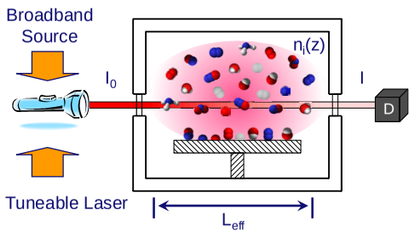

- Complex gas mixtures (+ spectral congestion)
- Gradients in temperatures and densities
- Reaction time-scales clearly below s
- Non-equilibrium ($T_g \sim T_{rot} < T_{vib}$)

$$I(\nu) = I_0(\nu) \cdot e^{-L_{eff} \cdot \sum_i n_i(z)\sigma_i(\nu,T)}$$

IR Laser Diagnostics

Gas Temperature

- *In-situ* sampling
  - Pulsed DC plasma (1% NO/N_2)
  - Single-pass ($L_{eff} \sim$ 0.5 m)
  - Pulsed quantum cascade laser
  - Time-resolved detection

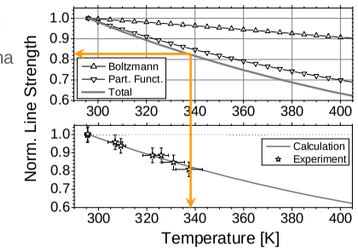

- **Challenges**
  - Convolution of changes in gas density and T_{gas}
  - Time-dependent T_{gas}
  - ↓
  - Time-dependent line strength $S(T_{gas})$
  - ↓
  - Temporal evolution of NO

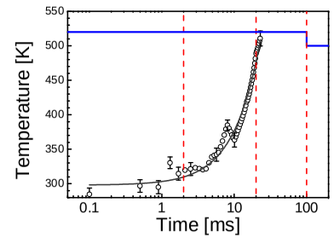

Cavity Enhanced Trace Gas Sensing

- Cavity-Enhanced Absorption Spectroscopy (CEAS)
  - High-R mirrors ($L_{eff} \sim$ 250 m)
  - CW quantum cascade laser
  - Calibration required with standardised gas samples
  - Monitoring of harmful species (e.g. $COCl_2$)

- **Challenges**
  - Small sample volumes preferred (Sensitivity)
  - Lack of high-resolution spectral line data (positions & strengths)
  - Broad and congested features

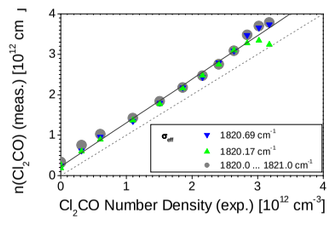

Broadband (FT-IR) Spectroscopy

Plasma-Enhanced Chemical Vapour Deposition

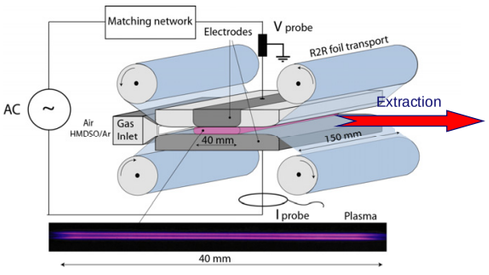

- *Ex-situ* sampling
  - 0.5 mm discharge gap
  - Multipass cell ($L_{eff} \sim$ 7.0 m)
- Gas mixture
  - Organosilicon precursor
  - N_2 / O_2 / Ar
- **Challenges**
  - Identification (PNNL-NWIR)
  - Spectral congestion
  - Quantification (HITRAN)

Qualitative & Quantitative Analysis

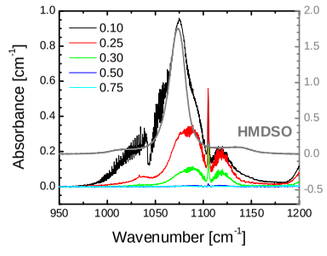

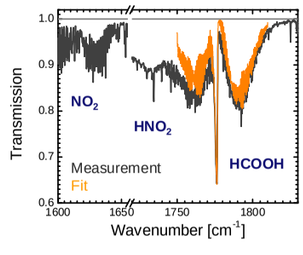

Plasma-Assisted Gas Conversion

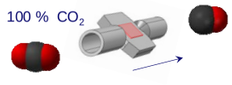

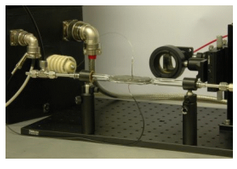

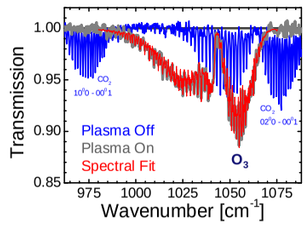

- *Ex-situ* sampling
  - Fibre-coupled cell ($L_{eff} \sim$ 0.5 m)
- **Challenges**
  - Quantification (HITRAN)
  - Line-broadening partners

Cavity-Enhanced Plasma Diagnostics

- *In-situ* CEAS
  - Ar / CH_4 / N_2 micro-wave plasma
  - Counter-measurements with IR-TDLAS
  - small(er) detection volumes

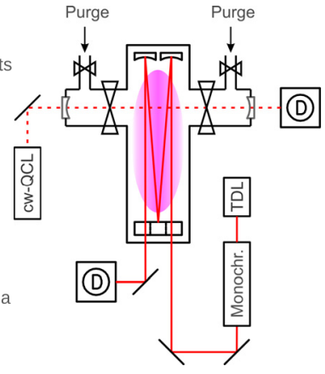

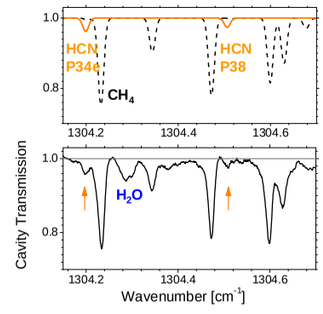

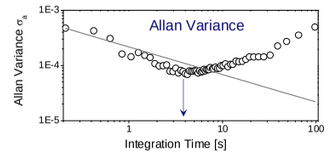

- **Challenges**
  - Convolution of changes and gradients in gas densities and temperatures across the plasma
  - Allan minimum determined by reactor expansion (sensitivity)
  - Non-equilibrium conditions (highly excited reaction products)

Herausgeber:
Physikalisch-Technische Bundesanstalt
Braunschweig und Berlin

Presse und Öffentlichkeitsarbeit

Bundesallee 100
38116 Braunschweig

Telefon: (05 31) 592-93 21
Telefax: (05 31) 592-92 92
www.ptb.de

Vertrieb:
Fachverlag NW in der
Carl Schünemann Verlag GmbH

Zweite Schlachtpforte 7
28195 Bremen

Telefon: (04 21) 369 03-0
Telefax: (04 21) 369 03-63
www.schuenemann-verlag.de